



Mitchell, Rebecca (2017) *Exploring BCR-ABL-independent mechanisms of TKI-resistance in chronic myeloid leukaemia*. PhD thesis.

<https://theses.gla.ac.uk/7977/>

Copyright and moral rights for this work are retained by the author

A copy can be downloaded for personal non-commercial research or study, without prior permission or charge

This work cannot be reproduced or quoted extensively from without first obtaining permission in writing from the author

The content must not be changed in any way or sold commercially in any format or medium without the formal permission of the author

When referring to this work, full bibliographic details including the author, title, awarding institution and date of the thesis must be given

Enlighten: Theses

<https://theses.gla.ac.uk/>
research-enlighten@glasgow.ac.uk

**Exploring BCR-ABL-independent mechanisms of
TKI-Resistance in Chronic Myeloid Leukaemia**

By

Rebecca Mitchell

BSc (Hons), MRes

Submitted in the fulfilment of the requirements for the degree of

Doctor of Philosophy

September 2016

Section of Experimental Haematology

Institute of Cancer Sciences

College of Medical, Veterinary and Life Science

University of Glasgow

Abstract

As the prevalence of Chronic Myeloid Leukaemia (CML) grows, due to the therapeutic success of tyrosine kinase inhibitors (TKI), we are witnessing increased incidences of drug resistance. Some of these patients have failed all currently licensed TKIs and have no mutational changes in the kinase domain that may explain the cause of TKI resistance. This poses a major clinical challenge as there are currently no other drug treatment options available for these patients. Therefore, our aim was to identify and target alternative survival pathways against BCR-ABL in order to eradicate TKI-resistant cells.

To investigate alternative survival mechanisms in TKI-resistant CML cells, ponatinib-resistant cell line models were generated, which show resistance to all current TKIs, despite complete inhibition of BCR-ABL activity. Additionally, DNA sequencing revealed no mutational changes within the BCR-ABL kinase domain, which may explain TKI resistance and RNA-sequencing showed an impaired transcriptional response following ponatinib treatment when compared with parental TKI-sensitive cells.

Using these models, we demonstrated that the TKI-resistant cells acquired alternative activation of mTOR. Using clinically relevant dual PI3K and mTOR inhibitors; NVP-Bez235, VS-5584, apitolisib and gedatolisib, we validated the PI3K-AKT-mTOR pathway as a therapeutic target in vitro in TKI-resistant CML cell lines and more importantly in bone marrow derived mononuclear cells from CML patients resistant to TKIs and with no known kinase domain mutational changes.

We demonstrated in vitro that TKI-resistant cell lines are highly sensitive to PI3K and mTOR inhibitors, with EC50 values less than 30 nM compared to ponatinib, 647.3 nM. These inhibitors reduced cell viability by causing a significant induction of apoptosis and significant decrease in the clonogenic growth of primary TKI-resistant CML patient samples.

Furthermore, we showed that NVP-Bez235 induced autophagy as a protective mechanism following PI3K/mTOR inhibition. The combination of NVP-Bez235 with pharmacological (Hydroxychloroquine (HCQ)) or specific autophagy inhibition, via ATG7 knockdown, the efficacy of NVP-Bez235 was enhanced shown by the dramatic reduction in clonogenic growth of TKI-resistant CML patient cells. In addition, we validated this in vivo using a murine model by transplanting luciferase tagged TKI-resistant cells, treated with NVP-

Bez235 in combination with HCQ, which significantly reduced tumour burden and increased survival rates compared to controls.

These data suggested that the PI3K-AKT-mTOR pathway may be a key player responsible for TKI-resistance and that pharmacological inhibition of this pathway, with the additional inhibition of autophagy, may represent a potential new treatment option for TKI-resistant CML patients, when resistance is driven by a BCR-ABL-independent mechanism.

Table of contents

Table of Contents

Abstract	2
List of Tables.....	11
List of Figures	12
Publications	16
Publications in Preparation	16
Acknowledgement.....	17
Author's declaration.....	18
Abbreviations	19
1 Introduction	23
1.1 History of haemopoietic stem cells.....	23
1.1.1 Development of the haemopoietic system.....	24
1.1.2 Haemopoietic hierarchy.....	24
1.1.3 HSC identification and isolation.....	25
1.1.4 Haemopoietic stem cell characteristics and regulation.....	27
1.1.5 CML is a stem cell disease	28
1.2 Chronic Myeloid Leukaemia	29
1.2.1 CML epidemiology and clinical characteristics	30
1.2.2 Diagnosis and monitoring.....	32
1.2.3 BCR-ABL structure	33
1.2.4 BCR-ABL functional domains	33
1.2.5 BCR-ABL oncogenic pathway	35
1.2.6 BCR-ABL mimics growth factor signalling.....	39
1.2.7 BCR-ABL alteration of the HSC niche	40
1.3 History of CML treatment.....	41
1.3.1 The development of tyrosine kinase inhibitors (TKIs).....	42

1.3.2	Imatinib in clinical trial.....	44
1.3.3	Treatment responses	45
1.4	Mechanisms of resistance.....	47
1.4.1	Intolerance and non-compliance	47
1.4.2	BCR-ABL-dependent mechanisms of resistance	48
1.4.3	BCR-ABL-independent mechanisms of resistance	51
1.5	Strategies to combat TKI resistance	55
1.5.1	Imatinib dose escalation.....	55
1.5.2	TKIs	55
1.5.3	Second-generation TKIs	55
1.5.4	Third-generation TKIs	58
1.5.5	An alternative experimental BCR-ABL inhibitor.....	60
1.5.6	Omacetaxine	61
1.6	Autophagy	62
1.6.1	Autophagy initiation	63
1.6.2	Autophagosome formation	63
1.6.3	Autophagosome completion	64
1.6.4	Autolysosome formation.....	65
1.6.5	Autophagy and Cancer.....	65
1.6.6	Autophagy and CML	66
1.6.7	Autophagy inhibition in CML	68
1.6.8	CHOICES clinical trial	69
1.6.9	New generation of autophagy inhibitors.....	69
2	Materials and Methods	73
2.1	Materials	73
2.1.1	Small molecule inhibitors	73
2.1.2	Tissue culture materials	73
2.1.3	Molecular biology supplies.....	76
2.1.4	FACS	80

2.1.5	Immunofluorescence.....	80
2.1.6	Seahorse.....	81
2.1.7	Animal work.....	81
2.1.8	PCR primer sequences.....	82
2.1.9	Equipment.....	83
2.2	Preparation of medium and solutions.....	84
2.2.1	Tissue culture mediums and solutions.....	84
2.2.2	Western blot solutions.....	87
2.2.3	Flow cytometry.....	90
2.2.4	Immunofluorescence solutions.....	90
2.2.5	PCR assay solutions.....	90
2.2.6	Transfection solutions.....	91
2.2.7	Microbiology solutions.....	92
2.3	Methods.....	93
2.3.1	Cell Culture.....	93
2.3.2	Cell proliferation assays.....	96
2.3.3	Colony Forming Cell (CFC) assay.....	97
2.3.4	Flow cytometry.....	98
2.3.5	Immunofluorescence microscopy.....	101
2.3.6	XTT cell viability assay.....	102
2.3.7	Repurposing NIH approved oncology drug screen.....	103
2.3.8	Western blotting.....	105
2.3.9	DNA sequencing.....	109
2.3.10	RNA-seq.....	111
2.3.11	shRNA constructs.....	112
2.3.12	Lentivirus transfection.....	112
2.3.13	Transduction of CML cell lines.....	113
2.3.14	CRISPR guide design.....	113
2.3.15	Target Guide Sequence Cloning Protocol.....	117

2.3.16	Animal work	119
3	Results (I): Identification and validation of suitable TKI-resistant models for the study of BCR-ABL-independent TKI-resistance	122
3.1	Aims and objectives	123
3.2	An assessment of current imatinib-resistant cell line models and their relevance for the study of BCR-ABL-independent TKI-resistance.....	123
3.3	The generation of a ponatinib-resistant CML cell model	126
3.3.1	Ponatinib resistant CML cell model is pan-TKI-resistant	131
3.3.2	Pre-clinical BCR-ABL inhibitor, ABL001, is ineffective against KCL22 ^{Pon-Res} and BaF3 ^{Pon-Res} cells	132
3.4	Characterisation of the mechanism causing TKI resistance in the ponatinib-resistant cell models	136
3.4.1	DNA sequencing reveals no kinase domain mutation.....	136
3.4.2	KCL22 ^{Pon-Res} cells have an impaired transcriptional response to TKI.....	137
3.4.3	mTOR activity is sustained in KCL22 ^{Pon-Res} cells despite BCR-ABL inhibition 139	
4	Results (II): Screening for potential novel drug target candidates for the treatment of BCR-ABL-independent TKI-resistant CML.....	141
4.1	Aim and objective	141
4.2	National Institute of Health (NIH) approved oncology drug screen	141
4.2.1	Confirmation that KCL22 ^{Pon-Res} cells are pan-TKI-resistant	143
4.2.2	37 clinically approved cancer drugs have the potential to induce cell death in TKI-resistant CML cells.....	143
4.2.3	KCL22 ^{Pon-Res} cells are highly sensitive to mTOR inhibitors.....	143
4.2.4	KCL22 ^{Pon-Res} cells are sensitive to HDAC inhibition	144
4.2.5	KCL22 ^{Pon-Res} cells are sensitive to MEK inhibition.....	145
4.3	Validation of the primary drug screen using the BaF3 ^{Pon-Res} cell model.....	148
4.3.1	mTORC1 inhibition is insufficient to affect cell viability in BaF3 ^{Pon-Res} cells	148
4.3.2	BaF3 ^{Pon-Res} cells are highly sensitive to dual PI3K and mTOR inhibition.....	150

4.3.3	Potential selectivity using trametinib against BaF3 ^{Pon-Res} cells compared to BaF3 ^{parental} cells	153
4.4	A tertiary screen was performed to assess toxicity of the drugs to normal haemopoietic cells	155
4.4.1	Dual PI3K and mTOR inhibitors may have a therapeutic window for treatment for BCR-ABL-independent TKI-resistant CML patients.....	155
4.4.2	MEK inhibition is not toxic to non-CML haemopoietic cells	158
5	Validation of mTOR inhibitors in ponatinib-resistant cell lines	160
5.1	Ponatinib resistant CML cells are sensitive to mTOR inhibition	161
5.2	mTOR inhibitors induce apoptosis and reduce CFC output in KCL22 ^{Pon-Res} cells 163	
5.3	KCL22 ^{Pon-Res} cells are highly sensitive to catalytic PI3K and mTOR inhibitors .	165
5.4	BaF3 ^{Pon-Res} cells are highly sensitive to NVP-Bez235	168
5.5	KCL22 ^{Pon-Res} cells transcriptional response is restored upon NVP-Bez235 treatment	170
6	Validation of mTOR inhibitors in primary TKI-resistant CML cells	178
6.1	MNCs derived from TKI-resistant CML patients are sensitive to NVP-Bez235-mediated mTOR inhibition ex vivo.....	178
6.2	Ponatinib is an effective treatment against BCR-ABL-dependent TKI-resistant CML cells	180
6.3	Ponatinib treatment causes different transcriptional responses in TKI sensitive CML, T315I CML and BCR-ABL-independent TKI-resistant CML	182
6.4	mTORC1 inhibition induces protective autophagy in KCL22 ^{Pon-Res} cells	192
6.5	NVP-Bez235 mediated mTOR inhibition induces autophagy in KCL22 ^{Pon-Res} cells 193	
6.6	ATG7 knock out mediated autophagy inhibition increases sensitivity of KCL22 ^{Pon-Res} cells to NVP-Bez235	195
6.7	Pharmacological autophagy inhibition enhances the effect of NVP-Bez235 against primary TKI-resistant CML cells	201
6.8	Autophagy inhibition enhances the effect of dual PI3K and mTOR inhibitors against primary TKI-resistant CML cells	203

6.9	Pharmacological inhibition of autophagy enhances the effect of NVP-Bez235 <i>in vivo</i>	205
6.10	The combination treatment of NVP-Bez235 and HCQ has minimal toxicity compared to omacetaxine in non-CML cells	207
6.11	The combination treatment of NVP-Bez235 and HCQ was well tolerated by NSG mice and significantly extended the survival of TKI-resistant CML xenograft mice.	210
7	Results: Establishing CRISPR as a genome-wide screening tool for the study of BCR-ABL-independent TKI-resistance	213
7.1	Gene knock-down	213
7.2	Clustered Regularly Interspaced Short Palindromic Repeat (CRISPR)/Cas system	214
7.2.1	CRISPR as a genome editing tool.....	217
7.2.2	CRISPR as a genome-wide forward screening tool.....	218
7.2.3	Method: Genome-wide forward CRISPR screen.....	221
7.2.4	CRISPR 2-vector screen	226
7.2.5	Preliminary results	236
7.2.6	Future work.....	239
8	Discussion	242
8.1	mTOR and autophagy	251
8.2	NVP-Bez235 and toxicity	253
8.3	Conclusion.....	255
8.4	Future work	256
9	Appendices	259
9.1	Plasmid maps	259
9.1.1	pLKO.1 puro	259
9.1.2	psPAX2 – Addgene (12260).....	260
9.1.3	pCMV-VSV-G – Addgene (8454).....	261
9.1.4	LentiCRISPR v2 Addgene (52961)	262
9.1.5	LentiCas9-Blast – Addgene (52962)	263
9.1.6	LentiGuide-Puro – Addgene (52963)	264

9.2	CRISPR data	265
9.2.1	gRNA lists from the KCL22 ^{WT} screen sample 1	265
9.2.2	gRNA lists from the KCL22 ^{WT} screen sample 2	292
10	List of references.....	310

List of Tables

Table 1-1: Immunophenotypes of haemopoietic cell populations.....	26
Table 2-1: Small molecule inhibitors ^(a) dimethyl sulfoxide; DMSO, ^(b) phosphate buffered saline; PBS	73
Table 2-2: Forward and reverse BCR-ABL primer sequences.	109
Table 2-3: PCR reaction mix.	109
Table 2-5: CRISPR single guide sequences for ATG7, mTOR, MEK and BCR-ABL.	116
Table 5-1: Clinically applicable dual PI3K and mTOR inhibitors. The drug name, name of pharmaceutical company developing the drug, EC50 (nM) in KCL22 ^{Pon-Res} cells calculated by graphpad from (figure 5-4) and the number of phase I and II clinical trials the drug is currently involved in. as shown on clinicaltrials.gov.	166
Table 5-2: A list of the different biological processes that occur in KCL22 ^{Pon-Res} cells following 24 hour NVP-Bez235 treatment and KCL22 ^{WT} following 24 hour ponatinib treatment obtained from the gene ontology enrichment analysis.....	176
Table 6-1: Clinical patient informations. Details of prior treatments, clinical trials and treatment responses.	180
Table 6-2: A differential list of the biological processes for CML TKI sensitive treated with ponatinib (green) and TKI-resistant CML treated with ponatinib (blue).....	188
Table 6-3: A differential list of the biological processes for CML T315I treated with ponatinib (light blue) and TKI-resistant CML treated with ponatinib (blue).....	191
Table 7-1: CRISPR screen gDNA concentrations.	234
Table 7-2: CRISPR screen PCR product concentrations.	236
Table 7-3: Guide RNAs with the highest reads from the CRISPR Screen.	236

List of Figures

Figure 1-1: The Haemopoietic Hierarchy.....	23
Figure 1-2: The Philadelphia Chromosome.....	30
Figure 1-3: Autophagy activation.....	70
Figure 1-4: The molecular mechanism of autophagy.....	71
Figure 2-1: Trypan blue method for cell counting and viability assessment with improved Neubauer counting chamber.....	96
Figure 2-2: 96 well plate XTT assay design for low concentration drug screening.....	102
Figure 2-3: BCR-ABL transcript.....	109
Figure 2-4: Design template for targeted guide sequences for CRISPR KO.....	114
Figure 2-5: Gel purification of BsmBI digested lentiCRISPRv2 and lentiGuide-puro.....	117
Figure 3-1: Imatinib-resistant cell lines.....	125
Figure 3-2: Illustrates the time course and increasing concentration of ponatinib used to generate the BaF3 ^{Pon-Res} cell line.....	126
Figure 3-3: KCL22 ^{WT} and KCL22 ^{Pon-Res} cells were seeded at 0.25x10 ⁶ /mL and treated with 0.1, 1, 10, 100, 1000 and 10000 nM ponatinib and 150 nM dasatinib.....	127
Figure 3-4: BaF3 ^{WT} and BaF3 ^{Pon-Res} cells were seeded at 0.25x10 ⁶ /ml and treated with 0.1, 1, 10, 100, 1000 and 10000 nM ponatinib and 150 nM dasatinib.....	128
Figure 3-5: XTT assay using ponatinib against KCL22 ^{WT} , KCL22 ^{Pon-Res} , BaF3 ^{parental} , BaF3 ^{WT} and BaF3 ^{Pon-Res} cells.....	130
Figure 3-6: KCL22 ^{Pon-Res} cells were treated with imatinib 2 μM, nilotinib 2 μM, dasatinib 150 nM, ponatinib 100 nM and omacetaxine 10 nM for 72 hours, and analysed by flow cytometry following annexin V and 7AAD staining.....	131
Figure 3-7: KCL22 ^{WT} and KCL22 ^{Pon-Res} cells were seeded at 0.25x10 ⁶ /ml and treated with 0.1, 1, 10, 100, 1000, 10000 nM ABL001 for 72 hours.....	133
Figure 3-8: BaF3 ^{parental} , BaF3 ^{WT} , BaF3 ^{T315I} and BaF3 ^{Pon-Res} cells were seeded at 0.25x10 ⁶ /ml and treated with 0.1, 1, 10, 100, 1000, 10000 nM ABL001 for 72 hours, and analysed by FACS following annexin V and 7AAD staining.....	135
Figure 3-9: Genomic sequencing of BaF3 ^{Pon-Res} revealed no mutations within the BCR-ABL kinase domain. Data shown here is for the position for the T315I mutation and no mutation change has occurred.....	136
Figure 3-10: Venn diagram showing the differential gene expression changes between KCL22 ^{WT} and KCL22 ^{Pon-Res} cells following 24 hours ponatinib treatment.....	138
Figure 3-11: A diagram of the PI3K/AKT/mTOR pathway, downstream of BCR-ABL.....	139
Figure 4-1: Workflow and depiction of the robotics used to pipette the drugs and the cells into the 96 well plates.....	142
Figure 4-2: Workflow and depiction of the robotics used to pipette the resazurin into the 96 well plates and the resazurin plate reader.....	142
Figure 4-3: Heat map of the top IC50 concentrations obtained from NIH approved oncology drug screen against KCL22 ^{Pon-Res} cells with and without ponatinib.....	147
Figure 4-4: BaF3 ^{parental} , BaF3 ^{WT} , BaF3 ^{Pon-Res} and BaF3 ^{Pon-Res} + 100 nM ponatinib cells were seeded at 0.25x10 ⁶ /mL and treated with the same equimolar concentration of drug ranging from 0.001 nM to 10 μM of sirolimus or everolimus.....	149
Figure 4-5: KCL22 ^{WT} , KCL22 ^{Pon-Res} , KCL22 ^{Pon-Res} +100 nM ponatinib, BaF3 ^{parental} , BaF3 ^{WT} , BaF3 ^{Pon-Res} and BaF3 ^{Pon-Res} + 100 nM ponatinib cells were seeded at 0.25x10 ⁶ /mL and treated with the same equimolar concentration of drug ranging from 0.001 nM to 10 μM of AZD8055.....	150

Figure 4-6: KCL22 ^{WT} , KCL22 ^{Pon-Res} , KCL22 ^{Pon-Res} +100 nM ponatinib, BaF3 ^{parental} , BaF3 ^{WT} , BaF3 ^{Pon-Res} and BaF3 ^{Pon-Res} + 100 nM ponatinib cells were seeded at 0.25x10 ⁶ / mL and treated with the same equimolar concentration of drug ranging from 0.001 nM to 10 μM of Apitolisib, VS-5584, NVP-Bez235 and Gedatolisib.	152
Figure 4-7: KCL22 ^{WT} , KCL22 ^{Pon-Res} , KCL22 ^{Pon-Res} +100 nM ponatinib, BaF3 ^{parental} , BaF3 ^{WT} , BaF3 ^{Pon-Res} and BaF3 ^{Pon-Res} + 100 nM ponatinib cells were seeded at 0.25x10 ⁶ / mL and treated with the same equimolar concentration of drug ranging from 0.001 nM to 10 μM of selumetinib and trametinib.	154
Figure 4-8: Non-CML cells from three different samples were seeded at 0.5x10 ⁶ / mL and treated with the same equimolar concentration of drug ranging from 0.001 nM to 10 μM of sirolimus, everolimus and AZD8055.	156
Figure 4-9: Non-CML cells from three different samples were seeded at 0.5x10 ⁶ / mL and treated with the same equimolar concentration of drug ranging from 0.001 nM to 10 μM of apitolisib, VS-5584, NVP-Bez235 and gedatolisib.	157
Figure 4-10: Non-CML cells from three different samples were seeded at 0.5x10 ⁶ / mL and treated with the same equimolar concentration of drug ranging from 0.001 nM to 10 μM selumetinib and trametinib.	158
Figure 5-1: Schematic of the PI3K/AKT/mTOR pathway, downstream of BCR-ABL. It illustrates the chosen clinically applicable mTOR inhibitors and their targets.	161
Figure 5-2: KCL22 ^{Pon-Res} were seeded at 0.2x10 ⁶ / mL and treated with the same equimolar concentration of drug ranging from 0.01 nM to 10 μM (ponatinib, NVP-Bez235, AZD8055, and BKM120).	162
Figure 5-3: KCL22 ^{Pon-Res} were seeded at 0.25x10 ⁶ / mL and treated with 2 μM imatinib, 2 μM nilotinib, 150 nM dasatinib, 100 nM ponatinib, 10 nM rapamycin, 500nM BKM120, AZD8055, 100 nM NVP-Bez235, 100 nM.	164
Figure 5-4: KCL22 ^{Pon-Res} were seeded at 0.2x10 ⁶ / mL and treated with the same equimolar concentration of drug ranging from 0.01 nM to 10 μM (gedatolisib, VS-5584, NVP-Bez235, apitolisib, and ponatinib). Colour coded by Table 5-1.	166
Figure 5-5: KCL22 ^{Pon-Res} were seeded at 0.25x10 ⁶ / mL and treated with 100 nM ponatinib, 100 nM apitolisib, 100 nM VS-5584, 100 nM NVP-Bez235, 100 nM gedatolisib for 72 hours.	167
Figure 5-6: KCL22 ^{WT} and KCL22 ^{Pon-Res} were seeded at 0.25x10 ⁶ /mL and treated with and 100 nM ponatinib, 100 nM NVP-Bez235 or 100 nM gedatolisib for 24 hours.	167
Figure 5-7: (a) BaF3 ^{WT} and BaF3 ^{Pon-Res} were seeded at 0.2x10 ⁶ / mL and treated with the same equimolar concentration of drug ranging from 0.01 nM to 10 μM (ponatinib and NVP-Bez235. Cell viability measured after 72 hours using an XTT assay and (b) EC50 was calculated using graphpad prism.	169
Figure 5-8: BaF3 ^{WT} and BaF3 ^{Pon-Res} were seeded at 0.25x10 ⁶ / mL and treated with 2μM imatinib, 150 nM dasatinib, 100 nM ponatinib or 100 nM NVP-Bez235.	170
Figure 5-9: A volcano plot showing the fold changes in gene expression patterns in KCL22 ^{Pon-Res} cells following 24 hour NVP-Bez235 treatment or a combination treatment of NVP-Bez235 and ponatinib, down-regulated genes in green and up-regulated genes in pink.	171
Figure 5-10: (a) Venn diagram showing the differential gene expression changes between KCL22 ^{WT} following 24 hour ponatinib treatment and KCL22 ^{Pon-Res} cells following 24 hour NVP-Bez235 treatment and (b) Relative correlation comparison of log changes in gene expression.	173
Figure 5-11: Venn diagram showing the comparison of the differential gene expression changes between KCL22 ^{WT} following 24 hour ponatinib treatment, KCL22 ^{WT} following 24 hour NVP-Bez235 treatment and KCL22 ^{Pon-Res} cells following 24 hour NVP-Bez235 treatment.	174

Figure 6-1: Bone marrow and peripheral blood derived MNCs from TKI-resistant CML patients were cultured in SFM supplemented with physiological growth factors.	179
Figure 6-2: Bone marrow and peripheral blood derived MNCs from CML patients carrying the T315I mutation.....	181
Figure 6-3: Volcano plots showing the fold changes in gene expression patterns in TKI sensitive CML cells, BCR-ABL-independent TKI-resistant CML cells and T315I CML cells following 24 hour ponatinib treatment, down-regulated genes (left) and up-regulated genes (right).	183
Figure 6-4: Venn diagram showing the differential gene expression changes between TKI sensitive CML cells, BCR-ABL-independent TKI-resistant CML cells and T315I CML cells following 24 hours ponatinib treatment. Genes up-regulated in red and genes down-regulated in green.....	183
Figure 6-5: Gene ontology enrichment of the biological processes that occur in KCL22 ^{Pon-Res} cells following 24 hour NVP-Bez235 treatment.....	185
Figure 6-6: A dot plot showing the functional response to ponatinib in CML TKI sensitive versus CML TKI-resistant cells.	186
Figure 6-7: A dot plot showing the functional response to ponatinib in CML T315I versus CML TKI-resistant cells.	189
Figure 6-8: Schematic of the PI3K/AKT/mTOR pathway, downstream of BCR-ABL and mTORC1's regulation of autophagy.	192
Figure 6-9: Schematic diagram of mRFP-GFP-LC3 system where different stages of autophagy can be measured as red+green=yellow puncta indicating autophagosomes and 'red only' signal indicates autolysosomes.....	194
Figure 6-10: KCL22 ^{Pon-Res} cells were lentivirally transduced with a CRISPR v2 vector containing an ATG7-targeting sequence or an empty vector control with unconcentrated virus.	196
Figure 6-11: The measurement of LC3BII in KCL22 ^{Pon-Res} ATG7 KO and control cells.....	197
Figure 6-12: KCL22 ^{Pon-Res} cells were lentivirally transduced with a CRISPR v2 vector containing an ATG7-targeting sequence or an empty vector control with unconcentrated virus.	198
Figure 6-13: KCL22 ^{Pon-Res} cells were lentivirally transduced with a pLKO.1-GFP vector carrying either a mock (shSCR) or an ATG7-targeting hairpin (shATG7) with unconcentrated virus.....	199
Figure 6-14: Bone marrow derived MNCs from TKI-resistant CML patients were cultured in SFM supplemented with physiological growth factors.....	202
Figure 6-15: Bone marrow derived MNCs from a TKI-resistant CML patient were cultured in SFM supplemented with physiological growth factors.....	204
Figure 6-16: KCL22 ^{Pon-Res} were labelled with lentiviral firefly luciferase and seeded at 0.25x10 ⁶ /ml and treated with 10 µM HCQ, 100 nM Ponatinib, 100 nM NVP-Bez235 or combination, in vitro for 72 hours.	206
Figure 6-17: BaF3 ^{Parental} and BaF3 ^{Pon-Res} cells were seeded at 0.25x10 ⁶ / mL and treated with 100 nM NVP-Bez235 or 100 nM gedatolisib. The percentage of apoptosis was measured following a 72 hour drug treatment.....	208
Figure 6-18: Bone marrow derived MNCs from a non-CML lymphoma patients were cultured in SFM supplemented with physiological growth factors.....	209
Figure 6-19: KCL22 ^{Pon-Res} were labelled with lentiviral firefly luciferase intravenously injected into NSG mice (5-6 mice per cohort).....	211
Figure 7-1: The functional mechanism of the type II CRISPR-Cas systems for adaptive immunity.	216
Figure 7-2: Lentiviral expression vectors for the one vector (lentiCRISPRv2) and two vector GeCKO systems (lentiCas9-Blast and lentiGuide-puro).....	220

Figure 7-3: Gel electrophoresis of PCR products from PCR 1 and 2. Gel purification of PCR 2 product 340pb.	225
Figure 7-4: The workflow of the GeCKO Library amplification Addgene.....	225
Figure 7-5: The workflow for the positive selection CRISPR Screen.....	226
Figure 7-6: Stable expression of LentiCas9-Blast in KCL22 ^{WT} cells.....	227
Figure 7-7: KCL22 ^{WT} cells under a ponatinib treatment time course.....	228
Figure 7-8: Virus titration on KCL22 ^{WT} -Cas9-Blast after 72 hours.....	230
Figure 7-9: KCL22 ^{WT} -Cas9-Blast FACS analysis post 10 days puromycin selection.....	231
Figure 7-10: : Ponatinib selection and FACS sorting of the CRISPR screen.....	233
Figure 7-11: Gel purification of PCR 2 product 340pb from KCL22 ^{WT} resistant screen day 0.....	235
Figure 7-12: Gel purification of PCR 2 product 340pb from KCL22 ^{WT} resistant screen day 0.....	236
Figure 7-13: The workflow for a negative CRISPR Screen.....	240
Figure 8-1: Our proposed drug treatment strategy for BCR-ABL-independent mechanism TKI-resistant CML.....	255

Publications

Isabel Ben-Batalla, Robert Erdmann, Heather Jørgensen, **Rebecca Mitchell**, Thomas Ernst, Gunhild von Amsberg, Philippe Schafhausen, Stephen Rankin, Richard E. Clark, Steffen Koschmieder, Alexander Schultze, Subir Mitra, Peter Vandenberghe, Tim Brümmendorf, Peter Carmeliet, Gudmundur Helgason, Andreas Hochhaus, Klaus Pantel, Carsten Bokemeyer, Tessa Holyoake and Sonja Loges. BGB324 Inhibits Pan-TKI-Resistant Chronic Myeloid Leukaemia. *Blood* 2015 126:1569

Karvela M, Baquero P, Kuntz EM, Mukhopadhyay A, **Mitchell R**, Allan EK, Chan E, Kranc KR, Calabretta B, Salomoni P, Gottlieb E, Holyoake TL and Helgason GV. ATG7 regulates energy metabolism, differentiation and survival of Philadelphia chromosome-positive cells. *Autophagy*. 2016. 12(6): 936–948.

Isabel Ben-Batalla, Robert Erdmann, Heather Jørgensen, **Rebecca Mitchell**, Thomas Ernst, Gunhild von Amsberg, Philippe Schafhausen, Stephen Rankin, Richard E. Clark, Steffen Koschmieder, Alexander Schultze, Subir Mitra, Peter Vandenberghe, Tim Brümmendorf, Peter Carmeliet, Gudmundur Helgason, Andreas Hochhaus, Klaus Pantel, Carsten Bokemeyer, Tessa Holyoake and Sonja Loges. AXL Blockade by BGB324 Inhibits BCR-ABL Tyrosine Kinase Inhibitor-Sensitive and -Resistant Chronic Myeloid Leukaemia. *Clinical Cancer Research*. Undergoing minor revisions.

Publications in Preparation

Rebecca Mitchell, Lisa E. M. Hopcroft, Elaine K. Allan, Key Hewit, Daniel James, Graham Hamilton, Arunima Mukhopadhyay, Pablo Baquero, Jim O’Prey, Alan Hair, Junia Melo, Edmond Chan, Kevin M. Ryan, Brian J. Druker, Richard Clark, Subir Mitra, Pawel Herzyk, Franck E. Nicolini, Paolo Salomoni, Emma Shanks, Bruno Calabretta, Tessa L. Holyoake, and G. Vignir Helgason. Combined mTOR and autophagy inhibition overcomes BCR-ABL-independent TKI resistance in chronic myeloid leukaemia

Acknowledgement

Undertaking this PhD has been great learning experience for me and I would like to thank all the people who made this thesis possible. Firstly, to my primary supervisor, Dr. Vignir Helgason who directed this project and supported me throughout the duration of the PhD. I'm also grateful of the kindness he and his family have shown over the years by involving me in family events and his generosity in times of success within the laboratory. It has been a great experience working alongside Vignir. As I am young scientist the knowledge and the support he has given me has encouraged me to maintain a career in academia.

I would also like to thank my second supervisor Professor Tessa Holyoake, whose knowledge and expertise in the CML field has allowed our research in the lab to excel. I am very thankful to her for her support over the years. I have been very lucky to have been picked to do this PhD under the supervision of two very talented scientists and in state of the art facilities. I have learnt so much over the years this opportunity has opened so many doors to me that I should be able to thrive as an academic researcher upon passing my PhD.

I would like to acknowledge several people who helped with aspects of the research presented in this thesis, namely, Dr Pablo Baquero, Ms Elaine Allan, Dr Alan Hair, Miss Jennifer Cassels, Mrs Karen Dunn, Dr Lisa Hopcroft, Dr Graham Hamilton, Dr Pawel Herzyk and his team at Glasgow Polyomics, Dr Emma Shanks, Dr Kay Hewitt, Dr Susan Rhodes, Dr Annie Latif, Dr Franck Nicolini, Dr Subir Mitra and Dr Richard Clark and a special thank you to the patients who donated their blood and bone marrow samples for experimentation in this thesis.

I would also like to acknowledge my advisor of studies, Professor Kevin Ryan and Dr Emilio Cosimo for useful discussions throughout the duration of my PhD. I would like to thank my examiners and convenor Professor Nick Cross, Dr Christina Halsey and Dr Heather Jørgensen for taking the time to examine my thesis. I would like to thank my colleagues at the Paul O'Gorman Leukaemia Research Centre for their continual support during the course of my PhD. I am lucky to have worked with such a wonderful group of people and in a fantastic laboratory environment. I would like to thank the University of Glasgow and the Scottish Universities Life Sciences Alliance (SULSA) for the funding of my research.

However, the most special thank you goes to my parents, family and friends. They have been there for me when it all seems too much and you always get me through it. I would not have been able to get to this stage without your unconditional love and support and I am so grateful for you all. x

Author's declaration

I declare that, except where explicit reference is made to the contribution of others, this dissertation is the result of my own work and has not been submitted for any other degree at the University of Glasgow or any other institution.

Abbreviations

Accelerated phase	AP
Activating Molecule in BECN1-regulated autophagy1	AMBRA1
Adenosine triphosphate	ATP
AMP-activated protein kinase	AMPK
ATP-binding cassette subfamily B member 1	ABCB1, Pgp, MDR1
Autophagy genes	ATG
Bicinchoninic acid	BCA
Blast crisis	BC
Bone marrow	BM
Bovine serum albumin	BSA
Breakpoint Cluster Region	BCR
Chloroquine	CQ
CHlOroquine and Imatinib Combination to Eliminate Stem cells	CHOICES
Chronic myeloid leukaemia	CML
Chronic phase	CP
Clustered Regularly Interspaced Short Palindromic Repeat	CRISPR
Coiled-coil	CC
Colony Formation Cell assay	CFC
Common lymphoid progenitors	CLP
Common myeloid progenitors	CMP
Complementary DNA	cDNA
Complete CyR	CCyR
Complete haematological response	CHR
Complete molecular response	CMR
CRISPR-associated	Cas
Cyclin-dependent kinase	CDK
Cytochrome P450	CYP
Cytogenetic responses	CyR
DEP domains interactor of mTOR	DEPTOR
Double stranded break	DSB
Dulbecco's modified eagle medium	DMEM
Endoplasmic reticulum	ER
Eukaryotic translation initiation factor 4E-binding protein 1	4E-BP1
European Leukaemia Net	ELN
Evaluation of ponatinib versus imatinib in CML trial	EPIC
Foetal calf serum	FBS

Fluorescence in-situ hybridization	FISH
Forkhead box subgroup O	FOXO
Genome-scale CRISPR Knock Out	GeCKO
Genomic DNA	gDNA
Granulocyte colony stimulating factor	G-CSF
Granulocyte macrophage-colony stimulating factor	GM-CSF
Grb-2-associated binding protein 2	GAB2
Green fluorescent protein	GFP
Guide RNAs	gRNA
Haemopoietic stem cells	HSCs
Hank's buffered salt solution	HBSS
Histone acetyltransferase	HAT
Histone deacetylases	HDACs
Homology Directed Repair	HDR
Human homologue of the Abelson Murine Leukaemia virus	ABL
Human organic cation transporter 1 transporter	hOCT-1
Hydroxychloroquine	HCQ
Insertions or deletions	InDels
Interferon α	IFN α
Interleukin-3	Il-3
International Randomized Study of Interferon and STI571 trial	IRIS
Isocove's modified Dulbecco's medium	IMDM
Janus-activated kinase	JAK
Kilobases	kb
Knock-down	KD
Knock-out	KO
Leukaemic stem cells	LSCs
Light chain 3	LC3
Long-term HSCs	LT-HSCs
Macrophage inflammatory protein 1 α	MIP-1 α
Magnesium chloride	MgCl ₂
Major cytogenetic response	MCyR
Major molecular response	MMR
Mammalian Target of Rapamycin	mTOR
Maximal tolerated doses	MTDs
Maximum measured plasma concentration	cMax
Micromolar	μ M

Mitogen-activated protein kinase	MAPK
Mononuclear cells	MNCs
mTOR complex 1	mTORC1
mTOR complex 2	mTORC2
Multi-Drug resistant gene 1	MDR1
Multiplicity of infection	MOI
Multipotent progenitors	MPP
Murine double mutant 2	MDM2
Nanomolar	nM
National Comprehensive Cancer Network	NCCN
National Institute of Health	NIH
natural killer	NK
NOD scid gamma	NSG
Non-Homologous End Joining	NHEJ
Open reading frame	ORF
Oxygen Consumption Rate	OCR
P-glycoprotein	Pgp
Philadelphia chromosome	Ph
Phosphate buffered saline	PBS
Phosphatidylethanolamine	PE
Phosphoinositide 3-kinase	PI3K
Phosphoinositide-4,5-bisphosphate	PIP2
Phosphoinositide-3,4,5-trisphosphate	PIP3
Platelet-derived growth factor	PDGF
Ponatinib Ph+ ALL and CML Evaluation trial	PACE
Protein kinase $C\alpha$	PKC α
Protospacer Adjacent Motif	PAM
Quantitative reverse-transcriptase polymerase chain reaction	qRT-PCR
Rac GTPase activating protein	Rac-GAP
Radio-immunoprecipitation assay buffer	RIPA
Rapamycin insensitive companion of mTOR	RICTOR
Reactive oxygen species	ROS
Red blood cells	RBCs
Regulatory-associated protein of mTOR	RAPTOR
Retinoblastoma	Rb
Rho guanine-nucleotide exchange factor	Rho-GEF
Ribosomal protein S6	RPS6

SCR homology domain	SH
SDS-polyacrylamide gel electrophoresis	SDS-PAGE
Serum free medium	SFM
SFM supplemented with high five growth factors	SFM+5GFs
SFM supplemented with physiological growth factors	SFM+PGFs
SH2-containing tyrosine phosphatase 1	SHP-1
short-hairpin RNA	shRNA
Short-term HSCs	ST-HSCs
Signal transducer and activator of transcription factor 5	STAT5
Sodium dodecyl sulphate	SDS
Son of Sevenless	SOS
SQSTM1	p62
Stem Cell Factor	SCF
Tuberous Sclerosis-2	TSC-2
Tyrosine Kinase Inhibitor	TKI
Ultraviolet	UV
Unc-51- like kinase 1	ULK1
Unc-51- like kinase 2	ULK2
United States Food and Drug Administration	FDA
UV radiation resistance-associated gene	UVRAG
Vacuolar protein sorting 34	VPS34
4',6-Diamidino-2-Phenylindole, Dihydrochloride	DAPI
7 aminoactinomycin D	7-AAD

1 Introduction

1.1 History of haemopoietic stem cells

Haemopoiesis is a beautiful example of the human body's ability to orchestrate highly complex and regulated processes that are vital for the maintenance of life. The haemopoietic system is responsible for producing blood cells from all blood cell lineages and replenishing these cells throughout an individual's lifetime. Most mature blood cells have short lifespans and therefore maintaining blood homeostasis relies heavily on the cells ability to self-renew and differentiate. These unique biological properties are held by a very rare but long lived cell population known as haemopoietic stem cells (HSCs).

HSCs stand at the apex of the hierarchy of the haemopoietic system and have the ability to maintain themselves and generate all types of mature blood cells through a series of progenitor cells that become progressively restricted to several or single lineages (Orkin, 2000). These progenitors create blood precursors devoted to unilineage differentiation and production of mature blood cells, including red blood cells, megakaryocytes, myeloid cells (monocyte/macrophage and neutrophil), and lymphocytes (figure 1-1).

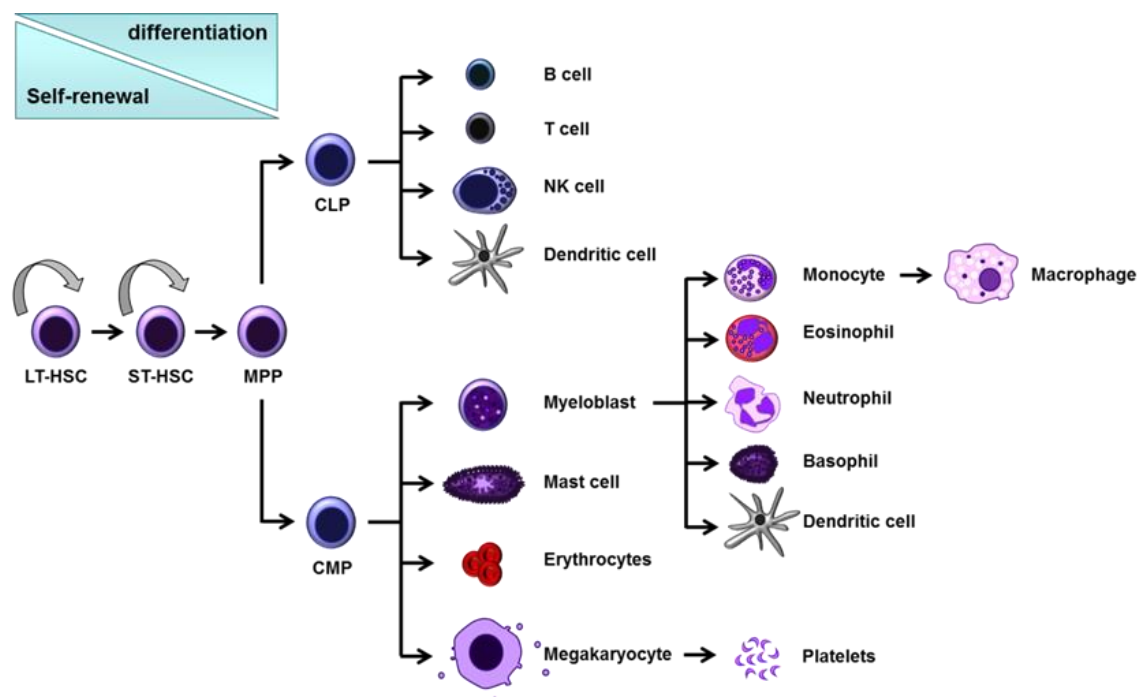


Figure 1-1: The Haemopoietic Hierarchy.

1.1.1 Development of the haemopoietic system

In mammals, the production of haemopoietic cells is accomplished in two waves of haemopoietic activity; a primitive wave and a definitive wave (Galloway and Zon, 2003). The primitive wave begins early in embryonic development, within the yolk sac. The purpose of this wave is to produce erythrocytes which are able to oxygenate the embryo and to support its rapid proliferation (Orkin and Zon, 2008). Although blood cells are produced during this wave, they are transitory and are only produced to provide support to the embryo within its early development.

The definitive wave is the first major phase of haemopoietic cell production and this occurs in the aorta, gonads and mesonephros (AGM) region. This occurs around day 23 during human gestation, where the initial transient progenitors are produced (Bertrand et al., 2007, McGrath et al., 2011). By day 27 cells with the characteristic hallmarks of a HSC begin to emerge from the human embryonic aorta (Tavian et al., 2001). The HSCs divide and soon after migrate to the primary foetal haemopoietic centre, the liver. The HSCs continue to divide in the foetal liver and migrate through to the spleen and thymus, and just before birth the HSCs migrate to the primary adult haemopoietic centre, the BM, where they engraft, self-renew and differentiate (Cumano and Godin, 2007).

1.1.2 Haemopoietic hierarchy

Human and mouse haemopoiesis are historically described as cellular hierarchies, which are maintained by HSCs that reside at the apex of the pyramidal structure of differentiating blood cells. In murine haemopoiesis the HSC pool has two functionally distinct subpopulations, long-term HSCs (LT-HSCs) and short-term HSCs (ST-HSCs) (Morrison and Weissman, 1994). LT-HSCs have an extensive renewing potential and provide long-term reconstitution of HSCs, while ST-HSCs have a limited self-renewal capacity.

The standard haemopoietic model begins with a single LT-HSC and upon activation can give rise to a less primitive ST-HSC. The HSC population produces stem cell intermediates with less durable self-renewal, termed multipotent progenitor cells (MPPs). This is the final step before oligopotent and unipotent progenitors are produced, which have shorter life spans, are of higher frequency and differentiate into many functional blood cell types. MPPs can differentiate into two different common lineages; one for myelopoiesis; a common myeloid progenitor (CMP) or one for lymphopoiesis; a common lymphoid progenitor (CLP) (Akashi et al., 2000, Kondo et al., 1997). CLPs then differentiate and the potential to produce B-cells, T-cells, Natural Killer (NK) cells and dendritic cells. During

myelopoiesis the CMP population, produce more mature lineage restricted progenitor populations, such as megakaryocyte and erythroid progenitors, which go on to make platelets and red blood cells (RBCs). CMPs also produce granulocyte and monocyte progenitors, which differentiate into mast cells, eosinophils, basophils, neutrophils, monocytes, dendritic cells and macrophages (figure 1-1).

1.1.3 HSC identification and isolation

The human haemopoietic hierarchical model was based on a similar differentiation scheme as that of mouse haemopoiesis. Human HSCs were isolated and validated using the same isolation strategy previously used for mouse HSCs using immunophenotypic cell surface markers (Table 1-1). Cell populations were isolated using FACS analysis against the cell's immunophenotypes and their activity was measured by conducting BM repopulation assays and methylcellulose colony-forming cell (CFC) assays. These experiments identified that different populations of cells vary in terms of their ability to reconstitute the haemopoietic system. However, the current model that human blood development occurs progressively through a series of multipotent, oligopotent, and then unilineage progenitor stages is being challenged (Notta et al., 2016). Recent studies in John Dick's Laboratory have proposed a redefined model, which includes a developmental shift in the progenitor cell architecture from the foetus, where many stem and progenitor cell types are multipotent, to the adult, where the stem cell compartment is multipotent but the progenitors are unipotent (Notta et al., 2016). Since the original experiments were carried out to identify and isolate haemopoietic cells, new markers have been identified and new isolation strategies are being proposed (Notta et al., 2016).

<i>Cell Type</i>	<i>Phenotype</i>
LT-HSC	CD34+ CD38- CD90+ CD45RA- CD49f+ Lineage -
MPP	CD34+ CD38- CD90- CD45RA- CD49f- Lineage -
CMP	CD34+ CD38+ CD45RA- CD135+ CD7- CD10-
CLP	CD34+ CD38+ CD45RA+ CD7- CD10+
Mature cells	CD34- Lineage+

Table 1-1: Immunophenotypes of haemopoietic cell populations

1.1.4 Haemopoietic stem cell characteristics and regulation

The HSCs are the most important cells in haemopoietic cell production, as these cells are ultimately responsible for repopulating the whole haemopoietic system throughout life. Although HSCs are a very rare cell population, accounting for only 0.05% of cells within total BM population (Morrison et al., 1995), they have the capacity to produce all types of mature blood cells due to their multipotency and ability to self-renew. In order to do so, HSCs can either divide asymmetrically; producing one daughter cell that differentiates and becomes a committed progenitor cell and one daughter cell that retains HSC characteristics or HSCs can divide symmetrically producing two daughter cells that are committed progenitor cells or two new HSCs (Marley and Gordon, 2005). The combination of asymmetric and symmetric cell divisions controls haemopoiesis by maintaining the stem cell pool and the producing more mature progenitors. The daughter cell's fate is highly regulated by many intrinsic factors as well as extrinsic factors, which are believed to come from the BM microenvironment, known also as the stem cell niche (Schofield, 1978).

Another fundamental characteristic of HSCs is quiescence. HSCs exist in a quiescent state within the BM microenvironment. Cellular division is very infrequent and it is thought a single cell division occurs every 40 weeks (Catlin et al., 2011). Therefore, HSCs predominantly reside outside of the cell cycle in the G0 phase. However, HSCs can be rapidly activated to enter the cell cycle to regulate haemopoiesis following physiological demands.

The maintenance of HSCs demands strict regulation between HSC quiescence and proliferation, which is maintained by a complex network of intrinsic and extrinsic factors. Essential intrinsic factors include cell cycle regulators, such as cyclin-dependent kinase (CDK) inhibitor p21^{Cip1} (Cheng et al., 2000), Rb family (Viatour et al., 2008), p53 (Liu et al., 2009), c-myc (Laurenti et al., 2008), PTEN (Yilmaz et al., 2006), RUNX1 (Jacob et al., 2010), FOXO (Miyamoto et al., 2007), PU.1 (Staber et al., 2013), C/EBPa (Ye et al., 2013) and epigenetic regulators; Bmi1 (Park et al., 2003) and Dnmt3a (Challen et al., 2012). Extrinsic factors also have an important role in the maintenance of quiescent HSCs. It is believed that osteoblasts within the niche produce growth factors, extracellular matrices and other intracellular signals that are crucial for the long-term maintenance of HSC quiescence. Various signalling pathways have been implicated such as; Wnt/ β -catenin signalling (Fleming et al., 2008), Notch signalling (Varnum-Finney et al., 1998), as well as Tie2/Angiopoietin-1 (Arai et al., 2004) and Mpl/Thrombopoietin (Qian et al., 2007, Yoshihara et al., 2007) interactions. The hypoxic environment of the niche is also a key

regulator of HSCs. Hypoxia-inducing factors, such as HIF-1 (Takubo et al., 2010) contribute to the maintenance of HSC quiescence (Simsek et al., 2010). Due to low levels of oxygen in the BM microenvironment HSCs have a low oxidative metabolism and therefore use glycolysis for energy production (Simsek et al., 2010). This also results in reduced reactive oxygen species (ROS) production, which is required to maintain self-renewal and genomic stability (Suda et al., 2011).

Another mechanism has been identified which allows HSCs to evade metabolic stress within the stem cell niche. It has been shown that quiescent HSCs require the efficient process of autophagy. Autophagy is a catabolic pathway, which sequesters unwanted cellular components into characteristic double-membrane vesicles, called autophagosomes, and delivers them to lysosomes for degradation (He and Klionsky, 2009). The energy produced through the degradation of the cellular components can then be used to maintain nutrient and energy levels during periods of metabolic starvation or stress (He and Klionsky, 2009). Through the ablation of essential autophagy gene, *ATG7*, it has been shown that efficient autophagy is required in order for quiescent HSCs to control mitochondrial mass, ROS levels, and genomic integrity (Mortensen et al., 2011). Warr and colleagues showed that autophagy was essential in protecting quiescent HSCs from growth factor fluctuations and nutrient deprivations that naturally occur in the BM microenvironment, especially after haemopoietic injury (Warr et al., 2013a). Any imbalance in these mechanisms could cause haematological disorders; (1) insufficient proliferation would impair haemopoiesis and cause BM failure, (2) whilst increased proliferation might lead to exhaustion of the HSC pool and therefore overproduction of various blood lineages, which could lead to the development of a haematological malignancy (Pietras et al., 2011).

1.1.5 CML is a stem cell disease

The concept of a cancer causing stem cell was first proposed in 1997 by Bonnet and Dick, when they were able to isolate different populations of haemopoietic stem and progenitor cells from acute myeloid leukaemia patients and assess their capacity to initiate leukaemia in NOD.Cg-PrkdcscidII2rgtm1Wjl/SzJ mice or more commonly known as the NOD scid gamma (NSG). Their study showed that only the most primitive stem cell population ($CD34^+CD38^-$) had the potential to induce leukaemia (Bonnet and Dick, 1997). Leukaemic stem cells (LSCs) have a similar phenotype to normal HSCs. It is thought that in CML the LSC arises from a HSC that has acquired mutations that promote leukaemic transformation, as LSCs retain stem cell characteristics such as the ability to self-renew,

but have also developed the ability to initiate leukaemia and cause metastasis and drug resistance (Reya et al., 2001).

1.2 Chronic Myeloid Leukaemia

Chronic myeloid leukaemia (CML) is one of the biggest success stories of modern medicine. Research in this field was the first to provide evidence of a genetic link to cancer. Historically, in 1960 Peter Nowell and David Hungerford identified that leukaemic leukocytes from patients suffering from CML had “small but definite chromosomal changes”. This study revealed an abnormally short chromosome 22, which they called the Philadelphia (Ph) chromosome (Nowell and Hungerford, 1960). Initially, Ph chromosome was thought to be caused by a genetic deletion, however in 1973, due to the development of new cytogenetic techniques, Dr. Janet Rowley karyotyped CML patients cells and demonstrated that the Ph chromosome developed as a consequence of a specific chromosomal translocation (Rowley, 1973). This abnormality resulted from the reciprocal translocation of the long arm of chromosome 9 replacing the long arm of chromosome 22, $t(9;22)(q34;q11)$ (Rowley, 1973) (figure 1-2). Consequentially, this leads to the generation of an abnormal fusion between *c-Abl*⁺ (human homologue of the Abelson Murine Leukaemia virus) a tyrosine kinase encoding oncogene, native to chromosome 9 and *Bcr*⁺ (Breakpoint Cluster Region), native to chromosome 22 (Groffen et al., 1984). This chimeric fusion gene encodes a 210 kDa oncoprotein (p210 BCR-ABL), which possesses increased and constitutively active tyrosine kinase activity (Konopka et al., 1984, Daley et al., 1990). It is this abnormal activity, which promotes cellular transformation and ultimately the development of leukaemia (Konopka et al., 1984, Daley et al., 1990).

The most striking evidence of this was shown by various mouse model experiments, where murine BM was infected with retrovirus encoding p210 BCR-ABL and was transplanted into recipient mice. Transplant recipients developed a myeloproliferative syndrome closely resembling the chronic phase (CP) of human CML. Therefore demonstrating that BCR-ABL is necessary and sufficient for the development and maintenance of the disease (Daley et al., 1990, Elefanty et al., 1990, Heisterkamp et al., 1990, Kelliher et al., 1990).

The origin of this myeloproliferative disorder has been shown to arise as a consequence of a rare event in a single haemopoietic stem cell. Evidence that CML is a clonal disease was first demonstrated in 1967 following a study of three female CML patients. These patients were heterozygous for an X-linked gene, glucose-6-phosphate dehydrogenase, however the CML cells from the patients only expressed one of the genes suggesting that these cells originated from a common stem cell and that CML cells are clonal in origin, which leads

to the expansion of transformed, primitive haemopoietic progenitor cells (Fialkow et al., 1967, Fialkow).

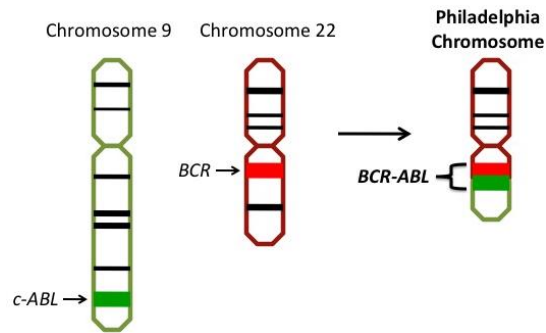


Figure 1-2: The Philadelphia Chromosome.

This mutation develops due to a translocation involving the long arm of chromosome 9 replacing that of chromosome 22 $t(9:22)(q34;q11)$ and vice versa. In doing so leads to the fusion of two genes *Bcr+* and *Abl+*, which encodes oncoprotein BCR-ABL.

1.2.1 CML epidemiology and clinical characteristics

The annual incidence rate of CML varies between countries, however current data from large scale studies, such as the European study EUTOS, showed an incident rate of 0.99 per 100,000/year (Hoffmann et al., 2015) and in the USA study, SEER, it was published that an incidence rate as high as 1.8 per 100,000 was predicted (Chen et al., 2013). However closer to home in the UK and more particularly Scotland it has been reported that incident rates are 0.7 per 100,000 (Smith et al., 2014) and 0.64 per 100,000 per year (Harrison et al., 2004) respectively, which is much lower than predicted globally. These incidences of CML account for 15% of all adult leukaemia diagnosed globally (Faderl et al., 1999b). The median age for patients at diagnosis is 45 to 55 years (Faderl et al., 1999b), however in the UK, Cancer Research UK state that 50% of diagnosed patients are 65 and over. It is thought that about 50% of these cases are diagnosed through routine check-ups as a significant number of patients are asymptomatic or present with mild symptoms, such as fatigue, weight loss, fever, abdominal fullness, bleeding, purpura, splenomegaly, leukocytosis, anaemia, and thrombocytosis, which are fairly general and could account for a number of benign disorders.

CML is characterised by its biphasic or triphasic progression and approximately 90% of patients who are newly diagnosed are in the first phase of the disease, known as chronic phase (CP). Patients in CP have fairly mild symptoms, if not asymptomatic. However, as CML develops leukaemic cells lose the ability to differentiate resulting in an expansion of primitive blast cells rather than mature granulocytes. CP patients typically have less than 10% blasts in their peripheral blood or BM, therefore the blood cells are mainly

differentiated and minimally invasive (Faderl et al., 1999b). Unless controlled, 3-5 years after the onset of CML the disease will progress. CP patients can advance to an intermediate phase called accelerated phase, however a quarter of patients are thought to progress straight to blast crisis (Kantarjian et al., 1993). Accelerated phase (AP) is characterised by 10-20% blasts in the peripheral blood and BM, a high basophil count of 20% or more in the peripheral blood and BM, a high WBC, thrombocytopenia, thrombocytosis, splenomegaly and cytogenetic clonal evolution (Kantarjian et al., 1993). Eventually patients progress to the terminal stage, blast crisis (BC), which can display as either myeloid or B-lymphoid. In this phase there is a further increase in the cellular expansion of the immature blasts to 30% or more in the peripheral blood and BM, due to newly developed cytogenetic changes. Blast cells also exhibit enhanced proliferation and have acquired the ability to evade apoptosis. At this end stage, blast cells have become so aggressive that they have infiltrated extramedullary sites. Patients in BC have a very poor prognosis with a median survival rate of 3-6 months (Kantarjian et al., 1987).

CML disease progression is a complex process characterised by the increase in proliferation, a block in differentiation and cytogenetic clonal evolution. Genomic instability causes the continuous generation of subclones (Jiang et al., 2007, Bolton-Gillespie et al., 2013), and inevitably the progression to BC. However, the molecular events that occur to trigger disease progression from CP CML to advanced AP or BC are unknown. The accumulation of various different chromosomal abnormalities have been implicated in the transition from CP to an advanced disease (AP or BC), such as double Ph chromosome, trisomy 8, and isochromosome 17 (Spiers and Baikie, 1968, Rowley, 1975). These abnormalities are found in 50-75% of advanced stage patients (Muehleck et al., 1984, Rowley, 1975, Spiers and Baikie, 1968, Spiers, 1979). As well as these chromosomal rearrangements, gene deletions, insertions and point mutations are also involved, which may suggest that a second hit is important for the transformation to an acute leukaemia. At the molecular level, the most common mutations to occur are of *p53*, *RUNX1*, *CDKN2A/B* and *IKAROS*. More recently *Jak1*, *Flt3*, *Nf1*, *Erg* and *Mll3* have also been implicated in disease progression (Giotopoulos et al., 2015). However, as these genetic changes are relatively common and none of these lesions occur solely in the majority of patients, it is likely that it is a combination of different mutations that result in BC (Perrotti et al., 2010).

One of the main markers of aggressive progression into BC is the overexpression of *BCR-ABL1* in committed progenitors, this leads to various genetic and epigenetic events. This has been shown to impact upon the transcriptome, resulting in altered gene expression of

SOC-2 (Schultheis et al., 2002), which is involved in PI3K and MAPK signalling, IGF-1, which is involved in RAS signalling, as well as genes involved in the WNT/ β -catenin pathway, all of which may play a role in BC (Radich et al., 2006). Overexpression of *BCR-ABL1* may also result in the constitutive activation of factors involved in mitogenic, anti-apoptosis and anti-differentiation, such as MAPK/ERK1/2, MYC, JAK2, YES-1, LYN, hnRNP-E2, MDM2, STAT5, BMI-1, and Bcl-2, as well as, inhibiting key tumour suppressors such as p53, C/EBP α and PP2A (Calabretta and Perrotti, 2004a, Melo and Barnes, 2007, Chang et al., 2007).

1.2.2 Diagnosis and monitoring

As previously discussed, the symptoms of CML are not specific and include; weight loss, weakness, fever, night sweats, and malaise. Therefore, an assumed diagnosis is usually made via blood counts indicating leukocytosis with basophilia with a more in depth assessment made with a blood film demonstrating immature granulocytes, mainly metamyelocytes, myelocytes and promyelocytes, and few or occasional myeloblasts being indicative of CML.

However the gold standard diagnostic observation for CML is the detection of the Ph chromosome, which is found in 95% of CML patients (Faderl et al., 1999b). The most sensitive methods for the identification of the Ph chromosome are cytogenetic analysis and fluorescence in-situ hybridization (FISH). Cytogenetic analysis allows for the screening of additional chromosomal abnormalities, which may be indicative of a more advanced stage of disease (Egan and Radich, 2015). Therefore these methods help establish a diagnosis of CML, the disease staging and the potential response to therapy (Egan and Radich, 2015). Quantitative reverse-transcriptase polymerase chain reaction (qRT-PCR) testing is the most sensitive method for detection of BCR-ABL mRNA. BCR-ABL transcripts in a single CML cell in a background of up to at least 100,000 normal cells can be detected using current methods (Egan and Radich, 2015). This high level of sensitivity allows for less invasive monitoring within the peripheral blood. BCR-ABL transcript levels determined by qRT-PCR are highly correlated with disease burden and is used along with FISH to monitor patients response after stem cell transplantations or the efficacy of treatment (Faderl et al., 1999b).

1.2.3 BCR-ABL structure

The Ph translocation forms the aberrant fusion gene *BCR-ABL* by adding a 3' end fragment of the *ABL* gene to part of the 5' end of the *BCR* gene. The *BCR* gene is located on chromosome 22 and spans over 130 kilobases (kb) and encodes two proteins, which are 160kDa and 130kDa in size. *BCR* is expressed ubiquitously, but the highest levels of mRNA are found in the brain and haemopoietic cells (Collins et al., 1987, Frit et al., 1999, Maru et al., 1999). Although the function of BCR is still not very well defined, it has been associated with the XPB protein, which has a role in DNA repair, transcription initiation and cell cycle regulation. The *c-ABL* (Abelson) gene is located on chromosome 9, it has 11 exons and is over 230 kb long. It encodes for a 145 kDa protein, which is a member of a family of non-receptor kinases (Kurzrock et al., 1988). *c-ABL* is also ubiquitously expressed and has a major role in regulating cell cycle progression (Van Etten, 1999). In quiescent cells retinoblastoma (Rb) protein binds to the ABL protein to inhibit ABL activity. When cells re-enter the cell cycle Rb is phosphorylated and dissociates from ABL, which then becomes activated and is subsequently phosphorylated by CDC2 kinases to allow progression through the cell cycle (Sawyers et al., 1994).

The break point of *ABL* usually occurs 5' of exon 2 and therefore exons a2-a11 are transposed into the major breakpoint cluster region of BCR. This usually occurs between exon 12 and 16, also known as b1 to b5. The breakpoint locations on *BCR* usually occur between b2 and b3 and this creates a BCR-ABL fusion gene with a b2a2 or b3a2 junction, which is transcribed into an 8.5 kb mRNA. The mRNA is then translated into a chimeric protein of 210 kDa called p210 BCR-ABL (Kurzrock et al., 1988).

1.2.4 BCR-ABL functional domains

Both BCR and ABL proteins possess structural elements, which work together or individually to promote the leukaemogenic transformation. ABL has important roles in regulation of cell growth but also in signal transduction, due to three functional domains at the N-terminus that have a similar homology to Scr family kinases. These are termed SCR homology domain (SH) 1, 2 and 3. SH1 possesses the tyrosine kinase activity of p210 BCR-ABL, and plays an important role in phosphorylating proteins. SH1 is flanked by SH2 and SH3, at the N-terminal end, and are both involved in protein-protein interactions required for the protein signalling (Pawson, 1995, Feller et al.).

In addition, at the c-terminus of ABL there is a nuclear localisation domain, DNA binding domain and actin binding domain (Van Etten et al., 1994). BCR has multiple functional domains, the most critical are; the dimerization domain, which has a coiled-coil (CC)

motif, and has been shown to increase tyrosine kinase activity (McWhirter et al., 1993), a serine-threonine kinase domain, which activates signalling pathways regulated by ABL tyrosine kinase activity, as well as BCR-ABL (Reuther et al., 1994). BCR also has a Rho guanine-nucleotide exchange factor (Rho-GEF) domain, a calcium- dependent lipid binding site and a Rac GTPase activating protein (Rac-GAP) domain (Boguski and McCormick, 1993, Diekmann et al., 1991).

The N-terminal fusion of BCR to ABL appends a large amino acid sequence to the SH2 domain of ABL, this deregulates the SH3 domain and allows the tyrosine kinase activity of ABL to become constitutively active (Pendergast et al., 1991, Kurzrock et al., 1988).

As well as being constitutively active, BCR-ABL has much higher tyrosine kinase activity compared to the native c-ABL protein (Kurzrock et al., 1988).

It is this constant high level of tyrosine kinase activity which causes malignant transformation. In order to understand the underlying molecular mechanisms that lead to this transformation, experiments have been performed mainly using retrovirally transduced cellular models (Daley et al., 1990). It has been shown that BCR-ABL has many targets and activates many signalling pathways to protect the cells from apoptosis and maintain their pathogenicity by altering cellular mechanisms such as proliferation and differentiation, cell adhesion and survival (Afar et al., 1994, Jiang et al., 2000, Puil et al., 1994, Sawyers, 1993, Bhatia et al., 1999, Gordon et al., 1987, Bedi et al., 1994, Cortez et al., 1995, Cotter, 1995, McGahon et al., 1994). This comes as no surprise, due to the number of diverse binding domains BCR-ABL possesses.

1.2.5 BCR-ABL oncogenic pathway

BCR-ABL targets a large variety of signalling pathways, however the major contributors to malignant transformation include; the Janus-activated kinase (JAK)-STAT pathway, which effects transcriptional response, Ras-mitogen-activated protein kinase (MAPK), effects proliferation, and the phosphoinositide 3-kinase (PI3K)/AKT/mTOR, which effects apoptosis (Raitano et al., 1995, Skorski et al., 1997, Skorski et al., 1995a, Warmuth et al., 1999, 1995).

It is a combination of these cellular signals, which leads to the characteristic phenotype of CML cells; increased proliferation, ability to evade apoptosis, growth factor independence and genomic instability.

BCR-ABL also effects adaptor proteins such as CRKL, c-CBL and cytoskeleton and cell membrane mediating proteins, such as actin, paxillin and FAK/PYK2, which cause cell adhesion and cytoskeleton defects and results in the abnormal entry of immature cells into the peripheral blood and extramedullary tissues (Salgia et al., 1997, Sattler et al., 2002b, Salesse and Verfaillie, 2002).

1.2.5.1 JAK-STAT pathway

The JAK-STAT pathway is an important signalling pathway, which regulates the transcription of genes in normal haemopoiesis. This pathway is activated when haemopoietic growth factors bind to their receptors. This in turn activates the intracellular tyrosine kinase JAK2, which subsequently phosphorylates the signal transducer and activator of transcription factor 5 (STAT5). JAK2 and STAT5 form a dimer and translocate to the nucleus, where STAT5 can regulate transcription (Ward et al., 2000). The importance of the JAK2/STAT5 pathway in haemopoiesis has been demonstrated in *in vivo* studies, as it was shown that JAK2^{-/-} embryos become anaemic and die around day 12.5 postcoitum (Neubauer et al., 1998, Grundschober et al., 2014, Park et al., 2013).

Several studies have shown that both JAK2 and STAT5 are constitutively active in BCR-ABL⁺ cells (Chai et al., 1997, 1996) and that this abnormal activity promotes leukaemogenesis. More specifically, STAT5 has been shown to support leukaemogenesis by assisting in the inhibition of apoptosis via the Bcl-2 family proteins such as MCL-1 and Bcl-X_L (Gesbert and Griffin, 2000, Mei Huang, 2002). Whereas, JAK2 has been reported to activate c-myc mRNA expression and protect c-myc protein from degradation, therefore acting as a cooperative oncogene (Shanghai Xie, 2002). JAK2 has also been implicated in

promoting leukaemogenesis in a study where BCR-ABL⁺ cells were transduced with an inactive form of JAK2, which reduced clonogenic potential and disease burden (Shanghai Xie, 2001).

1.2.5.2 The GRB2 adaptor

One of the most critical pathways for leukaemic transformation is induced by BCR via the tyrosine residue at position 177 (Y177). BCR-ABL induces autophosphorylation of this site, which has been identified as a major Grb-2-binding site (Pendergast et al., Puil et al., 1994). Grb-2 acts as an adaptor molecule, which activates the Ras and PI3K signalling pathways (Cortez et al., 1995, Goga et al.).

The importance of this process was shown *in vivo* where a mutation at the Y177 site, changing tyrosine to phenylalanine (Y177F) abolished Grb-2 binding and turns off BCR-ABL-driven activation of Ras, which extended the life expectancy of the mice (Million and Van Etten, 2000).

1.2.5.3 Activation of the RAS pathway

Ras proteins are responsible for regulating cell signalling pathways involved in cell growth, migration, adhesion, cytoskeletal integrity, survival and differentiation. Ras was first discovered as a retroviral oncogene in a study of the Harvey sarcoma virus and Kirsten sarcoma virus (Chang et al., 1982). Ras proteins sit at the top of a signalling cascade known as the Ras-Raf-MEK-MAPK pathway, which is thought to be deregulated in approximately 20% of all human cancers, promoting tumour growth and disease progression (Rajalingam et al., 2007).

As explained the Grb-2 adaptor molecule binds to the Y177 residue of BCR-ABL to create the BCR-ABL-Grb-2 complex, which recruits Son of Sevenless (SOS) (David Cortez, 1997). The BCR-ABL-Grb-2- SOS complex then stimulates the conversion of the inactive GDP-bound form of Ras to its active GTP bound form (Ren, 2005). The BCR-ABL-Grb-2-SOS complex also activates Grb-2-associated binding protein 2 (GAB2), which is also recruited to the complex. As a result, the Grb-2/GAB2/SOS complex is formed, and this causes a constitutive activation of Ras and its signalling pathway (Sattler et al., 2002a). The pathway begins with the active form of Ras activating a serine/threonine-selective protein, Raf. Raf then phosphorylates MEK and ultimately leads to the activation of ERK, now known as MAP kinase (MAPK). MAPK is involved in regulating transcription and translation of genes important for the cell cycle, via an indirect activation of the ribosomal protein S6 (RPS6). Therefore, deregulation within this pathway will alter cell cycle regulation and promote abnormal cell proliferation.

1.2.5.4 PI3K-AKT-mTOR signalling pathway

The PI3K-AKT-mTOR signalling pathway is involved in many essential cellular processes such as survival, proliferation, differentiation, metabolism and motility (Fruman et al., 1998). It has been found to be deregulated in a high percentage of human cancers (Kapeller and Cantley, 1994), including CML, where PI3K has been shown to play an essential role in BCR/ABL leukaemogenesis. The major mode of activation of the PI3K signalling pathway in CML is via the Grb-2 adaptor molecule. As previously described Grb-2 binds to the Y177 residue of BCR-ABL, this leads to the recruitment of GAB2. GAB2 possesses a YXXM motif, which is phosphorylated by BCR-ABL and this then acts as a binding site for PI3K regulatory subunits, which activates the PI3K/AKT/mTOR pathway (Sattler et al., 2002a). PI3K is an intracellular lipid kinase that phosphorylates phosphatidylinositol. There are various classes of PI3Ks; however, the ones involved in BCR-ABL signalling are class IA. PI3Ks are heterodimers consisting of a catalytic and a regulatory subunit. There are three genes that code for the 110-kDa catalytic subunits (p110 α , p110 β , and p110 δ) and three genes that code for regulatory subunits (p85 α , p85 β , and p55 γ) (Kharas and Fruman, 2005). It is not yet clear, which PI3K isoforms are essential for BCR-ABL transformation as haemopoietic cells express all three class IA PI3K catalytic isoforms as well as the class IB isoform (p110 γ) (Gritsman et al., 2015). Once activated via the regulatory subunit, PI3K, with the use of the catalytic domain, converts phosphoinositide-4,5-bisphosphate (PIP₂) to phosphoinositide-3,4,5-trisphosphate (PIP₃), an important second adaptor molecule (Vanhaesebroeck et al., 2001). PIP₃ creates a docking site for proteins that contain pleckstrin homology domains, such as AKT and PDK1 (Divecha and Irvine, 1995). AKT is localised to the lipid membrane and binds to PIP₃, this allows PDK-1 to activate AKT via phosphorylation at the threonine 308 residue (Alessi et al., 1996, Alessi et al., 1997).

AKT is a serine/threonine kinase and was first isolated in its active form from the cells of leukaemia and lymphoma prone mice (Staal, 1987, 1988). AKT has a number of potentially important substrates that link it to a number of biological processes, which may be important in leukaemogenesis. Such substrates include; the forkhead box subgroup O (FOXO) transcription factors, which regulate cell cycle and promote cell survival, growth and proliferation in CML cells (Komatsu et al., 2003). Bad, which inhibits apoptosis via Bcl-2 and Bcl-X_L dissociation, which allows Bcl-X_L to bind to Bax molecules and prevent the formation of pro-apoptotic Bax homodimers (Datta et al., 1997, M Andreeff, 1999). Murine double mutant 2 (MDM2) oncogene, which is phosphorylated by AKT to suppress p53 expression, which inhibits p53 mediated apoptosis (Mayo and Donner, 2001, Goetz et

al., 2001, Trotta et al., 2003). However, the substrate of AKT, which is most important in CML leukaemogenesis, is Tuberous Sclerosis-2 (TSC-2) as it activates the Mammalian Target of Rapamycin (mTOR) pathway. Active AKT phosphorylates TSC-2, which blocks TSC-1/2 complex formation and therefore its ability to inhibit Rheb. Rheb is then free to activate mTOR. mTOR is a highly conserved serine threonine kinase, which is composed of two complexes. The first is mTOR complex 1 (mTORC1), which is made up mTOR, regulatory-associated protein of mTOR (RAPTOR), the mammalian LST8/G-protein β -subunit like protein (mLST8/G β L), PRAS40 and the DEP domains interactor of mTOR (DEPTOR) (Kim et al., 2003, Kim et al., 2002). mTORC1 is a master growth regulator that senses diverse nutritional and environmental cues, including growth factors, energy levels, cellular stress, and amino acids (Koo and Squazzo, 1994). It then uses these signals to promote cell growth by phosphorylating substrates that potentiate anabolic processes, such as mRNA translation and lipid synthesis, as well as processes such as autophagy (Bhaskar and Hay, 2007, Wullschleger et al., 2006).

Two important targets of mTOR are ribosomal S6 kinase (RPS6K) and the eukaryotic translation initiation factor 4E-binding protein 1 (4E-BP1). mTOR phosphorylates 4EBP-1, which blocks its ability to inhibit eIF4E. This releases the eIF4E protein, which is then free to bind to the 5'-cap structure of mRNAs and increase in cap-dependent translation efficiency (Pause et al., 1994).

mTOR also phosphorylates RPS6K and is further phosphorylated by PDK1 to initiate activation of RPS6K (Pullen et al., 1998). This then activates RPS6 protein of 40S ribosomes to allow protein synthesis (Peterson and Schreiber, 1998). RPS6K can also feedback to mTORC1 to stimulate mTOR activity (Chiang and Abraham, 2005).

The second complex, mTOR complex 2 (mTORC2), is composed of mTOR, (RAPA; aka sirolimus)-insensitive companion of mTOR (RICTOR), mLST8/G β L and the mammalian stress-activated protein kinase interacting protein 1 (mSIN1) (Frias et al., 2006, Dos et al., 2004). mTORC2 promotes cell survival by forming a feedback loop, which phosphorylates and activates AKT via the serine 473 residue (Sarbasov et al., 2005). It also regulates cytoskeleton dynamics by activating protein kinase C α (PKC α) and the small GTPases (RHOA, CDC42 and RAC1) as well as controlling ion transport and growth via SGK1 (Mori et al., 2014).

The importance of PI3K-AKT-mTOR pathway in CML leukaemogenesis has been shown in a study expressing an inactive form of AKT, which greatly diminished BCR-ABL-

dependent myeloid colony formation (Skorski et al., 1997) It has also been discussed that cancer cells that are highly dependent of AKT, also rely on the subsequent activation of mTOR for tumourigenesis and are thought to be addicted to mTOR activity (Guertin and Sabatini, 2007).

The PI3K pathway is negatively regulated by phosphatases, specifically PTEN. PTEN is a lipid and protein phosphatase that removes the 3-phosphate from the PIP₃ to produce PIP₂, which prevents AKT activation (Wu et al., 1998). PTEN is considered a tumour suppressor and is frequently mutated in human cancer (Dahia et al., 1999).

1.2.5.5 CRKL adaptor protein

CRKL is an adaptor protein for BCR-ABL (ten Hoeve et al., 1994). It is ubiquitously expressed and expresses high tyrosine phosphorylation activity during embryogenesis, however this activity becomes more restricted in adult tissues (de Jong et al., 1995). However, in CML patients, CRKL is constitutively tyrosine phosphorylated (ten Hoeve et al., 1994, Oda et al., 1994, Nichols et al., 1994). CRKL contains an SH2 domain and two SH3 domains and has been shown to be an important BCR-ABL target, as its high phosphorylation activity was found in neutrophils from the peripheral blood of CML patients (Oda et al., 1994). Since this study, further information has been elucidated, and it has been demonstrated that CRKL interacts with BCR-ABL through a SH3 domain and is phosphorylated on tyrosine 207 (de Jong et al., 1995). Although the main function of CRKL in CML is still unknown, it has been linked to paxillin, which may imply a role in cytoskeleton reorganization and integrin-mediated signalling pathways (Salgia et al., 1995). CRKL has also been implicated in PI3K binding and therefore may also initiate the PI3K/AKT/mTOR signalling pathway (Sattler et al., 1997). Despite the main function of CRKL in CML being unknown, it is still a prominent substrate of BCR-ABL and is the gold standard marker for measuring BCR-ABL activity (Grumbach et al., 2001, Druker et al., 2001b).

1.2.6 BCR-ABL mimics growth factor signalling

Another survival mechanism used by CML cells to promote cell proliferation and survival is growth factor mimicking. Normal haemopoietic cells cannot survive without the support of growth factors. They use cytokines, such as Interleukin-3 (IL-3) and granulocyte colony stimulating factor (G-CSF), which bind to receptors on the cells and upon activation of signalling pathways such as RAS-MEK-ERK, PI3K-AKT-mTOR and JAK-STAT, promote proliferation and differentiation. However, one very obvious feature observed *in vitro* when studying the effect BCR-ABL has on normal cytokine-dependent cell lines is

they no longer need cytokines to proliferate (Daley and Baltimore, 1988, Lugo and Witte, 1989, Kabarowski et al., 1994). This observation was further supported by later studies, which showed *in vivo* that mice with a CML-like disease induced by BCR-ABL have developed an autocrine mechanism to produce IL-3 and GM-CSF (Zhang and Ren, 1998, Li et al., 1999). In order to prove this mechanism was also true for primary CML cells proved difficult. However, in 1986 Eaves and colleagues showed that CML cells were actively cycling, whether cultured in the presence of supportive stromal cells or as a single cell suspension. Since this observation and due to the generation of more sensitive techniques it was found that CD34⁺ CML cells from CP patients had consistent activation of IL-3 and G-CSF associated with growth factor independent proliferation (Jiang et al., 1999). Mimicking of physiological growth factor stimulation, obviously gives cells a growth advantage and must play a significant part in malignant transformation and maintenance of CML cells (Jiang et al., 1999).

1.2.7 BCR-ABL alteration of the HSC niche

Increasing evidence from current research shows that the BM microenvironment is also an important factor to consider in order to fully understand leukaemic cells survival mechanisms. It has been shown that LSCs can reprogram the environment in order to favour their growth above normal HSCs. An example of this was shown when Schepers and colleagues found that when BCR-ABL is expressed in haemopoietic cells secondary genetic changes occur within the microenvironmental cells which would support the survival of the leukaemic cells. They demonstrated that upon BCR-ABL transformation there was a marked decrease in osteolineage mesenchymal cell expression of molecules that support normal haemopoiesis, such as CXCL12 and Kit ligand (Schepers et al., 2013). This shifted the balance in favour of leukaemic cells and provides evidence that BCR-ABL cells can effectively remodel the niche for their advantage adding more complexity to the molecular mechanisms used by leukaemic cells for their survival.

Furthermore, a recent study conducted by Welner and colleagues showed that the exposure to chronic myeloid leukaemia (CML) caused normal mouse hematopoietic progenitor cells to increase division, alter their differentiation, and reduce their reconstitution and self-renewal potential. They also reported that the normal cells also acquired gene expression patterns similar to that of the CML cells, which implied the leukaemia signature was mediated by extrinsic factors. In this study, IL-6 was deemed responsible for most of these changes as neutralization of IL-6 prevented these changes and treated the disease (Welner et al., 2015).

1.3 History of CML treatment

The first known treatment of a CML patient was described in 1882 by Arthur Conan Doyle, a physician from Birmingham, UK. He described his patient as presenting with “leucocythaemia”, which was thought to be due to malaria. He first prescribed a malaria treatment of quinine and iron for the anaemia; however, no change was seen in the patient’s symptoms. Another known treatment at that time, for malaria, was a 1% arsenic trioxide solution. The arsenic solution was reported to improve the clinical condition of CML patients, as at an appropriate dose it controlled fever, reduced the white blood cell count, reduced the size of the spleen, relieved pruritus, and reduced the degree of anaemia (CE, 1938), however for the treatment of CML these effects were short-lived.

In the early 1900s with the discovery of x-rays, it was found that if irradiation was directed to the spleen of patients with CML it reduced splenomegaly and to a degree normalised the patient’s blood cell counts and general health status (WA, 1902, Senn, 1903). Although this treatment gave patients a better quality of life it did not cure patients nor prolong the life expectancy of these patients (Hoffman and Craver, 1931, Minot et al., 1924).

The increased understanding of cancer biology throughout the 1900s led to cancer drug discovery programmes becoming more focused on DNA synthesis and cell division. This resulted in the generation of chemotherapeutic agents. The first chemotherapy used to treat leukaemia came from chemical weapons created in WWII. It was known that mustard gas had myelosuppressive effects and therefore provided a good rationale for its use in the treatment of leukaemia (Goodman et al., 1984, Jacobson et al., 1946). Although it showed some efficacy, it was highly toxic. Therefore, this spurred on studies to produce a variety of antimetabolites, alkylating agents and microtubule destabilizers that were less toxic, such as busulphan. Although they proved highly effective in controlling clinical features of CML for long periods of time, they were still highly toxic due to their non-specificity, which left patients with severe side effects (Galton, 1953, Galton, 1959, Haddow and Timmis, 1953).

In the 1979, the first successful BM transplantations were recorded in CML patients. They were treated with high-dose chemoradiotherapy followed by a transfusion of BM cells from their genetically identical, normal twins (Fefer et al., 1979). This led to the initiation of programs for treating CML patients by allogeneic stem cell transplantation (Champlin et al., 1982, Clift et al., 1982, Goldman et al., 1982, McGlave et al., 1982). Although, transplantation resulted in great survival rates, it could only be offered to 20% of CML patients due to limitations, in age, physical health, and donor availability (Goldman, 1998).

It also only showed high 5-year survival rates in low-risk patients, 72%, which was reduced to 20% in high-risk patients (Gratwohl et al., 1998). Patients undergoing transplantation also demonstrated increased morbidity and mortality due to infections, mucositis, graft failure or graft-versus-host disease (Faderl et al., 1999a, Sawyers, 1999).

In the 1980s, came the discovery of biological agents, interferons which have immunomodulatory, antiviral, and antiproliferative properties, all of which make them highly attractive prospects for anti-cancer therapy. The cytokine interferon α (IFN α) offered an alternative less toxic treatment for the management of CML, compared to previous chemotherapies. IFN α effectively stabilised CML symptoms and prolonged life expectancy. One of the most significant observations in patients following IFN α treatment was that many patients became Ph negative and transformation rates into BC were much reduced (Talpaz et al., 1983).

However, the most significant breakthrough occurred due to the discovery of BCR-ABL and its constitutive tyrosine kinase activity being the driving force of cellular transformation in CML. The enzymatic activity of this deregulated gene could plausibly be defined as an attractive drug target for addressing BCR-ABL-positive leukaemia (Lugo et al., 1990). In 1992 it was reported that by treating CML cells with tyrphostin, a tyrosine kinase inhibitor, it was possible to inhibit the tyrosine kinase activity of BCR-ABL. This discovery opened up the possibility of creating an ABL specific drug for the treatment of ABL-associated human leukaemia (Anafi et al., 1992, Anafi et al., 1993).

1.3.1 The development of tyrosine kinase inhibitors (TKIs)

The discovery of BCR-ABL meant that for the first time a drug target was identified that distinguished between normal cells and leukaemic cells. BCR-ABLs enzymatic activity functions by transferring a phosphate from ATP to tyrosine residues of its protein substrates and this could be targeted pharmacologically.

In the late 1980s Lydon and Matter from Novartis, initiated projects to identify compounds with inhibitory activity against protein kinases. They profiled a library of compounds and initially focused on a Protein Kinase C inhibitor. However low potency and poor specificity led to further tweaks in the compound, such as: the addition of a 3'-pyridyl group at the 3'-position of the pyrimidine, which enhanced potency. The introduction of a benzamide group at the phenyl ring, which enhanced the activity specifically against tyrosine kinases. The addition of a flag-methyl group at the anilino phenyl ring, which led to the loss of activity against PKC, but further enhanced activity against tyrosine kinases

and finally with the attachment of a highly polar side chain, N-methylpiperazine for solubility, imatinib was born (Zimmermann et al., 1996, Zimmermann et al., 1997).

Imatinib is a competitive ATP inhibitor and has the ability to inhibit c-ABL kinase at a concentration of 85 nM (Sandra et al., 2004). Imatinib interacts with ABL via its kinase domain, when ABL is in its kinase inactive conformation and therefore the A-loop and the major regulatory element occlude the catalytic centre. This specific way of binding is important for imatinib's selectivity towards ABL, as there is higher structural diversity in kinases in their inactive state (Nagar et al., 2002, Manley et al., 2002, Schindler et al., 2000). Therefore, imatinib stabilises the inactive form of BCR-ABL and inhibits autophosphorylation, which blocks the kinase activity and the subsequent phosphorylation of downstream substrates.

In collaboration with Brian Druker, the selective inhibitory activity of imatinib was shown at the cellular level on the constitutively active p210BCR-ABL tyrosine kinase in *in vitro* and *in vivo* studies (Druker et al., 1996). Further studies revealed that the inhibition of BCR-ABL autophosphorylation was closely related to the anti-proliferative activity of imatinib. These also showed that even treatment with low micromolar concentrations of imatinib, was enough to selectively induced apoptosis in BCR-ABL+ cell lines, and induced cell death in primary leukaemia cells from patients with Ph+ CML. *In vivo* treatment with 160 mg/kg⁻¹ daily of imatinib over three doses for 11 days inhibited p210 BCR-ABL tyrosine phosphorylation, and resulted in tumour free survival. This was specific for BCR-ABL positive cells, as minimal toxicity was seen in BCR-ABL negative cells (Druker et al., 1996, Beran et al., 1998, Gambacorti-Passerini et al., 1997, Deininger et al., 1997, Shingo Dan, 1998, le Coutre et al., 1999).

As well as imatinib's ability to potently inhibit all of the ABL tyrosine kinases, including c-ABL, v-ABL, and BCR-ABL (Buchdunger et al., 1996, Druker et al., 1996, Buchdunger et al., 2000), it has also been shown that it can target c-KIT and ligand-activated platelet-derived growth factor (PDGF) receptor (Buchdunger et al., 2000, Heinrich et al., 2000).

1.3.2 Imatinib in clinical trial

Due to its success in *in vitro* and *in vivo* models of CML, imatinib entered clinical trials. A phase I clinical trial began in 1998 in order to assess the maximal tolerated dose that would produce a clinical benefit. Patients eligible for the trial were CP CML patients, who had failed IFN- α . Patients were treated with imatinib as a daily oral therapy, with doses ranging from 25 to 1000 mg. Imatinib treatment was well tolerated and had remarkable effects. Out of 54 patients receiving at least 300 mg/day, 53 achieved a complete haematological response (CHR). Even more impressive was that at doses of 300 mg/day and higher, cytogenetic responses (CyR) were achieved in 31% of patients, with 13% achieving a major cytogenetic response (MCyR) (Druker et al., 2001b).

The success of the Phase I trial moved imatinib into a Phase II trial in late 1999. This study involved using imatinib as a single agent for all stages of CML (Sawyers et al., 2002). Treatment with imatinib in late CP CML patients, that had previously failed IFN α , allowed 95% of the patients to achieve a MCyR and, after an 18 month follow up, 89.2% of the patients had not progressed to AP or BC (Kantarjian et al., 2002). Unsurprisingly as disease progressed the efficacy of imatinib on patients decreased (Talpaz et al., 2002).

In 2000 a Phase III trial began to assess the efficacy of imatinib versus the current standard therapy for CML patients. The trial was called International Randomized Study of Interferon and STI571 (IRIS) trial. In this trial newly diagnosed CP CML patients received either 400 mg/ day of imatinib or the standard treatment of IFN- α and cytarabine, a chemotherapeutic agent that inhibits DNA synthesis. This trial recruited 1106 patients from 16 different countries. In the 19 month follow up patients treated with imatinib had gained much higher MCyR rates, 87.1%, versus 34.7% in the IFN- α and cytarabine treated group. Even more encouraging was that 76.2% of imatinib treated patients had achieved a complete CyR (CCyR) compared to 14.5% in the IFN- α and cytarabine treated. In 2001, with the success in clinical trial, imatinib received approval from the United States Food and Drug Administration (FDA) to be used as a frontline treatment for Ph+ CML (O'Brien et al., 2003, Hochhaus et al., 2009, O'Brien and Deininger, 2003).

1.3.3 Treatment responses

Although TKIs are highly effective in treating CML, some patients fail to respond, respond sub-optimally or can relapse due to acquired resistance. Patients are monitored closely, by cytogenetic and molecular techniques, during treatment to ensure an optimal response is being achieved. If patients become unresponsive this can be caught early and treatment regimens can be changed to control disease progression.

Treatment responses have been officially categorised by the European Leukemia Net (ELN) and the U.S. National Comprehensive Cancer Network (NCCN) guidelines (Baccarani et al., 2009, (NCCN), 2010). Response profiles are categorised into haematological, cytogenetic and molecular. A haematological response indicates an improvement in the peripheral blood cell counts. A complete haematological response (CHR) indicates normalised peripheral blood counts; a white blood cell count below $10 \times 10^9/L$, platelets below $450 \times 10^9/L$, immature cells absent or normalized differential and no signs and symptoms of disease. A CyR refers to the amount of Ph⁺ cells in the BM or peripheral blood. A complete or major cytogenetic response (CCyR) is the complete absence of Ph⁺ cells. The loss of a CyR is indicated by an increase in Ph⁺ cells to 30% or more in the BM or PB. A molecular response is the level of *BCR-ABL* transcripts relative to an established baseline, which is determined by measuring *BCR-ABL* transcripts levels in the blood of the patient upon diagnosis. The transcript level is then standardised according to an international scale (Hughes et al., 2006). A complete molecular response (CMR) indicates the absence of transcripts and a major molecular response (MMR) is defined as a 3-log decrease or a reduction to 0.1% compared with the baseline level of *BCR-ABL* transcripts (Hughes et al., 2006). The time a patient takes to respond to treatment haematologically, cytogenetically and molecularly is also very important in determining whether drug therapy is effective. The ELN also provide guidelines for the times that it should take to reach certain levels of response and warning signs of suboptimal responses or relapses (Baccarani et al., 2009). Patients that do not achieve a timely response to drug treatment are at higher risk of disease progression due to ineffective drug treatment. Failure to respond to TKI is indicated by the patient not achieving a CHR by 3 months, or having *BCR-ABL* transcripts >10% and/or Ph⁺ >35% at 6 months, or at 12 months *BCR-ABL* transcripts >1% and/or Ph⁺ >0%. Then at any time loss of CHR, CCyR, loss of MMR and the detection of mutations all indicate TKI failure. Failure to respond is also indicated in relapse if there is a loss of CHR or CCyR at any point. If this occurs, it means continuing with the current treatment regime is no longer appropriate. A suboptimal response is defined by the patient having *BCR-ABL* transcripts

>10% and Ph⁺ 36-95% at 3 months, or at 6 months having BCR-ABL transcripts 1-10% and Ph⁺ 1-35%, or at 12 months having BCR-ABL transcripts 0.1-1% (Baccarani et al., 2013).

The current practice for CML patients is to continue treatment indefinitely as the ability of imatinib to completely eradicate the CML clone is uncertain. However, it was thought that patients who had achieved a CMR for at least 2 years may have completely eradicated CML cells from their body and could potentially discontinue treatment. Therefore, the STIM and the Australian TWISTER studies were launched. In the STIM study, imatinib was discontinued in 69 patients and of these 61% of them relapsed (Mahon et al., 2010). Similar results were obtained in the TWISTER study, which also demonstrated that all patients in the trial, even patients that did not relapse after stopping imatinib treatment, still harboured residual leukaemia (Ross et al., 2013). These two trials support the hypothesis that there is a population of leukaemic stem cells (LSCs) that are resistant to TKI and their persistence can replenish the leukaemic cell pool upon drug withdrawal and cause relapse. However, it is still thought that imatinib can be safely discontinued in patients, which have achieved a CMR for at least 2 years' duration, as imatinib discontinuation in this type of patient population has resulted in molecular relapse-free survival for many patients in the trial. These patients potentially could be cured of CML by TKI. Additionally, patients who did suffer a relapse still responded well to the reintroduction of imatinib (Ross et al., 2013, Mahon et al., 2010, Nicolini et al., 2013).

1.4 Mechanisms of resistance

Although the majority of CML patients have excellent response rates to imatinib, there is a significant subset of patients who experience primary or secondary resistance to imatinib treatment. Primary or intrinsic resistance is the lack of efficacy of imatinib from the outset. Secondary resistance is an acquired resistance which occurs following an initial response to imatinib treatment. A significant amount of research has been directed towards understanding the mechanisms that cause imatinib resistance. Initial studies were conducted using BCR-ABL+ cell line models that had been exposed to prolonged and progressive escalation dosing of imatinib in order to cause a cellular change, which may resemble resistance seen in the clinic (le Coutre et al., 2000, Mahon et al., 2000b, Weisberg and Griffin, 2000). This has led to the discovery of numerous mechanisms which are associated with resistance, and can be classified into BCR-ABL-dependent and independent. Resistant mechanisms classed as BCR-ABL-dependent include; genetic mutations in BCR-ABL, BCR-ABL amplification and drug trafficking. Those associated with BCR-ABL-independent mechanisms are epigenetics, clonal evolution and activation of alternative signalling pathways.

1.4.1 Intolerance and non-compliance

A very simple and yet unfortunate reason that a patient may suffer from a sub-optimal response to imatinib treatment is poor compliance or intolerance. A large study conducted in 2011, showed that out of 422 patients that took part in the study, 25-30% of the patients suffered quite highly from side effects, which ranged from fatigue, muscle cramps, musculoskeletal pain and oedema (Efficace et al., 2011). Only 20% of patients in this study reported not to experience any side effects (Efficace et al., 2011). Continuous side effects of this nature are enough to impact upon a patient's ability to comply with their treatment regime. A study conducted in 2009, the Adherence Assessment with Glivec: Indicators and Outcomes (ADAGIO) demonstrated that although 15% of patients on imatinib took more than the prescribed dose, 71% of patients took less than their prescribed dose (Noens et al., 2009). This information is very disconcerting as there is a very strong negative correlation between patients taking less than 90% of their imatinib dosage compared to patients taking over 90% and reaching an optimal MMR, 28.4% and 94.5% respectively (Marin et al., 2010). This is also even more apparent in patients' ability to achieve a CMR, 0% and 43.8% respectively (Marin et al., 2010). Although these side effects can be fairly manageable, patients can suffer more serious life threatening complications after long term

treatment with TKIs. These complications include myelosuppression and infection, fluid retention including pleural and pericardial effusions, liver toxicity, pancreatitis, cardiac effects such as; cardiac failure, arrhythmias, vascular events including hypertension, myocardial infarction, peripheral vascular occlusion and stroke, pulmonary hypertension, and gastrointestinal bleeding. If these sorts of life threatening events occur, TKI treatment must be discontinued, however the frequency of occurrence and severity are associated with the more potent inhibitors (Holyoake and Helgason, 2015).

1.4.2 BCR-ABL-dependent mechanisms of resistance

1.4.2.1 BCR-ABL amplification

One of the first mechanisms of resistance to be established using TKI-resistant CML cell line models, was increased levels of BCR-ABL kinase activity compared to the original TKI sensitive CML cell lines. This was shown to be due to BCR-ABL gene amplification and was shown in three independent studies (le Coutre et al., 2000, Mahon et al., 2000b, Weisberg and Griffin, 2000). Although this had only been shown in cell lines, Gorre and colleagues performed cytogenetic testing on 11 samples collected from patient resistant to imatinib and showed that 3 of these had multiple copies of the BCR-ABL gene (Gorre et al., 2001). In all three cases, additional copies of the Ph chromosome were observed as imatinib treatment was continued. Quantitative PCR analysis of genomic DNA (gDNA) obtained from these three patients confirmed increased ABL gene copy number at relapse when compared to a patient without BCR-ABL gene amplification (Gorre et al., 2001). This drug resistance mechanism is associated with BCR-ABL signal transduction at higher levels. It is possible that the original imatinib dose is no longer sufficient to inhibit the higher levels of BCR-ABL signalling therefore allowing cells to continue proliferating. High levels of BCR-ABL activity are also associated with genomic instability, due to increased levels of ROS (Sattler et al., 2000, Koptyra et al., 2008). This would increase the likelihood of a mutation to occur, which may lead to the development of imatinib resistance. However, there is a low frequency of CML patients who are found with BCR-ABL gene amplification (A Hochhaus, 2002). This may be due to high levels of BCR-ABL being toxic to CML cells and these cells die before analysis. With this in mind it has been hypothesised that the first step in the development of imatinib resistance is the overexpression of BCR-ABL, which subsequently leads to a mutation. It is thought that the highly expressing BCR-ABL clone dies and leaves the clones which have lower levels of BCR-ABL and a mutation which gives them a growth advantage and drives imatinib resistance (Tang et al., 2011).

1.4.2.2 Mutations affecting the BCR-ABL kinase domain

The most common cause of imatinib resistance is due to the cells ability to evolve and develop point mutations. These mutations usually cluster within the kinase domain of BCR-ABL, which is the binding site for imatinib. This disrupts the contact points between imatinib and BCR-ABL or induces conformational changes from inactive to active, which makes imatinib no longer able to bind to BCR-ABL and renders it ineffective (von Bubnoff et al., 2002, Gorre et al., 2001, Branford et al., 2003, Shah et al., 2002). BCR-ABL mutations are found in 50–80% of patients with CML at time of development of resistance (Gorre et al., 2002, Soverini et al., 2005, Jabbour et al., 2006, Jones et al., 2008). The list of point mutations in BCR-ABL has grown to include more than 90 which confer imatinib resistance. Some of these occur at a higher frequency than others and cause varying degrees of imatinib resistance (Corbin et al., 2003, Soverini et al., 2011). The degree of resistance caused depends on the proximity to the kinase domain, ranging from moderate to severe resistance, which significantly increases imatinib's IC₅₀, half the maximal inhibitory concentration. Mutations that are associated with high levels of resistance to imatinib include mutations on the P-loop of BCR-ABL, specifically between amino acids 244 and 255, such as; Q252R/H, Y253F/H, E255K/V (O'Hare et al., 2005). However the most common mutation, which causes a high level of imatinib resistance and occurs within the BCR-ABL kinase domain, is the T315I mutation and is known as the 'gatekeeper' mutation (O'Hare et al., 2005). Of all the CML patients that develop an imatinib resistant mutation, 20% will develop the T315I mutation (Aaron Shaver, 2014). The development of mutations not only affects imatinib binding, but also causes genomic instability, which promotes DNA damage and impairment of DNA repair mechanisms (Stoklosa et al., 2008).

In the majority of CML patients, 1 mutation will occur in the BCR-ABL kinase domain. However, there is a subset of patients susceptible to ≥ 2 mutations, which can be caused by multiple BCR-ABL clones, polyclonal mutations, or ≥ 2 mutations in the same BCR-ABL molecule, which are termed compound mutations. Each of the individual mutants from the polyclonal mutant population is expected to retain a certain amount of sensitivity to imatinib, depending on the mutation. However, compound mutations, due to the multiple mutational changes, impose a higher risk of dramatic changes to BCR-ABL, which can have extremely negative effects in terms of drug binding and therefore imatinib sensitivity (Shah et al., 2007, Eide et al., 2015). Patients harbouring highly imatinib resistant compound mutants, such as BCR-ABL^{E255V/T315I}, have limited therapeutic options (Eide et al., 2015).

1.4.2.3 Pharmacokinetics & drug delivery issues

Another proposed mechanism underlying resistance to imatinib can be due to pharmacokinetics and ineffective drug delivery. One simple reason for a suboptimal response to imatinib may be due to low imatinib plasma levels resulting from exposure to inadequate imatinib dosage. Metabolism of imatinib occurs through the cytochrome (CYP) P450 system to which CYP isoenzyme 3A4 (CYP3A4) is the major enzyme that metabolises imatinib and its levels can vary highly between patients, therefore it is important to monitor plasma levels carefully (Larson et al., 2008, Peng et al., 2004, Picard et al., 2007).

However low plasma levels could also be due to dysfunctional drug import and export pumps on the target cell membrane. The multidrug efflux transporter, ATP-binding cassette subfamily B member 1 (ABCB1), also known as P-glycoprotein and MDR1, has been implicated in imatinib resistance in CML (Mahon et al., 2003). ABCB1 is a transmembrane protein that belongs to the ATP-binding cassette subfamily (ABC). ABC transporters use ATP hydrolysis to open and close ion channels to allow the movement of endogenous substrates across the plasma membrane. ABC transporters also participate in the movement of most drugs and their metabolites across cell surface and cellular organelle membranes and therefore defects in these genes have been implicated in drug resistance (Vasiliou et al., 2009). ABCB1 has been shown to mediate multidrug resistance by increasing the efflux of imatinib from haemopoietic cells (Raaijmakers, 2007, Burger et al., 2004). Mahon and colleagues showed that overexpression of the MDR1/ABCB1 gene in a CML cell line led to imatinib resistance, which could be reversed by treatment with a P-glycoprotein inhibitor (Mahon et al., 2003). To further understand this mechanisms in a clinical setting, a study was conducted analysing 33 CML patients which concluded that overexpression of ABCB1 was linked to more advanced phases of disease, such as AP and BC CML patients (Mahon et al., 2000a, Galimberti et al., 2005). However, the importance of this has been put into question due to later studies from our laboratory, which demonstrated that inhibition of ABCB1 could neither enhance the effect of imatinib nor did it significantly increase imatinib's efficiency in eliminating CD34+ CML cells, which was thought to be due to low expression levels of ABCB1 in this primitive cell fraction (Hatzieremia et al., 2009).

A second membrane transporter that has been implicated in imatinib resistance is human organic cation transporter 1 transporter (hOCT-1), which has been shown to induce imatinib influx into cells and its inhibition was shown to directly impact imatinib uptake in leukaemic cells (Thomas et al., 2004). In clinical studies, the activity of hOCT-1 and the

mRNA expression of *OCT-1* correlate with the imatinib response (White et al., 2010, Wang et al., 2008, Eechoute et al., 2011). Patients with high hOCT-1 expression achieved superior response rates to imatinib, with regards to CCyR and progression-free and overall survival (Wang et al., 2008). However, patients with imatinib resistant CML have been shown to have lower levels of hOCT-1 (Kim et al., 2014). In addition, a study analysing 33 newly diagnosed CML patients identified a hOCT-1 single nucleotide deletion, M240del, which was associated with an increased probability of imatinib treatment failure (Giannoudis et al., 2013). Dose escalation of imatinib may overcome the pharmacokinetics and drug influx and efflux issues to increased imatinib plasma levels and allow the patient to achieve better response (White et al., 2007).

1.4.3 BCR-ABL-independent mechanisms of resistance

However, there are a sub set of patients who are treated with TKI and despite BCR-ABL inhibition the CML cells retain the ability to survive and proliferate. These patients are described as having a BCR-ABL-independent resistance to TKIs. This can either occur due to epigenetic changes, clonal expansion, microenviromental factors or by activation of a secondary oncogenic mechanism. Patients with BCR-ABL-independent TKI resistance are of major clinical concern. As unlike BCR-ABL-dependent resistance mechanisms, these patients have very limited treatment options and it is thought that 50% or more imatinib resistant CML patients may develop BCR-ABL-independent imatinib resistance mechanisms. Therefore, increased effort is being made to investigate these alternative mechanisms of resistance.

1.4.3.1 Clonal evolution

As CML progresses patients acquire additional cytogenetic anomalies, which has been coined “clonal evolution”. The most frequent abnormalities that are associated with clonal evolution are trisomy 8 (34%), isochromosome 17 (20%), and duplicate Ph chromosome (38%) (Johansson et al., 2002). These aberrations have been linked to c-myc overexpression, loss of p53 and BCR-ABL overexpression, respectively (Jennings and Mills, 1998, Calabretta and Perrotti, 2004b, Gaiger et al., 1995). Loss of p53 occurs at a high rate and is found mutated in 25-30% of BC CML patients (Calabretta and Perrotti, 2004b). The inactivation of p53 has also been shown to augment disease progression by blocking the response to imatinib and therefore causing imatinib resistance (Wendel et al., 2006). Clonal evolution reflects the high level of genetic instability that occurs during disease progression and ultimately leads to advanced stages of CML.

1.4.3.2 Epigenetic modifications

Recent evidence suggests that abnormal epigenetic regulation of the expression of CML-associated genes may play a critical role in its pathogenesis and in the mechanisms modulating therapeutic responsiveness (Jelinek et al., 2011, Machova Polakova et al., 2013). Epigenetic events include; DNA methylation and post-translation modifications in histone, including acetylation, deacetylation and phosphorylation (Jenuwein and Allis, 2001, Matzke et al., 2001).

DNA methylation of CpG islands is a transcription inhibiting mechanism that balances the levels of gene expression that is frequently deregulated in leukaemia. A large number of genes, which are mostly tumour suppressors, are inactivated by hypermethylation of CpG islands mainly in the promoter regions, while other genes, such as oncogenes are hypomethylated. Hypomethylation has been shown to cause genomic instability in CML and leads to disease progression (Roman-Gomez et al., 2008). Genes that have been found to be hypermethylated in CML and correlate with a poor prognosis are HOXA4 and HOXA5 (Strathdee et al., 2007), and DNA-damage-inducible transcript 3 (DDIT3) gene, from the CEBP family of transcription factors (Wang et al., 2010), which are associated with cell growth and differentiation in haemopoiesis. As well as tumour suppressor genes p15, a cyclin independent kinase inhibitor (Nguyen et al., 2000), Cadherin-13, responsible for selective cell recognition and adhesion (Roman-Gomez et al., 2003), Metastasis suppressor 1 (MTSS) (Schemionek et al., 2016) and SHP1 (Esposito et al., 2011b).

Further epigenetic mechanisms that are important for cellular transformation in leukaemia are histone acetylation and deacetylation. Studies have shown that alterations in the pattern of acetylation of non-histone proteins can promote abnormal cellular proliferation and resistance to apoptosis. Using imatinib resistant CML cell line models it was shown that these cells undergo aberrant acetylation of nonhistone proteins, such as p53, Ku70, and Hsp90, which was due to upregulation of histone deacetylases (HDACs) and down-regulation of histone acetyltransferase (HAT) (Lee et al., 2007). This occurs due to upregulation of HDAC1, 2, and 3 and SIRT1 and the down regulation of CBP/p300 and PCAF with HAT. The aberrant acetylation therefore down-regulates p53 and cytoplasmic Ku70 (Lee et al., 2007). Ku70 is a known acetylation-sensitive binding partner for pro-apoptotic protein, Bax. This allows Ku70 to sequester Bax and inhibit stress-induced apoptotic cell death (Sawada et al., 2003, Cohen et al., 2004).

Treatment of CML cells with the HDAC inhibitors restores the acetylation of several proteins and the cell's ability to undergo apoptosis. In addition, the use of HDAC inhibitors

in combination with TKIs showed a synergistic effect by increasing the level of apoptosis in primary cells isolated from CML patients (Kircher et al., 2009, Fiskus et al., 2006). One phase II/III clinical study has been conducted using HDAC inhibitors for the treatment of patients suffering from CP CML with resistant disease following treatment with at least two BCR-ABL targeting TKIs, NCT00451035. The results of this trial have not yet been published. However, toxicity of HDAC inhibitor to normal stem cells is a potential concern. Another potential therapeutic option is to target SIRT1 (Li et al., 2012). Currently available HDAC inhibitors do not target SIRT1, which has been shown to play an important role in maintaining self-renewal and differentiation of HSC especially under conditions of stress (Narala et al., 2008, Ou et al., 2011, Han et al., 2008). SIRT1 is over expressed in CML stem cells and as discussed is associated with aberrant acetylation of p53 (Luo et al., 2001), Ku70 and Foxos (Brooks and Gu, 2009). Inhibition of SIRT1 was shown not to affect normal HSC but importantly, increase apoptosis and reduce proliferation of CML stem cells and this effect was significantly enhanced by the addition of imatinib (Li et al., 2012).

An interesting study was performed using a BCR-ABL positive CML cell line (KBM7), to generate iPSCs, which showed that when the KBM7 cells were reprogrammed they lost their dependency on BCR-ABL and became insensitive to imatinib. The authors hypothesise that imatinib must target cells in a specific epigenetic context, which may contribute to the inability of imatinib to fully eradicate CML cells (Carette et al., 2010). However a similar study performed more recently by Amabile and colleagues shows that reprogramming CML cells back to an iPSC state erased the CML DNA-methylation signature and these cells were no longer effective in producing CML when subsequently transplanted into immunocompromised mice (Amabile et al., 2015). This shows the complexity involved of epigenetic mechanisms in CML and that it is context dependent.

1.4.3.3 Activation of alternative signalling pathways

Aberrant activation of alternative cellular pathways can also be responsible for BCR-ABL-independent imatinib resistance. The exact mechanism that may cause this is unclear, however it seems to vary depending on the individual as studies conducted with mouse models and human primary samples have shown much variability. The main pathways and their associated mechanisms that have been implicated so far include; (1) deregulation of apoptotic proteins, such as down-regulation of pro-apoptotic protein BIM (Ng et al., 2012) or up-regulation of anti-apoptotic protein Bcl-2 (Dai et al., 2004), (2) down-regulation of SH2-containing tyrosine phosphatase 1 (SHP-1) (Esposito et al., 2011a), (3) over-expression of SRC kinases, such as LYN, HCK and FYN, which promote survival and proliferation (Donato et al., 2003, Grosso et al., 2009) and (4) maintenance of survival signals such as the activation of the PI3K/AKT/mTOR pathway (Quentmeier et al., 2011), FOXO1 and FOXO3A (Wagle et al., 2016, Pellicano et al., 2014), STAT3 (Eiring et al., 2015) and RAS-independent activation of RAF (Hentschel, 2011) and Wnt/ β -catenin (Zhang et al., 2013, Neviani et al., 2013, McWeeny et al., 2010). Despite the complexity of this type of resistance it is hoped that through further research a common alternative drug target will be identified that can be exploited for treatment of this patient population.

The PI3K/AKT/mTOR pathway is a frequently deregulated pathway in cancer (Gallardo et al., 2012, Shukla et al., 2007). Activation of this pathway has been shown to positively regulate cellular proliferation, differentiation, survival and mRNA translation, which is regulated via phosphorylation of the mTOR complex 1 (mTORC1), which phosphorylates the downstream targets ribosomal protein S6 (RPS6) and eukaryotic translation initiation factor 4E-binding factor (4E-BP1) in CML cells (Ly et al., 2003). In CML, it has been shown that BCR-ABL can regulate the activity of the PI3K/AKT/mTOR pathway (Skorski et al., 1995b) and the aberrant activity was important for supporting BCR-ABL mediated cellular transformation and disease progression (Skorski et al., 1997). It has also been reported that the PI3K/AKT/mTOR pathway is involved in promoting TKI-resistance. A study conducted using BCR-ABL-independent imatinib resistant CML cell line models, showed that after treatment with imatinib, ERK1/2 and STAT5 were dephosphorylated, however PI3K/AKT1/mTOR activity remained unaffected. In addition, targeting this pathway with inhibitors against PI3K, AKT or mTOR, induced a high level of apoptosis (Quentmeier et al., 2011, Okabe et al., 2014). This makes the PI3K/AKT/mTOR pathway an attractive signalling pathway for investigation of TKI-resistance in CML patients.

1.5 Strategies to combat TKI resistance

1.5.1 Imatinib dose escalation

In the first instance, to overcome TKI resistance a dose escalation of imatinib can be given to patients. This can be beneficial to patients who have BCR-ABL over expression, an amplification of *BCR-ABL* transcripts, BCR-ABL mutation and drug influx and efflux issues, which can be targeted at higher imatinib concentrations.

The standard of care for imatinib treatment is 400 mg daily. If a patient is having a slow or inadequate response to 400 mg of imatinib then dose escalation to a daily dose of 600-800 mg daily has been shown to benefit a proportion of patients (Kantarjian et al., 2003).

106 patients from the IRIS clinical trial experienced a suboptimal cytogenetic response or resistance to the 400 mg imatinib treatment. These patients were then entered into a trial to assess the effects of dose escalation to either 600 mg or 800 mg of imatinib daily. Dose escalation was beneficial as 42% of these patients achieved a cytogenetic response. The dose increase also prevented disease progression to AP or BC in 89% of patients and overall survival was 84% following 3 years of increased imatinib treatment. Imatinib dose escalation was deemed an appropriate initial treatment option for patients with CP CML who had experienced suboptimal CyR or resistance (Kantarjian et al., 2009).

1.5.2 TKIs

Resistance to TKIs is one of the primary reasons for the failure of therapy in patients with CML. In an effort to overcome this more potent and mutation targeted TKIs have been designed. Second generation TKIs, dasatinib and nilotinib, were designed to be more potent than imatinib, to bind more effectively to the BCR-ABL kinase domain and allow binding to BCR-ABL mutant isoforms. Although very effective the elusive T315I BCR-ABL mutation was not targeted by second-generation TKIs. This led to third generation TKIs, bosutinib and ponatinib, which exhibited increasing specificity and potency towards BCR-ABL. Ponatinib, was specifically designed to overcome resistance-inducing mutations, including the T315I mutation, in the ABL kinase domain.

1.5.3 Second-generation TKIs

1.5.3.1 Dasatinib

Dasatinib was developed as a more advanced BCR-ABL kinase inhibitor than imatinib and differed due to dasatinib's slightly less stringent binding requirements. This enables dasatinib to bind to both the inactive and the active conformations of BCR-ABL. It can also

bind the Src family kinases given their similar geometry to the Abl active conformation, and maybe most importantly it has activity against many imatinib-resistant kinase domain mutations of BCR-ABL. In vitro studies using cell line models showed that dasatinib could inhibit 18-19 known imatinib-resistant BCR-ABL mutations, within a narrow clinically achievable concentration range. The only mutation that is able to evade dasatinib treatment is a single point mutation deep within the ATP-binding domain, T315I. It has been shown to have a high resistance against imatinib and second generation TKIs. It is thought that this occurs as all current TKIs directly interact with threonine-315 via hydrogen bonding, therefore if this site is mutated the inhibitors can no longer bind (Shah et al., 2004, Lombardo et al., 2004, O'Hare et al., 2005, Tokarski et al., 2006).

Dasatinib went into a dose escalation Phase I clinical trial in 2003 and patients were recruited in various stages of CML disease progression that were resistant to imatinib. Patients received 15 to 240 mg/day in four-week treatment cycles, once or twice daily. The results of this trial showed that 37 out of 40 CP CML patients achieved a complete haematological response, with 95% of patients maintaining their response at 12 months (Talpaz et al., 2006).

A phase II trial followed recruiting 387 CP CML patients resistant to imatinib. Patients were dosed at 70 mg twice daily and after a median follow-up of 15.2 months 91% of patients had attained and maintained a CHR, 59% achieved a MCyR and of these patients 49% achieved CCyR (Hochhaus et al., 2008).

The efficacy of dasatinib versus imatinib treatment was then evaluated in newly diagnosed CML patients in the DASISION trial (Kantarjian et al., 2010). In this trial 519 CP CML patients were recruited and randomised into two groups. One group received 100 mg of dasatinib and the second 400 mg of imatinib per day. After 12 months a higher percentage of patients treated with dasatinib achieved CCyR at a much faster rate than imatinib treated patients (dasatinib 77%, imatinib 66%; $p = 0.007$). Also a higher percentage of dasatinib treated patients achieved a Major Molecular Response (MMR) compared to imatinib (Dasatinib 46%, imatinib 28%; $p < 0.0001$) (Kantarjian et al., 2010). After a 5 year follow up, the final results from the trial continue to support dasatinib 100 mg once daily as a safe and effective first line therapy for the long-term treatment of CP CML (Cortes et al., 2016). In 2006, with the success of the clinical trials dasatinib was approved by the FDA for the treatment of newly diagnosed CML patients and patients who were resistant to previous therapy. Although dasatinib treatment had enhanced effects over imatinib in CP CML patients, in more progressive phase of the disease, these effects were limited and response

rates were poor and short lived (Cortes et al., 2008, Apperley et al., 2009). Dasatinib has also been shown, due to its increased potency, to target an earlier CML progenitor population than imatinib, however it still fails to eliminate the persistent LSCs within the BM (Copland et al., 2006a).

1.5.3.2 Nilotinib

It was hypothesized that more potent and selective compounds could be developed by reengineering the structure of imatinib to incorporate elements designed to capitalise upon the elucidation of the imatinib-ABL binding mode (Manley et al., 2004). Nilotinib is based on the chemical structure of imatinib and exhibits the same binding mode (Sandra et al., 2004). Nilotinib has one important structural difference, which is the replacement of an N-methylpiperazinyl group, which gave nilotinib a slightly different structure to fit better within the kinase domain of BCR-ABL and therefore enhances binding efficiency. This increased potency of nilotinib by 30-fold compared to imatinib. It also increased its binding affinity for BCR-ABL compared to other kinases, such as c-KIT and PDGFR. The enhancement in binding affinity also improves inhibitory activity against most of the common kinase domain mutations that cause imatinib resistance, with the exception of the T315I mutation (Weisberg et al., 2005, Bradeen et al., 2006, Ray et al., 2007).

Through Phase I and II clinical trials nilotinib has shown greater efficacy than imatinib in newly diagnosed CP CML patients. A phase III trial ENESTnd further emphasised this effect, as patients in a three arm randomised trial where patients were treated with either 300 mg nilotinib or 400 mg nilotinib twice daily or 400 mg imatinib daily. A 2 year follow up of this trial concluded that significantly more patients treated with nilotinib had achieved a MMR compared to imatinib; 71% of 300 mg nilotinib treated patients, 67% 400 mg nilotinib and 44% of 400 mg imatinib patients. Overall a significantly higher number of nilotinib treated patients achieved CMR compared to imatinib (Kantarjian et al., 2011, Hochhaus et al., 2016). In 2010, with the success shown in the clinical trials, the FDA granted accelerated approval for nilotinib treatment in patients with newly diagnosed CP CML. However, like imatinib and dasatinib, nilotinib is also unable to eliminate the persistent population of LSCs (Jørgensen et al., 2007b).

1.5.4 Third-generation TKIs

1.5.4.1 Ponatinib

Ponatinib was designed through computational modelling and structure-based experiments in order to develop a TKI that could inhibit BCR-ABL, including the T315I mutation. To overcome this problematic mutation, ponatinib has a novel triple-bond linkage that avoids the steric hindrance caused by the bulky isoleucine residue at position 315 in the BCR-ABL T315I mutant (Zhou et al., 2011). Ponatinib is therefore a pan-TKI inhibitor, which can inhibit all known BCR-ABL mutants; it also targets Flt3 and SRC kinases. Additionally preclinical experiments showed that ponatinib could suppress tyrosine to phenylalanine (T177F) the emergence of any mutation at a low concentration of 40 nM (O'Hare et al., 2009).

A phase I clinical trial was conducted in 2008 to evaluate the toxicity and safety of ponatinib for clinical use. This dose escalation trial recruited CML patients who had previously failed at least two TKIs. 43 CP CML patients entered this trial and of these patients 98% achieved a CHR, 63% a CCyR and 44% MMR. Ponatinib was generally well tolerated and on the basis of the safety, pharmacokinetic, and pharmacodynamic data, 45 mg of ponatinib was determined to be the maximum tolerated dose suggested for further clinical studies (Cortes et al., 2012b).

The encouraging phase I results led to the launch of a phase II clinical trial in 2010, the Ponatinib Ph+ ALL and CML Evaluation (PACE) trial. PACE recruited 271 CP CML patients and 79 AP CML patients, who had experienced resistance to or unacceptable side effects from dasatinib or nilotinib or harboured the T315I mutation. Patients received 45 mg/day of ponatinib and the results showed that ponatinib had significant anti-leukaemic activity across categories of disease stages and especially with patients harbouring the T315I mutation. Overall 46% of the CP CML patients achieved a CCyR response of whom 34% achieved a MMR (Cortes et al., 2013).

Ponatinib was becoming a very attractive treatment option for patient's resistant to all current TKIs. Further clinical studies were performed to assess whether ponatinib would result in a superior outcome compared with imatinib in newly diagnosed CP CML patients. A phase III trial commenced in 2012, called the Evaluation of ponatinib versus imatinib in CML (EPIC) trial. 307 patients were entered into randomised groups and either treated with 45 mg of ponatinib or 400 mg imatinib daily. However, the trial was terminated early, following concerns about thrombotic vascular adverse events that were observed in patients given ponatinib in other trials. The trial termination meant limited data was

available for the primary endpoint of the trial, MMR at 12 months. Only 10 patients in the ponatinib arm and 13 in the imatinib could be assessed at the 12 month time point. The small number of patients means interpretation of the data was taken with caution, however the preliminary data suggested ponatinib maybe more beneficial. 80% of ponatinib patients and only 38% of the imatinib patients achieved MMR within 12 months (Lipton et al., 2016).

Due to the concerns of thrombotic vascular events, ponatinib was briefly withdrawn from the US market in October 2013 on the recommendation of the FDA, however it was soon re-introduced in January 2014. Ponatinib is currently approved for CML patients with the T315I mutation or for CML patients who are unresponsive to all TKIs (National Institute of Health, 2013).

1.5.4.2 Bosutinib

Bosutinib is a dual inhibitor of ABL and SRC kinases, which showed potent inhibitory activity against BCR-ABL in imatinib-resistant CML cell lines. It is a much more potent inhibitor than imatinib, with several studies showing a 15-100 fold lower IC₅₀(Puttini et al., 2006, Golas et al., 2003).

Unlike other TKIs bosutinib exhibits a lower activity against c-Kit or PDGFR, which are non-specific targets of TKIs, which are thought to be associated with toxicities (Puttini et al., 2006, Rensing Rix et al., 2008, Konig et al., 2008, Bartolovic et al., 2003).

The FDA approved Bosutinib in 2012 for the treatment of CP, AP and BC CML patients with resistance to prior therapy.

An on-going phase III clinical trial BELA is evaluating the efficacy of bosutinib compared to imatinib in newly diagnosed CP CML patients. The patients were randomised into two groups one received 500 mg of bosutinib and the other 400 mg of imatinib. Data from a 2 year follow-up showed that the CCyR rates were the same for the two treatment groups; 50% for bosutinib and 49% for imatinib. However a higher percentage of bosutinib treated patients achieved MMR compared to imatinib, 59% and 49%, respectively (Brümmendorf et al., 2015).

1.5.5 An alternative experimental BCR-ABL inhibitor

1.5.5.1 ABL001

ABL001 is an allosteric inhibitor of BCR-ABL. It binds to the myristoyl pocket of the BCR-ABL kinase domain. The normal substrate for this pocket is the myristoylated N-terminus of ABL, which serves as an autoregulatory mechanism for ABL signalling, however this domain is lost in the formation of BCR-ABL. Therefore, ABL001 has been designed to fit the myristoyl pocket to mimic the autoregulatory role of the myristoylated N-terminus of ABL and restore negative regulation of kinase activity. As this inhibitor does not bind with the kinase domain of BCR-ABL, where many mutations occur to cause TKI resistance, it is thought this could potentially be an alternative drug treatment for TKI-resistant patients.

Preclinical studies showed that ABL001 was potent and selectively inhibited the growth of BCR-ABL+ CML cells. These inhibitory effects were also extended to mutated isoforms of BCR-ABL, including T315I. *In vivo* treatment of xenograft models with ABL001 revealed potent anti-tumour activity and complete tumour regression (Ottmann et al., 2015). Additionally, a combination treatment of ABL001 and nilotinib achieved sustained tumour regression even after treatment discontinuation (Wylie et al., 2014). ABL001 is currently undergoing a phase I dose-escalation study to examine the safety of the drug in the clinic. Patients have been recruited who have CP or AP CML that is not responding to two or more TKIs due to resistance. The patients have been treated with ABL001 in doses ranging from 10 to 150 mg twice daily (Ottmann et al., 2015).

Thirty-five patients were recruited to the study, however at the time of publication data was only available for 20 of the patients. Patients had received treatment for ≥ 3 months at the time of analysis and evidence of BCR-ABL inhibition was observed in doses ≥ 10 mg. Five of these patients had suffered a haematological relapse and all of these patients achieved a CHR within three months of ABL001 treatment. Nine of the 20 patients that were in cytogenetic relapse at trial entry achieved a MCyR by 3 months, and 6 of these patients also achieved CCyR. Five of the 20 patients achieved a MMR after 5 months of ABL001 treatment. All patients that achieved a CHR, CCyR or MMR maintained their responses. Therefore ABL001 has proven itself to have rapid dose-dependent anti-tumour activity and to-date has been well tolerated in CML patients, providing evidence that ABL001 could have the potential to benefit CML patients resistant to TKIs (Ottmann et al., 2015).

1.5.6 Omacetaxine

Omacetaxine also known as homoharringtonine is an alkaloid derived from the plant *Cephalotaxus harringtonia*, which has anti-tumour properties. It has been reported that omacetaxine has the ability to reversibly inhibit the initial stages of protein translation of important anti-apoptotic and cell cycle mediators, such as MCL-1, Cyclin D1, c-myc, XIAP and β -catenin, and therefore promotes apoptosis and cell cycle arrest (Tang et al., 2006, Meir and David, 2011). Although omacetaxine cannot selectively target cancer cells, protein translation has been shown to be markedly upregulated in cancer cells along with high levels of proteins involved in cell division and survival, compared to normal cells (Hershey and Miyamoto, 2000).

Omacetaxine has been assessed in several phase II clinical trials involving CML patients, who are either TKI-resistant (ClinicalTrials.gov identifier: NCT00462943) or for CML patients that carry the BCR–ABL T315I mutation and have failed TKI treatment (ClinicalTrials.gov identifier: NCT00375219) (Cortes et al., 2012a). The study which assessed the effects of omacetaxine treatment in CML patients carrying the T315I mutation was carried out in the pre-ponatinib era, when no TKI was effective against the T315I mutation. 66 patients were enrolled in the study and 77% of the patients achieved a CHR, 23% achieved a MCyR and 16% of these patients achieved CCyR. Omacetaxine was deemed a safe and effective treatment option for these patients. The clinical trial for CP and AP CML patients resistant to TKI recruited 46 CP-CML patients, who had received 2 or more prior TKIs. Haematological response was achieved in 67%, however a CCyR was only achieved by 4% of patients. Although this treatment is not so effective in these patients it was given approval by the FDA in 2012 for treatment for CP or AP CML patients with resistance or intolerance to two or more TKIs, as treatment options were very limited for CML patients who were resistant to TKIs at that time. Omacetaxine is seen as a last resort treatment option for CML patients. Due to its non-specific mode of action it has the ability to potently target both normal and leukaemic cells (Allan et al., 2011). This makes it highly toxic and causes many adverse effects, such as cardiac toxicity, which raises concerns for its use as a CML treatment. However, there is another clinical trial still recruiting patients which hopes to evaluate the pharmacokinetics, safety, and efficacy of Omacetaxine to patients with CP or AP CML (Referred to as the SYNSINCT Study) (ClinicalTrials.gov identifier: NCT02078960).

1.6 Autophagy

Eukaryotic cells orchestrate many finely balanced biological processes in order to maintain cellular homeostasis. One of the main regulators of cellular homeostasis is the lysosome. The lysosome contains acidic hydrolases, which the cell utilises to degrade unwanted materials. In stressful conditions, such as nutrient deprivation, cells can employ a highly regulated self-eating process called autophagy. Autophagy is an intracellular recycling mechanism that regulates lysosomal degradation of organelles, protein aggregates, cytoplasmic proteins and lipids (DeBerardinis et al., 2008). This allows for the generation of new cellular building blocks, such as amino acids, fatty acids and acetyl-CoA, that can be utilised by the cell for energy and the synthesis of macromolecules (DeBerardinis et al., 2008).

Autophagy is an essential mechanism for the maintenance of cellular homeostasis (Amaravadi et al., 2011). Cells have a basal rate of autophagy that is critical for the degradation and recycling of aberrant protein aggregates and damaged organelles that will otherwise accumulate and cause cellular damage (Amaravadi et al., 2011, Jung et al., 2009). However in stressful cellular conditions, such as nutrient deprivation, hypoxia or following chemotherapeutic drugs, autophagy can be upregulated in order to maintain a balanced cellular environment (Amaravadi et al., 2011).

The term autophagy was first introduced in 1963 by Christian de Duve, who used this word to describe observations from electron microscopy studies, which showed single or double membrane vesicles that contained parts of the cytoplasm, including organelles, in various degrees of degradation (Ashford and Porter, 1962, Clark, 1957, de Duve and Wattiaux, 1966, Novikoff, 1959). However, it wasn't until the late 1990s, that the molecular mechanisms of how autophagy functions began to become clearer. This started with genetic screens using budding yeast, *Saccharomyces cerevisiae*, which led to the identification of 32 autophagy (ATG) related genes. Of these genes 11 were found to have unambiguous orthologues in mammalian cells and most of these genes mediate the highly regulated autophagosome formation (Nakatogawa et al., 2009).

There are three general types of autophagy; chaperone-mediated, microautophagy and macroautophagy (Huang and Klionsky, 2007, Majeski and Fred Dice, 2004, Reggiori and Klionsky, 2002, Wang and Klionsky, 2003). This piece of work focuses on macroautophagy, which will from hereon be referred to as autophagy.

The autophagy process begins with the formation of the phagophore, which is a cup shaped membrane that is generated upon induction of autophagy. The phagophore elongates to form a double membrane vesicle, known as an autophagosome. As it does so it engulfs cytoplasmic components that have been primed for degradation. Autophagosomes are able to move by sliding along cytoskeletal structures to deliver the waste material to the lysosome. The outer membrane of the autophagosome fuses with the lysosome to create an autolysosome. The inner membrane along with the waste cargo is then degraded by the acidic hydrolases from the lysosome. The broken down waste products can be recycled back to the cytosol for reuse (Tooze and Yoshimori, 2010).

Basal levels of autophagy are low under normal conditions, but are upregulated following cellular stress. The autophagy pathway can be divided into sequential steps; initiation, autophagosome formation, fusion and degradation, each highly regulated by different protein complexes.

1.6.1 Autophagy initiation

The major regulator of autophagy in mammalian cells is mTORC1, which is activated in a Rheb-dependent manner under nutrient rich conditions to inhibit membrane targeting of the autophagic initiation complex (Hosokawa et al., 2009). The initiation complex is made up of several components; Unc-51- like kinase 1 (ULK1), ULK2, ATG13, ATG101 and FIP200. mTORC1 is able to negatively regulate autophagy initiation by phosphorylating ULK1 and ATG13 (Jung et al., 2009). In stressful condition, such as nutrient deprivation, mTORC1 is inhibited and dissociates from the initiation complex, freeing the complex to allow energy sensor AMP-activated protein kinase (AMPK) to phosphorylate ULK1 and thereby induce autophagy (Kim et al., 2011). Activated ULK1, phosphorylates and activates ATG13 and FIP200, and the active ULK-ATG13-FIP200 complex is recruited to the phagophores (Hosokawa et al., 2009).

1.6.2 Autophagosome formation

The formation of the phagophore is regulated by a second multi-protein complex, referred to as the class III PI3K complex (Liang et al., 2008). This complex comprises the class III PI3K vacuolar protein sorting 34 (VPS34), the regulatory unit VPS15 and BECLIN1 (Mizushima, 2007, Itakura et al., 2008, Simonsen and Tooze, 2009). VPS34 is essential for the developmental progression of a phagophore to an autophagosome (Liang et al., 2008).

The PI3K complex has many different binding partners that regulate autophagy and depending upon the interaction the complex will function in a specific manner. Most of

these interactions occur via binding with BECLIN1 and therefore BECLIN1 is also an essential protein for autophagosome biogenesis. One such interaction occurs between BECLIN1 and ATG14L. It is believed that ATG14L targets the PI3K complexes to an endoplasmic reticulum (ER) subdomain and therefore mediates the localisation of the PI3K complexes to the site of the autophagosome formation (Itakura and Mizushima, 2010, Matsunaga et al., 2010). BECLIN1 can also form a complex with apoptosis regulators Bcl-2 or Bcl-xL, via its BH3 domain, which has an inhibitory effect on BECLIN1 (Maiuri et al., 2007). However, upon starvation BECLIN1 disassociates and can induce autophagy (Levine et al., 2008). In addition, BECLIN1 can also form a complex with Activating Molecule in BECN1-regulated autophagy1 (AMBRA1). This interaction allows the PI3K complex to dock to the cytoskeleton via dyneins. However upon autophagy induction, ULK1 phosphorylates AMBRA1, which disrupts this interaction and allows the PI3K complex to detach and migrate to the ER to initiate autophagosome formation (Di Bartolomeo et al., 2010). Other BECLIN1 regulators include the UV radiation resistance-associated gene (UVRAG) and Rubicon, which can either positively or negatively regulate autophagy (Yang and Klionsky, 2010).

Although the autophagosome is thought to form near the ER, the origin of the autophagosome membrane is still unclear. However, studies have suggested the ER, Golgi apparatus, mitochondria or even de novo generation (Tooze and Yoshimori, 2010).

1.6.3 Autophagosome completion

Autophagosome completion is controlled by two essential ubiquitin-like conjugation systems: ATG12-ATG5 (Mizushima et al., 1998) and LC3-PE (Ichimura et al., 2000). The ATG12-ATG5 conjugation forms with the aid of a homodimeric E1-like enzyme, ATG7. ATG7 activates ATG12, which covalently conjugates ATG12 to ATG10, an E2-like enzyme, and then to ATG5. ATG10 then interacts with ATG16 to form the ATG12-ATG5-ATG16 complex (Nakatogawa et al., 2009). This large complex promotes the recruitment and conversion of cytosolic-associated protein light chain 3 (LC3-I) to the membrane bound lipidated form; LC3-II (Matsushita et al., 2007, Kabeya et al., 2000). LC3-I conjugation begins with the cleavage of the carboxyl-terminal by cysteine protease ATG4. Upon autophagy activation, ATG7 activates LC3-I and transfers it to ATG3, an E2-like enzyme (Yamada et al., 2007). Finally, the ATG12-ATG5-ATG16 complex facilitates the conjugation of LC3-I to phosphatidylethanolamine (PE) to generate the lipidated form, LC3-II, which is integrated into the double membrane of the autophagosome. ATG4 can also cleave LC3 from the outer membrane of the autophagosome for recycling (Kirisako et

al., 2000). When autophagosome formation is complete the ATG proteins are recycled, with the exception of LC3-II, which remains bound to the mature autophagosome until fusion with a lysosome has been completed. LC3-II is the main marker of autophagy and it is the LC3 conversion that is used as a marker to monitor autophagy (Klionsky et al., 2016).

Although it is thought that autophagosomes engulf cellular material non-specifically, it can be semi selective. A cargo selector receptor, known as SQSTM1 (p62) delivers ubiquitinated substrates to the autophagosomes for autophagic degradation. p62 contains a c-terminal ubiquitin-associated domain that binds ubiquitin and also a LC3 interaction region that allows direct binding with LC3 (Pankiv et al., 2007). p62 is also useful when analysing autophagy as it is degraded during autophagy, but accumulates when autophagy is inhibited (Klionsky et al., 2016).

1.6.4 Autolysosome formation

Maturation of the autophagosome involves the fusion of the outer membrane of the autophagosome with a lysosome, to form an autolysosome (Liang et al., 2008). Upon the formation of the autolysosome the inner membrane and the sequestered cellular debris are lysed by lysosomal hydrolases, such as cathepsins, and are subsequently degraded to their monomeric units and released back into the cytosol. Therefore the cell gains new building blocks for energy generation and macromolecule synthesis (Xie and Klionsky, 2007). This maturation/degradative process is not fully understood, but is known to require lysosomal protein LAMP-2, the small GTPase RAB7 and UVRAG for completion (Rosenfeldt and Ryan, 2009) (figure 1-4).

1.6.5 Autophagy and Cancer

The first strong piece of evidence that linked autophagy to cancer was in 1999 when it was shown that BECLIN1 expression in MCF7 breast cancer cell line inhibited cell proliferation *in vitro* and inhibited tumourigenesis in nude mice (Liang et al., 1999). This data was interestingly supported by data showing that BECLIN1 was mono-allelically deleted in 40-70% of sporadic human breast and ovarian cancer patients (Aita et al., 1999). It was later shown that BECLIN1 haploinsufficient mice were prone to tumour development (Qu et al., 2003, Yue et al., 2003). Since these findings it has also been shown that other autophagy related genes have links to cancer. For example, frameshift mutations of ATG2B, ATG5, ATG9B and ATG12 in gastric and colorectal cancers (Kang et al., 2009) and deletion of other key autophagy regulators, such as ATG7, in mice

promote malignant transformation in the liver and HSCs (Mortensen et al., 2011, Takamura et al., 2011).

1.6.6 Autophagy and CML

Increasing evidence is emerging that autophagy is an essential mechanism involved in the maintenance of HSCs and may protect against leukaemia development (Liu et al., 2010, Mortensen et al., 2011, Warr et al., 2013b). The first studies to show this were conducted by Lui *et al* and Mortensen *et al*, which showed, that deleting essential autophagy genes *FIP200* and *Atg7* had negative effects on the function and maintenance of HSCs (Liu et al., 2010, Mortensen et al., 2011). *FIP200* was shown to be essential for foetal HSC maintenance and function, as its deletion caused increased mitochondrial mass and high levels of ROS production and as a consequence these mice suffered from severe anaemia and perinatal lethality (Liu et al., 2010). Similarly, the conditional deletion of *ATG7* in the haemopoietic system led to the accumulation of mitochondria, increased ROS production, DNA damage and the loss of HSC function (Mortensen et al., 2011). The loss of *ATG7* also affected the production of myeloid and lymphoid progenitor cells and the mice developed a myeloproliferative disorder and only had a mean survival of 12 weeks (Mortensen et al., 2010), therefore suggesting that autophagy may protect the cells against leukaemogenesis. This has been supported more recently by Warr *et al*, who demonstrated that *FOXO3A* is essential for life-long maintenance of HSCs via its critical role in poising HSCs for rapid induction of autophagy upon starvation (Warr et al., 2013b). These data indicate just how important basal autophagy is to maintain homeostasis in normal cells, as it allows the cells to adapt to changing environments.

Strong evidence linking autophagy with leukaemia development has led to several studies publishing links specifically to CML (Bellodi et al., Salomoni and Calabretta, 2009, Yan et al., 2006, Kamitsuji et al., 2008).

As discussed CML cells depend on growth factoring mimicking of BCR-ABL for their survival. One major pathway which BCR-ABL signals through for growth and survival is the PI3K/AKT/mTOR pathway, therefore mTOR is constitutively active in CML cells. mTOR is a negative regulator of autophagy and an *in vivo* study has shown that BCR-ABL expressing haemopoietic precursor cells have low levels of autophagic activity, however, the cells are highly dependent on this process (Altman et al., 2011).

Strong data shows that although standard treatments for CML cause apoptosis in the majority of cells, a small persistent reservoir of BCR-ABL expressing CML cells survive, which is responsible for disease progression. Treatment of CML cells with TKIs has been

shown to induce autophagy, presumably due to the inhibition of BCR-ABL signalling, which therefore leads to down regulation of the PI3K/AKT/mTOR pathway. The induction of autophagy is thought to make CML cells become metabolically inactive, which allows them to evade TKI stress. A hypothesis, was drawn by Calabretta and Salomoni, that if CML cells induce autophagy as a survival mechanism against TKI, the inhibition of autophagy would eliminate this pro-survival mechanism and could potentially restore TKI sensitivity in these CML cells (Calabretta and Salomoni, 2011).

The first evidence of autophagy induction in CML cells was shown in 2006, when a lab used a neurotoxin; crotoxin, as an anti-cancer treatment against the CML cell line K562. They showed that crotoxin induced autophagy in the K562 cells and by blocking autophagy, this further sensitised the K562 cells to the crotoxin treatment, thereby increasing the cytotoxic effect (Yan et al., 2006). The following year, with the development of more specific CML therapeutics, it was shown that specifically inhibiting BCR-ABL induced autophagy in CML cells. This study used a potent c-ABL and LYN kinase inhibitor, bafetinib (INNO-406) to treat K562 cells and this led to the induction of autophagy (Kamitsuji et al., 2008). The autophagic response had a protective role in the surviving cell population as a treatment with autophagy inhibitor chloroquine (CQ) enhanced the cytotoxic effect of bafetinib. Upon the generation of imatinib this data was further supported as, imatinib was also shown to induce autophagy in CML cells and a combination treatment with CQ substantially enhanced imatinib-induced cell death (Mishima et al., 2008). However the strongest evidence that demonstrates that autophagy inhibition enhances imatinib treatment of primary CML cells was conducted by Bellodi and colleagues in 2009 (Bellodi et al., 2009). They showed that combining a TKI, imatinib, dasatinib or nilotinib, with autophagy inhibition, enhanced TKI treatment to the extent that there was a near complete elimination of phenotypically and functionally defined CML stem cells (Bellodi et al., 2009). This was supported by an *in vivo* study, which conditionally deleted *ATG3* to inhibit autophagy in BCR-ABL expressing haemopoietic cells (Altman et al., 2011). These cells were then transplanted into lethally irradiated mice and due to the *ATG3* deletion the BCR-ABL cells failed to induce leukaemia (Altman et al., 2011).

Studies within our own laboratory have shown that CD34⁺ CML cells express lower levels of essential autophagy genes compared to normal CD34⁺ cell populations. However, upon TKI treatment and subsequent BCR-ABL inhibition, these same genes are shown to be upregulated in the CD34⁺ CML cells. This suggests that BCR-ABL not only suppresses autophagy post-transcriptionally by increased PI3K/AKT/mTOR signalling, but also leads

to down-regulated transcription of key autophagy genes. This data further supports the hypothesis made by Bellodi *et al*, that at the primitive stem cell level, autophagy is induced as a protective mechanism specifically against TKI induced BCR-ABL inhibition (Bellodi et al., 2009).

A collaboration between our laboratory and Calabretta and Salomoni, has identified autophagy as a potential survival pathway that CML stem cells activate in response to TKI-induced cellular stress (Calabretta and Salomoni, 2011). Autophagy is thought to help CML stem cells escape TKI induced death and there evade eradication. Therefore, autophagy has become a key research area in CML stem cell research.

1.6.7 Autophagy inhibition in CML

In the clinic the most common treatment given to patients to inhibit autophagy is an antimalarial drug called CQ, or its derivative, HCQ which is increasingly potent and associated with lower retinal toxicity (Solomon and Lee, 2009, Levy et al., 1997).

HCQ is a lysosomotropic weak bases, which raises the pH within lysosomes and impairs lysosomal function. This can therefore effect the end stage of the autophagy process; due to the inhibition of lysosomal acidification it can no longer degrade the autophagic cargo. In addition to this effect it can also inhibit autophagy flow by preventing the fusion of the autophagosome to the lysosome. HCQ's primary use is as an anti-malarial drug, but it has also been used to treat patients with autoimmune diseases, such as rheumatoid arthritis. HCQ has been well tolerated in the clinic and due to its FDA approval it has allowed a number of clinical trials to be launched investing its efficacy in inhibiting autophagy function, either as a sole cancer treatment or in combination with cytotoxic agents.

There are other pharmacological drugs that are available that can target the early stages of autophagy, such PI3K-III inhibitor, 3-methyladenine and wortmannin (Blommaert et al., 1997). Chemical inhibitors are also available and these target the later stages of autophagy, such as lysosomal protease inhibitors E64d and pepstatin, which effects degradation of the autophagosome (Tanida et al., 2005). However, none of these inhibitors are specific to autophagy and some of them are associated with high toxicity at clinically relevant doses.

1.6.8 CHOICES clinical trial

The significance of the previously mentioned data has led to the initiation of the phase II CHOICES (CHIOroquine and Imatinib Combination to Eliminate Stem cells) randomised clinical trial (NTC01227135). CHOICES is a preliminary study evaluating the response of imatinib versus imatinib and HCQ, in CML patients who have been on imatinib for over 1 year and are in MCyR with residual disease detectable by qRT-PCR. The primary objectives of this trial are (1) to determine if imatinib or imatinib in combination with HCQ is more effective in lowering BCR-ABL levels in patients with CML in MCyR with residual BCR-ABL positive cells detectable by qRT-PCR after at least one year of imatinib treatment, and (2) to determine the safety and tolerance of this treatment regime in CML patients. Patients were randomised into 2 different treatment arms; in arm A patients received oral imatinib daily and arm B patients received oral imatinib daily and oral HCQ twice daily. In both treatment arms the treatment was given continuously for up to 12 months in the absence of disease progression or unacceptable toxicity. The patients then received oral imatinib daily for a further 12 months during the follow up period of the study. Patients' blood samples will be analysed at baseline, during and upon completion of the treatment for pharmacological and laboratory testing. After the completion of the study, patients undergo follow-up testing at 3, 6, 9 and 12 months.

Data from the CHOICES clinical trial will be invaluable in the understanding of the regulation of autophagy in CML and if this is an effective future therapeutic option for CML patients.

1.6.9 New generation of autophagy inhibitors

Although, HCQ has been shown to effectively inhibit autophagy *in vitro* there is uncertainty whether the same effect can be achieved in the clinic. Therefore, we are continuing to investigate different autophagy inhibitors, as more potent and specific compounds are becoming increasingly available. Currently we are interested in analysing the effects of Lys05, a CQ derivative, which has been shown to be 10x more potent than HCQ (McAfee et al., 2012) and therefore more likely to show the desired inhibitory effect needed for CML patients. Lys05 is an autophagy inhibitor, which has also shown to have single agent antitumour activity, unlike HCQ (McAfee et al., 2012). *In vivo* investigations using mouse models have shown that at a high dosage level Lys05 reproduced a similar phenotype as humans with genetic defects in autophagy gene ATG16L1, therefore supporting its specificity to autophagy inhibition (McAfee et al., 2012).

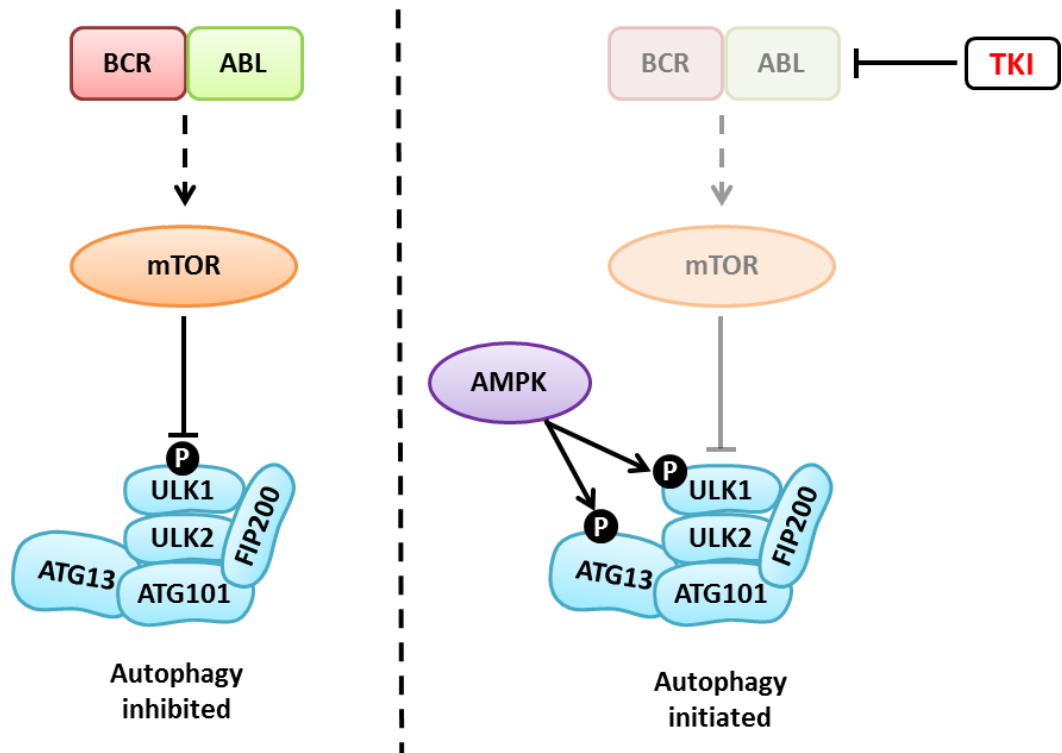


Figure 1-3: Autophagy activation.

Autophagy is induced by the activation of the initiation complex. This occurs when mTOR is inhibited, as seen with the inhibition of BCR-ABL signalling by TKIs. This allows ULK1 and ATG13 to be phosphorylated by AMPK and activate the initiation complex, which is then recruited to the phagophore.

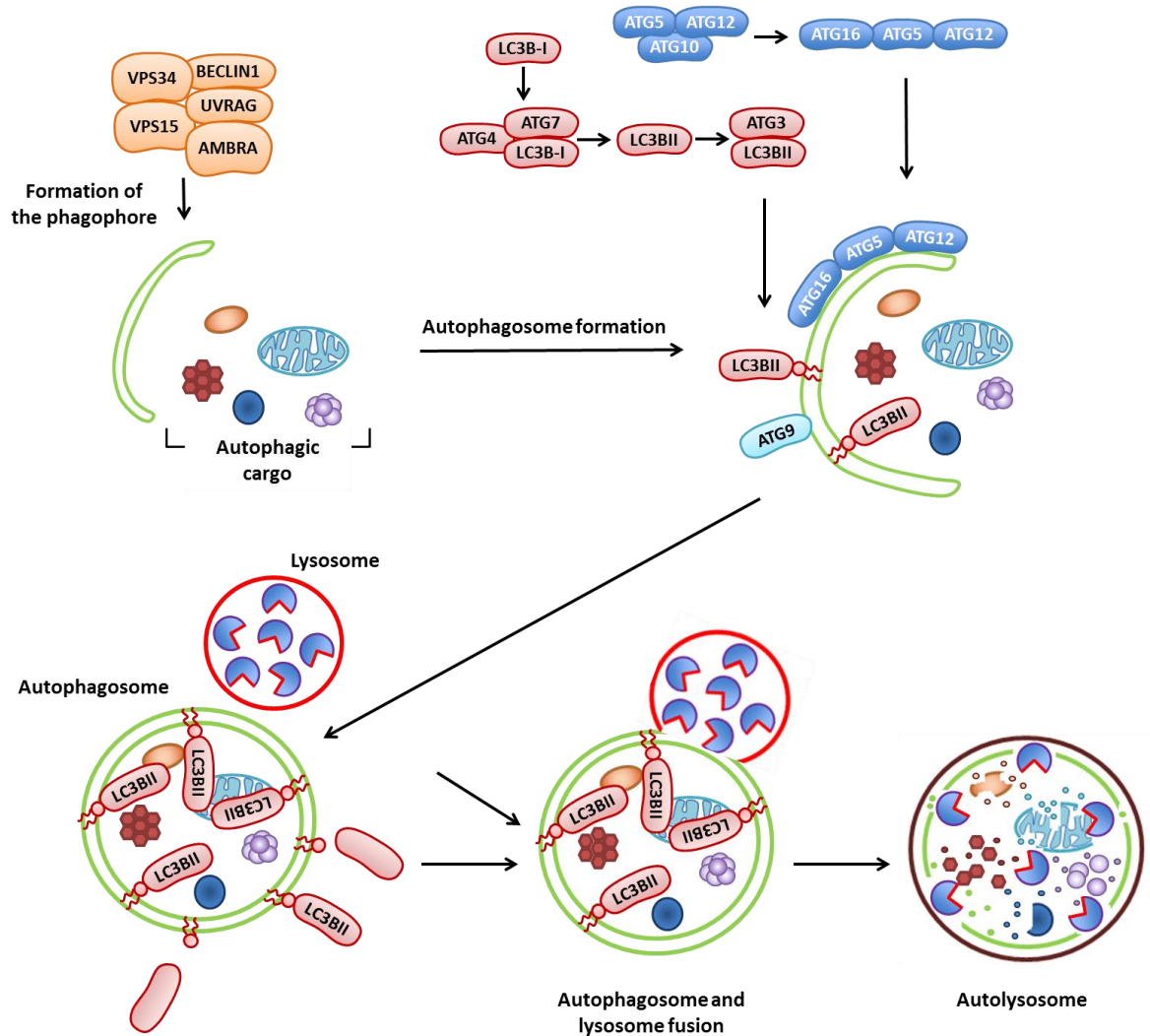


Figure 1-4: The molecular mechanism of autophagy.

Activation of the initiation complex promotes autophagosome formation. An essential autophagy protein for autophagosome formation is VPS34, which forms a complex with VPS15, BECLIN1, UVRAG and AMBRA1. Autophagosome completion is regulated by LC3 and ATG12-ATG5 conjugation systems, which mediate lipid modification of LC3-I, allowing LC3-II to bind to the autophagosomal double membrane. Completed autophagosomes contain cellular debris that is ready for degradation. The completed autophagosome fuses with a lysosome and forms an autolysosome, which uses the lysosomal enzymes to degrade and recycle the debris to allow for the generation of energy and new building blocks for protein synthesis. Adapted from (He and Klionsky, 2009b).

1.7 Summary

As has been discussed in this chapter, TKIs have greatly improved the life expectancy of CML patients, however their success has been tarnished by the development of drug intolerance, CML stem cell insensitivity to TKIs (Graham et al., 2002, Jørgensen et al., 2007a, Copland et al., 2006b, Corbin et al., 2011, Hamilton et al., 2012) and drug resistance (Karvela et al., 2012). A significant subset of CML patients suffer from TKI resistance and despite efforts to combat known resistant mechanisms such as *ABL* kinase domain mutations (Druker et al., 1996) with the development of more potent TKIs (Corbin et al., 2002, Lombardo et al., 2004, Brümmendorf et al., 2015, O'Hare et al., 2009) there is still a patient population, which have an acquired TKI resistance, which is not due to a kinase domain mutation and yet are resistant to all current TKI treatments. These patients are believed to have a BCR-ABL-independent mechanism of resistance. Evidence has been shown from several reputable publications (Thomas et al., 2004, Mahon et al., 2003, Mahon et al., 2008) that BCR-ABL-independent TKI resistance may stem from the activation of a secondary oncogenic mechanism. Patients with a BCR-ABL-independent mechanism of TKI resistance are of major clinical concern, as although a number of mechanisms have been proposed, not one common mechanism has been discovered, which leaves these patients with very limited treatment options. In this study we hope to gain a further understanding of the mechanisms causing BCR-ABL-independent TKI resistance. In order to do so we generate ponatinib resistant cell line models and attempt to characterise their mechanism of resistance using different screening methods. It is hoped that information gained from these experiments will guide us towards the identification of a common weakness in primary TKI-resistant CML cells. Results from our study propose the PI3K-AKT-mTOR pathway as a key player responsible for TKI resistance and that pharmacological inhibition of this pathway in combination with the inhibition of survival mechanism, autophagy, may represent a potential new treatment for TKI-resistant CML patients.

2 Materials and Methods

2.1 Materials

2.1.1 Small molecule inhibitors

Imatinib and ABL001 were provided as a white powder under a Materials Transfer Agreement (MTA) from Novartis Pharma (Basel, Switzerland). Dasatinib was provided as a white powder under a MTA from Bristol-Myers Squibb (Princeton, NJ, USA). Ponatinib was provided as a white powder under a MTA from ARIAD Pharmaceuticals Inc. (Massachusetts, USA). Details of the suppliers, stock concentrations, and diluents of all drugs and inhibitors used are listed in Table 2-1. All stock aliquots were stored at -20°C, with the exception of HCQ and CQ, which were stored at 4°C. All small molecule inhibitors were made up fresh for each experiment and diluted to the appropriate concentration with appropriate medium prior to use.

Molecule	Vehicle	Stock Concentration	Supplier
Imatinib	Water	100 mM	Novartis
Dasatinib	DMSO ^(a)	20 mM	Bristol-Myers Squibb
Nilotinib	DMSO	10 mM	Novartis
Ponatinib	DMSO	10 mM	ARIAD Pharma
ABL001	DMSO	10 mM	Novartis
Omacetaxine	DMSO	10 mM	Chemgenex
Chloroquine	Water	100 mM	Sigma-Aldrich
Hydroxychloroquine	PBS ^(b)	100 mM	SigmaAldrich
Rapamycin	Ethanol	2 mM	Sigma-Aldrich
Rad001	DMSO	5 mM	Novartis (MTA)
PP242	DMSO	10 mM	Seleckchem
AZD8055	DMSO	10 mM	Seleckchem
NVP-Bez235	DMSO	1 mM	LC laboratories
VS-5584	DMSO	10 mM	Seleckchem
Gedatolisib	DMSO	1 mM	Seleckchem
XL765	DMSO	10 mM	Seleckchem
Apitolisib	DMSO	10 mM	Seleckchem
BKM120	DMSO	10 mM	Seleckchem
PI-103	DMSO	10 mM	Seleckchem
AZD6244	DMSO	10 mM	Seleckchem
Trametinib	DMSO	10 mM	Seleckchem
Vorinostat	DMSO	10 mM	Seleckchem
Belinostat	DMSO	10 mM	Seleckchem
Sunitinib	DMSO	10 mM	Seleckchem

Table 2-1: Small molecule inhibitors ^(a)dimethyl sulfoxide; DMSO, ^(b)phosphate buffered saline; PBS

2.1.2 Tissue culture materials

BD Biosciences, Oxford, UK

20G needles

Syringes: 1 mL, 5 mL, 10 mL, 20 mL, 50 mL

Biolegend, London, UK

Mouse recombinant IL-3

Corning, Amsterdam, Netherlands

Pipettes: 5 mL, 10 mL and 25 mL

Sterile plastic falcon tubes: 15 mL and 50 mL

Tissue culture flasks: 25 cm², 75 cm², 175 cm² and 225 cm².

Tissue culture plates: 35 mm², 10 cm², 6-well, 12-well, 24-well and 96-well

Chugai Pharma, London, UK

Human recombinant G-CSF

Gilson, Middleton, USA

Yellow and blue pipette tips

Greiner, Bio-One, Gloucestershire, UK

BIJOU BOTTLE 7 mL

Culture dish TC treated 145 mm deep base 20 mm

Cryotubes

EASYstrainer 40 µm mesh

Eppendorf Tubes: 0.5 mL and 1.5 mL

Hendley, Essex, UK

Multi-spot microscope slides

Invitrogen, Paisley, UK

Ampicillin

Blastocidin

Dulbecco's modified eagle medium (DMEM)

Dulbecco's phosphate buffered saline (PBS)

Foetal calf serum (FCS) heat inactivated

Hank's buffered salt solution (HBSS)

Isocove's modified Dulbecco's medium (IMDM)

L-glutamine (200 mM)

Penicillin-Streptomycin (10,000 U/mL)

Puromycin

RPMI 1640

Trypsin-EDTA (0.05%), phenol red

Nalgene Labware, Roskilde, Denmark

Cryo freezing container 'Mr Frosty'

Non-adherent tissue culture flasks: 25 cm² and 75 cm²

Peptotech, London, UK

Human recombinant FLT-3L

Human recombinant granulocyte macrophage-colony stimulating factor (GM-CSF)

Human recombinant IL-3

Human recombinant IL-6

Human recombinant LIF

Human recombinant Macrophage inflammatory protein 1 α (MIP-1 α)

Human recombinant Stem Cell Factor (SCF)

Sartorius, Hannover, Germany

Minisart 0.2 μ M sterile filters

Minisart 0.45 μ M sterile filters

Sigma-Aldrich, Dorset, UK

2-mercaptoethanol (2-ME)
Bovine serum albumin (BSA)
DMSO
Ficoll/Histopaque®-1077
Hydrochloric acid (HCl)
Magnesium chloride (MgCl₂)
Potassium chloride (KCl₂)
Trypan blue
XTT salt

StemCell™ Technologies, Grenoble, France

(DNase) 1 mg/mL
BSA/insulin/transferrin (BIT)
Low density lipoprotein (LDL)
Methocult (human) H4034
Methocult (human) H4230
Methocult (murine) M3434

2.1.3 Molecular biology supplies**Applied Biosystems, Foster City, CA, USA**

GeneAmp® RNA PCR Core Kit

Bioline, London, UK

HyperPAGE prestained protein marker
α-select competent cells (gold and silver efficiency)

Bio-Rad Laboratories Ltd, Sussex, UK

Precision plus protein dual xtra standard ladder
Mini Trans-Blot® Cell

Cambridge bioscience, UK

Endura™ ElectroCompetent Cells (DUOs) Lucigen

Cell Signaling Technology®, New England Biolabs, Hitchin, UK

100 BP DNA ladder

1 kB DNA ladder

Anti-rabbit IgG HRP linked secondary antibody

Rabbit anti-human-p-CrkL antibody

Rabbit anti-human p-ERK1/2 antibody

Rabbit anti-human-LC3b antibody

Rabbit anti-human-p-RPS6 antibody

Rabbit anti-human- β -Tubulin antibody

Quick DNA ligation kit

T4 DNA ligase

T4 Polynucleotide kinase

Chemical Store, University of Glasgow, Glasgow, UK

EtOH

Methanol

Isopropanol

Epitomics-Abcam, Burlingame, CA, USA

ATG7 antibody

GE Healthcare Life Sciences, Buckinghamshire, UK

Hybond-P (14 × 16 cm) PVDF membrane 1 box

IDT, Leuven, Belgium

Oligonucleotides

PCR primers

Invitrogen, Paisley, UK

Agarose

DH5 ALPHA CELLS SUBCLONING EFF/1 mL

Empty Gel Cassettes, mini, 1.0 mm

Empty Gel Cassette Combs, mini, 1.0 mm, 10 well

NuPage® MES sodium dodecyl sulphate (SDS) running buffer (20x)

NuPage® MOPS sodium dodecyl sulphate (SDS) running buffer (20x)

Nupage® Novex® Bis-Tris 4-12% gel

NuPage® transfer buffer (20x)

SYBR®Safe

XCell II™ Blot module

Qiagen, West Sussex, UK

HiSpeed® plasmid maxi kit

QIAamp DNA blood mini kit

QIAquick gel extraction kit

RNeasy mini kit

Sigma-Aldrich, Dorset, UK

4-(2-hydroxyethyl)-1-piperazineethanesulfonic acid (HEPES)

Agar

Ammonium persulfate (APS)

Boric acid

CaCl₂*2H₂O

COMPLETE ULTRA, MINI, EDTA-Free easypack

DTT

EDTA

Glucose

Glycine

PhosSTOP

Potassium chloride

SOC media

Sodium chloride

Sodium phosphate

Sodium dodecyl sulphate (SDS)

Tetramethylethylenediamine (TEMED)

Tris base

TWEEN 20

Thermo Fisher Scientific

Bicinchoninic acid (BCA)TM protein assay kit

CL-XPosure Film, 7 x 9.5 inches (18 x 24 cm)

FastAP Thermosensitive Alkaline Phosphatase (1 U/L)

FastDigest Esp3I (BsmBI)

FILTER PAPER 3MM CHROMATOGRAPHY 46x57cm

PierceTM ECL Western Blotting Substrate

Phusion Flash High Fidelity PCR Master Mix

ProtoGel (30%) 37.5:1 Acrylamide to Bisacrylamide

RIPA Buffer

SuperSignalTM West Femto Maximum Sensitivity Substrate

Thistle Scientific, Glasgow, UK

PCR tubes

2.1.4 FACS

BD Biosciences, Oxford, UK

FACS flow/FACS clean

Mouse Anti-Human-annexin-V-APC antibody

Via-Probe™- 7 aminoactinomycin D (7-AAD)

PerCP-Cy™5.5 Mouse Anti-Human CD45

Sterile capped FACS tubes

Elkay Laboratories, Basingstoke, UK

FACS tubes

Merck Millipore

FlowCelect™ Autophagy LC3 Antibody-based Assay Kit

2.1.5 Immunofluorescence

Carl Zeiss, Jena, Germany

AxioVision software

Sigma-Aldrich, Dorset, UK

Formaldehyde solution (36.5%)

Poly-L-lysine

Vector Laboratories Ltd, Peterborough, UK

VECTASHIELD® mounting medium with 4',6-diamidino-2- phenylindole (DAPI)

2.1.6 Seahorse

Corning, Amsterdam, Netherlands

Cell Tak

Seahorse Bioscience, Copenhagen, Denmark

Seahorse XF96 Flux Analyser

XF96-well plate

XF Assay Medium

XF Cell Mito Stress Test Kit

Sigma-Aldrich, Dorset, UK

Oligomycin

Carbonyl cyanide 4-(trifluoromethoxy)phenylhydrazone (FCCP)

Antimycin A

Rotenone

2.1.7 Animal work

Perkin Elmer, Seer Green, UK

D-Luciferin, Potassium salt

Sigma-Aldrich, Dorset, UK

Citric acid

N-Methyl-2-pyrrolidone

Sodium citrate

Polyethylene glycol (PEG) 300

2.1.8 PCR primer sequences

CRISPR Screen PCR 1 primers:

v2Adaptor_F: AATGGACTATCATATGCTTACCGTAACTTGAAAGTATTTCCG

v2Adaptor_R: TCTACTATTCTTTCCCTGCACTGTtgtggcgatgtgcgctctg

CRISPR Screen PCR 2 primers:

Forward

F01:AATGATACGGCGACCACCGAGATCTACACTCTTTCCCTACACGACGCTCTT
CCGATCTtAAGTAGAGtcttgtggaaggacgaaacaccg

F02:AATGATACGGCGACCACCGAGATCTACACTCTTTCCCTACACGACGCTCTT
CCGATCTatACACGATCtcttgtggaaggacgaaacaccg

F03:AATGATACGGCGACCACCGAGATCTACACTCTTTCCCTACACGACGCTCTT
CCGATCTgatCGCGCGGTtcttgtggaaggacgaaacaccg

F04:AATGATACGGCGACCACCGAGATCTACACTCTTTCCCTACACGACGCTCTT
CCGATCTcgatCATGATCGtcttgtggaaggacgaaacaccg

F05:AATGATACGGCGACCACCGAGATCTACACTCTTTCCCTACACGACGCTCTT
CCGATCTtcgatCGTTACCAtcttgtggaaggacgaaacaccg

F06:AATGATACGGCGACCACCGAGATCTACACTCTTTCCCTACACGACGCTCTT
CCGATCTatcgatTCCTTGGTtcttgtggaaggacgaaacaccg

F07:AATGATACGGCGACCACCGAGATCTACACTCTTTCCCTACACGACGCTCTT
CCGATCTgatcgatAACGCATTtcttgtggaaggacgaaacaccg

F08:AATGATACGGCGACCACCGAGATCTACACTCTTTCCCTACACGACGCTCTT
CCGATCTcgatcgatACAGGTATtcttgtggaaggacgaaacaccg

F09:AATGATACGGCGACCACCGAGATCTACACTCTTTCCCTACACGACGCTCTT
CCGATCTacgatcgatAGGTAAGGtcttgtggaaggacgaaacaccg

F10:AATGATACGGCGACCACCGAGATCTACACTCTTTCCCTACACGACGCTCTT
CCGATCTtAACAATGGtcttgtggaaggacgaaacaccg

F11:AATGATACGGCGACCACCGAGATCTACACTCTTTCCCTACACGACGCTCTT
CCGATCTatACTGTATCtcttgtggaaggacgaaacaccg

F12:AATGATACGGCGACCACCGAGATCTACACTCTTTCCCTACACGACGCTCTT
CCGATCTgatAGGTTCGCAtcttgtggaaggacgaaacaccg

Reverse

R01:CAAGCAGAAGACGGCATAACGAGATAAGTAGAGGTGACTGGAGTTCAGAC
GTGTGCTCTTCCGATCTtTCTACTATTCTTTCCCCTGCACTGT

R02:CAAGCAGAAGACGGCATAACGAGATACACGATCGTGACTGGAGTTCAGAC
GTGTGCTCTTCCGATCTatTCTACTATTCTTTCCCCTGCACTGT

R03:CAAGCAGAAGACGGCATAACGAGATCGCGCGGTGTGACTGGAGTTCAGAC
GTGTGCTCTTCCGATCTgatTCTACTATTCTTTCCCCTGCACTGT

R04:CAAGCAGAAGACGGCATAACGAGATCATGATCGGTGACTGGAGTTCAGAC
GTGTGCTCTTCCGATCTcgatTCTACTATTCTTTCCCCTGCACTGT

R05:CAAGCAGAAGACGGCATAACGAGATCGTTACCAGTGACTGGAGTTCAGAC
GTGTGCTCTTCCGATCTtcatTCTACTATTCTTTCCCCTGCACTGT

R06:CAAGCAGAAGACGGCATAACGAGATTCCTTGGTGTGACTGGAGTTCAGACG
TGTGCTCTTCCGATCTatcgatTCTACTATTCTTTCCCCTGCACTGT

2.1.9 Equipment**Kell-Strom, Wethersfield, USA**

Branson 200 Ultrasonic cleaner

BD Biosciences, San Jose, CA, USA

FACSAria II

FACSCanto

FACSVerse

Gilson, Middleton, USA

Gilson pipetman single channel pipettes

Weber Scientific International, West Sussex, UK

Hawksley Neubauer counting chamber

Carestream Health, Rochester, NY, USA

Kodak X-OMAT 1000

Thermo Fisher Scientific, Loughborough, UK

Bio-Rad Hercules, CA, USA PowerPac300

NanoDrop ND-2000 spectrophotometer

Bio-Rad Laboratories Ltd., UK

Molecular Imager® ChemiDoc™ XRS

Carl Zeiss, Jena, Germany

Fluorescence microscope

Light microscope

2.2 Preparation of medium and solutions**2.2.1 Tissue culture mediums and solutions****RPMI media**

RPMI 1640 440 mL

FCS 50 mL

L-glutamine (200 mM) 5 mL

Penicillin/streptomycin solution (10,000 U/mL-1/10,000 gmL-1) 5 mL

DMEM media

DMEM 440 mL

FCS 50 mL

L-glutamine (200 mM) 5 mL

Penicillin/streptomycin solution (10,000 U/mL-1/10,000 gmL-1) 5 mL

DAMP solution for thawing cryopreserved CD34+ or mononuclear cell (MNC) aliquots from -150°C

DNase I (2 vials at approximately 2500 U/1 mL/vial) 2 mL

Magnesium chloride (400X, 1.0 M stock) 1.25 mL

Trisodium citrate (0.155 M) 53 mL

Human serum albumin (20%, SNBTS) 25 mL

Dulbecco's PBS (magnesium/calcium free) 418.75 mL

Serum free medium (SFM)

BIT (bovine serum albumin, insulin, transferrin) 25 mL

L-glutamine (200 mM) 1.25 mL

Penicillin/streptomycin solution (10,000 U/mL-1/10,000 gmL-1) 1.25 mL

2-mercaptoethanol (50 mM) 250 μ L

Low density lipoprotein (10 mg/mL) 500 μ L

IMDM 97.25 mL

SFM supplemented with high five growth factors (SFM+5GFs)

SFM 10 mL

IL-3 (50 μ g/mL) 4 μ L

IL-6 (50 μ g/mL) 4 μ L

G-CSF (20 μ g/mL) 10 μ L

FLT3L (50 μ g/mL) 20 μ L

SCF (50 μ g/mL) 20 μ L

*Filter through 0.22 μ M filter

SFM supplemented with physiological growth factors (SFM+PGFs)

SFM 10 mL

SCF (0.5 μ g/mL) 4 μ L

G-CSF (2 μ g/mL) 5 μ L

GM-CSF (0.1 μ g/mL) 20 μ L

IL-6 (5 μ g/mL) 2 μ L

LIF (0.1 μ g/mL) 5 μ L

MIP-1 α (0.1 μ g/mL) 20 μ L

*Filter through 0.22 μ M filter

IMDM for the maintenance of mouse c-kit enriched cells

IMDM 440 mL

FCS 50 mL

L-glutamine (200 mM) 5 mL

Penicillin/streptomycin solution (10,000 U/mL-1/10,000 gmL-1) 5 mL

Mouse SCF 50 ng/mL

Mouse IL-6 25 ng/mL

Mouse IL-3 10 ng/mL

1% FBS/ PBS

PBS 99 mL

FBS 1 mL

Freezing media 10% DMSO FBS

DMSO 5 mL

FBS 45 mL

2.2.2 Western blot solutions

Lysis buffer for protein lysates (radio-immunoprecipitation assay; RIPA)

Distilled sterile water (dsH₂O) 7.75 mL

1.5 M NaCl 1 mL

1 M Tris-HCl 0.5 mL

150 mM EDTA 333 µL

NP-40 50 µL

10% (w/v) Sodium deoxycholate 250 µL

*Immediately prior to use, one protease inhibitor tablet added per 10 mL of buffer

2x SDS Sample buffer (Laemmli)

1.5 M Tris-HCl, pH 6.8 10 mL

Glycerol 30 mL

20% (w/v) SDS 6 mL

Bromophenol blue 1.8 mg

2-mercaptoethanol 15 mL

Distilled H₂O to 100 mL

10X TBS buffer

NaCl 8.76 g

Tris 6.05 g

In 800 mL upH₂O

Adjust pH to 7.5 with 1M HCL (9.5 mL)

Adjust to 1 L with Ultra pure H₂O

1x TBS-Tween (TBST) buffer

10x Tris-buffered saline (TBS) buffer 100 mL

TWEEN20 1 mL

dH₂O 899 mL

Homemade gels - 1.5 mm mini gels**10% Resolving gel**

30% Acrylamide 5 mL

upH₂O 4.35 mL

1 M Tris (pH 8.8) 5.6 mL

10% SDS 0.25 mL

10% APS 0.1 mL

TEMED 0.02 mL

15% Resolving gel

30% Acrylamide 10.0 mL

dsH₂O 2.5 mL

1.5 M Tris (pH 8.8) 7.5 mL

10% SDS 0.35 mL

10% APS 0.1 mL

TEMED 0.02 mL

Stacking gel

30% Acrylamide 1.67 mL

dsH₂O 6 mL

1M Tris (pH 6.8) 1.25 mL

10% SDS 0.15 mL

10% APS 0.05 mL

TEMED 0.02 mL

10x Tris-Glycine Buffer

Tris 30.3 g

Glycine 144.1 g

Up H₂O to 1 L

1x Running buffer

10x Tris-Glycine Buffer 100 mL

10% SDS 10 mL

upH₂O 890 mL

1x Transfer buffer

10x Tris-Glycine Buffer 100 mL

Methanol 200 mL

upH₂O 700 mL

5% BSA/TBST blocking buffer

1X TBST buffer 100 mL

BSA 5 g

5% Milk/TBST blocking buffer

1X TBST buffer 100 mL

Marvel 5 g

2.2.3 Flow cytometry

Annexin-V and 7AAD solution per sample

Annexin-V APC 2.5 μ L

7AAD 2.5 μ L

HBSS 45 μ L

2.2.4 Immunofluorescence solutions

3.65% Formaldehyde

36.5% Formaldehyde solution 1 mL

PBS 9 mL

2.2.5 PCR assay solutions

10x Tris/Borate/EDTA (TBE) buffer

Boric acid 55 g

EDTA (0.5 M, pH 8.0) 40 mL

Tris base 108 g

Ultra pure (up)H₂O to 1L

2% Agarose gel

1x TBE 200 mL

Agarose 4 g

* The solution was boiled using a microwave until the agarose powder was completely dissolved. After cooling, 20 μ L of SYBR[®]Safe DNA gel stain was added to the solution and gel was poured into casting trays and allowed to set before use.

2.2.6 Transfection solutions

2x HEPES-buffered saline (HBS)

NaCl 8 g

KCl 0.37 g

Na₂HPO₄ 0.2 g

Glucose 1.0 g

HEPES 5 g

upH₂O to 500 mL

pH to 7.04

*Sterile filter through 0.22 µM filter

2 M CaCl₂

CaCl₂*2H₂O 147 g

upH₂O to 500 mL

Transfection solution/10cm² petri dish

dsH₂O 1280 µL

2X HBS 1.5 mL

2M CaCl₂ (dropwise) 183 µL

psPAX2 plasmid 12.45 µg

pCMV-VSV-G plasmid 4.5 µg

Plasmid for transfection 14.2 µg

2.2.7 Microbiology solutions

LB Broth

LB broth 20 g

upH₂O to 1 L

Autoclave

Ampicillin (100 mg/mL) 1 mL

LB Agar

LB broth 20 g

Agar 15 g

upH₂O to 1 L

Autoclave

Ampicillin (100 mg/mL) 1 mL

30% Glycerol

Glycerol 3 mL

upH₂O to 7 mL

Bacterial glycerol stocks

Bacteria in LB broth 500 µL

30% glycerol 500 µL

2.3 Methods

2.3.1 Cell Culture

2.3.1.1 Culture of cell lines

2.3.1.1.1 Suspension cells

The human CML Blast Crisis cell line KCL22^{WT} was available from our own laboratory. KCL22 cells expressing BCR-ABL^{T315I} were kindly donated by Professor Bruno Calabretta. The murine haemopoietic cell line, BaF3^{Parental}, is an IL-3 dependent pro-B cell line. BaF3^{Parental} transfected with a retroviral construct encoding BCR-ABL^{p210} or BCR-ABL^{p210} with the T315I kinase domain mutation to generate CML cell lines BaF3^{WT} or BaF3^{T315I} respectively, were donated as a kind gift from Professor Junia Melo.

2.3.1.1.2 Imatinib resistant cell lines

KCL22 imatinib-sensitive (KCL22-S), KCL22 imatinib-resistant (KCL22^{Im-Res}), human CML blast crisis cell lines K562-S, K562^{Im-Res}, Lama88-S and Lama88^{Im-Res} were also kindly gifted by Professor Junia Melo.

2.3.1.1.3 Ponatinib resistant cell lines

Ponatinib resistant cell line models were generated in our own lab, using KCL22^{WT} and BaF3^{WT}, which were grown in increasing concentrations of ponatinib, until 100 nM ponatinib resistant, for a prolonged period of time. KCL22^{Pon-Res} generated by Dr. G. V. Helgason and BaF3^{Pon-Res} generated by R. Mitchell.

All suspension cells were cultured in complete RPMI 1640 media in tissue culture flasks. BaF3^{Parental} cells were supplemented with 10 ng/ml recombinant mouse IL-3. The cells were counted and passaged every two days with fresh warm medium, to maintain a density of between 0.1×10^6 - 1×10^6 cells/mL.

2.3.1.1.4 Adherent cells

Human Embryonic Kidney 293 (HEK 293) cells were available from our own lab. HEK293 cells were cultured in complete DMEM media in tissue flasks. The cells were passaged every two days with fresh warm medium, to maintain confluency between 50-80%.

All cell lines were maintained at 37°C with 5% CO₂.

2.3.1.2 Isolating sub clones

Background: KCL22^{Pon-Res} cells are made up of a heterogeneous cell population. In order for us to understand the underlying mechanism of resistance we isolated individual clones.

Method: KCL22^{Pon-Res} cells were counted and 1000 cells were added to 1.5 mL of MethocultTM (H4230), transferred to 35 mm tissue culture plates and incubated for 10 days at 37°C, 5% CO₂. Following this incubation, individual colonies were plucked from the MethocultTM and added to 100 µL of RPMI in a 96 well plate to allow for expansion of the clones.

2.3.1.3 Primary samples

All samples were collected with the approval of the Local Research and Ethics Committee (LREC) and all human participants gave written informed consent.

Research Ethics Committee: West of Scotland REC 4

Research Tissue Bank: Haematological cell research bank

REC reference number: 15/WS/0077

2.3.1.3.1 CML cells

Peripheral blood or bone marrow samples from newly diagnosed untreated patients with CP CML, or patients with CML^{T3151} or TKI-resistant CML were collected and processed by Alan Hair or myself. Purification of the MNC fraction was performed using a method based on density gradients. The samples were diluted in PBS and layered onto Histopaque®-1077. The suspension was centrifuged at 400 x g for 30 min and the layer containing the MNC fraction was isolated and washed in PBS. This technique allows the isolation of MNC only, leaving the plasma, granulocytes and RBC.

2.3.1.3.2 Non-CML samples

Peripheral blood samples were obtained from patients undergoing autologous stem cell collection for either non-Hodgkin's lymphoma or multiple myeloma. Patient stem cells were mobilised with G-CSF following chemotherapy and the excess cells remaining after those required for clinical use were donated for research purposes.

2.3.1.4 Cryopreservation of cells

Primary CML, non-CML and cell lines were centrifuged at 300 x g for 10 minutes and resuspended by gently adding 10% DMSO/FBS dropwise with agitation. The cells were aliquoted into cryotubes and transferred to a cryofreezing container ("Mr Frosty") and kept at -80°C overnight in order to lower the temperature slowly. The next day the cryotubes were transferred to a -150°C liquid nitrogen freezer for long-term storage.

2.3.1.5 Recovery of frozen samples

Primary CML and non-CML cells were removed from liquid nitrogen and immediately thawed at 37°C in a water bath until ice crystals disappeared. The cells were transferred to a 15 mL sterile tube and recovered by adding dropwise 10 mL of pre-warmed at 37°C DAMP thawing solution over 20 minutes. This step was performed at room temperature to enhance the activity of the DNase I, with constant agitation to avoid clumping of the cells. The cells were then centrifuged 250 x g for 10 minutes and the supernatant removed. This was repeated twice more, to remove traces of DMSO. Subsequently, the cells were transferred to appropriate volume of SFM with Physiological Growth Factors (PGF) for CML samples or SFM with a high growth factor (5GF) cocktail for non-CML samples. The cells were seeded in a 25 cm² non-adherent tissue culture flasks at a cell density of 1x10⁶ cells/mL and incubated overnight to allow the cells to recover.

Cell lines were thawed immediately in a 37°C water bath and recovered by slowly adding RPMI with agitation. The cells were centrifuged at 300 x g for 5 minutes and the supernatant was removed. This step was repeated to wash off the DMSO. The cells were then resuspended in RPMI and seeded in a 25cm² tissue culture flask.

2.3.1.6 Primary cell culture

Primary CML mononuclear cells (MNCs) were cultured in SFM comprising Iscove's modified Dulbecco's medium with BIT, 1 mmol/l glutamine, 1 mmol/l streptomycin/penicillin, 40 ng/ml low-density lipoprotein and 0.1 mmol/l 2-mercaptoethanol (all, Invitrogen Ltd, Paisley, UK), further supplemented with a Physiological Growth Factor cocktail (0.2 ng/mL SCF, 1.0 ng/mL G-CSF, 0.2 ng/mL GM-CSF, 1.0 ng/mL IL6, 0.05 ng/mL LIF and 0.2 ng/mL MIP- α ; Stem Cell Technologies, Vancouver, BC, Canada). The cells were seeded in 25 cm² or 75 cm² non-adherent tissue culture flasks at an initial concentration of 1x10⁶ cells/mL and maintained in an incubator at 37°C, 5% CO₂.

Non-CML cells are cultured in SFM supplemented with a high growth factor cocktail (20 ng/mL IL-3, 20 ng/mL IL-6, 20 ng/mL G-CSF, 100 ng/mL Flt3-L, 100 ng/mL SCF).

2.3.2 Cell proliferation assays

2.3.2.1 Trypan blue dye exclusion method

Background: The trypan blue dye exclusion method was used for cell counting and assessment of viability. Non-viable cells have damaged membranes, which are porous and can therefore absorb the trypan blue dye, appearing dark blue under a light microscope. Viable cells with an intact membrane do not absorb the dye. To determine the viable cell counts only the unstained cells were counted and the remaining stained dead cells were deemed non-viable.

Method: Trypan blue dye was first diluted 1:10 with PBS and 50 μ L was added to 50 μ L of cell suspension to give a 1:1 dilution of cells. Approximately 10 μ L of the mixture was transferred to a counting chamber, an improved Neubauer haemocytometer, and the four squares (1, 2, 3 and 4 indicated in figure 2-1) were counted to give a statistically significant count. The number of cells was determined by using the formula shown in figure 2-1.

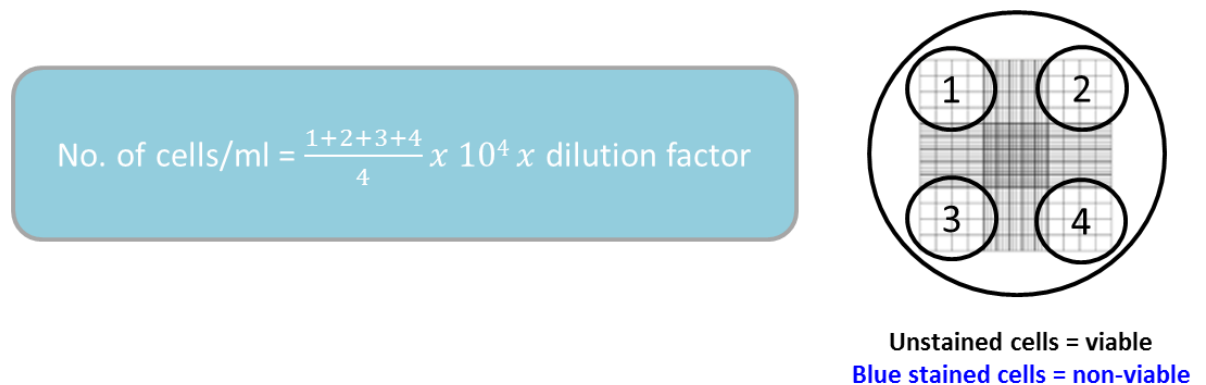


Figure 2-1: Trypan blue method for cell counting and viability assessment with improved Neubauer counting chamber.

2.3.2.2 Automated cell counter using the CASY® Cell Counter and Analyser System

Background: The Casy® cell counter and analyser system was also used to measure cell counts and cell viability. Casy® cell counter utilises electric current exclusion and pulse area analysis to count and analyse the cells in an efficient and precise manner.

2.3.3 Colony Forming Cell (CFC) assay

Background: The CFC assay is an *in vitro* functional assay used to detect and quantify haemopoietic stem and progenitor cells, based on their ability to proliferate and differentiate into different cell lineages to produce colonies in semisolid medium. Each colony is derived from a single progenitor cell and the number of colonies provides a measure of the number of viable and functional progenitors in the cell sample being tested. This assay can be of particular use for monitoring the activity of cells in response to treatment in culture or genetic manipulation. We also use this assay with cell lines, to determine the functionality of a leukaemic cell after drug treatment and whether it still has leukaemic potential.

Method: In order to carry out a CFC assay primary human cells or cell lines were cultured either in SFM with the addition of physiological growth factors or complete RPMI, respectively, with the appropriate drug treatment for 72 hours. After the 72 hour incubation cell counts were performed on all treatment arms. In order to gain a relative insight to the cell response to drug treatment, the number of cells were calculated so they were relative to the untreated arm, 100,000 cells in the case of primary samples and 1,000 cells for cell lines. Duplicate CFC assays were set up for each treatment arm, the appropriate volume of cell suspension was calculated and was added to 1.5 mL of Methocult™ (H4434 for primary human samples, M3434 for mouse cells and H4230 for cell lines). Cell suspensions were then pulse vortexed to allow for homogenous mixing of the cells and left for 10 minutes for the bubbles to dissipate. The mixture was then transferred into 35mm tissue culture plates using a 1 mL syringe. Two 35mm plates plus one 35mm filled with sterile PBS were put inside a 10cm plate, to ensure a humid environment during the long incubation period. The cells were incubated for 10-14 days at 37°C, 5% CO₂. At the end of this time, the total number of viable colonies was counted in each dish and this allowed a comparison of the primitive cells present in the different treatment conditions.

2.3.4 Flow cytometry

Flow cytometry is a laser based technology that can simultaneously measure and analyse multiple physical characteristics of a cell, such as size, using forward-angle light scatter (FSC) and granularity, using side angle light scatter (SSC). It can also determine the phenotype of the cell by staining with antigen specific fluorescent antibodies and measuring the fluorescence intensity. These cellular characteristics are determined by the way in which the cell scatters incident laser light and emits fluorescence. A flow cytometer is made up of three main components: (1) fluidics, which transports the cells in a stream to the laser beam, (2) optics, which is a complex system of lasers that illuminate the particles and optical filters that direct the light signals back to detectors, and (3) electronics, which converts the light signals to the computer for processing. All the flow cytometric analyses herein described were carried out on a Becton Dickinson FACSCanto or FACSVerse and the data was analysed using FlowJo software.

2.3.4.1 Analysis of apoptotic and necrotic cell death

Background: Apoptosis, or programmed cell death, is a normal process that occurs within a tissue to maintain homeostasis. This process is initiated when cells undergo stress that causes damage to the cells, such as cytotoxic drug treatments. One of the earliest features of apoptosis is the loss of asymmetry of the plasma membrane, during this event an important membrane phospholipid component phosphatidylserine (PS) translocates from the inner to the outer plasma membrane. Annexin V is calcium-dependent phospholipid binding protein that has a high affinity for PS and therefore binds to the exposed PS on apoptotic cells. Annexin V can be conjugated to fluorochrome and still retain its integrity and binding affinity to PS, therefore Annexin V is a useful tool to analyse early apoptotic events by fluorescence-activated cell sorting (FACS). As the apoptotic pathway proceeds the plasma membrane becomes porous, this is indicative of late stage apoptosis or necrosis. By staining the cells with a nucleic acid dye, such as 7-Amino-Actinomycin D (7AAD), we can determine whether membrane integrity has been lost, as the dye can enter the cell through the damaged plasma membrane. Therefore, cells that are stained both with Annexin V and 7AAD are said to be in late apoptosis. This assay can distinguish between viable cells, (annexin V- 7AAD-) and cells in early (annexin V+ 7AAD-) or late (annexin V+ 7AAD+) apoptosis.

Method: Apoptosis assay was used to analyse the effect of a drug on CML cells after 72 hours. In cell line experiments, cells were plated at a concentration of 0.25×10^6 /mL and for primary samples MNC were plated at 1×10^6 /mL in multi-well plates. Cells were then

treated, in triplicate, with the appropriate drugs and incubated for 72 hours. After 72 hours, 200 μ L was taken from each well and transferred to FACS tubes, cells were centrifuged at 300 x g for 5 minutes to remove the medium. The cells were resuspended in a solution made up of; 2.5 μ L annexin-V-APC (BD, Cat no. 550475) and 2.5 μ L 7-AAD (BD, Cat no. 559925) in 45 μ L 1x HBSS binding buffer (Thermo Fisher Scientific, Gibco Cat no. 14025100). Cells were incubated for 20 minutes in the dark at room temperature, then washed with 500 μ L 1x HBSS binding buffer and centrifuged at 300 x g for 5 minutes. The buffer was poured off and cells were resuspended in the residual buffer (~100 μ L) and analysed by FACS within an hour, to identify percentages of necrotic and apoptotic cells. The lasers used for analysis of fluorochromes were 633nm Annexin V-APC, 488 nm for 7AAD).

2.3.4.2 Measurement of cell death using DAPI

Background: 4',6-Diamidino-2-Phenylindole, Dihydrochloride (DAPI) is a nucleic acid dye that binds to A-T rich regions of DNA. Like 7AAD, DAPI cannot permeate through an intact plasma membrane of a living cell. Therefore, DAPI can be used to measure viability to discriminate between live cells and membrane damaged cells, i.e. dead cells.

Method: DAPI was used to analyse cell viability in cell lines post lenti-viral transduction or drug treatment. Cell line assays were set up at 0.25×10^6 /mL, 200 μ L of the cell suspension was taken for analysis, at each time point. The cells were transferred to FACS tubes and DAPI was added to the cells 1:100 dilution, making the final DAPI concentration 10 ng/mL. The cells were incubated for 5 minutes and analysed by FACS using laser 405 nm, to identify the percentage of DAPI stained cells, non-viable.

2.3.4.3 Flow cytometry cell sorting

Cells were counted using the CASY® Cell Counter to get an approximate cell number, and then washed with 2%FCS/PBS, centrifuged at 300 x g for 5 minutes. The cells were resuspended in 2%FCS/PBS and filtered through a nylon sterile filter cup. Cells were sorted using a FACS Aria III (BD Biosciences). Very stringent sorting parameters were set up with the help of FACS technician Jennifer Cassels. Cells were sorted back into a FACS tube containing 500 μ L of 2%FCS/PBS. Cell numbers were taken by the FACS Aria III and the cells were put in the appropriate volume of media and put back into culture overnight to recover from stress caused by sorting.

2.3.4.4 FlowCelect™ Autophagy LC3 Antibody-based Assay Kit (Millipore, Cat no. FCCH100171)

Background: As previously described; when autophagy is induced the LC3 protein is translocated from the cytoplasm to the autophagosome, where it is then targeted by the lysosome for degradation.

Autophagy is a hard process to analyse and interpret, however the FlowCelect™ kit allows us to specifically quantify lipidated LC3-II.

The kit selectively permeabilises the cell membrane and flushes out the cytosolic LC3 by a series of washing steps. However, the LC3 that has translocated into the autophagosome is protected and remains intact inside autophagosomes. The intact LC3 is stained with a FITC tagged LC3 antibody and the fluorescence is measured by flow cytometry. An increase in lipidated LC3 would imply an induction of autophagy.

Method: KCL22^{Pon-Res} cells were seeded at 0.25×10^6 /mL in RPMI and incubated at 37°C at 5% CO₂ for 24 hours with the appropriate drug; 100 nM ponatinib, 100 nM NVP-Bez235 or 4 hours with 10 µM HCQ. Each parameter was set up in triplicate. 100,000 cells were harvested per sample and collected into FACS tubes, the cells were centrifuged at 300 x g for 5 minutes and the supernatant was discarded. Wash cells with 1% FBS/PBS. Dilute Autophagy Reagent B at a 1:10 dilution in water and add 100 µL to each sample. Immediately centrifuge samples and discard the supernatant. The samples were then stained with anti-LC3-FITC antibody. The antibody is diluted 1:5 with assay buffer, with a final volume of 50 µL being added to each sample. The samples were incubated with the antibody for 30 minutes at 4°C. Following the incubation, the 150 µL of assay buffer was added to each sample and centrifuged at 300 x g for 5 minutes. The supernatant was discarded and the cells were resuspended in 200 µL of 1% FBS/PBS and analysed via FACS.

2.3.5 Immunofluorescence microscopy

Poly-L-lysine coated multi-spot microscope slides were prepared in advance; poly-L-lysine is adhesive and it facilitates suspension cells binding to glass microscope slides. Poly-L-lysine solution (Sigma-Aldrich, Cat no. P8920) was diluted 1:10 in distilled water, and multisport microscope slides were immersed in the dilution in a Coplin jar for 10 minutes. Excessive poly-L-lysine solution was removed, and the slides were air-dried and kept in a box for future use. 37,500 cells per treatment were added to each well of a poly-L-lysine-coated multi-spot slide. The samples were allowed to adhere to the slide for 90 minutes in a tissue culture incubator. Following the 90 minutes, the excess medium was gently removed by blotting carefully with tissue paper. The cells were fixed by cross-linking protein molecules by adding 30 μ L of 3.65% formaldehyde solution onto each well. The slides were incubated for 15 minutes at room temperature and washed 2x 5 minutes by spotting on PBS to the wells. The slides were then air-dried for 15 minutes and mounted with two drops of VECTASHIELD® mounting medium with DAPI (Vector, Cat no. H-1200) added to the centre of each slide and a coverslip placed on the top. The coverslip was carefully placed over the wells, so that the mounting medium covered each well of the slide and the edges of the cover slip were sealed with nail varnish. The slides were stored at 4°C until analysis. All slides were analysed using a Zeiss Imager M1 microscope at 100x magnification using oil immersion and AxioVision software. Images were captured with multiple layers from the top to the bottom of cells with optimal distance (0.25 μ M) between adjacent layers. Captured images were subjected to deconvolution to remove non-specific fluorescence and sharpen images. Deconvolution was performed by utilising the deconvolution program in the AxioVision software; the iterative algorithm and clip normalisation methods were used.

One row of wells was left free for 100 μ L of media only so the background level of XTT absorbance could be established and subtracted from the final results. The cells were left to incubate for 72 hours at 37°C and 5% CO₂. Following, the 72 hour incubation XTT salt was prepared: 1 mg XTT salt per 1 mL of media. The solution was placed at 37°C for 20 minutes until the salt had dissolved. In the meantime, 1 mg of PMS was dissolved in 715 μ L of PBS. 5 μ L of PMS is added to 1 mL of XTT solution. 25 μ L of the XTT and PMS solution was added to each well and incubated for 2 hours at 37°C. After the 2 hour incubation period, the absorbance of the XTT salt was read via spectrophotometer at a wavelength of 490 nm. A high absorbance indicates cells are un-affected by the drug and able to reduce the formazan dye. A low absorbance means the cells are metabolically inactive and the drug has cytotoxic effects at that concentration.

2.3.7 Repurposing NIH approved oncology drug screen

Background: In collaboration with the Beatson Drug Screening facility, we screened a total of 119 clinically tested drugs from the DTP-Approved Oncology Library (NIH), and 14 selected drugs of interest; dual PI3K/mTOR inhibitor: NVP-Bez235, apitolisib, VS-5584, voxtalisib (XL765) and gedatolisib; PI3K inhibitor: BKM120; mTORC1+2 inhibitor: AZD8055; MEK inhibitor: selumetinib (AZD6244); tyrosine kinase inhibitor: ponatinib; Autophagy inhibitors: hydroxychloroquine sulfate (HCQ), This library was screened initially in KCL22^{WT} and KCL22^{Pon-Res} cells. Prior to commencing screening, an appropriate cell seeding density for each cell line was determined in 96-well plate format, with minimal intra-plate variation. The appropriate cell density was 0.25×10^6 /mL. Internal plate controls were included to allow statistical assessment of screening performance, namely vehicle control (DMSO), a lethality control (omacetaxine (1 μ M)), and a positive control (ponatinib (100 nM)). Cells were counted using a Countess Cell counting System (Invitrogen) and plated at 25000 cpw (+/- 100 nM ponatinib) using an XRD automated reagent dispenser (FluidX). Drugs were diluted in medium and added to cell plates at a final concentration of 10, 1, 0.1 and 0.01 μ M using an automated JANUS system (Perkin Elmer). Drug effects were quantified by cellular metabolic output using resazurin, and scanning plates using an EnVision multiplate reader (Perkin Elmer).

Secondary screen was carried out taking the top hits from the initial screen. These drugs were validated using Ba/F3^{parental}, Ba/F3^{p210} and Ba/F3^{Pon-Res} cells. The same parameters were used as in the initial experiment; however, a drug curve was carried out with a larger

range of concentrations. Final drug concentrations were: 10, 5, 2.5, 1.25, 0.6, 0.3, 0.15, 0.08, 0.04 and 0.02 μM .

Drug toxicity was tested on normal blood cells, non-CML cells; non-CML024, 026 and 027 samples gained from the Holyoake Bio-bank. Cells were thawed using DAMP, and cultured for 3 days in SFM supplemented with high growth factors. Cell density experiment had previously been performed by Dr. D. Vetrie's group, using the same samples. Therefore, a seeding density of $0.5 \times 10^6/\text{mL}$ was used as per their experiment. Drugs tested included; omacetaxine (control), ponatinib (control), NVP-BEZ235, apitolisib, gedatolisib, VS-5584, AZD8055, rapamycin, RAD001, AZD6244 and trametinib. The same parameters were used as in the secondary experiment, with final drug concentrations of 10, 5, 2.5, 1.25, 0.6, 0.3, 0.15, 0.08, 0.04 and 0.02 μM .

2.3.8 Western blotting

Western blotting is a molecular technique used to identify specific proteins from a complex mixture of proteins that have been extracted from cells. This technique uses three steps to accomplish this: (1) gel electrophoresis to separate the proteins by size, (2) transfer of the proteins from the gel to a solid support, in this case a PVDF membrane, and (3) staining of the target protein using a specific primary antibody and a secondary HRP tagged antibody to visualize the expression of the protein of interest.

2.3.8.1 Protein lysate preparation

In order to analyse the proteins of interest, first, the cells need to be lysed. However as soon as the cells are lysed; proteolysis, dephosphorylation and denaturation also initiate. These events can be significantly inhibited by keeping the samples on ice and by adding appropriate protease and phosphatase inhibitors to the lysis buffer.

Ice-cold RIPA lysis buffer (Thermo-Scientific Cat no. 89900) was used for this application with an increased percentage of SDS from 0.1% to 1%, in order to increase the strength of the buffer and therefore enhance its ability to solubilise proteins. Protease and phosphatase inhibitors were added immediately prior to use.

Method: An equal numbers of cells were washed twice with ice cold PBS (300 x g for 5 mins). The cells were then transferred to a 1.5 mL eppendorf and washed again in ice cold PBS. RIPA buffer was added to the cell pellet, using approximately 100 μ L per 1×10^6 cells, homogenised by vigorous pipetting and incubated for 15 minutes on ice. Following the incubation, the cell lysates were centrifuged (21,000 x g for 20 minutes at 4°C) to pellet nucleic acids and cellular debris, leaving the supernatant containing protein. The supernatant was transferred to a new 1.5 ml eppendorf and stored at -20°C.

2.3.8.2 Protein quantification

Bicinchoninic acid (BCATM) protein assay (Thermo-Scientific Cat no. 23227) was used to quantify RIPA-lysed protein sample concentrations according to the manufacturer's instructions. This is a two-step process (1) reduction of Cu^{2+} to Cu^{1+} by protein in an alkaline medium to form a light blue complex. (2) Bicinchoninic acid (BCA) reacts with Cu^{1+} formed in step one. The intense purple colour produced is due to the chelation of two molecules of BCA with one Cu^{1+} ion. The BCA/ Cu^{1+} complex has a strong absorbance at 562 nm and correlates linearly with increasing protein concentrations from 20 to 2000 $\mu\text{g/mL}$.

Method: BSA standards were prepared by serially diluting 2000 µg/mL BSA in dH₂O. BSA concentrations were prepared: 2000, 1000, 400, 200, 100, 80 µg/mL and dH₂O only as a blank. These BSA standards were stored at - 20°C and used multiple times.

To a 96-well plate 10µL of each BSA standard concentration was added to each well in triplicate, and 10 µL of protein samples was added in duplicate. The BCA working solution was prepared according to manufacturer's instructions by thoroughly mixing reagents A and B (50:1). 200µL of this solution was then added to each well of a 96-well plate and incubated at 37°C for 30 minutes. The colorimetric reaction was read by a spectrophotometer at absorbance 562 nm. The protein concentrations were calculated according to the BSA standards and so equal quantities of protein from each lysate could be loaded for analysis by western blotting.

2.3.8.3 Sample preparation for SDS-PAGE

Background: 4X SDS sample buffer. 4x SDS sample buffer contains 4 main ingredients: SDS, 2-mercaptoethanol, glycerol and bromophenol blue.

(1) SDS denatures proteins by binding around their polypeptide backbone in a mass ratio of 1.4:1, giving the protein a negative charge that is proportional to their length. Therefore, during gel electrophoresis separation is not only determined by intrinsic electrical charge but by molecular weight. (2) 2-mercaptoethanol is used as a reducing agent; it reduces disulphide bridges in proteins before they adopt the random-coil configuration so that all the constituent polypeptides can be analysed separately. (3) Glycerol is added to the buffer to increase the weight of the sample so when loading the sample stays at the bottom of the well. (4) Bromophenol blue is a dye that enables the visualisation of the migration of proteins during gel electrophoresis.

An equal quantity of protein (20-30 µg) from each lysate was calculated from the BCATM assay. Protein samples were thawed on ice and the correct volume of lysates transferred into a new 1.5 mL eppendorf. Sample volumes were made up to 50 µL by adding 4x SDS sample buffer (12.5 µL) to each sample and the remaining volume made up with dH₂O.

Prior to loading the protein samples were boiled at 95°C for 10 minutes to denature the sample and briefly centrifuged.

2.3.8.4 SDS-polyacrylamide gel electrophoresis (SDS-PAGE)

Background: SDS-PAGE is a denaturing separation method used for the analysis of protein. When carrying out electrophoresis the samples are loaded into the wells and an electrical current is applied, the negatively charge proteins will travel towards the positive electrode through a gel matrix, which can separate out the proteins according to size. This technique uses two different types of gel: (1) stacking and (2) separating gel, which makes up the composition of the gel 1:2. The proteins first migrate through the stacking gel. This is slightly acidic, pH 6.8, and has a lower acrylamide concentration making it a porous gel, which separates protein poorly but allows them to form thin, sharply defined bands. The lower gel is called the separating, or resolving gel, is basic, pH 8.8, and has a higher polyacrylamide content, which makes the gel's pores narrower. The proteins are therefore separated by their size more so in this gel, as the smaller proteins can travel more easily, and hence rapidly, than larger proteins.

Method: SDS-PAGE method was used for the separation of proteins based on their size. Denatured protein samples were loaded into homemade 10% or 15% gels or into Nupage® Novex® Bis-Tris 4-12% (Invitrogen, Cat no. NP0321BOX) gradient gels. Alongside a pre-stained protein standard ladder (Bio-Rad Cat no. 1610377 or Bioline, Cat no. BIO33066) to determine the molecular weight of the proteins within the samples. Gels were run in 1X NuPAGE® MOPS or MES SDS running buffer for the precast gels, or homemade 1X running buffer for the homemade gels, at 80V for the first 30mins and at 120V for the remaining time, in an Invitrogen XCell SureLock™ mini-cell electrophoresis system.

2.3.8.5 Transfer to PVDF membrane

Following gel electrophoresis, proteins were transferred from the gel to a solid support, a PVDF membrane. The PVDF membrane was activated by soaking into methanol for 2 minutes and then equilibrated in 1x transfer buffer for 15 minutes. The sponges, Whatman paper and the gel were also soaked in transfer buffer before use. Methanol is added to the transfer buffer, to maintain the stability of the gel, and also to remove SDS from proteins and increase protein binding to the membrane. The transfer sandwich was assembled inside the gel cassette. The transfer sandwich was built upon the cathode side (black); 1 soaked foam pad, 3 soaked Whatman papers, the equilibrated gel, the equilibrated PVDF membrane, 3 soaked Whatman papers and 1 soaked foam pad. A blot roller removed any trapped air between the layers, then the cassette was closed and locked. The cassette was

inserted into the blotting module, along with an ice pack and the tank was filled with 1x transfer buffer. A magnetic stirrer was added to the tank and the tank was placed on top of a magnetic stir plate. Proteins were transferred at 120V for 2 hours in a Mini Trans-Blot[®] Cell module at 4°C.

2.3.8.6 Immunolabelling

Once the transfer was completed the membrane was blocked in either 5% Marvel/ 1xTBST or for the analysis of phospho-antibodies 5% BSA/1xTBST blocking buffer. This was performed at room temperature for 1 hour with constant agitation. Blocking is an important step as it prevents nonspecific binding of antibodies to unoccupied protein-binding sites on the membrane. After blocking, the membrane was incubated with a primary antibody solution diluted in the blocking buffer (e.g. p-CrkL, p-RPS6, p-ERK1/2, LC3B, ATG7, β -Tubulin; 1:500-1000 dilution) overnight at 4°C with gentle rotation. The next day, the membrane was incubated in primary antibody for an hour at room temperature with gentle rotation. The membrane was then washed in the 1X TBST buffer for 3x 15 minutes to get rid of unbound primary antibody and reduce background. After washing, the membrane was incubated with the appropriate HRP-conjugated secondary antibody solution (rabbit or mouse) using a 1:5000 dilution in 1% blocking solution for 1 hour at room temperature with agitation. Following secondary antibody incubation, the membrane was washed in the 1xTBST buffer 3x 15 minutes to remove unbound secondary antibody.

Finally, the Pierce[™] ECL Western Blotting Substrate (Thermo Scientific, Cat no. 32106) was used according to the manufacturer's instructions for development of the membrane. This involved the membrane being incubated with the mixture of equal amounts of an enhanced luminol solution and a peroxide solution for 2 minutes. In the presence of HRP, from the secondary antibody, and the peroxide buffer, luminol oxidises and forms an excited state, that emits light as it decays to a ground state. When oxidised luminol returns back to its initial state, light is emitted. The chemiluminescent signal was captured by using light sensitive photographic film, CL-Xposure[™] Film (Thermo Scientific, Cat no. 34097) and developed using a Kodak X-OMAT.

In order to incubate the PVDF membrane with a different primary antibody, such as against a housekeeping protein β -Tubulin, the membrane was reactivated in methanol for 2 minutes then thoroughly washed in 1x TBST for 3x 15 minutes. The membrane was re-blocked in blocking buffer for 1 hour before incubation with another primary antibody.

2.3.9 DNA sequencing

Genomic DNA (gDNA) was extracted from BaF3^{Pon-Res} cells using a QIAamp DNA mini kit (Qiagen, Cat no. 51304). PCR was performed using primers designed to cover the BCR-ABL splice junction, including the ABL kinase domain, in order to detect any common mutations which may cause TKI resistance. These primers were designed by Dr. Arunima Mukhopadhyay.

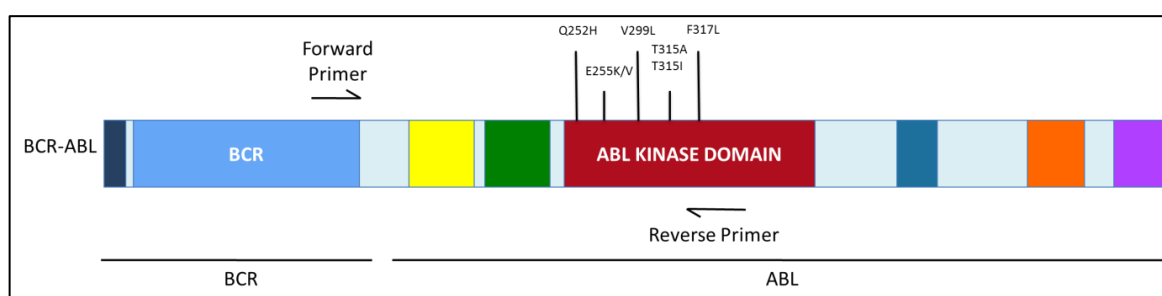


Figure 2-3: BCR-ABL transcript.

BCR-ABL indicating known mutations in the kinase domain, which affect TKI binding. It also indicates the regions of BCR-ABL that the forward and reverse primers span, allowing the sequencing of the kinase domain.

T315I Primer sequence F	T315I Primer sequence R
G TTCCTGATCTCCTCTGACTATGAGCGTG	G CATGGGCTGTGTAGGTGTCC

Table 2-2: Forward and reverse BCR-ABL primer sequences.

For each PCR reaction the following mix was made using the GeneAmp® RNA PCR Core Kit (Applied Biosystems, Cat no. N8080143):

Reagent	Volume (µL)
10x Buffer	5
dNTPs (10 mM)	10
Taq polymerase	2.5
F Primer (10 µM)	2.5
R Primer (10 µM)	2.5
MgCl ₂ (25 mM)	5
DNA template	1 µg
Nuclease free H ₂ O	Up to 50 µL

Table 2-3: PCR reaction mix.

2.3.9.1 Cycling parameters

The PCR tubes were heated to 95°C for 5 minutes to denature the double stranded DNA, and then 35 cycles of 95°C for 30 seconds, 52°C for 1 minute and 72°C for 1 minute were set in a PCR Thermo Cycler. After all cycles finished, the tubes were heated to 72°C for 5 minutes for final extension, and then held at 4°C.

2.3.9.2 Gel electrophoresis

The PCR products were run on an agarose gel in order to visualise the DNA bands. A 1% agarose gel was prepared by diluting 1 g of agarose powder in 100 mL of 1x TBE buffer (10x TBE buffer - diluted in dH₂O). The mixture was heated in a conical flask in a microwave for 2 minutes until the agarose powder had completely dissolved. When the gel cooled down, 2 µL of ethidium bromide (10 mg/mL) was added and mixed well. The gel was poured into a casting tray with a comb inserted to create wells and the gel was left to set. The gel was placed in a gel tank and filled with 1x TBE buffer so as to cover completely the gel and the comb was removed. 10µL of PCR product mixed with 2µL loading dye (6x) was loaded into each well of the gel, 5 µL of 100 bp DNA ladder was loaded in a separate lane, and then the gel was run at 100V for 1 hour. After running, the gel was viewed by an ultraviolet (UV) transilluminator (ChemiDoc).

DNA sequencing was performed by DNA Sequencing & Services (MRC I PPU, College of Life Sciences, University of Dundee, Scotland, www.dnaseq.co.uk) using Applied Biosystems Big-Dye Ver 3.1 chemistry on an Applied Biosystems model 3730 automated capillary DNA sequencer.

2.3.10 RNA-seq

RNA-Seq allows for the detection of transcript isoforms, gene fusions, single nucleotide variants, allele-specific gene expression in one single assay.

2.3.10.1 Cell lines

KCL22^{WT} or KCL22^{Pon-Res} cells were seeded at 0.25×10^6 /mL in RPMI and untreated, treated with 100 nM ponatinib, 100 nM NVP-Bez235 or a combination of ponatinib and NVP-Bez235 for 24 hours at 37°C at 5% CO₂. 1×10^6 cells were harvested from each sample and RNA was extracted using an RNeasy Mini kit (Qiagen, Cat no. 74104) as per the manufacturer's instructions. The RNA quantification was analysed by a nanodrop, ND-2000.

2.3.10.2 CML samples

MNCs were seeded at 1×10^6 /mL in SFM supplemented physiological growth factors. The cells were either untreated or treated with 100 nM ponatinib for 24 hours at 37°C at 5% CO₂. 2×10^6 cells were harvested from each sample and RNA was extracted using an RNeasy Mini kit (Qiagen, Cat no. 74104) as per the manufacturer's instructions. The RNA quantification was analysed by a nanodrop, ND-2000.

Quantification of RNA by the qubit revealed DNA contamination; therefore, samples underwent DNase treatment using the DNase Set - RNase free kit (Qiagen, Cat no. 79254) as per the manufacturer's instructions. Once again the RNA quantification was analysed by a nanodrop, ND-2000.

The samples were sent to Glasgow Polyomics who performed the RNA-seq experiment. Glasgow Polyomics prepared the RNA using polyA selection to enrich for mRNA. Subsequently, they prepared libraries by converting the mRNA to double-stranded complementary DNA (cDNA) and adding on the Illumina "adaptor" sequences. The samples were sequenced using an Illumina NextSeq™500. The samples were sequenced using paired end reads, with a read length of 75 and a read depth of 30 million. The sequencing data was analysed by Dr. Graham Hamilton and Dr. Lisa Hopcroft. In order to analyse the data first the sequences were demultiplexed, filtered, and trimmed. The reads were then assembled into transcripts and aligned to reference sequences. The transcripts were then annotated and the number of reads per transcript was quantified and a statistical comparison of transcript abundance across samples and treatment arms was performed.

2.3.11 shRNA constructs

pLKO.1-shATG7-GFP and pLKO.1-shATG7-PURO vectors carrying hairpins targeting *ATG7* were used along with the packaging vectors; psPAX2 and pCMV-VSV-G (see Appendix 9.1 for plasmid maps). Vectors pLKO.1-shSCR-GFP and pLKO.1-shSCR-PURO carried scrambled - non-targeting- hairpins and were used as control. The plasmid pCMV-VSV-G was kindly donated by Professor John Rossi. pLKO.1-PURO-shATG7 was donated by Professor Kevin Ryan. Plasmids pLKO.1-GFP-shCtrl and psPAX2 were donated by Dr Kamil Kranc. The pLKO.1-shATG7-GFP plasmid was generated in our lab by Dr. Maria Karvela.

2.3.12 Lentivirus transfection

Lentivirus was produced by transfecting HEK293 cells using the CaCl₂ method.

1x10⁶ HEK293 cells were plated in a 10 cm² cell culture dish in 10 mL DMEM three days prior to the transfection to allow the cells to adhere to the plate. After three days 70% confluency should have been achieved and the cell media was replaced by adding 9ml of DMEM plus 30 µM of chloroquine, which inhibits DNA degradation by lysosomes by raising their pH.

Lentiviral DNA mixes were made by adding 14.2 µg of the lentiviral vector, 12.45 µg psPAX2, and 4.5 µg pCMV-VSV-G into a 1.5 mL eppendorf. This was added to a 15 mL falcon tube along with 1280 µL of sterile water and 183 µL 2M CaCl₂. This mix was then added to 1.5 mL of 2xHBSS and mixed very thoroughly. The transfection mixes were incubated at 37°C for 20 minutes and then added dropwise to the HEK293 cells. Each mix made was for one 10cm² cell culture dish. After 8 hours the medium was replaced with 8 mL of DMEM, to wash off the CaCl₂ precipitate. The following morning the medium was changed again and 6 mL of DMEM was added to the cells. For GFP tagged plasmids, cells were checked under an inverted fluorescent microscope for the presence of green cells. Virus was harvested at 24 and 48 hours by collecting media, centrifuging at 300 x g for 5 minutes and filter sterilising the supernatant using a 0.45 µM filter before being used to directly transfect KCL22 cell lines.

2.3.13 Transduction of CML cell lines

After 24 hours of incubation, the viral DMEM medium was collected from the HEK293 cells and used for the transduction of KCL22 CML cell lines. 6 mL of fresh medium was placed on the HEK293 cells for harvesting at a 48 hour time point.

The 6 mL of viral medium was filter sterilised and KCL22 cells were resuspended in the virus at a cell concentration of 0.25×10^6 /mL and incubated for 24 hours. Following the incubation, the viral medium was removed and replaced with the 48 hour viral medium and incubated for a further 24 hours. Following these two rounds of infection the cells were centrifuged at $300 \times g$ for 5 minutes to remove the viral medium and the cells were resuspended in 6 mL of RPMI. Cells transduced with puromycin resistant selection marker would be immediately treated with $2.5 \mu\text{g}/\text{mL}$ puromycin for 72 hours then $5 \mu\text{g}/\text{mL}$ for a further 11 days before cells were used experimentally. Cells were continually grown in the presence of puromycin. Cells transduced with plasmid constructs tagged with GFP would be analysed under an inverted fluorescent microscope for the presence of green fluorescent cells.

2.3.14 CRISPR guide design

Background: See results chapter 4.

Specific oligonucleotides were designed for ATG7, BCR-ABL, mTOR and MEK CRISPR KO. First, the human gene transcripts were identified using Ensembl genome database. The transcripts chosen were verified from more than one reference database (Ensembl and Havana, yellow labelled merged genes in Ensembl database). Ref-seq was then used to gain the coding sequence of the gene (CDS). In order to create Indels that will cause a frameshift mutation that will ablate gene function it is important to generate CRISPR guides that target coding sequence early in the gene transcript. Therefore, sequences were taken from exons from the start of the coding sequence. 23-1000bp of the DNA sequence of interest were entered into the CRISPR Design Tool, designed by the Zhang laboratory at MIT <http://crispr.mit.edu/>.

This tool identifies 20 nucleotide DNA sequences followed by a Cas9 target site (PAM site 5' NGG) within the input sequence (Cong et al., 2013). The results provide the user with a rank ordered list of target sequences based on their predicted likelihood of off-target genome modifications. The algorithm used by the program is based on [Hsu et al., Nature Biotechnology 2013](#).

The 20 nucleotide guide sequences were chosen based on the quality score given by the design tool (Hsu et al., 2013). Sequences that scored $>90\%$ were chosen and their reverse

complimentary strands were established. These sequences were verified using NCBI/Nucleotide-Blast (Blastn). In order for those sequences to be cloned into the lenti-CRISPRv2 (Addgene, Cat no. 52961) or the lenti-Guide-puro (Addgene, Cat no. 52963) vectors, the two oligonucleotides must be synthesized with the addition of overhangs compatible with BsmBI digestion. Also if the target sequence did not start with guanidine (G), a G nucleotide is added 5' to make the sequence a 20+1 guide RNA. Guanidine will improve U₆-mediated transcription and will not affect the function of the gRNA. The PAM site is not included in the synthesis of the oligos. Therefore, oligos were designed using the following format:

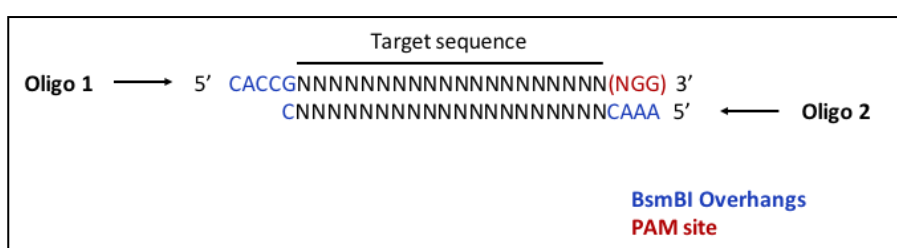


Figure 2-4: Design template for targeted guide sequences for CRISPR KO.

A 20 nucleotide target sequence, with 5' overhangs added for cloning using BsmBI restriction sites. The PAM site has been indicated but is not included in the design of the guide.

Name	Sequence	Exon	Quality score	Off target sites
CrispR ATG7 1-1	CACCGGAAGCTGAACGAGTATCGGC	2	95	33 (8 are in genes)
CrispR ATG7 1-2	AAACGCCGATACTCGTTCAGCTTCC			
CrispR ATG7 2-1	CACCGTGCCCTTTTAGTAGTGCCT	2	80	130 (9 are in genes)
CrispR ATG7 2-2	AAACAGGCACTACTAAAAGGGGCAC			
CrispR ATG7 3-1	CACCGAACTCCAATGTTAAGCGAGC	3	91	51 (8 are in genes)
CrispR ATG7 3-2	AAACGCTCGCTTAACATTGGAGTTC			
CrispR mTOR 1-1	CACCGTGGCCTAAAGAGCCGGAATG	2	90	104 (12 are in genes)
CrispR mTOR 1-2	AAACCATTCCGGCTCTTTAGGCCAC			
CrispR mTOR 2-1	CACCGCACTTTTACCGCTGAGTACG	4	92	40 (5 are in genes)
CrispR mTOR 2-2	AAACCGTACTCAGCGGTAAAAGTGC			
CrispR mTOR 3-1	CACCGGGTGGGAATGCCACCCGAAT	4	90	73 (7 are in genes)
CrispR mTOR 3-2	AAACATTCGGGTGGCATTCCCACCC			
CrispR MEK 1-1	CACCGCGTAACTGCAGAGCCGTCG	1	96	27 (5 are in genes)
CrispR MEK 1-2	AAACCGACGGCTCTGCAGTTAACGC			
CrispR MEK 2-1	CACCGTGGAGATCAAACCCGCAATC	3	93	61 (6 are in genes)
CrispR MEK 2-2	AAACGATTGCGGGTTTGATCTCCAC			
CrispR MEK 3-1	CACCGACATCCTAGTCAACTCCCGT	6	91	46 (2 are in

CrispR MEK 3-2	AAACACGGGAGTTGACTAGGATGTC			genes)
CrispR BCR- ABL 1-1	CACCGACGTGTAACCTTGCCGTTG	bcr- abl1	90	40 (5 are in genes)
CrispR BCR- ABL 1-2	AAACCAACGGCAAGAGTTACACGTC	e13a2		
CrispR BCR- ABL 2-1	CACCGGTCTGAGTGAAGCCGCTCGT	bcr- abl1	96	54 (17 are in genes)
CrispR BCR- ABL 2-2	AAACACGAGCGGCTTCACTCAGACC	e13a2		
CrispR BCR- ABL 3-1	CACCGATCATTCAACGGTGGCCGAC	bcr- abl1	93	31 (5 are in genes)
CrispR BCR- ABL 3-2	AAACGTCGGCCACCGTTGAATGATC	e13a2		

Table 2-4: CRISPR single guide sequences for ATG7, mTOR, MEK and BCR-ABL.

Both vectors have the same BsmBI digestion sites for cloning and therefore the same oligos can be used for cloning into lentiCRISPRv2 and lentiGuide-Puro vectors.

Standard desalted oligonucleotides were ordered for synthesis from IDT. On arrival the DNA was resuspended in sterile water at a concentration of 100 μ M.

2.3.15 Target Guide Sequence Cloning Protocol

In order to clone the guide sequences into the CRISPR lentiviral vectors the ‘targeted guide sequence cloning protocol’ was used from the Zhang lab. This protocol gives a detailed method of Lentiviral vector digestion, oligo annealing and cloning into digested vector. One amendment was made to the protocol; Step 1: vector digestion at 37°C overnight instead of for 30 minutes as stated.

5 µg of lentiCRISPRv2 or lentiGuide-puro were digested and dephosphorylated, using FastDigest *BsmBI*, FastAP, 10xFastDigest Buffer, freshly prepared 100 mM DTT and made up to 60 µL with H₂O. This reaction was incubated at 37°C overnight, in order to ensure cuts were made at the *BsmBI* digestion sites and to dephosphorylate its overhanging complementary ends and inhibit annealing between them. This reaction made two cuts, either side of an 1880bp filler sequence of the vectors, leaving this site available for the target sequences. The digestion products were then separated on a 1% agarose gel. The fragments of interest, lentiCRISPRv2 (12993 bp) and lentiGuide-puro (8297 bp) backbone fragments, were isolated under long-wave UV light using a clean scalpel. The products were gel-purified by using the QIAquick Gel Extraction Kit (Qiagen, Cat no. 28704) according to manufacturer’s instructions. The concentration and quality of extracted DNA were measured with a NanoDrop ND-2000 spectrophotometer.

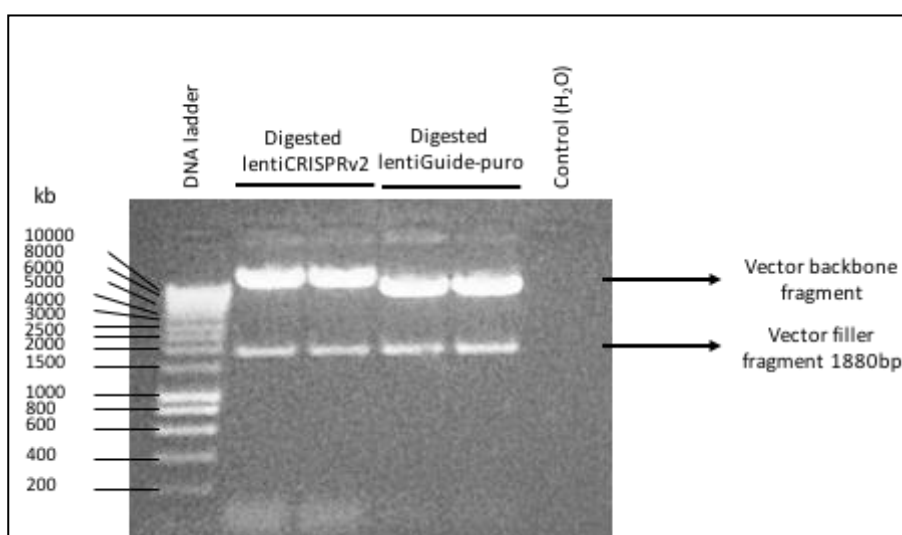


Figure 2-5: Gel purification of *BsmBI* digested lentiCRISPRv2 and lentiGuide-puro.

At the same time each pair of oligonucleotides for the target sequence were annealed and phosphorylated. This was performed by setting up a reaction containing; 100 μ M oligo 1 (sense) and 100 μ M oligo 2 (antisense), 10x ligation buffer (NEB), T4 Polynucleotide Kinase and ddH₂O. (10x Ligation buffer from NEB was used as it contains ATP required for the phosphorylation reaction). The reaction was put in a thermocycler under the following parameters: 37°C for 30 minutes, up to 95°C for 5 minutes and then down 5°C every 60 seconds until reaching 25°C. Following the thermocycler, the annealed oligos were diluted 1:200 in sterile water.

The ligation reaction performed by mixing; 50 ng of the BsmBI digested plasmid, 1 μ L of the diluted oligo duplex, 2x Quick ligase buffer (NEB), ddH₂O to make it up to 10 μ L and 1 μ L of quick ligase (NEB M2200S). The ligation reaction was incubated at room temperature for 10 minutes. A negative control was also performed.

After the incubation period the ligation was transformed into Subcloning Efficiency™ DH5 α ™ Competent Cells (Thermo Fisher Scientific Cat no. 18265017), following manufacturer's instructions. 5 μ L of the ligation reaction was carefully mixed with 50 μ L of bacteria and incubated on ice for 30 minutes. A positive control was also performed by adding 50 ng of undigested plasmid vector to the bacteria for transformation. The bacteria and DNA were heat shocked at 42°C for 20 seconds, then immediately placed on ice for 2 minutes. 950 μ L of pre-warmed S.O.C. media (Sigma, Cat no. S1797) was added to the tube and incubated at 37°C for 1 hour at 225 rpm. 200 μ L from each transformation, including the negative controls, was spread out on pre-warmed LB agar plates containing 100 μ g/mL ampicillin. The plates were incubated overnight at 37°C. After incubation, the plates were checked for bacterial growth, the positive control, which had intact plasmid DNA had high transformation efficiency with many bacterial colonies grown. The negative control contained digested plasmid DNA and the addition of ddH₂O, the DNA is therefore not intact and the bacteria cannot grow as they do not have the ampicillin resistant gene, which comes from the plasmid. The bacteria transformed with the lentiCRISPRv2 backbone fragment and the ATG7 oligos had a low number of colonies, indicating low transformation efficiency. However, 3 single colonies were randomly selected and incubated in 5 mL of LB broth for 4 hours at 37°C with constant agitation; the cultures were then transferred into 250 mL of LB broth and cultured overnight at 37°C with constant agitation.

The plasmid DNA was collected from the bacterial cells 24 hours later by using the Maxi Prep Kit (Qiagen, Cat no. 12163) as described by the manufacturer's instructions or by the Beatson services. 2mL of each culture were stored as bacterial glycerol stock (30% glycerol/ sterile H₂O).

2.3.16 Animal work

2.3.16.1 Ethical issues

All animal work was carried out in accordance with regulations set by the Animals Scientific Procedures Act 1986 and UK Home Office regulations. Animals were housed at the Beatson Institute for Cancer Research or at the Veterinary Research Facility at the University of Glasgow. All experiments were carried out under my personal licence (60/12683) and Dr Alison Michie's project licence (60/4076). Tumour initiating CML cell transplants were carried out on animals between 8 and 12 weeks. The details of the numbers of animals used and gender for each experiment is provided in each figure legend.

2.3.16.2 Mouse models

NOD.Cg-Prkdc^{scid}Il2rg^{tm1Wjl}/SzJ or more commonly known as the NOD scid gamma (NSG).

Background: This animal model combines the characteristics of the NOD/ShiLtJ background (deficiencies in innate immunity), severe combined immune deficiency mutation, scid, and an IL2 receptor gamma chain deficiency, which disables cytokine signalling. As a result, these mice lack mature T cells, B cells, functional NK cells, and are also deficient in cytokine signalling, making these mice very good transplant models.

2.3.16.3 Bioluminescent *in vivo* imaging of tumour initiating CML cells

KCL22 cells were labelled with lentiviral firefly luciferase, by G. V. Helgason, and selected based on antibiotic resistance, hygromycin. The cells were cultured in RPMI at a cell concentration of 0.25×10^6 /mL. Cells were untreated or treated with 100 nM ponatinib, 10 μ M HCQ, 100 nM NVP-Bez235 or the combination of 10 μ M HCQ and 100 nM NVP-Bez235. Cells were cultured for 72 hours. In a previous cell titration study performed by Dr. L. Mukherjee, 1×10^6 cells per mouse was the lowest number of cells to transplant to maintain efficacy. Cells were counted and based on the combination treatment; the volume of cell suspension required for 1×10^6 cells per mouse was harvested. Therefore, different number of cells will be transplanted per mouse depending on the drug cytotoxicity. Cells were centrifuged at 300 x g for 5 minutes and washed in PBS/ 0.5% FBS and centrifuged a second time at 300 x g for 5 minutes. Each cell sample was resuspended in 200 μ L of PBS/ 0.5% FBS and filtered through a 30 μ M filter cup, before being transplanted via tail vein into an 8-12 week old female NSG mouse. In order to activate the bioluminescent reaction, the chemical substrate D-Luciferin (Perkin Elmer, Cat no. 122799) must be injected into

the mice. The luciferin oxidises under catalytic effects of the firefly luciferase and ATP and emits light, which is captured by the IVIS spectral range between 550 nm and 620 nm. D-Luciferin was dissolved in PBS and injected subcutaneously at a dose of 3 mg per mouse 5 minutes before measuring the light emission. 30 minutes after the transplantation of the cells the mice were injected subcutaneously with D-luciferin and analysed by luciferase bioimaging via an IVIS Spectrum *In Vivo* Imaging System (PerkinElmer, Cat no. 124262), to measure the efficiency of transplantation. The engraftment of these cells was subsequently measured weekly, until tumour burden reached the threshold and the animals were sacrificed using appropriate schedule 1 methods.

2.3.16.4 *In vivo* drug treatment experiments

NSG mice were transplanted with 1×10^6 KCL22^{Pon-Res} cells per mouse, the cells were transplanted via tail vein into 8–12-week-old female NSG mice. The mice were monitored as previously described in 2.3.16.3. After 1 week, the mice were treated with vehicle control (citrate buffer or NMP/PEG300 (1:10)), ponatinib (5 mg/kg, oral gavage once daily), HCQ (60mg/kg, intraperitoneally once daily), NVP-Bez235 (40mg/kg, oral gavage once daily) or the combination of NVP-Bez235 and HCQ for 4-5 weeks. 5 mice were assigned per drug arm per experiment. Results presented represent data from both experiments.

2.3.16.5 Drug formulation

40mg/kg NVP-Bez235 (LC Labs, Cat no. N-4288)

10ml/kg = 54.67mg/kg BEZ235 salt

For 7 days of treatment a stock solution of 54.67 mg/mL of N-Methyl-2-pyrrolidone (NMP) was prepared.

Using a small glass beaker, 109.4 mg of NVP-BEZ235 was dissolved in 2 ml NMP by heating the solution in a water bath 80°C for 20 minutes followed by sonication. The solution was made into 0.25mL aliquots and frozen at -20°C. For each day of treatment, one aliquot was defrosted and resuspended in 2.25 mL of Polyethylene glycol 300 (PEG 300). Each mouse was treated 10 mL/kg, each mouse weighs on average 20g therefore each mouse will be treated with ~ 200 µL via oral gavage.

60 mg/kg HCQ (Sigma, Cat no. 1327000)

200 mg vial was dissolved in 40 mL of PBS making a stock solution of 5 mg /mL. Each mouse weighs on average 20g, therefore each mouse will be treated with ~ 240 μ L of HCQ intraperitoneally.

2.3.16.6 Dissection

Animals were sacrificed using appropriate schedule 1 methods. Femur, tibia, hip bones, spleen and tumours were dissected and stored in PBS/2%FBS on ice. Peripheral blood was taken from femoral vein post sacrifice and collected into tubes containing EDTA to ensure anti-coagulation, stored at RT and analysed within several hours.

2.3.16.7 Cell extraction

Bones from femur, tibia and hips were crushed in PBS/2% FBS using a mortar and pestle and made into a single cells suspension through filtering through a sterile 0.2 μ m filter. Spleen and tumours were homogenised in PBS/2% FCS using a sterile plunger and filtered. Peripheral blood (PB) was analysed neat for cellularity analyses.

2.3.16.8 Analysis

Cell suspensions from each tissue were spun and resuspended in appropriate antibodies and analysed by flow cytometry. Tumour and spleen sizes were measure and photographed.

3 Results (I): Identification and validation of suitable TKI-resistant models for the study of BCR-ABL-independent TKI-resistance

Although the discovery of TKIs has significantly improved the life expectancy of CML patients, its success has been marred by the development of drug intolerance, CML stem cell insensitivity to TKIs (Graham et al., 2002, Jørgensen et al., 2007a, Copland et al., 2006b, Corbin et al., 2011, Hamilton et al., 2012) and drug resistance (Karvela et al., 2012). Drug resistance affects a significant subset of CML patients and although the most common cause of drug resistance is due to mutations within the *ABL* kinase domain, which inhibit TKI binding (Druker et al., 1996), this is being combatted by the development of more potent TKIs (Corbin et al., 2002, Lombardo et al., 2004, Brümmendorf et al., 2015, O'Hare et al., 2009). However, there is a patient population, which have an acquired TKI resistance, which is not due to a kinase domain mutation and yet are resistant to all current TKI treatments. These patients are said to have a BCR-ABL-independent mechanism of resistance. Evidence shows that BCR-ABL-independent TKI resistance may stem from the activation of a secondary oncogenic mechanism (Thomas et al., 2004, Mahon et al., 2003, Mahon et al., 2008). These patients are of major clinical concern as a number of mechanisms have been proposed, yet not one common mechanism has been discovered, which leaves these patients with very limited treatment options. Therefore, increased effort is being made to investigate these alternative mechanisms of resistance. Recent studies by our laboratory suggest that classic imatinib-resistant cell line models are not ideal to investigate acquired resistance to all available TKIs (including ponatinib). Therefore, in this chapter we describe the development of ponatinib-resistant cell lines with acquired BCR-ABL-independent resistance and attempt to characterise the mechanism of resistance using different screening methods. With the hope that the information gained from these experiments will guide us towards the identification of a common weakness in primary TKI-resistant CML cells. By doing so we propose the PI3K-AKT-mTOR pathway as a key player responsible for TKI resistance and that pharmacological inhibition of this pathway in combination with the inhibition of survival mechanism, autophagy, may represent a potential new treatment for TKI-resistant CML patients.

3.1 Aims and objectives

- I. Generate a suitable ponatinib-resistant model for the study of BCR-ABL-independent TKI-resistance
- II. Characterise the mechanism causing TKI-resistance in the ponatinib-resistant cell models

3.2 An assessment of current imatinib-resistant cell line models and their relevance for the study of BCR-ABL-independent TKI-resistance

Classically, imatinib is used to generate TKI-resistant cell lines and several CML imatinib-resistant cell lines have been generated and published such as K562^{Im-Res}, KCL22^{Im-Res} and LAMA84^{Im-Res} (kindly donated by Bruno Calabretta and Junia Melo). These imatinib-resistant models have had their mechanisms of resistance previously characterised. K562^{Im-Res} is a BCR-ABL-independent cell line established by Donato and colleagues (Donato et al., 2003), which they established that the over-expression and activation of the SRC-related kinase, LYN was causing imatinib resistance. LAMA84^{Im-Res} established by Mahon and colleagues (Mahon et al., 2000a) showed that these cells developed two mechanisms which may owe to imatinib resistance, one being the up-regulation of the BCR-ABL protein, associated with amplification of the BCR-ABL gene, and the second is the over-expression of the multidrug resistance P-glycoprotein (Pgp). The KCL22^{Im-Res} cells were also established by Mahon and colleagues (Mahon et al., 2000a), however they were unable to establish the exact mechanism causing imatinib resistance in this cell line.

Although, imatinib is still the first-line therapy for CML patients, the development of more efficient and potent TKIs, along with improved drug regimens, has opened the question to whether using imatinib resistant cell lines is relevant in order to study BCR-ABL-independent resistant CML.

In the clinic, if a patient does not achieve an optimal response to imatinib treatment, they can be treated with an increased concentration of imatinib or a 2nd generation TKI such as dasatinib or nilotinib. Poor response to 1st and 2nd generation TKIs leads to treatment with 3rd generation TKI, ponatinib.

In order to investigate whether imatinib resistant cell lines are suitable models to study BCR-ABL-independent TKI-resistant mechanisms, we first wanted to treat these cells such as it would occur in the clinic. Therefore, we tested how the imatinib resistant cell lines respond to imatinib escalation and more potent TKIs; nilotinib, dasatinib and ponatinib, all

treated with concentrations within the maximal tolerated doses (MTDs) achieved in patients. Pharmacokinetic studies show that the MTD for imatinib is 800 mg, which equates to a maximum measured plasma concentration (cMax) of 3.9 μM (Peng et al., 2004). Patients treated with 400 mg of nilotinib achieve a cMax of 3.6 μM (Jabbour et al., 2009a). The maximal concentration achievable for dasatinib shown in phase I trials is 180 nM (Copland et al., 2006b). Ponatinib has shown to completely suppress the emergence of BCR-ABL transcripts at concentrations as low as 40 nM (O'Hare et al., 2009), however the maximal tolerated dose was 30 mg per day, which equates to a cMax of 120 nM (Cortes et al., 2012b). Therefore, for our experiments we used drug concentrations within the cMax ranges, imatinib 2 μM , nilotinib 2 μM , dasatinib 150 nM and ponatinib 100 nM. In addition, previous experiments in our lab had shown that at these concentrations BCR-ABL activity is inhibited, as reflected by a reduction in CRKL phosphorylation (Karvela, 2013). The effectiveness of imatinib, nilotinib dasatinib and ponatinib was also assessed with regards to cell proliferation, ability to induce apoptosis and reduce the number of leukaemic cells with colony forming potential.

K562^{Im-Res}, KCL22^{Im-Res}, and LAMA84^{Im-Res} (figure 3-1) cell lines were treated with TKIs. Following 72 hours of continuous treatment the K562^{Im-Res} cell line had significant induction of apoptosis in all TKI treatments (figure 3-1). The KCL22^{Im-Res} cell line was developed by growing the cells increasing amounts of imatinib up to 1 μM , however the KCL22^{Im-Res} cells had retained their resistance even to an increased concentration of imatinib (2 μM), shown by no induction of apoptosis over the untreated sample. However, the 2nd and 3rd generation TKIs induced a significant apoptotic response (figure 1b). The LAMA84^{Im-Res} cell line was resistant to first and second generation TKIs but ponatinib induced a striking and highly significant apoptotic affect even at 24 hours (figure 3-1).

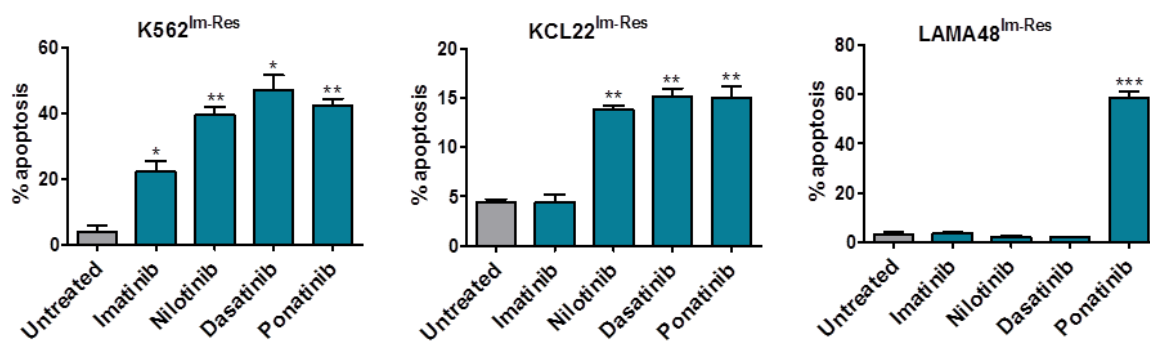


Figure 3-1: Imatinib-resistant cell lines.

K562^{Im-res}, KCL22^{Im-res} and Lama84^{Im-res} cells were seeded at 0.25×10^6 /mL and treated with 2 μ M imatinib, 2 μ M nilotinib, 150 nM dasatinib, and 100 nM ponatinib. The histogram represents early and late apoptosis and numbers are presented as mean \pm SEM (n=3). The percentage of apoptosis was measured following 24-72 hour drug treatment by flow cytometry following annexin V and 7AAD staining. Statistical analysis was performed by using paired t-test. Annotation above a bar refers to statistical significance between the bar and the untreated control. (**; $p \leq 0.01$, ***; $p \leq 0.001$).

Although TKIs have a potent inhibitory affect against BCR-ABL activity, they also have the ability to target other tyrosine kinases of similar structure, such as KIT and platelet-derived growth factor receptor (PDGFR). Each TKI shows slightly different effects in terms of cytotoxicity and anti-proliferation, which may be due to their ability to inhibit alternative kinases. Particularly dasatinib and ponatinib, which are less specific due to their design, which enables them to target mutated forms of BCR-ABL. For example, dasatinib, even at low nM concentrations inhibits SCR family kinases, including SRC, LCK, LYN, FGR, BLK, FYN, YES and HCK (Deguchi et al., 2008).

Similarly, ponatinib also inhibits SCR and LYN at low concentrations, as well as members of the VEGFR, FGFR, and PDGFR families of receptor tyrosine kinases (O'Hare et al., 2009). This may explain the increased cytotoxic effect caused by dasatinib and ponatinib compared to imatinib treatment against these cell lines. Ponatinib also has activity against many mutant forms of BCR-ABL including the T315I mutation and has the ability to completely suppress the outgrowth of BCR-ABL resistant clones (O'Hare et al., 2009). As ponatinib is so effective against imatinib resistant cell models, it puts into question whether these models are relevant for the study of BCR-ABL-independent TKI resistance. Therefore, we propose using ponatinib to generate a TKI-resistant model, as it would be more likely that the resistant cells selected by ponatinib treatment would have a BCR-

ABL-independent TKI-resistance. Given the limited availability of primary human TKI-resistant samples, the generation of TKI-resistant BCR-ABL positive cell line models provide us with a relevant tool to perform large-scale screens in order to identify mechanism(s) that the cells develop to become TKI-resistant, which would enable us to establish an effective drug target for treatment for these patients.

3.3 The generation of a ponatinib-resistant CML cell model

KCL22^{WT} cells and BaF3^{WT} cells, initially sensitive to TKIs, were grown in increasing concentrations of ponatinib over a long period of time (figure 3-2).

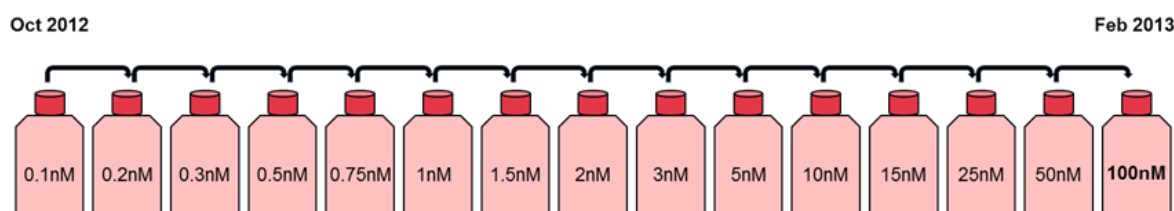


Figure 3-2: Illustrates the time course and increasing concentration of ponatinib used to generate the BaF3^{Pon-Res} cell line.

The parental BaF3^{WT} cell line was treated with 0.1 nM ponatinib in October, once the cells were happily proliferating, the cells were exposed to a gradual increase in concentration until they were resistant to 100 nM ponatinib.

Our data shows that the original TKI sensitive CML cell lines, KCL22^{WT} and BaF3^{WT}, were sensitive to ponatinib treatment (figure 3-3 and 3-4). An anti-proliferative effect was observed after 48 hours of treatment at concentrations as low as 1 nM of ponatinib for both cell lines. 150 nM dasatinib inhibited proliferation of KCL22^{WT} cells after 48 hours of treatment. The proliferation IC50 values for ponatinib against KCL22^{WT} and BaF3^{WT} cells, based on the cell counts following 72 hour of treatment ponatinib, are 2.5 nM and 0.95 nM respectively. The activity of BCR-ABL was analysed by its ability to phosphorylate and activate downstream proteins such as CRKL. Western blot analysis revealed that although proliferation can be impeded at low concentrations of ponatinib treatment in both cell lines, BCR-ABL activity was reduced, but not switched off until 10 nM treatment in KCL22^{WT} and 100 nM in BaF3^{WT} cells. This is in contrast to the newly generated KCL22 ponatinib-resistant (KCL22^{Pon-Res}) and BaF3^{WT} ponatinib-resistant (BaF3^{Pon-Res}) clones, which continue to proliferate in up to concentrations of 100 nM ponatinib (figure 3-3 and 3-4). In addition, 150 nM dasatinib had no effect on proliferation in both the KCL22^{Pon-Res} and

BaF3^{Pon-Res} cells (figure 3-3 and 3-4). The proliferation IC₅₀ values for ponatinib against KCL22^{Pon-Res} and BaF3^{Pon-Res} cells were 303.6 nM and 987.4 nM respectively. Therefore, the new ponatinib-resistant cell line KCL22^{Pon-Res} has over a 120 fold tolerance for ponatinib compared to its original counterpart, KCL22^{WT}, and BaF3^{Pon-Res} has over 1000 fold resilience against ponatinib compared to BaF3^{WT} cells. Although BCR-ABL activity is much reduced at 10 nM ponatinib treatment, as seen in KCL22^{WT} cells, a complete switch off does not occur until 100 nM treatment of ponatinib, despite cellular proliferation being unaffected (figure 3-3). The BaF3^{Pon-Res} cells do not show a reduction in signalling until 1 μ M ponatinib treatment, which corresponds with the high IC₅₀. However, despite, the reduction in BCR-ABL signalling the BaF3^{Pon-Res} cells continue to proliferate at this concentration (figure 3-4). (KCL22^{Pon-Res} cell line was generated by G.V. Helgason).

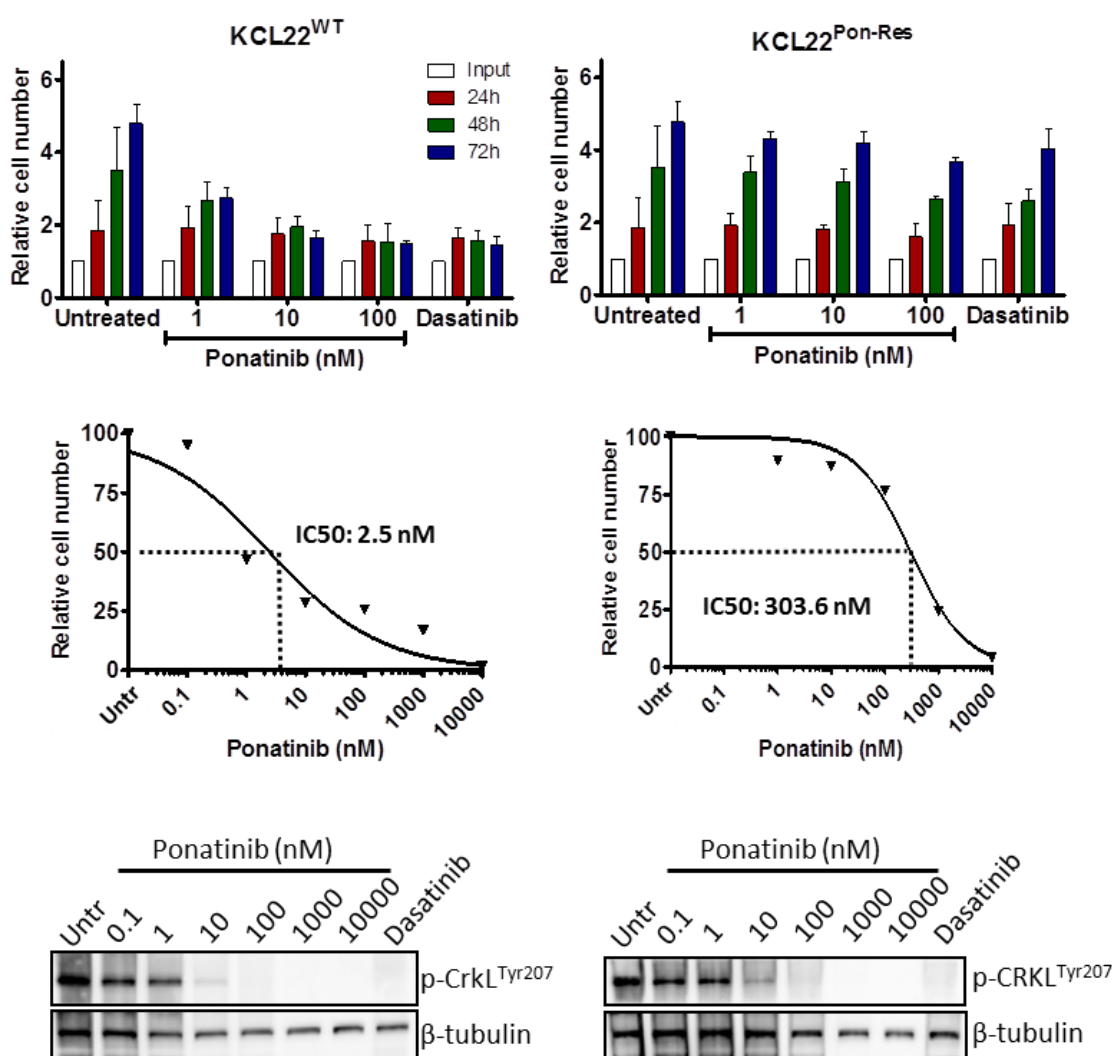


Figure 3-3: KCL22^{WT} and KCL22^{Pon-Res} cells were seeded at 0.25×10^6 /mL and treated with 0.1, 1, 10, 100, 1000 and 10000 nM ponatinib and 150 nM dasatinib.

Cell proliferation and viability were analysed by trypan blue cell counts at 24, 48 and 72 hours. IC₅₀s were calculated using 72 hour cell count data using prism. BCR-ABL kinase activity of

KCL22^{WT} and KCL22^{Pon-Res} cells after 24 hours TKI treatment was assessed by the level of phosphorylated CRKL protein expression via western blot. (Figures by G. V. Helgason).

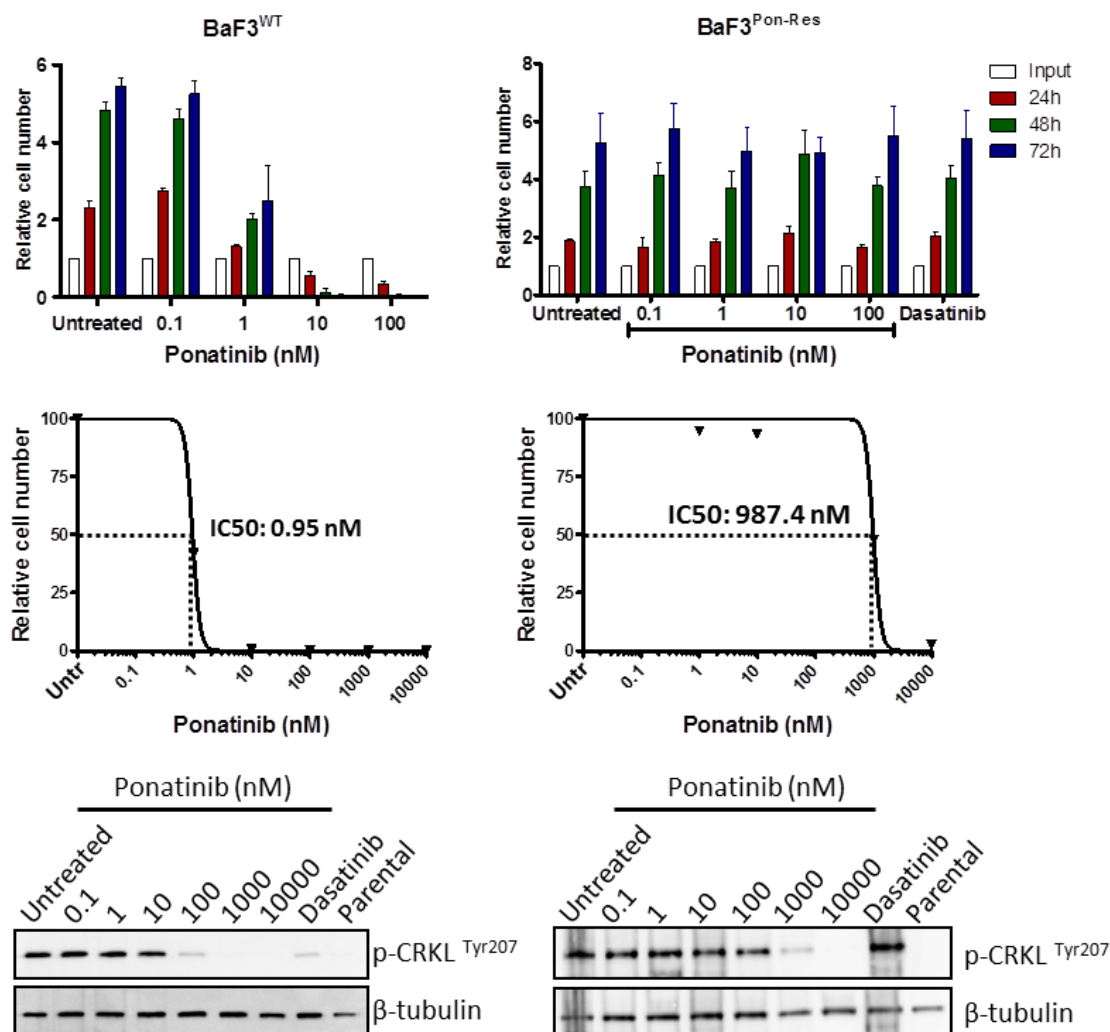
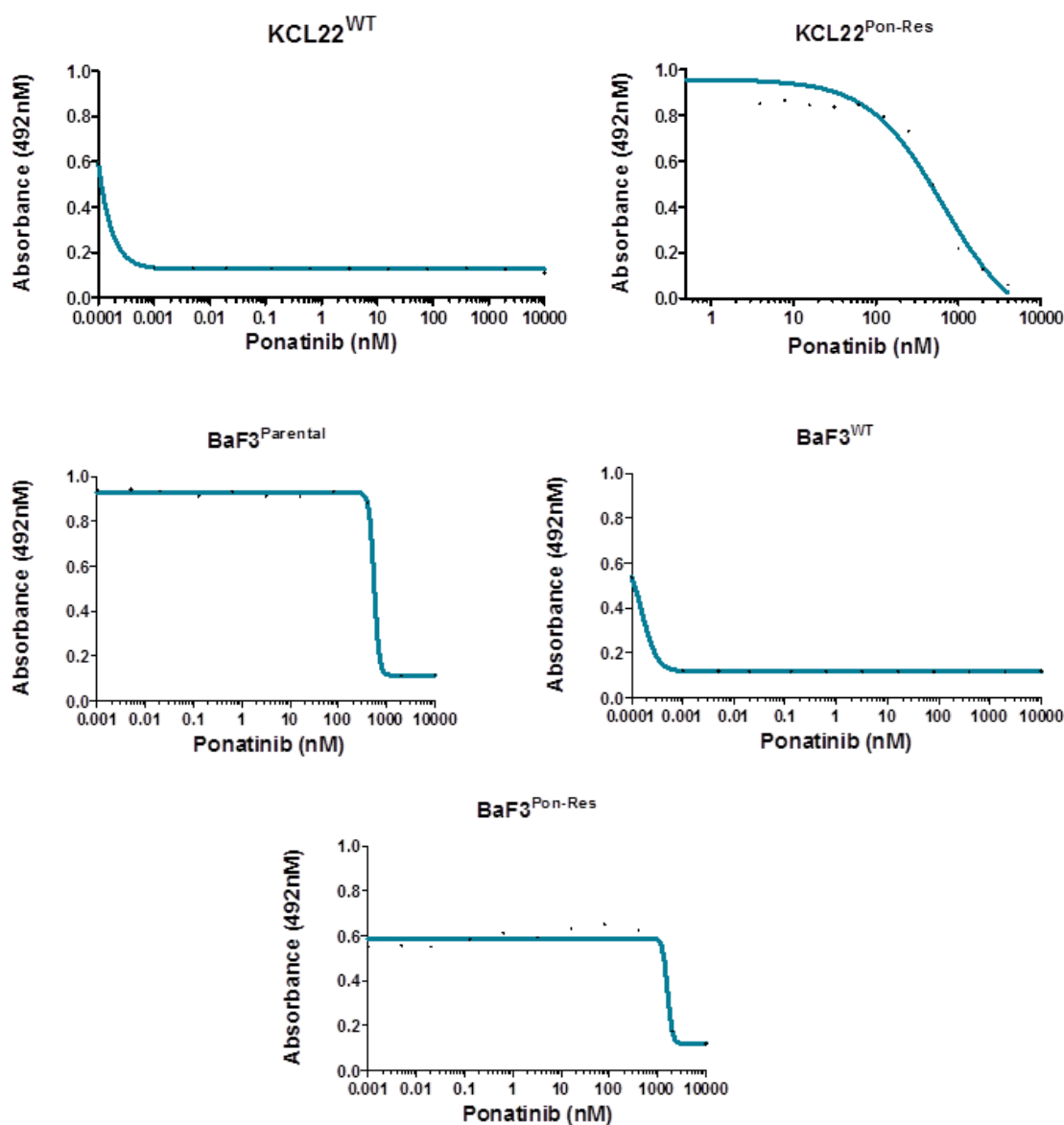


Figure 3-4: BaF3^{WT} and BaF3^{Pon-Res} cells were seeded at 0.25×10^6 /ml and treated with 0.1, 1, 10, 100, 1000 and 10000 nM ponatinib and 150 nM dasatinib.

Cell proliferation and viability were analysed by trypan blue cell counts at 24, 48 and 72 hours. IC50s were calculated using 72 hour cell count data using prism. BCR-ABL kinase activity of KCL22^{WT} and KCL22^{Pon-Res} cells after 24 hours TKI treatment was assessed by the level of phosphorylated CRKL protein expression via western blot. (Figures by Vignir Helgason).

To further analyse the level of ponatinib resistance gained by the KCL22^{Pon-Res} and BaF3^{Pon-Res} cells we performed XTT assays, to determine how this affected the cell viability by measuring the number of metabolically active cells. metabolic activity. The assay was carried out using a broad range of equimolar concentrations of ponatinib against KCL22^{WT} and KCL22^{Pon-Res} cells. The KCL22^{WT} cells were highly sensitive to ponatinib achieving a half maximal effective concentration (EC50) of 0.00004 nM. An EC50 refers to concentration of a drug that gives half-maximal response. The KCL22^{Pon-Res} cells had a much higher EC50 of 647.3 nM (figure 3-5). XTT assays were also performed on BaF3^{parental}, BaF3^{WT} and BaF3^{Pon-Res} cells. The BaF3^{parental} cell line does not express BCR-ABL and acted as a normal cell control. The BaF3 cells were treated with the same equimolar ranges of ponatinib. The BaF3^{WT} cells showed high sensitivity, similar to the KCL22^{WT} cells, with an EC50 of 0.0002 nM, which was in comparison to the BaF3^{Pon-Res} cells which had an EC50 of 1598 nM. BaF3^{parental} cells do not express BCR-ABL and therefore are not effected by TKIs until much higher doses, which are likely to be causing off target affects and inhibiting other important kinase activity. BaF3^{parental} cells exhibited a much higher tolerance to ponatinib treatment, with an EC50 of 552.1 nM, which is a similar concentration to the ponatinib-resistant cell lines, lower than the BaF3^{Pon-Res}, further strengthening the evidence that the KCL22^{Pon-Res} and the BaF3^{Pon-Res} no longer use BCR-ABL for their survival (figure 3-3 and 3-4).



Cell Type	Drug	EC50 (nM)
KCL22 ^{WT}	Ponatinib	0.00004
KCL22 ^{Pon-Res}	Ponatinib	647.3
BaF3 ^{Parental}	Ponatinib	552.1
BaF3 ^{WT}	Ponatinib	0.0002
BaF3 ^{Pon-Res}	Ponatinib	1598

Figure 3-5: XTT assay using ponatinib against KCL22^{WT}, KCL22^{Pon-Res}, BaF3^{parental}, BaF3^{WT} and BaF3^{Pon-Res} cells.

Cells were seeded at 0.2×10^6 /mL and treated with the same equimolar concentration of drug ranging from 0.01 nM to 10 μ M ponatinib. Cell viability measured after 72 hours using an XTT assay and (b) EC50s were calculated using graphpad prism.

3.3.1 Ponatinib resistant CML cell model is pan-TKI-resistant

The apoptotic effect of all available TKIs and the highly toxic protein translation inhibitor, omacetaxine, which is used in patients as a last resort treatment, were investigated in KCL22^{Pon-Res} cells. KCL22^{Pon-Res} cells were treated with TKIs; imatinib 2 μ M, nilotinib 2 μ M, dasatinib 150 nM, ponatinib 100nM and omacetaxine 10 nM for 72 hours. Apoptosis was analysed by FACS following annexin V and 7AAD staining. Figure 3-6 shows that TKIs did not induce apoptosis in the KCL22^{Pon-Res} cells. The low level of apoptosis shown reflects that seen in the untreated cell population. However, although pan-TKI-resistant, very low concentrations of omacetaxine are able induce highly significant levels of apoptosis within this pan-TKI-resistant cell line highlighting that the KCL22^{Pon-Res} cells still remain their ability to activate the apoptotic machinery and undergo programmed cell death.

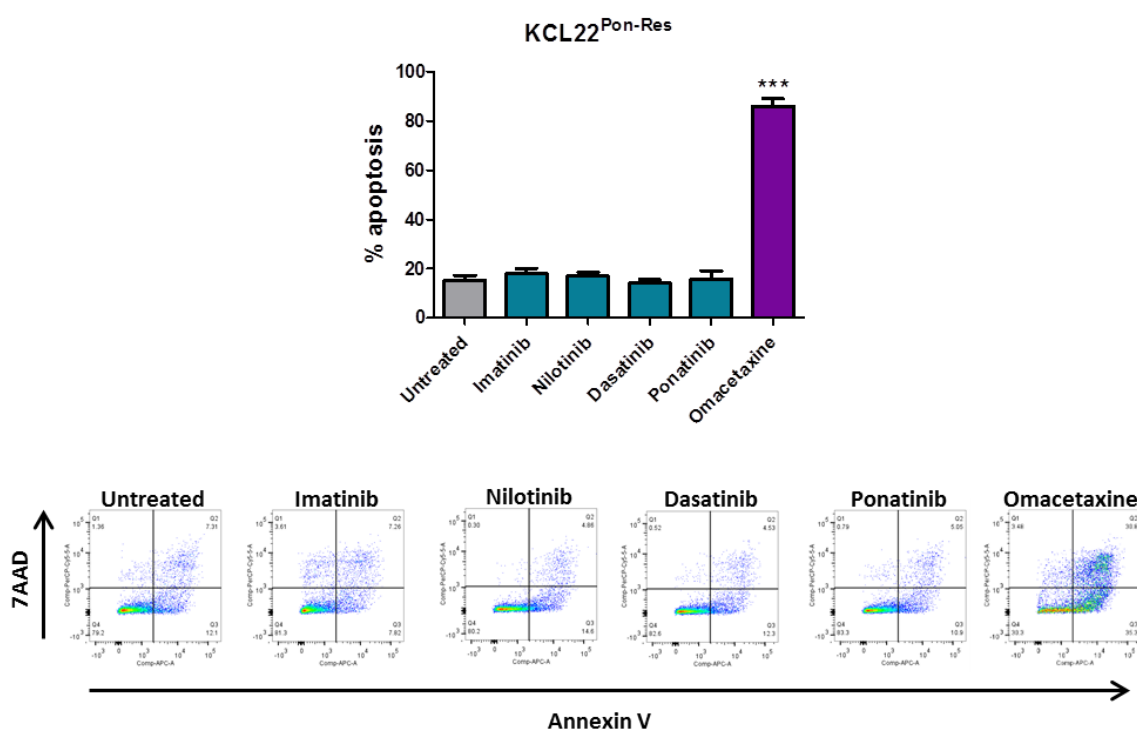


Figure 3-6: KCL22^{Pon-Res} cells were treated with imatinib 2 μ M, nilotinib 2 μ M, dasatinib 150 nM, ponatinib 100 nM and omacetaxine 10 nM for 72 hours, and analysed by flow cytometry following annexin V and 7AAD staining.

The histogram represents early and late apoptosis and numbers are presented as mean \pm SEM. Statistical analysis was performed by using paired t-test. Annotation above a bar refers to statistical significance between the bar and the untreated sample. (***) $p \leq 0.001$ $n=3$. The FACS plots show the live cell population in the lower left quadrant, early apoptotic cells in the lower right quadrant and the late apoptotic cells within the upper right hand quadrant.

3.3.2 Pre-clinical BCR-ABL inhibitor, ABL001, is ineffective against KCL22^{Pon-Res} and BaF3^{Pon-Res} cells

The previous experiments demonstrate the TKIs are redundant in the treatment of these pan-TKI-resistant cells. A new drug that exhibits an alternative mode of action against BCR-ABL is currently being investigated in a Phase I clinical trial, ABL001 (Ottmann et al., 2015). Unlike TKIs, which bind to the kinase domain, ABL001 binds to the myristoyl pocket of BCR-ABL and forces a conformational change that disables the kinase domain. Since this type of drug does not bind within the kinase domain of BCR-ABL, where most TKI-resistant mutations occur, it is thought that this could potentially be an alternative drug treatment for TKI-resistant patients (Ottmann et al., 2015). Hence, we wanted to investigate whether the KCL22^{Pon-Res} and BaF3^{Pon-Res} cells would be sensitive to this alternative drug. KCL22^{WT} and KCL22^{Pon-Res} cells were treated for 72 hours with a range of concentrations of ABL001. ABL001 proved to have antiproliferative effects in KCL22^{WT} cells in concentrations equal to 10 nM and above. However, ABL001 had no effect on proliferation of KCL22^{Pon-Res} cells, even in concentrations up to 1000 nM. In KCL22^{WT} cells, even low concentrations of 1 nM caused a modest induction of apoptosis after 72 hours of treatment, which significantly increased to 40% in concentrations 10 nM and above. Increased concentrations of 100 nM and 1000 nM did not further increase the level of apoptosis. ABL001 exhibited no apoptotic effect on the KCL22^{Pon-Res} cells, even at high concentrations of 1000 nM. The sensitivity of KCL22^{WT} and the resistance of KCL22^{Pon-Res} cells to ABL001 were reiterated in a XTT assay, which showed that KCL22^{WT} had an EC50 of 0.00005 nM and KCL22^{Pon-Res} cells had an EC50 of 6000 nM.

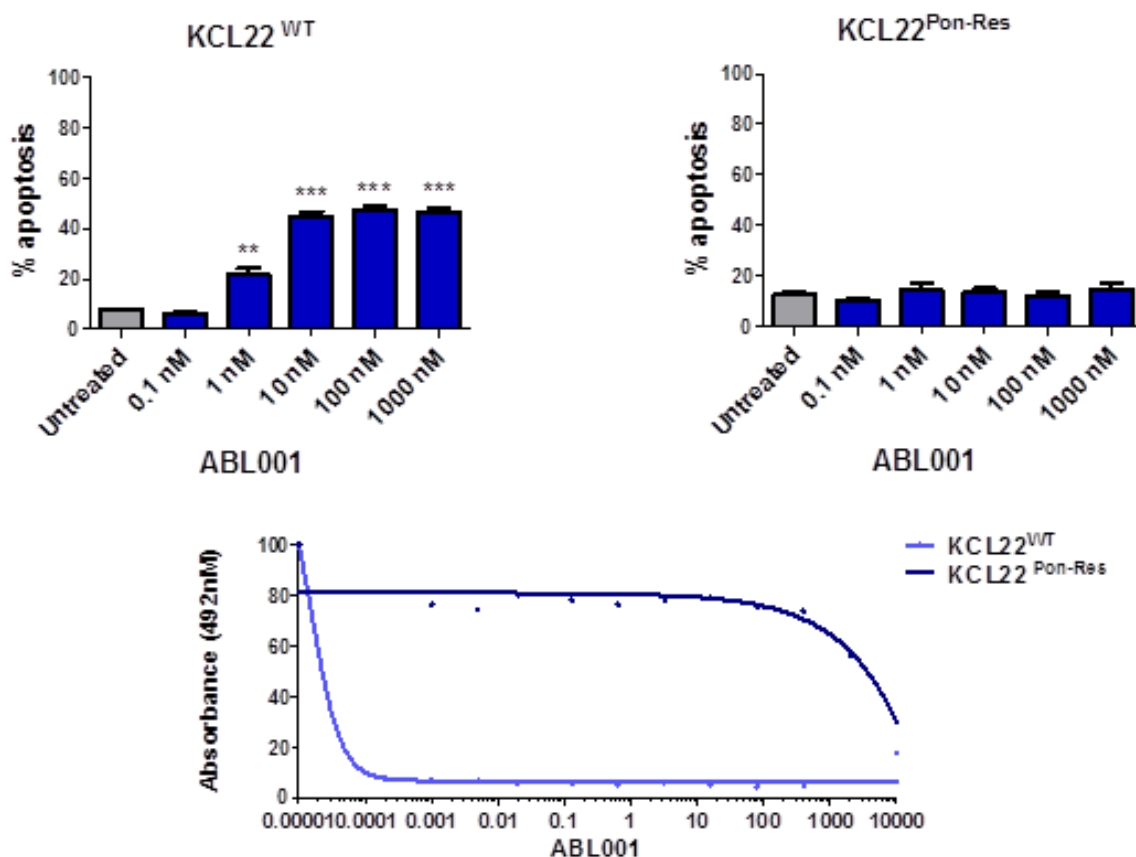


Figure 3-7: KCL22^{WT} and KCL22^{Pon-Res} cells were seeded at 0.25×10^6 /ml and treated with 0.1, 1, 10, 100, 1000, 10000 nM ABL001 for 72 hours.

Apoptosis was analysed via flow cytometry following annexin V and 7AAD staining. The histogram represents early and late apoptosis and numbers are presented as mean \pm SEM (n=3). Statistical analysis was performed by using paired t-test. Annotation above a bar refers to statistical significance between the bar and the untreated control. (**; $p \leq 0.01$, ***; $p \leq 0.001$). (c) KCL22^{WT} and KCL22^{Pon-Res} cells were seeded at 0.2×10^6 /mL and treated with the same equimolar concentration of drug ranging from 0.001 nM to 10 μ M ponatinib. Cell viability measured after 72 hours using an XTT assay and the EC50 was calculated using graphpad prism.

An apoptosis assay using a range of concentrations from 0.1 nM to 1000 nM was also performed on the BaF3 cell lines; BaF3^{parental}, BaF3^{WT}, BaF3^{T315I} and BaF3^{Pon-Res} cells. As expected, ABL001 had no impact upon the non-BCR-ABL expressing cell line, BaF3^{parental}. In the BaF3^{WT} cell line a modest induction of apoptosis was caused with 10 nM of ABL001, however treatment with 100 nM and 1000 nM of ABL001 induced a significant level of apoptosis, 85% and 90% respectively. Due to the design of ABL001, it has been shown to have inhibitory effects with CML patients harbouring the T315I mutation. Here we showed that 100 nM and 1000 nM induced apoptosis in the BaF3^{T315I} cells, to levels of 40% and 50% respectively. This is almost a 50% reduction in apoptosis compared to that observed in the BaF3^{WT} cells, using the same concentrations. This implies that BCR-ABL carrying the T315I mutation is less sensitive to ABL001 and may need treatment with higher concentrations to eradicate the cells (Thomas et al., 2015). As seen with the KCL22^{Pon-Res} cell line, ABL001 had no apoptotic effect on BaF3^{Pon-Res} cells, even at high concentrations of 1000 nM. These observations were supported by a cell viability assay, using resazurin. A broad range of equimolar concentrations of ABL001 were used against BaF3^{parental}, BaF3^{WT} and BaF3^{Pon-Res} cells, which showed that only the BaF3^{WT} cell were sensitive to ABL001 with a IC50 of 80 nM. The BaF3^{parental} and BaF3^{Pon-Res} cells did not show any response to ABL001 even at 10 µM, the highest concentration used within this assay. Even the combination of ABL001 and 100 nM ponatinib had no addition effect on the BaF3^{Pon-Res} cells. Given that both KCL22^{Pon-Res} and BaF3^{Pon-Res} cells are highly resistant to ABL001 reinforces the evidence that these cell lines do not have a kinase domain mutation which may infer the TKI resistance and that these cell line models truly survive due to a BCR-ABL-independent mechanism.

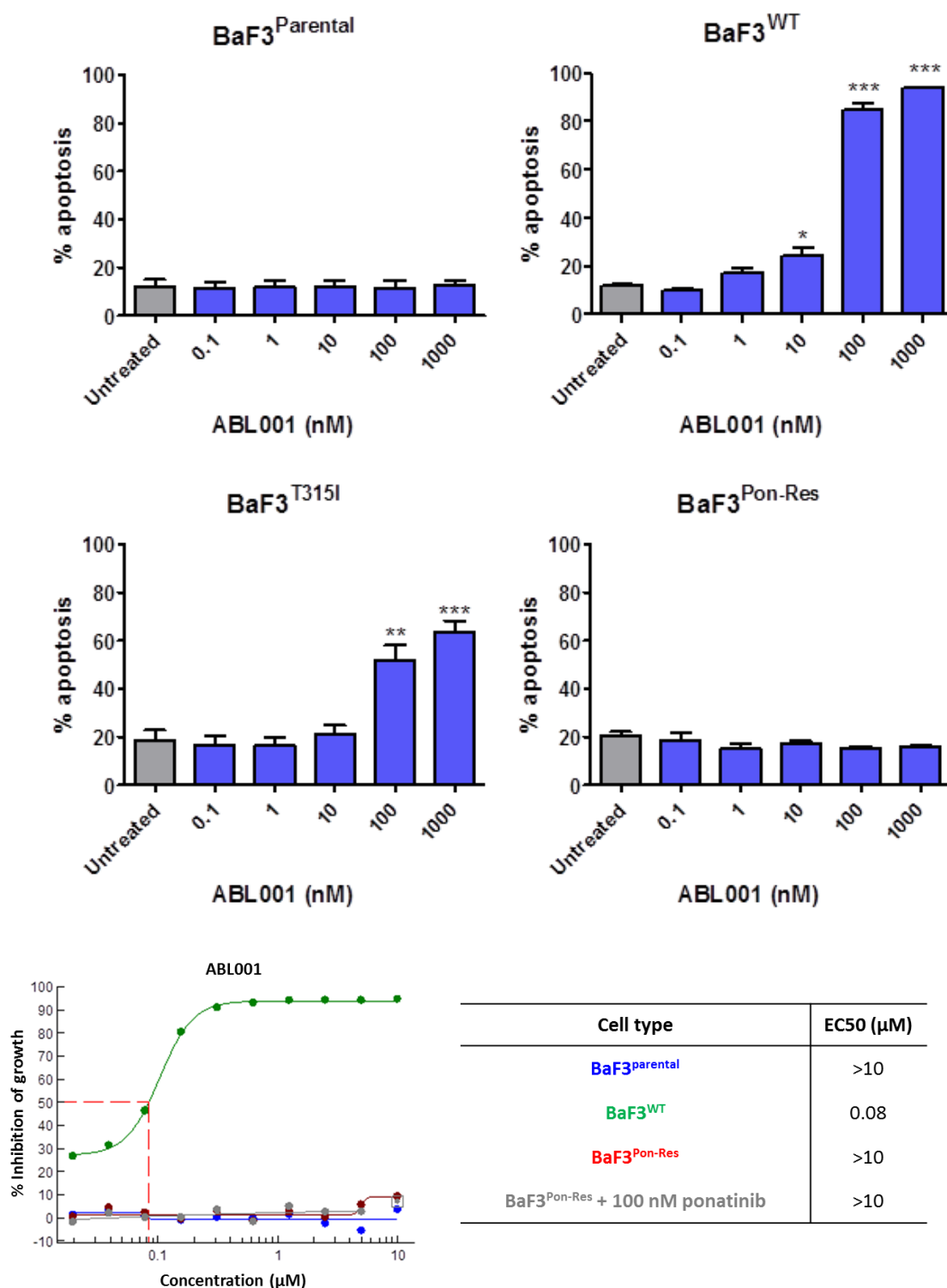


Figure 3-8: BaF3^{parental}, BaF3^{WT}, BaF3^{T315I} and BaF3^{Pon-Res} cells were seeded at 0.25×10^6 /ml and treated with 0.1, 1, 10, 100, 1000, 10000 nM ABL001 for 72 hours, and analysed by FACS following annexin V and 7AAD staining.

The histogram represents early and late apoptosis and numbers are presented as mean \pm SEM (n=3). Statistical analysis was performed by using paired t-test. Annotation above a bar refers to statistical significance between the bar and the untreated control (*; p \leq 0.05, **; p \leq 0.01, ***; p \leq 0.001).. BaF3^{parental}, BaF3^{WT}, BaF3^{Pon-Res} and BaF3^{Pon-Res} + 100 nM ponatinib cells were seeded at 0.25×10^6 /mL and treated with the same equimolar concentration of drug ranging from 0.001 nM to 10 μ M ABL001. Cell viability measured after 72 hours using a resazurin assay and the IC50 was calculated using graphpad prism (Beatson drug screening facility).

3.4 Characterisation of the mechanism causing TKI resistance in the ponatinib-resistant cell models

In order to understand the molecular mechanism driving the TKI resistance, both the KCL22^{Pon-Res} and BaF3^{Pon-Res} cells underwent several screening experiments.

3.4.1 DNA sequencing reveals no kinase domain mutation

Firstly, to confirm that the ponatinib-resistant cell models did not acquire kinase mutations, we sequenced the BCR-ABL kinase domain. As previously discussed, the BCR-ABL kinase domain is an area renowned for mutational changes, which affect TKI binding and ultimately cause TKI resistance. This is the most common cause of TKI resistance in CML patients. The T315I mutation is the most threatening mutation as 1st and 2nd generation TKIs are not able to bind to the BCR-ABL kinase domain due to this change. However, ponatinib has now been generated and was specifically designed to treat patients harbouring this mutation. The western blot previously showing the BCR-ABL activity of the BaF3^{Pon-Res} cells treated with increasing concentrations of ponatinib and dasatinib, showed that ponatinib could switch off BCR-ABL signalling, however dasatinib did not. Therefore, we were interested to know if during the generation of the BaF3^{Pon-Res} cells a T315I mutation had occurred. However, sequencing revealed no mutations within the kinase domain in either of the cell lines, which included no T315I mutation. As ponatinib is a more potent ABL inhibitor and the cells are highly resistant to ponatinib, perhaps higher concentrations of dasatinib are needed to inhibit BCR-ABL signalling in the BaF3^{Pon-Res} cell model. Data shown for BaF3^{Pon-Res} only (figure 3-9), KCL22^{Pon-Res} sequencing had been performed previously within our laboratory.

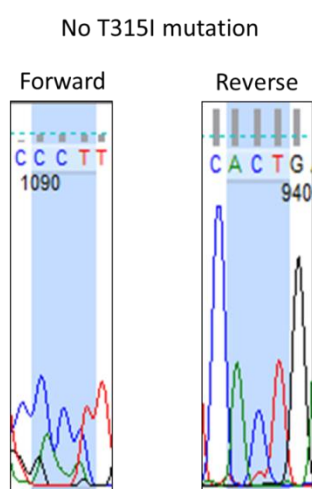


Figure 3-9: Genomic sequencing of BaF3^{Pon-Res} revealed no mutations within the BCR-ABL kinase domain. Data shown here is for the position for the T315I mutation and no mutation change has occurred.

3.4.2 KCL22^{Pon-Res} cells have an impaired transcriptional response to TKI

As mutational changes of the kinase domain had been ruled out as the mechanism of resistance for the TKI-resistant cells, we wanted to understand what mechanism the cells were using for their survival. With the recent advancements in sequencing we were interested in performing a transcriptomic screen to analyse the differences in gene transcription between the original KCL22^{WT} and KCL22^{Pon-Res} cells hoping to find the potential mechanism(s) of BCR-ABL-independent TKI resistance. The KCL22^{WT} and KCL22^{Pon-Res} cells were left untreated or treated with 100 nM ponatinib for 24 hours to switch off BCR-ABL signalling, and subsequently RNA and protein were generated. The transcriptomic analysis was performed using RNA-seq (performed by Glasgow Polyomics) to gain an understanding of the gene expression patterns between KCL22^{WT} and KCL22^{Pon-Res} cells and what effect switching off BCR-ABL signalling had to gene transcription in these two different cell lines. This analysis identified that KCL22^{WT} cells underwent many transcriptional changes, with 1658 genes being significantly up-regulated and significantly down-regulated following BCR-ABL inhibition by ponatinib (figure 3-10). However, the response in KCL22^{Pon-Res} cells to BCR-ABL inhibition was vastly different, with only two genes up-regulated and three down-regulated follow ponatinib treatment (figure 3-10). This suggested that although BCR-ABL has been inhibited, signalling pathways for cell survival remain unaffected and therefore no transcriptional changes occur, highlighting KCL22^{Pon-Res} cells lack of transcriptional response following ponatinib treatment.

This lack of transcriptional response was also shown clearly in the volcano plot, which showed the KCL22^{WT} cells with a large magnitude of fold changes in genes up-regulated (pink) and genes down-regulated (green). However, KCL22^{Pon-Res} cells show very few changes and what has changed is of very low magnitude. The linear correlation (r) between gene expression changes in KCL22^{WT} and KCL22^{Pon-Res} cells following 24 hour ponatinib treatment was 0.6. This means that there is no positive correlation between the two samples, as anything below 0.7 is deemed meaningless, and therefore this is not a significant correlation. Statistically this demonstrates that TKI sensitive KCL22^{WT} cells and TKI-resistant KCL22^{Pon-Res} cells have very different transcriptional responses to ponatinib treatment.

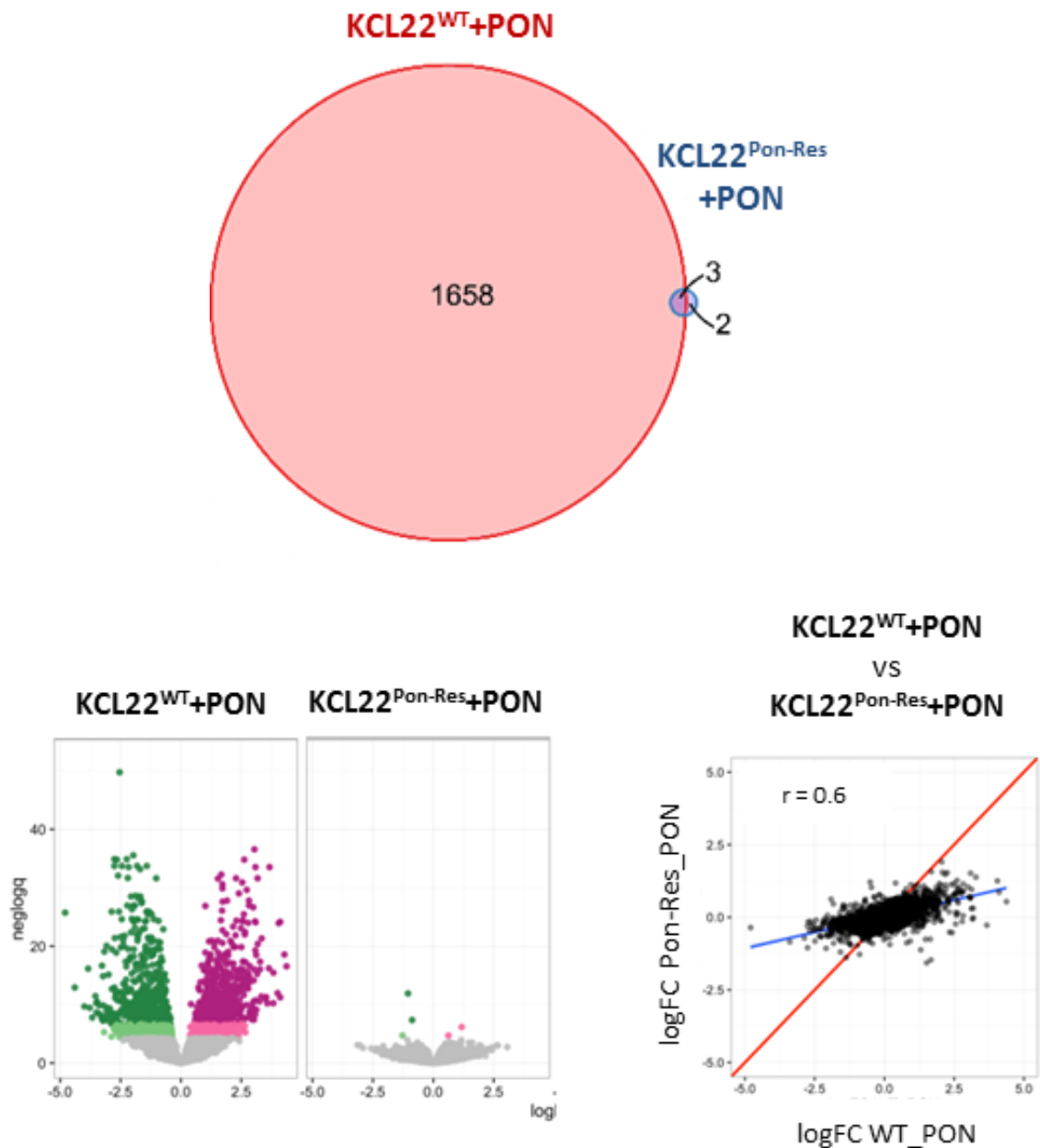


Figure 3-10: Venn diagram showing the differential gene expression changes between $KCL22^{WT}$ and $KCL22^{Pon-Res}$ cells following 24 hours ponatinib treatment.

A volcano plot showing the fold changes in gene expression patterns in $KCL22^{WT}$ and $KCL22^{Pon-Res}$ cells following 24 hours ponatinib treatment, down-regulated genes in green and up-regulated genes in pink. Comparison of log changes in gene expression between $KCL22^{WT}$ and $KCL22^{Pon-Res}$ cells following 24 hours ponatinib treatment.

3.4.3 mTOR activity is sustained in KCL22^{Pon-Res} cells despite BCR-ABL inhibition

As previously described PI3K/AKT/mTOR pathway is an important signalling pathway activated by BCR-ABL to help drive cell growth and proliferation (figure 3-11). Due to mTOR's involvement in protein translation it was hypothesised that deregulation of this pathway may have led to the impaired transcriptional response observed in the KCL22^{Pon-Res} cells following ponatinib treatment as seen in the RNA-seq experiment. In order to investigate this concept, we performed a western blot to analyse the activity mTOR in ponatinib sensitive CML cells (KCL22^{WT} and KCL22^{T315I}) and TKI-resistant CML cells (KCL22^{Pon-Res}) following treatment with TKIs, dasatinib or ponatinib. Treatment of the cells with TKI showed complete inhibition of BCR-ABL, shown by the absence of phosphorylated CRKL (KCL22^{T315I} with ponatinib treatment only). In the TKI sensitive CML cells, inhibition of BCR-ABL stops the signalling of the PI3K/AKT/mTOR pathway shown here by the inhibition of phosphorylated Ribosomal Protein S6 (RPS6), which is phosphorylated and activated by the mTOR pathway via S6 kinase (figure 3-11). However, we observed in the KCL22^{Pon-Res} cell line, despite the complete inhibition of BCR-ABL, there was sustained phosphorylation of RPS6. This indicates that mTOR is still active within the KCL22^{Pon-Res} cells. This activation is not via BCR-ABL therefore it suggests an alternative survival factor is activating mTOR complex 1 (mTORC1) (Ly et al., 2003), which is a common protein involved in multiple oncogenic signalling pathways.



Figure 3-11: A diagram of the PI3K/AKT/mTOR pathway, downstream of BCR-ABL.

KCL22^{WT}, KCL22^{T315I} and KCL22^{Pon-Res} were seeded at 0.25×10^6 /ml and treated with 150 nM dasatinib and 100 nM ponatinib for 24 hours. A western blot which assess the activity of BCR-ABL shown by phosphorylation of CRKL and mTOR activity shown by the phosphorylation of RPS6 (figure B by G. V. Helgason however n=3, 2 performed by Rebecca Mitchell).

3.5 Key findings

In this chapter we discuss the use of cellular models to study BCR-ABL independent TKI resistance in CML and the potential flaws of the imatinib resistant cell line models. One of the most significant results in this chapter was the development of truly BCR-ABL independent TKI resistant CML cellular models. We generated two ponatinib resistant cell lines; KCL22^{Pon-Res} and BaF3^{Pon-Res}, both of these models maintained the ability to proliferate under the treatment of high concentrations of 1st, 2nd and 3rd generation TKIs as well as the pre-clinical BCR-ABL inhibitor, ABL001. It was also shown that despite continued proliferation and survival, under 100 nM ponatinib treatment, BCR-ABL signalling was switched off, as seen with the inhibition of the phosphorylation of CRKL by western blotting. These findings led us to believe that these CML cells are using an alternative survival pathway for their survival.

In an attempt to characterise the mechanism of TKI resistance both models were screened for *ABL* kinase domain mutations, however both cell lines were negative for any known mutations which may cause TKI resistance. A transcriptomic screen was performed on KCL22^{WT} and KCL22^{Pon-Res} cells using RNA-seq to determine gene transcriptional changes between the two cell lines, which may infer the mechanism of resistance. There were very few transcriptional differences between the two cell lines at baseline. However, when BCR-ABL is inhibited, by ponatinib the KCL22^{WT} cells had a significant amount of transcriptional changes, whereas the KCL22^{Pon-Res} cells had no transcriptional response to ponatinib. This impaired response, highlights the redundancy of BCR-ABL signalling as a survival mechanism.

Although results from the RNA-seq were inconclusive, through western blotting we discovered of sustained mTOR signalling in the KCL22^{Pon-Res} cells despite the complete inhibition of BCR-ABL. Therefore, this led us to believe that mTOR was being activated by an alternative survival pathway. This was a very significant result from the chapter and led us to continue to investigate the PI3K/AKT/mTOR pathway as a potential drug target for BCR-ABL independent TKI resistant CML.

4 Results (II): Screening for potential novel drug target candidates for the treatment of BCR-ABL-independent TKI-resistant CML

4.1 Aim and objective

- III. Search for potential drug targets for BCR-ABL-independent TKI-resistant CML by performing a drug screen using National Institute of Health (NIH) approved oncology drugs

4.2 National Institute of Health (NIH) approved oncology drug screen

As a mutational change in BCR-ABL kinase domain had been ruled out as the mechanism of resistance for these TKI-resistant cells, we utilised a large scale screening programme in conjunction with the Beatson Drug Screening Facility. This facility possesses a library of 119 National Institute of Health (NIH) approved oncology drugs, which can be tested against cells via high throughput screening methods. This library includes inhibitors that target many pathways known to be deregulated in cancer, such as RAS/MEK/ERK and PI3K/AKT/mTOR, inhibitors against HDACs and tyrosine kinases and as well as many other conventional chemotherapy drugs. We wanted to use this screen not only to find an alternative treatment for BCR-ABL-independent TKI resistance, but also as a parallel approach to uncover the underlying molecular pathophysiology. The initial experiment was an analysis of KCL22^{WT} and KCL22^{Pon-Res} cells against the large library of inhibitors. KCL22^{Pon-Res} cells were analysed with and without 100 nM ponatinib treatment. Cells were plated at a density of 0.25×10^6 /mL in 96 well plates and treated with 4 concentrations of each drug (10 μ M, 1 μ M, 0.1 μ M, 0.01 μ M) in triplicate (figure 4-1). Following 72 hours of incubation, a resazurin cell viability assay was performed (figure 4-2).

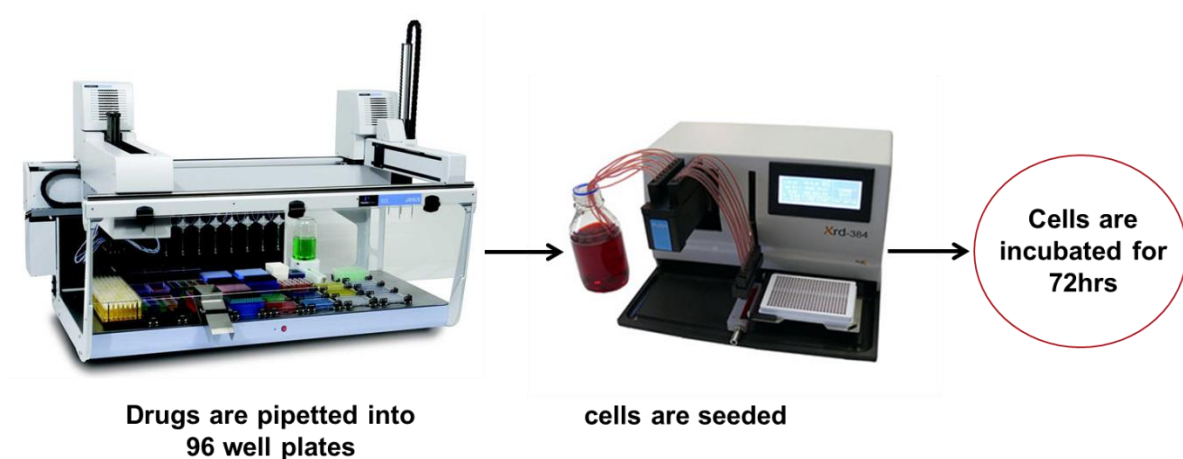


Figure 4-1: Workflow and depiction of the robotics used to pipette the drugs and the cells into the 96 well plates.

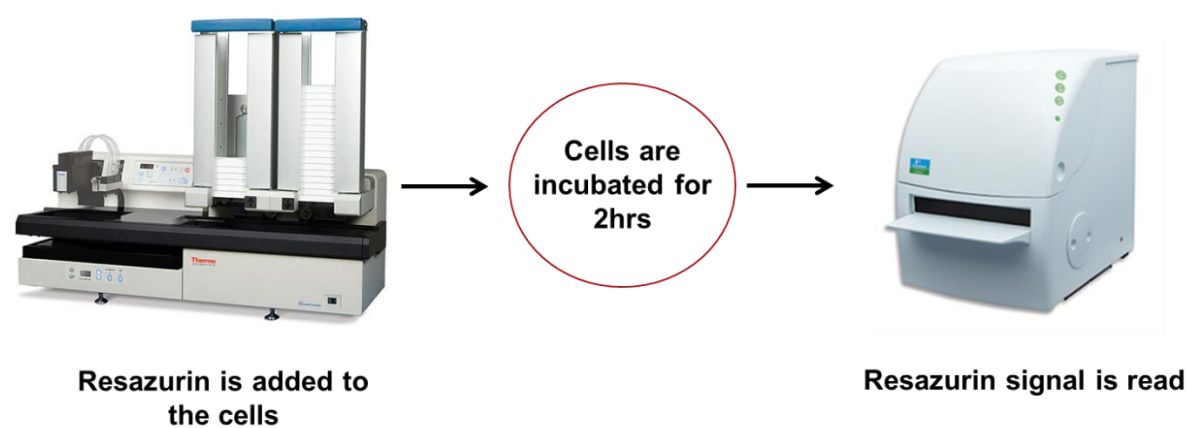


Figure 4-2: Workflow and depiction of the robotics used to pipette the resazurin into the 96 well plates and the resazurin plate reader.

4.2.1 Confirmation that KCL22^{Pon-Res} cells are pan-TKI-resistant

Importantly the screen confirmed that KCL22^{Pon-Res} cells are pan-TKI-resistant, as cell viability tests against the majority of FDA-approved TKIs never achieving an IC₅₀ under 10 µM, the maximum drug concentration used in the screen (figure 4-3), with the exception of bosutinib, which had an IC₅₀ of 8.123 µM, which would be an unachievable in patients and still denoted a resistant phenotype (figure 4-3).

4.2.2 37 clinically approved cancer drugs have the potential to induce cell death in TKI-resistant CML cells

The primary aim of this screen was to identify a drug(s) that could kill TKI-resistant CML cells. Our secondary aim was to find an inhibitor, which would exhibit a level of specificity towards the KCL22^{Pon-Res} cell line to help to uncover the mechanism of resistance. However, the results of the screen showed that all of the drugs that were effective against KCL22^{Pon-Res} cells also exerted their activity against KCL22^{WT} cells. Despite the non-selectivity towards the KCL22^{Pon-Res} cells, of the 119 drugs tested in the screen, 37 were shown to have an effect on cell viability of KCL22^{Pon-Res} cells within the drug concentration range (0.001-10 µM). Many of these drugs were non-specific chemotherapy drugs, such as vincristine sulphate, ixabepilone, docetaxel, cabazitaxel, vinblastine sulphate, paclitaxel and dactinomycin. All of these conventional chemotherapy treatments were within the top 10 drugs, which were able to reduce cell viability using very low drug concentrations. All of the IC₅₀s were under 100 nM (figure 4-3). Another chemotherapeutic, omacetaxine, as previously shown in figure 3-6, used as our positive control in this assay, was also highly effective against KCL22^{Pon-Res} cells, with an IC₅₀ of 42 nM (figure 4-3).

4.2.3 KCL22^{Pon-Res} cells are highly sensitive to mTOR inhibitors

The most prominent target highlighted from the screen was the inhibition of mTOR. mTOR had three consistent hits from allosteric inhibitors; everolimus, sirolimus and temsirolimus. These drugs were ranked highly for their low IC₅₀s against KCL22^{Pon-Res} cells (12th, 13th and 16th) (figure 4-3). The IC₅₀s of everolimus, sirolimus and temsirolimus were 115 nM, 118 nM and 158 nM, respectively (figure 4-3). The addition of ponatinib treatment to the cells had no additional effect on the IC₅₀s. Of all the drug targets in the screen, mTOR was the only target that had 3 consecutive hits from drugs which were highly effective in reducing cell viability (figure 4-3). mTOR inhibitors are of great interest, as PI3K/AKT mTOR is deregulated in many cancers. Sirolimus is more widely known as

rapamycin, and everolimus and temsirolimus are rapamycin analogues. Clinical trials have been conducted with mTOR inhibitors, one of which tested the effect of everolimus and imatinib in treating patients with CP CML who were not in CCyR after previous imatinib treatment (NCT00093639). This trial has now been completed, however no data is currently available. While sirolimus and rapamycin analogues have had moderate success in cancer therapy for solid tumours, only modest efficacy was achieved in patients, where it was thought it would provide great benefit (Sillaber et al., 2008, Wander et al., 2011). It is thought that the reason for the suboptimal response is due to rapamycin and its analogues only targeting mTORC1 and not the secondary subunit mTORC2, which can feedback to AKT and provide further stimulus for activation of mTOR (Choo and Blenis, 2009). However, this issue is being tackled by the development of catalytic inhibitors, one of which is about to open in a phase I clinical trial. This trial is a dose-finding study of NVP-Bez235 in adult patients with relapsed or refractory acute leukaemia, which is also open to BC CML patients (NCT01756118). NVP-Bez235 is a potent dual inhibitor of PI3K and mTOR (Maira et al., 2008). Dual PI3K and mTOR inhibitors are particularly effective in blocking PI3K/AKT/mTOR activation because they can also prevent the feedback activation of PI3K signalling normally observed with mTORC1 inhibitors, such as rapamycin and its analogues (Mukherjee et al., 2012).

4.2.4 KCL22^{Pon-Res} cells are sensitive to HDAC inhibition

However, very interestingly the drug that showed the highest sensitivity towards the KCL22^{Pon-Res} cells was romidepsin. This is a HDAC inhibitor currently approved for the treatment of cutaneous T-cell lymphoma (CTCL) and other peripheral T-cell lymphomas (PTCLs) (Iyer and Foss, 2015, Prince and Dickinson, 2012). The IC₅₀ obtained for this drug against the KCL22^{Pon-Res} cells was below the lowest drug concentration performed in the assay, 10 nM (figure 4-3). Other HDAC inhibitors were also screened against the KCL22^{Pon-Res} cells, however belinostat and vorinostat did not show the same level of sensitivity, having IC₅₀s of 1.039 µM and 3.41 µM, respectively (figure 4-3). The addition of ponatinib treatment to the cells had a varied effect on the IC₅₀s. In the scope of this experiment, as the concentration range did not go lower than 10 nM for romidepsin, it was unclear whether HDAC inhibition further sensitised cells to ponatinib. The addition of ponatinib had very little effect on belinostat, however it reduced the IC₅₀ of vorinostat by ~ 70% (figure 4-3).

4.2.5 KCL22^{Pon-Res} cells are sensitive to MEK inhibition

Another interesting specific drug target was the MEK inhibitor, trametinib. As previously described, MEK is part of the RAS/MEK/ERK signalling pathway, which is an important pathway downstream of BCR-ABL. Trametinib was within the top 20 drugs that affected KCL22^{Pon-Res} cell viability (figure 4-3). Sensitivity to this drug may be understandable due to it being one of the main survival pathways used by BCR-ABL. The main reason we found this particular drug so interesting was because as a single treatment it had an IC50 of 287 nM against KCL22^{Pon-Res} cells. However, when this was combined with 100 nM of ponatinib treatment it lowered the IC50 to 34 nM (figure 4-3). Therefore, ponatinib treatment further sensitises the KCL22^{Pon-Res} cells to the MEK inhibitor, suggesting that there may be a secondary oncogenic source activating MEK for KCL22^{Pon-Res} cell survival. This additive effect may allow for a more specific treatment towards TKI-resistant CML cells versus normal cells (figure 4-3).

KCL22^{Pon-Res}

Ponatinib - +

Repurposing Drug	IC50 -	IC50 +
Romidepsin	<0.01	<0.01
Vincristine sulfate	0.013	0.017
Ixabepilone	0.014	0.014
Docetaxel	0.015	0.016
Cabazitaxel	0.016	0.013
Vinblastine sulfate	0.016	0.014
Paclitaxel	0.016	0.014
Bortezomib	0.019	0.020
Omacetaxine mepesuccinate	0.042	0.023
Dactinomycin	0.071	0.073
Vinorelbine tartrate	0.115	0.370
Everolimus	0.115	0.126 *
Sirolimus	0.118	0.110 *
Carfilzomib	0.142	0.142
Clofarabine	0.143	>10
Temsirolimus	0.158	0.189 *
Plicamycin	0.174	0.174
Idarubicin hydrochloride	0.217	0.249
Trametinib	0.287	0.034
Topotecan hydrochloride	0.345	0.356
Doxorubicin hydrochloride	0.426	0.793
Gemcitabine hydrochloride	0.458	>10
Daunorubicin hydrochloride	0.478	0.602
Epirubicin hydrochloride	0.498	0.896
Mitoxantrone	0.529	0.919
Pralatrexate	0.804	>10
Thioguanine	0.980	1.339
Belinostat	1.039	0.840
Teniposide	1.193	2.511
Cytarabine hydrochloride	1.964	>10
Mitomycin	2.468	3.615
Valrubicin	3.410	5.123
Crizotinib	4.697	9.238
Vorinostat	5.170	1.549
Mercaptopurine	5.203	>10
Sunitinib	6.521	9.877
Bleomycin sulfate	6.730	>10
Bosutinib	8.123	>10
Ponatinib	>10	>10
Nilotinib	>10	>10
Imatinib	>10	>10
Dasatinib	>10	>10

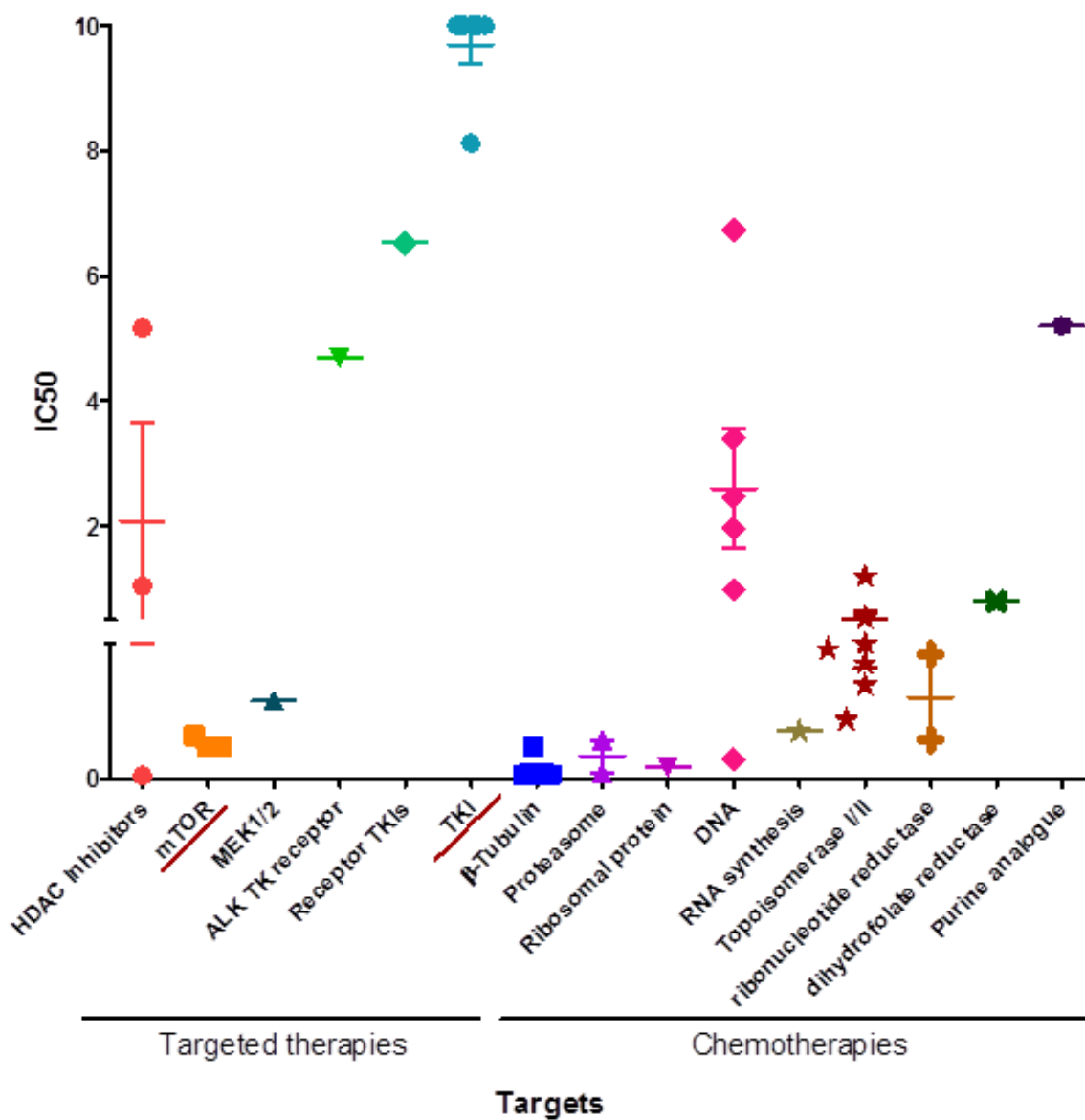


Figure 4-3: Heat map of the top IC50 concentrations obtained from NIH approved oncology drug screen against KCL22Pon-Res cells with and without ponatinib.

mTOR inhibitors highlighted by asterisks within the heat map. Dot plot of the drugs with the top IC50 concentrations against KCL22^{Pon-Res} cells grouped into their target/mode of action.

4.3 Validation of the primary drug screen using the BaF3^{Pon-Res} cell model

A secondary screen was conducted using the BaF3^{Pon-Res} cell model to validate that the hits from the first screen could be translated to other TKI-resistant models and wasn't specific to KCL22^{Pon-Res} cells. Several pre-clinical mTOR inhibitors were added to the screen, including dual PI3K and mTOR inhibitors, to assess whether they were more effective than the rapamycin analogues used in the primary screen. In the secondary screen BaF3^{parental}, BaF3^{WT} and BaF3^{Pon-Res} cells were analysed. The BaF3^{parental} were used as a “normal” haemopoietic cell control in order to understand if the drugs were toxic to normal cells or were specific to CML cells. The experiment was set up as previously described.

4.3.1 mTORC1 inhibition is insufficient to affect cell viability in BaF3^{Pon-Res} cells

mTOR inhibitors, everolimus and sirolimus, were very effective in the primary drug screen and were able to inhibit 50% of cell growth at 115 nM and 118 nM. However, in the BaF3^{Pon-Res} cell model the mTORC1 inhibitors were ineffective (figure 4-4). No IC50 was achieved for either sirolimus or everolimus in any of the BaF3 cell lines up to the maximum concentration, 10 µM (figure 4-4). Sirolimus in combination with 100 nM ponatinib, achieved an IC50 of 7.4 µM in the BaF3^{Pon-Res} cells, however this is a very high concentration, which may not be achievable in the clinic. The failure of the mTORC1 inhibitors in this setting, may be due to the partial effect on the mTOR pathway, which therefore once more highlights the need for more effective mTOR inhibitors, such as the catalytic inhibitors (Mukherjee et al., 2012).

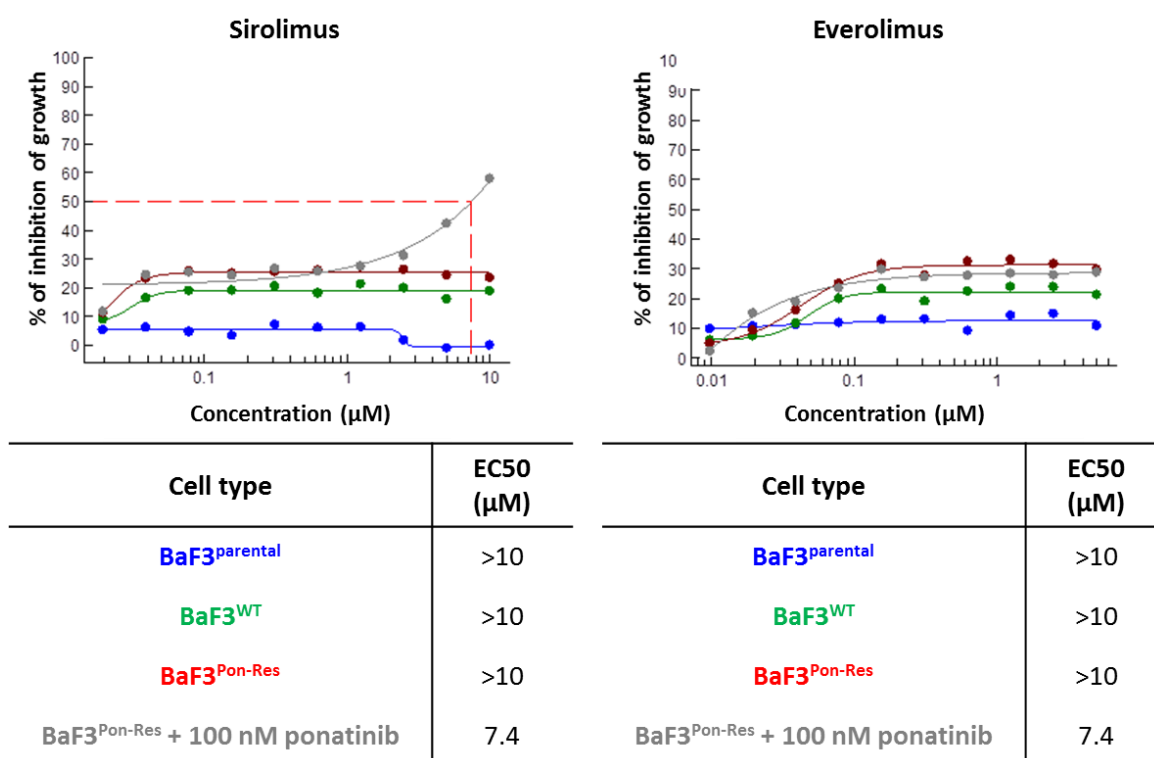


Figure 4-4: BaF3^{parental}, BaF3^{WT}, BaF3^{Pon-Res} and BaF3^{Pon-Res} + 100 nM ponatinib cells were seeded at 0.25×10^6 / mL and treated with the same equimolar concentration of drug ranging from 0.001 nM to 10 μM of sirolimus or everolimus.

Cell viability was measured after 72 hours using a resazurin assay and the IC50s were calculated using graphpad prism

4.3.2 BaF3^{Pon-Res} cells are highly sensitive to dual PI3K and mTOR inhibition

The PI3K-mTOR inhibitors may establish a deeper mTORC1 inhibition due to the targeting of both mTORC1 and mTORC2 as well as all PI3K isoforms (Maira et al., 2008). Therefore, we analysed the effects of catalytic inhibitors, AZD8055, (an mTORC1 and mTORC2 inhibitor that does not affect PI3K at the concentrations used), as well as several dual PI3K and mTORC1/2 inhibitors; apitolisib, VS-5584, NVP-Bez235 and gedatolisib. The sensitivity of KCL22^{WT} and KCL22^{Pon-Res} to AZD8055 was very similar to the mTOR inhibitors used in the primary screen, with the regards to the IC₅₀ drug concentrations. More importantly, AZD8055 had a significantly greater effect on growth inhibition in all three BaF3 cell lines, shown by the low IC₅₀ compared to the allosteric inhibitors. Although AZD8055 also affects the BaF3^{parental}, lower concentrations of AZD8055 are needed to inhibit the growth of BaF3^{WT} and BaF3^{Pon-Res} cells. BaF3^{parental} cells have an IC₅₀ of 320 nM, BaF3^{WT} cells 150 nM and BaF3^{Pon-Res} cells 240 nM (figure 4-5). The addition of ponatinib did not give AZD8055 any increased affect against the ponatinib-resistant cells (figure 4-5).

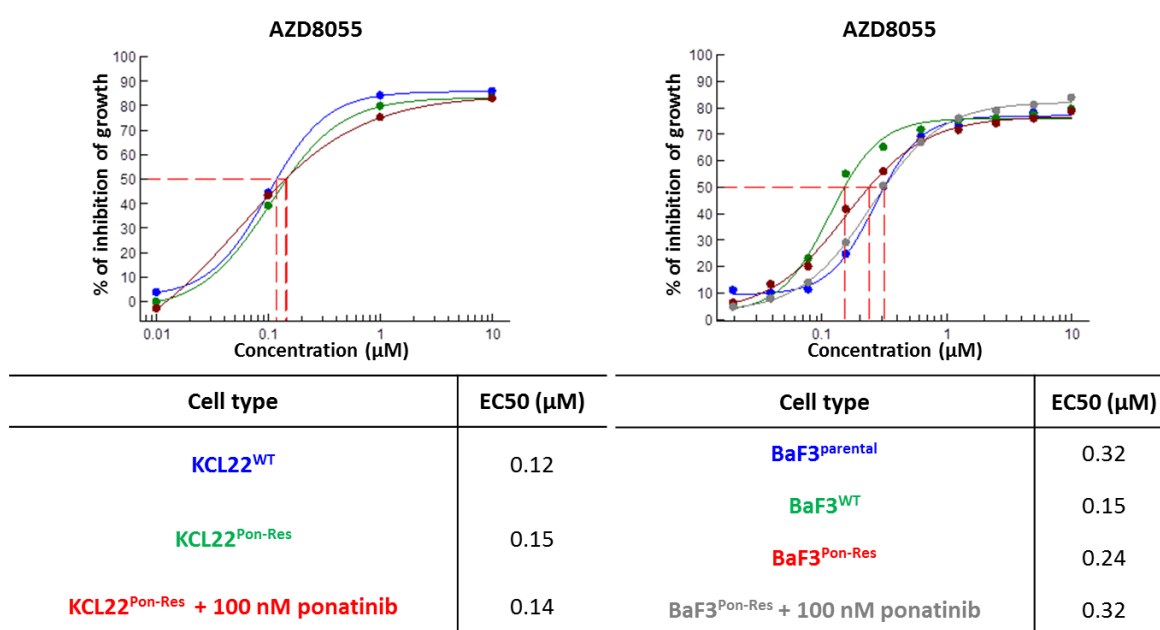
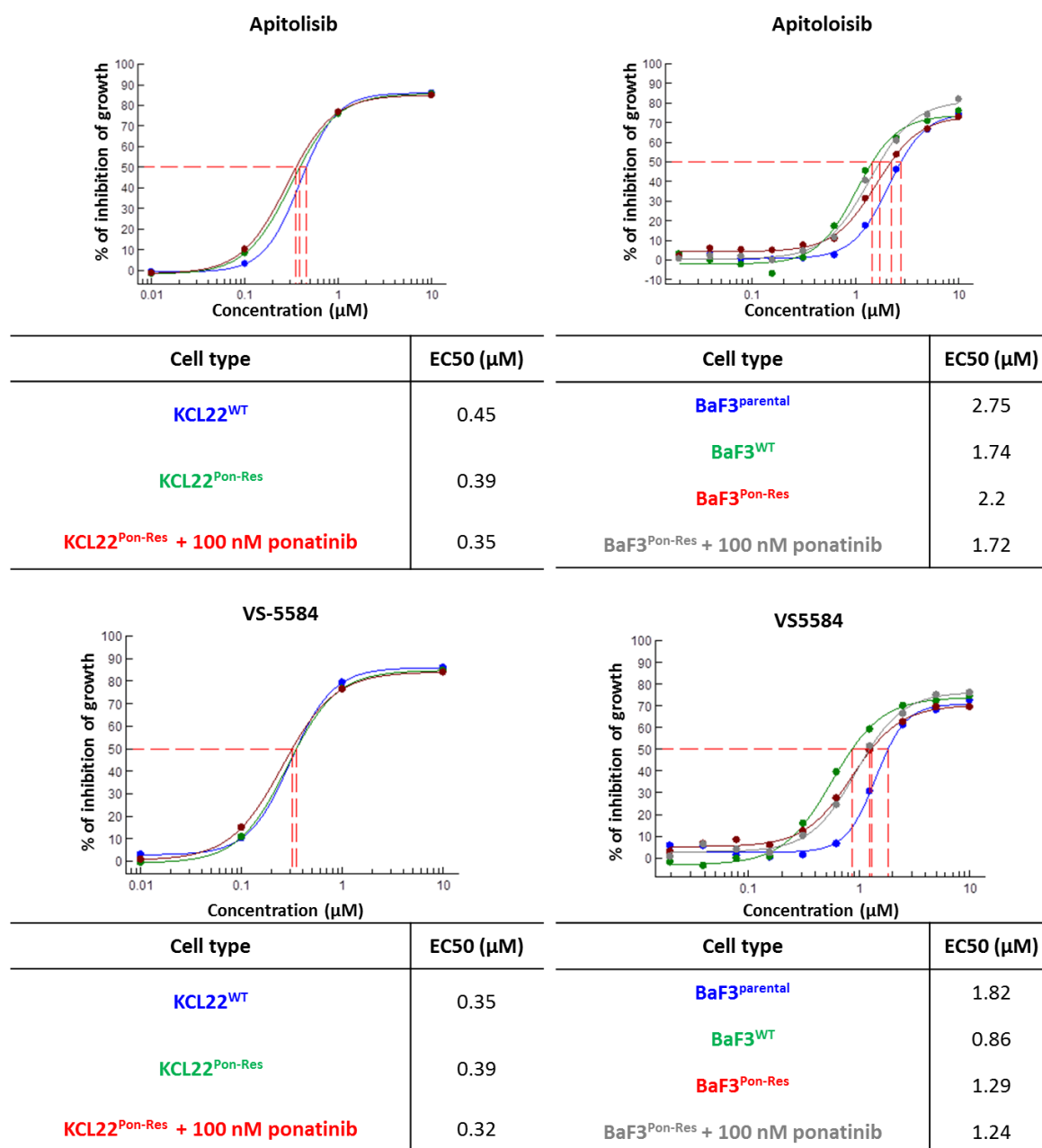


Figure 4-5: KCL22^{WT}, KCL22^{Pon-Res}, KCL22^{Pon-Res} +100 nM ponatinib, BaF3^{parental}, BaF3^{WT}, BaF3^{Pon-Res} and BaF3^{Pon-Res} + 100 nM ponatinib cells were seeded at 0.25×10^6 /mL and treated with the same equimolar concentration of drug ranging from 0.001 nM to 10 μM of AZD8055.

Cell viability was measured after 72 hours using a resazurin assay and the IC₅₀s were calculated using graphpad prism.

The KCL22^{Pon-Res} and the BaF3^{Pon-Res} cells were also highly sensitive to treatment with dual PI3K and mTOR inhibitors; apitolisib, VS-5584, NVP-Bez235 and gedatolisib. KCL22^{Pon-Res} 390 nM, 390 nM, 6 μ M and 1.4 μ M and BaF3^{Pon-Res} cells 2.2 μ M, 1.29 μ M, 0.94 μ M, 460 nM, respectively (figure 4-6).



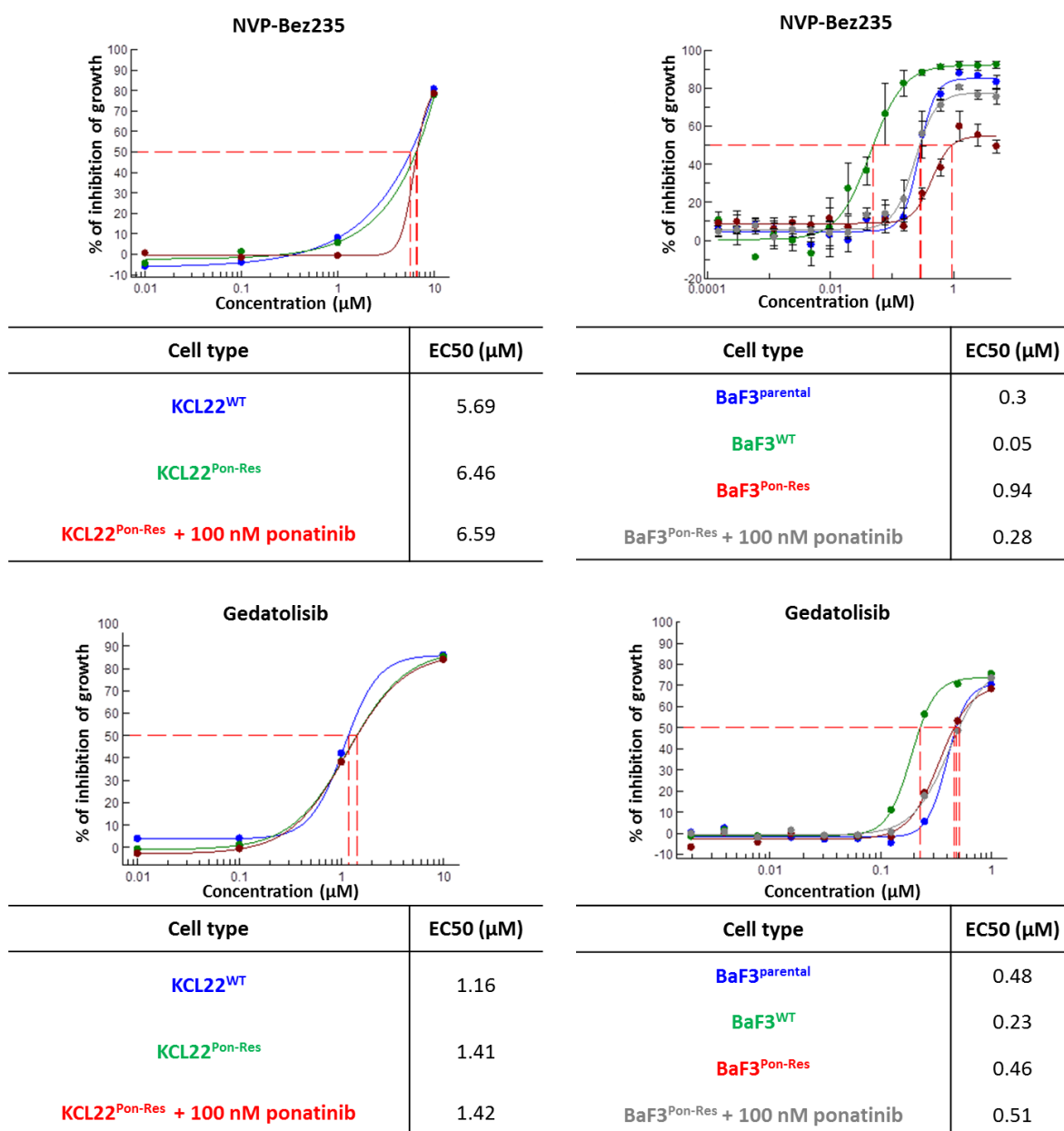


Figure 4-6: KCL22^{WT}, KCL22^{Pon-Res}, KCL22^{Pon-Res} + 100 nM ponatinib, BaF3^{parental}, BaF3^{WT}, BaF3^{Pon-Res} and BaF3^{Pon-Res} + 100 nM ponatinib cells were seeded at 0.25×10^6 / mL and treated with the same equimolar concentration of drug ranging from 0.001 nM to 10 µM of Apatolisib, VS-5584, NVP-Bez235 and Gedatolisib.

Cell viability was measured after 72 hours using a resazurin assay and the IC50s were calculated using graphpad prism.

4.3.3 Potential selectivity using trametinib against BaF3^{Pon-Res} cells compared to BaF3^{parental} cells

With the success of trametinib in the primary drug screen we wanted to ensure these results translated to the BaF3^{Pon-Res} cell model. This revealed that trametinib was a specific drug target for CML cells, as an IC50 for the BaF3^{parental} cells was not achieved within the drug concentration range (0.001 to 10 μ M) and IC50s for the BCR-ABL expressing cells, BaF3^{WT} and BaF3^{Pon-Res} were 230 nM and 1.83 μ M respectively (figure 4-7). Once again as seen in the KCL22^{Pon-Res} cell model, BaF3^{Pon-Res} cells were further sensitised to MEK inhibition with the addition of ponatinib treatment, reducing the IC50 from 1.83 μ M to 440 nM (figure 4-7). We also wanted to analyse whether MEK inhibition was a reproducible target, as only one MEK inhibitor was used in the primary screen. In the secondary screen we added selumetinib, which is also referred to as AZD6244. The efficacy of selumetinib was tested in the KCL22^{WT}, KCL22^{Pon-Res}, KCL22^{Pon-Res} +100 nM ponatinib, BaF3^{parental}, BaF3^{WT}, BaF3^{Pon-Res} and BaF3^{Pon-Res} +100 nM ponatinib cells. Selumetinib also showed greater efficacy against the KCL22^{Pon-Res} cells, IC50 480 nM, compared to KCL22^{WT}, IC50 >10 μ M (figure 4-7). As seen previously with trametinib, the addition of ponatinib treatment in combination with selumetinib treatment further sensitised the KCL22^{Pon-Res} cells to cell death, decreasing the IC50 to 70 nM (figure 4-3). However, this failed to translate to the BaF3 cell models, as selumetinib did not reach an IC50 within the drug concentration range (0.001 to 10 μ M) (figure 4-7).

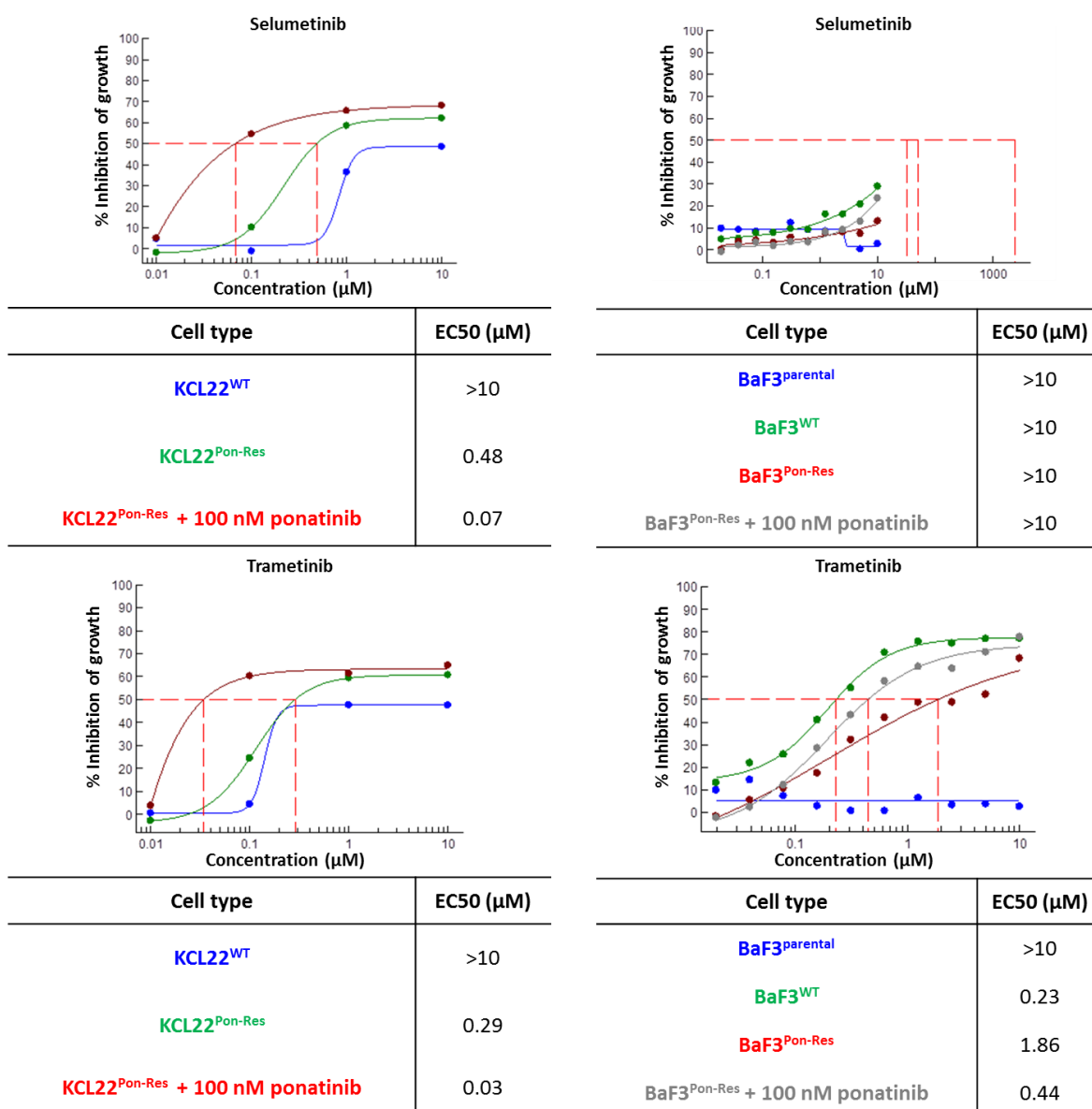


Figure 4-7: KCL22^{WT}, KCL22^{Pon-Res}, KCL22^{Pon-Res}+100 nM ponatinib, BaF3^{parental}, BaF3^{WT}, BaF3^{Pon-Res} and BaF3^{Pon-Res}+100 nM ponatinib cells were seeded at 0.25×10^6 / mL and treated with the same equimolar concentration of drug ranging from 0.001 nM to 10 μM of selumetinib and trametinib.

Cell viability was measured after 72 hours using a resazurin assay and the IC50s were calculated using graphpad prism.

4.4 A tertiary screen was performed to assess toxicity of the drugs to normal haemopoietic cells

Due to the similarity in IC₅₀ drug concentrations against BaF3^{parental} cells, TKI-sensitive and TKI-resistant CML cells in the cell line models we wanted to repeat the drug screen to test the toxicity of the mTOR and MEK inhibitors in primary non-CML CD34⁺ cells from three separate patients. The assay was set up very similarly to the cell line experiments.

4.4.1 Dual PI3K and mTOR inhibitors may have a therapeutic window for treatment for BCR-ABL-independent TKI-resistant CML patients

The results of the screen showed that mTOR inhibitors, sirolimus and everolimus, were not toxic to the “normal” cells, as IC₅₀s for sirolimus were in the high micromolar range 4.63, 2.27 and 8.97 μ M for each patient. As for treatment with everolimus a 50% reduction in growth was never achieved in any of the patient samples. PI3K/AKT/mTOR is an important pathway in normal cells as well as cancer cells, therefore the inhibition of mTOR should cause some growth inhibitory response. As this had not been observed within the assay, it also reinforces the theory that these allosteric mTOR inhibitors are inefficient. Due to their rarity, it would be impossible for us to carry out a drug screen using BCR-ABL-independent TKI-resistant CML samples. Therefore, our nearest comparison was human cell line, KCL22^{Pon-Res}. IC₅₀ concentrations have been plotted alongside the non-CML samples as a vague comparison. As seen with the KCL22^{Pon-Res} cells, the non-CML cells were also very sensitive to AZD8055 with all three samples having IC₅₀ concentrations within the nM range. These concentrations were very similar to the KCL22^{Pon-Res} model, which demonstrates a level of toxicity. IC₅₀ values for non-CML samples, < 20 nM, 100 nM and 210 nM compared to 160 nM for KCL22^{Pon-Res} cells (figure 4-8). The non-CML cells were also sensitive to the dual PI3K and mTOR inhibitors, however the IC₅₀ concentrations were higher than that of the KCL22^{Pon-Res} model. Apitolisib non-CML samples IC₅₀s: 670 nM, 430 nM and 850 nM compared to 390 nM achieved in KCL22^{Pon-Res} cells. VS-5584 IC₅₀s: 1.02 μ M, 610 nM, 1.31 μ M compared to 340 nM in KCL22^{Pon-Res} cells. NVP-Bez235: 320 nM, 520 nM, >1 μ M compared to 630 nM in KCL22^{Pon-Res} cells. Gedatolisib: 730 nM, 530 nM, 630 nM compared to 160 nM in KCL22^{Pon-Res} cells (figure 4-9). Therefore, this requires further investigation and may be best tested in an in vivo model (refer to chapter 6.12).

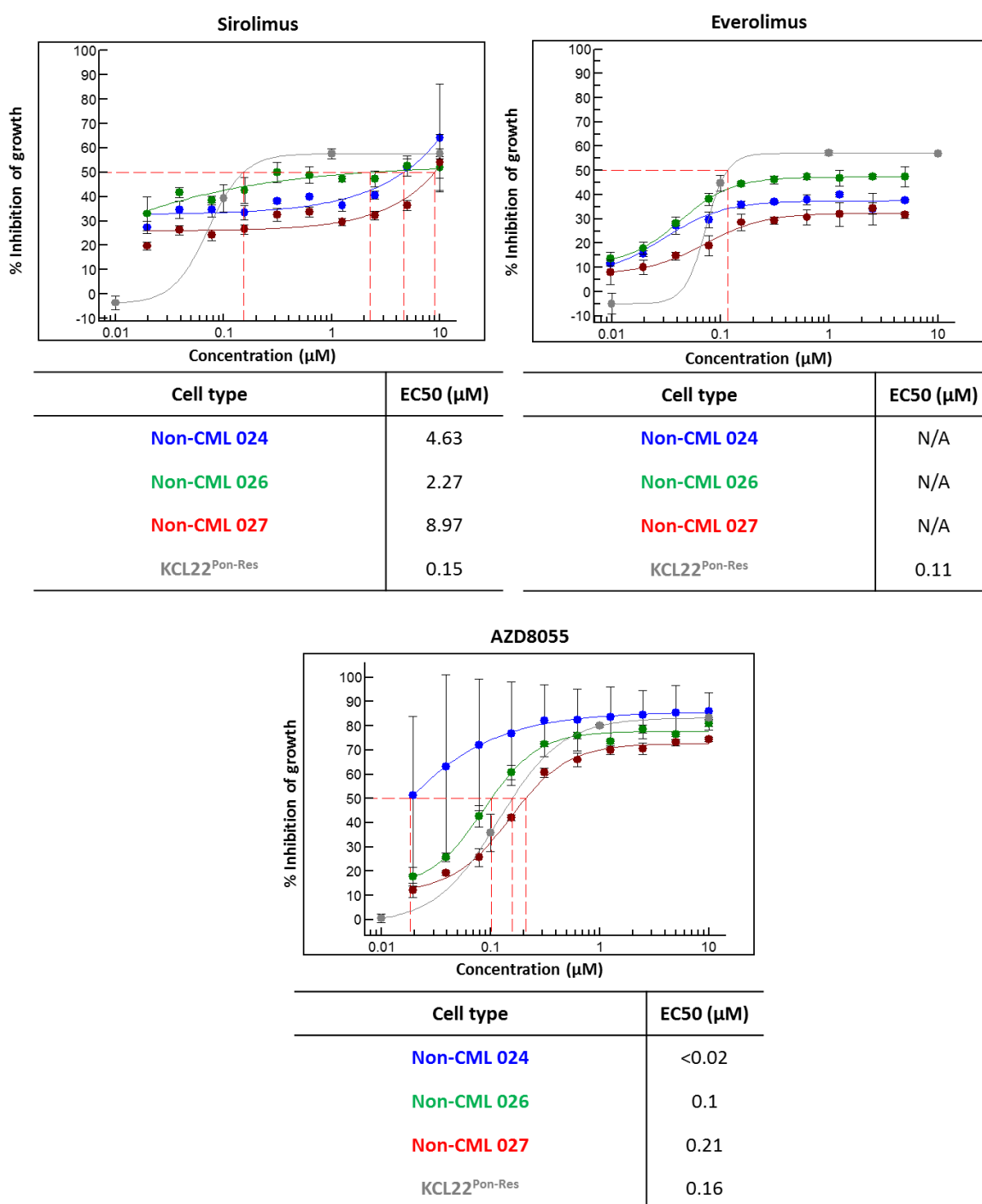


Figure 4-8: Non-CML cells from three different samples were seeded at 0.5×10^6 / mL and treated with the same equimolar concentration of drug ranging from 0.001 nM to 10 µM of sirolimus, everolimus and AZD8055.

Cell viability was measured after 72 hours using a resazurin assay and the IC50s were calculated using graphpad prism.

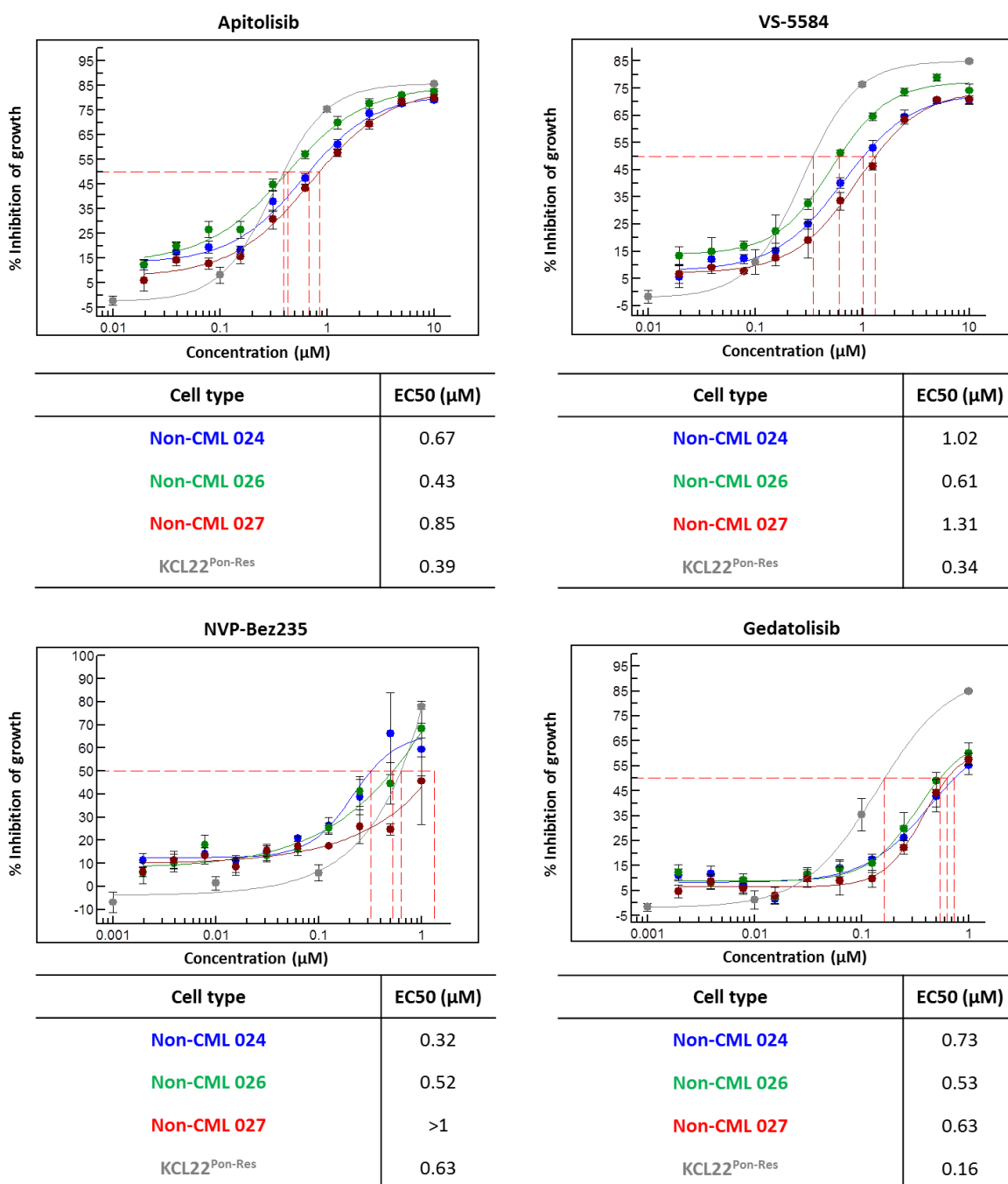


Figure 4-9: Non-CML cells from three different samples were seeded at 0.5×10^6 / mL and treated with the same equimolar concentration of drug ranging from 0.001 nM to 10 µM of apatolisib, VS-5584, NVP-Bez235 and gedatolisib.

Cell viability was measured after 72 hours using a resazurin assay and the IC50s were calculated using graphpad.

4.4.2 MEK inhibition is not toxic to non-CML haemopoietic cells

Despite the inconsistent translation between cell line models shown with the MEK inhibitors, we thought further investigation was still worthwhile as a potential therapeutic against BCR-ABL-independent TKI-resistant CML. Therefore, we also tested the toxicity of selumetinib and trametinib against non-CML haemopoietic cells. In this assay it showed that selumetinib and trametinib did not reach 50% cell growth inhibition, apart from one patient sample treated with trametinib which had a high IC₅₀ of 3.72 μ M (figure 4-10). Therefore, it suggests that MEK inhibition is not toxic to “normal” haemopoietic cells and could be a potential specific drug target for BCR-ABL-independent TKI-resistant CML.

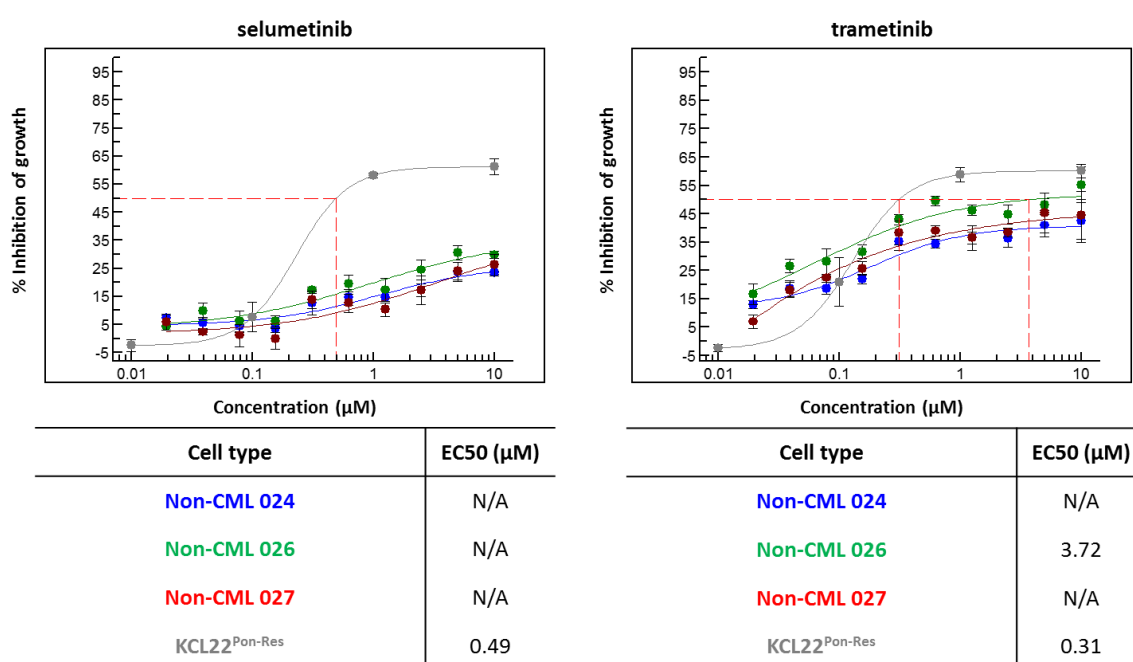


Figure 4-10: Non-CML cells from three different samples were seeded at 0.5×10^6 / mL and treated with the same equimolar concentration of drug ranging from 0.001 nM to 10 μ M selumetinib and trametinib.

Cell viability was measured after 72 hours using a resazurin assay and the IC₅₀s were calculated using graphpad prism.

4.5 Key findings

In this chapter we perform a drug screen in conjunction with the Beatson Drug Screening Facility. The facility possessed a library of 119 National Institute of Health (NIH) approved oncology drugs.

Our main aim for the screen was to find an alternative treatment for BCR-ABL-independent TKI resistant CML. By identifying an alternative target we hoped this may also lead to uncovering the underlying molecular pathophysiology.

The initial screen was conducted using KCL22^{WT} and KCL22^{Pon-Res} cells, which identified 37 clinically approved drugs that had the potential to induce cell death in TKI-resistant CML cells. The most significant result from this chapter was that the KCL22^{Pon-Res} cells were no longer sensitive to TKI treatment however were highly sensitive to mTORC1 inhibitors, which complimented data from chapter 3 where we saw sustained mTOR activity despite BCR-ABL inhibition. The primary drug screen results were validated using the BaF3^{Pon-Res} cell model and although the allosteric mTORC1 inhibitors from the primary experiment had a suboptimal effect on BaF3^{Pon-Res} cell viability, the use of novel dual PI3K and mTOR catalytic inhibitors, were highly effective at reducing cell viability in the BaF3^{Pon-Res} cell model, therefore further strengthening the concept that the PI3K/AKT/mTOR pathway may be a potential drug target for BCR-ABL independent TKI resistant CML.

5 Results (III): Validation of mTOR inhibitors in ponatinib-resistant cell lines

5.1 Aim and objective

IV. Validation of mTOR inhibitors in ponatinib-resistant cell lines

Although mTOR was not the only target discovered within the drug screen, the positive data that was collated from the primary and secondary screen showed that both the KCL22^{Pon-Res} and the BaF3^{Pon-Res} cells were highly sensitive to mTOR inhibition. Along with the impaired transcriptional response highlighted in the RNA-seq data (figure 3-10), as well as the sustained mTOR activity (figure 3-11), all provide a strong rationale for further investigation into mTOR as a therapeutic target for BCR-ABL-independent TKI-resistant CML. Therefore, we wanted to gain a deeper understanding of the importance of the PI3K/AKT/mTOR pathway's role in BCR-ABL-independent TKI-resistant CML.

Initially within the laboratory, we treated the ponatinib-resistant cell lines with clinically relevant mTOR inhibitors. As previously described mTORC2 can feed back to AKT to further activate mTOR. Therefore, the inhibitors we selected for the assays had slightly different targets, to establish whether inhibiting mTOR alone was sufficient to induce cell death or if the full PI3K/AKT/mTOR pathway had to be inhibited in order for full response to occur (figure 5-1). The inhibitors used included; BKM120, a catalytic inhibitor for class IA PI3Ks, rapamycin, a mTORC1 only allosteric inhibitor, AZD8055, acatalytic inhibitor that target mTORC1 and mTORC2 complexes of mTOR and NVP-Bez235, a catalytic mTOR inhibitor that inhibits both mTOR complexes and also has strong activity against all PI3K isoforms (figure 5-1). By using inhibitors against different proteins within the pathway, we were able to establish the best target that would affect cellular survival.

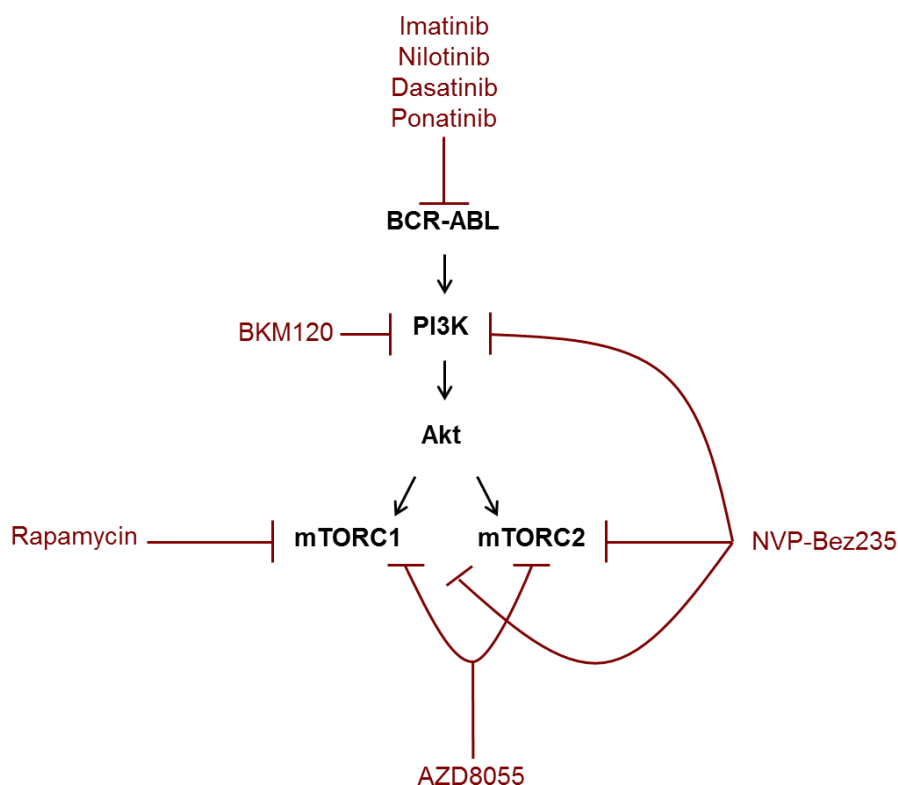
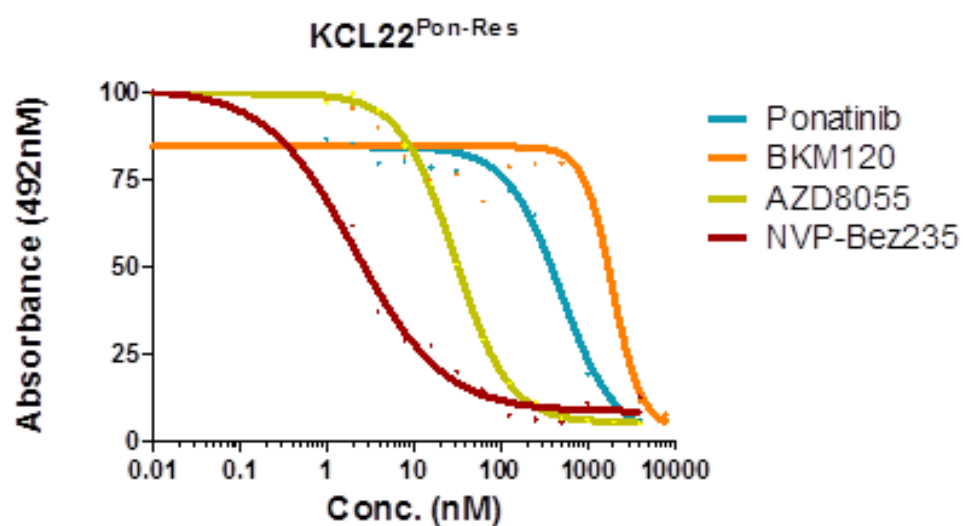


Figure 5-1: Schematic of the PI3K/AKT/mTOR pathway, downstream of BCR-ABL. It illustrates the chosen clinically applicable mTOR inhibitors and their targets.

5.2 Ponatinib resistant CML cells are sensitive to mTOR inhibition

Preliminary studies tested the efficacy of catalytic inhibitors BKM120 (PI3K), AZD8055 (mTORC1+2) and NVP-Bez235 (PI3K and mTORC1+2) against the KCL22^{Pon-Res} cell model by performing XTT assays and calculating the EC₅₀s. The KCL22^{Pon-Res} cells were highly sensitive to NVP-Bez235 and AZD8055 treatment. NVP-Bez235 had the greatest effect by decreasing proliferation at very low concentrations achieving an EC₅₀ concentration of 2.22 nM. An EC₅₀ of 28.28 nM was achieved in KCL22^{Pon-Res} cells against AZD8055. However, PI3K inhibition alone, by BKM120 required a much higher concentration and achieved an EC₅₀ at 1.928 μM. Therefore, mTOR inhibitors are capable of reducing cell viability at low concentrations in the KCL22^{Pon-Res} cell model, which provides increasing evidence that mTOR is important for TKI-resistant CML cellular survival (figure 5-2).



Drug	EC50 (nM)
NVP-Bez235	2.22
AZD8055	28.28
ponatinib	647.3
BKM120	1928

Figure 5-2: KCL22^{Pon-Res} were seeded at 0.2×10^6 / mL and treated with the same equimolar concentration of drug ranging from 0.01 nM to 10 μ M (ponatinib, NVP-Bez235, AZD8055, and BKM120).

Cell viability measured after 72 hours using an XTT assay and EC50 was calculated using graphpad prism.

5.3 mTOR inhibitors induce apoptosis and reduce CFC output in KCL22^{Pon-Res} cells

To further validate the results from the drug screen and the XTT assays we assessed how the inhibition of the PI3K/AKT/mTOR survival pathway affected the TKI-resistant cell viability following 72 hours of drug treatment by performing apoptosis and long term-survival assays (figure 5-3). The drug concentrations used in the assay were all clinically achievable in patients.

As expected none of the TKIs, imatinib, nilotinib, dasatinib and ponatinib, had an effect on either the induction of apoptotic cell death or the leukaemic colony formation shown from CFC assays (Figure 5-3). The efficacy of the panel of mTOR and PI3K inhibitors was analysed in parallel. Following the 72 hour drug treatment, rapamycin and BKM120 had exerted a very minimal effect on the overall survival of the KCL22^{Pon-Res} cells. However, treatment with the mTORC1 and mTORC2 inhibitor AZD8055 and dual inhibitor, NVP-Bez235, induced apoptosis by 25 and 30%, respectively (Figure 5-3). Although AZD8055 reduced leukaemic colony formation by 50%, NVP-Bez235 had the most significant effect and was able to reduce leukaemic colony forming potential by approximately 66% (Figure 5-3). The efficiency of NVP-Bez235 of inhibiting the PI3K/AKT/mTOR pathway highlights the importance of a complete inhibition of this pathway to switch off pro-survival signals. Complete inhibition of mTOR signalling by NVP-BE235 provided a much more effective treatment against BCR-ABL-independent TKI-resistant CML cells.

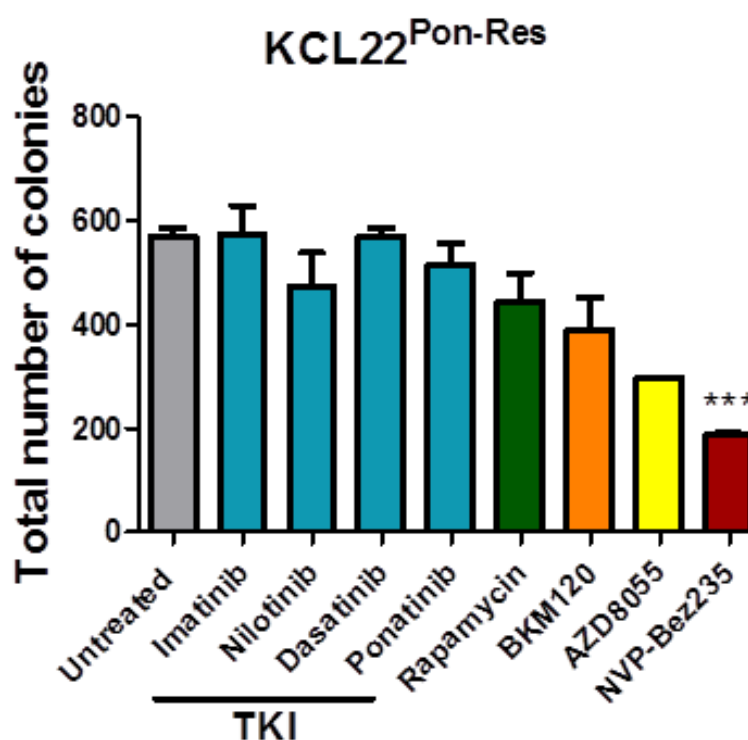
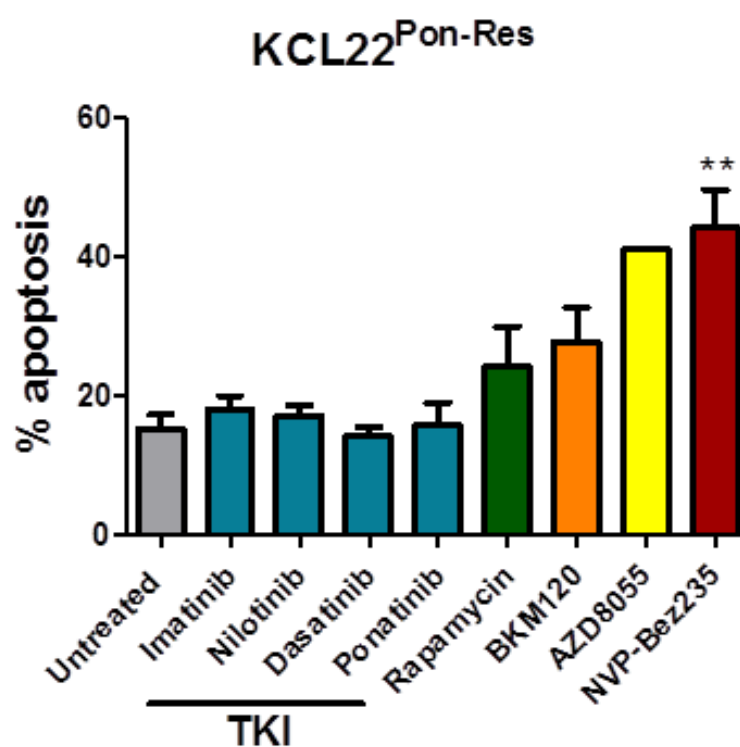


Figure 5-3: KCL22^{Pon-Res} were seeded at 0.25×10^6 / mL and treated with 2 μ M imatinib, 2 μ M nilotinib, 150 nM dasatinib, 100 nM ponatinib, 10 nM rapamycin, 500nM BKM120, AZD8055, 100 nM NVP-Bez235, 100 nM.

The percentage of apoptosis and the colony forming potential were measured following a 72 hour drug treatment. The numbers are presented as mean \pm SEM (n=3). Statistical analysis was performed by using paired t-test. Annotation above a bar refers to statistical significance between the bar and the untreated control. (**; $p \leq 0.01$, ***; $p \leq 0.001$)

5.4 KCL22^{Pon-Res} cells are highly sensitive to catalytic PI3K and mTOR inhibitors

Due to the success of the NVP-Bez235 compound against TKI-resistant cells in our *in vitro* studies, we wanted to validate the NVP-Bez235 effect by testing a further three clinically relevant catalytic dual PI3K and mTOR inhibitors against the KCL22^{Pon-Res} cells. The three new inhibitors are; gedatolisib, apitolisib and VS-5584. All of these inhibitors are currently undergoing investigation in phase I and II clinical trials against numerous blood and solid tumour cancers (table 5-1). Efficacy of these new inhibitors were first tested by XTT assays to gain an understanding of the drug concentration needed to produce half the maximal effective concentration (EC50) (figure 5-4). As it was seen NVP-Bez235, KCL22^{Pon-Res} cells were highly sensitive to all of the catalytic PI3K and mTOR inhibitors. All the EC50s achieved were comparable to that of NVP-Bez235 (EC50: 2.15 nM), gedatolisib; EC50: 0.168 nM, VS-5584; EC50: 1.742 nM and apitolisib; EC50: 29.15 nM. All the inhibitors exerted their inhibitory effects at very low concentration.

Using low nM concentrations of the inhibitors; gedatolisib, apitolisib and VS-5584, and treating the KCL22^{Pon-Res} cells for 72 hours, a significant amount of apoptosis was induced above the untreated cells for all PI3K and mTOR inhibitors. Additionally, VS-5584 and more so NVP-Bez235 and gedatolisib were able to significantly increase apoptotic death of KCL22^{Pon-Res} cells above treatment with TKI, ponatinib 18, 35 and 38% respectively (figure 5-5). In order to validate the mode of action of the catalytic PI3K and mTOR inhibitors in the KCL22 cells, we treated the KCL22^{WT} and KCL22^{Pon-Res} cells with 100 nM ponatinib, as a control, 100 nM NVP-Bez235 and 100 nM gedatolisib and analysed mTOR signalling, through RPS6 phosphorylation and BCR-ABL signalling via the phosphorylation of CRKL. This showed that in TKI sensitive, KCL22^{WT} cells that ponatinib switches off BCR-ABL signalling (no phosphorylated CRKL), which subsequently switches off downstream pathway PI3K/AKT/mTOR signalling, shown by the absence of phosphorylated RPS6. This is the part of the mechanism that induces cell death in TKI-sensitive cells. However, in the KCL22^{Pon-Res} cells, ponatinib inhibits BCR-ABL (no phosphorylated CRKL), but mTOR signalling is still present, RPS6 is phosphorylated and the cells continue to survive and proliferate. Treatment of both the KCL22^{WT} and KCL22^{Pon-Res} cells with NVP-Bez235 and gedatolisib completely inhibits mTOR signalling, as shown by the absence of phosphorylated RPS6. The complete inhibition of this pathway in the KCL22^{Pon-Res} leads to high levels of cellular death as seen in the apoptosis assay (figure 5-5). Therefore, further strengthening the importance of the PI3K/AKT/mTOR pathway for KCL22^{Pon-Res} cell survival. As NVP-Bez235 is the most

highly investigated catalytic dual PI3K and mTOR inhibitor currently on the market and the efficacy seen in the *in vitro* thus far, we focus on this compound in our experiments for the remainder of the study.

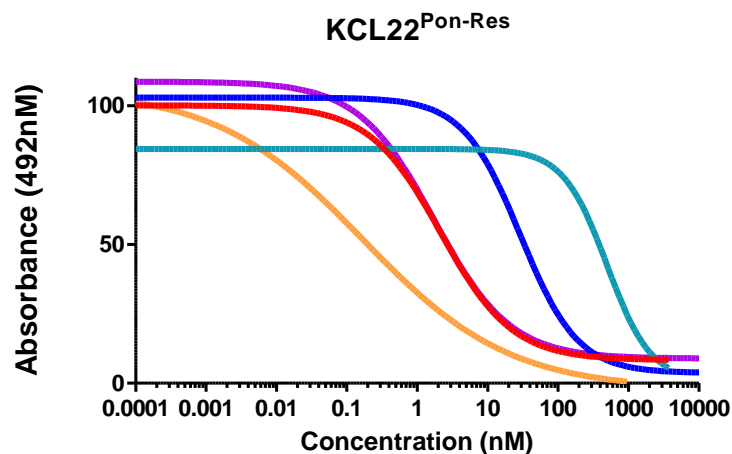


Figure 5-4: KCL22^{Pon-Res} were seeded at 0.2×10^6 / mL and treated with the same equimolar concentration of drug ranging from 0.01 nM to 10 μ M (gedatolisib, VS-5584, NVP-Bez235, apitolisib, and ponatinib). Colour coded by Table 5-1.

Cell viability measured after 72 hours using an XTT assay.

Drug	Company	EC50 (nM)	Phase I Clinical Trials	Phase II Clinical Trials
gedatolisib	Pfizer	0.168	4	1
VS-5584	Verastem	1.742	2	-
NVP-Bez235	Novartis	2.15	10	5
apitolisib	Genentech	29.15	8	4
ponatinib	Ariad	647.3		

Table 5-1: Clinically applicable dual PI3K and mTOR inhibitors. The drug name, name of pharmaceutical company developing the drug, EC50 (nM) in KCL22^{Pon-Res} cells calculated by graphpad from (figure 5-4) and the number of phase I and II clinical trials the drug is currently involved in. as shown on clinicaltrials.gov.

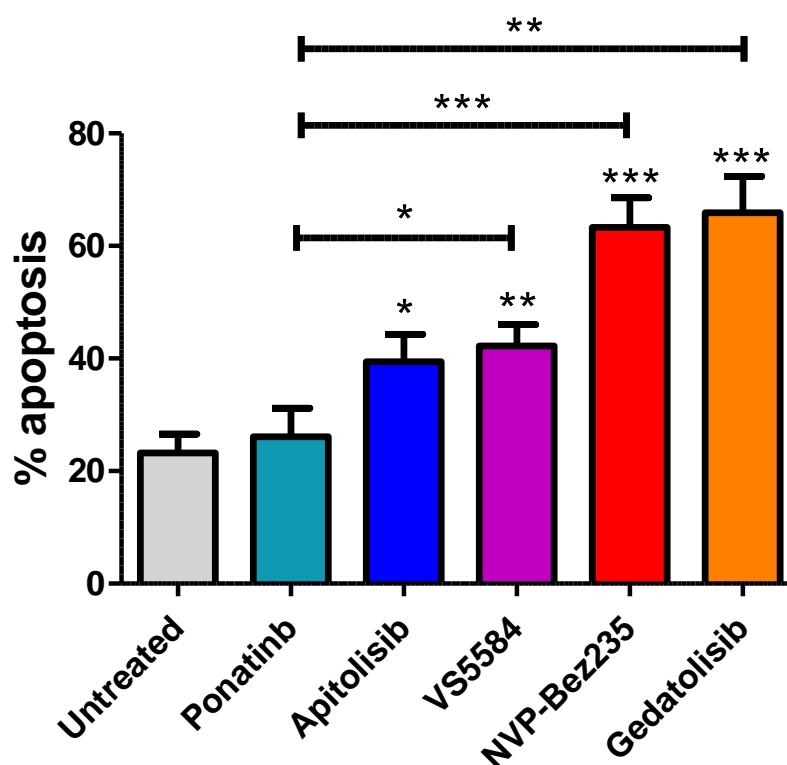


Figure 5-5: KCL22^{Pon-Res} were seeded at 0.25×10^6 /mL and treated with 100 nM ponatinib, 100 nM apitolisib, 100 nM VS-5584, 100 nM NVP-Bez235, 100 nM gedatolisib for 72 hours.

Following treatment, the level of apoptosis induced was analysed by flow cytometry. The histogram represents early and late apoptosis and numbers are presented as mean \pm SEM (n=3). Statistical analysis was performed by using paired t-test. Annotation above a bar refers to statistical significance between the bar and the untreated control (*; p \leq 0.05, **; p \leq 0.01, ***; p \leq 0.001).

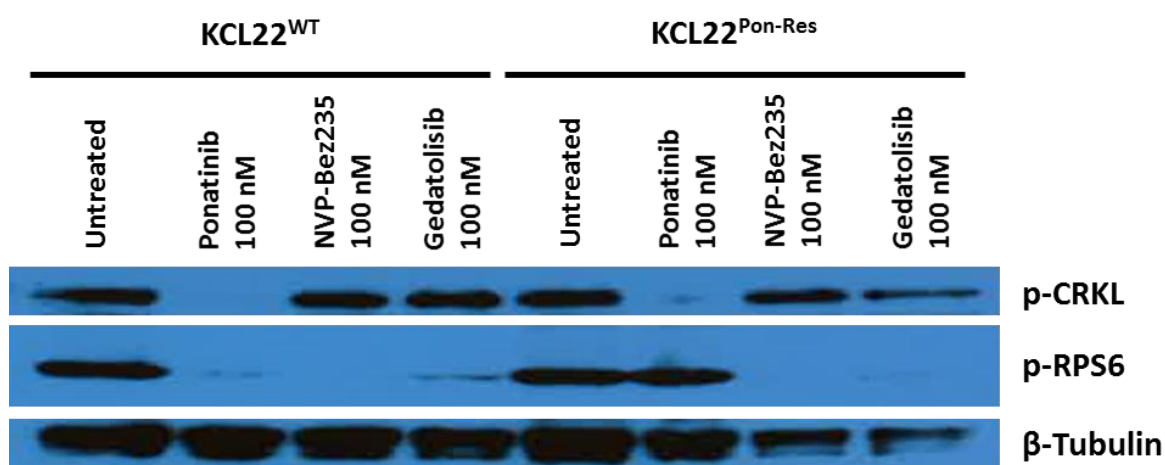


Figure 5-6: KCL22^{WT} and KCL22^{Pon-Res} were seeded at 0.25×10^6 /mL and treated with and 100 nM ponatinib, 100 nM NVP-Bez235 or 100 nM gedatolisib for 24 hours.

Western blot analysis assessed the activity of BCR-ABL shown by phosphorylation of CRKL and mTOR activity shown by the phosphorylation of RPS6.

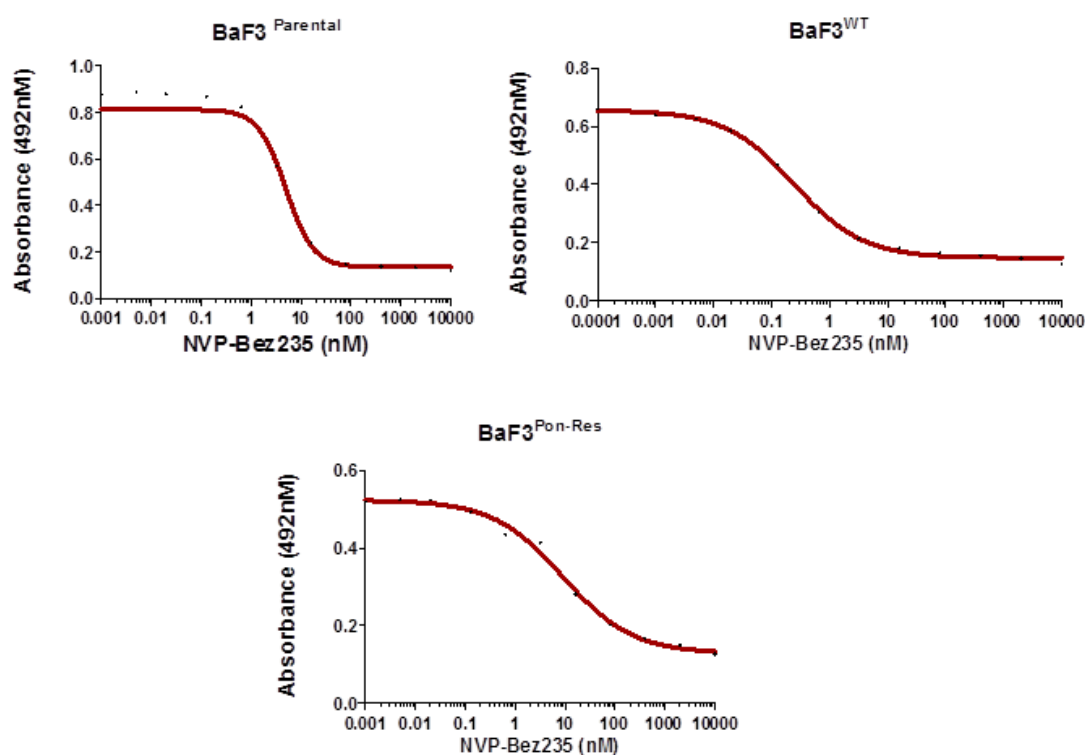
5.5 BaF3^{Pon-Res} cells are highly sensitive to NVP-Bez235

The efficacy of dual PI3K and mTOR inhibitor; NVP-Bez235 was validated in the BaF3^{Pon-Res} cell model. Previous experiments showed that NVP-Bez235 was the most effective mTOR drug against KCL22^{Pon-Res} cells, which is likely due to inhibition of both mTOR complexes and PI3K. This should inhibit any regulatory feedback loops within the pathway and results in a complete inhibition of PI3K/AKT/mTOR signalling.

In order to gain further insight into the NVP-Bez235 effect on BaF3^{Pon-Res} cell viability an XTT assay was performed and EC50s calculated. This experiment was performed on both the original BaF3^{WT} and BaF3^{Pon-Res} cells to establish whether sensitivity to mTOR inhibition was a trait gained in the generation of the ponatinib-resistant cell line, or if the original BaF3^{WT} cells, which are TKI sensitive, were also sensitive to NVP-Bez235 treatment. As shown previously, BaF3^{WT} cells were highly sensitive to ponatinib treatment with an EC50 of 0.0002 nM and the BaF3^{Pon-Res} cells were much more resistant with an EC50 of 1.598 µM (figure 5-7). The BaF3^{WT} cells also showed some sensitivity to NVP-Bez235 treatment, however NVP-Bez235 (EC50:0.24 nM) was not as effective as ponatinib (EC50:0.0002 nM) (figure 5-7 and 3-5).

Most importantly, BaF3^{Pon-Res} cells retain their sensitivity to the NVP-Bez235 compound with an EC50: 8.971 nM compared to 1.598 µM with ponatinib, which is an unachievable concentration for patient treatment. The increased concentration of NVP-Bez235 needed to achieve an EC50 increased from 0.24 nM in BaF3^{WT} cells to 8.971 nM in BaF3^{Pon-Res} cells, which may imply increased activation of mTOR signalling in the BaF3^{Pon-Res} cells.

In parallel with the XTT assay, following 72 hours of treatment, NVP-Bez235 also induced a considerable amount of apoptosis in both BaF3^{WT} cells and BaF3^{Pon-Res} cells of 70 and 60%, respectively. The original BaF3^{WT} cells remain most sensitive to TKI treatment, due to their BCR-ABL dependency. Apoptosis levels achieved with imatinib were 45%, dasatinib 78% and ponatinib 75%. The BaF3^{Pon-Res} cells lost their sensitivity to all TKIs tested as the level of apoptosis achieved was equal or less than the untreated cells (figure 5-8). However, the BaF3^{Pon-Res} cells retained their sensitivity to the inhibition of PI3K/AKT/mTOR.



Cell Type	Drug	EC50 (nM)
BaF3 ^{Parental}	NVP-Bez235	4.935
BaF3 ^{WT}	NVP-Bez235	0.2435
BaF3 ^{Pon-Res}	NVP-Bez235	8.971

Figure 5-7: (a) BaF3^{WT} and BaF3^{Pon-Res} were seeded at 0.2×10^6 / mL and treated with the same equimolar concentration of drug ranging from 0.01 nM to 10 μ M (ponatinib and NVP-Bez235). Cell viability measured after 72 hours using an XTT assay and (b) EC50 was calculated using graphpad prism.

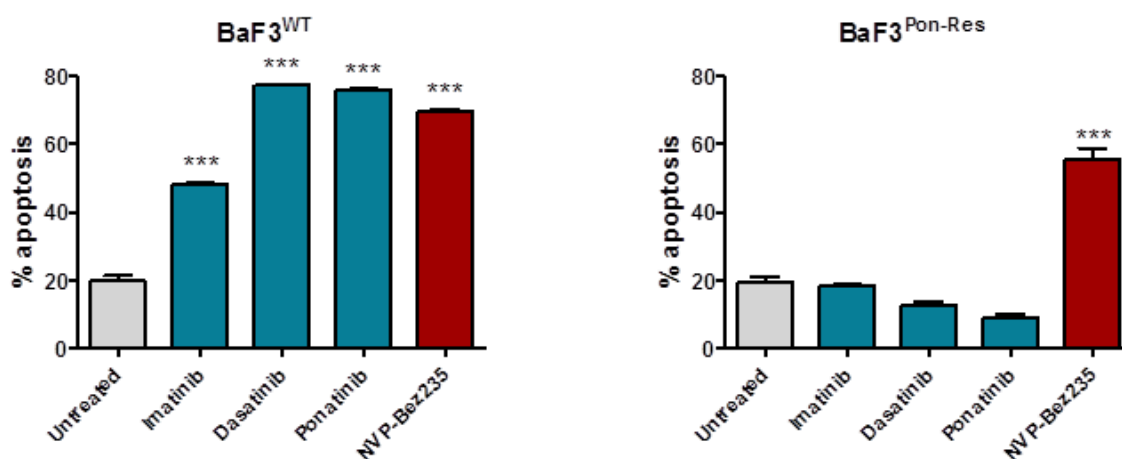


Figure 5-8: BaF3^{WT} and BaF3^{Pon-Res} were seeded at 0.25x10⁶/ mL and treated with 2 μ M imatinib, 150 nM dasatinib, 100 nM ponatinib or 100 nM NVP-Bez235.

The percentage of apoptosis was measured following a 72 hour drug treatment. The histogram represents early and late apoptosis and numbers are presented as mean \pm SEM (n=3). Statistical analysis was performed by using paired t-test. Annotation above a bar refers to statistical significance between the bar and the untreated control (***, p \leq 0.001).

5.6 KCL22^{Pon-Res} cells transcriptional response is restored upon NVP-Bez235 treatment

To gain further insight into how mTOR inhibition induces cell death in BCR-ABL-independent TKI-resistant CML we performed RNA-seq using KCL22^{WT} and KCL22^{Pon-Res} cells. The cells were treated with 100 nM NVP-Bez235 with or without the combination of 100 nM ponatinib for 24 hours, to switch off mTOR and BCR-ABL signalling. Inhibition of BCR-ABL by ponatinib treatment had no effect on the KCL22^{Pon-Res} cells transcriptionally (figure 3-10), however, treatment with NVP-Bez235 caused a large number of transcriptional changes in genes up-regulated and down-regulated, similar to that number of the number of genes regulated in the KCL22^{WT} cells following ponatinib treatment (figure 5-9).

Of the 5 genes which were upregulated in response to ponatinib treatment, all 5 overlapped with the response to NVP-Bez235 treatment, which may imply these transcriptional changes were not ponatinib mediated BCR-ABL inhibition specific and occur in the response to any drug treatment or are artifacts from the experimental method.

However, the combination treatment of NVP-Bez235 and ponatinib did not enhance the NVP-Bez235 effect, as seen in the volcano plot (figure 5-9). The Venn diagram shows that 1039 (~88%) genes from the NVP-Bez235 only and the combination treatment overlap (figure 5-9), with only just over 10% of genes being upregulated by NVP-Bez235 treatment alone and 10% with the combination treatment.

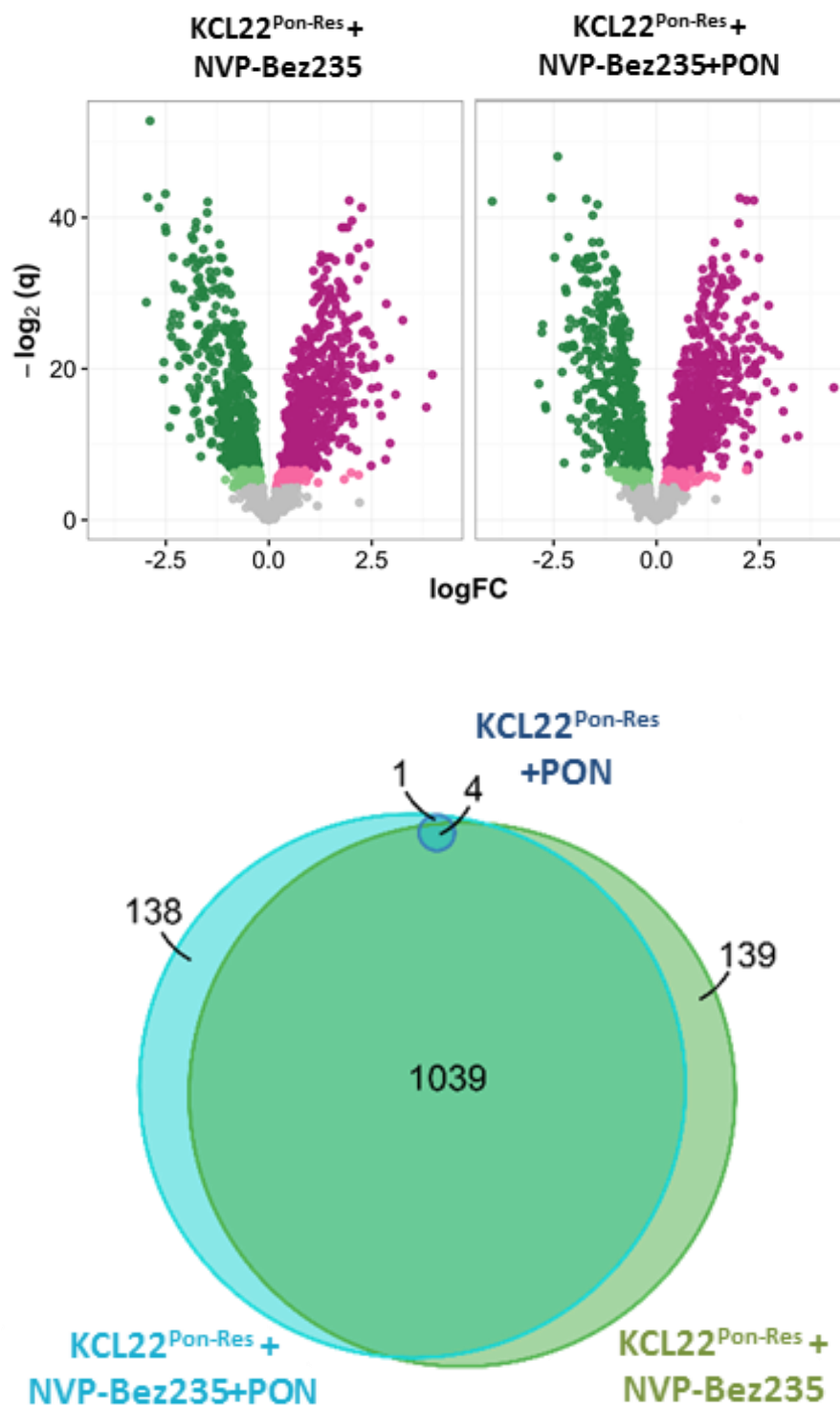


Figure 5-9: A volcano plot showing the fold changes in gene expression patterns in KCL22^{Pon-Res} cells following 24 hour NVP-Bez235 treatment or a combination treatment of NVP-Bez235 and ponatinib, down-regulated genes in green and up-regulated genes in pink.

Venn diagram showing the differential gene expression changes between 3 scenarios; KCL22^{Pon-Res} cells following 24 hour ponatinib treatment, KCL22^{Pon-Res} cells following 24 hour NVP-Bez235 treatment and KCL22^{Pon-Res} cells following a 24 hour combination treatment of NVP-Bez235 and ponatinib.

In a comparison between KCL22^{WT} cells treated with ponatinib and KCL22^{Pon-Res} cells treated with NVP-Bez235, the majority of transcription changes that occurred in the KCL22^{WT} cells following ponatinib mediated BCR-ABL inhibition also occurred in the KCL22^{Pon-Res} cells following NVP-Bez235 mediated mTOR inhibition. Although more transcriptional changes occurred following NVP-Bez235 treatment in KCL22^{Pon-Res} cells, the proportion of overlap implies that NVP-Bez235 triggers a similar transcriptional response as ponatinib does in TKI sensitive cells (figure 5-10). This was corroborated by statistical analysis of the linear correlation between gene expression changes in ponatinib treated KCL22^{WT} and the NVP-Bez235 treated KCL22^{Pon-Res} cells. This showed a correlation (r) = 0.78, which means there was a meaningful positive linear association that was statistically significant. Again the importance of mTOR was highlighted in CML when further analysis showed that KCL22^{WT} cells treated with NVP-Bez235 had a very similar transcriptional response as ponatinib treated KCL22^{WT} and the NVP-Bez235 treated KCL22^{Pon-Res} cells (figure 5-10), further demonstrating that targeting mTOR downstream of BCR-ABL can rescue the impaired transcription response seen in TKI-resistant cells following TKI treatment. Analysis of the KCL22^{Pon-Res} cells treated with both NVP-Bez235 and ponatinib revealed very few additional gene changes compared to the NVP-Bez235 only treated cells. (figure 5-11) (Bioinformatics performed by Graham Hamilton and Lisa Hopcroft).

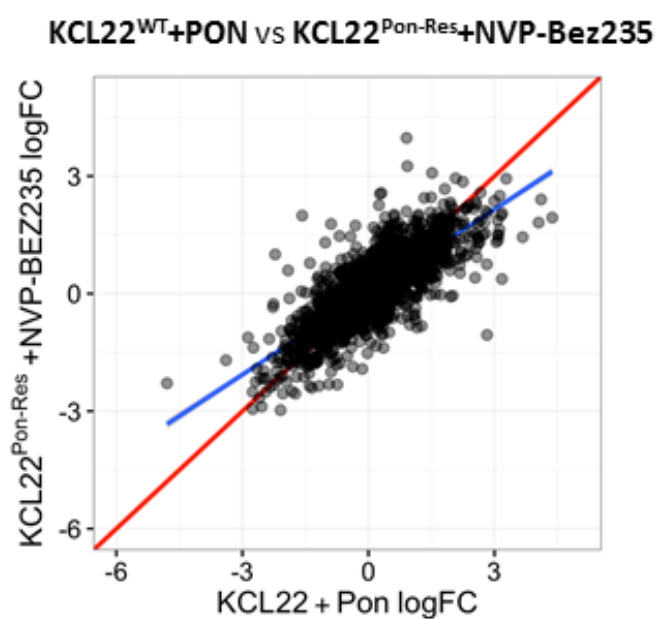
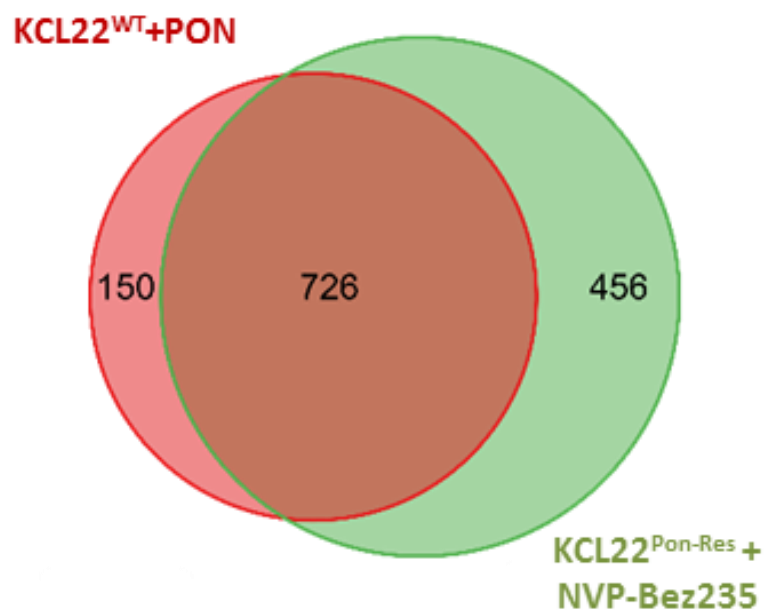


Figure 5-10: (a) Venn diagram showing the differential gene expression changes between KCL22^{WT} following 24 hour ponatinib treatment and KCL22^{Pon-Res} cells following 24 hour NVP-Bez235 treatment and (b) Relative correlation comparison of log changes in gene expression.

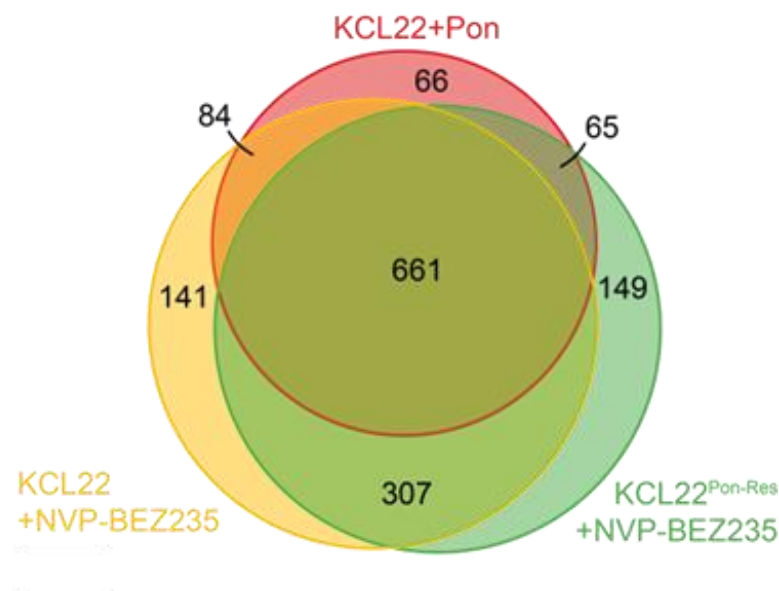


Figure 5-11: Venn diagram showing the comparison of the differential gene expression changes between KCL22^{WT} following 24 hour ponatinib treatment, KCL22^{WT} following 24 hour NVP-Bez235 treatment and KCL22^{Pon-Res} cells following 24 hour NVP-Bez235 treatment.

As many of the transcriptional changes that occurred in the KCL22^{WT} cells treated with ponatinib also occurred in the KCL22^{Pon-Res} cells treated with NVP-Bez235, we were interested to establish whether the same pathways were being induced by NVP-Bez235 in the KCL22^{Pon-Res} cells as ponatinib did in the KCL22^{WT} cells.

Gene ontology enrichment analysis was performed, in which the genes of interest are assigned to predefined biological processes depending on their functional characteristics. Of the transcriptional changes that occurred in the KCL22^{WT} cells treated with ponatinib, which also overlapped with the KCL22^{Pon-Res} treated with NVP-Bez235 only 6 biological processes were significantly up-regulated. These processes were involved in apoptosis, DNA damage repair and cellular response to stress. These biological processes are all pathways expected to be induced following cytotoxic drug treatment. However, 54 additional biological processes that were up-regulated only in the KCL22^{Pon-Res} cells treated with NVP-Bez235, which were processes associated with protein translation and metabolism (Table 5-2). The induction of these processes would be expected due to the NVP-Bez235 mediated inhibition of mTOR. The difference in biological processes upregulated in the two different cell lines seems heavily dependent on the MOA of the drugs; ponatinib and NVP-Bez235, as TKIs and mTOR inhibitors have different targets. Although, TKIs do inhibit mTOR indirectly, which may account for the lack of differential biological processes upregulated in the KCL22^{WT} cells treated with ponatinib compared to the KCL22^{Pon-Res} cells treated with NVP-Bez235. The additional biological processes enriched in the KCL22^{Pon-Res} cells treated with NVP-Bez235 must be mTOR inhibition specific.

<i>Sample</i>	<i>Biological Processes</i>
<p>KCL22^{WT}+PON and KCL22^{Pon-Res}+Bez</p>	<p>Execution phase of apoptosis Cellular component disassembly involved in the execution of apoptosis Double-strand break repair via homologous recombination Recombinational repair DNA repair Cellular response to stress</p>
<p>KCL22^{Pon-Res}+Bez</p>	<p>Nuclear-transcribed mRNA catabolic process, nonsense-mediated decay Translational elongation Protein localization to endoplasmic reticulum Translational termination Establishment of protein localization to endoplasmic reticulum Cotranslational protein targeting to membrane SRP-dependent cotranslational protein targeting to membrane Protein targeting to ER Translational initiation Protein targeting to membrane Nuclear-transcribed mRNA catabolic process mRNA catabolic process Viral gene expression Cellular protein complex disassembly Multi-organism metabolic process Viral transcription Amide biosynthetic process Translation Peptide biosynthetic process RNA catabolic process Protein complex disassembly Peptide metabolic process</p>

Establishment of protein localization to membrane
 Macromolecular complex disassembly
 Establishment of protein localization to organelle
 Cellular amide metabolic process
 Protein transport
 Protein localization
 Protein targeting
 Protein localization to organelle
 Organonitrogen compound biosynthetic process
 Macromolecule localization
 Viral life cycle
 Protein localization to membrane
 Organic substance transport
 Establishment of protein localization
 Protein complex subunit organization
 Cytoplasmic transport
 Intracellular protein transport
 Membrane organization
 Single-organism membrane organization
 Nucleobase-containing compound catabolic process
 Aromatic compound catabolic process
 Heterocycle catabolic process
 Organic cyclic compound catabolic process
 Single-organism cellular localization
 Cellular nitrogen compound catabolic process
 Cellular protein localization
 Cellular macromolecule localization
 Cytoplasmic translation
 Macromolecular complex subunit organization
 Cellular localization
 Establishment of localization in cell
 Transport

Table 5-2: A list of the different biological processes that occur in KCL22^{Pon-Res} cells following 24 hour NVP-Bez235 treatment and KCL22^{WT} following 24 hour ponatinib treatment obtained from the gene ontology enrichment analysis.

5.7 Key findings

In this chapter we tested clinically relevant PI3K and mTOR inhibitors against ponatinib resistant cell lines to establish the most effective drug target against this pathway. We tested several different inhibitors including, BKM120, a catalytic inhibitor for class IA PI3Ks, rapamycin, a mTORC1 only allosteric inhibitor, AZD8055, a catalytic inhibitor that targets mTORC1 and mTORC2 complexes of mTOR and NVP-Bez235, a catalytic mTOR inhibitor that inhibits both mTOR complexes and also has strong activity against all PI3K isoforms (figure 5-1).

Through different types of cell viability assays we identified the catalytic dual PI3K and mTOR inhibitor, NVP-Bez235 as the most effective drug at inducing apoptosis and reducing cell viability in ponatinib resistant CML cells. This was validated by testing a further three clinically relevant dual PI3K and mTOR inhibitors; gedatolisib, apitolisib and VS-5584. Both NVP-Bez235 and gedatolisib induced significant amounts of apoptosis in the KCL22^{Pon-Res} cells and despite not effecting BCR-ABL signalling they did switch off mTOR signalling, which we saw with the inhibition of phosphorylated RPS6 by western blotting.

Also, importantly we show through RNA-seq analysis that a transcriptional response is restored in the KCL22^{Pon-Res} cells upon treatment with NVP-Bez235 and that this response to mTOR inhibition caused very similar gene transcription changes as ponatinib does to TKI sensitive CML cells, KCL22^{WT} cells. The data from this chapter thereby, increases the evidence that the PI3K/AKT/mTOR pathway is important for BCR-ABL independent TKI resistant CML cell survival.

6 Results (IV): Validation of mTOR inhibitors in primary TKI-resistant CML cells

6.1 Aim and objective

- V. Validation of mTOR inhibitors in primary TKI-resistant CML cells.

6.2 MNCs derived from TKI-resistant CML patients are sensitive to NVP-Bez235-mediated mTOR inhibition *ex vivo*

In order to test the predictive value of our cell line model we investigated whether mTOR inhibition would also target CML cells from patients known to have BCR-ABL-independent TKI-resistant CML. To do this, bone marrow was collected from three patients who had failed to achieve a CCyR despite treatment with 1st, 2nd and 3rd generation TKIs. The MNCs were extracted from the samples and the effects of TKIs and catalytic mTOR inhibitors were analysed. The cells were treated with the TKIs imatinib or ponatinib, and mTOR inhibitors; AZD8055, BKM120 and NVP-Bez235 for 72 hours and apoptosis and the colony forming potential of progenitor cells were analysed.

Importantly, mTOR inhibition mediated by treatment with AZD8055 and more potently NVP-Bez235 had a significant effect on the survival of the progenitor cells from these patients. In all 3 patients NVP-Bez235 caused an induction of apoptosis, which was increased by 12-22% above that of untreated or TKI treated cells. The most dramatic results were seen in the reduction in the potential of colony formation following drug treatment.

Although the patients have been clinically diagnosed as TKI-resistant and have failed to achieve a CCyR with ponatinib treatment, as there are no alternative treatments the patients are currently being treated with ponatinib, which has at least enabled a haematological response. The partial response to ponatinib may explain the slight reduction in colony formation in the cells treated with TKIs imatinib and ponatinib. However, NVP-Bez235 mediated mTOR inhibition had the greatest affect at reducing colony numbers.

NVP-Bez235 treatment on MNCs derived from TKI-resistant CML patients 1 and 3 significantly reduced colony formation by 63 and 88%, respectively. Data from patient 1 also showed a significant decrease, 83%, in colony numbers compared to ponatinib treatment (figure 6-1). The data from the two different cell lines and more importantly the

patient samples demonstrate just how important the PI3K/AKT/mTOR pathway is for TKI-resistant CML cellular survival.

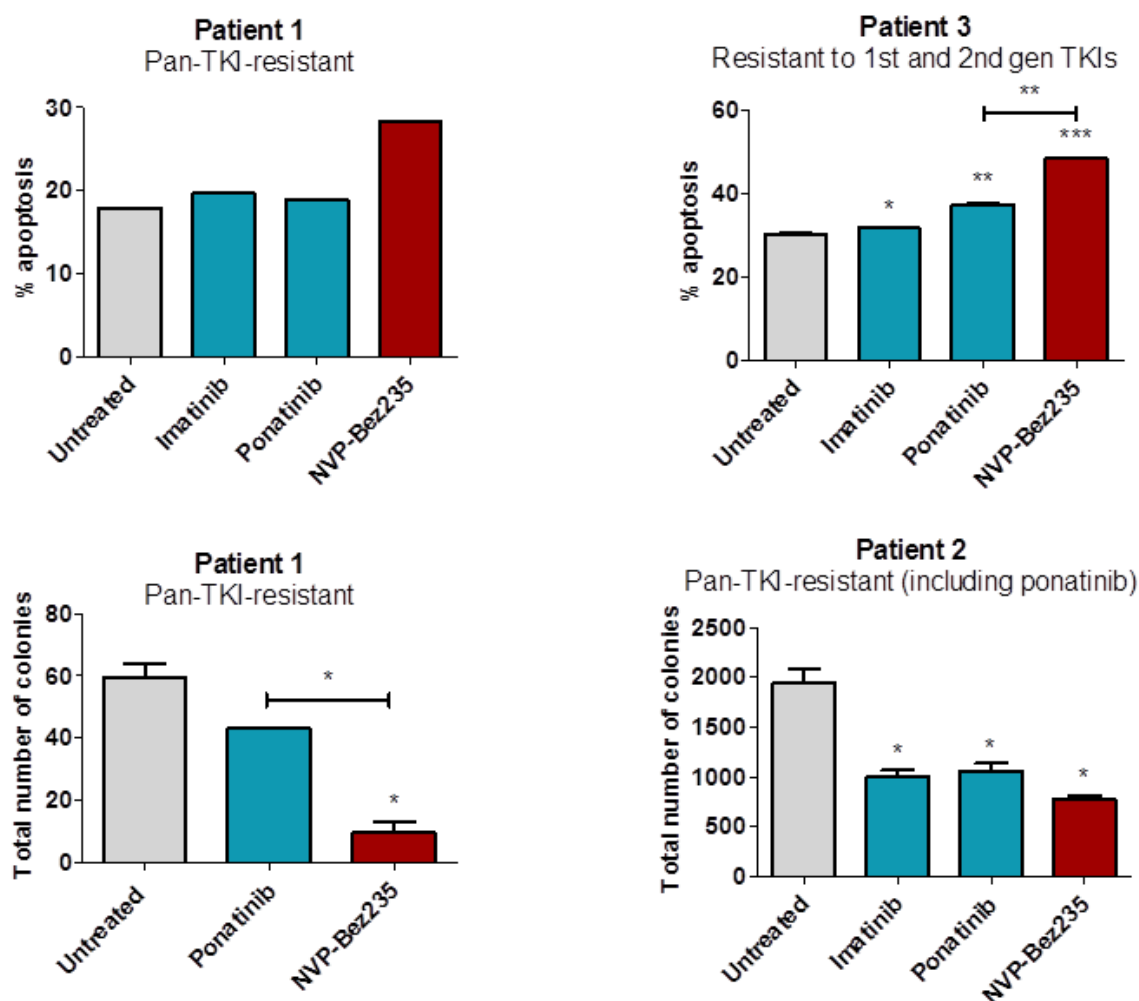


Figure 6-1: Bone marrow and peripheral blood derived MNCs from TKI-resistant CML patients were cultured in SFM supplemented with physiological growth factors.

Cells were treated with 2 μ M imatinib, 100 nM ponatinib and 100 nM NVP-Bez235 and the apoptosis and colony forming potential were measured following a 72 hour drug treatment. $n=2$ patients. The histogram numbers are presented as mean \pm SEM. Statistical analysis was performed by using paired t-test. Annotation above a bar refers to statistical significance between the bar and the untreated control (*; $p \leq 0.05$, **; $p \leq 0.01$, ***; $p \leq 0.001$).

Clinical patient information	
Patient 1	Resistant to two TKIs. The patient was ponatinib naïve at the time the sample was taken, with no known kinase domain mutation
Patient 2	No response to imatinib. Dasatinib started 2006. Ponatinib since 2011 (PACE trial). No CCyR or MMR on ponatinib.
Patient 3	Dasatinib and nilotinib failure. Achieved CHR but no CYR on ponatinib.
Patient 4	CHR but not CyR on imatinib. Dasatinib started 2007. BCR-ABL 16% in July 2013.

Table 6-1: Clinical patient informations. Details of prior treatments, clinical trials and treatment responses.

6.3 Ponatinib is an effective treatment against BCR-ABL-dependent TKI-resistant CML cells

To allow us to compare treatment regimens between patients harbouring a BCR-ABL-dependent mechanism of TKI-resistant CML or patients with a BCR-ABL-independent mechanism of TKI-resistant CML, we collected bone marrow samples from two patients, clinically confirmed to have the BCR-ABL T315I mutation. These patients therefore have a BCR-ABL-dependent mechanism of TKI-resistant CML. These cells were treated with TKIs; dasatinib or ponatinib and mTOR inhibitor, NVP-Bez235 for 72 hours or 6 days. Following drug treatment, the cells were assessed for the induction of apoptosis and their colony forming potential in a CFC assay. As expected 2nd generation TKI, dasatinib had no effect on the T315I samples, as the drug is not able to bind and inhibit BCR-ABL. However, ponatinib, which was designed to target CML cells with the BCR-ABL T315I mutation, induced apoptosis by 10% within 72 hours and to 20% after 6 days of treatment. mTOR inhibition by NVP-Bez235 treatment induced a similar apoptotic response and reduction in colony formation to ponatinib. However, although the response to ponatinib and NVP-Bez235 was similar in both samples, the treatment with ponatinib was more significant statistically, which highlights that TKIs are the most effective treatment for patients suffering from a BCR-ABL-dependent form of TKI-resistant CML.

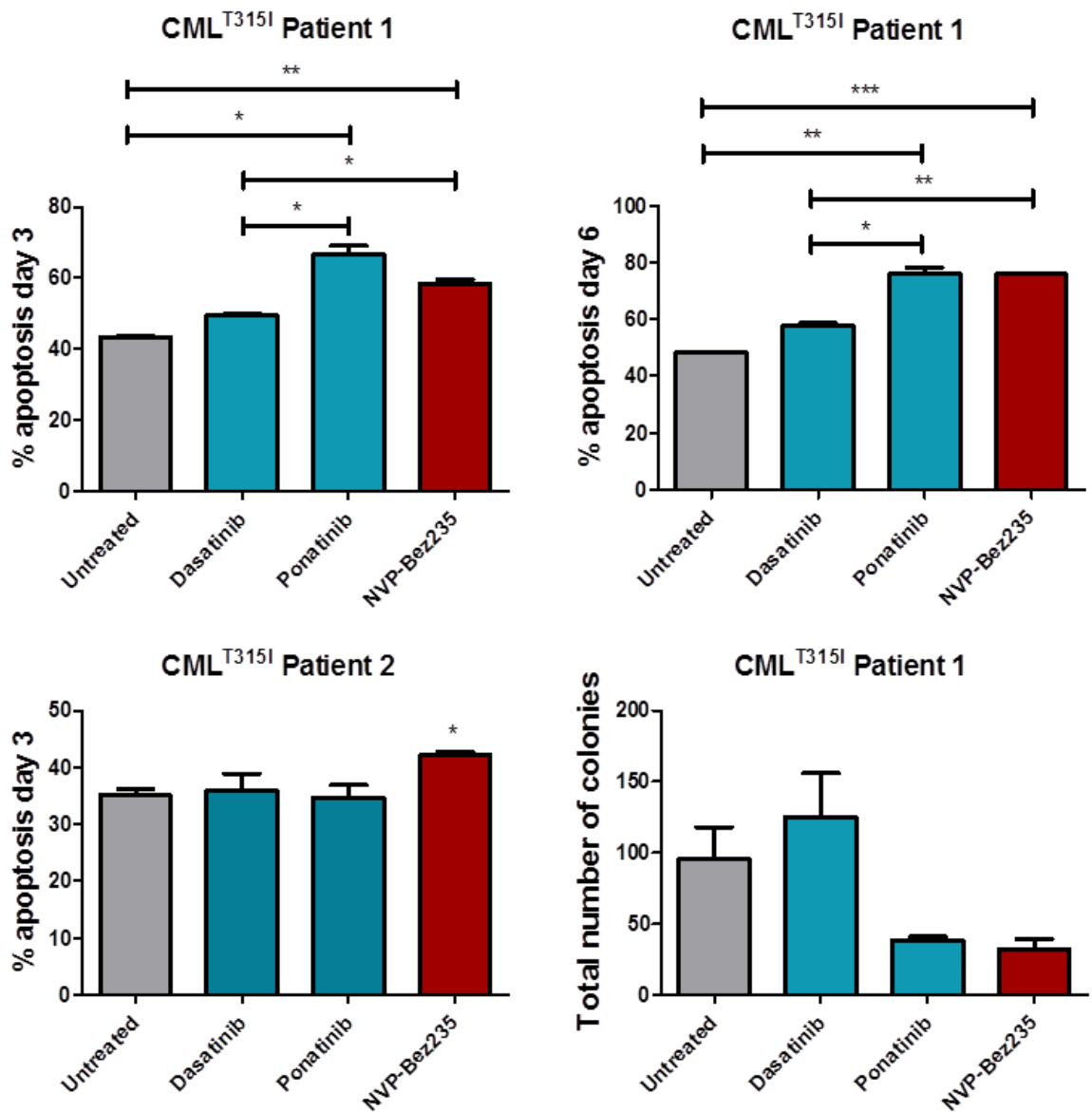


Figure 6-2: Bone marrow and peripheral blood derived MNCs from CML patients carrying the T315I mutation.

The cells were cultured in SFM supplemented with physiological growth factors and treated with 150 nM dasatinib, 100 nM ponatinib and 100 nM NVP-Bez235 and the apoptosis and colony forming potential were measured following a 72 hour or 6 days of drug treatment. n=2 patients. The histogram numbers are presented as mean±SEM. Statistical analysis was performed by using paired t-test. Annotation above a bar refers to statistical significance between the bar and the untreated control (*; p≤0.05, **; p≤0.01, ***; p≤0.001).

6.4 Ponatinib treatment causes different transcriptional responses in TKI sensitive CML, T315I CML and BCR-ABL-independent TKI-resistant CML

Access to primary samples gave us a cellular tool to investigate BCR-ABL-independent mechanisms of TKI-resistant in current patients CML cells. Although the experiments are performed in an ex vivo environment the response would much closer mimic what happens to CML cells in patients. However due to the rarity and limited size of these samples we were restricted in the type of experiments that could be conducted. However, one screening method which was possible was RNA-seq. By performing RNA-seq this allowed us to identify potential gene transcriptional changes which may enable us to decipher potential mechanism(s) of BCR-ABL-independent TKI resistance. We performed this experiment by analysing 3 different CML patient groups (1) TKI sensitive, (2) BCR-ABL-dependent TKI-resistant; T315I mutation, (3) BCR-ABL-independent TKI-resistant. Bone marrow was collected from these patients and the MNCS were isolated. The cells were untreated or ponatinib treated for 24 hours to switch off BCR-ABL signalling and subsequently RNA was generated from the samples. BCR-ABL was switched off in the different sample types to gain an understanding what additional transcriptional changes, if any, occur in the BCR-ABL-independent TKI-resistant samples to allow the continued survival and proliferation despite BCR-ABL inhibition. Three samples were obtained from each patient group, except T315I patients, which has two. Analysis of the gene transcriptional changes from the 3 groups showed subtle changes in all groups. The volcano plots for each of the three groups showed very low magnitude fold changes in genes up-regulated and down-regulated (figure 6-2). Gene transcription changes were then compared in all 3 groups following ponatinib mediated BCR-ABL inhibition. This revealed that the response in each group was vastly different, with the majority of gene changes occurring being specific to that patient group, with very little overlap between each group (figure 6-3). Although only a low magnitude of gene expression changes occurred in the CML TKI-resistant cells, the level of transcriptional response was comparable to the ponatinib sensitive cells; CML TKI sensitive and CML T315I samples, which was inconsistent with the cell line data which showed KCL22^{Pon-Res} cells have an impaired transcriptional response following 24 hour ponatinib treatment (figure 3-10).

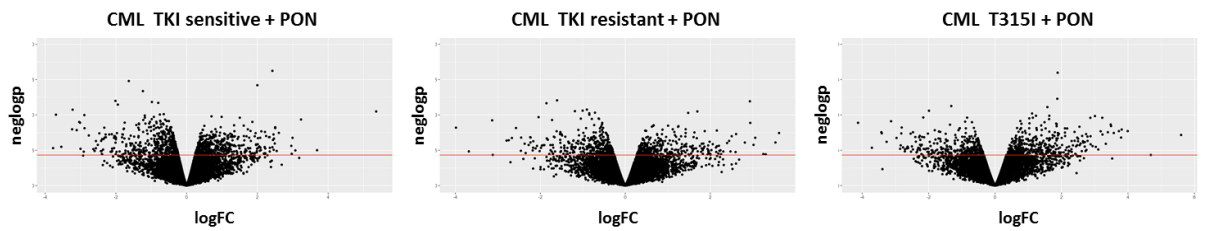


Figure 6-3: Volcano plots showing the fold changes in gene expression patterns in TKI sensitive CML cells, BCR-ABL-independent TKI-resistant CML cells and T315I CML cells following 24 hour ponatinib treatment, down-regulated genes (left) and up-regulated genes (right).

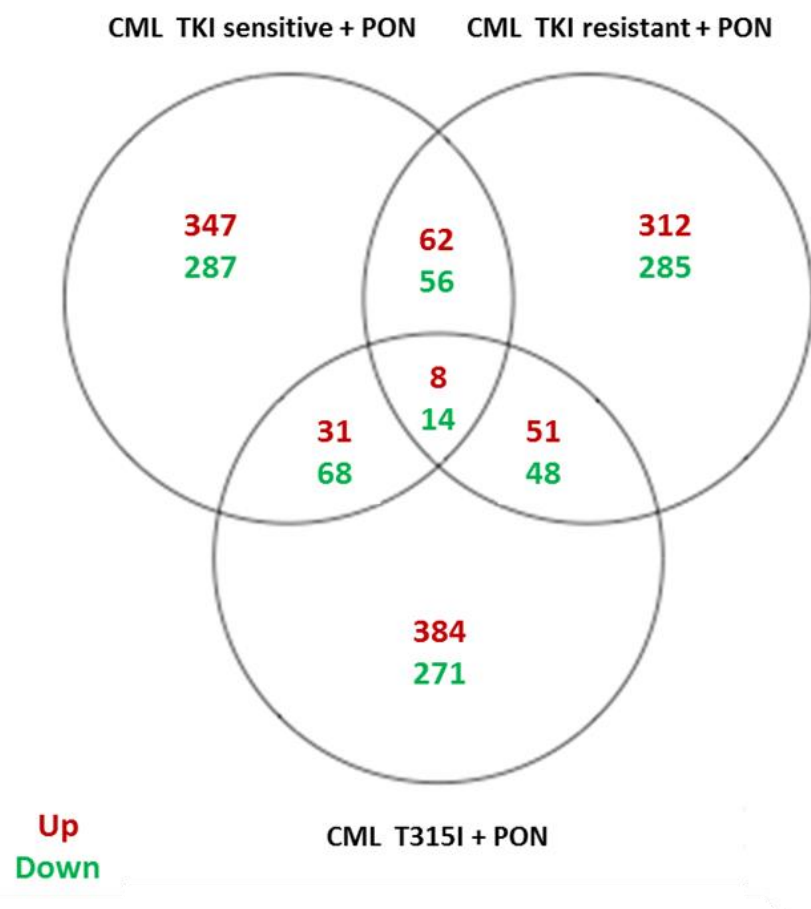


Figure 6-4: Venn diagram showing the differential gene expression changes between TKI sensitive CML cells, BCR-ABL-independent TKI-resistant CML cells and T315I CML cells following 24 hours ponatinib treatment. Genes up-regulated in red and genes down-regulated in green.

Despite the disparity in the transcriptional changes between groups gene ontology enrichment analysis was performed to assess whether there was an overlap in the biological processes regulated in the cells following ponatinib treatment.

Analysis of gene ontology from data gathered from the BCR-ABL-independent TKI-resistant CML cell samples significantly upregulate many biological processes following ponatinib treatment. These processes included multicellular processes, cell to cell signalling, signal transduction, G-coupled receptor signalling, ion transportation and cell adhesion. Also one of the processes was 'response to stimulus' which implies the cells may sense the cytotoxic ponatinib treatment, but have the mechanisms to overcome treatment and evade cell death (figure 6-4).

To understand if TKI-resistant CML cells upregulated different biological processes for their survival against TKI a comparison was made between TKI sensitive CML and TKI-resistant CML following ponatinib treatment. This revealed that the majority of biological processes that are activated in the TKI-resistant cells are also activated TKI sensitive CML group. Only four biological processes differed despite the differences in gene transcription between the two sample groups (figure 6-5 and table 6-2). However, the TKI-resistant CML group had 35 biological processes that were regulated that were not used by the TKI sensitive CML sample group, these additional processes may account for the survival of the TKI-resistant CML cells.

In order to identify the differences between a BCR-ABL-dependent TKI-resistant cells and BCR-ABL-independent TKI-resistant cells, the same comparison was made between the CML T315I group and the TKI-resistant CML following ponatinib treatment. This analysis revealed that 22 biological processes were regulated in the CML T315I group that were different to the TKI-resistant CML group. These biological processes included; growth factor activity, locomotion, movement of cell or subcellular component, differentiation, ion transport and regulation of cell proliferation. Similarly, 22 biological processes were regulated in the TKI-resistant CML group in response to ponatinib that differed from the CML T315I group. These included; antigen binding, cellular response to stimulus, G-protein coupled receptor binding, G-protein coupled receptor signalling pathway, ligand-gated ion channel activity, positive regulation of cell adhesion, regulation of ion transport, regulation of localization, regulation of secretion and signal transduction. Therefore, implying that mechanistically the biological processes used by the CML T315I (BCR-ABL-dependent TKI-resistant cells and TKI-resistant CML (BCR-ABL-independent TKI-resistant cells) are vastly different, although small similarities did occur, grey dots in (figure 6-6 and table 6-3).

Although small changes had occurred between the patient groups, the low magnitude of transcriptional changes and the level of disparity have left the results from these experiments inconclusive. This is most possibly due to the cell heterogeneity within the MNC population, which has “masked” the effect of the TKI treatment.

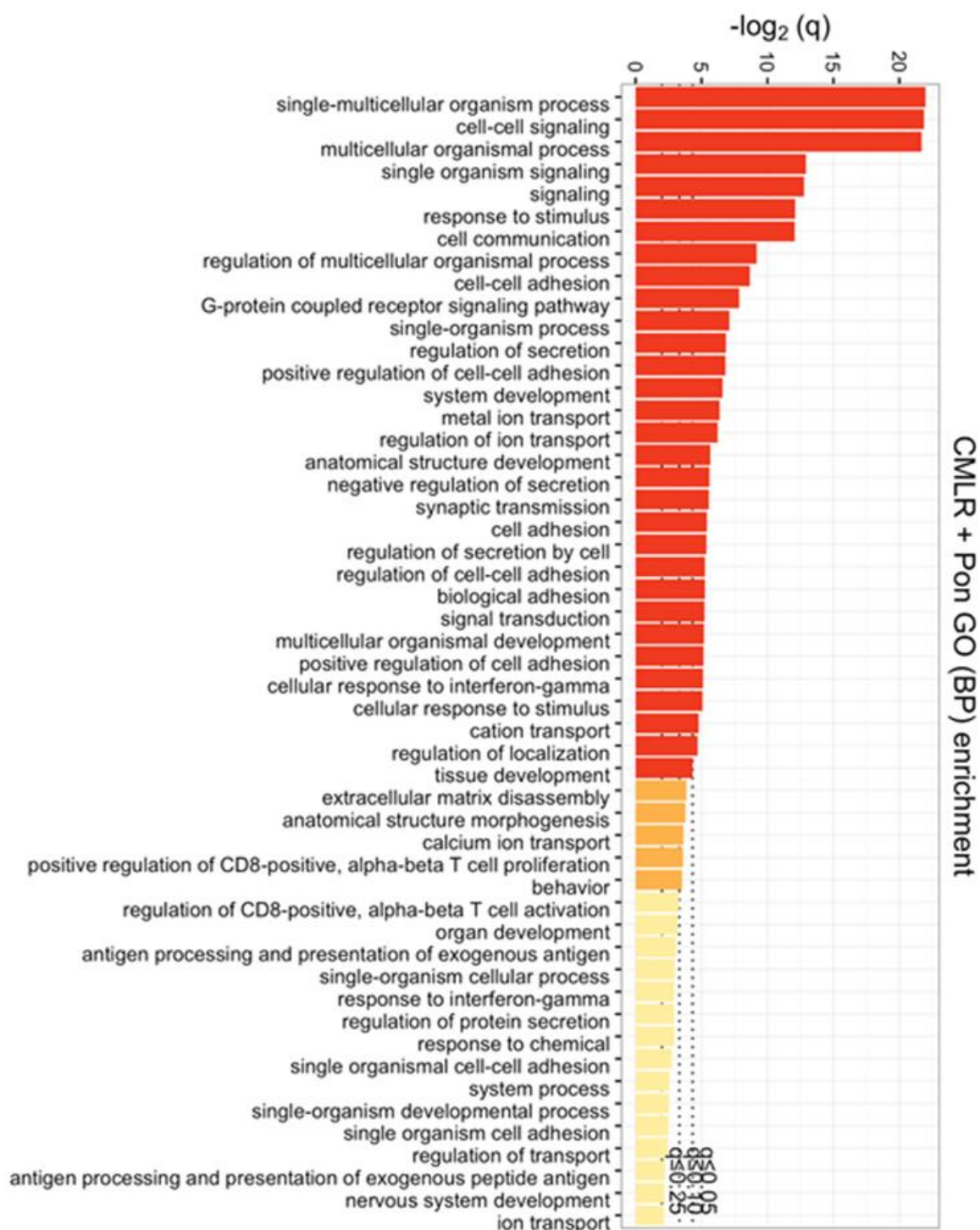


Figure 6-5: Gene ontology enrichment of the biological processes that occur in KCL22^{Pon-Res} cells following 24 hour NVP-Bez235 treatment.

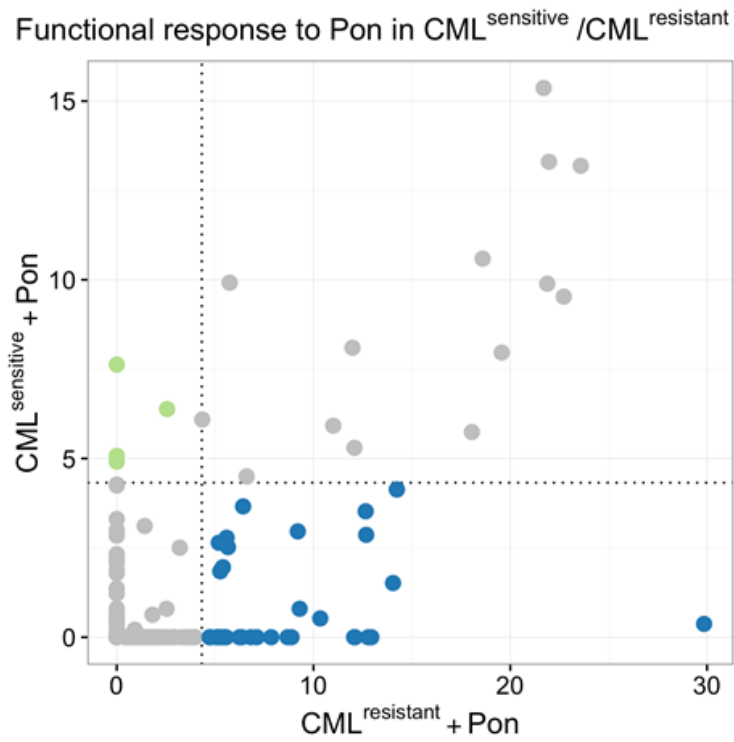


Figure 6-6: A dot plot showing the functional response to ponatinib in CML TKI sensitive versus CML TKI-resistant cells.

The dots represent a biological response either specifically upregulated in the CML TKI sensitive cells (green) or specifically upregulated in the CML TKI-resistant cells (blue), which occur in TKI sensitive CML and not BCR-ABL-independent TKI-resistant CML following 24 hour ponatinib treatment.

CML TKI Sensitive + PON

Biological Processes

Neurological System Process
Response to Lipid
Sensory Perception
System Process

CML TKI Resistant + PON

Biological Processes

Anatomical Structure Development
Antigen Binding
Biological Adhesion
Cation Channel Activity
Cation Transport
Cell Adhesion
Cell Communication
Cell-Cell Adhesion
Cellular Response to Interferon-Gamma
Cellular Response to Stimulus
Channel Activity
G-Protein Coupled Receptor Activity
G-Protein Coupled Receptor Binding
G-Protein Coupled Receptor Signaling Pathway
Hormone Activity
Ligand-Gated Channel Activity
Ligand-Gated Ion Channel Activity
Metal Ion Transmembrane Transporter Activity
Metal Ion Transport
MHC Class II Receptor Activity
Multicellular Organismal Development
Passive Transmembrane Transporter Activity
Positive Regulation of Cell Adhesion
Positive Regulation of Cell-Cell Adhesion
Receptor Binding
Regulation of Cell-Cell Adhesion
Regulation of Ion Transport

Regulation of Localization
Regulation of Multicellular Organismal Process
Response to Stimulus
Signal Transducer Activity
Signal Transduction
Signaling
Single Organism Signaling
Single-Organism Process
Synaptic Transmission

Table 6-2: A differential list of the biological processes for CML TKI sensitive treated with ponatinib (green) and TKI-resistant CML treated with ponatinib (blue).

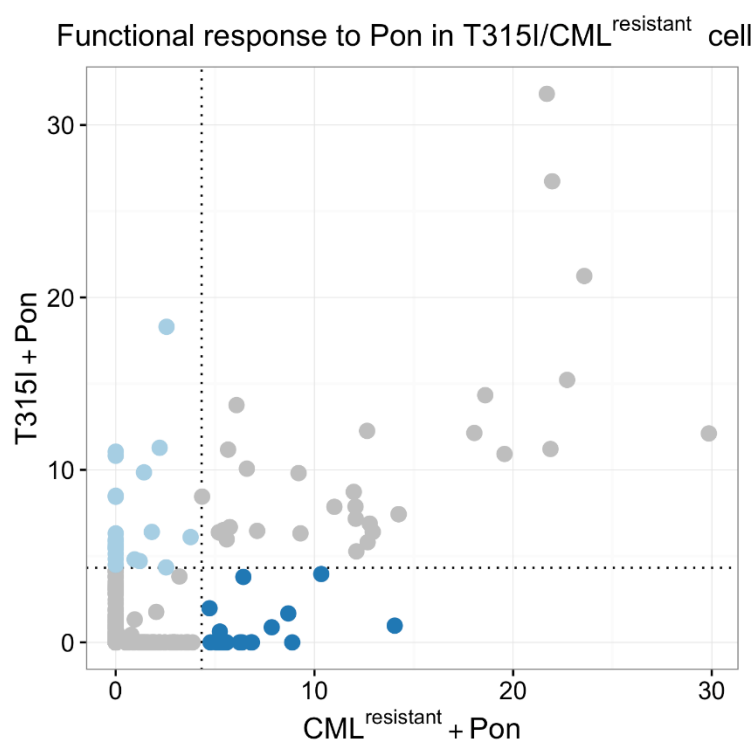


Figure 6-7: A dot plot showing the functional response to ponatinib in CML T315I versus CML TKI-resistant cells.

The dots represent a biological response either specifically upregulated in the CML T315I cells (light blue) or specifically upregulated in the CML TKI-resistant cells (blue), which occur in TKI sensitive CML and not BCR-ABL-independent TKI-resistant CML following 24 hour ponatinib treatment.

CML T315I + PON

Biological Processes

Anatomical Structure Morphogenesis
Blood Circulation
Circulatory System Process
Developmental Process
Generation of Neurons
Growth Factor Activity
Locomotion
Movement of Cell or Subcellular Component
Myotube Differentiation
Nervous System Development
Neurogenesis
Neurological System Process
Neuron Differentiation
Organ Morphogenesis
Positive Regulation of Developmental Process
Positive Regulation of Multicellular Organismal Process
Potassium Ion Transport
Regulation of Cell Proliferation
Response to Retinoic Acid
Response to Wounding
Single-Organism Developmental Process
System Process

CML TKI Resistant + PON

Biological Processes

Antigen Binding
Cation Transport
Cell-Cell Adhesion
Cellular Response to Interferon-Gamma
Cellular Response to Stimulus
G-Protein Coupled Receptor Binding
G-Protein Coupled Receptor Signaling Pathway
Hormone Activity
Ligand-Gated Channel Activity

Ligand-Gated Ion Channel Activity
Metal Ion Transmembrane Transporter Activity
Metal Ion Transport
Negative Regulation of Secretion
Positive Regulation of Cell Adhesion
Positive Regulation of Cell-Cell Adhesion
Regulation of Cell-Cell Adhesion
Regulation of Ion Transport
Regulation of Localization
Regulation of Secretion
Regulation of Secretion by Cell
Signal Transduction
Synaptic Transmission

Table 6-3: A differential list of the biological processes for CML T315I treated with ponatinib (light blue) and TKI-resistant CML treated with ponatinib (blue).

6.5 mTORC1 inhibition induces protective autophagy in KCL22^{Pon-Res} cells

As discussed previously, mTORC1 not only regulates translation, but is also the main regulator of the catabolic process, autophagy. mTORC1 is a negative regulator of autophagy in nutrient rich conditions, however in stressful conditions such as nutrient deprivation or following drug stress, autophagy can be induced as a protective mechanism for the cell to evade cell death. The induction of protective autophagy has been observed in CP CML CD34⁺ cells as a mechanism to evade drug treatment, which leads to drug resistance (Bellodi et al., 2009). Therefore, we asked the question whether NVP-Bez235 would induce protective autophagy in TKI-resistant CML cells (figure 6-7).

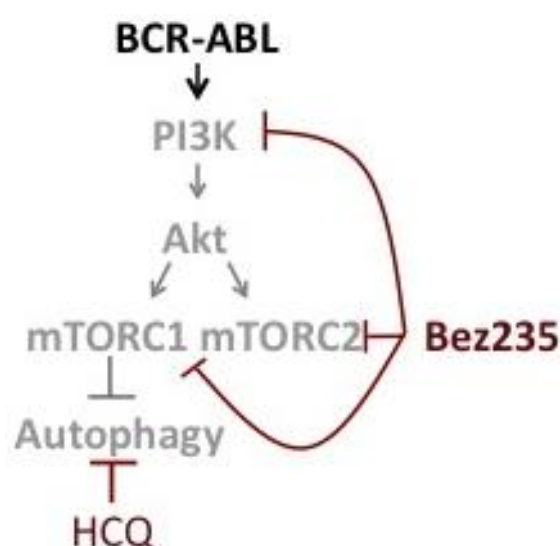


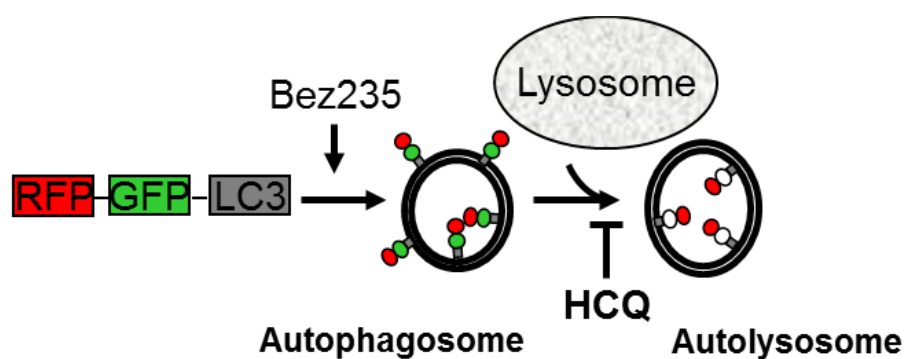
Figure 6-8: Schematic of the PI3K/AKT/mTOR pathway, downstream of BCR-ABL and mTORC1's regulation of autophagy.

This illustrates our hypothesis that NVP-Bez235 may induce autophagy due to the inhibition of mTORC1. This may in turn provide opportunities to further sensitise cells to NVP-Bez235 using HCQ, a late stage autophagy inhibitor.

6.6 NVP-Bez235 mediated mTOR inhibition induces autophagy in KCL22^{Pon-Res} cells

The assessment of autophagy induction can be hard to interpret, however previously in our laboratory a cellular tool was developed to help us assess the effects of autophagy flow. KCL22^{Pon-Res} cell line that stably expressed fluorescently tagged human LC3B-II, mRFP-GFP-LC3B enables the visualization of different stages of autophagy by fluorescent microscopy (Shunsuke Kimura, 2007). The RFP-GFP signal (red+green=yellow) is expressed when the LC3 is bound to the autophagosome. When the autophagy process continues and the lysosome binds to the autophagosome the pH is decreased and this quenches GFP leaving only an RFP signal (red), which indicates autolysosomes (figure 6-8). Autophagy flow can be inhibited pharmacologically by HCQ, which prevents the fusion of the autophagosome and the lysosome. This leads to an accumulation of autophagosomes and therefore a build-up of a yellow fluorescent signal (figure 6-8).

Using the KCL22^{Pon-Res}-RFP-GFP-LC3 cell model to determine if NVP-Bez235 induced autophagy, we treated the KCL22^{Pon-Res}-RFP-GFP-LC3 cells with 100 nM NVP-Bez235, 10 μ M HCQ and the combination treatment, NVPBez235 and HCQ. Following 24 hours treatment the cells were analysed under a fluorescent microscope. The untreated cells allowed us to visualise the basal level of autophagy occurring within the KCL22^{Pon-Res} cells (figure 6-8). The single treatment of NVP-Bez235 dramatically increased puncta expressing a red signal, indicating that a high level of autophagic flow is being completed (figure 6-8). HCQ only treatment resulted in the accumulation of yellow puncta, therefore providing proof that autophagy can be pharmacologically inhibited in KCL22^{Pon-Res} cells (figure 6-8). The combination treatment of NVP-Bez235 and HCQ also resulted in the accumulation of yellow puncta. This indicates that NVP-Bez235 mediated inhibition of mTORC1 induces autophagy and that protective autophagy can be successfully inhibited with combined treatment with HCQ (figure).



Red+green puncta (yellow) = Autophagosomes = autophagy inhibition

Red only = Autolysosomes (GFP degraded) = increased autophagy

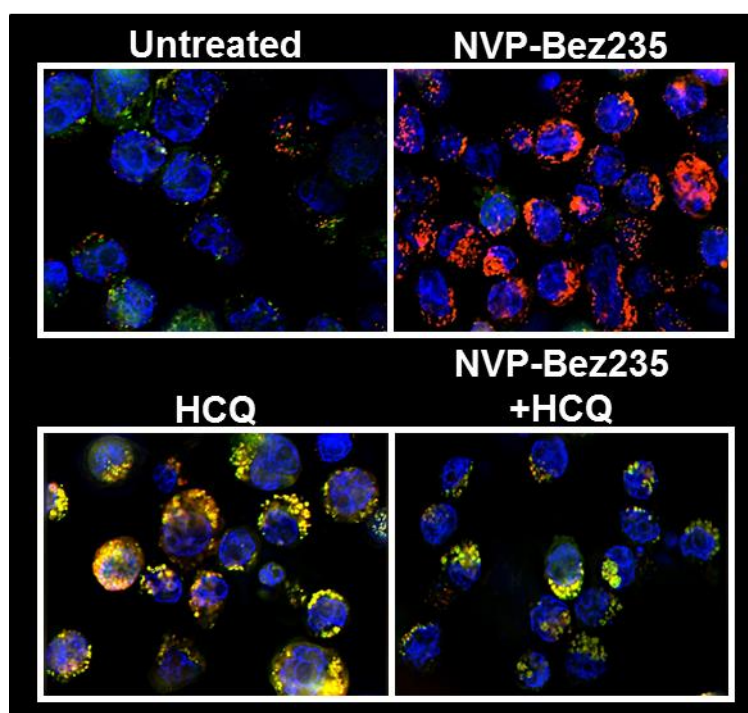


Figure 6-9: Schematic diagram of mRFP-GFP-LC3 system where different stages of autophagy can be measured as red+green=yellow puncta indicating autophagosomes and 'red only' signal indicates autolysosomes.

KCL22^{Pon-Res} expressing mRFP-GFP-LC3 were treated for 24 hours with 100 nM NVP-Bez235, 10 μ M HCQ or combination treatment, NVP-Bez235+HCQ. Autophagy flow and inhibition of autophagy were visualised using a fluorescent microscope. Image produced by Elaine Allan.

6.7 *ATG7* knock out mediated autophagy inhibition increases sensitivity of *KCL22*^{Pon-Res} cells to NVP-Bez235

Next we investigated if autophagy induced by NVP-Bez235 has a protective role following drug treatment in TKI-resistant cells. However HCQ is a non-specific autophagy agent and has been proposed to affect cancer cells in an autophagy independent manner (Maycotte et al., 2012). Therefore, we employed two complimentary approaches; CRISPR-Cas9 and RNAi techniques to test if specific inhibition of autophagy could enhance the effects of NVP-Bez235 on *KCL22*^{Pon-Res} cell death. In order to inhibit autophagy, we targeted an essential autophagy gene, *ATG7*, an E1-like enzyme required for the lipidation of LC3B. First we generated two CRISPR-Cas9 plasmids containing single guide RNAs specific for *ATG7* (see methods 2.3.14-15). These plasmids were used to knock out (KO) *ATG7* in *KCL22*^{Pon-Res} cells using CRISPR. The level of *ATG7* KO was analysed by western blot against the *ATG7* protein. The complete KO of *ATG7* by KO2 and partial KO by KO1 was associated with the inhibition of the formation of the lipidated form of LC3, LC3B-II, as well as a build-up of the autophagy substrate SQSTM1/p62. The *KCL22*^{Pon-Res} *ATG7* KO and the complementary control cells were treated with 100 nM NVP-Bez235, 10 μ M HCQ and the combination treatment. As the *KCL22*^{Pon-Res} *ATG7* KO cells already had autophagy fully inhibited no effect was seen with the treatment with HCQ (figure 6-9). However, in the control cells HCQ caused a build-up of LC3BII, due to the inhibition of autophagosome degradation, which was complemented with an increase in SQSTM1/p62 (figure 6-9). The treatment of both the *ATG7* KO cells and the control cells with NVP-Bez235 led to full inhibition of phosphorylated RPS6 and therefore evidence that NVP-Bez235 can inhibit mTOR signalling within the *KCL22*^{Pon-Res} *ATG7* KO cell model (figure 6-9).

This data was complemented with a secondary assay measuring lipidated LC3BII by flow cytometry. The assay washes out cytoplasmic LC3BI and detects membrane bound LC3BII by using a fluorescent tagged (FITC) antibody. Flow cytometry detected very low levels of FITC fluorescent, which correlates with low levels of LC3BII in *ATG7* KO cells. This is consistent with the protein expression analysis, which shows that *ATG7* KO cells no longer have the potential to convert LC3BI to LC3BII, which implies that autophagy has been inhibited in these cells (figure 6-10). Low levels of fluorescence were observed with all treatment conditions in *ATG7* KO cells. In comparison, the control cells, when treated with HCQ there is a striking increase in LC3BII as seen with an increase in FITC fluorescence (figure 6-10). HCQ inhibits the formation of the autolysosome, which causes a build-up of autophagosomes and therefore membrane bound LC3BII (figure 6-10). By using these two complimentary assays we can show that autophagy flow is impaired in the *ATG7* KO cells.

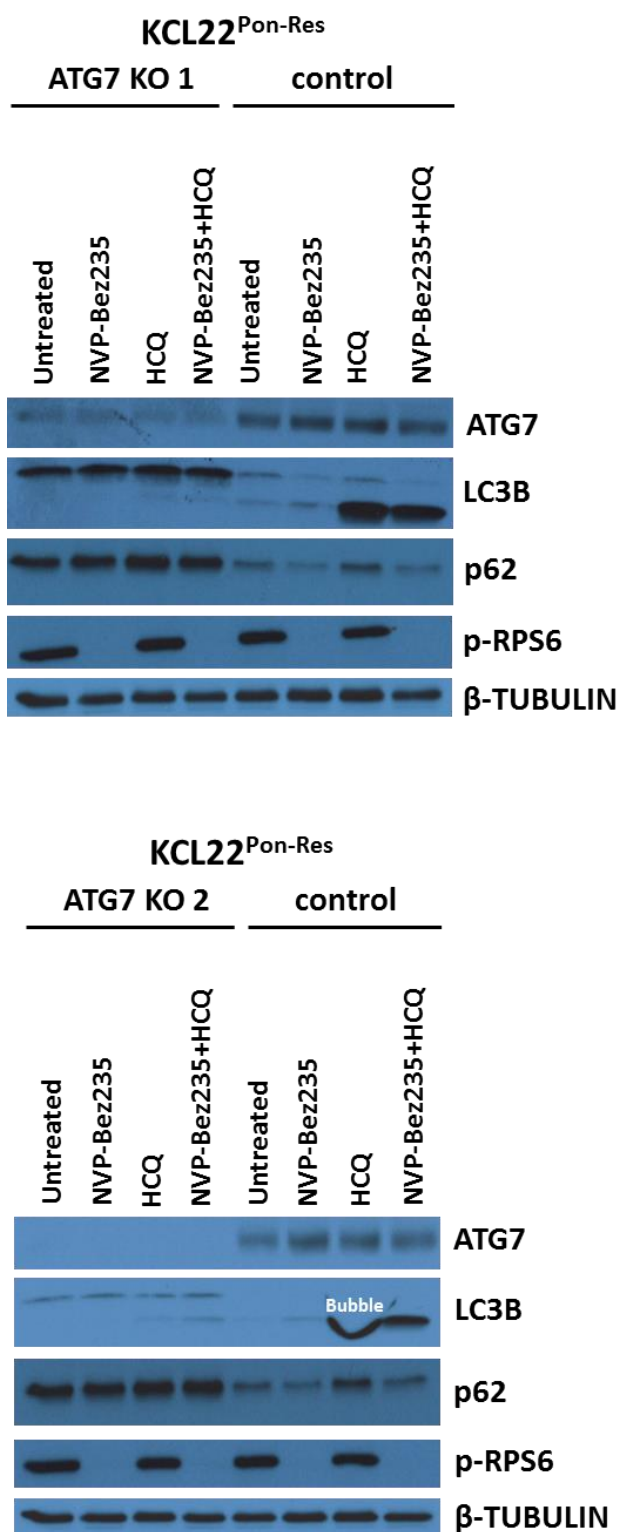


Figure 6-10: KCL22^{Pon-Res} cells were lentivirally transduced with a CRISPR v2 vector containing an *ATG7*-targeting sequence or an empty vector control with unconcentrated virus.

The KCL22^{Pon-Res} cells transduced with the control v2 vector, CRISPR v2 *ATG7*-1 or CRISPR v2 *ATG7*-2 were then treated with 100 nM NVP-Bez235, 10 μM HCQ or the combination for 24 hours.

Western blot analysis assessed the level of ATG7 KO achieved and other autophagy associated proteins, such as LC3B and p62. The mTOR activity was assessed by the phosphorylation of RPS6.

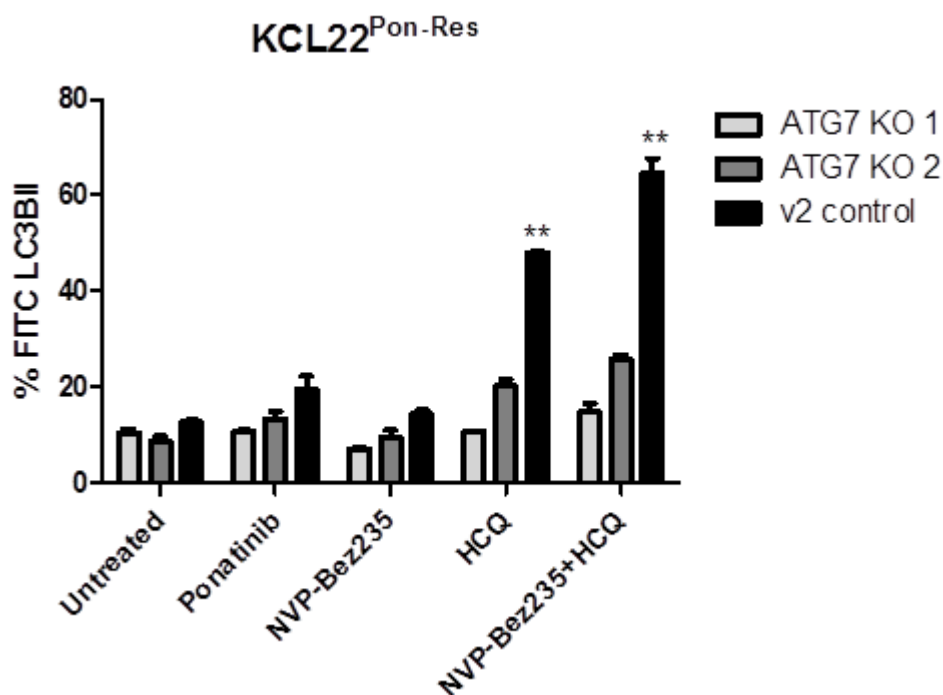


Figure 6-11: The measurement of LC3BII in KCL22^{Pon-Res} ATG7 KO and control cells.

The KCL22^{Pon-Res} cells were seeded at 0.25×10^6 /mL for 24 hours with the appropriate drug; 100 nM ponatinib, 100 nM NVP-Bez235 or 4 hours with 10 μ M HCQ. The FlowCollect™ Autophagy LC3 Antibody-based Assay Kit was performed as per the protocol. FITC fluorescence was detected via flow cytometry. Statistical analysis was performed by using paired t-test. Annotation above a bar refers to statistical significance between the bar and the untreated control (**; $p \leq 0.01$)(n=2).

The generation of a specific autophagy null TKI-resistant CML cell line, KCL22^{Pon-Res} ATG7 KO cells, provided us with a tool to assess whether the inhibition of autophagy enhances the NVP-Bez235 mediated cell death in KCL22^{Pon-Res} cells. The KCL22^{Pon-Res} ATG7 KO cells and the control cells were treated with 100 nM ponatinib or 100 nM NVP-Bez235 and following 72 hours of treatment apoptosis and CFC assays were performed. Ponatinib treatment had no apoptotic effect on either the KCL22^{Pon-Res} ATG7 KO cells or the control cells, however caused a modest reduction in colony forming potential in the CFC assay (Figure 6-11). NVP-Bez235 caused a high level of apoptosis in both the KCL22^{Pon-Res} ATG7 KO cells and the control cells (Figure 6-11). The apoptotic response in the controls cells was increased by 32% above the untreated cells, which was enhanced in the KCL22^{Pon-Res} ATG7 KO cells as the apoptotic response increased to 42% following NVP-Bez235 treatment (Figure 6-11). Therefore, the inhibition of autophagy enhanced the apoptotic response to NVP-Bez235 treatment by 10%. This enhanced effect was mirrored

in the CFC. The *ATG7* KO in the $KCL22^{Pon-Res}$ cells significantly reduced the amount of colonies formed following NVP-Bez235 treatment compared to $KCL22^{Pon-Res}$ control cells treated with NVP-Bez235, which was a 37.5% reduction (figure 6-11).

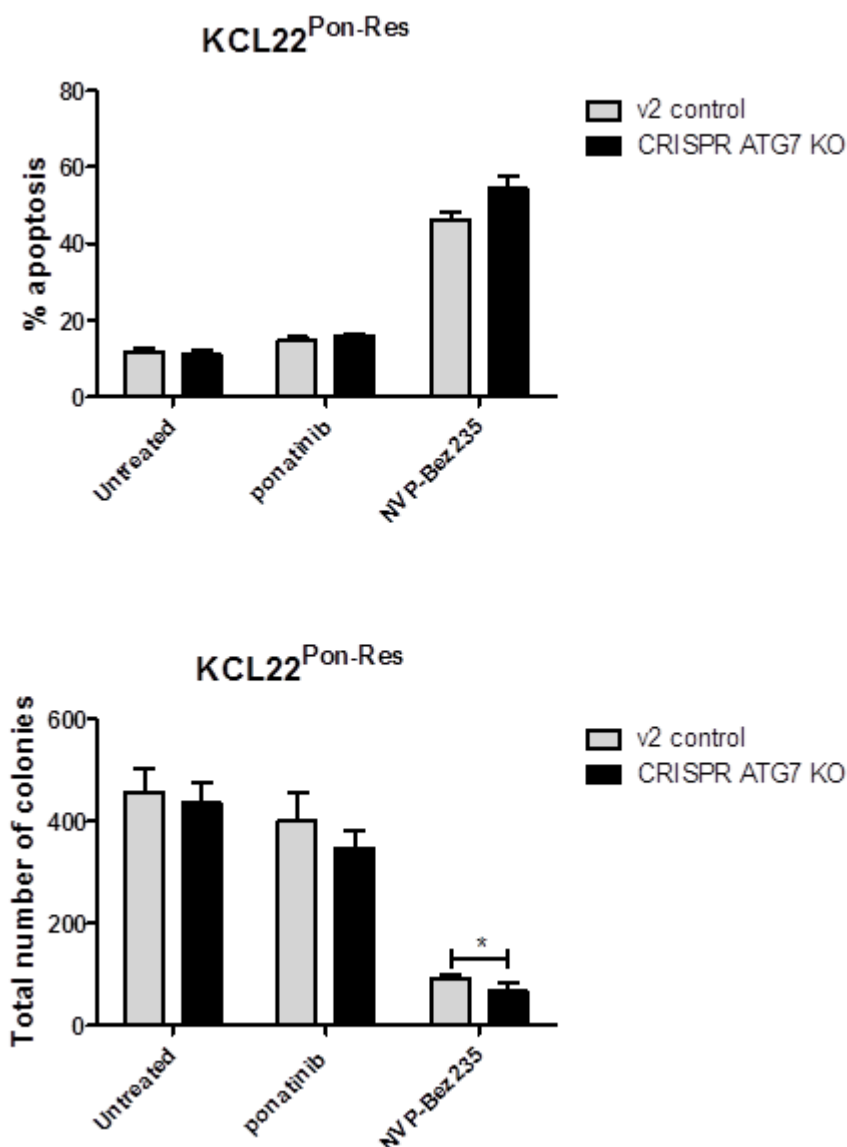


Figure 6-12: $KCL22^{Pon-Res}$ cells were lentivirally transduced with a CRISPR v2 vector containing an *ATG7*-targeting sequence or an empty vector control with unconcentrated virus.

The cells were transduced for 48 hours and underwent puromycin selection for 14 days. The $KCL22^{Pon-Res}$ cells transduced with the control v2 vector, CRISPR v2 *ATG7*-1 or CRISPR v2 *ATG7*-2 were treated with 100 nM NVP-Bez235 for 72hrs and apoptosis was measured by staining the cells with annexin V and 7AAD and analysed using flow cytometry. The histograms represent the average of both the results from *ATG7* KO 1 and 2. Statistical analysis was performed by using paired t-test. Annotation above a bar refers to statistical significance between the bar and the untreated control (*; $p \leq 0.05$) (n=3).

Due to possibility of off target effects occurring when generating a specific KD or KO, a secondary complementary approach was performed, which similarly used a pLKO-GFP shRNA vector system to knock down (KD) *ATG7* in the KCL22^{Pon-Res} cells. KCL22^{Pon-Res} cell lines were transduced with either a pLKO-GFP shATG7 vector or a pLKO-GFP shSCR (Scrambled) control vector. The level of *ATG7* KD obtained was assessed at the protein level by western blot, which showed the complete inhibition of *ATG7* protein expression, indicating that the *ATG7* had been silenced in the sh-ATG7 KD KCL22^{Pon-Res} cells (figure 6-12). To establish whether the *ATG7* KD could also enhance the NVP-Bez235 mediated cell death in the KCL22^{Pon-Res} cells, we treated the cells with 100 nM NVP-Bez235 for 72 hours and analysed apoptosis. NVP-Bez235 induced apoptosis in both the KCL22^{Pon-Res} control and *ATG7* KD cells. However, the level of apoptosis was significantly increased within the autophagy redundant cells by more than 20% compared to the control cells treated with NVP-Bez235 (figure 6-12).

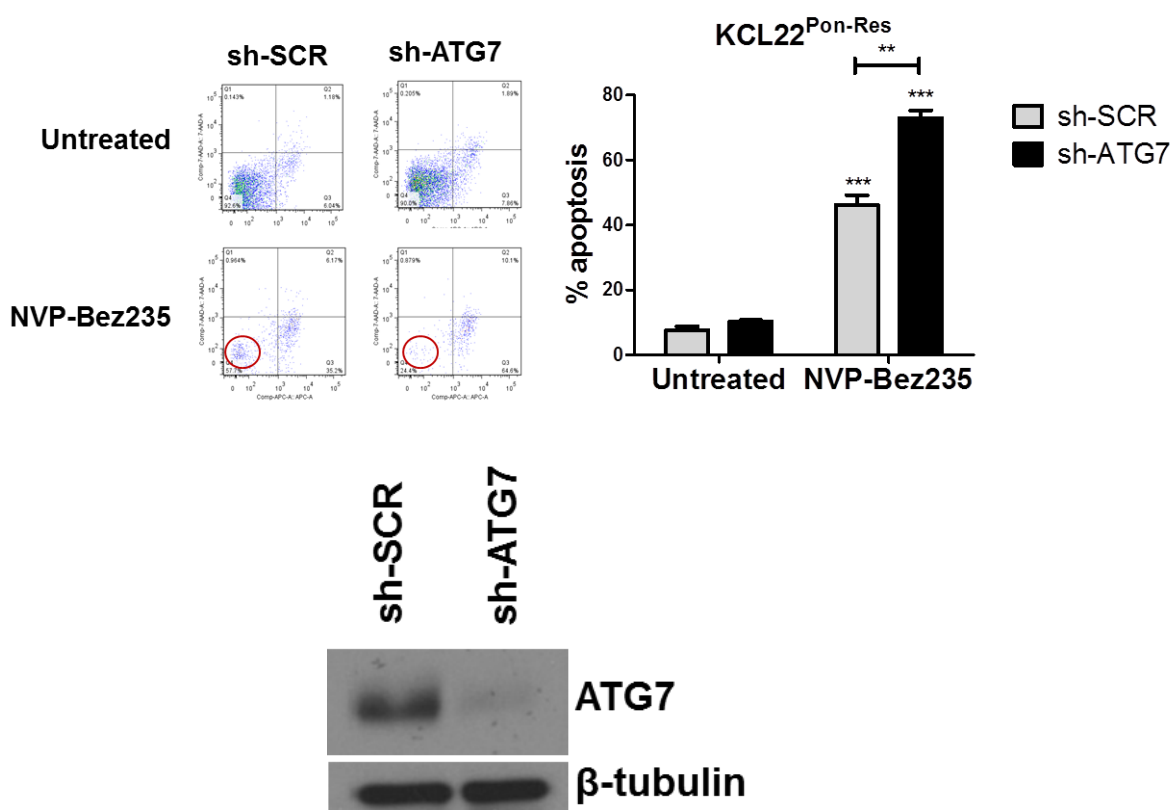


Figure 6-13: KCL22^{Pon-Res} cells were lentivirally transduced with a pLKO.1-GFP vector carrying either a mock (shSCR) or an *ATG7*-targeting hairpin (shATG7) with unconcentrated virus.

Cells were transduced over 48 hours and GFP was measured by flow cytometry analysis, which showed >99% transduction efficiency for both vectors. The KCL22^{Pon-Res} cells transduced with shSCR or shATG7 were treated with NVP-Bez235 for 72hrs and apoptosis was measured. The level of *ATG7* knockdown achieved was assessed by western blot. The histogram represents early and late apoptosis and numbers are presented as mean±SEM (n=3). Statistical analysis was

performed by using paired t-test. Annotation above a bar refers to statistical significance between the bar and the untreated control (**; $p \leq 0.01$, ***; $p \leq 0.001$).

6.8 Pharmacological autophagy inhibition enhances the effect of NVP-Bez235 against primary TKI-resistant CML cells

Our previous study using the KCL22^{Pon-Res} cell model showed that NVP-Bez235 mediated mTORC1 inhibition induces protective autophagy. We were able to inhibit autophagy in the KCL22^{Pon-Res} cells pharmacologically by HCQ treatment or specifically by knocking out or knocking down essential autophagy gene, ATG7. The combination of NVP-Bez235 treatment and autophagy inhibition led to the significant enhancement of NVP-Bez235 induced cell death.

As a result of these promising data we wanted to investigate whether autophagy inhibition could also enhance NVP-Bez235 induced cell death in primary BCR-ABL-independent TKI-resistant CML cells.

To do this we extracted MNCs from the bone marrow of three patients who have failed to achieve CCyR following 1st, 2nd and 3rd generation TKI treatments. We then treated these cells with 100 nM ponatinib, as a control for TKI-resistance, 10 μ M HCQ, 100 nM NVP-Bez235 and the combination of NVP-Bez235 and HCQ. Following 72 hours treatment the colony forming potential of the leukaemic cells and their ability to form colonies post treatment were assessed by performing CFC assays.

As shown previously NVP-Bez235 had a significantly greater effect at reducing the colony forming potential than ponatinib. NVP-Bez235 reduced the number of colonies formed by 60%, whilst ponatinib reduced colonies by 40-45% (figure 6-13). Most importantly this assay confirmed that HCQ treatment could significantly enhance that effect of NVP-Bez235 by reducing the number of colonies formed by 80%, which was highly significant in both patients. This combination treatment proved to be significantly more effective than ponatinib treatment and the treatment of NVP-Bez235 alone in all patients analysed (figure 6-13).

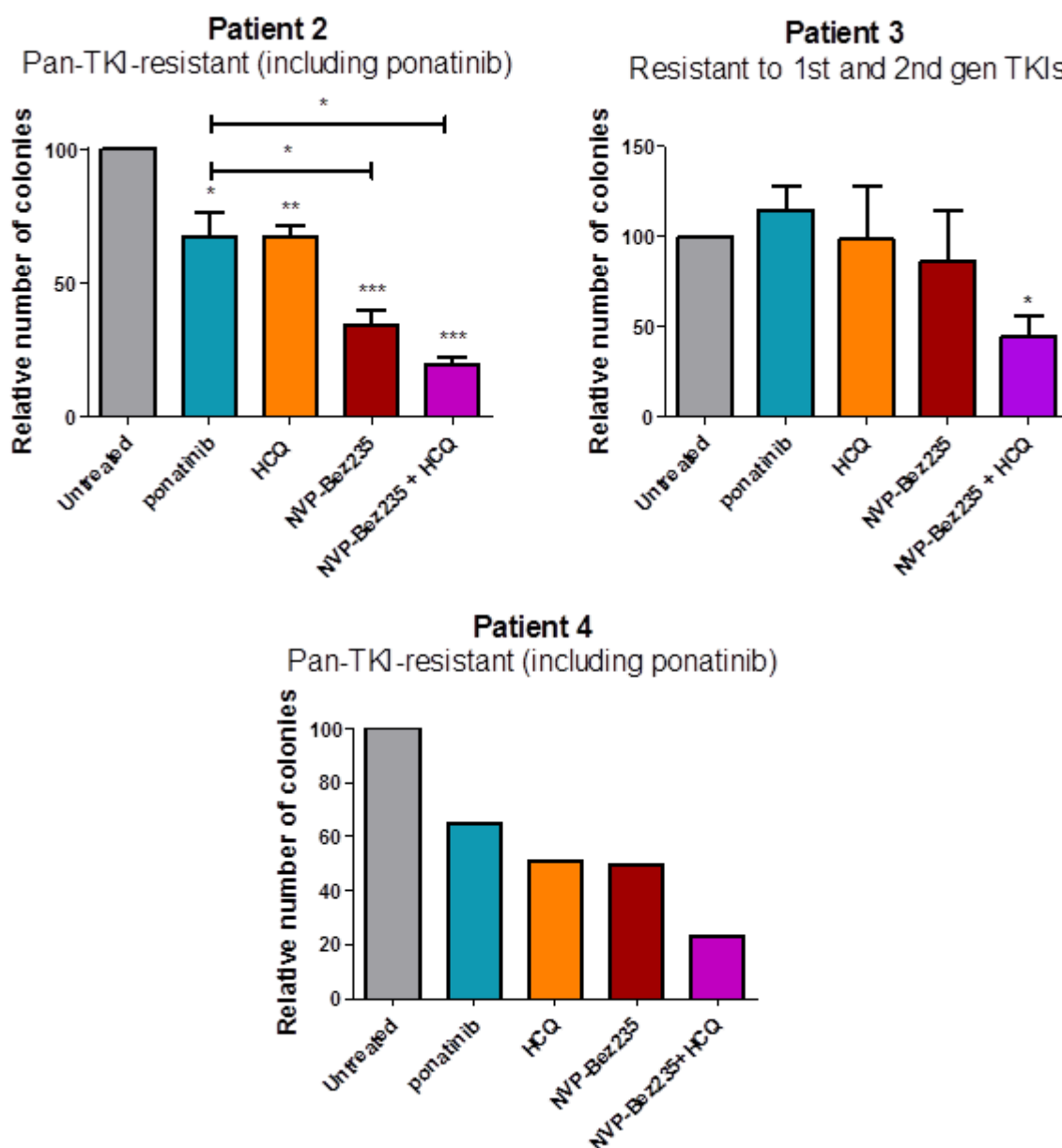


Figure 6-14: Bone marrow derived MNCs from TKI-resistant CML patients were cultured in SFM supplemented with physiological growth factors.

Cells were treated with 100 nM ponatinib, 10 μ M HCQ, 100 nM NVP-Bez235 and combination treatment of NVP-Bez235 and HCQ. The colony forming potential was measured following a 72 hour drug treatment. (n=3 patients). Statistical analysis was performed by using paired t-test. Annotation above a bar refers to statistical significance between the bar and the untreated control (*; $p \leq 0.05$, **; $p \leq 0.01$, ***; $p \leq 0.001$).

6.9 Autophagy inhibition enhances the effect of dual PI3K and mTOR inhibitors against primary TKI-resistant CML cells

A preliminary experiment investigating the effect of the novel dual PI3K and mTOR inhibitors and combination treatment with HCQ was performed on one patient sample. The MNCs were extracted from the patient's bone marrow and were treated with 100 nM ponatinib, 10 μ M HCQ, 100 nM NVP-Bez235, 100 nM gedatolisib, 100 nM apitolisib and 100 nM VS-5584. All the dual PI3K and mTOR inhibitors were analysed as single treatments or in combination with 10 μ M HCQ. Following 72 hours of treatment cell viability was assessed by apoptosis and CFC assays. Ponatinib was used as a control for TKI resistance. This experiment showed that ponatinib treatment had no effect on cell death or colony forming potential in the primary TKI-resistant CML cells. As single treatments, the dual PI3K and mTOR inhibitors all induced a modest level of apoptosis, between 5-12% above untreated and ponatinib treatment, NVP-Bez235 being the most effective (figure 6-14). However, the most striking effect was seen in the CFC assay, which assesses the cells colony forming potential following drug treatment. All single treatments with the dual PI3K and mTOR inhibitors reduced the number of colonies formed. NVP-Bez235 and gedatolisib had the greatest effects compared to untreated control, 70 and 39% reduction, respectively (figure 6-14). However, the combination treatment with the PI3K and mTOR inhibitors and HCQ showed the most striking effects, all combination treatments significantly reduced the number of colonies. The combination of NVP-Bez235 plus HCQ most significantly decreased colony formation (85% reduction), which was also significantly reduced compared to ponatinib, the patient's current treatment. The combination treatment of gedatolisib and HCQ also significantly reduced colony formation compared to ponatinib treatment alone. The combination of gedatolisib and HCQ decreased colony formation by 53%. Apitolisib and HCQ reduced colony formation by 65% and VS5585 and HCQ by 61.5% (figure 6-14).

This experiment highlights the importance of our concept of treatment with dual PI3K and mTOR inhibitors in combination with an autophagy inhibitor for treatment against BCR-ABL-independent TKI-resistant CML. Although all combination treatments effectively induced cell death and reduced the long-term survival of the leukaemic cells, NVP-Bez235 and HCQ remained the most effective drug treatment option.

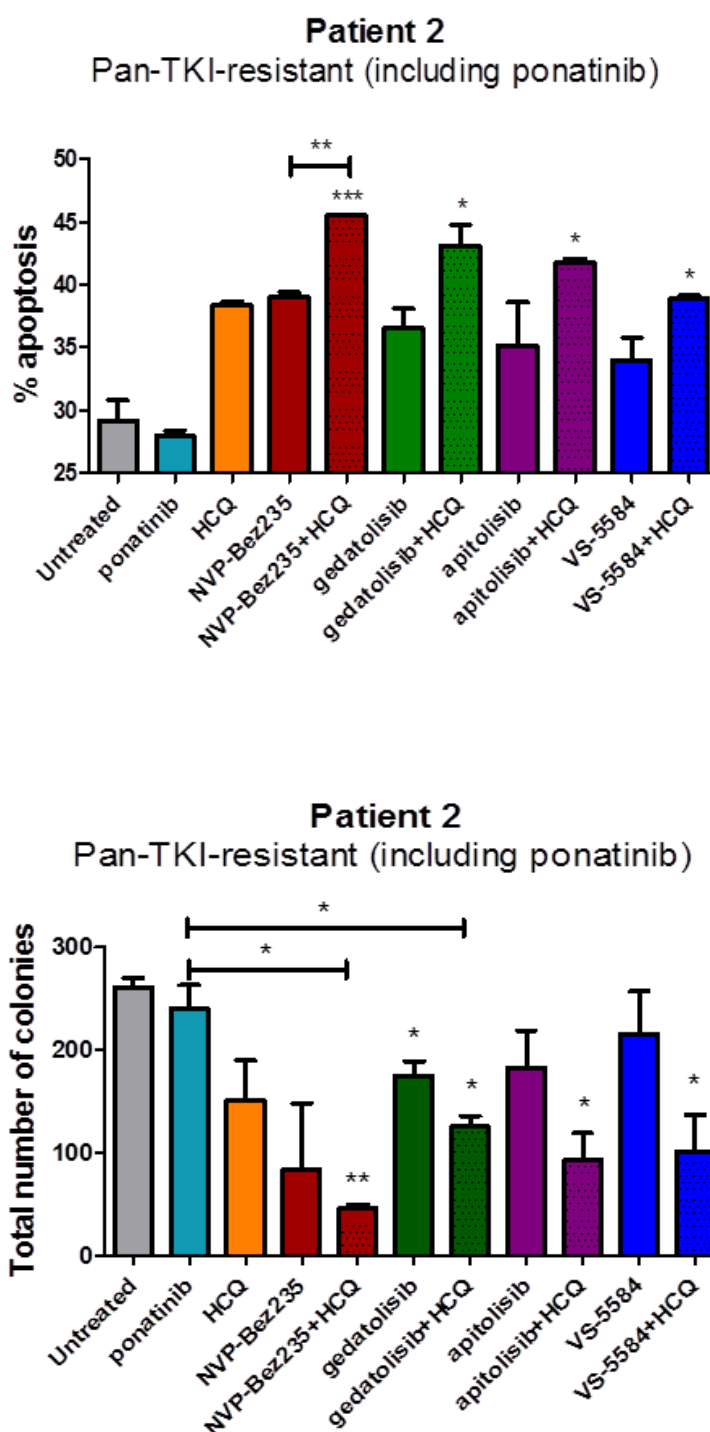


Figure 6-15: Bone marrow derived MNCs from a TKI-resistant CML patient were cultured in SFM supplemented with physiological growth factors.

Cells were treated with 100 nM ponatinib, 10 μ M HCQ, 100 nM NVP-Bez235, 100 nM gedatolisib, 100 nM apitolisib and 100 nM VS-5584. All the dual PI3K and mTOR inhibitors were analysed as single treatments or in combination with 10 μ M HCQ. The induction of apoptosis and the colony forming potential was measured following a 72 hour drug treatment. (n=1 patient). Statistical analysis was performed by using paired t-test. Annotation above a bar refers to statistical significance between the bar and the untreated control (*; $p \leq 0.05$, **; $p \leq 0.01$, ***; $p \leq 0.001$).

6.10 Pharmacological inhibition of autophagy enhances the effect of NVP-Bez235 *in vivo*

Previously we have shown in *in vitro* and *ex vivo* studies that the combination of mTOR and autophagy inhibition is an effective treatment, which induces high levels of apoptosis and also reduces long-term cell viability against BCR-ABL-independent TKI-resistant CML cells.

To analyse this further, we investigated whether the mTOR inhibition, when combined with autophagy inhibition, could inhibit leukaemia initiation in TKI-resistant cells. To do this we used KCL22^{Pon-Res} cells, expressing firefly luciferase (previously generated by G. V. Helgason). These cells were treated *in vitro* with 10 μ M HCQ, 100 nM ponatinib, 100 nM NVP-Bez235 and combination treatments of ponatinib and HCQ and NVP-Bez235 and HCQ. Following a 72 hours drug treatment cell counts were performed, and taking into account cell death, the relative number of cells were transplanted intravenously into sub-lethally irradiated NOD/SCID/IL-2R γ ^{-/-} (NSG) mice (Ishikawa et al., 2005). Thirty minutes after the transplant the mice were injected with D-luciferin substrate to activate the firefly luciferase and the mice were imaged using a bioluminescent imager, IVIS, to ensure the success of the transplantation and the cell viability. Subsequently the mice were imaged weekly to assess leukaemia development. By week 4 there was a significant reduction in the luciferase expression in the mice transplanted with the combination treatment of NVP-Bez235 and HCQ (figure 6-15). This suggests that mTOR and autophagy inhibition can delay leukaemia development. The NVP-Bez235 and HCQ drug treatment combination also significantly prolonged the survival of the NSG mice, compared to the cohort of mice transplanted with untreated control cells and mice transplanted with ponatinib treated cells ($p=0.0004$ and $p=0.0054$, respectively) (figure 6-15). All 4 mice in the combination arm were sacrificed at day 42 with little evidence of leukaemia (figure 6-15).

The NVP-Bez235 treatment alone also reduced the development of leukaemia significantly compared to the untreated cohort of mice, however it only increased survival by 1-5 days

(figure 6-15). Ponatinib, HCQ and the combination treatment had very little effect against the development of the leukaemia in this model and only prolonged survival by 1 or 2 days (figure 6-15).

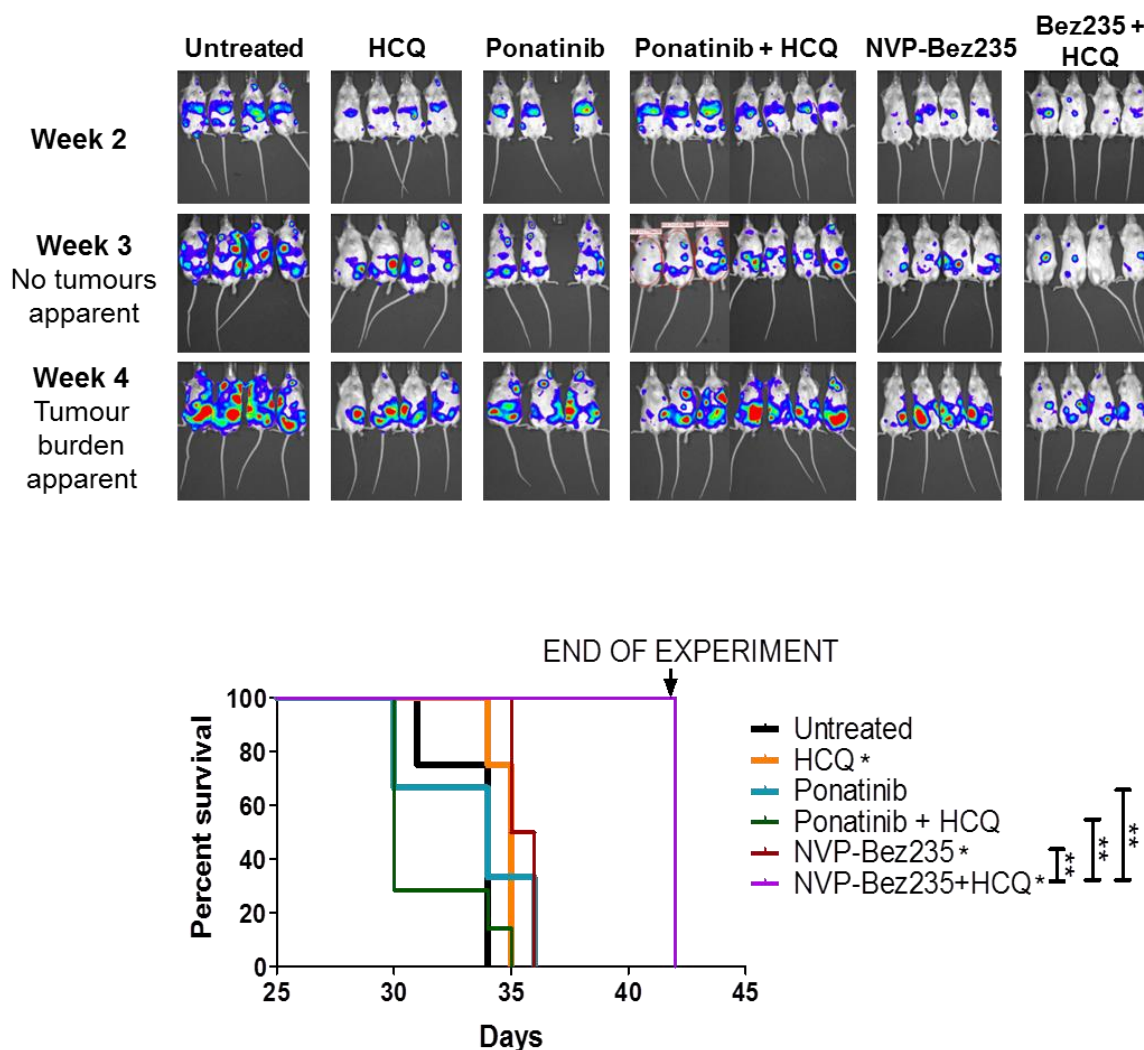


Figure 6-16: KCL22^{Pon-Res} were labelled with lentiviral firefly luciferase and seeded at 0.25×10^6 /ml and treated with 10 μ M HCQ, 100 nM Ponatinib, 100 nM NVP-Bez235 or combination, in vitro for 72 hours.

Cell counts were performed to taking into account cell death from the drug treatments. The relative numbers of cells compared to the NVP-Bez235+HCQ treatment were injected into sublethally irradiated NSG mice (4-7 mice per cohort) i.e. if the untreated cells had expanded 3 fold over the 72 hour treatment time compared to the NVP-Bez235+HCQ treated cells, the mice in the untreated cohort were transplanted with 3×10^6 cells and the mice in the NVP-Bez235+HCQ cohort would receive 1×10^6 cells. Leukaemic burden and engraftment was recorded by IVIS bioluminescent imaging weekly. Overall survival was monitored and measured by Kaplan-Meier analysis using graphpad prism. Annotation above a bar refers to statistical significance between the bar and the untreated control (*; $p \leq 0.05$, **; $p \leq 0.01$, ***; $p \leq 0.001$).

6.11 The combination treatment of NVP-Bez235 and HCQ has minimal toxicity compared to omacetaxine in non-CML cells

Despite the successful anti-leukaemic effects NVP-Bez235 has shown in this study, treatment of NVP-Bez235 in the clinics has taken a precautionary approach, as reports have been made that some patients have suffered from adverse effects. NVP-Bez235 is currently under investigation in many clinical trials against a wide range of solid and blood cancers, to ascertain whether NVP-Bez235 could be an effective and safe treatment for patients from different disease backgrounds. Due to the toxicities reported from the clinic and some of our preclinical data from the drug screen, which showed non-CML CD34⁺ cells were sensitive to low drug concentrations of the PI3K and mTOR inhibitors, we tested the effect of NVP-Bez235 and the combination treatment of NVP-Bez235 and HCQ on normal cells. Firstly, due to lack of clinical material we tested the effects of NVP-Bez and gedatolisib on normal BaF3^{Parental} cells and compared it to the cytotoxic effects caused in the TKI-resistant BaF3^{Pon-Resl} cells. This preliminary study suggested that NVP-Bez235 and gedatolisib were more selective towards the TKI-resistant BaF3^{Pon-Resl} cells, by increasing apoptosis 25-30% higher in these cells compared to the normal cells (figure 6-16). Further investigation was performed using non-CML CD34⁺ cells, derived from patients with a Ph negative haematological malignancy, lymphoma. The non-CML cells were treated with ponatinib, NVP-BEZ235, alone and in combination with HCQ, and compared with cytotoxicity of 10 nM omacetaxine treatment. This revealed that omacetaxine significantly affected the colony forming potential of normal progenitor cells, as no colonies were formed, the combination of NVP-BEZ235 and HCQ had a less than maximal effect (figures 6-17).

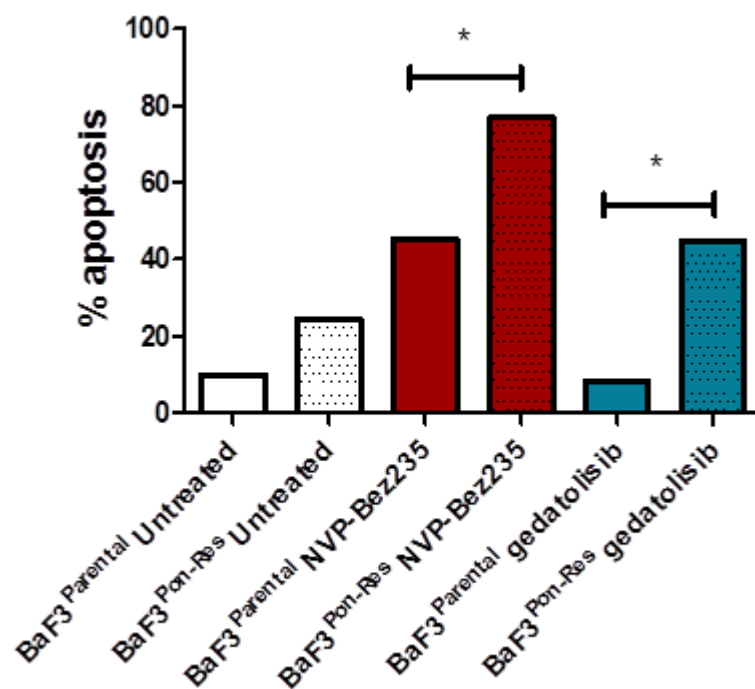


Figure 6-17: BaF3^{Parental} and BaF3^{Pon-Res} cells were seeded at 0.25×10^6 / mL and treated with 100 nM NVP-Bez235 or 100 nM gedatolisib. The percentage of apoptosis was measured following a 72 hour drug treatment.

Statistical analysis was performed by using paired t-test. Annotation above a bar refers to statistical significance (*; $p \leq 0.05$).

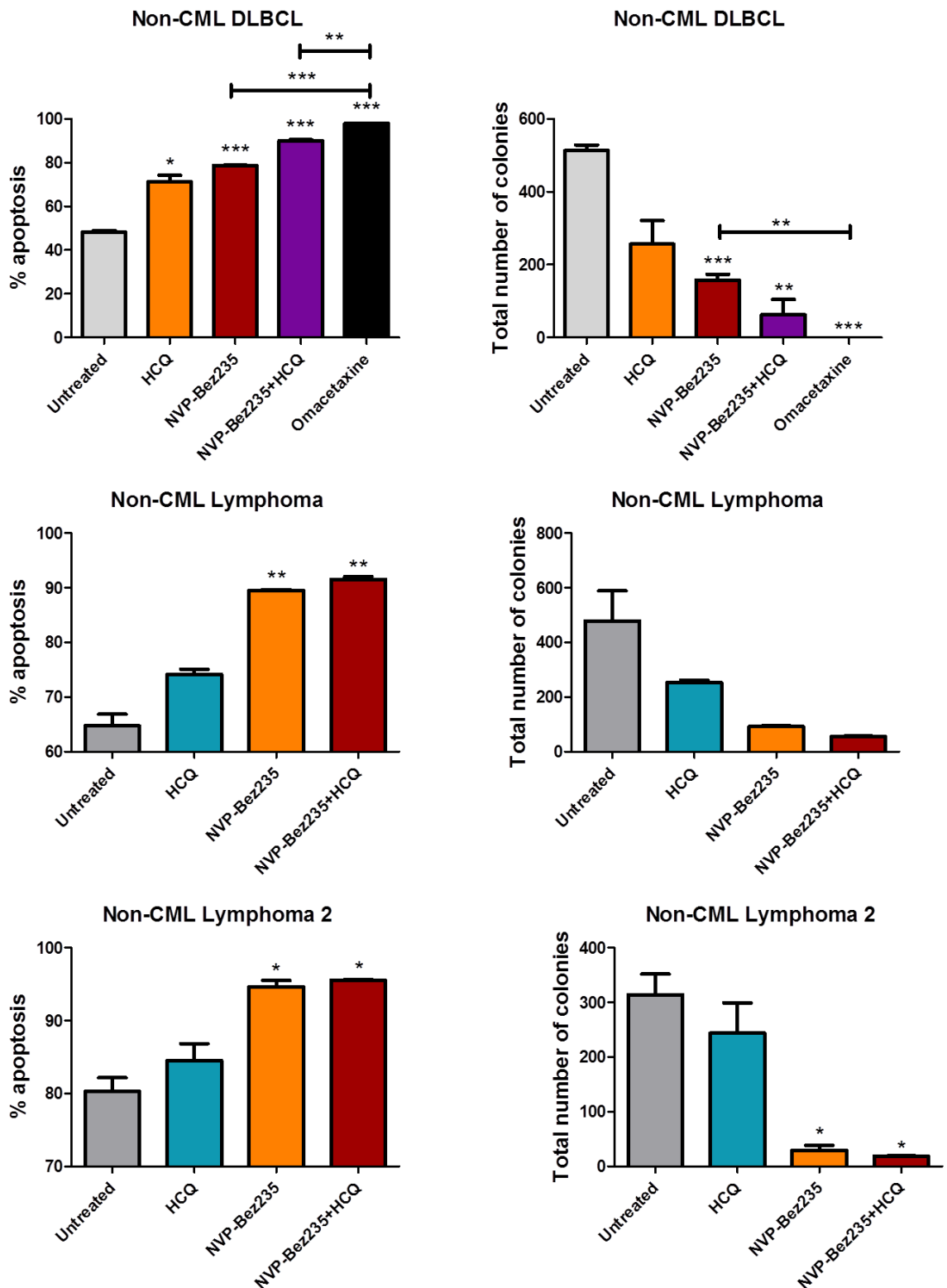


Figure 6-18: Bone marrow derived MNCs from a non-CML lymphoma patients were cultured in SFM supplemented with physiological growth factors.

Cells were treated with 10 μ M HCQ, 100 nM NVP-Bez235, NVP-Bez235 in combination with HCQ and 10 nM omacetaxine. The induction of apoptosis and the colony forming potential was measured following a 72 hour drug treatment. (n=3 patients). Statistical analysis was performed by using paired t-test. Annotation above a bar refers to statistical significance between the bar and the untreated control (*; $p \leq 0.05$, **; $p \leq 0.01$, ***; $p \leq 0.001$).

6.12 The combination treatment of NVP-Bez235 and HCQ was well tolerated by NSG mice and significantly extended the survival of TKI-resistant CML xenograft mice.

As a result of the concerns raised about the toxic effects of NVP-bez235 we tested the tolerability and efficacy of this drug combination with HCQ *in vivo*. In this study we used the KCL22^{Pon-Res} luciferase positive cells and transplanted them intravenously into NSG mice. Evidence of engraftment of the KCL22^{Pon-Res} cells was assessed 7 days after transplantation by bioluminescent imaging. Following confirmation of engraftment, the mice were treated with NVP-Bez235, HCQ and the combination treatment. The NVP-Bez235 treated mice received a daily dose of 45mg/kg by oral gavage and the HCQ treated mice received a daily dose of 60 mg/kg by intraperitoneal injection. One mouse in the NVP-Bez235 treated arm was culled for reasons unrelated to disease development or drug treatment. After 3 weeks of treatment bioluminescent imaging revealed the untreated (vehicle control) mice and the HCQ treated mice had a high level of bioluminescent signal, indicating the development of leukaemia and by week 4, due to the level of disease burden, the untreated and HCQ treated mice were sacrificed (figure 6-18). At week 5, two of the 5 NVP-Bez235 treated mice were sacrificed due to the leukaemic burden. Bioluminescent imaging indicated an increased level of bioluminescence in the remaining NVP-Bez235 only treated mice compared to the combination treatment mice (figure 6-18). The mice treated with the combination of NVP-Bez235 and HCQ tolerated the treatment well with no signs of toxicity, observed by weight of the mice, appearance, behaviour, eating and drinking. The combination treatment slowed the kinetics of disease development, shown by the reduced levels of bioluminescence, and significantly extended the survival of the mice compared to the single NVP-Bez235 treatment (figure 6-18).

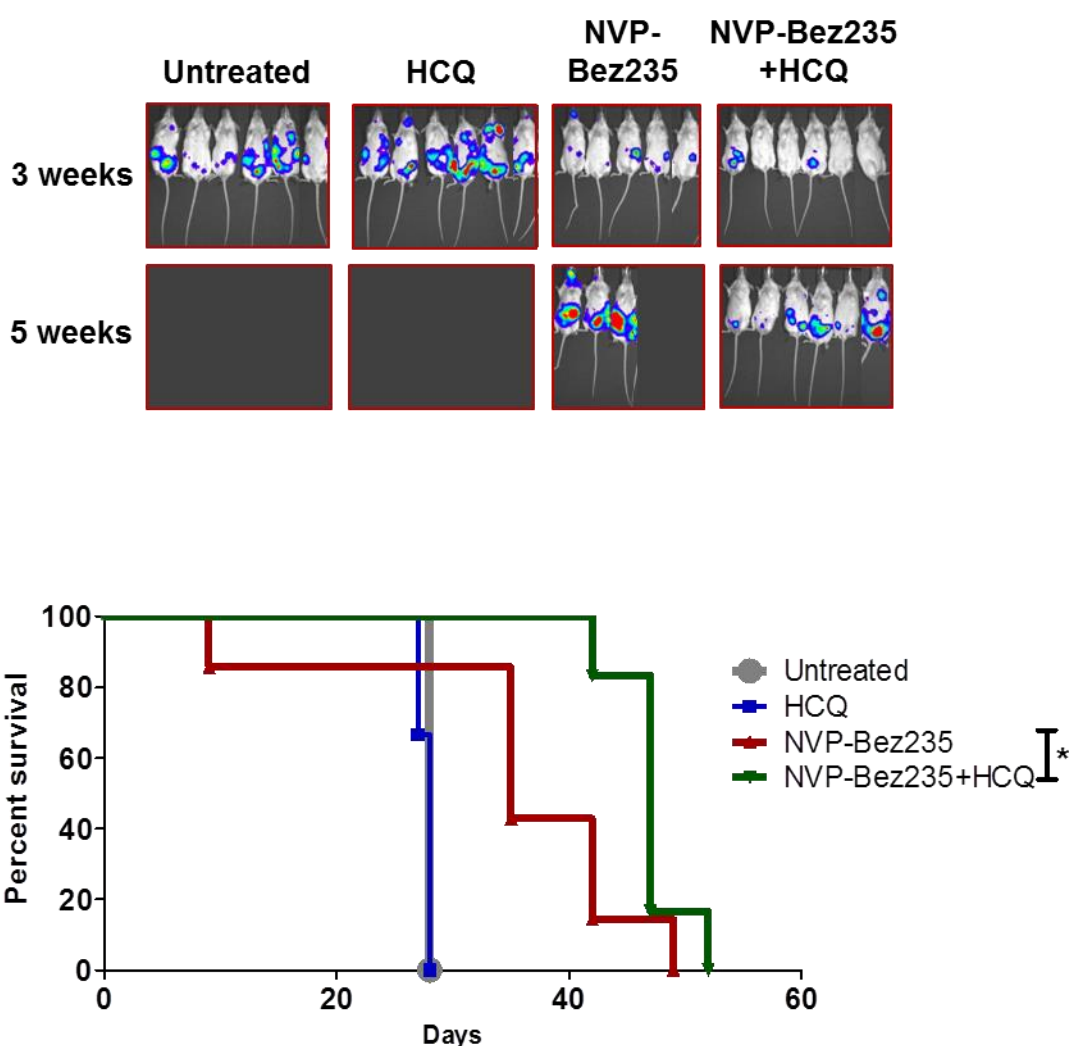


Figure 6-19: KCL22^{Pon-Res} were labelled with lentiviral firefly luciferase intravenously injected into NSG mice (5-6 mice per cohort).

The mice were treated once daily with vehicle control, 60 mg/ml HCQ by IP injection, 45 mg/kg of NVP-Bez235 or the combination of NVP-Bez235 and HCQ. (a) Disease burden and engraftment were recorded weekly by IVIS bioluminescent imaging. (b) Overall survival was monitored and measured by Kaplan-Meier analysis using graphpad prism. Annotation above a bar refers to statistical (*; $p \leq 0.05$).

Overall our data showed that TKI resistance can occur through the aberrant activation of alternative survival pathways. This was observed in our ponatinib-resistant KCL22 cell model which no longer required BCR-ABL for survival. Instead this cell model was highly dependent on mTOR, which was shown by the sustained mTOR activation and sensitivity to mTOR inhibition by catalytic inhibitor NVP-Bez235. We also showed the potent mTOR inhibition by NVP-Bez235 induced protective autophagy. Furthermore, pharmacological inhibition of autophagy, in combination with NVP-Bez235, enhanced the NVP-Bez235

induced cell death, which we therefore propose as an alternative treatment option to tackle the problem of BCR-ABL-independent mechanism TKI-resistant CML.

6.13 Key findings

Very importantly in this chapter we show that MNCs derived from three TKI-resistant CML patients, who are thought to have a BCR-ABL independent mechanism of TKI resistance, are also sensitive to NVP-Bez235-mediated mTOR inhibition *ex vivo*. NVP-Bez235 significantly increased apoptosis above TKI treatment as well as significantly reducing colony formation.

Additionally we showed that NVP-Bez235-mediated mTOR inhibition induces protective autophagy in KCL22^{Pon-Res} cells, which could be inhibited via lentiviral KO and KD methods targeting essential autophagy gene *ATG7* and pharmacologically by treatment with HCQ, which increased the sensitivity of KCL22^{Pon-Res} cells to treatment with NVP-Bez235. Importantly we showed that HCQ mediated autophagy inhibition enhances the effect of dual PI3K and mTOR inhibitors against primary TKI-resistant CML cells. This was validated *in vivo* by transplanting KCL22^{Pon-Res} cells tagged with firefly luciferase into NSG mice and treating the mice with a combination treatment of NVP-Bez235 and HCQ, which significantly reduced the development of leukaemia and prolonged the survival of the NSG mice. This study provides strong pre-clinical data that this drug combination would improve the treatment of BCR-ABL independent TKI resistant CML compared to current drug regimes, which is shown to be a safe and tolerable treatment *in vivo*. Therefore, this study provides a rationale for testing this drug combination in the clinic for BCR-ABL independent TKI resistant CML patients who are not responding to TKIs.

7 Results (V): Establishing CRISPR as a genome-wide screening tool for the study of BCR-ABL-independent TKI-resistance

7.1 Gene knock-down

RNA interference is a very powerful tool in cellular biology and a widely used approach to study specific gene function (Hannon, 2002). The technique of “knocking down” a gene degrades the target’s gene expression and therefore impacts upon the translation of the targets protein product. The inhibition of the translation of the protein allows investigations into the function of the gene by analysing the resulting change, if any, in the cells phenotype. This is carried out by editing the cell’s DNA, through sequence specific degradation of the host mRNA, meaning that this gene can no longer be translated into a functional protein. Traditionally, this technique uses short-hairpin RNAs (shRNAs), which contain a sequence specific to the target gene. The shRNA is delivered into the cells via lentiviral vectors and is integrated into the host’s genome, which allows for long-term knockdown of the target gene. However, by using this strategy gene function is reduced, but not eliminated.

Therefore, with recent advancements in genome editing using Clustered Regularly Interspaced Short Palindromic Repeat (CRISPR) as an exciting tool not only to knockout single genes, but with the potential to be used as a whole genome screening tool, we established protocols and designed experiments for the use of CRISPR within our laboratory. Our intention was to use the CRISPR whole genome knockout screen to infect a CML cell line and knock out 1 gene from the whole genome in each cell and treat the cells with TKI to assess if the deletion of single gene could cause drug resistance against TKIs. We hoped this may provide an effective tool to uncover new gene targets, which may be the main cause of BCR-ABL-independent TKI resistance, as so far many different mechanisms have been implicated.

7.2 Clustered Regularly Interspaced Short Palindromic Repeat (CRISPR)/Cas system

Background: The interpretation of gene function and that of their variants requires precise genome editing technologies. Although protein-based targeting methods, such as Zinc Finger Nucleases (Gonzalez et al., 2010) and Transcription Activator-Like Effector Nucleases (TALEN) (Zhang et al., 2011), had enabled targeted genome modifications, a need still remained for new technologies that were affordable and easy to design, which would not be limited in large scale use.

In 2013 a new system was introduced to the field, Clustered Regularly Interspaced Short Palindromic Repeat (CRISPR)/Cas system (Cong et al., 2013, Hsu et al., 2013, Mali et al., 2013b). This has given the research community the ability to precisely edit the genome of a living cell, which has opened up an exciting range of possibilities for future research, including the potential for therapeutic and biotechnological application.

The new CRISPR technology is based on a naturally occurring biological mechanism, first discovered in bacteria and archaea, used as a novel defence mechanism against environmental stresses, such as viral infections (Barrangou et al., 2007).

CRISPR repeat sequences were initially discovered in *E.Coli* in 1987 (Ishino et al., 1987). However, very little was known about them until 2002, when these genomic sequences were characterised and subsequently coined 'CRISPR' after similar sequences had been observed in genomes of various bacteria and archaea (Jansen et al., 2002, Mojica et al., 2000). At this time the biological function of the CRISPR region had still eluded researchers until in silico studies of the spacers revealed sequence homology corresponding to foreign elements, such as bacteriophage and plasmid sequences (Makarova et al., 2006, Mojica et al., 2005). These studies hypothesised that the function of the CRISPR region was to provide immunity against genetic material, via a RNA interference based mechanism. This was confirmed by Barrangou and colleagues in 2007, where they reported that after a viral challenge, bacteria integrated new spacer sequences derived from phage genomic DNA into the CRISPR region. The CRISPR spacer content along with the CRISPR-associated (Cas) enzymatic machinery, provided the bacteria with a specific nucleic acid based immunity against phages containing the particular sequence (Barrangou et al., 2007). The system is made up of two main components; the CRISPR array, which is composed of spacer sequences corresponding to invading viral or plasmid sequences and is located on the host genome often next to the Cas genes (Barrangou et al.,

2007, Ishino et al., 1987, Jansen et al., 2002, Makarova et al., 2006, Mojica et al., 2005, Mojica et al., 2000) and the second component: Cas protein complex which is a large and heterogeneous family of proteins that carry functional domains typical of nucleases, helicases, polymerases, and polynucleotide-binding protein. CRISPR, in combination with Cas proteins, forms the CRISPR/Cas systems (Haft et al., 2005, Jansen et al., 2002, Makarova et al., 2006).

Through further study, much more is now known about the CRISPR/Cas system and its function in bacteria and archaea. This defence mechanism has the ability to incorporate foreign genetic material in specific locations within a CRISPR region of the host genome (Barrangou et al., 2007, Ishino et al., 1987, Jansen et al., 2002, Makarova et al., 2006, Mojica et al., 2000, Mojica et al., 2005). The foreign gene sequences are processed into non-coding RNAs and in conjunction with Cas proteins can bind to invading foreign genetic material with the same sequence (Jinek et al., 2012). This sequence recognition informs nucleases in the Cas protein complex to cleave the invading nucleic acids and prevent the viral attack (Jinek et al., 2012). This exposure provides the host with heritable immunity (figure 7-1).

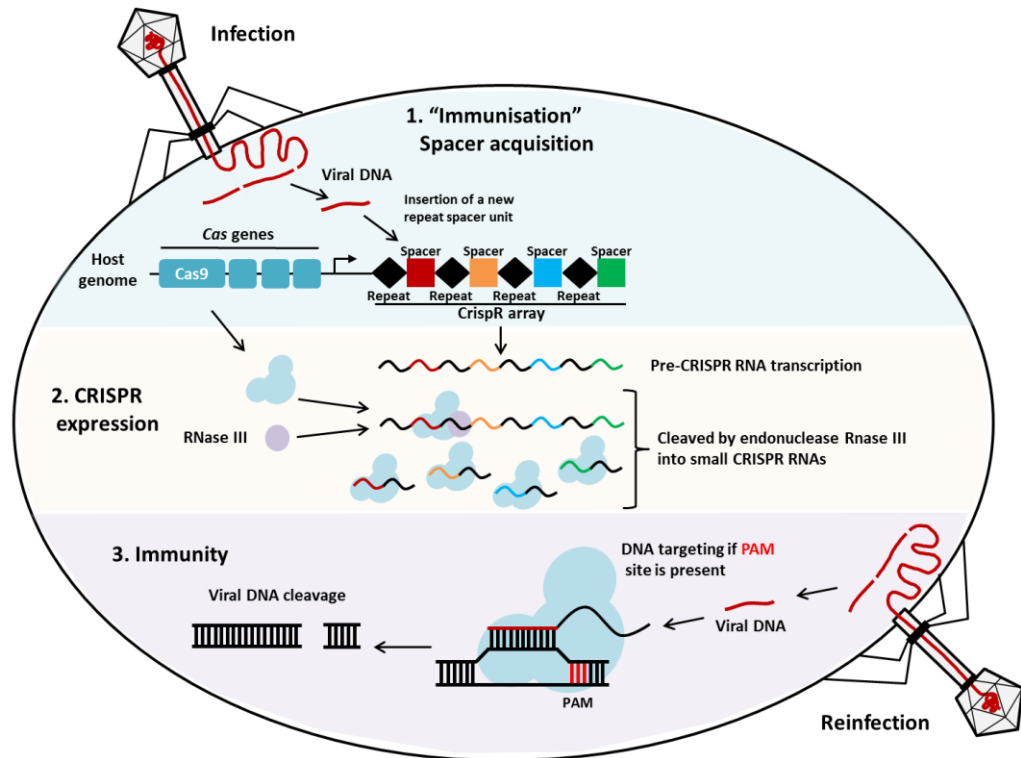


Figure 7-1: The functional mechanism of the type II CRISPR-Cas systems for adaptive immunity.

CRISPR can be separated into stages, first is the "immunisation step" or spacer acquisition. This is when the host recognises an invading virus and subsequently integrates short sequences of DNA from the invading virus's genome into the CRISPR region of its own genome. These foreign 'spacer' sequences are only 20 nucleotides long and are integrated between two repeat units to form the CRISPR array. The corresponding sequence of the spacer on the viral genome is known as the 'protospacer'. In most cases following the protospacer there is a short conserved nucleotide sequence, referred to as the Protospacer Adjacent Motif (PAM) and this is a recognition motif required for acquisition of the viral DNA fragment. This process requires the use of nucleases, which are present in the Cas protein complex. The second stage is 'CRISPR expression' where, RNA polymerase transcribes the CRISPR array into a pre-CRISPR RNA. The pre-CRISPR RNA is cleaved by endonucleases into small CRISPR RNAs or otherwise known as guide RNAs (gRNA). In the final stage, 'immunity', the gRNAs, within the multi protein complex recognise and bind specifically with complimentary regions of the foreign DNA. This then initiates cleavage of the gRNA and foreign nucleic acid complex. Adapted from (Mali et al., 2013a).

7.2.1 CRISPR as a genome editing tool

In 2013 the Feng Zhang and George Church laboratories at the Broad Institute and Massachusetts Institute of Technology successfully engineered the CRISPR-Cas9 system for mammalian genome editing (Cong et al., 2013, Hsu et al., 2013, Mali et al., 2013b). The method consists of the same two components: a gRNA, specific to the gene target and the Cas proteins. This particular system uses the type II CRISPR system, which is unique as it only uses one Cas protein for gene silencing; Cas9 (Deltcheva et al., 2011, Jinek et al., 2012).

The gRNA must contain a 20 nucleotide sequence specific to the target gene, otherwise known as the 'spacer'. The sequence must also be immediately upstream of a PAM sequence, as this is crucial for targeted binding (Sternberg et al., 2014, Swarts et al., 2012). PAM sequences are specific to the species in which the endonuclease originated. In this specific protocol, the Cas9 endonuclease, which was isolated from *Streptococcus pyogenes* is exploited. The PAM sequence for this species is: 5' NGG 3' (Cong et al., 2013, Mali et al., 2013b).

Once expressed the Cas9 proteins and gRNA form a riboprotein complex, and Cas9 undergoes a conformational change, which shifts it from being in an inactive non-DNA binding formation, to an active DNA binding formation (Jinek et al., 2012). The 'spacer' sequence of the gRNA remains available for binding with the target DNA (Nishimasu et al., 2014). The gRNA-Cas9 complex will bind any genomic sequence with a PAM site, but will only cleave the sequence if there is a high homology between the gRNA and the target DNA (Jinek et al., 2012). Once the gRNA-Cas9 complex binds the target, the 3' end of the gRNA anneals to the target DNA in a 3' to 5' direction. This zipper like annealing mechanism starting from the 3' end may explain why low homology stops Cas9 cleavage, as 3' end pairing needs to be more precise than 5' pairing, which decreases the chances of off target effects. Cas9 has two functional nuclease domains, RuvC and HNH (Jinek et al., 2012). When Cas9 binds to the target DNA it undergoes a second conformation change which positions the nuclease domains to cleave opposite strands of the target DNA, resulting in a double stranded break (DSB) around 3-4 nucleotides upstream of the PAM site (Jinek et al., 2012). The DSB can be repaired by either (1) an efficient but error-prone Non-Homologous End Joining (NHEJ) pathway or (2) the less efficient but high fidelity Homology Directed Repair (HDR) pathway (Jinek et al., 2013, Lin et al., 2014).

The NHEJ pathway is the most active repair mechanism capable of rapidly repairing DSBs, but due to its high activity this process frequently incurs mistakes (Shrivastav et al., 2008). However, this becomes useful for gene editing. NHEJ most commonly creates small insertions or deletions (InDels) in the target DNA, which can cause in-frame insertions or deletions, or frameshift mutations leading to premature STOP codons within the open reading frame (ORF) (Shrivastav et al., 2008). This can cause a loss-of-function mutation, rendering the gene inactive and therefore knock-out the target gene (Jinek et al., 2013).

CRISPR has opened up many different possibilities for genome editing. It was originally thought to be a useful tool to knockout (KO) a target gene in mammalian cells, but has now had its use extended to selectively activate or repress target genes, to purify specific regions of DNA, to image DNA in live cells using fluorescent tags and also for genome-wide screens.

7.2.2 CRISPR as a genome-wide forward screening tool

Due to the simplicity of generating custom gRNAs to repress almost any gene in the genome, CRISPR-Cas9 has become an ideal genome editing system for large-scale genetic screening. Forward genetic screens are very useful tools to study disease phenotypes, when there is no known underlying cause. By using this method, we can take parental cells and knockout genes in the cell population to try and identify if any particular gene KO can mimic the same phenotype as the disease. Before the discovery of CRISPR, shRNA screens were used in this context, but these screens were not so reliable due to incomplete knock-downs of the target genes. However, CRISPR is capable of generating a population of cells that have a homogenous gene knock-out, which gives it a higher sensitivity for screening, especially, in cases where reduced gene expression can still allow gene function, as seen with autophagy genes. In 2014, the Zhang lab at MIT showed that by delivery of pooled single gRNA-Cas9 CRISPR libraries using lentivirus it was possible to conduct both positive and negative loss-of-function screens in mammalian cells (Sanjana et al., 2014, Shalem et al., 2014). Pooled CRISPR libraries are heterogeneous populations of lentiviral vectors, that each contains one gRNA to target a single gene within the genome. The gRNAs are designed *in silico* and synthesised. These individual gRNAs are then cloned into CRISPR lentiviral vectors and pooled.

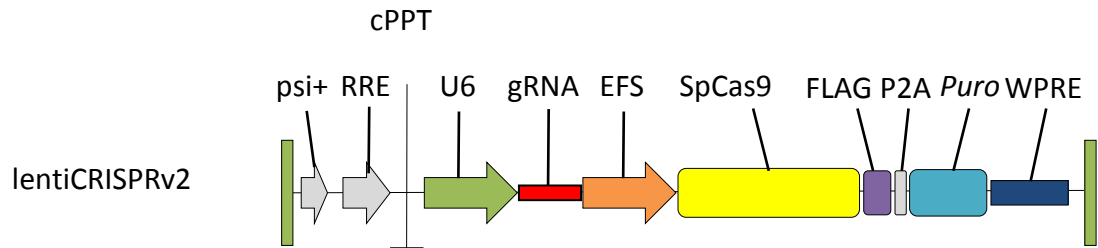
In this study we used the human Genome-scale CRISPR Knock Out (GeCKO) v2 library to help us uncover whether the loss of a single gene may cause TKI resistance in CML cells and potentially mimic what is seen with patients in the clinic. The GeCKO v2 library was

generated by the Zhang lab (Sanjana et al., 2014, Shalem et al., 2014) and consists of 122,411 unique gRNAs for gene KO on two separate plasmids, 65,383 in Library A and 58,028 in Library B. This targets 19,050 genes in the human genome. The two libraries (A and B) are used together so there are 6 gRNAs to target each gene to ensure there is sufficient coverage of each gene. Both of the libraries contain 1000 control gRNAs designed not to target the genome, and library A also contains gRNAs to target 1864 miRNAs, 4 gRNAs per miRNA (Sanjana et al., 2014, Shalem et al., 2014). Complete sequences of all the gRNAs in library A and B are available on the Zhang laboratories website <http://www.genome-engineering.org/gecko/>.

The GeCKO v2 library is available either in a 1 vector system, using lentiCRISPRv2, which has Cas9 in the plasmid constructs, or as a 2 vector system, where first cells are made Cas9 competent using the lentiCas9-Blast plasmid, then the gRNA libraries are added using lentiGuide-Puro plasmids. Although the 2 vector format requires more steps, the lentiGuide-Puro plasmid has the advantage of higher titer for the library virus (figure 7-2) (Sanjana et al., 2014, Shalem et al., 2014).

The GeCKO screening systems have been shown to have very high modification efficiency, low off target modification, high consistency between unique sgRNAs targeting the same genes and high validation rate of screen hits (Sanjana et al., 2014, Shalem et al., 2014).

One vector lentiviral GeCKO system



Two vector lentiviral GeCKO system

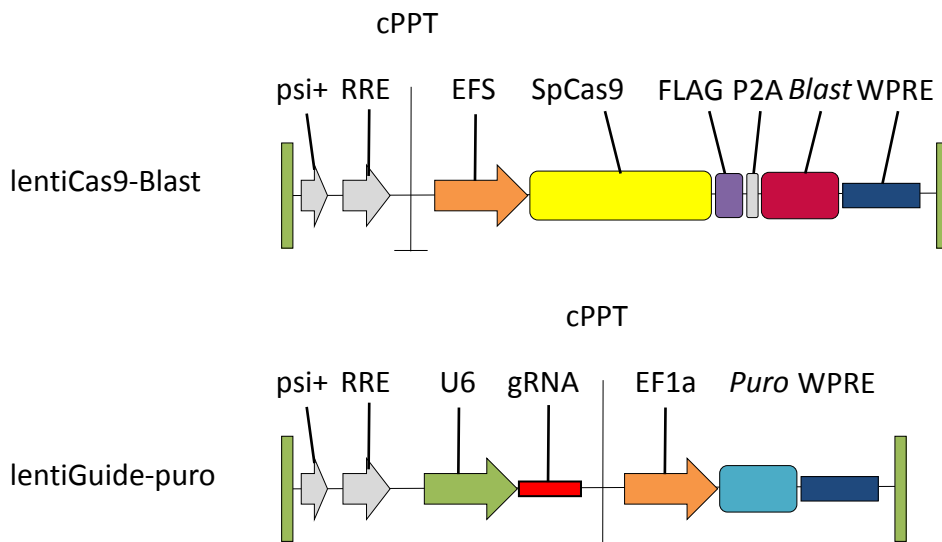


Figure 7-2: Lentiviral expression vectors for the one vector (lentiCRISPRv2) and two vector GeCKO systems (lentiCas9-Blast and lentiGuide-puro).

Puro, puromycin selection marker, Blast, blastocidin selection marker; psi+, psi packaging signal; RRE, rev response element; cPPT, central polypurine tract; U6, U6 promoter element; EFS, elongation factor-1a short promoter; P2A, 2A self-cleaving peptide; WPRE, posttranscriptional regulatory element. Figure from (Sanjana et al., 2014)

7.2.3 Method: Genome-wide forward CRISPR screen

GeCKO CRISPR pooled libraries were bought from Addgene. Here I will explain my experimental design for a pooled CRISPR screen in KCL22 parental cells.

7.2.3.1 GeCKO pooled electroporation, plating, determination of transformation efficiency and maxi prep

The pooled libraries are provided at a quantity that is too low for immediate large screening application. Therefore, the first step is to amplify the library to a concentration that is sufficient to be used to generate lentivirus.

In order to amplify the DNA of the pooled libraries received from Addgene the ‘GeCKO pooled electroporation, plating, and determination of transformation efficiency and maxi prep’ protocol was used, which was published by the Zhang lab.

The following protocol was followed to amplify and prepare each library, A and B separately.

First the DNA concentrations of GeCKO libraries A and B were determined using the NanoDrop ND-2000 spectrophotometer. The GeCKO libraries were both diluted to 50 ng/ μ L in water. DNA was amplified using Lucigen EnduraTM electrocompetent cells and electroporation as per the manufacturer’s instructions. Four transformations per library were set up.

The 0.1 cm gap Electroporation cuvettes (Bio-Rad, Cat no. 1652089) and microcentrifuge tubes were chilled on ice. 25 μ L of the EnduraTM cells were aliquoted into a chilled microcentrifuge tube. 100ng of library A and B DNA was electroporated into 25 μ L aliquots of Lucigen EnduraTM electrocompetent cells (Lucigen, Cat no. 60242-1) with efficiency 1×10^{10} cfu/ μ g. The mixture was stirred carefully with a pipette tip and transferred into a chilled 0.1cm electroporation cuvette. The cuvette was flicked downwards to deposit cells at the bottom of the cuvette and electroporated using the following instructions: 10 μ F, 600 Ohms, 1800 Volts for 3.5 to 4.5 milliseconds. Immediately following the pulse 975 μ L of room temperature Recovery Medium was added to the cuvette, the cells were resuspended and transferred to a culture tube containing a further 1 ml of Recovery Medium. The culture tubes were incubated at 37°C for 1 hour with constant agitation.

In order to calculate the transformation efficiency a dilution plate was set up. 8 mL of the electroporated cells was pooled and mixed well. 10 μ L of cells was transferred to 1 mL of

recovery medium, mixed and plated 20 μL onto a pre-warmed LB agar plates containing 100 $\mu\text{g}/\text{mL}$ ampicillin. This was performed separately for library A and B. This was a 40,000 fold dilution of the transformation and allowed for an estimation of the transform efficiency to ensure full representation of the library.

The rest of the transformation cultures were plated out on 20 10cm^2 LB agar plates containing 100 $\mu\text{g}/\text{mL}$ ampicillin. 400 μL of the culture was plated per LB plate. The cultures were grown for 14 hours at 32°C ; the lower temperature reduces recombination between the lentiviral long-term repeats.

Following a 14 hour incubation the transformation efficiency was calculated. The number of colonies was counted for library A and library B. The number of colonies was multiplied by 40,000, to correct for the dilution factor. The colony number should be 3×10^6 , this equates to 50x colonies per construct in the GeCKO library.

The transformation plates were then harvested by pipetting 500 μL of LB broth onto each plate and the colonies were scraped off using a cell scraper. The liquid culture was then pipetted into and tube and repeated on the same plate. The culture was then centrifuged at 6,000 xg for 20 minutes at 4°C and the supernatant was discarded. The bacterial pellets were frozen at -20°C and taken to the Beatson services for DNA extraction.

Following DNA extraction, the gRNA representation was checked using next generation sequencing, to ensure no guides have been lost or over amplified, which may introduce bias to the screen.

7.2.3.2 DNA sequencing

The DNA sequencing protocol was followed from the supplementary methods of improved lentiviral vectors and genome-wide libraries for CRISPR screening (Sanjana et al., 2014).

To analyse the guides from the DNA, 2 PCR steps were performed. The first PCR amplifies lentiCRISPR gRNAs and the second PCR step attaches the Illumina adaptors and barcodes the samples.

In the first PCR reaction, two separate reactions were set up for library A and library B. The primers sequences used to amplify lentiCRISPR gRNAs were used, which were designed by the Zhang lab and the sequences are publicly available on the GeCKO website http://genome-engineering.org/gecko/?page_id=15.

v2Adaptor_F: **AATGGACTATCATATGCTTACCGTAACTTGAAAGTATTTTCG**

v2Adaptor_R: **TCTACTATTCTTTCCCCTGCACTGTtgtggcgatgtgcgctctg**

These primers were ordered as standard desalted oligonucleotides from IDT and on arrival were resuspended in sterile water at a stock concentration of 100 μ M, for the PCR step the stock was diluted 1:10 for a working concentration of 10 μ M.

Each PCR reaction was set up with a total volume of 50 μ L. First 10 μ g of template DNA was added to a chilled PCR tube, to this 2.5 μ L of 10 μ M of v2Adaptor_F and v2Adaptor_R, final concentration 0.5 μ M. This was made up to 25 μ L with Nuclease free water (Qiagen, Cat no. 129114) and then 25 μ L 2xPhusion Flash High-Fidelity PCR Master Mix (Thermo Scientific, F548S) was added and mixed carefully by pipetting. A negative control was also set up minus the template DNA.

The PCR tubes were immediately put on a thermocycler with conditions:

Initial denaturation: 98°C for 10 seconds, denaturation: 98°C for 1 second, annealing: 61°C for 5 seconds, extension: 72°C for 15 seconds, repeated for 20 cycles. Final extension: 72°C for 1 minute then held at 4°C.

The second PCR step was performed to attach the Illumina adaptors and to barcode the samples. These primers were ordered as Ultramers from IDT for high-fidelity synthesis of

very long oligos. Each sample is set up in 12 reactions using 12 different forward primers (F01-F12). The forward primers have a staggered sequence, which are 1-9bp different in order to increase the complexity of the library to avoid problems during sequencing. The same reverse primer is used in the 12 reactions for 1 sample; therefore, it is specific for that biological condition. For example: Sample 1: F01+R01, F02+R01, F03+R01, F04+R01, F05+R01, F06+R01, F07+R01, F08+R01, F09+R01, F10+R01, F11+R01 and F12+R01. If sequencing multiple samples, different reverse primers are used 12 reverse primer sequences (R01-R12) can be found on the GeCKO website.

Once again this PCR reaction was set up as a 50 μ L reaction, and 4 μ L of the PCR product from the first PCR was used in each of the 12 reactions. Using the entire DNA sample from the first step helps to keep representation of the guides.

Therefore, 4 μ L from PCR 1 was added to a chilled PCR tube, as before 2.5 μ L of 10 μ M F01 primer and R01 primer, final concentration 0.5 μ M was added. This was made up to 25 μ L with Nuclease free water and then 25 μ L 2xPhusion Flash High-Fidelity PCR Master Mix was added and mixed carefully by pipetting. A negative control was also set up minus the template DNA. The same thermocycler parameters were used, apart from one change which was 24 cycles, instead of 20.

The resulting amplicon from the second PCR had an expected length of 340bp. This was run on a 2% agarose gel, for gel extraction, to remove the excess of primers. The gel was stained with SYBR safe and imaged under UV light, the 340bp product was excised, gel extracted using a QIAquick gel extraction kit as per the manufacturer's instructions, bearing in mind the instructions for a 2% gel (figure 7-3).

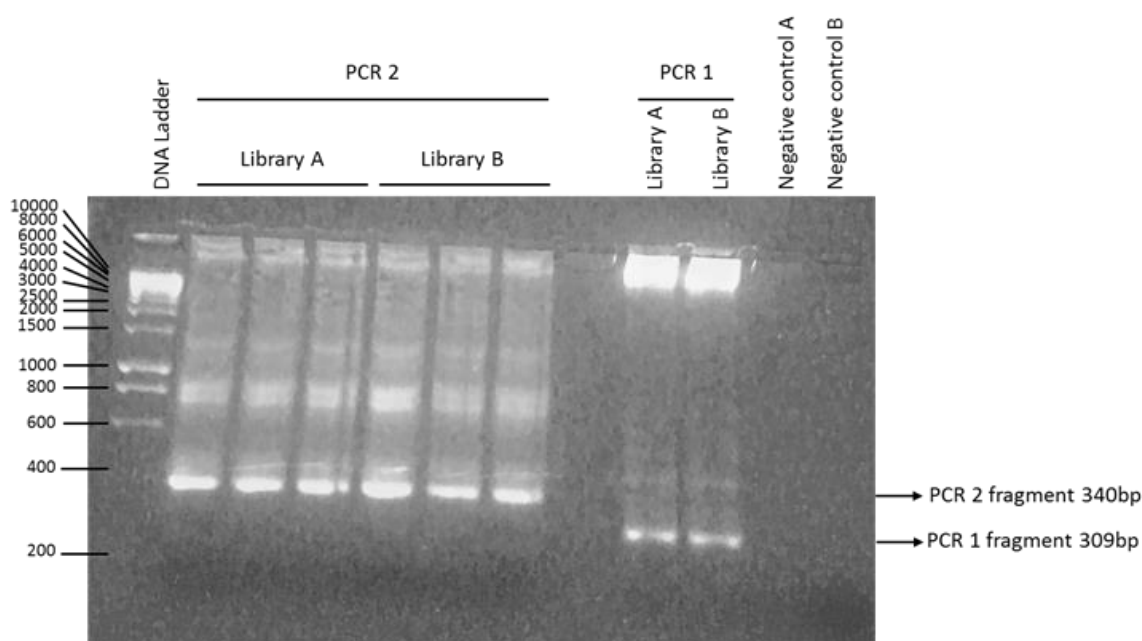


Figure 7-3: Gel electrophoresis of PCR products from PCR 1 and 2. Gel purification of PCR 2 product 340pb.

The PCR products from the same biological condition were mixed and the DNA concentration was measured using a NanoDrop ND2000.

The samples were given to Glasgow Polyomics for sequencing on a HiSeq 2500 (Illumina) and analysis performed by Dr. Pawel Herzyk.

Analysis of the sequencing showed 99.98% representation in both Library A and Library B. All gRNAs were well represented and no skewed bias was shown (figure 7-4).

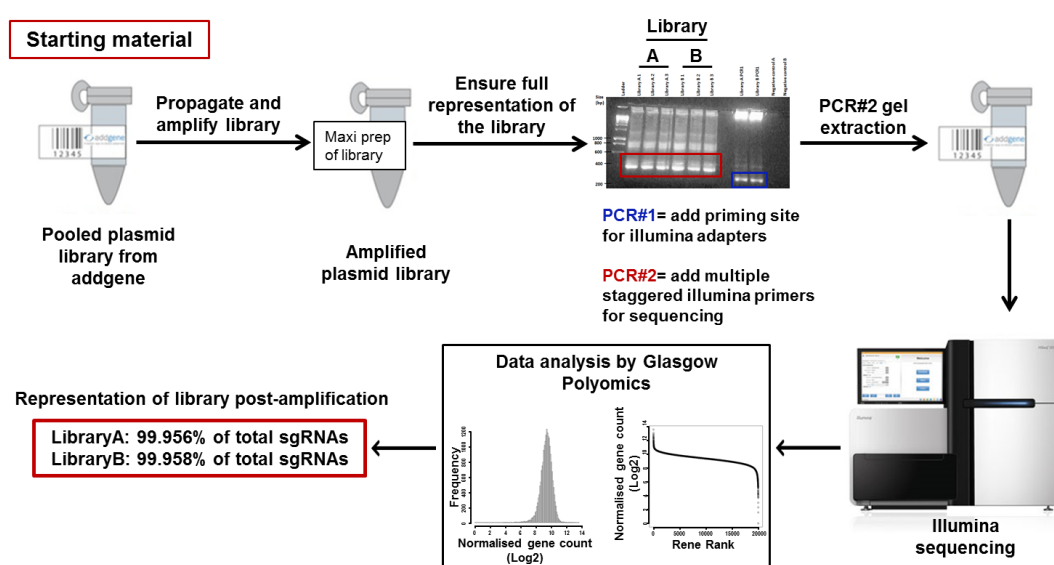


Figure 7-4: The workflow of the GeCKO Library amplification Addgene.

7.2.4 CRISPR 2-vector screen

In this study we used the human CML cell line, KCL22^{WT} as our model. The human GeCKO v2 library was used to transduce the cells and knockout one gene per cell/ within the entire human genome. The cells then underwent ponatinib selection to investigate, whether any TKI-resistant clones could overcome ponatinib treatment.

Our aim in doing so was to uncover whether the loss of a single gene may cause TKI resistance in CML cells.

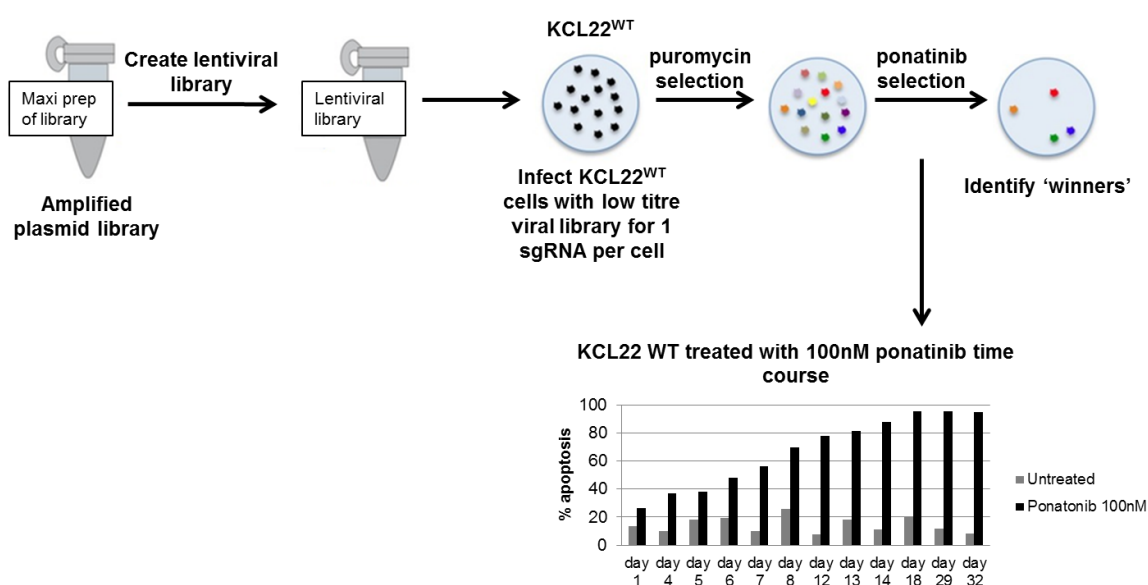


Figure 7-5: The workflow for the positive selection CRISPR Screen.

7.2.4.1 KCL22^{WT} Cas9 competent cells

The first step of the GeCKO CRISPR screen 2 vector is to establish a Cas9 competent cell line, by infecting cells with the lentiCas9-Blast construct.

Lentivirus was produced by transfecting HEK293 cells using the CaCl₂ method as previously described 2.3.12. The virus was used to transduce the KCL22^{WT} CML cell line, using the transduction protocol previously discussed 2.3.13. This construct has a blastocidin selection marker; therefore, these cells were selected in 10 µg/ml blastocidin for 14 days. To allow for an assessment of Cas9 expression the Cas9 protein was FLAG-tagged (DYKDDDDK Tag) and the protein expression was analysed by western blot. Therefore, follow selection, protein was extracted from the KCL22^{WT} cells, as per protocol, and analysed for Cas9 expression via a FLAG antibody (Sigma, Cat no. F3165).

KCL22 cells stably expressing Cas9



Figure 7-6: Stable expression of LentiCas9-Blast in KCL22^{WT} cells.

In order to assess the ponatinib treatment period needed to kill TKI-sensitive CML cells, a ponatinib treatment time course was performed.

7.2.4.2 Ponatinib treatment time course

KCL22^{WT} cells were seeded at $0.25 \times 10^6/\text{mL}$ grown in RPMI in the presence of 100 nM ponatinib. An apoptosis assay was performed every few days to analysis the effect of ponatinib on cell death. Cells were also imaged after four weeks to observe the morphology of the cells. After 5 weeks of ponatinib treatment, the drug was washed out and cultured in RPMI only, for a further 10 days; however, no cells were able to repopulate the culture following treatment (figure 7-7).

KCL22^{WT} cells under a ponatinib treatment time course

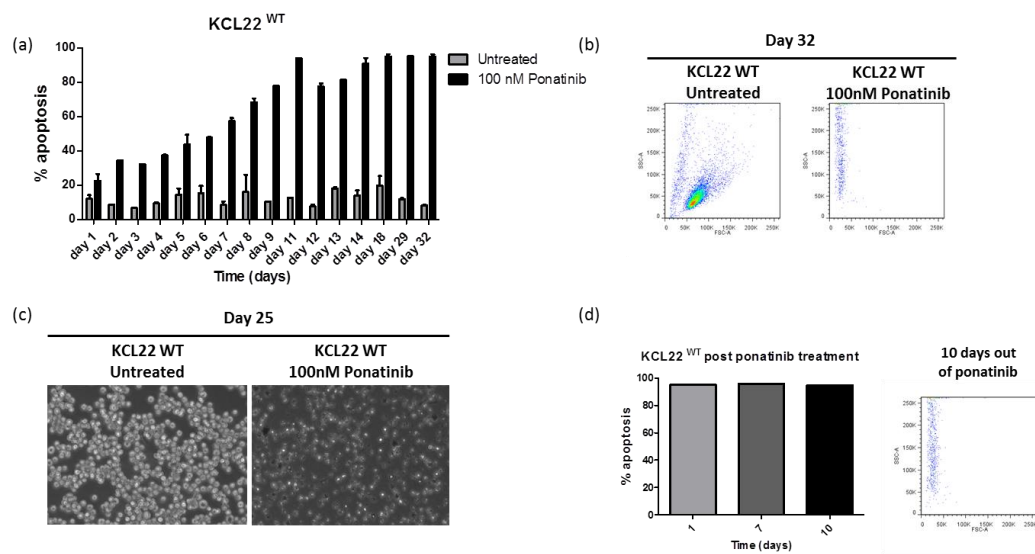


Figure 7-7: KCL22^{WT} cells under a ponatinib treatment time course.

7.2.4.3 Lentivirus production

A large quantity of virus was needed to perform the whole screen, including enough for replicates. Lentivirus was produced by transfecting HEK293 cells using the CaCl₂ method.

14 cm² cell culture dishes were used for viral production. These plates have a 2.8x bigger surface area than a 10 cm² dish, therefore conditions previously discussed for lentivirus production were multiplied by 2.8.

2.8x10⁶ HEK293 cells were plated in eight 14 cm² cell culture dishes in 28 ml DMEM three days prior to the transfection to allow the cells to adhere to the plate. After three days 70% confluency was achieved and the media was replaced by adding 23.8 ml of DMEM plus 30 µM of chloroquine.

Lentiviral DNA mixes were made for each 14 cm² plate by adding 39.76 µg of library A and 39.76 µg of library B, 34.86 µg psPAX2 and 12.6 µg pCMV-VSV-G into a 15 mL falcon tube. To the DNA mix 2560 µL of sterile water and 512.4 µL 2M CaCl₂ were added and mixed thoroughly. This mix was then added to 4.2 mL of 2xHBSS and mixed very thoroughly. The transfection mixes were incubated at 37°C for 30 minutes and then added dropwise to the HEK293 cells. Each mix made was for one 14cm² cell culture dish. This was allowed to incubate at 37°C for 8 hours, and then medium was replaced with 28 mL of DMEM. The following morning the medium was changed again and 16.8 mL of DMEM was added to the cells. The virus was harvested after 48 hours by collecting media, centrifuging at 300 xg for 5 minutes and filter sterilising the viral supernatant using a 0.45 µM filter. The virus was pooled and immediately snap frozen in dry ice and transferred to a -80°C for storage.

7.2.4.4 CRISPR library virus titration

In order to understand how a single gene knockout will affect a cells phenotype in this whole genome targeted format, only one gene can be knocked out per cell. Therefore, a very low multiplicity of infection (MOI) is required to ensure only 1 gene is knocked out per cell. An MOI of 0.3-0.5 was the recommended infection rate (Shalem et al., 2014).

To find the optimal virus volumes for achieving an MOI of 0.3-0.5 the Cas9 competent cells, KCL22^{WT}-Cas9-Blast, were infected with different volumes of virus. 1×10^6 KCL22^{WT}-Cas9-Blast cells were plated per well in a 6 well plate. The frozen virus was defrosted and pre-warmed. Six different volumes of virus were added to the cells 0.1 mL, 0.2 mL, 0.5 mL, 1 mL, 2 mL, 4 mL, total volume of 4 mL per well made up with RPMI medium. The cells were incubated with the virus for 24 hours. Following the 24 hour incubation the viral medium was removed by centrifugation and replaced with RPMI. Each well was split into duplicate wells and one replicate received 5 μ g/mL puromycin for 72 hours. The cells were counted and analysed by FACS using DAPI staining to evaluate the % of cells that had died post puromycin selection. A MOI of 0.3-0.5 equates to 50-70% cell death. Erring on the side of caution, a virus volume of 0.5 mL was chosen for large-scale screening (figure 7-8).

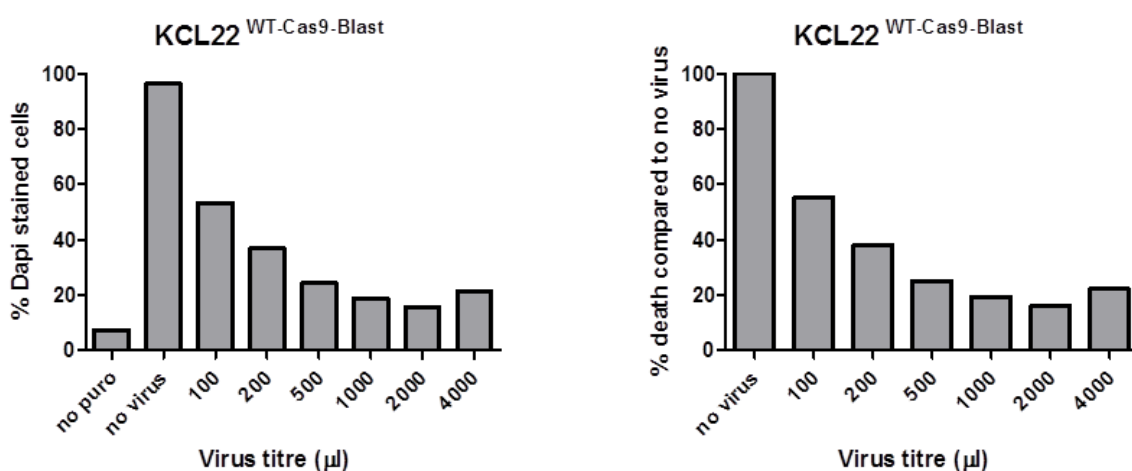


Figure 7-8: Virus titration on KCL22^{WT}-Cas9-Blast after 72 hours

7.2.4.5 KCL22^{WT} resistant screen

In order to have good representation of all the guides in a population of cells, a calculation was made to ensure 400x coverage for each guide. The GeCKO Library's A and B together contain over 120,000 gRNAs, therefore in theory, 120×10^6 cells are needed per infection. Using an MOI of 0.4, after puromycin selection leaves 48×10^6 cells. This equates to over 400 cells with every single gRNA.

Therefore, 120×10^6 KCL22^{WT}-Cas9-Blast cells were seeded, at a cell concentration of 0.5×10^6 /mL. The total volume of media need equates to 240 mL, therefore, cells were resuspended in 210 mL of RPMI and 30 mL of viral supernatant. The cells were incubated for 24 hours with the virus and following the incubation period the viral medium was removed by centrifugation and replaced with RPMI, supplemented with 2.5 μ g/mL puromycin for selection. The cells were initially incubated for 72 hours and then the concentration of puromycin was increased to 5 μ g/ml for a further 7 days to ensure a thorough selection of cells, which had been transduced with the lentivirus (figure 7-9).

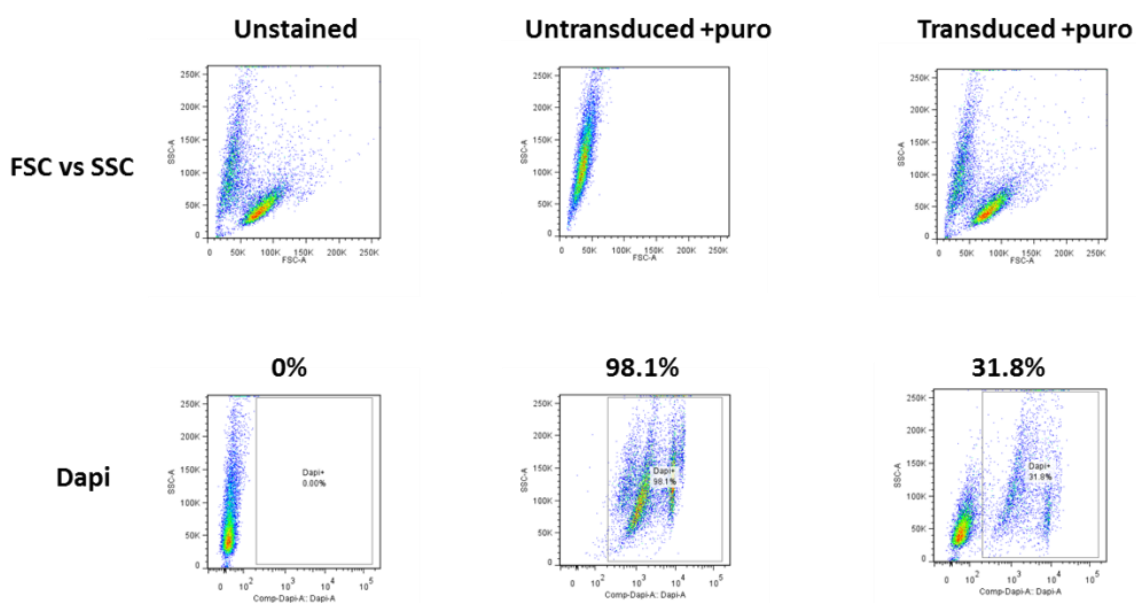


Figure 7-9: KCL22^{WT}-Cas9-Blast FACS analysis post 10 days puromycin selection.

On day 10, 10×10^6 cells were taken for genomic DNA analysis to ensure the coverage of the gRNAs post transduction. 48×10^6 cells were cultured in RPMI supplemented with 100 nM ponatinib, with the exception of a control flask without ponatinib treatment. All the rest of the cells were frozen down. Another important control for the screen was KCL22^{WT}-Cas9-Blast cells not transduced with the library treated with ponatinib. The cells were either passaged or fresh media and ponatinib replaced every 3 days. Cells were FACS analysed with Dapi staining once a week. After 4 weeks of ponatinib treatment a population of cells in the GeCKO library transduced KCL22^{WT} cells had survived, unlike the non-transduced cells. The surviving cell population was FACS sorted (figure 7-10).

These cells were allowed to recover overnight in culture and the following day genomic DNA was extracted using a QIAamp DNA Mini Kit (Qiagen, Cat no. 51304) as per the manufacturer's instructions. The DNA concentration was measured using a nanodrop ND2000 (Table 7-1).

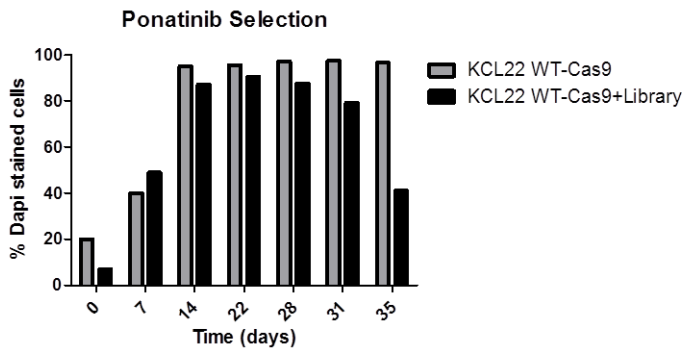
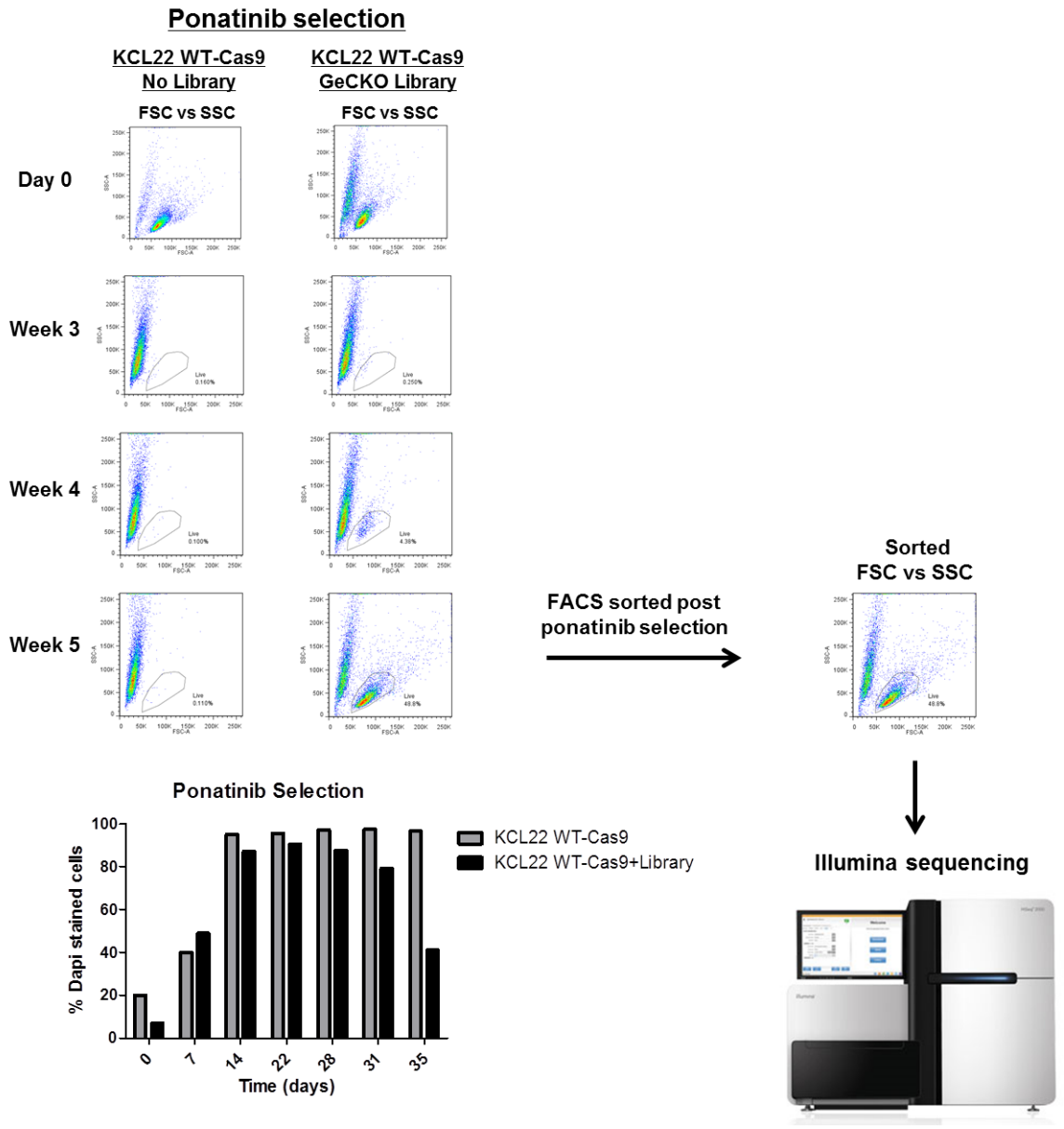


Figure 7-10: : Ponatinib selection and FACS sorting of the CRISPR screen.

Sample	DNA concentration ng/ μ L	Quality (260/280)
CRISPR screen day 0 1	427.4	1.98
CRISPR Screen day 0 2	457	1.93
CRISPR screen post ponatinib 1	507.8	1.98
CRISPR screen post ponatinib 2	884.4	1.91
CRISPR Screen post ponatinib 3-1	660.2	2
CRISPR Screen post ponatinib 3-2	1992.9	1.99
CRISPR Screen post ponatinib 3-3	1935.4	1.95
CRISPR Screen post ponatinib 3-4	1094.7	1.94
CRISPR Screen post ponatinib 3-5	1942.2	2
CRISPR Screen post ponatinib 3-6	1990.2	2
CRISPR Screen post ponatinib 3-7	1523.6	1.98
CRISPR Screen post ponatinib 3-8	2036.7	1.99
CRISPR Screen post ponatinib 3-9	1985.8	1.95
CRISPR Screen post ponatinib 3-10	2317.5	1.99
CRISPR Screen post ponatinib 3-11	1948	1.99

Table 7-1: CRISPR screen gDNA concentrations.

7.2.4.6 Genomic DNA sequencing

As previously discussed, PCR was performed in two steps. For the first PCR, in order to achieve 300x coverage over the GECKO library, the amount of input genomic DNA (gDNA) for each sample, the calculation was described by Shalem et al, 2014. It was recommended that 130 μg of DNA was used per sample. Therefore, for each sample, 13 separate 50 μl reactions were performed with 10 μg genomic DNA in each reaction using 2xPhusion Flash High-Fidelity PCR Master Mix as previously described for PCR 1.

The second PCR was performed as previously described, in a 50 μL reaction volume using 5 μl of the product from the first PCR (figure 7-11 and 7-12).

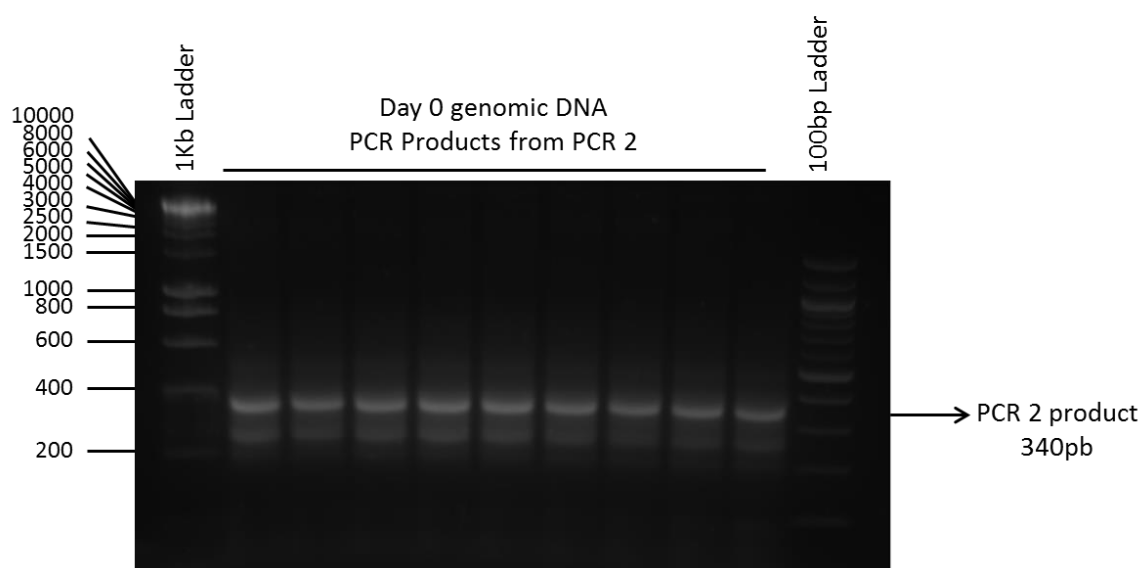


Figure 7-11: Gel purification of PCR 2 product 340pb from KCL22^{WT} resistant screen day 0.

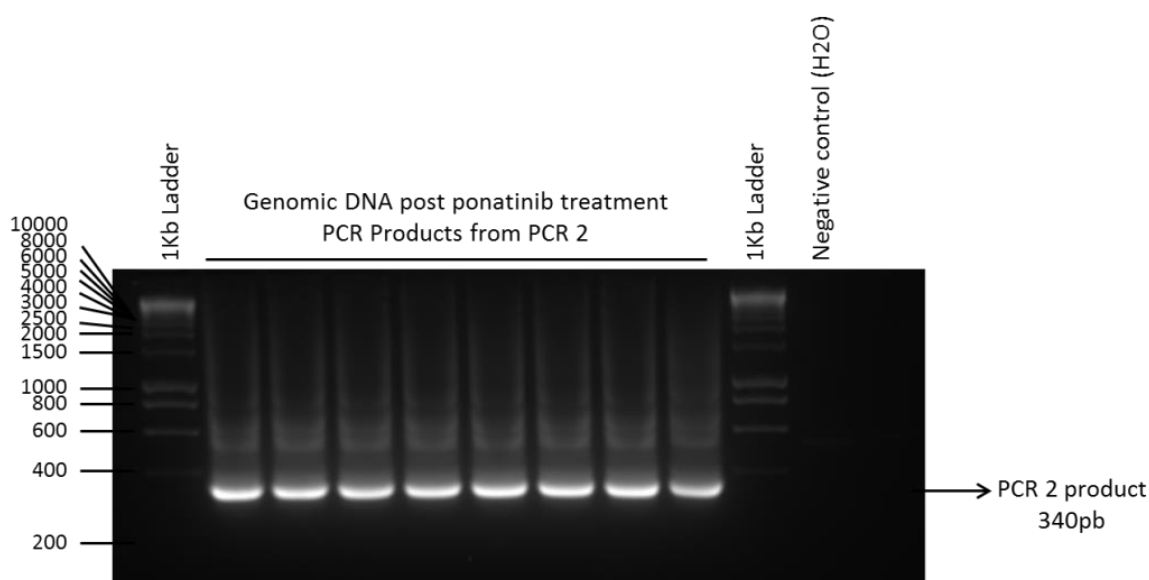


Figure 7-12: Gel purification of PCR 2 product 340pb from KCL22^{WT} resistant screen day 0.

Sample	DNA concentration ng/ μ L	260/280
CrispR screen day 0 PCR 2	194.0	1.87
CrispR Screen post ponatinib 1 PCR 2	116.5	1.89
CrispR Screen post ponatinib 2 PCR 2	170.0	1.89

Table 7-2: CRISPR screen PCR product concentrations.

Preliminary results

The resulting PCR products from the second PCR were gel extracted, quantified, mixed and sequenced using a HiSeq 2500 (Illumina). The sequencing was single ended and 75 bp in length, with a depth of 33 million.

In the preliminary experiment, sequencing revealed 4 dominant gRNAs from the population of KCL22^{WT} cells after 5 weeks of ponatinib treatment (Table 7-3), suggesting that loss of these particular genes may contribute to ponatinib resistance.

Top hits		
Gene	Reads	% of clones in sample
*EDARADD	16128536.39	Sample 1 - 45
TBC1D9	9628072.508	Sample 1 - 27
MRFAP1L1	9595178.017	Sample 1 - 27
CDH4	35415241.35	Sample 2 - 98

Table 7-3: Guide RNAs with the highest reads from the CRISPR Screen.

The results from this preliminary screen showed the top hit was EDARADD, which comprised 45% of the TKI resistant clones from the samples. No evidence has so far been that implicates EDARADD in the development of leukaemia or in drug resistance. However, it is associated with NF- κ B signalling, RelA, which is involved in lymphogenesis, survival and proliferation, the Wnt and BMP signalling and Sonic hedgehog (Shh) signalling. NF- κ B, Wnt, BMP and Shh signalling pathways have all been implicated in TKI resistance or disease persistence in CML. Therefore, pathway modelling to help identify the most likely mechanism causing the resistance could be performed, as well as *in vitro* studies to analysis the response of these 3 pathways when EDARADD is KO in KCL22^{WT} cells compared to the scrambled control.

One unexplained result from the screen, which is hard to interpret is the out growth of clones with a TBC1D9 KO. This gene is more commonly known as Multi-drug resistance 1 (MDR1). Overexpression of MDR1 is known to cause TKI resistance in CML due to increased drug efflux from the cell causing suboptimal concentrations being achieved within the CML cells. Therefore, the reduced expression of this gene causing drug resistance is hard to interpret. Purely, speculator, however there is the possibility a compensatory mechanism has been activated due to the low levels of MRD1, which may lead to the drug resistance.

27% of the clones that became ponatinib resistant had a MRFAP1L1 KO. MRFAP1L1 has not been implicated in the development of leukaemia either, however has been associated with the following: Motility factor 1 like 1, Ubiquitin C, smu-1 suppressor of mec-8 and unc-52 homolog, transmembrane protein 126B, which is involved in assembly of the mitochondrial NADH-ubiquinone oxidoreductase complex, translin-associated factor X; protein kinase C, delta binding protein; which seems to have an immune potentiation function, cyclin-dependent kinase 2 associated protein 2 and RAD52 motif 1. Some of these proteins are associated with CML development such as RAD52 and protein kinase C. Therefore, the KO of MRFAP1L1 may also cause TKI resistance indirectly through one of these associated pathways. Once again, pathway modelling and *in vitro* studies would give us a better understanding of the resistant mechanism.

In the second technical replicate cells with a CDH4 KO comprise 98% of the clones in that sample. CDH4 encodes R-cadherin, which so far has not been implicated in leukaemia, unlike N-cadherin. However, a study in colorectal and gastric cancer showed that promoter methylation of CDH4 results in the loss of gene expression, which could be restored with the treatment with a demethylating agent. Methylation of CDH4 was not detected in

normal patients, and has therefore been considered an early event in tumour progression. This study concluded that CDH4 may act as a tumour suppressor gene in human gastrointestinal tumours, which may also make sense of the result of our CRISPR screen (Miotto et al., 2004). Knocking out a tumour suppressor gene would give the cells a growth and survival advantage, which may be strong enough to cause the CML cells to become drug resistant.

However, high variability in the two technical replicates compelled further investigation (see appendix 9.2). In light of this the remaining cells from the experiment had been frozen down, these cells have now been defrosted and put into culture. The cells underwent the same experimental protocol, 100 nM ponatinib selection for 5 weeks, sorted under the same parameters, genomic DNA extracted, and PCR reactions were performed as previously stated. However, we are still awaiting sequencing to be performed by Glasgow Polyomics, which will be performed using the same parameters.

7.2.5 Future work

7.2.5.1 Design a secondary library

The next conventional step would be to validate the hits confirmed from the primary screen. In order to do so a secondary screen would be performed, by generating a new library that targets the top genes in the analysis of the primary screen.

The guide sequences from the GeCKO libraries are available publicly, http://genome-engineering.org/gecko/?page_id=15.

For construction of the library, the previously published protocol from Shalem et al., 2014, would be followed. However, in brief, the oligos would be synthesized, and amplified using the following primers:

Forward:

**TAACTTGAAAGTATTTTCGATTTCTTGGCTTTATATATCTTGTGGAAAGGAC
GAAACACCG**

Reverse:

**ACTTTTTCAAGTTGATAACGGACTAGCCTTATTTTAACTTGCTATTTCTAG
CTCTAAAAC**

Following amplification, the oligos would then be cloned into the lentiGuide-Puro plasmid (Addgene, Cat no. 52963) using the Gibson ligation reaction (NEB, Cat no, E5510S). The ligation reaction is performed using molar ratio of 1:5 of the vector to insert. The ligated DNA is then transformed into Lucigen EnduraTM electrocompetent cells (Lucigen, Cat no. 60242-1) according to the parameters previously described in GeCKO pooled electroporation, plating, determination of transformation efficiency and maxi prep. 10 parallel transformations are performed and plated onto 10 cm² plates with 100 µg/mL ampicillin for 14 hours at 32°C. Following incubation, bacterial colonies would be collected and plasmid DNA extracted. Virus production and all subsequent steps would be performed as described for the primary screen.

A secondary screen has greater specificity and sensitivity and therefore represents an effective strategy for increasing the rate of true positives. However, as we obtained so few dominant clones from our primary screen it would be within our capabilities to generate single guide RNAs to KO out each individual gene to validate these hits.

7.2.5.2 Negative Screen

A second way of validating the hits in the primary positive screen is to perform a negative screen. The negative screen is essentially an inverse of the primary screen. This screen would utilise the KCL22^{Pon-Res} cell line, therefore these cells are already TKI-resistant. The same whole genome GeCKO library would be used to KO one gene in each cell. The KCL22^{Pon-Res} cells would then undergo ponatinib selection and observed by FACS and DAPI staining to see if the cells become re-sensitised to the TKI. The remaining cell population would then be sequenced and analysed against an untreated population to see what guides had been lost and were therefore responsible for the re-sensitisation.

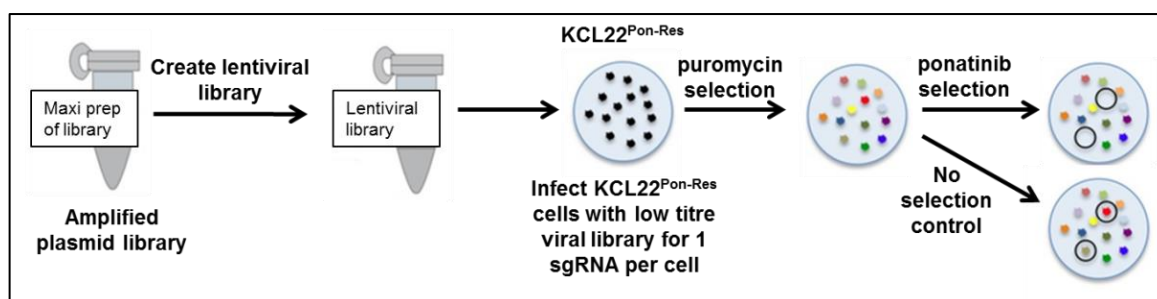


Figure 7-13: The workflow for a negative CRISPR Screen.

7.2.5.3 Single guide RNAs

Final validation of the hits found through the screening methods will be performed by generating 6 single gRNAs for the specific genes as outlined in methods 2.3.14. This will allow us to establish a TKI-resistant CML cell line with the specific single gene KO. This will provide us with a tool to study the change in the cells phenotype in response to the gene silencing and if this re-sensitises the whole population of cells to TKI.

Performing a thorough screening experiment in cell lines narrows down the potential candidates that may be the cause of TKI resistance in CML patients. This makes the candidate gene pool smaller, which helps when designing an experiment using TKI-resistant CML patient samples, as there is a limited number of cells available that would make it very difficult to perform a whole genome KO screen in primary samples. Therefore, a smaller library or single guide knockouts would be advantageous for furthering our research using primary patient samples.

If a successful candidate(s) gene is found from the CRISPR screen and could be validated by single guide KOs in cell lines and in primary samples this would be considered an extremely important gene for the development of TKI resistance in CML and worthy of further validation.

If the KO of this gene can cause TKI resistance, analysis of the gene's products and their interactions may need to be considered, in order to find a mechanism to target that would oppose the KO effect. This could have the potential to lead to the discovery of novel drug therapies against TKI-resistant CML, which can be further validated by therapeutic inhibition in *in vitro* studies, as well as in *in vivo* models.

8 Discussion

CML is driven by the aberrant tyrosine kinase activity of the fusion oncoprotein BCR-ABL. TKIs were designed to target BCR-ABL and inhibit its kinase activity and therefore induce cell death within the CML cell population. TKIs were one of the first successful targeted drug therapies developed for the treatment of cancer. They proved a very successful treatment strategy and clinical trials reported >87% of patients treated with imatinib (1st generation TKI) achieved MCyR in the IRIS study (O'Brien et al., 2003).

Although most patients treated with TKIs achieve a MCyR, it has been reported that approximately 30% of patients with newly diagnosed CP CML who receive imatinib did not achieve a CCyR within 1 year of treatment (O'Brien et al., 2003). In addition, approximately 10% of patients experienced relapse during 5 years of follow-up, including approximately 10% who had achieved a CCyR (Druker et al., 2006).

Another limitation of imatinib which hampers successful treatment is minimal residual disease (MRD). This has been observed in a number of patients who fail to achieve CMR due to the continued detection of BCR-ABL transcripts (Druker et al., 2006). Imatinib is also much less effective in treating more advanced stages of CML, if any response to imatinib does occur it is only transient (Druker et al., 2001a).

Unfortunately, the development of resistance has become the Achilles' heel of TKIs, with both primary and acquired TKI resistance remaining major clinical problems. Due to no alternative targeted treatment the disease may progress and become harder to treat. The only effective treatment options for these patients are either an invasive stem cell transplantation, but this is only if the patient is eligible and has a matched donor available or treatment with omacetaxine, which is highly toxic.

So far, many mechanisms have been reported to lead to imatinib resistance, which is most commonly due to BCR-ABL kinase domain mutations that affect imatinib binding. Acquired resistance can also arise due to BCR-ABL-independent mechanisms, such as activation of alternative survival pathways, as discussed in more detail below. In an attempt to overcome these issues, increasing the dose of imatinib was suggested in resistant CML patients, i.e. patients originally treated with 400 mg/day were treated with up to 800 mg/day (Kantarjian et al., 2003, Jabbour et al., 2009b). However, although response rates were often improved, this was not sufficient to eliminate resistance in many cases.

In the aim to overcome imatinib resistance, 2nd generation TKIs dasatinib and nilotinib were developed, which were much more potent and designed to target BCR-ABL mutants and conformations of the drug pocket which were unattainable by imatinib. Both the 2nd generation TKIs had a superior affect compared to the standard dose of imatinib in the clinic, shown in the DASISION and the ENESTnd clinical trials. However, some patients still had primary resistance or acquired resistance to both dasatinib and nilotinib. One reason for this was that neither of the 2nd generation TKIs were effective in targeting the T315I mutation (Shah et al., 2004, O'Hare et al., 2005).

This has led to the more recently developed 3rd generation TKI ponatinib, which was specifically designed to inhibit BCR-ABL and its mutant form, T315I. Ponatinib is a pan-TKI inhibitor and has been shown to exert its effects on additional targets, such as SRC kinases. It has also been shown to be highly effective in suppressing the emergence of any BCR-ABL mutations, even at low concentrations, such as 40 nM (O'Hare et al., 2009). The PACE clinical trial reported that ponatinib induced rapid and durable responses in CP CML patients, as well as, having significant anti-leukaemic activity in patients harbouring the T315I mutation and patients in more advanced disease stages (Cortes et al., 2013).

Despite promising results from clinical trials such as PACE, which showed that ponatinib induced rapid and durable responses in CP CML patients, there is still a significant number of patients which are unresponsive to all current TKIs. For these patients it is thought that they have developed a mechanism of resistance that is not related to BCR-ABL, i.e. BCR-ABL-independent mechanism of TKI resistance. Such mechanisms of resistance are often thought to occur due to the activation of alternative oncogenic mechanisms (Quentmeier et al., 2011, Hentschel, 2011), which protect CML cells against cell death by maintaining pro-survival pathways, even when BCR-ABL signalling is inhibited. Patients diagnosed with BCR-ABL-independent TKI-resistant CML currently have very few treatment options and therefore have a poor prognosis. With further research it is hoped that an alternative drug target can be identified, that is shared by this patient population, and could be inhibited by a novel drug therapy.

Many studies that have been conducted so far investigating BCR-ABL-independent TKI resistance have used cell line models that have had prolonged exposure to imatinib in order to acquire TKI resistance. Studies using imatinib resistant CML cell lines have led to the implication of many different mechanistic pathways that contribute to TKI-resistance. One of which was the over-expression of SRC kinases, such as LYN, HCK and FYN, which promote survival and proliferation (Donato et al., 2003, Grosso et al., 2009). However, in

our study we have shown that even though imatinib resistant CML cell lines have a durable imatinib resistance they are sensitive to imatinib dose escalation, nilotinib, dasatinib and ponatinib (figure 3-1). The primary reason may be that while TKIs have a potent inhibitory effect against BCR-ABL activity, they also have the ability to target other tyrosine kinases of similar structure, such as KIT and platelet-derived growth factor receptor (PDGFR). Each TKI shows slightly different effects in terms of cytotoxicity and anti-proliferative activities, which are due to their ability to inhibit alternative kinases. Particularly dasatinib and ponatinib, which are less specific due to their design, which enables them to target mutated forms of BCR-ABL. For example dasatinib, even at low nanomolar concentrations, is able to inhibit SRC family kinases, including SRC, LCK, LYN, FGR, BLK, FYN, YES and HCK (Deguchi et al., 2008).

Similarly, ponatinib can also inhibit SRC and LYN at low concentrations, as well as members of the VEGFR, FGFR, and PDGFR families of receptor tyrosine kinases (O'Hare et al., 2009). This may explain the increased cytotoxic effect caused by dasatinib and ponatinib compared to imatinib treatment against these cell lines. Ponatinib also has activity against many mutant forms of BCR-ABL, including the T315I mutation and has the ability to completely suppress the outgrowth of BCR-ABL resistant clones (O'Hare et al., 2009). Due to ponatinib's effectiveness against imatinib resistant cell models, the question arises as to whether imatinib models are currently relevant to study BCR-ABL-independent TKI resistance. Therefore, we proposed that using ponatinib to generate a TKI-resistant model would be more likely to result in a pan-TKI-resistant BCR-ABL-independent phenotype.

Consequently, to allow us to investigate the exact mechanism(s) of BCR-ABL-independent TKI-resistance, we generated a TKI-resistant cell model using the human KCL22^{WT} cell line and the murine BaF3^{WT} cell line (KCL22^{Pon-Res} and BaF3^{Pon-Res}) by growing them in increasing concentrations of ponatinib for a prolonged period of time until the cells showed a resistant phenotype. To the best of our knowledge this is the first time that ponatinib-resistant CML cell lines have been generated for the study of TKI resistance. The BaF3^{Pon-Res} and KCL22^{Pon-Res} cell lines were validated as TKI-resistant CML cell models due to their tolerance of up to 100 nM ponatinib and 150 nM dasatinib, which under these conditions would be toxic to the original parental cells.

Most importantly this study showed that 100 nM ponatinib switched off BCR-ABL signalling in KCL22^{Pon-Res} cells and 1 μ M switched off BCR-ABL in the BaF3^{Pon-Res} cells; however, the cells continued to proliferate, despite the absence of BCR-ABL activity

(figure 3-11). This infers that both of these cell lines have adapted and are using a mechanism independent of BCR-ABL for their cellular survival.

In addition, we convincingly showed that BCR-ABL inhibition via TKIs (imatinib, nilotinib, dasatinib, or ponatinib) or the experimental BCR-ABL inhibitor ABL001, which inhibits BCR-ABL via a different binding pocket, had no effect on the KCL22^{Pon-Res} and BaF3^{Pon-Res} cell lines. An exhaustive series of cell viability assays showed that TKI or ABL001 mediated BCR-ABL inhibition was unable to induce apoptosis, reduce cell proliferation or inhibit colony forming potential of TKI-resistant CML cells (Figures 3-3 – 3-8).

The implication that the BaF3^{Pon-Res} and KCL22^{Pon-Res} cell lines were utilising BCR-ABL-independent mechanisms for their survival was strengthened by genomic DNA sequencing of the ABL kinase domain, which was negative for any mutation which may confer a BCR-ABL-dependent TKI resistance.

The generation of these ponatinib-resistant CML cell models therefore provided us with a unique tool to investigate the mechanism(s) which drive a truly BCR-ABL-independent resistance in CML.

In an effort to tease out the molecular mechanism(s) which may be the driving force for survival of the ponatinib-resistant cells, a transcriptomics analysis was performed to investigate the gene transcription differences between the original KCL22^{WT} cell line and the KCL22^{Pon-Res} cell line at basal levels and following ponatinib mediated BCR-ABL inhibition. By analysing the transcriptional response with and without BCR-ABL signalling we hoped to see genes responses that were normalised in KCL22^{WT} following ponatinib treatment, which were still being aberrantly expressed in the KCL22^{Pon-Res} cell line despite BCR-ABL inhibition. Results showed that, although, there were very few differences comparatively at basal level, following 24 hours of ponatinib treatment, unsurprisingly a vast number of genes were up-regulated or down-regulated in the KCL22^{WT} cell line. Gene ontology analysis revealed that the genes were associated with biological processes involved in apoptosis, DNA damage repair and cellular response to stress. These biological processes are all typical pathways expected to be induced following cytotoxic drug treatment. However, no transcriptional response was observed in the KCL22^{Pon-Res} cells following ponatinib treatment. The lack of transcriptional response added to the evidence that BCR-ABL signalling is redundant in the KCL22^{Pon-Res} due to the gain of an alternative survival pathway. There may be a possibility mTOR is involved as although, mTOR is known to be a major regulator of translation, it also has links to gene

transcription regulation (Laplane and Sabatini, 2013, Mayer and Grummt, 0000, Yecies and Manning, 2011).

The PI3K/AKT/mTOR pathway is a downstream pathway in BCR-ABL signalling and is known to be deregulated in a number of different types of cancers. PI3K/AKT/mTOR signalling plays a central role in regulating proliferation, survival and differentiation events in haemopoiesis and has also been linked with functions of HSCs and the process of lineage commitment (Martelli et al., 2010). PI3K/AKT/mTOR signalling is involved in many important processes and any change in the signal transduction could have dramatic effects on the phenotype of the cell, which is the possible reason why deregulation of this pathway is so common in cancer, including leukaemia.

In our model, western blot analysis of the KCL22^{Pon-Res} cells revealed sustained mTOR activity despite TKI mediated BCR-ABL inhibition. This data is in agreement with previous studies, which showed that the PI3K/AKT/mTOR pathway was activated by imatinib treatment in LAMA84 cells as well as primary leukaemia cells *in vitro*, and also mediated the early stages of imatinib resistance (Burchert et al., 2005). More recently it has been shown that PI3K and mTOR inhibition can re-sensitise both CML progenitors and stem cells to nilotinib (Airiau et al., 2013). It has also been reported that PI3K is constitutively activated in a high percentage of patients with chronic leukaemia (Ringshausen et al., 2002).

Therefore this data implies that the generation of the KCL22^{Pon-Res} cell line has resulted in the BCR-ABL-independent activation of mTORC1, which is in agreement with other studies which have also disclosed that the activation of PI3K/AKT/mTOR may be the cause of TKI resistance and sub-optimal response to TKIs in CML cells (Burchert et al., 2005, Airiau et al., 2013, Ringshausen et al., 2002). This makes the PI3K/AKT/mTOR pathway an attractive potential therapeutic target for CML patients.

In order to facilitate the identification of clinically relevant drugs with potential efficacy and selectivity against TKI-resistant CML cells, we screened a panel of NIH approved anti-cancer drugs. This screen included inhibitors that target signalling pathways known to be deregulated in cancer, such as RAS/MEK/ERK and PI3K/AKT/mTOR, inhibitors against tyrosine kinases as well as many other conventional chemotherapy drugs. The results of this screen pulled out 37 drugs which had inhibitory effects against the KCL22^{Pon-Res} cells. Most of the hits were non-specific chemotherapy drugs, such as vincristine sulphate, ixabepilone, docetaxel, cabazitaxel, vinblastine sulphate and paclitaxel. The mechanism of action of these drugs is to bind to tubulin, which then affects the

microtubule formation in the mitotic spindle and results in a cell cycle arrest. Other chemotherapies that showed a high efficacy against the KCL22^{Pon-Res} cells were protein translation inhibitors, such as omacetaxine and dactinomycin. However, none of these chemotherapy drugs target the actual mechanism driving the leukaemia and are non-selective as they also target normal cells so create high levels of toxicity and side effects for patients.

In spite of this, three specific drug targets were discovered from the initial drug screen; HDAC, MEK and mTOR inhibitors. The top hit in the drug screen was to an HDAC inhibitor, romidepsin, which is currently approved for the treatment of CTCL and PTCLs (Iyer and Foss, 2015, Prince and Dickinson, 2012). HDAC inhibitors have previously been reported to have a synergistic effect when combined with BCR-ABL inhibition in treatment against imatinib resistant CML cells (Nguyen et al., 2011). In this study the HDAC inhibitor vorinostat was used which was also used in our drug screen as well as belinostat. Both vorinostat and belinostat had much higher IC50s, both within the μM range compared to romidepsin. Although as a single treatment vorinostat had a very high IC50 ($>5 \mu\text{M}$), when combined with ponatinib it was reduced to $1.5 \mu\text{M}$, which may just be achievable. As cMax for vorinostat in studies have ranged from $1\text{-}1.5 \mu\text{M}$ (Rubin et al., 2006, Ramalingam et al., 2010, Doi et al., 2013).

A second promising target that was highlighted in the drug screen was MEK. In the initial screen the MEK inhibitor trametinib was the 19th most effective drug against the KCL22^{Pon-Res} cell line, having an IC50 of 287 nM. A second MEK inhibitor was added to the screen, selumetinib, which had a greater efficacy against the TKI-resistant cells than the TKI sensitive cells. However, this was not translated to the BaF3^{Pon-Res} cell model, where only trametinib was effective and required a much higher concentration to achieve an IC50: $1.86 \mu\text{M}$. Despite the inconsistency between the inhibitors and the cell models, neither of the MEK inhibitors affected the non-CML cells, which never reached an IC50 within the $10 \mu\text{M}$ concentration range, suggesting that this could be a potential specific treatment for TKI-resistant CML. However, subsequent experiments in the laboratory showed that despite 72 hours of MEK inhibition it had very little effect on the apoptotic response and colony forming potential TKI-resistant CML cells. This is in keeping with previous studies, which have also reported that TKI-resistant CML cells (or CML cells having a sub-optimal response to TKIs), are sensitive to MEK inhibition, due to re-activation of the RAS-MEK-ERK signalling pathway (Pietarinen et al., 2015, Packer et al., 2011, Asmussen et al., 2014, Ma et al., 2014). In line with our study they also witnessed a

synergistic affect with combination MEK inhibition and TKI treatment (Ma et al., 2014, Packer et al., 2011).

In addition, it has also been reported that there is cross-talk between the MEK/ERK and PI3K/AKT/mTOR pathways, which is involved in the maintenance of self-renewal and tumorigenicity of glioblastoma stem-like cells (Sunayama et al., 2010). Due to the sensitivity of the KCL22^{Pon-Res} cell to both mTOR and MEK inhibition, aberrant activity of these two pathways, working together, may be the potential mechanism driving survival and growth of these TKI-resistant CML cells.

The most conclusive data obtained from the drug screen was the sensitivity of TKI-resistant CML cells to mTOR inhibition. Three different allosteric mTOR inhibitors were all tested against the TKI-resistant cells and had strong anti-proliferative effects at very low drug concentrations. The three mTOR inhibitors from the drug screen were everolimus, sirolimus and temsirolimus, each achieving similar IC50s at 115 nM, 118 nM and 158 nM, respectively. Three consecutive hits for the same target suggests the importance of this pathway to the TKI-resistant CML cells. This was in line with the fact that mTOR was still active despite BCR-ABL inhibition (figure 3-11), strengthening the concept that activation of the mTOR signalling pathway was promoting cell proliferation and survival in the TKI-resistant CML cells.

Currently the only mTOR inhibitors that are FDA approved are the allosteric inhibitors; everolimus, sirolimus and temsirolimus. These inhibitors are currently approved for the treatment of renal cancer, and have been deemed safe and have been relatively well tolerated (Teachey et al., 2009). A very small trial was conducted assessing the efficacy of mTOR inhibition in patients suffering with imatinib-resistant CML. Four of the subjects were treated with 2 mg of sirolimus for 14 days. Due to the low number of subjects the results were inconclusive; two patients achieving a major response and two others achieving a minor response (Sillaber et al., 2008). Larger trials have been conducted in CML to gain more conclusive data but the results are not yet available; sirolimus (rapamycin) (NCT00780104) and rapamycin derivative, everolimus (RAD001) (NCT00093639 and NCT00081874).

However, there are results available from clinical trials analysing the effect of allosteric mTOR inhibitors against other types of malignancies, such as breast cancer, a cancer known for its high frequency of patients with a deregulated PI3K/AKT/mTOR pathway. These trials reported surprisingly poor response rates, when it was expected to provided significant benefit (Wander et al., 2011).

Although the allosteric mTOR inhibitors showed great efficacy in our initial drug screen, subsequent validation of the mTOR inhibitors in the secondary screen using the BaF3^{Pon-Res} cell model was unsuccessful, as both everolimus and sirolimus failed to achieve an IC₅₀ within 10 μ M. This poor response rate is similar to the results we observed in our *in vitro* studies, in which rapamycin induced minimal apoptosis compared to our untreated control and had no effect on the colony forming potential of BaF3^{Pon-Res} cells or the KCL22^{Pon-Res} cells. The insensitivity of cells to rapamycin may be explained by its selective inhibitory action against only one of the mTOR complexes, mTORC1, and its inability to fully inhibit phosphorylation of downstream targets, such as 4EBP1 (Choo et al., 2008), which therefore gives an incomplete inhibition of the mTOR pathway. It has also been suggested that because mTORC2 is still active it creates a feedback loop, which activates AKT and allows further phosphorylation of both the mTOR complexes therefore opposing the effect of rapamycin (O'Reilly et al., 2006).

Due to the suboptimal response of allosteric inhibitors observed in the clinic, new catalytic mTOR inhibitors have now been developed; PP242 and AZD8055, which target both mTOR complexes and NVP-Bez235, which is a dual inhibitor that targets PI3K and both the mTOR complexes. By using catalytic inhibitors against mTOR we hoped to increase efficacy of mTOR inhibition as they utilise competitive inhibition and directly inhibit kinase activity rather than a non-competitive method of inhibition used by allosteric inhibitors.

The drug screen showed that the increased potency of the catalytic inhibitors AZD8055 and NVP-Bez235 against mTOR kinase activity was more effective as the inhibitors were able to exert their anti-proliferative effects on both the KCL22^{Pon-Res} and BaF3^{Pon-Res} cells. In order to further test the efficacy of the PI3K/mTOR inhibitors, subsequent analysis was performed in the laboratory to gain an understanding of which target within the PI3K/AKT/mTOR pathway would provide the most effective inhibition. XTT assays were performed testing AZD8055, BKM120 and NVP-Bez235 against the human KCL22^{Pon-Res} cells. This showed that the TKI-resistant cells were very sensitive to mTOR inhibition (AZD8055 EC₅₀:28.28 nM) and even more so to the mTOR and PI3K inhibition (NVP-Bez235 EC₅₀:2.22 nM). The reduced sensitivity of AZD8055 compared to NVP-Bez235 may be due to a feedback mechanism between mTORC2 and PI3K as the inhibition of mTOR leads to a feedback activation of PI3K (Carracedo and Pandolfi, 2008), which may have a role in imposing resistance against AZD8055. However, AZD8055 may just be less efficient at inhibiting mTOR. These cells were less affected by PI3K inhibition alone

(BKM120 EC₅₀:1928 nM). This highlights the sensitivity of TKI-resistant CML cells to catalytic mTOR inhibition.

These results correlate with apoptosis data, where rapamycin (mTORC1 only inhibitor) and BKM120 (PI3K only inhibitor) had a very minimal effect on cell death. AZD8055 (mTORC1+2 inhibitor) increased apoptosis to more than 40%, which is almost double that in response to rapamycin. However, NVP-Bez235, induced the highest levels of apoptosis and significantly reduced the leukaemic colony forming potential of the TKI-resistant cells following 72 hours of treatment. Rapamycin and BKM120 had a minimal effect on CFC. AZD8055 reduced the CFC by ~50%. However, NVP-Bez235 had the ability to reduce CFC by approximately 66% (Figure 5-3). This data was supported by a second TKI-resistant cell line BaF3^{Pon-Res}, where mTORC1 inhibition by rapamycin showed a minimal increase in apoptosis compared to untreated, but no effect on CFC of CML cells. PP242 (mTORC1+2 inhibitor) surprisingly, unlike AZD8055, had no effect on cell death nor CFC, which may be due to its decreased efficacy (IC₅₀: 8 nM (Apsel et al., 2008)) compared to AZD8055 (IC₅₀: 0.8 nM (Chresta et al., 2010)) against mTOR activity. However, even low concentrations of NVP-Bez235 caused a striking and very significant increase in apoptotic events and significantly reduced the CFC potential of these TKI-resistant CML cells.

Importantly, this translated to clinical samples, as NVP-Bez235 was also highly effective in both inducing cell death and reducing clonogenic growth in primary TKI-resistant CML patient samples. Therefore, treating TKI-resistant cells with NVP-Bez235 became more attractive as this targets both mTOR and PI3K and may be able to overcome the feedback mechanisms within this pathway and produce a better inhibitory action against the whole PI3K/AKT/mTOR pathway.

Due to the success of PI3K and mTOR inhibitors, such as NVP-Bez235, at inhibiting the PI3K/AKT/mTOR pathway, more dual inhibitors were developed such as apitolisib, VS-5584 and gedatolisib. Therefore, we used these inhibitors to validate that the effects of NVP-Bez235 were due to PI3K and mTOR inhibition and not off target effects, which should not occur due to the low concentrations used in the assays. XTT assays revealed that the human KCL22^{Pon-Res} cells were just as sensitive to apitolisib (EC₅₀: 29.15 nM), VS-5584 (EC₅₀: 1.742 nM) and gedatolisib (EC₅₀: 0.168 nM) as they were to NVP-Bez235 (EC₅₀: 2.15 nM). This data also corresponded with a significant induction in apoptosis, especially with gedatolisib, which achieved a similarly high level of apoptosis as NVP-Bez235. Once again this data successfully transferred to clinical samples, where we

showed at low concentrations that apitolisib, VS-5584 and gedatolisib can induce apoptosis and reduce clonogenic growth in primary TKI-resistant CML patient samples, increasingly more so than ponatinib.

Subsequent testing of catalytic mTOR inhibitors revealed that NVP-Bez235 treatment led to the complete inhibition of RPS6 phosphorylation, indicating a potent inhibition of mTOR activity and therefore an effective inhibition of protein translation. This suggests that the cell death occurring in the TKI-resistant CML cells when treated with NVP-Bez235 is due to mTOR inhibition.

The importance of targeting mTOR was again highlighted in the RNA-seq experiment. KCL22^{Pon-Res} cells were shown to have an impaired transcriptional response when treated with ponatinib, however NVP-Bez235-mediated mTOR inhibition had a dramatic impact on the cells causing a large number of transcriptional changes, which mimicked the response seen in TKI sensitive CML cells following BCR-ABL inhibition (as many of the transcriptional changes that occurred in the KCL22^{WT} cells following ponatinib mediated BCR-ABL inhibition also occurred in the KCL22^{Pon-Res} cells following NVP-Bez235 mediated mTOR inhibition).

The ability of these compounds to inhibit proliferation at low nanomolar concentrations and induce a high apoptotic response further enhances the notion that TKI-resistant CML cells are highly dependent on mTOR signalling for their survival. Taken together, this therefore provides a rationale for testing dual PI3K/mTOR inhibitors in the clinic, for patients that don't respond to BCR-ABL inhibitors.

8.1 mTOR and autophagy

It is evident that the depth of response to TKI is insufficient in TKI-resistant patients to inhibit leukaemic burden and therefore there is a clinical need for treatments which target the resistant clones or preferably target the primitive CML stem cells from which TKI-resistant clones may arise (Bolton-Gillespie et al., 2013).

In addition to the survival signals previously described, the PI3K/AKT/mTOR pathway is also linked to another survival mechanism; autophagy. Autophagy maintains cellular homeostasis by regulating recycling of intracellular waste in order to generate energy and new materials needed for cell survival (DeBerardinis et al., 2008, Amaravadi et al., 2011). This process is a fundamental cellular pathway for the survival and maintenance of HSCs (Warr et al., 2013b). Autophagy is specifically regulated by mTORC1, which when active, binds to the initiation complex to inhibit the induction of autophagy (Kim et al., 2011).

Therefore, by treating the TKI-resistant cells with mTOR inhibitors it may induce autophagy and protect cells against cell death and lead to a sub-optimal response to mTOR inhibitors.

We tested this hypothesis using the KCL22^{Pon-Res}-RFP-GFP-LC3 cell model and observed that treatment with NVP-Bez235 induced a striking increase in autophagy flow. Moreover, the NVP-Bez235 mediated autophagy induction could be inhibited through pharmacological intervention by HCQ. For this reason, we examined the response of TKI-resistant cells to the combination of autophagy inhibition and NVP-Bez235 treatment and whether this could enhance the effects of NVP-Bez235 treatment alone.

To address our hypothesis and test whether this effect could be reproduced in primary patient samples, we tested the combination treatment of NVP-Bez235 and HCQ on bone marrow derived MNCs from three different TKI-resistant CML patients. The combination treatment caused a dramatic and highly significant reduction in clonogenic growth by ~80% in both patients. Autophagy inhibition, using HCQ, enhanced the effect of NVP-Bez235 alone, which had a great impact on cell survival.

HCQ mediated autophagy inhibition also enhanced the efficacy of NVP-Bez235 in an *in vivo* xenograft model of TKI-resistant CML. The NVP-Bez235 and HCQ combination treatment had a significant impact on reducing the number of leukaemia initiating cells, which significantly reduced disease progression, tumour burden and prolonged survival rates beyond that of ponatinib +/- HCQ and NVP-Bez235 as a single agent treatment in NSG mice. The combination treatment of NVP-Bez235 and HCQ was also well tolerated by NSG mice, which makes it a promising treatment for going forward to clinical trial.

HCQ is currently being tested in 27 active clinical trials for autophagy inhibition (Helgason et al., 2013). However, HCQ is not a specific autophagy inhibitor and exerts its effect by inhibiting lysosomal function and therefore has the potential to influence other pathways and cellular processes. Therefore, to validate that the effects of HCQ treatment were due to autophagy inhibition, we used two complimentary approaches; CRISPR and shRNA, to KO/KD the essential autophagy gene *ATG7* in the KCL22^{Pon-Res} cells. *ATG7* plays an essential role in the lipidation of LC3; which is vital for the complete formation of the autophagosome.

KCL22^{Pon-Res} transduced with CRISPR-*ATG7* or sh*ATG7* were treated with NVP-Bez235, which caused significant apoptosis in both the control cells and the *ATG7* knockdown cells. However, the addition of *ATG7* knockdown mediated autophagy inhibition greatly

enhanced the apoptotic response and reduced CFC potential when compared with the control cells treated with NVP-Bez235. Importantly, this shows that autophagy inhibition further sensitises CML cells to NVP-Bez235 induced cell death, which confirms that autophagy was induced following NVP-Bez235 mediated mTOR inhibition and that autophagy was causing a cytoprotective effect against NVP-Bez235 treatment. This also suggests that the additive effect of HCQ, when used in combination with mTOR inhibitors, was due to blocking the autophagy process.

8.2 NVP-Bez235 and toxicity

As mTOR has many important roles in normal physiological conditions, such as protein translation, there are concerns that mTOR inhibition will also effect viability of normal cells as well as the leukaemic cells, which may cause a level of toxicity in patients. Results from the drug screen do infer a level of toxicity due to the sensitivity of the primary non-CML cells to the dual PI3K and mTOR inhibitors, however not having a direct comparison with primary TKI-resistant CML cells makes it hard to assess whether there may still be a therapeutic window for treatment using the catalytic dual PI3K and mTOR inhibitors. However, drug concentrations needed to achieve an IC50 were higher in non-CML cell than in the TKI-resistant cell line models. Further assessment of NVP-Bez235 treatment on non-CML cells did result in an 80% induction of apoptosis and a reduction in colony formation, only 40% of colonies remained compared to untreated. This outcome not optimal however it may have potential as it was less toxic than last resort treatment omacetaxine, which at extremely low concentrations, 10 nM, induced 90% apoptosis and affected “normal” cell viability to the point that no cells survived to form colonies within the CFC assay.

Additionally, there are concerns that mTOR inhibitors may also cause immunosuppression in the clinic. Critically, our primary objective for using mTOR inhibitors was to modulate aberrant mTOR activity in the TKI-resistant cells; however, mTOR inhibitors were originally developed as antifungal agents, which were later found to have immunosuppressive and anti-proliferative properties. The mode of action of sirolimus and its analogues is to target mTOR activity, which then inhibits interleukin-2 signal transduction, which inevitably results in a G1/S phase cell cycle arrest (Hardinger et al., 2004, Kelly et al., 1997). Due to the inhibition of interleukin-2 and the subsequent cytokine production they also block the activation of T-cells and B-cells, causing immunosuppression (Kelly et al., 1997). However, previous clinical trials with allosteric inhibitors; everolimus, sirolimus and temsirolimus have considered them safe and relatively well tolerated (Teachey et al., 2009) and have subsequently been FDA approved.

Currently, many early phase clinical trials are being conducted to test the safety and efficacy of the catalytic inhibitors. AZD8055 has been tested in 4 trials for solid and advanced phase tumours. The dual PI3K and mTOR inhibitors are also undergoing early phase safety testing in clinical trials; NVP-Bez235 is currently being tested in 13 trials, one of which is recruiting CML patients (NCT01756118), gedatolisib is being tested in two trials for breast cancer, VS-5584 is also being tested in two trials, one of which is recruiting lymphoma patients, and apitolisib has been tested in 12 clinical trials, 2 of which included non-Hodgkin's lymphoma patients.

8.3 Conclusion

In this study we have reported that TKI-resistant cells are highly sensitive to inhibition of the PI3K/AKT/mTOR pathway. Moreover, NVP-Bez235 is most effective at targeting TKI-resistant cells by inducing apoptosis and reducing the survival of TKI-resistant cells, which was shown in both ponatinib-resistant cell line models, in cells derived from a TKI-resistant CML patients as well as in an *in vivo* model. Importantly, our data also suggests that NVP-Bez235 is more effective against TKI-resistant cells compared to current TKI treatments dasatinib and ponatinib.

As NVP-Bez235 is the most effective PI3K/AKT/mTOR inhibitor it highlights the importance of a complete inhibition of the pathway, as targeting mTOR and PI3K together is more effective against TKI-resistant cell survival compared to mTOR or PI3K inhibition alone, as seen with rapamycin, PP242, AZD8055 and BKM120 treatments. In addition, our results demonstrate that NVP-Bez235 treatment can be enhanced with the pharmacological inhibition of autophagy, providing a rationale for testing this combination in the clinic for CML patients with BCR-ABL-independent resistance mechanisms.

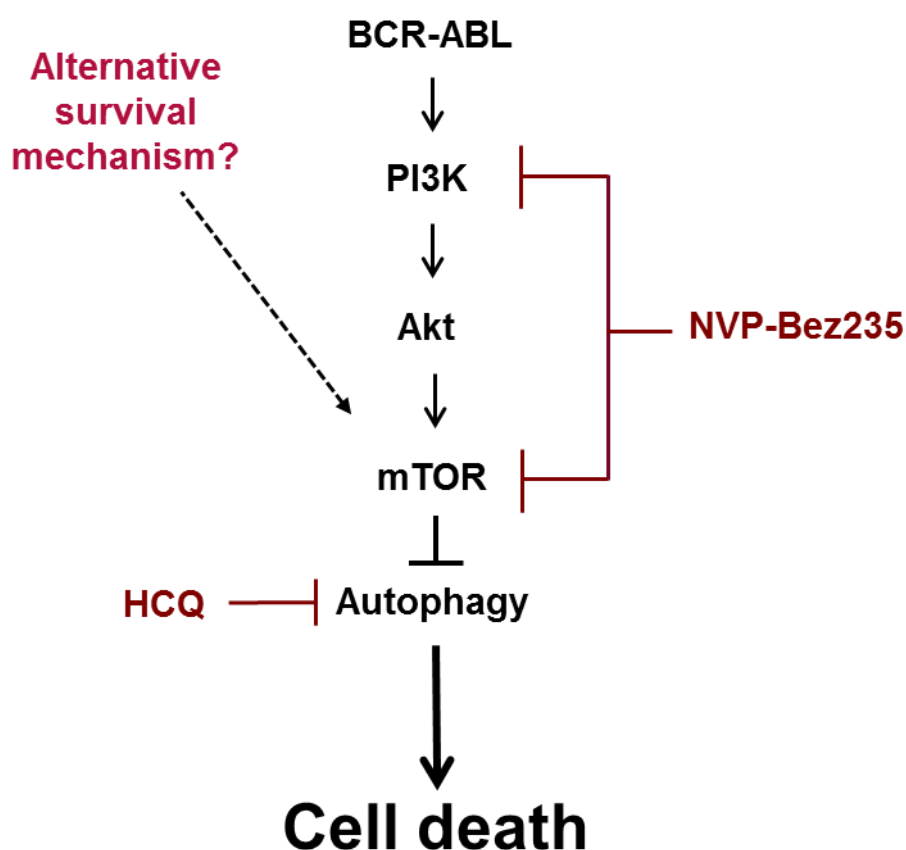


Figure 8-1: Our proposed drug treatment strategy for BCR-ABL-independent mechanism TKI-resistant CML

8.4 Future work

Despite our attempts to identify the underlying mechanism causing BCR-ABL independent TKI resistance, we were unable to find the source of the aberrant pro-survival and proliferation signalling. Different experimental approaches were tried such as the (1) NIH repurposing drug screen, which included many inhibitors that target pathways that are already deregulated in cancer, (2) RNA-seq was performed to understand the differential gene expression between TKI-sensitive and TKI-resistant CML, and (3) CRISPR whole genome KO screen was carried out using TKI-sensitive CML cells (KCL22^{WT}), which were subsequently treated with ponatinib to assess whether a single gene KO (a secondary genetic hit) could cause TKI resistance.

With the development of CRISPR protocols within the lab an attempt was made to KO mTOR in the KCL22^{Pon-Res} cells, to gain a more specific mTOR inhibition. Due to the sensitivity of KCL22^{Pon-Res} cells to mTOR inhibition it is hypothesised that this may result in 100% death. However, despite successful transduction of the virus containing CRISPR gRNAs against mTOR, no KO was achieved. This is presumably due to complications in the generation of gRNAs against mTOR. In order to generate an mTOR KO KCL22^{Pon-Res} model more time will need to be invested to design guides which are more efficient.

In keeping with this study, we also made an attempt to further validate the BCR-ABL independent TKI-resistant CML model, by designing gRNAs, which would KO BCR-ABL only, in KCL22^{Pon-Res} cells, as these cells can survive without BCR-ABL signalling. Despite designing 3 gRNAs against the BCR-ABL junction, none of the gRNAs were efficient to KO BCR-ABL signalling, which was analysed by the phosphorylation of CRKL via western blot. Once again further experiments are required to understand the BCR-ABL sequence in more detail and find an optimum target sequence. However, if this approach is successful, we will have generated a CML cell line, which can grow and proliferate despite not expressing BCR-ABL, which will give us a true BCR-ABL independent CML model.

The most substantial data we gathered during our study was that mTOR activity is sustained, despite BCR-ABL inhibition, possibly leading to the aberrant transcriptional response following TKI treatment. In an attempt to answer the question whether primary cells had an aberrant transcriptional response following BCR-ABL inhibition we performed RNA-seq on MNCs from TKI-resistant patients. However, the results from these

experiments were inconclusive, possibly due to the cell heterogeneity within the MNC population, which “masked” the effect of the TKI treatment.

The majority of our screening processes focussed on gene transcription, however with the advancements technology in large proteomics screens there could be a potential to analyse differential protein expression between TKI-sensitive and TKI-resistant CML using mass spectrometry. This data can then be processed and used to identify any functionally active proteins and networks.

It is also possible to perform phosphoproteomic analysis on the TKI-resistant cells, which is a method that has already gained some success in investigating drug resistance in breast cancer (Oyama et al., 2011, Rexer et al., 2011). Protein phosphorylation, is involved in signal transduction and it requires coherent activation of protein kinases and phosphatases, which leads to the defined functions. In imatinib-resistant CML many kinases have already been implicated in development of TKI-resistance, therefore this could be an interesting experiment to perform understanding the signalling pathways involved in BCR-ABL independent TKI-resistance CML and how mTOR fits into the scenario.

Another screening method, which is of high priority, to facilitate the characterisation of the resistance mechanism in the KCL22^{Pon-Res} cells is whole genome sequencing (WGS). This technology has the potential to give us invaluable data such as; potential sequence variants, mutations, gene copy numbers, as well as structural changes such as chromosomal translocations and fusion genes, which may be the source of pro- survival signalling. A comparison between the original KCL22^{WT} and the TKI-resistant KCL22^{Pon-Res} to see what mutations have been gained to cause TKI-resistance. BCR-ABL independent TKI-resistance CML samples are scarce, however if a mechanism of resistance is found in the cell lines, validating this using WGS in primary patient cells would be the next step.

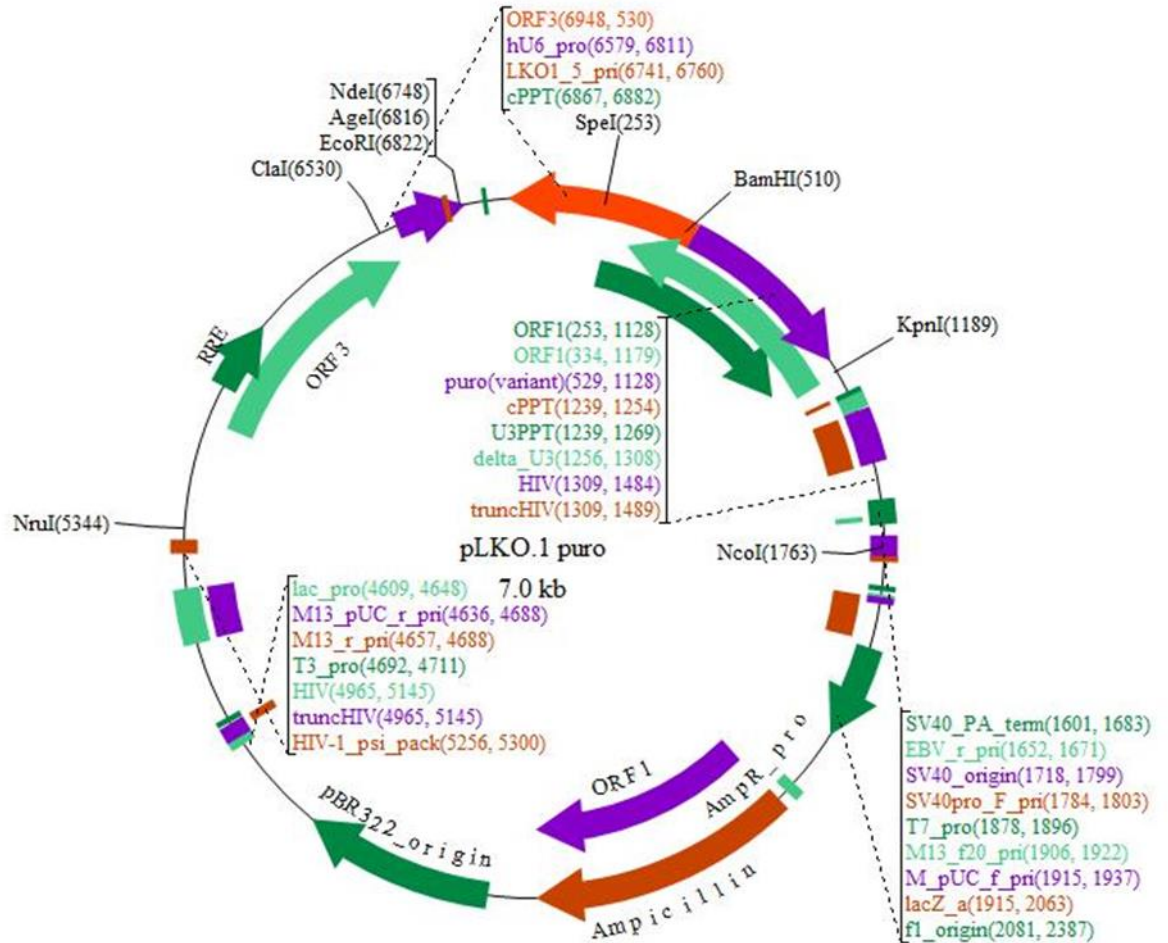
From translational point of view, we hope to continue the search for the most suitable catalytic mTOR inhibitor and initiate discussion with pharmaceutical companies and clinical scientist about ways to test our hypothesis in the clinic. In this setting, the most likely clinical trial scenario would involve testing tolerability of adding mTOR inhibitors to TKI treatment in patients who are failing 1-3rd gen TKIs. Although TKI are not effective in this group of patients, being granted ethical approval to stop TKI and give them a treatment that does not target BCR-ABL specifically would be challenging and require an in depth screening process to track disease progression or regression in these patients, which would require a lot of resources. However, progressing this study to a clinical trial has already been briefly discussed with my second supervisor Tessa Holyoake, who is

involved in designing and leading clinical trials in CML and therefore already has the knowledge and expertise to help guide this project to the level required to translate it into a clinical trial.

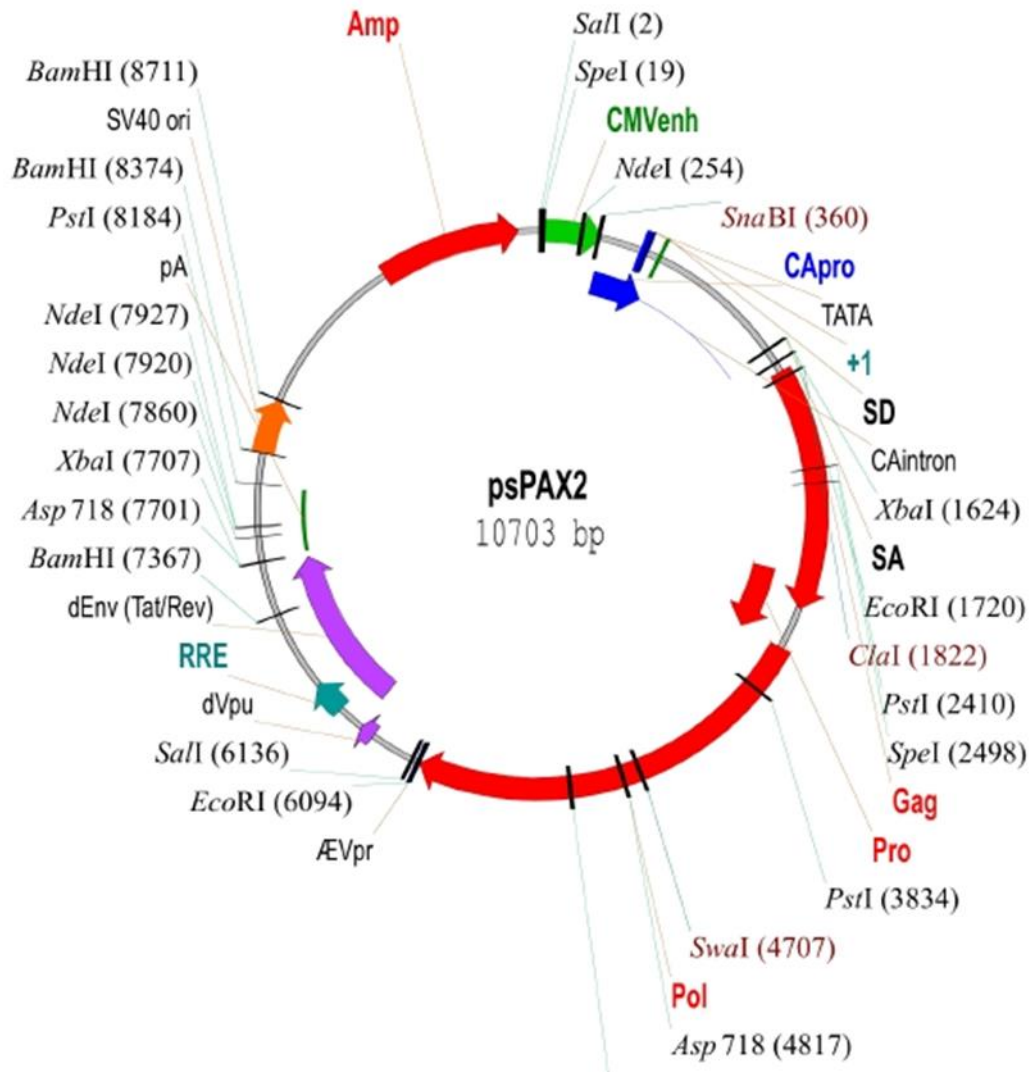
9 Appendices

9.1 Plasmid maps

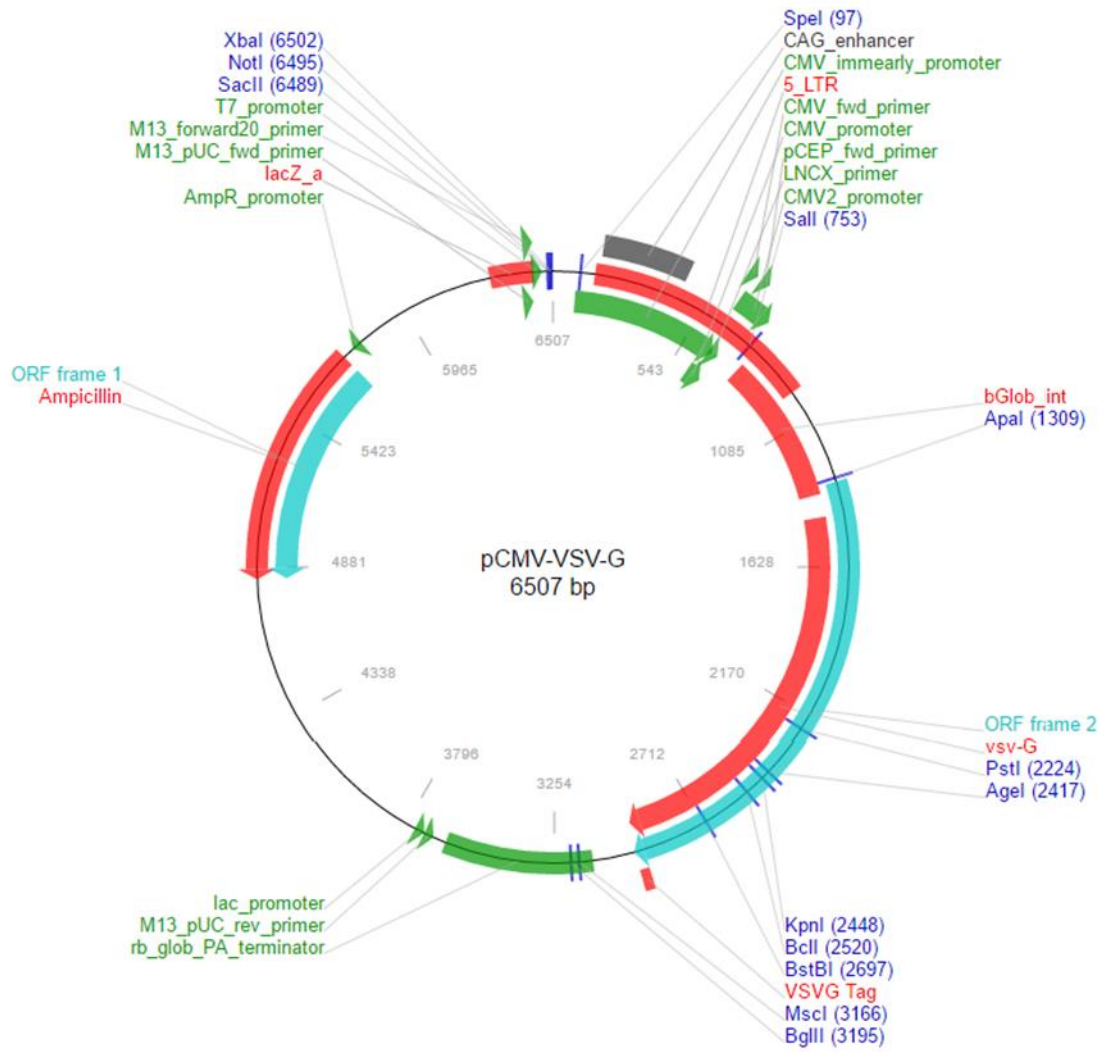
9.1.1 pLKO.1 puro



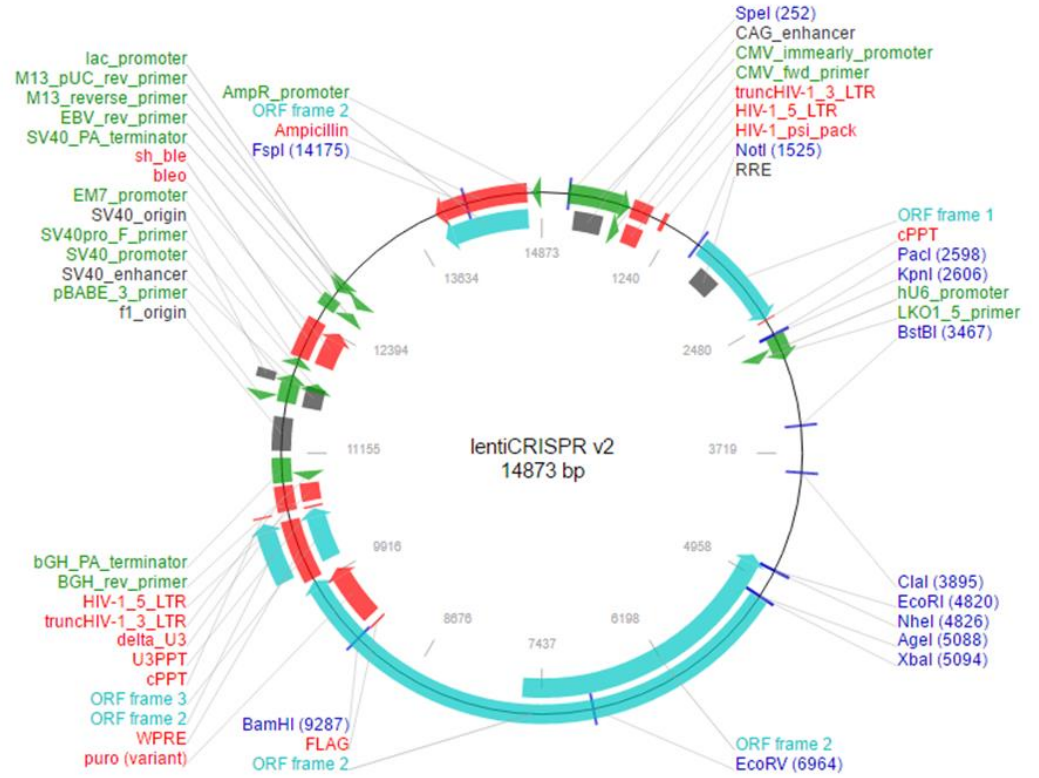
9.1.2 psPAX2 – Addgene (12260)



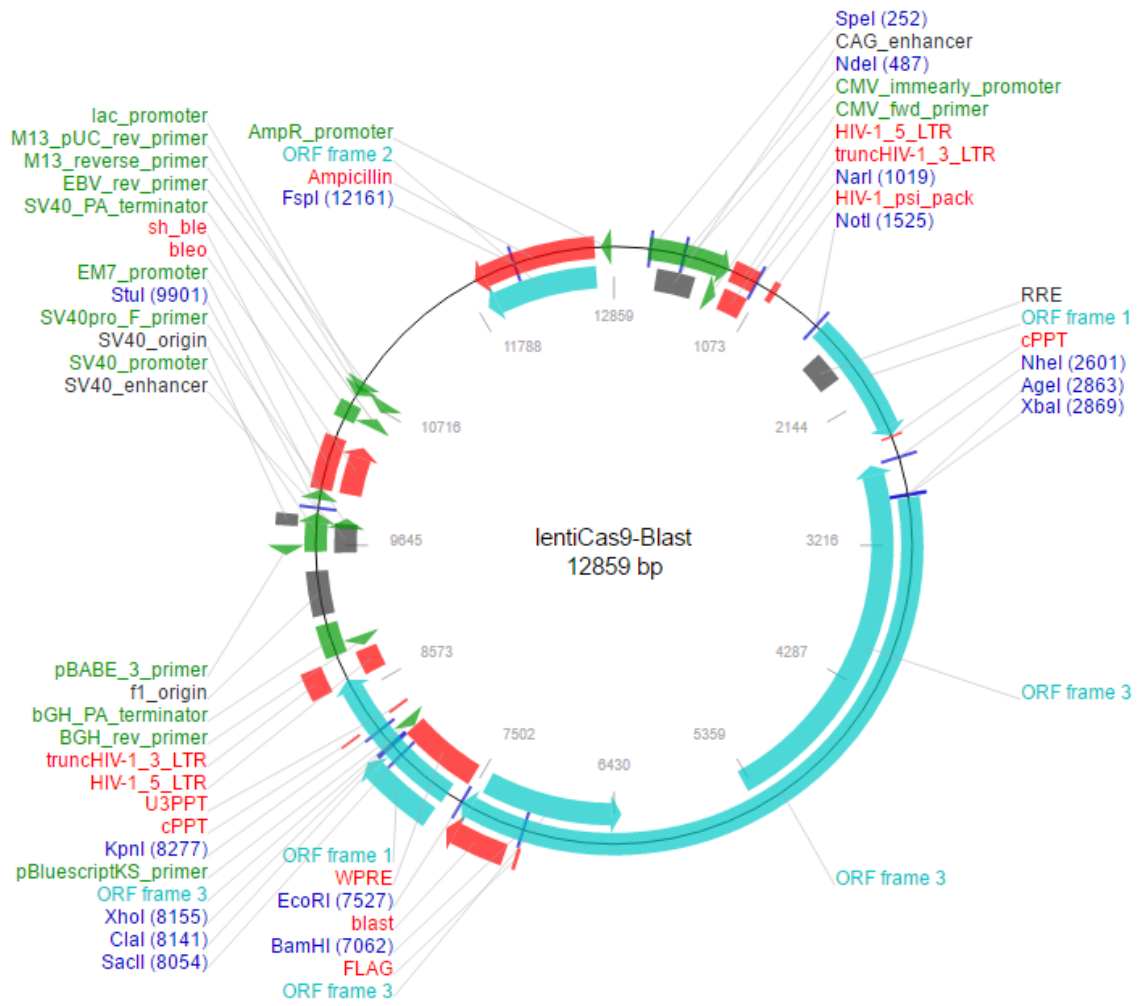
9.1.3 pCMV-VSV-G – Addgene (8454)



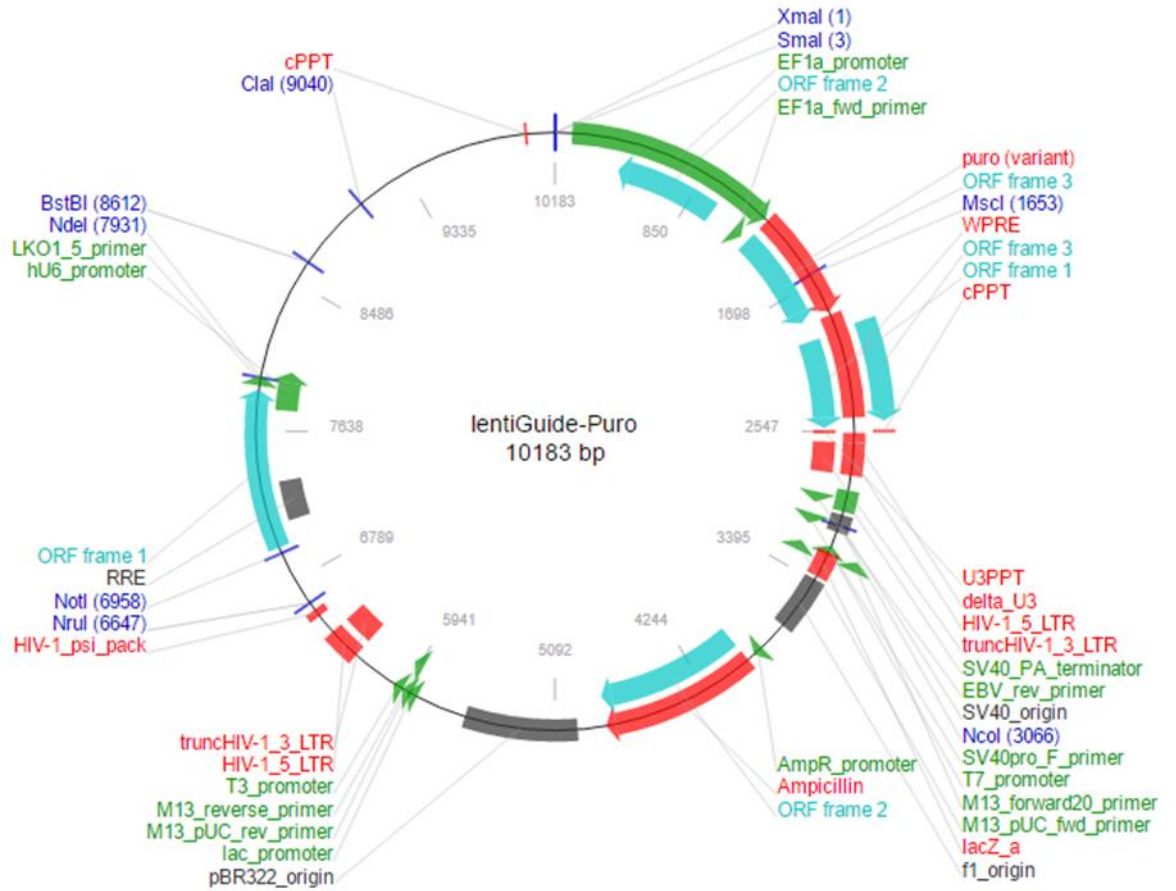
9.1.4 LentiCRISPR v2 Addgene (52961)



9.1.5 LentiCas9-Blast – Addgene (52962)



9.1.6 LentiGuide-Puro – Addgene (52963)



9.2 CRISPR data

9.2.1 gRNA lists from the KCL22^{WT} screen sample 1

Gene	WGKO-S1	WGKO-S1 %
EDARADD	16128536.39	45.34378387
TBC1D9	9628072.508	27.068373
MRFAP1L1	9595178.017	26.97589339
MAP3K7	4345.029167	0.012215619
OR5D14	621.5791667	0.001747508
C6	618.5666667	0.001739039
HCAR1	614.55	0.001727747
PRPS1	607.5208333	0.001707985
CCKAR	600.4916667	0.001688223
DFNB31	586.4333333	0.001648699
TMEM200C	578.4	0.001626114
KIAA0513	574.3833333	0.001614822
SNTB1	568.3583333	0.001597883
HS6ST3	565.3458333	0.001589414
NARG2	565.3458333	0.001589414
TRIM58	564.3416667	0.001586591
TMEM55A	563.3375	0.001583768
ABCB6	555.3041667	0.001561183
F2R	543.2541667	0.001527305
OXA1L	541.2458333	0.001521659
ZNF283	539.2375	0.001516013
GJA8	537.2291667	0.001510367
RYBP	534.2166667	0.001501897
HIPK4	524.175	0.001473666
ZCCHC17	523.1708333	0.001470843
NR4A1	522.1666667	0.00146802
hsa-mir-618	522.1666667	0.00146802
ITCH	520.1583333	0.001462374
FRG2B	516.1416667	0.001451081
ACTL8	515.1375	0.001448258
CXCR1	512.125	0.001439789
GFOD1	510.1166667	0.001434143

NRTN	507.1041667	0.001425673
RUSC1	499.0708333	0.001403088
ARG1	498.0666667	0.001400265
GFER	497.0625	0.001397442
RPL32	496.0583333	0.001394619
PHF16	495.0541667	0.001391796
RPRM	495.0541667	0.001391796
FAM107B	492.0416667	0.001383326
ZNF517	492.0416667	0.001383326
RBMY1D	488.025	0.001372034
JKAMP	487.0208333	0.001369211
FOXK1	487.0208333	0.001369211
CCDC97	483.0041667	0.001357918
ALS2CL	480.9958333	0.001352272
RAD21L1	480.9958333	0.001352272
MED11	479.9916667	0.001349449
RPH3AL	479.9916667	0.001349449
CYP4A22	478.9875	0.001346626
HECTD1	477.9833333	0.001343803
FXR2	476.9791667	0.00134098
DEFB133	468.9458333	0.001318395
SPATA9	468.9458333	0.001318395
SLC19A2	468.9458333	0.001318395
TCF3	463.925	0.001304279
FAM216A	459.9083333	0.001292987
hsa-mir-548a-3	454.8875	0.001278871
LRRC40	453.8833333	0.001276048
VCX2	453.8833333	0.001276048
ELMOD1	451.875	0.001270402
EEA1	450.8708333	0.001267579
SBNO2	448.8625	0.001261932
ATP6V1C1	447.8583333	0.001259109
ISOC1	447.8583333	0.001259109
PDCD6	447.8583333	0.001259109
FARSA	446.8541667	0.001256286

hsa-mir-7-3	443.8416667	0.001247817
ITM2C	442.8375	0.001244994
OLFML3	441.8333333	0.001242171
PPCDC	439.825	0.001236524
GCSAM	438.8208333	0.001233701
LOC100287036	429.7833333	0.001208293
KREMEN1	428.7791667	0.00120547
OR52H1	428.7791667	0.00120547
RORC	423.7583333	0.001191355
PPP3CB	420.7458333	0.001182885
TBX15	420.7458333	0.001182885
YPEL1	418.7375	0.001177239
C2orf44	415.725	0.00116877
HIST1H2AA	415.725	0.00116877
SUPT20HL1	415.725	0.00116877
GRIN2B	411.7083333	0.001157477
DAAM2	409.7	0.001151831
DUSP7	408.6958333	0.001149008
LOC81691	408.6958333	0.001149008
NLRP8	408.6958333	0.001149008
ATXN1	407.6916667	0.001146185
SF1	404.6791667	0.001137715
SLC12A5	404.6791667	0.001137715
POLN	403.675	0.001134892
KIDINS220	402.6708333	0.001132069
TCTN1	399.6583333	0.0011236
C1QBP	396.6458333	0.001115131
C7orf60	394.6375	0.001109484
NR1I3	393.6333333	0.001106661
MCOLN3	391.625	0.001101015
CES5A	390.6208333	0.001098192
FKBP15	390.6208333	0.001098192
SLC17A9	389.6166667	0.001095369
CACNA1G	388.6125	0.001092546
IL10RB	386.6041667	0.001086899

PTPN3	384.5958333	0.001081253
PSPH	383.5916667	0.00107843
ZNF558	379.575	0.001067138
CD300A	378.5708333	0.001064314
KIAA1704	377.5666667	0.001061491
SLC25A35	375.5583333	0.001055845
FGFR1	374.5541667	0.001053022
LIPT1	374.5541667	0.001053022
DIAPH2	372.5458333	0.001047376
FAM60A	372.5458333	0.001047376
KPNA3	371.5416667	0.001044553
FBXW12	362.5041667	0.001019145
MS4A7	362.5041667	0.001019145
OR4K14	361.5	0.001016321
CHRNA3	361.5	0.001016321
ZCCHC16	360.4958333	0.001013498
CLDN17	358.4875	0.001007852
HELB	357.4833333	0.001005029
WNT5B	355.475	0.000999383
ACLY	355.475	0.000999383
GCSH	354.4708333	0.00099656
CEP57	352.4625	0.000990913
TTC29	351.4583333	0.00098809
IQCB1	349.45	0.000982444
TYRP1	346.4375	0.000973975
MCM9	345.4333333	0.000971152
SNCB	345.4333333	0.000971152
CEP170	344.4291667	0.000968329
SRBD1	343.425	0.000965505
GHSR	342.4208333	0.000962682
MCM3	342.4208333	0.000962682
C6orf57	341.4166667	0.000959859
AP1G2	340.4125	0.000957036
STON1-GTF2A1L	335.3916667	0.00094292
ZDHHC13	335.3916667	0.00094292

C4orf19	330.3708333	0.000928805
MTMR12	330.3708333	0.000928805
TMEM39A	330.3708333	0.000928805
CTNNBIP1	330.3708333	0.000928805
LRRC19	329.3666667	0.000925982
ARPC4-TTLL3	327.3583333	0.000920336
SFTPD	327.3583333	0.000920336
CIAO1	326.3541667	0.000917512
RPUSD2	324.3458333	0.000911866
TBC1D24	324.3458333	0.000911866
FBXW8	323.3416667	0.000909043
COMMD2	322.3375	0.00090622
SALL2	321.3333333	0.000903397
hsa-mir-597	321.3333333	0.000903397
C1orf198	320.3291667	0.000900574
TDGF1	320.3291667	0.000900574
COMP	318.3208333	0.000894928
NR4A1	318.3208333	0.000894928
hsa-mir-3689f	316.3125	0.000889281
MRGPRD	315.3083333	0.000886458
DNAJB3	315.3083333	0.000886458
hsa-mir-8074	314.3041667	0.000883635
HP	313.3	0.000880812
POP1	312.2958333	0.000877989
RNF4	312.2958333	0.000877989
WDR4	312.2958333	0.000877989
SESN3	311.2916667	0.000875166
SH3RF3	311.2916667	0.000875166
ZNF280D	311.2916667	0.000875166
ATP6V0E1	310.2875	0.000872343
CD6	310.2875	0.000872343
PLA2R1	310.2875	0.000872343
SLAIN1	310.2875	0.000872343
hsa-mir-6073	310.2875	0.000872343
OTOP1	309.2833333	0.000869519

EAPP	308.2791667	0.000866696
MPPED1	308.2791667	0.000866696
SMIM15	307.275	0.000863873
DRC1	306.2708333	0.00086105
LHFPL2	306.2708333	0.00086105
PSMC6	306.2708333	0.00086105
PCDHGB6	305.2666667	0.000858227
SUPT4H1	304.2625	0.000855404
ATRX	303.2583333	0.000852581
FAM193A	303.2583333	0.000852581
TRIM40	303.2583333	0.000852581
C19orf26	302.2541667	0.000849758
CDCA3	302.2541667	0.000849758
EBP	302.2541667	0.000849758
PRH1	302.2541667	0.000849758
CCR3	301.25	0.000846935
RRH	301.25	0.000846935
OR7D4	300.2458333	0.000844111
UGT2B7	300.2458333	0.000844111
NonTargetingControlGuideForHuman_0068	300.2458333	0.000844111
C6orf48	300.2458333	0.000844111
USP30	300.2458333	0.000844111
GAL3ST1	299.2416667	0.000841288
GDPD2	299.2416667	0.000841288
GYLTL1B	299.2416667	0.000841288
MSX2	299.2416667	0.000841288
OR6K6	299.2416667	0.000841288
S100A4	299.2416667	0.000841288
TNFSF11	299.2416667	0.000841288
AEBP1	298.2375	0.000838465
MRPL22	298.2375	0.000838465
TCTN2	298.2375	0.000838465
SEC24A	298.2375	0.000838465
CACNB3	297.2333333	0.000835642
CRIP1	297.2333333	0.000835642

NRARP	297.2333333	0.000835642
TMEM167B	297.2333333	0.000835642
TRAPPC8	297.2333333	0.000835642
ITGA7	296.2291667	0.000832819
CNTN1	295.225	0.000829996
KLK3	295.225	0.000829996
NonTargetingControlGuideForHuman_0755	295.225	0.000829996
COPRS	294.2208333	0.000827173
LMTK2	294.2208333	0.000827173
STRIP1	294.2208333	0.000827173
HAPLN4	294.2208333	0.000827173
GJA3	293.2166667	0.00082435
HTR3A	293.2166667	0.00082435
INSRR	293.2166667	0.00082435
PPP1R21	293.2166667	0.00082435
TRA2A	293.2166667	0.00082435
hsa-mir-4519	293.2166667	0.00082435
GAR1	293.2166667	0.00082435
UCHL1	293.2166667	0.00082435
EVC2	292.2125	0.000821527
SIGLEC8	292.2125	0.000821527
TMEM258	292.2125	0.000821527
ACTG1	291.2083333	0.000818703
C9orf117	291.2083333	0.000818703
CHMP1B	291.2083333	0.000818703
ETV2	291.2083333	0.000818703
NDUFB11	291.2083333	0.000818703
PPP1R13B	291.2083333	0.000818703
ZKSCAN3	291.2083333	0.000818703
GPD2	290.2041667	0.00081588
INS	290.2041667	0.00081588
OTUB2	290.2041667	0.00081588
ACTG1	289.2	0.000813057
SFXN1	289.2	0.000813057
GAB1	289.2	0.000813057

C1orf229	288.1958333	0.000810234
ZNF775	288.1958333	0.000810234
NonTargetingControlGuideForHuman_0191	288.1958333	0.000810234
CD59	287.1916667	0.000807411
ID2	287.1916667	0.000807411
SLC25A21	287.1916667	0.000807411
POLR2G	287.1916667	0.000807411
hsa-mir-4787	286.1875	0.000804588
CDC45	286.1875	0.000804588
FAM110C	285.1833333	0.000801765
C22orf42	285.1833333	0.000801765
MYL7	285.1833333	0.000801765
Sep-08	285.1833333	0.000801765
TRAPPC13	285.1833333	0.000801765
FOXA2	284.1791667	0.000798942
GHRH	284.1791667	0.000798942
SQRDL	284.1791667	0.000798942
YTHDC2	284.1791667	0.000798942
KIAA0101	283.175	0.000796118
C7orf57	282.1708333	0.000793295
C9orf114	282.1708333	0.000793295
LY6D	282.1708333	0.000793295
SIGLEC8	282.1708333	0.000793295
TRMT2B	282.1708333	0.000793295
ADCK4	281.1666667	0.000790472
MAP3K6	281.1666667	0.000790472
MORN5	281.1666667	0.000790472
MYLK4	281.1666667	0.000790472
GAGE12D	281.1666667	0.000790472
PPP5D1	281.1666667	0.000790472
ZNF506	281.1666667	0.000790472
MUC12	280.1625	0.000787649
UBQLNL	280.1625	0.000787649
hsa-mir-374c	280.1625	0.000787649
ECI1	279.1583333	0.000784826

IZUMO1	279.1583333	0.000784826
NIPBL	279.1583333	0.000784826
PRKAG1	279.1583333	0.000784826
hsa-mir-4781	279.1583333	0.000784826
PCID2	279.1583333	0.000784826
GALNT16	278.1541667	0.000782003
GPX8	278.1541667	0.000782003
HYOU1	278.1541667	0.000782003
TNFSF14	278.1541667	0.000782003
NEU3	277.15	0.00077918
OARD1	277.15	0.00077918
PCF11	277.15	0.00077918
CYP4A11	276.1458333	0.000776357
MSGN1	276.1458333	0.000776357
OR51Q1	276.1458333	0.000776357
TTC19	276.1458333	0.000776357
hsa-mir-181d	276.1458333	0.000776357
HNRNPL	276.1458333	0.000776357
NINJ1	275.1416667	0.000773534
SLC29A2	275.1416667	0.000773534
hsa-mir-503	275.1416667	0.000773534
hsa-mir-548an	275.1416667	0.000773534
PMM1	275.1416667	0.000773534
LIPA	274.1375	0.00077071
CFHR5	274.1375	0.00077071
GPR37	274.1375	0.00077071
KRTAP16-1	274.1375	0.00077071
NME4	274.1375	0.00077071
SDR9C7	274.1375	0.00077071
EEF2	274.1375	0.00077071
SLC1A3	274.1375	0.00077071
FTH1	273.1333333	0.000767887
CDY2B	273.1333333	0.000767887
PLOD3	273.1333333	0.000767887
hsa-mir-3973	273.1333333	0.000767887

PDLIM4	273.1333333	0.000767887
KCNQ2	272.1291667	0.000765064
OXR1	272.1291667	0.000765064
RGS22	271.125	0.000762241
KDSR	270.1208333	0.000759418
BEND2	269.1166667	0.000756595
FARSB	269.1166667	0.000756595
TSHZ3	269.1166667	0.000756595
ZNF697	269.1166667	0.000756595
TMEM74B	269.1166667	0.000756595
CARD16	268.1125	0.000753772
DDIT4L	268.1125	0.000753772
EPHX1	268.1125	0.000753772
KCNN4	268.1125	0.000753772
LCN6	268.1125	0.000753772
P2RX6	268.1125	0.000753772
APOL3	268.1125	0.000753772
DSC2	267.1083333	0.000750949
MS4A14	267.1083333	0.000750949
hsa-mir-4255	267.1083333	0.000750949
LUZP2	266.1041667	0.000748126
RPAP2	266.1041667	0.000748126
AKIRIN2	265.1	0.000745302
CRYBA1	265.1	0.000745302
NRDE2	265.1	0.000745302
NTSR1	265.1	0.000745302
RHBDD3	265.1	0.000745302
TRAT1	265.1	0.000745302
DPPA5	264.0958333	0.000742479
OR2B3	264.0958333	0.000742479
PTPRJ	264.0958333	0.000742479
RIMS1	264.0958333	0.000742479
HOXA11	263.0916667	0.000739656
LCAT	263.0916667	0.000739656
NDUFB6	263.0916667	0.000739656

ZNF729	263.0916667	0.000739656
hsa-mir-548e	263.0916667	0.000739656
C14orf183	263.0916667	0.000739656
FCER1G	263.0916667	0.000739656
NXPE3	263.0916667	0.000739656
CACUL1	262.0875	0.000736833
COL22A1	262.0875	0.000736833
GTPBP4	262.0875	0.000736833
TCEAL8	262.0875	0.000736833
DFFA	261.0833333	0.00073401
EFS	261.0833333	0.00073401
LIN54	261.0833333	0.00073401
VGf	261.0833333	0.00073401
ZNF189	261.0833333	0.00073401
LGALS7	261.0833333	0.00073401
REPIN1	261.0833333	0.00073401
CST2	260.0791667	0.000731187
DDX19A	260.0791667	0.000731187
SMN2	260.0791667	0.000731187
IDNK	259.075	0.000728364
KCNMB2	259.075	0.000728364
OR8G5	259.075	0.000728364
C19orf44	258.0708333	0.000725541
NPAS3	258.0708333	0.000725541
RGPD4	258.0708333	0.000725541
DPAGT1	257.0666667	0.000722717
KLK1	257.0666667	0.000722717
P2RX1	257.0666667	0.000722717
SP5	257.0666667	0.000722717
NonTargetingControlGuideForHuman_0301	257.0666667	0.000722717
CHSY3	256.0625	0.000719894
HRASLS5	256.0625	0.000719894
KIAA1239	256.0625	0.000719894
VGLL2	256.0625	0.000719894
hsa-mir-16-2	256.0625	0.000719894

hsa-mir-4470	256.0625	0.000719894
CHRNA4	256.0625	0.000719894
BAG5	255.0583333	0.000717071
EIF4E2	255.0583333	0.000717071
LRFN2	255.0583333	0.000717071
MMP8	255.0583333	0.000717071
MRPL2	255.0583333	0.000717071
PDHA2	255.0583333	0.000717071
hsa-mir-6740	255.0583333	0.000717071
BEND7	254.0541667	0.000714248
LACTB2	254.0541667	0.000714248
TBC1D2B	254.0541667	0.000714248
hsa-mir-4288	254.0541667	0.000714248
FBXO9	253.05	0.000711425
KIAA0895	253.05	0.000711425
MAP2K7	253.05	0.000711425
PRSS16	253.05	0.000711425
KCNJ15	253.05	0.000711425
GRN	252.0458333	0.000708602
PRB2	252.0458333	0.000708602
hsa-mir-6764	252.0458333	0.000708602
EXOSC9	252.0458333	0.000708602
MLL3	252.0458333	0.000708602
NCOR2	252.0458333	0.000708602
PPP1R10	252.0458333	0.000708602
GLIS3	251.0416667	0.000705779
MVP	251.0416667	0.000705779
WASH1	251.0416667	0.000705779
ZNHIT6	251.0416667	0.000705779
hsa-mir-4452	251.0416667	0.000705779
FAM177B	251.0416667	0.000705779
MTL5	250.0375	0.000702956
PRELID1	250.0375	0.000702956
STAG3	250.0375	0.000702956
TBK1	250.0375	0.000702956

TTC40	250.0375	0.000702956
hsa-mir-5096	249.0333333	0.000700133
BANF1	248.0291667	0.000697309
DISP2	248.0291667	0.000697309
HKR1	248.0291667	0.000697309
CD1D	248.0291667	0.000697309
CPSF7	248.0291667	0.000697309
ATP6V1G3	247.025	0.000694486
CCL23	247.025	0.000694486
LONP1	247.025	0.000694486
WIP1	247.025	0.000694486
TMEM159	247.025	0.000694486
CSN3	246.0208333	0.000691663
CST9L	246.0208333	0.000691663
DOC2B	246.0208333	0.000691663
MCM4	246.0208333	0.000691663
NPW	246.0208333	0.000691663
HMGN1	245.0166667	0.00068884
MAT1A	245.0166667	0.00068884
WWC3	245.0166667	0.00068884
hsa-mir-1-2	245.0166667	0.00068884
C16orf78	245.0166667	0.00068884
SLC16A5	245.0166667	0.00068884
ZIC3	245.0166667	0.00068884
C1orf61	244.0125	0.000686017
CHRM4	244.0125	0.000686017
SEC31B	244.0125	0.000686017
ASIC1	244.0125	0.000686017
H2AFX	243.0083333	0.000683194
LAMB3	243.0083333	0.000683194
OR6C6	243.0083333	0.000683194
PUS3	243.0083333	0.000683194
RPL5	243.0083333	0.000683194
hsa-mir-7112-1	243.0083333	0.000683194
TMEM11	243.0083333	0.000683194

UNC79	242.0041667	0.000680371
ANKRD7	242.0041667	0.000680371
ITGB1	242.0041667	0.000680371
TAS2R4	242.0041667	0.000680371
USP18	242.0041667	0.000680371
USE1	242.0041667	0.000680371
CDAN1	241	0.000677548
KRT3	241	0.000677548
RNF166	241	0.000677548
hsa-mir-6859-2	241	0.000677548
ACOT6	239.9958333	0.000674725
ACTR2	239.9958333	0.000674725
HIST1H2AJ	239.9958333	0.000674725
SLC25A39	239.9958333	0.000674725
SH3BGRL2	239.9958333	0.000674725
FOXK1	238.9916667	0.000671901
OR6F1	238.9916667	0.000671901
PPP1R11	238.9916667	0.000671901
PRAMEF2	238.9916667	0.000671901
TNFSF14	238.9916667	0.000671901
TRA2A	238.9916667	0.000671901
ZFC3H1	238.9916667	0.000671901
C10orf76	238.9916667	0.000671901
CYP2F1	238.9916667	0.000671901
OPRD1	237.9875	0.000669078
TAGLN2	237.9875	0.000669078
FAM45A	237.9875	0.000669078
ASB17	236.9833333	0.000666255
MICALCL	236.9833333	0.000666255
FTSJD2	236.9833333	0.000666255
GTPBP6_X	236.9833333	0.000666255
G6PC2	235.9791667	0.000663432
GJA10	235.9791667	0.000663432
NODAL	235.9791667	0.000663432
hsa-mir-7111	235.9791667	0.000663432

KCNJ13	234.975	0.000660609
P2RY1	234.975	0.000660609
POLR2K	234.975	0.000660609
SMC1A	234.975	0.000660609
hsa-mir-635	234.975	0.000660609
NonTargetingControlGuideForHuman_0207	234.975	0.000660609
DMXL2	234.975	0.000660609
MOB1B	234.975	0.000660609
CACNA1S	233.9708333	0.000657786
CRIPAK	233.9708333	0.000657786
PRAMEF8	233.9708333	0.000657786
TEX14	233.9708333	0.000657786
TVP23C-CDRT4	233.9708333	0.000657786
BPIFB2	233.9708333	0.000657786
FKBP1A	233.9708333	0.000657786
ATP13A2	232.9666667	0.000654963
PAIP2	232.9666667	0.000654963
PAXBP1	232.9666667	0.000654963
SYN2	232.9666667	0.000654963
hsa-mir-3689c	232.9666667	0.000654963
TMEM129	232.9666667	0.000654963
ZNF610	232.9666667	0.000654963
DEPTOR	231.9625	0.00065214
NPLOC4	231.9625	0.00065214
PBK	231.9625	0.00065214
BCAS3	230.9583333	0.000649316
UGT2A1	230.9583333	0.000649316
SPRTN	230.9583333	0.000649316
OPRM1	229.9541667	0.000646493
C13orf45	229.9541667	0.000646493
SAPCD2	229.9541667	0.000646493
C7orf34	228.95	0.00064367
CLEC1A	228.95	0.00064367
CRHR1	228.95	0.00064367
KCNK4	228.95	0.00064367

PLGRKT	228.95	0.00064367
SLC30A6	228.95	0.00064367
hsa-mir-4298	228.95	0.00064367
hsa-mir-562	228.95	0.00064367
LYRM2	227.9458333	0.000640847
PCGF5	227.9458333	0.000640847
UGT3A2	227.9458333	0.000640847
FAM64A	227.9458333	0.000640847
HYKK	227.9458333	0.000640847
BAG2	226.9416667	0.000638024
EPS8L2	226.9416667	0.000638024
MUC2	226.9416667	0.000638024
TMEM130	226.9416667	0.000638024
PMPCB	226.9416667	0.000638024
CCNI	225.9375	0.000635201
DNTTIP1	225.9375	0.000635201
FFAR1	225.9375	0.000635201
STX2	225.9375	0.000635201
FAM25G	224.9333333	0.000632378
BEST4	224.9333333	0.000632378
COL3A1	224.9333333	0.000632378
MAGEB18	224.9333333	0.000632378
ZNF585A	224.9333333	0.000632378
NonTargetingControlGuideForHuman_0221	224.9333333	0.000632378
hsa-mir-26b	223.9291667	0.000629555
SCO1	223.9291667	0.000629555
DGKD	222.925	0.000626732
UTF1	222.925	0.000626732
CYP4F3	221.9208333	0.000623908
HGFAC	221.9208333	0.000623908
LARP6	221.9208333	0.000623908
RFNG	221.9208333	0.000623908
RSPO4	221.9208333	0.000623908
TUSC3	221.9208333	0.000623908
MAN2A1	220.9166667	0.000621085

MMP1	220.9166667	0.000621085
CCL25	220.9166667	0.000621085
EPPIN	220.9166667	0.000621085
CDH8	219.9125	0.000618262
TMPRSS6	219.9125	0.000618262
hsa-mir-126	219.9125	0.000618262
hsa-mir-1915	219.9125	0.000618262
DLL3	219.9125	0.000618262
ABCG4	218.9083333	0.000615439
BSG	218.9083333	0.000615439
F2RL2	218.9083333	0.000615439
PDE2A	218.9083333	0.000615439
CASP12	217.9041667	0.000612616
DPH3P1	217.9041667	0.000612616
FCAMR	217.9041667	0.000612616
NHEJ1	217.9041667	0.000612616
USP25	217.9041667	0.000612616
LIPA	217.9041667	0.000612616
MAGED2	216.9	0.000609793
OR6F1	216.9	0.000609793
TNFRSF13C	216.9	0.000609793
hsa-mir-542	216.9	0.000609793
ENTPD1	215.8958333	0.00060697
hsa-mir-6815	215.8958333	0.00060697
EIF4E1B	215.8958333	0.00060697
OXSRI	214.8916667	0.000604147
WFDC2	214.8916667	0.000604147
FRMD3	213.8875	0.000601324
LRBA	213.8875	0.000601324
hsa-mir-582	213.8875	0.000601324
HIGD2A	213.8875	0.000601324
OR4K15	213.8875	0.000601324
TRIM74	213.8875	0.000601324
FRMPD1	212.8833333	0.0005985
HOXC10	212.8833333	0.0005985

LSM12	212.8833333	0.0005985
MMRN1	212.8833333	0.0005985
USP28	212.8833333	0.0005985
WDR49	212.8833333	0.0005985
hsa-mir-4712	212.8833333	0.0005985
DDX11	212.8833333	0.0005985
MYBPC3	212.8833333	0.0005985
OR2T4	211.8791667	0.000595677
ABLIM2	211.8791667	0.000595677
EIF3D	211.8791667	0.000595677
GID4	210.875	0.000592854
ZNF335	210.875	0.000592854
HIST1H2BK	208.8666667	0.000587208
NOXO1	208.8666667	0.000587208
LRP4	208.8666667	0.000587208
C6orf201	207.8625	0.000584385
TUBE1	207.8625	0.000584385
SLC30A9	207.8625	0.000584385
DTNBP1	206.8583333	0.000581562
ENDOG	206.8583333	0.000581562
ARFRP1	206.8583333	0.000581562
CRYZL1	206.8583333	0.000581562
KIAA1430	206.8583333	0.000581562
MAGEB1	206.8583333	0.000581562
SLC25A22	206.8583333	0.000581562
SPARCL1	206.8583333	0.000581562
PKN3	205.8541667	0.000578739
ASB8	205.8541667	0.000578739
OSTM1	205.8541667	0.000578739
SLC38A2	205.8541667	0.000578739
CACFD1	205.8541667	0.000578739
HBA1	205.8541667	0.000578739
OR6K6	205.8541667	0.000578739
RPH3AL	205.8541667	0.000578739
PLCE1	204.85	0.000575916

TNKS	204.85	0.000575916
MAP1LC3B	203.8458333	0.000573092
RAB2B	203.8458333	0.000573092
SYNDIG1L	203.8458333	0.000573092
ZNF804B	203.8458333	0.000573092
MAGOHB	201.8375	0.000567446
TMED10	201.8375	0.000567446
NKX2-3	201.8375	0.000567446
CT47A5	200.8333333	0.000564623
TCEA1	200.8333333	0.000564623
TP53TG3B	200.8333333	0.000564623
ADAM33	199.8291667	0.0005618
DACT2	199.8291667	0.0005618
DMRTC1B	199.8291667	0.0005618
EIF4G3	199.8291667	0.0005618
ITGA8	198.825	0.000558977
OR13C8	198.825	0.000558977
PGK1	198.825	0.000558977
AGGF1	198.825	0.000558977
STAMBPL1	198.825	0.000558977
ATP6V0A4	197.8208333	0.000556154
COX14	197.8208333	0.000556154
HNRNPH3	196.8166667	0.000553331
FFAR2	195.8125	0.000550507
hsa-let-7a-1	195.8125	0.000550507
DEPDC1	195.8125	0.000550507
SCNN1A	195.8125	0.000550507
hsa-mir-432	194.8083333	0.000547684
EBP	193.8041667	0.000544861
CNIH4	193.8041667	0.000544861
FASTK	193.8041667	0.000544861
hsa-mir-3174	192.8	0.000542038
DCXR	192.8	0.000542038
INSIG1	192.8	0.000542038
INSM2	192.8	0.000542038

LRIT3	191.7958333	0.000539215
NPHP4	191.7958333	0.000539215
CLTB	190.7916667	0.000536392
RAD18	189.7875	0.000533569
ERMP1	188.7833333	0.000530746
R3HCC1L	188.7833333	0.000530746
HHIP	186.775	0.000525099
TRMT5	186.775	0.000525099
FATE1	185.7708333	0.000522276
MATN1	185.7708333	0.000522276
TBX19	185.7708333	0.000522276
TTC19	185.7708333	0.000522276
IRX3	184.7666667	0.000519453
NAV2	183.7625	0.00051663
C10orf54	183.7625	0.00051663
PITRM1	183.7625	0.00051663
ACP6	182.7583333	0.000513807
BOC	182.7583333	0.000513807
GSTO1	181.7541667	0.000510984
KIAA1191	181.7541667	0.000510984
LEPROTL1	181.7541667	0.000510984
NAE1	180.75	0.000508161
RHOT1	180.75	0.000508161
C4orf33	179.7458333	0.000505338
DISP1	179.7458333	0.000505338
UEVLD	179.7458333	0.000505338
MPHOSPH6	177.7375	0.000499691
SEMA5A	177.7375	0.000499691
ITGA1	177.7375	0.000499691
DEPDC1	176.7333333	0.000496868
GUF1	176.7333333	0.000496868
MOSPD1	176.7333333	0.000496868
ZNF25	175.7291667	0.000494045
VPS37A	173.7208333	0.000488399
MED31	173.7208333	0.000488399

hsa-mir-585	172.7166667	0.000485576
UNC13B	171.7125	0.000482753
OIP5	171.7125	0.000482753
hsa-mir-4799	170.7083333	0.00047993
ARSF	170.7083333	0.00047993
OGT	170.7083333	0.00047993
RNF6	170.7083333	0.00047993
hsa-mir-6723	169.7041667	0.000477106
KLF12	167.6958333	0.00047146
METTL21A	165.6875	0.000465814
OR11H12	165.6875	0.000465814
TENM2	162.675	0.000457345
CA2	160.6666667	0.000451698
FABP5	159.6625	0.000448875
OR6K6	158.6583333	0.000446052
BRINP2	155.6458333	0.000437583
NLRP13	153.6375	0.000431937
MLX	153.6375	0.000431937
XPO1	152.6333333	0.000429114
NRG3	150.625	0.000423467
NR4A3	150.625	0.000423467
TRIM34	149.6208333	0.000420644
ARL8A	147.6125	0.000414998
PRKRA	145.6041667	0.000409352
BCKDK	145.6041667	0.000409352
MYOD1	144.6	0.000406529
UBE2L6	144.6	0.000406529
CPNE5	144.6	0.000406529
HMGB2	143.5958333	0.000403705
SETD5	143.5958333	0.000403705
COL5A3	142.5916667	0.000400882
IFITM5	142.5916667	0.000400882
SMIM22	142.5916667	0.000400882
ACTN4	142.5916667	0.000400882
KRT24	141.5875	0.000398059

PICALM	138.575	0.00038959
CMYA5	137.5708333	0.000386767
KCNMA1	137.5708333	0.000386767
FAM153B	136.5666667	0.000383944
ABL2	135.5625	0.000381121
hsa-mir-151b	134.5583333	0.000378297
EIF2B4	133.5541667	0.000375474
ZMAT2	133.5541667	0.000375474
CYP26A1	131.5458333	0.000369828
SIGLEC12	131.5458333	0.000369828
TIGD1	129.5375	0.000364182
SERPINB9	128.5333333	0.000361359
hsa-mir-4795	127.5291667	0.000358536
SLC47A2	127.5291667	0.000358536
SGPP1	125.5208333	0.000352889
DPEP2	123.5125	0.000347243
TMEM33	123.5125	0.000347243
ZNF442	122.5083333	0.00034442
OR8U1	122.5083333	0.00034442
TP73	120.5	0.000338774
CSMD2	119.4958333	0.000335951
TTC33	119.4958333	0.000335951
PYCRL	118.4916667	0.000333128
ZFP90	116.4833333	0.000327481
APOB	115.4791667	0.000324658
FLNB	114.475	0.000321835
BAI1	113.4708333	0.000319012
NPC1L1	113.4708333	0.000319012
RHOJ	113.4708333	0.000319012
SETD4	113.4708333	0.000319012
SMTN	113.4708333	0.000319012
NUDT15	112.4666667	0.000316189
CEP128	110.4583333	0.000310543
DCAF8L2	105.4375	0.000296427
LBP	103.4291667	0.000290781

IL27RA	102.425	0.000287958
FERMT3	101.4208333	0.000285135
hsa-mir-3913-2	101.4208333	0.000285135
ZNF213	101.4208333	0.000285135
OR5V1	100.4166667	0.000282312
INSL6	96.4	0.000271019
NonTargetingControlGuideForHuman_0578	96.4	0.000271019
hsa-mir-3682	95.39583333	0.000268196
hsa-mir-513b	91.37916667	0.000256903
PTGES3L-AARSD1	90.375	0.00025408
REV3L	89.37083333	0.000251257
ZSCAN21	87.3625	0.000245611
REV1	85.35416667	0.000239965
MSRB3	84.35	0.000237142
TBC1D10C	82.34166667	0.000231495
DISC1	79.32916667	0.000223026
RLF	77.32083333	0.00021738
KIAA0930	76.31666667	0.000214557
CRTAM	74.30833333	0.000208911
OOEP	73.30416667	0.000206087
ADSS	71.29583333	0.000200441
NonTargetingControlGuideForHuman_0631	71.29583333	0.000200441
CCHCR1	68.28333333	0.000191972
CAMTA2	67.27916667	0.000189149
LPAR6	67.27916667	0.000189149
ARAF	66.275	0.000186326
DDX49	65.27083333	0.000183502
SLC39A13	63.2625	0.000177856
ARL2BP	61.25416667	0.00017221
FAM184A	60.25	0.000169387
SLC15A4	57.2375	0.000160918
PAFAH2	55.22916667	0.000155271
hsa-mir-4679-1	52.21666667	0.000146802
HADH	50.20833333	0.000141156
LOC100144595	50.20833333	0.000141156

OR14I1	50.20833333	0.000141156
TRIM15	50.20833333	0.000141156
TSPAN9	50.20833333	0.000141156
SLC7A11	50.20833333	0.000141156
BCL2L1	49.20416667	0.000138333
GM2A	48.2	0.00013551
HNF1A	48.2	0.00013551
PDE4B	47.19583333	0.000132686
CARS2	44.18333333	0.000124217
GNRH2	44.18333333	0.000124217
MYOZ2	44.18333333	0.000124217
VPS11	44.18333333	0.000124217
MTRNR2L5	41.17083333	0.000115748
CCL2	40.16666667	0.000112925
PITPNM2	37.15416667	0.000104455
C4orf32	35.14583333	9.8809E-05
LHFPL5	35.14583333	9.8809E-05
LOC391322	34.14166667	9.59859E-05
OR5K4	33.1375	9.31628E-05
CDKL3	32.13333333	9.03397E-05
MON1B	32.13333333	9.03397E-05
CYHR1	31.12916667	8.75166E-05
IFNL3	30.125	8.46935E-05
ATP1A1	27.1125	7.62241E-05
KIAA1967	27.1125	7.62241E-05
POU2F3	26.10833333	7.3401E-05
MBD3L2	25.10416667	7.05779E-05
CNRIP1	22.09166667	6.21085E-05
ESYT2	21.0875	5.92854E-05
RAB11FIP2	21.0875	5.92854E-05
HMG3	19.07916667	5.36392E-05
USP7	19.07916667	5.36392E-05
MTRNR2L7	18.075	5.08161E-05
OR10A2	17.07083333	4.7993E-05
MXRA7	16.06666667	4.51698E-05

XPNPEP1	16.06666667	4.51698E-05
ZNF812	16.06666667	4.51698E-05
hsa-mir-105-1	16.06666667	4.51698E-05
CLMP	16.06666667	4.51698E-05
OR2G3	15.0625	4.23467E-05
POLR3H	15.0625	4.23467E-05
NDUFS5	14.05833333	3.95236E-05
ZMAT5	13.05416667	3.67005E-05
hsa-mir-512-2	13.05416667	3.67005E-05
ACPT	11.04583333	3.10543E-05
PGAP1	11.04583333	3.10543E-05
IMMT	11.04583333	3.10543E-05
RUNDC3B	11.04583333	3.10543E-05
HBD	10.04166667	2.82312E-05
HMMR	10.04166667	2.82312E-05
KCNK16	10.04166667	2.82312E-05
CEACAM7	8.03333333	2.25849E-05
WWP1	8.03333333	2.25849E-05
DDOST	8.03333333	2.25849E-05
PSORS1C2	8.03333333	2.25849E-05
SFTPC	8.03333333	2.25849E-05
CDH4	7.029166667	1.97618E-05
GNAT3	7.029166667	1.97618E-05
HTR1F	7.029166667	1.97618E-05
USP17L20	7.029166667	1.97618E-05
VSTM4	7.029166667	1.97618E-05
hsa-mir-4491	7.029166667	1.97618E-05
CYP4Z1	7.029166667	1.97618E-05
HEYL	7.029166667	1.97618E-05
DAZ2	6.025	1.69387E-05
MAPK13	6.025	1.69387E-05
MCM4	6.025	1.69387E-05
SNCAIP	6.025	1.69387E-05
PPIL2	6.025	1.69387E-05
HMCES	5.020833333	1.41156E-05

DDB1	5.020833333	1.41156E-05
CTH	4.016666667	1.12925E-05
IFI30	4.016666667	1.12925E-05
KPNA2	4.016666667	1.12925E-05
CHRFAM7A	4.016666667	1.12925E-05
MRGPRD	4.016666667	1.12925E-05
FBXW4	3.0125	8.46935E-06
C7orf10	3.0125	8.46935E-06
GPATCH8	3.0125	8.46935E-06
KRTAP5-5	3.0125	8.46935E-06
PLB1	3.0125	8.46935E-06
PRPF31	3.0125	8.46935E-06
SLC20A1	3.0125	8.46935E-06
WDR96	3.0125	8.46935E-06
hsa-mir-920	3.0125	8.46935E-06
BAGE2	3.0125	8.46935E-06
C19orf81	3.0125	8.46935E-06
SERPINB1	3.0125	8.46935E-06
EFCAB4B	2.008333333	5.64623E-06
ETV3	2.008333333	5.64623E-06
RBM45	2.008333333	5.64623E-06
SPATA31A5	2.008333333	5.64623E-06
TTK	2.008333333	5.64623E-06
CENPP	2.008333333	5.64623E-06
COMMD9	2.008333333	5.64623E-06
E2F3	2.008333333	5.64623E-06
PAPOLB	2.008333333	5.64623E-06
SLC51A	2.008333333	5.64623E-06
TTC3	2.008333333	5.64623E-06
CBFA2T3	1.004166667	2.82312E-06
DNMT1	1.004166667	2.82312E-06
KCNT2	1.004166667	2.82312E-06
SF3B4	1.004166667	2.82312E-06
SLC9B1	1.004166667	2.82312E-06
STK36	1.004166667	2.82312E-06

TMOD2	1.004166667	2.82312E-06
ZNF212	1.004166667	2.82312E-06
hsa-mir-3130-2	1.004166667	2.82312E-06
hsa-mir-4487	1.004166667	2.82312E-06
hsa-mir-7152	1.004166667	2.82312E-06
ADRA2C	1.004166667	2.82312E-06
HP1BP3	1.004166667	2.82312E-06
OR2F2	1.004166667	2.82312E-06
PTRH2	1.004166667	2.82312E-06
QDPR	1.004166667	2.82312E-06
RANBP6	1.004166667	2.82312E-06
UBE3C	1.004166667	2.82312E-06
UGT2B28	1.004166667	2.82312E-06
UHRF2	1.004166667	2.82312E-06

9.2.2 gRNA lists from the KCL22^{WT} screen sample 2

Gene	WGKO-S2	WGKO-S2 %
CDH4	35415241.35	98.98672400
FAM3A	55706.65448	0.15570187
MRFAP1L1	43845.00914	0.12254819
TBC1D9	38425.11883	0.10739943
ATG13	15337.98903	0.04287017
ZBTB38	1316.402194	0.00367939
ID3	1309.389397	0.00365978
DEPTOR	1234.252285	0.00344977
ZNF135	1205.199269	0.00336857
CALU	1203.195612	0.00336297
XAF1	1180.153565	0.00329857
VWA3B	1172.13894	0.00327617
ZFAND3	1169.133455	0.00326777
ENKUR	1168.131627	0.00326496
TTI1	1158.113346	0.00323696
DMRT3	1157.111517	0.00323416
AMIGO3	1152.102377	0.00322016
IRX5	1136.073126	0.00317536
TEX14	1130.062157	0.00315856
CHST11	1127.056673	0.00315016
RSPH10B	1106.018282	0.00309136

AURKA	1086.983547	0.00303815
GABARAPL1	1081.974406	0.00302415
S1PR2	1080.972578	0.00302135
NonTargetingControlGuideForHuman_0696	1080.972578	0.00302135
ARHGEF4	1077.967093	0.00301295
SEPHS2	1077.967093	0.00301295
KRT26	1074.961609	0.00300455
NonTargetingControlGuideForHuman_0447	1066.946984	0.00298215
MMP9	1054.925046	0.00294855
CNTROB	1053.923218	0.00294575
PSMB5	1051.919561	0.00294015
C3orf83	1047.912249	0.00292895
NPFFR2	1043.904936	0.00291775
UCN3	1033.886654	0.00288975
SLC12A4	1031.882998	0.00288415
KIF6	1014.85192	0.00283654
KAAG1	1010.844607	0.00282534
EPS8L3	1004.833638	0.00280854
GAST	1003.83181	0.00280574
FZD6	1001.828154	0.00280014
KLK8	999.8244973	0.00279454
DNAJC3	997.820841	0.00278894
EEF2K	996.8190128	0.00278614

LHFPL5	994.8153565	0.00278054
hsa-mir-648	985.7989031	0.00275534
PRSS56	976.7824497	0.00273014
ANKH	976.7824497	0.00273014
GRID2IP	973.7769653	0.00272174
OR6N2	966.7641682	0.00270214
CCL4L2	964.7605119	0.00269654
FBXL4	960.7531993	0.00268534
DCAF5	956.7458867	0.00267414
ZNF383	954.7422303	0.00266853
LRP5L	953.7404022	0.00266573
hsa-mir-7849	951.7367459	0.00266013
KLRC2	951.7367459	0.00266013
MAP2K6	948.7312614	0.00265173
TMED7-TICAM2	946.7276051	0.00264613
MMGT1	941.7184644	0.00263213
HSD17B8	938.7129799	0.00262373
SKA2	929.6965265	0.00259853
LFNG	923.6855576	0.00258173
PCDH19	919.678245	0.00257053
CNNM3	913.6672761	0.00255373
OR51B2	905.6526508	0.00253133
ZCCHC24	902.6471664	0.00252293

CAPZB	899.6416819	0.00251453
LOC100652824	896.6361974	0.00250613
hsa-mir-4478	894.6325411	0.00250053
hsa-mir-642a	894.6325411	0.00250053
CDKN2AIP	870.5886654	0.00243332
SAAL1	863.5758684	0.00241372
C16orf80	858.5667276	0.00239972
FAM189B	857.5648995	0.00239692
hsa-mir-5572	855.5612431	0.00239132
CDY2A	843.5393053	0.00235772
ACVRL1	842.5374771	0.00235492
NonTargetingControlGuideForHuman_0694	842.5374771	0.00235492
MTRNR2L7	840.5338208	0.00234932
RBM14	831.5173675	0.00232412
HLTF	824.5045704	0.00230452
MFSD2B	823.5027422	0.00230172
PDGFB	822.5009141	0.00229892
NOTUM	820.4972578	0.00229332
NEFM	819.4954296	0.00229052
XPO7	817.4917733	0.00228492
LOXL3	809.4771481	0.00226251
CDHR2	807.4734918	0.00225691
C15orf60	796.4533821	0.00222611

GSTP1	795.4515539	0.00222331
SPAG1	785.4332724	0.00219531
GOLGA8A	781.4259598	0.00218411
PLSCR3	779.4223035	0.00217851
DGAT2L6	772.4095064	0.00215891
KIAA1551	764.3948812	0.00213651
DEFB115	763.393053	0.00213371
FAM209A	763.393053	0.00213371
AP2A2	762.3912249	0.00213091
TMEM97	757.3820841	0.00211691
MIER1	751.3711152	0.00210011
PLEKHH1	750.369287	0.00209731
SLC43A3	750.369287	0.00209731
CYP17A1	749.3674589	0.00209451
HACL1	744.3583181	0.00208051
RPS19	743.3564899	0.00207770
SEL1L3	739.3491773	0.00206650
CPA6	730.3327239	0.00204130
IQSEC2	726.3254113	0.00203010
SYTL1	723.3199269	0.00202170
HCST	719.3126143	0.00201050
MCTP1	714.3034735	0.00199650
RTN4	711.297989	0.00198810

FANCD2	709.2943327	0.00198250
PPP1R1C	708.2925046	0.00197970
SUCO	705.2870201	0.00197130
SCN5A	704.285192	0.00196850
EFNB2	703.2833638	0.00196570
PRPF6	694.2669104	0.00194050
C15orf52	692.2632541	0.00193490
FCAR	691.261426	0.00193210
RD3L	690.2595978	0.00192930
ZNF311	689.2577697	0.00192650
VSX1	685.250457	0.00191530
MYOCD	683.2468007	0.00190970
HVCN1	681.2431444	0.00190410
RSG1	679.2394881	0.00189850
GRAP2	674.2303473	0.00188450
SMPD2	672.226691	0.00187889
PIGQ	661.2065814	0.00184809
KRT2	659.202925	0.00184249
hsa-mir-194-2	656.1974406	0.00183409
KAAG1	647.1809872	0.00180889
CD1D	645.1773309	0.00180329
hsa-mir-550b-2	643.1736746	0.00179769
ZNF696	641.1700183	0.00179209

VN1R1	637.1627057	0.00178089
HES1	635.1590494	0.00177529
hsa-mir-6778	633.1553931	0.00176969
GALNT1	629.1480804	0.00175849
FAM212A	626.142596	0.00175009
MIS18A	626.142596	0.00175009
SERHL2	623.1371115	0.00174169
BAI3	621.1334552	0.00173609
CELF2	617.1261426	0.00172489
CALCR	616.1243144	0.00172209
GNGT1	616.1243144	0.00172209
ZNF878	612.1170018	0.00171089
TFF2	611.1151737	0.00170809
CDK12	611.1151737	0.00170809
KLRC2	610.1133455	0.00170529
C9orf37	609.1115174	0.00170249
ACOX1	607.1078611	0.00169689
SLC24A1	607.1078611	0.00169689
WASF2	606.1060329	0.00169409
MAB21L1	605.1042048	0.00169129
TBC1D17	605.1042048	0.00169129
ZMYM4	603.1005484	0.00168569
EMD	603.1005484	0.00168569

C9orf91	601.0968921	0.00168008
LASP1	600.095064	0.00167728
C5orf28	596.0877514	0.00166608
PASD1	594.0840951	0.00166048
HS3ST2	593.0822669	0.00165768
ANP32D	593.0822669	0.00165768
PPP2R1A	593.0822669	0.00165768
LTK	592.0804388	0.00165488
ZNF30	587.071298	0.00164088
PKN3	584.0658135	0.00163248
MAEA	584.0658135	0.00163248
MKRN2	584.0658135	0.00163248
KCNJ8	583.0639854	0.00162968
ARHGEF10L	582.0621572	0.00162688
EHMT2	581.0603291	0.00162408
GPR97	581.0603291	0.00162408
PC	580.0585009	0.00162128
KLHL15	578.0548446	0.00161568
DAPL1	577.0530165	0.00161288
hsa-mir-7107	574.047532	0.00160448
CCL4L2	572.0438757	0.00159888
OR2G3	571.0420475	0.00159608
FKRP	570.0402194	0.00159328

RPL3	570.0402194	0.00159328
CRTAM	567.0347349	0.00158488
SNRPN	567.0347349	0.00158488
CDK10	566.0329068	0.00158208
NGB	559.0201097	0.00156248
UNC79	556.0146252	0.00155408
HYAL4	555.0127971	0.00155128
GPR56	554.0109689	0.00154848
TOMM6	553.0091408	0.00154568
NAA38	553.0091408	0.00154568
OR3A2	552.0073126	0.00154288
TMEM192	550.0036563	0.00153728
AGPAT4	549.0018282	0.00153448
hsa-mir-1233-1	548	0.00153168
ZNF675	546.9981718	0.00152888
ABCF3	543.9926874	0.00152048
MC4R	543.9926874	0.00152048
CCDC54	541.9890311	0.00151488
OR6V1	540.9872029	0.00151208
NonTargetingControlGuideForHuman_0263	537.9817185	0.00150368
SMIM13	537.9817185	0.00150368
NonTargetingControlGuideForHuman_0842	534.976234	0.00149528
IGSF5	532.9725777	0.00148968

PALLD	532.9725777	0.00148968
RGS12	530.9689214	0.00148407
ERVMER34-1	530.9689214	0.00148407
USP31	530.9689214	0.00148407
hsa-mir-4717	528.9652651	0.00147847
LILRB2	527.9634369	0.00147567
MED31	527.9634369	0.00147567
IQCF6	524.9579525	0.00146727
ZKSCAN4	520.9506399	0.00145607
SMIM14	519.9488117	0.00145327
SNX14	519.9488117	0.00145327
ABCA9	518.9469835	0.00145047
FAM50B	517.9451554	0.00144767
SHC2	513.9378428	0.00143647
COMMD6	512.9360146	0.00143367
FAM122B	509.9305302	0.00142527
CPT1A	508.928702	0.00142247
PLAC1L	506.9250457	0.00141687
GPR33	504.9213894	0.00141127
DDOST	504.9213894	0.00141127
PTPN20A	503.9195612	0.00140847
FANCD2OS	502.9177331	0.00140567
PLCB4	502.9177331	0.00140567

PODNL1	501.9159049	0.00140287
CLDN24	500.9140768	0.00140007
SLC35G1	500.9140768	0.00140007
FTH1	499.9122486	0.00139727
CDH20	499.9122486	0.00139727
TECPR1	499.9122486	0.00139727
MLIP	495.904936	0.00138607
KIAA0907	494.9031079	0.00138327
UHRF1BP1	491.8976234	0.00137487
DUSP27	488.8921389	0.00136647
OR11A1	487.8903108	0.00136367
RAB11A	487.8903108	0.00136367
BTG4	485.8866545	0.00135807
EFHD2	480.8775137	0.00134407
KLHL15	479.8756856	0.00134127
RNF152	479.8756856	0.00134127
CKAP5	473.8647166	0.00132447
PROS1	471.8610603	0.00131887
C21orf58	468.8555759	0.00131047
PSORS1C2	467.8537477	0.00130767
TTN	466.8519196	0.00130487
RNF144A	460.8409506	0.00128807
HSPA9	459.8391225	0.00128526

LAT2	458.8372943	0.00128246
IFI30	457.8354662	0.00127966
SLC7A2	456.833638	0.00127686
hsa-mir-642a	450.8226691	0.00126006
CCBE1	448.8190128	0.00125446
ATP5SL	447.8171846	0.00125166
CCL25	442.8080439	0.00123766
TCEAL1	441.8062157	0.00123486
ZNF254	436.797075	0.00122086
POGLUT1	430.786106	0.00120406
CDYL2	427.7806216	0.00119566
LSS	425.7769653	0.00119006
ZFHX3	423.773309	0.00118446
PYGB	422.7714808	0.00118166
SCUBE2	417.76234	0.00116766
SNAPC5	417.76234	0.00116766
PHLPP2	417.76234	0.00116766
CRTC3	413.7550274	0.00115646
MZT1	403.7367459	0.00112846
IGF2BP1	402.7349177	0.00112566
BEND2	401.7330896	0.00112286
CKM	399.7294333	0.00111726
LRRC25	396.7239488	0.00110886

GPR15	392.7166362	0.00109766
THBS2	390.7129799	0.00109206
ZCCHC11	388.7093236	0.00108645
XKRY	386.7056673	0.00108085
MMRN2	380.6946984	0.00106405
ZNF593	380.6946984	0.00106405
YBEY	374.6837294	0.00104725
C18orf54	372.6800731	0.00104165
PRM3	372.6800731	0.00104165
ZNF736	365.6672761	0.00102205
hsa-mir-4742	364.6654479	0.00101925
SLC2A7	363.6636197	0.00101645
NOTCH4	361.6599634	0.00101085
MBD3L4	358.654479	0.00100245
ZNF229	355.6489945	0.00099405
TLR8	354.6471664	0.00099125
NT5DC1	351.6416819	0.00098285
ZFH3	351.6416819	0.00098285
NCOA7	349.6380256	0.00097725
ZNF675	346.6325411	0.00096885
PTCHD2	344.6288848	0.00096325
SYTL5	339.6197441	0.00094925
CDH3	326.5959781	0.00091285

SNN	325.5941499	0.00091005
MELK	318.5813528	0.00089044
NEK4	317.5795247	0.00088764
PRSS21	313.5722121	0.00087644
PLSCR5	310.5667276	0.00086804
RNPS1	309.5648995	0.00086524
OR2T1	302.5521024	0.00084564
RBM34	301.5502742	0.00084284
CMKLR1	300.5484461	0.00084004
TMEM218	292.5338208	0.00081764
STX17	292.5338208	0.00081764
DCPS	284.5191956	0.00079524
PRR20A	283.5173675	0.00079244
ZNF799	278.5082267	0.00077844
C16orf80	272.4972578	0.00076164
TRIM69	270.4936015	0.00075604
RGPD1	269.4917733	0.00075324
DUSP3	259.4734918	0.00072524
AKAP17A_Y	255.4661792	0.00071404
KLRF2	247.4515539	0.00069163
CACNG2	246.4497258	0.00068883
ZNF551	237.4332724	0.00066363
GPR87	234.4277879	0.00065523

hsa-mir-1266	234.4277879	0.00065523
UBXN4	227.4149909	0.00063563
TMSB10	217.3967093	0.00060763
QPCT	206.3765996	0.00057683
NOX4	197.3601463	0.00055163
RFC2	187.3418647	0.00052363
BANF1	187.3418647	0.00052363
HMSD	185.3382084	0.00051803
SCAND3	178.3254113	0.00049843
TAF1C	177.3235832	0.00049563
MLL3	177.3235832	0.00049563
PKLR	173.3162706	0.00048442
DPM1	172.3144424	0.00048162
ZNF607	167.3053016	0.00046762
SNRPA	140.2559415	0.00039202
PHC1	138.2522852	0.00038642
NKIRAS2	132.2413163	0.00036962
CCHCR1	123.2248629	0.00034442
CAPN2	104.190128	0.00029121
DNAJC19	76.13893967	0.00021281
SNTB2	64.11700183	0.00017921
MRPS25	53.09689214	0.00014841
hsa-mir-4799	47.08592322	0.00013161

FAM25C	47.08592322	0.00013161
SCNN1A	44.08043876	0.00012321
CCR1	40.07312614	0.00011201
FBXW4	39.07129799	0.00010921
RALGPS1	33.06032907	0.00009240
OR4C45	31.05667276	0.00008680
NPIPL3	27.04936015	0.00007560
HAUS1	26.04753199	0.00007280
C19orf44	21.03839122	0.00005880
GFPT2	21.03839122	0.00005880
CAST	18.03290676	0.00005040
CEPT1	14.02559415	0.00003920
EDARADD	13.023766	0.00003640
RAB11FIP4	13.023766	0.00003640
ZSCAN2	12.02193784	0.00003360
LIPA	11.02010969	0.00003080
SCRN3	9.016453382	0.00002520
NAP1L5	6.010968921	0.00001680
RGMB	6.010968921	0.00001680
TOB1	6.010968921	0.00001680
C14orf80	5.009140768	0.00001400
RNF212	5.009140768	0.00001400
PEX19	5.009140768	0.00001400

COMMD2	4.007312614	0.00001120
KIF2A	4.007312614	0.00001120
IL16	3.005484461	0.00000840
LOC643037	3.005484461	0.00000840
NCAPD3	2.003656307	0.00000560
hsa-mir-384	2.003656307	0.00000560
TNNT1	2.003656307	0.00000560
ZNF330	2.003656307	0.00000560
DUSP7	1.001828154	0.00000280
APITD1-CORT	1.001828154	0.00000280
BRS3	1.001828154	0.00000280
IL17RA	1.001828154	0.00000280
LRRC41	1.001828154	0.00000280
MYO16	1.001828154	0.00000280
NPY4R	1.001828154	0.00000280
SAMD8	1.001828154	0.00000280
SLC16A11	1.001828154	0.00000280
SPRY4	1.001828154	0.00000280
hsa-mir-4437	1.001828154	0.00000280
ARMCX4	1.001828154	0.00000280
FAM96A	1.001828154	0.00000280
PLA2G4F	1.001828154	0.00000280
SP140L	1.001828154	0.00000280

TMEM42	1.001828154	0.00000280
TOMM34	1.001828154	0.00000280
WBSCR28	1.001828154	0.00000280

10 List of references

1988. Thymic lymphoma induction by the AKT8 murine retrovirus. *The Journal of Experimental Medicine*, 167, 1259-1264.
1994. The COOH terminus of the c-Abl tyrosine kinase contains distinct F- and G-actin binding domains with bundling activity [published erratum appears in *J Cell Biol* 1994 Mar;124(5):865]. *The Journal of Cell Biology*, 124, 325-340.
1995. Genetic requirement for Ras in the transformation of fibroblasts and hematopoietic cells by the Bcr-Abl oncogene. *The Journal of Experimental Medicine*, 181, 307-313.
1996. Tyrosyl phosphorylation and DNA binding activity of signal transducers and activators of transcription (STAT) proteins in hematopoietic cell lines transformed by Bcr/Abl. *The Journal of Experimental Medicine*, 183, 811-820.
- (NCCN), N. C. C. N. 2010. National Comprehensive Cancer Network (NCCN) Clinical Practice Guidelines in Oncology: Chronic Myelogenous Leukemia. V.2.2010. Fort Washington, PA.
- A HOCHHAUS, S. K., A S CORBIN, P LA ROSÉE, M C MÜLLER, T LAHAYE, B HANFSTEIN, C SCHOCH, N C P CROSS, U BERGER, H GSCHAIDMEIER, B J DRUKER AND R HEHLMANN 2002. Molecular and chromosomal mechanisms of resistance to imatinib (STI571) therapy. *Leukemia*, 16, 2190-2196.
- AARON SHAVER, M. J. 2014. *BCR-ABL1 c.944C>T (T315I) Mutation in Chronic Myeloid Leukemia* [Online]. My cancer genome. Available: <https://www.mycancergenome.org/content/disease/chronic-myeloid-leukemia/bcr-abl1/231/> [Accessed 17/08 2016].
- AFAR, D. E., GOGA, A., MCLAUGHLIN, J., WITTE, O. N. & SAWYERS, C. L. 1994. Differential complementation of Bcr-Abl point mutants with c-Myc. *Science*, 264, 424-426.
- AIRIAU, K., MAHON, F. X., JOSSELIN, M., JEANNETEAU, M. & BELLOC, F. 2013. PI3K/mTOR pathway inhibitors sensitize chronic myeloid leukemia stem cells to nilotinib and restore the response of progenitors to nilotinib in the presence of stem cell factor. *Cell Death Dis*, 4, e827.
- AITA, V. M., LIANG, X. H., MURTY, V. V. V. S., PINCUS, D. L., YU, W., CAYANIS, E., KALACHIKOV, S., GILLIAM, T. C. & LEVINE, B. 1999. Cloning and Genomic Organization of Beclin 1, a Candidate Tumor Suppressor Gene on Chromosome 17q21. *Genomics*, 59, 59-65.
- AKASHI, K., TRAVER, D., MIYAMOTO, T. & WEISSMAN, I. L. 2000. A clonogenic common myeloid progenitor that gives rise to all myeloid lineages. *Nature*, 404, 193-197.
- ALBERTO M. MARTELLI, F. C., CAMILLA EVANGELISTI, CECILIA GRIMALDI, ANDREA OGNIBENE, LUCIA MANZOLI, ANNA MARIA BILLI AND JAMES A. MCCUBREY 2010. The phosphatidylinositol 3-kinase/AKT/mammalian target of rapamycin signaling network and the control of normal myelopoiesis. *Histol Histopathol* 25, 669-680.
- ALESSI, D. R., ANDJELKOVIC, M., CAUDWELL, B., CRON, P., MORRICE, N., COHEN, P. & HEMMINGS, B. A. 1996. Mechanism of activation of protein kinase B by insulin and IGF-1. *The EMBO Journal*, 15, 6541-6551.
- ALESSI, D. R., JAMES, S. R., DOWNES, C. P., HOLMES, A. B., GAFFNEY, P. R. J., REESE, C. B. & COHEN, P. 1997. Characterization of a 3-phosphoinositide-dependent protein kinase which phosphorylates and activates protein kinase Ba. *Current Biology*, 7, 261-269.
- ALLAN, E. K., HOLYOAKE, T. L., CRAIG, A. R. & JORGENSEN, H. G. 2011. Omacetaxine may have a role in chronic myeloid leukaemia eradication through downregulation of Mcl-1 and induction of apoptosis in stem/progenitor cells. *Leukemia*, 25, 985-994.
- ALTMAN, B. J., JACOBS, S. R., MASON, E. F., MICHALEK, R. D., MACINTYRE, A. N., COLOFF, J. L., ILKAYEVA, O., JIA, W., HE, Y. W. & RATHMELL, J. C. 2011. Autophagy is essential to suppress cell stress and to allow BCR-Abl-mediated leukemogenesis. *Oncogene*, 30, 1855-1867.
- AMABILE, G., DI RUSCIO, A., MÜLLER, F., WELNER, R. S., YANG, H., EBRALIDZE, A. K., ZHANG, H., LEVANTINI, E., QI, L., MARTINELLI, G., BRUMMELKAMP, T., LE BEAU, M. M., FIGUEROA, M. E., BOCK, C. & TENEN, D. G. 2015. Dissecting the role of aberrant DNA methylation in human leukaemia. *Nature Communications*, 6, 7091.
- AMARAVADI, R. K., LIPPINCOTT-SCHWARTZ, J., YIN, X.-M., WEISS, W. A., TAKEBE, N., TIMMER, W., DIPAOLO, R. S., LOTZE, M. T. & WHITE, E. 2011. Principles and Current Strategies for Targeting Autophagy for Cancer Treatment. *Clinical cancer research : an official journal of the American Association for Cancer Research*, 17, 654-666.
- ANAFI, M., GAZIT, A., GILON, C., BEN-NERIAH, Y. & LEVITZKI, A. 1992. Selective interactions of transforming and normal abl proteins with ATP, tyrosine-copolymer substrates, and tyrophostins. *Journal of Biological Chemistry*, 267, 4518-4523.
- ANAFI, M., GAZIT, A., ZEHAZI, A., BEN-NERIAH, Y. & LEVITZKI, A. 1993. Tyrophostin-induced inhibition of p210bcr-abl tyrosine kinase activity induces K562 to differentiate. *Blood*, 82, 3524-3529.

- APPERLEY, J. F., CORTES, J. E., KIM, D.-W., ROY, L., ROBOZ, G. J., ROSTI, G., BULLORSKY, E. O., ABRUZZESE, E., HOCHHAUS, A., HEIM, D., DE SOUZA, C. A., LARSON, R. A., LIPTON, J. H., KHOURY, H. J., KIM, H.-J., SILLABER, C., HUGHES, T. P., ERBEN, P., VAN TORNOUT, J. & STONE, R. M. 2009. Dasatinib in the Treatment of Chronic Myeloid Leukemia in Accelerated Phase After Imatinib Failure: The START A Trial. *Journal of Clinical Oncology*, 27, 3472-3479.
- APSEL, B., BLAIR, J. A., GONZALEZ, B. Z., NAZIF, T. M., FELDMAN, M. E., AIZENSTEIN, B., HOFFMAN, R., WILLIAMS, R. L., SHOKAT, K. M. & KNIGHT, Z. A. 2008. Targeted polypharmacology: Discovery of dual inhibitors of tyrosine and phosphoinositide kinases. *Nature chemical biology*, 4, 691-699.
- ARAI, F., HIRAO, A., OHMURA, M., SATO, H., MATSUOKA, S., TAKUBO, K., ITO, K., KOH, G. Y. & SUDA, T. 2004. Tie2/Angiopoietin-1 Signaling Regulates Hematopoietic Stem Cell Quiescence in the Bone Marrow Niche. *Cell*, 118, 149-161.
- ASHFORD, T. P. & PORTER, K. R. 1962. CYTOPLASMIC COMPONENTS IN HEPATIC CELL LYSOSOMES. *The Journal of Cell Biology*, 12, 198-202.
- ASMUSSEN, J., LASATER, E. A., TAJON, C., OSES-PRIETO, J., JUN, Y.-W., TAYLOR, B. S., BURLINGAME, A., CRAIK, C. S. & SHAH, N. P. 2014. MEK-Dependent Negative Feedback Underlies BCR-ABL-Mediated Oncogene Addiction. *Cancer discovery*, 4, 200-215.
- BACCARANI, M., CORTES, J., PANE, F., NIEDERWIESER, D., SAGLIO, G., APPERLEY, J., CERVANTES, F., DEININGER, M., GRATWOHL, A., GUILHOT, F., HOCHHAUS, A., HOROWITZ, M., HUGHES, T., KANTARJIAN, H., LARSON, R., RADICH, J., SIMONSSON, B., SILVER, R. T., GOLDMAN, J. & HEHLMANN, R. 2009. Chronic Myeloid Leukemia: An Update of Concepts and Management Recommendations of European LeukemiaNet. *Journal of Clinical Oncology*, 27, 6041-6051.
- BACCARANI, M., DEININGER, M. W., ROSTI, G., HOCHHAUS, A., SOVERINI, S., APPERLEY, J. F., CERVANTES, F., CLARK, R. E., CORTES, J. E., GUILHOT, F., HJORTH-HANSEN, H., HUGHES, T. P., KANTARJIAN, H. M., KIM, D.-W., LARSON, R. A., LIPTON, J. H., MAHON, F.-X., MARTINELLI, G., MAYER, J., MÜLLER, M. C., NIEDERWIESER, D., PANE, F., RADICH, J. P., ROUSSELOT, P., SAGLIO, G., SAUßELE, S., SCHIFFER, C., SILVER, R., SIMONSSON, B., STEEGMANN, J.-L., GOLDMAN, J. M. & HEHLMANN, R. 2013. European LeukemiaNet recommendations for the management of chronic myeloid leukemia: 2013. *Blood*, 122, 872.
- BARRANGOU, R., FREMAUX, C., DEVEAU, H., RICHARDS, M., BOYAVAL, P., MOINEAU, S., ROMERO, D. A. & HORVATH, P. 2007. CRISPR Provides Acquired Resistance Against Viruses in Prokaryotes. *Science*, 315, 1709-1712.
- BARTOLOVIC, K., BALABANOV, S., HARTMANN, U., KOMOR, M., BOEHMLER, A. M., BÜHRING, H.-J., MÖHLE, R., HOELZER, D., KANZ, L., HOFMANN, W.-K. & BRÜMMENDORF, T. H. 2003. Inhibitory effect of imatinib on normal progenitor cells in vitro. *Blood*, 103, 523-529.
- BEDI, A., ZEHNBAUER, B. A., BARBER, J. P., SHARKIS, S. J. & JONES, R. J. 1994. Inhibition of apoptosis by BCR-ABL in chronic myeloid leukemia. *Blood*, 83, 2038-2044.
- BELLODI, C., LIDONNICI, M. R., HAMILTON, A., HELGASON, G. V., SOLIERA, A. R., RONCHETTI, M., GALAVOTTI, S., YOUNG, K. W., SELMI, T., YACOBI, R., VAN ETTEN, R. A., DONATO, N., HUNTER, A., DINSDALE, D., TIRR, X.F., ELENA, VIGNERI, P., NICOTERA, P., DYER, M. J., HOLYOAKE, T., SALOMONI, P. & CALABRETTA, B. Targeting autophagy potentiates tyrosine kinase inhibitor-induced cell death in Philadelphia chromosome-positive cells, including primary CML stem cells. *The Journal of Clinical Investigation*, 119, 1109-1123.
- BERAN, M., CAO, X., ESTROV, Z., JEHA, S., JIN, G., O'BRIEN, S., TALPAZ, M., ARLINGHAUS, R. B., LYDON, N. B. & KANTARJIAN, H. 1998. Selective inhibition of cell proliferation and BCR-ABL phosphorylation in acute lymphoblastic leukemia cells expressing Mr 190,000 BCR-ABL protein by a tyrosine kinase inhibitor (CGP-57148). *American Association for Cancer Research*, 4, 1661-1672.
- BERTRAND, J. Y., KIM, A. D., VIOLETTE, E. P., STACHURA, D. L., CISSON, J. L. & TRAVER, D. 2007. Definitive hematopoiesis initiates through a committed erythromyeloid progenitor in the zebrafish embryo. *Development*, 134, 4147-4156.
- BHASKAR, P. T. & HAY, N. 2007. The Two TORCs and Akt. *Developmental Cell*, 12, 487-502.
- BHATIA, R., MUNTHE, H. A. & VERFAILLIE, C. M. 1999. Role of abnormal integrin-cytoskeletal interactions in impaired $\beta 1$ integrin function in chronic myelogenous leukemia hematopoietic progenitors. *Experimental Hematology*, 27, 1384-1396.
- BLOMMAART, E. F. C., KRAUSE, U., SCHELLENS, J. P. M., VREELING-SINDELÁROVÁ, H. & MEIJER, A. J. 1997. The Phosphatidylinositol 3-Kinase Inhibitors Wortmannin and LY294002 Inhibit Autophagy in Isolated Rat Hepatocytes. *European Journal of Biochemistry*, 243, 240-246.
- BOGUSKI, M. S. & MCCORMICK, F. 1993. Proteins regulating Ras and its relatives. *Nature*, 366, 643-654.
- BOLTON-GILLESPIE, E., SCHEMIONEK, M., KLEIN, H.-U., FLIS, S., HOSER, G., LANGE, T., NIEBOROWSKA-SKORSKA, M., MAIER, J., KERSTIENS, L., KOPTYRA, M., MÜLLER, M. C., MODI, H., STOKLOSA, T., SEFERYSKA, I., BHATIA, R., HOLYOAKE, T. L.,

- KOSCHMIEDER, S. & SKORSKI, T. 2013. Genomic instability may originate from imatinib-refractory chronic myeloid leukemia stem cells. *Blood*, 121, 4175-4183.
- BONNET, D. & DICK, J. E. 1997. Human acute myeloid leukemia is organized as a hierarchy that originates from a primitive hematopoietic cell. *Nat Med*, 3, 730-737.
- BRADEEN, H. A., EIDE, C. A., O'HARE, T., JOHNSON, K. J., WILLIS, S. G., LEE, F. Y., DRUKER, B. J. & DEININGER, M. W. 2006. Comparison of imatinib mesylate, dasatinib (BMS-354825), and nilotinib (AMN107) in an N-ethyl-N-nitrosourea (ENU)-based mutagenesis screen: high efficacy of drug combinations. *Blood*, 108, 2332-2338.
- BRANFORD, S., RUDZKI, Z., WALSH, S., PARKINSON, I., GRIGG, A., SZER, J., TAYLOR, K., HERRMANN, R., SEYMOUR, J. F., ARTHUR, C., JOSKE, D., LYNCH, K. & HUGHES, T. 2003. Detection of BCR-ABL mutations in patients with CML treated with imatinib is virtually always accompanied by clinical resistance, and mutations in the ATP phosphate-binding loop (P-loop) are associated with a poor prognosis. *Blood*, 102, 276-283.
- BROOKS, C. L. & GU, W. 2009. How does SIRT1 affect metabolism, senescence and cancer? *Nature reviews. Cancer*, 9, 123-128.
- BRÜMMENDORF, T. H., CORTES, J. E., DE SOUZA, C. A., GUILHOT, F., DUVILLIÉ, L., PAVLOV, D., GOGAT, K., COUNTOURIOTIS, A. M. & GAMBACORTI-PASSERINI, C. 2015. Bosutinib versus imatinib in newly diagnosed chronic-phase chronic myeloid leukaemia: results from the 24-month follow-up of the BELA trial. *British Journal of Haematology*, 168, 69-81.
- BUCHDUNGER, E., CIOFFI, C. L., LAW, N., STOVER, D., OHNO-JONES, S., DRUKER, B. J. & LYDON, N. B. 2000. Abl Protein-Tyrosine Kinase Inhibitor STI571 Inhibits In Vitro Signal Transduction Mediated by c-Kit and Platelet-Derived Growth Factor Receptors. *Journal of Pharmacology and Experimental Therapeutics*, 295, 139-145.
- BUCHDUNGER, E., ZIMMERMANN, J., METT, H., MEYER, T., MÜLLER, M., DRUKER, B. J. & LYDON, N. B. 1996. Inhibition of the Abl Protein-Tyrosine Kinase in Vitro and in Vivo by a 2-Phenylaminopyrimidine Derivative. *Cancer Research*, 56, 100-104.
- BURCHERT, A., WANG, Y., CAI, D., VON BUBNOFF, N., PASCHKA, P., MULLER-BRUSSELBACH, S., OTTMANN, O. G., DUYSER, J., HOCHHAUS, A. & NEUBAUER, A. 2005. Compensatory PI3-kinase//Akt//mTor activation regulates imatinib resistance development. *Leukemia*, 19, 1774-1782.
- BURGER, H., VAN TOL, H., BOERSMA, A. W. M., BROK, M., WIEMER, E. A. C., STOTER, G. & NOOTER, K. 2004. Imatinib mesylate (STI571) is a substrate for the breast cancer resistance protein (BCRP)/ABCG2 drug pump. *Blood*, 104, 2940.
- CALABRETTA, B. & PERROTTI, D. 2004a. The biology of CML blast crisis. *Blood*, 103, 4010-4022.
- CALABRETTA, B. & PERROTTI, D. 2004b. The biology of CML blast crisis. *Blood*, 103, 4010.
- CALABRETTA, B. & SALOMONI, P. 2011. Inhibition of autophagy: a new strategy to enhance sensitivity of chronic myeloid leukemia stem cells to tyrosine kinase inhibitors. *Leukemia & Lymphoma*, 52, 54-59.
- CARETTE, J. E., PRUSZAK, J., VARADARAJAN, M., BLOMEN, V. A., GOKHALE, S., CAMARGO, F. D., WERNIG, M., JAENISCH, R. & BRUMMELKAMP, T. R. 2010. Generation of iPSCs from cultured human malignant cells. *Blood*, 115, 4039-4042.
- CARRACEDO, A. & PANDOLFI, P. P. 0000. The PTEN-PI3K pathway: of feedbacks and cross-talks. *Oncogene*, 27, 5527-5541.
- CATLIN, S. N., BUSQUE, L., GALE, R. E., GUTTORP, P. & ABKOWITZ, J. L. 2011. The replication rate of human hematopoietic stem cells in vivo. *Blood*, 117, 4460-4466.
- CE, F. 1938. *Leukemia and allied disorders*, New York.
- CHAI, S. K., NICHOLS, G. L. & ROTHMAN, P. 1997. Constitutive activation of JAKs and STATs in BCR-Abl-expressing cell lines and peripheral blood cells derived from leukemic patients. *The Journal of Immunology*, 159, 4720-4728.
- CHALLEN, G. A., SUN, D., JEONG, M., LUO, M., JELINEK, J., BERG, J. S., BOCK, C., VASANTHAKUMAR, A., GU, H., XI, Y., LIANG, S., LU, Y., DARLINGTON, G. J., MEISSNER, A., ISSA, J.-P. J., GODLEY, L. A., LI, W. & GOODELL, M. A. 2012. Dnmt3a is essential for hematopoietic stem cell differentiation. *Nat Genet*, 44, 23-31.
- CHAMPLIN, R., HO, W., ARENSON, E. & GALE, R. P. 1982. Allogeneic bone marrow transplantation for chronic myelogenous leukemia in chronic or accelerated phase. *Blood*, 60, 1038-1041.
- CHANG, E. H., GONDA, M. A., ELLIS, R. W., SCOLNICK, E. M. & LOWY, D. R. 1982. Human genome contains four genes homologous to transforming genes of Harvey and Kirsten murine sarcoma viruses. *Proceedings of the National Academy of Sciences of the United States of America*, 79, 4848-4852.
- CHANG, J. S., SANTHANAM, R., TROTTA, R., NEVIANI, P., EIRING, A. M., BRIERCHECK, E., RONCHETTI, M., ROY, D. C., CALABRETTA, B., CALIGIURI, M. A. & PERROTTI, D. 2007. High levels of the BCR/ABL oncoprotein are required for the MAPK-hnRNP-E2-dependent suppression of C/EBP α -driven myeloid differentiation. *Blood*, 110, 994-1003.

- CHEN, Y., WANG, H., KANTARJIAN, H. & CORTES, J. 2013. Trends in chronic myeloid leukemia incidence and survival in the United States from 1975 to 2009. *Leukemia & Lymphoma*, 54, 1411-1417.
- CHENG, T., RODRIGUES, N., SHEN, H., YANG, Y.-G., DOMBKOWSKI, D., SYKES, M. & SCADDEN, D. T. 2000. Hematopoietic Stem Cell Quiescence Maintained by p21^{cip1}/waf1. *Science*, 287, 1804-1808.
- CHIANG, G. G. & ABRAHAM, R. T. 2005. Phosphorylation of Mammalian Target of Rapamycin (mTOR) at Ser-2448 Is Mediated by p70S6 Kinase. *Journal of Biological Chemistry*, 280, 25485-25490.
- CHOO, A. Y. & BLENIS, J. 2009. Not all substrates are treated equally: Implications for mTOR, rapamycin-resistance, and cancer therapy. *Cell Cycle*, 8, 567-572.
- CHOO, A. Y., YOON, S.-O., KIM, S. G., ROUX, P. P. & BLENIS, J. 2008. Rapamycin differentially inhibits S6Ks and 4E-BP1 to mediate cell-type-specific repression of mRNA translation. *Proceedings of the National Academy of Sciences of the United States of America*, 105, 17414-17419.
- CHRESTA, C. M., DAVIES, B. R., HICKSON, I., HARDING, T., COSULICH, S., CRITCHLOW, S. E., VINCENT, J. P., ELLSTON, R., JONES, D., SINI, P., JAMES, D., HOWARD, Z., DUDLEY, P., HUGHES, G., SMITH, L., MAGUIRE, S., HUMMERSON, M., MALAGU, K., MENEAR, K., JENKINS, R., JACOBSEN, M., SMITH, G. C. M., GUICHARD, S. & PASS, M. 2010. <http://www.w3.org/1999/xhtml> Is a Potent, Selective, and Orally Bioavailable ATP-Competitive Mammalian Target of Rapamycin Kinase Inhibitor with In vitro and In vivo Antitumor Activity. *Cancer Research*, 70, 288.
- CLARK, S. L. 1957. CELLULAR DIFFERENTIATION IN THE KIDNEYS OF NEWBORN MICE STUDIED WITH THE ELECTRON MICROSCOPE. *The Journal of Biophysical and Biochemical Cytology*, 3, 349-362.
- CLIFT, R. A., THOMAS, E. D., FEFER, A., SINGER, J., STEWART, P., DEEG, J., BUCKNER, C. D., DONEY, K., NEIMAN, P. E., SANDERS, J., SULLIVAN, K. M. & STORB, R. 1982. Originally published as Volume 2, Issue 8299 TREATMENT OF CHRONIC GRANULOCYTIC LEUKAEMIA IN CHRONIC PHASE BY ALLOGENEIC MARROW TRANSPLANTATION. *The Lancet*, 320, 621-623.
- COHEN, H. Y., LAVU, S., BITTERMAN, K. J., HEKKING, B., IMAHIYEROBO, T. A., MILLER, C., FRYE, R., PLOEGH, H., KESSLER, B. M. & SINCLAIR, D. A. 2004. Acetylation of the C Terminus of Ku70 by CBP and PCAF Controls Bax-Mediated Apoptosis. *Molecular Cell*, 13, 627-638.
- COLLINS, S., COLEMAN, H. & GROUDINE, M. 1987. Expression of bcr and bcr-abl fusion transcripts in normal and leukemic cells. *Molecular and Cellular Biology*, 7, 2870-2876.
- CONG, L., RAN, F. A., COX, D., LIN, S., BARRETTO, R., HABIB, N., HSU, P. D., WU, X., JIANG, W., MARRAFFINI, L. A. & ZHANG, F. 2013. Multiplex Genome Engineering Using CRISPR/Cas Systems. *Science (New York, N.Y.)*, 339, 819-823.
- COPLAND, M., HAMILTON, A., ELRICK, L. J., BAIRD, J. W., ALLAN, E. K., JORDANIDES, N., BAROW, M., MOUNTFORD, J. C. & HOLYOAKE, T. L. 2006a. Dasatinib (BMS-354825) targets an earlier progenitor population than imatinib in primary CML but does not eliminate the quiescent fraction. *Blood*, 107, 4532-4539.
- COPLAND, M., HAMILTON, A., ELRICK, L. J., BAIRD, J. W., ALLAN, E. K., JORDANIDES, N., BAROW, M., MOUNTFORD, J. C. & HOLYOAKE, T. L. 2006b. Dasatinib (BMS-354825) targets an earlier progenitor population than imatinib in primary CML but does not eliminate the quiescent fraction. *Blood*, 107, 4532.
- CORBIN, A. S., AGARWAL, A., LORIAUX, M., CORTES, J., DEININGER, M. W. & DRUKER, B. J. 2011. Human chronic myeloid leukemia stem cells are insensitive to imatinib despite inhibition of BCR-ABL activity. *The Journal of Clinical Investigation*, 121, 396-409.
- CORBIN, A. S., BUCHDUNGER, E., PASCAL, F. & DRUKER, B. J. 2002. Analysis of the Structural Basis of Specificity of Inhibition of the Abl Kinase by STI571. *Journal of Biological Chemistry*, 277, 32214-32219.
- CORBIN, A. S., ROSÉE, P. L., STOFFREGEN, E. P., DRUKER, B. J. & DEININGER, M. W. 2003. Several Bcr-Abl kinase domain mutants associated with imatinib mesylate resistance remain sensitive to imatinib. *Blood*, 101, 4611-4614.
- CORTES, J., KIM, D. W., RAFFOUX, E., MARTINELLI, G., RITCHIE, E., ROY, L., COUTRE, S., CORM, S., HAMERSCHLAK, N., TANG, J. L., HOCHHAUS, A., KHOURY, H. J., BRUMMENDORF, T. H., MICHALLET, M., REGE-CAMBRIN, G., GAMBACORTI-PASSERINI, C., RADICH, J. P., ERNST, T., ZHU, C., VAN TORNOUT, J. M. A. & TALPAZ, M. 2008. Efficacy and safety of dasatinib in imatinib-resistant or -intolerant patients with chronic myeloid leukemia in blast phase. *Leukemia*, 22, 2176-2183.
- CORTES, J., LIPTON, J. H., REA, D., DIGUMARTI, R., CHUAH, C., NANDA, N., BENICHOU, A.-C., CRAIG, A. R., MICHALLET, M., NICOLINI, F. E. & KANTARJIAN, H. 2012a. Phase 2 study of

- subcutaneous omacetaxine mepesuccinate after TKI failure in patients with chronic-phase CML with T315I mutation. *Blood*, 120, 2573-2580.
- CORTES, J. E., KANTARJIAN, H., SHAH, N. P., BIXBY, D., MAURO, M. J., FLINN, I., O'HARE, T., HU, S., NARASIMHAN, N. I., RIVERA, V. M., CLACKSON, T., TURNER, C. D., HALUSKA, F. G., DRUKER, B. J., DEININGER, M. W. N. & TALPAZ, M. 2012b. Ponatinib in Refractory Philadelphia Chromosome-Positive Leukemias. *New England Journal of Medicine*, 367, 2075-2088.
- CORTES, J. E., KIM, D. W., PINILLA-IBARZ, J., LE COUTRE, P., PAQUETTE, R., CHUAH, C., NICOLINI, F. E., APPERLEY, J. F., KHOURY, H. J., TALPAZ, M., DIPERSIO, J., DEANGELO, D. J., ABRUZZESE, E., REA, D., BACCARANI, M., MÜLLER, M. C., GAMBACORTI-PASSERINI, C., WONG, S., LUSTGARTEN, S., RIVERA, V. M., CLACKSON, T., TURNER, C. D., HALUSKA, F. G., GUILHOT, F., DEININGER, M. W., HOCHHAUS, A., HUGHES, T., GOLDMAN, J. M., SHAH, N. P. & KANTARJIAN, H. 2013. A Phase 2 Trial of Ponatinib in Philadelphia Chromosome-Positive Leukemias. *New England Journal of Medicine*, 369, 1783-1796.
- CORTES, J. E., SAGLIO, G., KANTARJIAN, H. M., BACCARANI, M., MAYER, J., BOQUÉ, C., SHAH, N. P., CHUAH, C., CASANOVA, L., BRADLEY-GARELIK, B., MANOS, G. & HOCHHAUS, A. 2016. Final 5-Year Study Results of DASISION: The Dasatinib Versus Imatinib Study in Treatment-Naïve Chronic Myeloid Leukemia Patients Trial. *Journal of Clinical Oncology*, 34, 2333-2340.
- CORTEZ, D., KADLEC, L. & PENDERGAST, A. M. 1995. Structural and signaling requirements for BCR-ABL-mediated transformation and inhibition of apoptosis. *Molecular and Cellular Biology*, 15, 5531-5541.
- COTTER, T. G. 1995. BCR-ABL: An Anti-Apoptosis Gene in Chronic Myelogenous Leukemia. *Leukemia & Lymphoma*, 18, 231-236.
- CUMANO, A. & GODIN, I. 2007. Ontogeny of the Hematopoietic System. *Annual Review of Immunology*, 25, 745-785.
- DAHIA, P. L. M., AGUIAR, R. C. T., ALBERTA, J., KUM, J. B., CARON, S., SILL, H., MARSH, D. J., RITZ, J., FREEDMAN, A., STILES, C. & ENG, C. 1999. PTEN Is Inversely Correlated With the Cell Survival Factor Akt/PKB and Is Inactivated Via Multiple Mechanisms in Haematological Malignancies. *Human Molecular Genetics*, 8, 185-193.
- DAI, Y., RAHMANI, M., COREY, S. J., DENT, P. & GRANT, S. 2004. A Bcr/Abl-independent, Lyn-dependent Form of Imatinib Mesylate (STI-571) Resistance Is Associated with Altered Expression of Bcl-2. *Journal of Biological Chemistry*, 279, 34227-34239.
- DALEY, G. Q. & BALTIMORE, D. 1988. Transformation of an interleukin 3-dependent hematopoietic cell line by the chronic myelogenous leukemia-specific P210bcr/abl protein. *Proceedings of the National Academy of Sciences of the United States of America*, 85, 9312-9316.
- DALEY, G. Q., VAN ETTEEN, R. A. & BALTIMORE, D. 1990. Induction of chronic myelogenous leukemia in mice by the P210bcr/abl gene of the Philadelphia chromosome. *Science*, 247, 824-830.
- DATTA, S. R., DUDEK, H., TAO, X., MASTERS, S., FU, H., GOTOH, Y. & GREENBERG, M. E. 1997. Akt Phosphorylation of BAD Couples Survival Signals to the Cell-Intrinsic Death Machinery. *Cell*, 91, 231-241.
- DAVID CORTEZ, G. R. A. A. M. P. 1997. The Bcr-Abl tyrosine kinase activates mitogenic signaling pathways and stimulates G1-to-S phase transition in hematopoietic cells. *Oncogene*, 15, 2333-2342.
- DE DUVE, C. & WATTIAUX, R. 1966. Functions of Lysosomes. *Annual Review of Physiology*, 28, 435-492.
- DE JONG, R., HAATAJA, L., VONCKEN, J. W., HEISTERKAMP, N. & GROFFEN, J. 1995. Tyrosine phosphorylation of murine Crkl. *Oncogene*, 11, 1469-1474.
- DEBERARDINIS, R. J., LUM, J. J., HATZIVASSILIOU, G. & THOMPSON, C. B. 2008. The Biology of Cancer: Metabolic Reprogramming Fuels Cell Growth and Proliferation. *Cell Metabolism*, 7, 11-20.
- DEGUCHI, Y., KIMURA, S., ASHIHARA, E., NIWA, T., HODOHARA, K., FUJIYAMA, Y. & MAEKAWA, T. 2008. Comparison of imatinib, dasatinib, nilotinib and INNO-406 in imatinib-resistant cell lines. *Leukemia Research*, 32, 980-983.
- DEININGER, M. W. N., GOLDMAN, J. M., LYDON, N. & MELO, J. V. 1997. The Tyrosine Kinase Inhibitor CGP57148B Selectively Inhibits the Growth of BCR-ABL-Positive Cells. *Blood*, 90, 3691-3698.
- DELTCHEVA, E., CHYLINSKI, K., SHARMA, C. M., GONZALES, K., CHAO, Y., PIRZADA, Z. A., ECKERT, M. R., VOGEL, J. & CHARPENTIER, E. 2011. CRISPR RNA maturation by trans-encoded small RNA and host factor RNase III. *Nature*, 471, 602-607.
- DI BARTOLOMEO, S., CORAZZARI, M., NAZIO, F., OLIVERIO, S., LISI, G., ANTONIOLI, M., PAGLIARINI, V., MATTEONI, S., FUOCO, C., GIUNTA, L., D'AMELIO, M., NARDACCI, R., ROMAGNOLI, A., PIACENTINI, M., CECCONI, F. & FIMIA, G. M. 2010. The dynamic interaction of AMBRA1 with the dynein motor complex regulates mammalian autophagy. *The Journal of Cell Biology*, 191, 155-168.

- DIEKMANN, D., BRILL, S., GARRETT, M. D., TOTTY, N., HSUAN, J., MONFRIES, C., HALL, C., LIM, L. & HALL, A. 1991. Bcr encodes a GTPase-activating protein for p21rac. *Nature*, 351, 400-402.
- DIVECHA, N. & IRVINE, R. F. 1995. Phospholipid signaling. *Cell*, 80, 269-278.
- DOI, T., HAMAGUCHI, T., SHIRAO, K., CHIN, K., HATAKE, K., NOGUCHI, K., OTSUKI, T., MEHTA, A. & OHTSU, A. 2013. Evaluation of safety, pharmacokinetics, and efficacy of vorinostat, a histone deacetylase inhibitor, in the treatment of gastrointestinal (GI) cancer in a phase I clinical trial. *International Journal of Clinical Oncology*, 18, 87-95.
- DONATO, N. J., WU, J. Y., STAPLEY, J., GALLICK, G., LIN, H., ARLINGHAUS, R. & TALPAZ, M. 2003. BCR-ABL independence and LYN kinase overexpression in chronic myelogenous leukemia cells selected for resistance to STI571. *Blood*, 101, 690.
- DOS, D. S., ALI, S. M., KIM, D.-H., GUERTIN, D. A., LATEK, R. R., ERDJUMENT-BROMAGE, H., TEMPST, P. & SABATINI, D. M. 2004. Rictor, a Novel Binding Partner of mTOR, Defines a Rapamycin-Insensitive and Raptor-Independent Pathway that Regulates the Cytoskeleton. *Current Biology*, 14, 1296-1302.
- DRUKER, B. J., GUILHOT, F., O'BRIEN, S. G., GATHMANN, I., KANTARJIAN, H., GATTERMANN, N., DEININGER, M. W. N., SILVER, R. T., GOLDMAN, J. M., STONE, R. M., CERVANTES, F., HOCHHAUS, A., POWELL, B. L., GABRILOVE, J. L., ROUSSELOT, P., REIFFERS, J., CORNELISSEN, J. J., HUGHES, T., AGIS, H., FISCHER, T., VERHOEF, G., SHEPHERD, J., SAGLIO, G., GRATWOHL, A., NIELSEN, J. L., RADICH, J. P., SIMONSSON, B., TAYLOR, K., BACCARANI, M., SO, C., LETVAK, L. & LARSON, R. A. 2006. Five-Year Follow-up of Patients Receiving Imatinib for Chronic Myeloid Leukemia. *New England Journal of Medicine*, 355, 2408-2417.
- DRUKER, B. J., SAWYERS, C. L., KANTARJIAN, H., RESTA, D. J., REESE, S. F., FORD, J. M., CAPDEVILLE, R. & TALPAZ, M. 2001a. Activity of a Specific Inhibitor of the BCR-ABL Tyrosine Kinase in the Blast Crisis of Chronic Myeloid Leukemia and Acute Lymphoblastic Leukemia with the Philadelphia Chromosome. *New England Journal of Medicine*, 344, 1038-1042.
- DRUKER, B. J., TALPAZ, M., RESTA, D. J., PENG, B., BUCHDUNGER, E., FORD, J. M., LYDON, N. B., KANTARJIAN, H., CAPDEVILLE, R., OHNO-JONES, S. & SAWYERS, C. L. 2001b. Efficacy and Safety of a Specific Inhibitor of the BCR-ABL Tyrosine Kinase in Chronic Myeloid Leukemia. *New England Journal of Medicine*, 344, 1031-1037.
- DRUKER, B. J., TAMURA, S., BUCHDUNGER, E., OHNO, S., SEGAL, G. M., FANNING, S., ZIMMERMANN, J. & LYDON, N. B. 1996. Effects of a selective inhibitor of the Abl tyrosine kinase on the growth of Bcr-Abl positive cells. *Nat Med*, 2, 561-566.
- EECHOUTE, K., SPARREBOOM, A., BURGER, H., FRANKE, R. M., SCHIAVON, G., VERWEIJ, J., LOOS, W. J., WIEMER, E. A. C. & MATHIJSSSEN, R. H. J. 2011. Drug Transporters and Imatinib Treatment: Implications for Clinical Practice. *Clinical Cancer Research*, 17, 406.
- EFFICACE, F., BACCARANI, M., BRECCIA, M., ALIMENA, G., ROSTI, G., COTTONE, F., DELILIERI, G. L., BARATÈ, C., ROSSI, A. R., FIORITONI, G., LUCIANO, L., TURRI, D., MARTINO, B., DI RAIMONDO, F., DABUSTI, M., BERGAMASCHI, M., LEONI, P., SIMULA, M. P., LEVATO, L., ULISCIANI, S., VENERI, D., SICA, S., RAMBALDI, A., VIGNETTI, M. & MANDELLI, F. 2011. Health-related quality of life in chronic myeloid leukemia patients receiving long-term therapy with imatinib compared with the general population. *Blood*, 118, 4554-4560.
- EGAN, D. & RADICH, J. 2015. Prognosis and Molecular Monitoring in Chronic Myeloid Leukemia. *Clinical Lymphoma Myeloma and Leukemia*, 15, Supplement, S109-S113.
- EIDE, C. A., ZABRISKIE, M. S., ADRIAN, L. T., LANGE, T., DEININGER, M. W., DRUKER, B. J. & HARE, T. 2015. Resistance Profiling of BCR-ABL Compound Mutations Linked to Tyrosine Kinase Inhibitor Therapy Failure in Chronic Myeloid Leukemia. *Blood*, 118, 1416.
- EIRING, A. M., PAGE, B. D. G., KRAFT, I. L., MASON, C. C., VELLORE, N. A., RESETCA, D., ZABRISKIE, M. S., ZHANG, T. Y., KHORASHAD, J. S., ENGAR, A. J., REYNOLDS, K. R., ANDERSON, D. J., SENINA, A., POMICTER, A. D., ARPIN, C. C., AHMAD, S., HEATON, W. L., TANTRAVAHU, S. K., TODIC, A., MORIGGL, R., WILSON, D. J., BARON, R., O'HARE, T., GUNNING, P. T. & DEININGER, M. W. 2015. Combined STAT3 and BCR-ABL1 Inhibition Induces Synthetic Lethality in Therapy-Resistant Chronic Myeloid Leukemia. *Leukemia*, 29, 586-597.
- ELEFANTY, A. G., HARIHARAN, I. K. & CORY, S. 1990. bcr-abl, the hallmark of chronic myeloid leukaemia in man, induces multiple haemopoietic neoplasms in mice. *The EMBO Journal*, 9, 1069-1078.
- ESPOSITO, N., COLAVITA, I., QUINTARELLI, C., SICA, A. R., PELUSO, A. L., LUCIANO, L., PICARDI, M., DEL VECCHIO, L., BUONOMO, T., HUGHES, T. P., WHITE, D., RADICH, J. P., RUSSO, D., BRANFORD, S., SAGLIO, G., MELO, J. V., MARTINELLI, R., RUOPPOLO, M., KALEBIC, T., MARTINELLI, G. & PANE, F. 2011a. SHP-1 expression accounts for resistance to imatinib treatment in Philadelphia chromosome-positive cells derived from patients with chronic myeloid leukemia. *Blood*, 118, 3634.

- ESPOSITO, N., COLAVITA, I., QUINTARELLI, C., SICA, A. R., PELUSO, A. L., LUCIANO, L., PICARDI, M., DEL VECCHIO, L., BUONOMO, T., HUGHES, T. P., WHITE, D., RADICH, J. P., RUSSO, D., BRANFORD, S., SAGLIO, G., MELO, J. V., MARTINELLI, R., RUOPPOLO, M., KALEBIC, T., MARTINELLI, G. & PANE, F. 2011b. SHP-1 expression accounts for resistance to imatinib treatment in Philadelphia chromosome-positive cells derived from patients with chronic myeloid leukemia. *Blood*, 118, 3634-3644.
- FADERL, S., TALPAZ, M., ESTROV, Z. & KANTARJIAN, H. M. 1999a. Chronic Myelogenous Leukemia: Biology and Therapy. *Annals of Internal Medicine*, 131, 207-219.
- FADERL, S., TALPAZ, M., ESTROV, Z., O'BRIEN, S., KURZROCK, R. & KANTARJIAN, H. M. 1999b. The Biology of Chronic Myeloid Leukemia. *New England Journal of Medicine*, 341, 164-172.
- FEFER, A., CHEEVER, M. A., THOMAS, E. D., BOYD, C., RAMBERG, R., GLUCKSBERG, H., BUCKNER, C. D. & STORB, R. 1979. Disappearance of pH1-Positive Cells in Four Patients with Chronic Granulocytic Leukemia after Chemotherapy, Irradiation and Marrow Transplantation from an Identical Twin. *New England Journal of Medicine*, 300, 333-337.
- FELLER, S. M., REN, R., HANAFUSA, H. & BALTIMORE, D. SH2 and SH3 domains as molecular adhesives: the interactions of Crk and Abl. *Trends in Biochemical Sciences*, 19, 453-458.
- FIALKOW, P. J. Chronic Myelocytic Leukemia: ORIGIN OF SOME LYMPHOCYTES FROM LEUKEMIC STEM CELLS. *The Journal of Clinical Investigation*, 62, 815-823.
- FIALKOW, P. J., GARTLER, S. M. & YOSHIDA, A. 1967. Clonal origin of chronic myelocytic leukemia in man. *Proceedings of the National Academy of Sciences of the United States of America*, 58, 1468-1471.
- FISKUS, W., PRANPAT, M., BALI, P., BALASIS, M., KUMARASWAMY, S., BOYAPALLE, S., ROCHA, K., WU, J., GILES, F., MANLEY, P. W., ATADJA, P. & BHALLA, K. 2006. Combined effects of novel tyrosine kinase inhibitor AMN107 and histone deacetylase inhibitor LBH589 against Bcr-Abl-expressing human leukemia cells. *Blood*, 108, 645-652.
- FLEMING, H. E., JANZEN, V., LO CELSO, C., GUO, J., LEAHY, K. M., KRONENBERG, H. M. & SCADDEN, D. T. 2008. Wnt Signaling in the Niche Enforces Hematopoietic Stem Cell Quiescence and Is Necessary to Preserve Self-Renewal In Vivo. *Cell Stem Cell*, 2, 274-283.
- FRIAS, M. A., THOREEN, C. C., JAFFE, J. D., SCHRODER, W., SCULLEY, T., CARR, S. A. & SABATINI, D. M. 2006. mSin1 Is Necessary for Akt/PKB Phosphorylation, and Its Isoforms Define Three Distinct mTORC2s. *Current Biology*, 16, 1865-1870.
- FRIT, P., BERGMANN, E. & EGLY, J.-M. 1999. Transcription factor IIIH: A key player in the cellular response to DNA damage. *Biochimie*, 81, 27-38.
- FRUMAN, D. A., MEYERS, R. E. & CANTLEY, L. C. 1998. PHOSPHOINOSITIDE KINASES. *Annual Review of Biochemistry*, 67, 481-507.
- GAIGER, A., HENN, T., HORTH, E., GEISSLER, K., MITTERBAUER, G., MAIER-DOBERSBERGER, T., GREINIX, H., MANNHALTER, C., HAAS, O. A. & LECHNER, K. 1995. Increase of bcr-abl chimeric mRNA expression in tumor cells of patients with chronic myeloid leukemia precedes disease progression. *Blood*, 86, 2371.
- GALIMBERTI, S., CERVETTI, G., GUERRINI, F., TESTI, R., PACINI, S., FAZZI, R., SIMI, P. & PETRINI, M. 2005. Quantitative molecular monitoring of BCR-ABL and MDR1 transcripts in patients with chronic myeloid leukemia during Imatinib treatment. *Cancer Genetics and Cytogenetics*, 162, 57-62.
- GALLARDO, A., LERMA, E., ESCUIN, D., TIBAU, A., MUÑOZ, J., OJEDA, B., BARNADAS, A., ADROVER, E., SÁNCHEZ-TEJADA, L., GINER, D., ORTIZ-MARTÍNEZ, F. & PEIRÓ, G. 2012. Increased signalling of EGFR and IGF1R, and deregulation of PTEN/PI3K/Akt pathway are related with trastuzumab resistance in HER2 breast carcinomas. *British Journal of Cancer*, 106, 1367-1373.
- GALLOWAY, J. L. & ZON, L. I. 2003. Ontogeny of hematopoiesis: Examining the emergence of hematopoietic cells in the vertebrate embryo. *Current Topics in Developmental Biology*. Academic Press.
- GALTON, D. A. G. 1953. Originally published as Volume 1, Issue 6753MYLERAN IN CHRONIC MYELOID LEUKÆMIA RESULTS OF TREATMENT. *The Lancet*, 261, 208-213.
- GALTON, D. A. G. 1959. TREATMENT OF THE CHRONIC LEUKAEMIAS. *British Medical Bulletin*, 15, 78-85.
- GAMBACORTI-PASSERINI, C., LE COUTRE, P., MOLOGNI, L., FANELLI, M., BERTAZZOLI, C., MARCHESI, E., DI NICOLA, M., BIONDI, A., CORNEO, G. M., BELOTTI, D., POGLIANI, E. & LYDON, N. B. 1997. Inhibition of the ABL Kinase Activity Blocks the Proliferation of BCR/ABL+Leukemic Cells and Induces Apoptosis. *Blood Cells, Molecules, and Diseases*, 23, 380-394.
- GESBERT, F. & GRIFFIN, J. D. 2000. Bcr/Abl activates transcription of the Bcl-X gene through STAT5. *Blood*, 96, 2269-2276.
- GIANNOUDIS, A., WANG, L., JORGENSEN, A. L., XINARIANOS, G., DAVIES, A., PUSHPAKOM, S., LILOGLOU, T., ZHANG, J.-E., AUSTIN, G., HOLYOAKE, T. L., FORONI, L., KOTTARIDIS, P. D., MÜLLER, M. C., PIRMOHAMED, M. & CLARK, R. E. 2013. The hOCT1 SNPs M420del and

- M408V alter imatinib uptake and M420del modifies clinical outcome in imatinib-treated chronic myeloid leukemia. *Blood*, 121, 628.
- GIOTOPOULOS, G., VAN DER WEYDEN, L., OSAKI, H., RUST, A. G., GALLIPOLI, P., MEDURI, E., HORTON, S. J., CHAN, W.-I., FOSTER, D., PRINJHA, R. K., PIMANDA, J. E., TENEN, D. G., VASSILIOU, G. S., KOSCHMIEDER, S., ADAMS, D. J. & HUNTLY, B. J. P. 2015. A novel mouse model identifies cooperating mutations and therapeutic targets critical for chronic myeloid leukemia progression. *The Journal of Experimental Medicine*, 212, 1551-1569.
- GOETZ, A. W., VAN DER KUIP, H., MAYA, R., OREN, M. & AULITZKY, W. E. 2001. Requirement for Mdm2 in the Survival Effects of Bcr-Abl and Interleukin 3 in Hematopoietic Cells. *Cancer Research*, 61, 7635-7641.
- GOGA, A., MCLAUGHLIN, J., AFAR, D. E. H., SAFFRAN, D. C. & WITTE, O. N. Alternative signals to RAS for hematopoietic transformation by the BCR-ABL oncogene. *Cell*, 82, 981-988.
- GOLAS, J. M., ARNDT, K., ETIENNE, C., LUCAS, J., NARDIN, D., GIBBONS, J., FROST, P., YE, F., BOSCHELLI, D. H. & BOSCHELLI, F. 2003. SKI-606, a 4-Anilino-3-quinolinecarbonitrile Dual Inhibitor of Src and Abl Kinases, Is a Potent Antiproliferative Agent against Chronic Myelogenous Leukemia Cells in Culture and Causes Regression of K562 Xenografts in Nude Mice. *Cancer Research*, 63, 375-381.
- GOLDMAN, J. 1998. Hematopoietic stem cell transplantation. *Current Opinion in Hematology*, 5, 417-418.
- GOLDMAN, J. M., MCCARTHY, D. M., HOWS, J. M., CATOVSKY, D., GOOLDEN, A. W. G., BAUGHAN, A. S. J., WORSLEY, A. M., GORDON-SMITH, E. C., BATCHELOR, J. R. & GALTON, D. A. G. 1982. Originally published as Volume 2, Issue 8299Marrow TRANSPLANTATION FOR PATIENTS IN THE CHRONIC PHASE OF CHRONIC GRANULOCYTIC LEUKAEMIA. *The Lancet*, 320, 623-625.
- GONZALEZ, B., SCHWIMMER, L. J., FULLER, R. P., YE, Y., ASAWAPORNMONGKOL, L. & BARBAS, C. F. 2010. Modular system for the construction of zinc-finger libraries and proteins. *Nat. Protocols*, 5, 791-810.
- GOODMAN, L. S., WINTROBE, M. M., DAMESHEK, W., GOODMAN, M. J., GILMAN, A. & MCLENNAN, M. T. 1984. Nitrogen mustard therapy: Use of methyl-bis(beta-chloroethyl)amine hydrochloride and tris(beta-chloroethyl)amine hydrochloride for hodgkin's disease, lymphosarcoma, leukemia and certain allied and miscellaneous disorders. *JAMA*, 251, 2255-2261.
- GORDON, M. Y., DOWDING, C. R., RILEY, G. P., GOLDMAN, J. M. & GREAVES, M. F. 1987. Altered adhesive interactions with marrow stroma of haematopoietic progenitor cells in chronic myeloid leukaemia. *Nature*, 328, 342-344.
- GORRE, M. E., ELLWOOD-YEN, K., CHIOSIS, G., ROSEN, N. & SAWYERS, C. L. 2002. BCR-ABL point mutants isolated from patients with imatinib mesylate-resistant chronic myeloid leukemia remain sensitive to inhibitors of the BCR-ABL chaperone heat shock protein 90. *Blood*, 100, 3041-3044.
- GORRE, M. E., MOHAMMED, M., ELLWOOD, K., HSU, N., PAQUETTE, R., RAO, P. N. & SAWYERS, C. L. 2001. Clinical Resistance to STI-571 Cancer Therapy Caused by BCR-ABL Gene Mutation or Amplification. *Science*, 293, 876-880.
- GRAHAM, S. M., JØRGENSEN, H. G., ALLAN, E., PEARSON, C., ALCORN, M. J., RICHMOND, L. & HOLYOAKE, T. L. 2002. Primitive, quiescent, Philadelphia-positive stem cells from patients with chronic myeloid leukemia are insensitive to STI571 in vitro. *Blood*, 99, 319.
- GRATWOHL, A., HERMANS, J., GOLDMAN, J. M., ARCESE, W., CARRERAS, E., DEVERGIE, A., FRASSONI, F., GAHRTON, G., KOLB, H. J., NIEDERWIESER, D., RUUTU, T., VERNANT, J. P., DE WITTE, T. & APPERLEY, J. 1998. Risk assessment for patients with chronic myeloid leukaemia before allogeneic blood or marrow transplantation. *The Lancet*, 352, 1087-1092.
- GRITSMAN, K., KAUR, I. & SINCLAIR, T. 2015. The Class IA PI3 Kinase Isoforms Have Distinct but Overlapping Roles in Adult Hematopoiesis. *Blood*, 126, 3587-3587.
- GROFFEN, J., STEPHENSON, J. R., HEISTERKAMP, N., DE KLEIN, A., BARTRAM, C. R. & GROSVELD, G. 1984. Philadelphia chromosomal breakpoints are clustered within a limited region, bcr, on chromosome 22. *Cell*, 36, 93-99.
- GROSSO, S., PUISSANT, A., DUFIES, M., COLOSETTI, P., JACQUEL, A., LEBRIGAND, K., BARBRY, P., DECKERT, M., CASSUTO, J. P., MARI, B. & AUBERGER, P. 2009. Gene expression profiling of imatinib and PD166326-resistant CML cell lines identifies Fyn as a gene associated with resistance to BCR-ABL inhibitors. *Molecular Cancer Therapeutics*, 8, 1924.
- GRUMBACH, I. M., MAYER, I. A., UDDIN, S., LEKMINE, F., MAJCHRZAK, B., YAMAUCHI, H., FUJITA, S., DRUKER, B. J., FISH, E. N. & PLATANIAS, L. C. 2001. Engagement of the CrkL adaptor in interferon α signalling in BCR-ABL-expressing cells. *British Journal of Haematology*, 112, 327-336.
- GRUNDSCHOBBER, E., HOELBL-KOVACIC, A., BHAGWAT, N., KOVACIC, B., SCHEICHER, R., ECKELHART, E., KOLLMANN, K., KELLER, M., GREBIEN, F., WAGNER, K. U., LEVINE, R. L. & SEXL, V. 2014. Acceleration of Bcr-Abl+ leukemia induced by deletion of JAK2. *Leukemia*, 28, 1918-1922.

- GUERTIN, D. A. & SABATINI, D. M. 2007. Defining the Role of mTOR in Cancer. *Cancer Cell*, 12, 9-22.
- HADDOW, A. & TIMMIS, G. M. 1953. Originally published as Volume 1, Issue 6753MYLERAN IN CHRONIC MYELOID LEUKÆMIA CHEMICAL CONSTITUTION AND BIOLOGICAL ACTION. *The Lancet*, 261, 207-208.
- HAFT, D. H., SELENGUT, J., MONGODIN, E. F. & NELSON, K. E. 2005. A Guild of 45 CRISPR-Associated (Cas) Protein Families and Multiple CRISPR/Cas Subtypes Exist in Prokaryotic Genomes. *PLoS Computational Biology*, 1, e60.
- HAMILTON, A., HELGASON, G. V., SCHEMIONEK, M., ZHANG, B., MYSSINA, S., ALLAN, E. K., NICOLINI, F. E., MÜLLER-TIDOW, C., BHATIA, R., BRUNTON, V. G., KOSCHMIEDER, S. & HOLYOAKE, T. L. 2012. Chronic myeloid leukemia stem cells are not dependent on Bcr-Abl kinase activity for their survival. *Blood*, 119, 1501.
- HAN, M.-K., SONG, E.-K., GUO, Y., OU, X., MANTEL, C. & BROXMEYER, H. E. 2008. SIRT1 regulates apoptosis and Nanog expression in mouse embryonic stem cells by controlling p53 subcellular localization. *Cell stem cell*, 2, 241.
- HANNON, G. J. 2002. RNA interference. *Nature*, 418, 244-251.
- HARDINGER, K. L., KOCH, M. J. & BRENNAN, D. C. 2004. Current and Future Immunosuppressive Strategies in Renal Transplantation. *Pharmacotherapy: The Journal of Human Pharmacology and Drug Therapy*, 24, 1159-1176.
- HARRISON, S. J., JOHNSON, P. R. E. & HOLYOAKE, T. L. 2004. The Scotland Leukaemia Registry Audit of Incidence, Diagnosis and Clinical Management of New Patients with Chronic Myeloid Leukaemia in 1999 and 2000. *Scottish Medical Journal*, 49, 87-90.
- HATZIIEREMIA, S., JORDANIDES, N. E., HOLYOAKE, T. L., MOUNTFORD, J. C. & JØRGENSEN, H. G. 2009. Inhibition of MDR1 does not sensitize primitive chronic myeloid leukemia CD34+ cells to imatinib. *Experimental Hematology*, 37, 692-700.
- HE, C. & KLIONSKY, D. J. 2009. Regulation Mechanisms and Signaling Pathways of Autophagy. *Annual Review of Genetics*, 43, 67-93.
- HEINRICH, M. C., GRIFFITH, D. J., DRUKER, B. J., WAIT, C. L., OTT, K. A. & ZIGLER, A. J. 2000. Inhibition of c-kit receptor tyrosine kinase activity by STI 571, a selective tyrosine kinase inhibitor. *Blood*, 96, 925-932.
- HEISTERKAMP, N., JENSTER, G., TEN HOEVE, J., ZOVICH, D., PATTENGAL, P. K. & GROFFEN, J. 1990. Acute leukaemia in bcr/abl transgenic mice. *Nature*, 344, 251-253.
- HELGASON, G. V., HOLYOAKE, T. L. & RYAN, K. M. 2013. Role of autophagy in cancer prevention, development and therapy. *Essays In Biochemistry*, 55, 133.
- HENTSCHEL, J., RUBIO, I., EBERHART, M., HIPLER, C., SCHIEFNER, J., SCHUBERT, K., LONCAREVIC, I. F., WITTIG, U., BANIAHMAD, A., VON EGGELING, F. 2011. BCR-ABL- and Ras-independent activation of Raf as a novel mechanism of Imatinib resistance in CML. *International Journal of Oncology*, 39, 585-591.
- HERSHEY, J. W. B. & MIYAMOTO, S. 2000. *20 Translational Control and Cancer*.
- HOCHHAUS, A., BACCARANI, M., DEININGER, M., APPERLEY, J. F., LIPTON, J. H., GOLDBERG, S. L., CORM, S., SHAH, N. P., CERVANTES, F., SILVER, R. T., NIEDERWIESER, D., STONE, R. M., DOMBRET, H., LARSON, R. A., ROY, L., HUGHES, T., MULLER, M. C., EZZEDDINE, R., COUNTOURIOTIS, A. M. & KANTARJIAN, H. M. 2008. Dasatinib induces durable cytogenetic responses in patients with chronic myelogenous leukemia in chronic phase with resistance or intolerance to imatinib. *Leukemia*, 22, 1200-1206.
- HOCHHAUS, A., O'BRIEN, S. G., GUILHOT, F., DRUKER, B. J., BRANFORD, S., FORONI, L., GOLDMAN, J. M., MULLER, M. C., RADICH, J. P., RUDOLTZ, M., MONE, M., GATHMANN, I., HUGHES, T. P. & LARSON, R. A. 2009. Six-year follow-up of patients receiving imatinib for the first-line treatment of chronic myeloid leukemia. *Leukemia*, 23, 1054-1061.
- HOCHHAUS, A., ROSTI, G., CROSS, N. C. P., STEEGMANN, J. L., LE COUTRE, P., OSSENKOPPELE, G., PETROV, L., MASSZI, T., HELLMANN, A., GRISKEVICIUS, L., WIKTOR-JEDRZEJCZAK, W., REA, D., CORIU, D., BRÜMMENDORF, T. H., PORKKA, K., SAGLIO, G., GASTL, G., MÜLLER, M. C., SCHULD, P., DI MATTEO, P., PELLEGRINO, A., DEZZANI, L., MAHON, F. X., BACCARANI, M. & GILES, F. J. 2016. Frontline nilotinib in patients with chronic myeloid leukemia in chronic phase: results from the European ENEST1st study. *Leukemia*, 30, 57-64.
- HOFFMAN, W. J. & CRAVER, L. F. 1931. Chronic myelogenous leukemia: Value of irradiation and its effect on the duration of life. *Journal of the American Medical Association*, 97, 836-840.
- HOFFMANN, V. S., BACCARANI, M., HASFORD, J., LINDOERFER, D., BURGSTALLER, S., SERTIC, D., COSTEAS, P., MAYER, J., INDRAK, K., EVERAUS, H., KOSKENVESA, P., GUILHOT, J., SCHUBERT-FRITSCHLE, G., CASTAGNETTI, F., DI RAIMONDO, F., LEJNIECE, S., GRISKEVICIUS, L., THIELEN, N., SACHA, T., HELLMANN, A., TURKINA, A. G., ZARITSKEY, A., BOGDANOVIC, A., SNINSKA, Z., ZUPAN, I., STEEGMANN, J. L., SIMONSSON, B., CLARK, R. E., COVELLI, A., GUIDI, G. & HELLMANN, R. 2015. The

- EUTOS population-based registry: incidence and clinical characteristics of 2904 CML patients in 20 European Countries. *Leukemia*, 29, 1336-1343.
- HOLYOAKE, T. L. & HELGASON, G. V. 2015. Do we need more drugs for chronic myeloid leukemia? *Immunological Reviews*, 263, 106-123.
- HOSOKAWA, N., HARA, T., KAIZUKA, T., KISHI, C., TAKAMURA, A., MIURA, Y., IEMURA, S.-I., NATSUME, T., TAKEHANA, K., YAMADA, N., GUAN, J.-L., OSHIRO, N. & MIZUSHIMA, N. 2009. Nutrient-dependent mTORC1 Association with the ULK1–Atg13–FIP200 Complex Required for Autophagy. *Molecular Biology of the Cell*, 20, 1981-1991.
- HSU, P. D., SCOTT, D. A., WEINSTEIN, J. A., RAN, F. A., KONERMANN, S., AGARWALA, V., LI, Y., FINE, E. J., WU, X., SHALEM, O., CRADICK, T. J., MARRAFFINI, L. A., BAO, G. & ZHANG, F. 2013. DNA targeting specificity of RNA-guided Cas9 nucleases. *Nat Biotech*, 31, 827-832.
- HUANG, J. & KLIONSKY, D. J. 2007. Autophagy and Human Disease. *Cell Cycle*, 6, 1837-1849.
- HUGHES, T., DEININGER, M., HOCHHAUS, A., BRANFORD, S., RADICH, J., KAEDA, J., BACCARANI, M., CORTES, J., CROSS, N. C. P., DRUKER, B. J., GABERT, J., GRIMWADE, D., HEHLMANN, R., KAMEL-REID, S., LIPTON, J. H., LONGTINE, J., MARTINELLI, G., SAGLIO, G., SOVERINI, S., STOCK, W. & GOLDMAN, J. M. 2006. Monitoring CML patients responding to treatment with tyrosine kinase inhibitors: review and recommendations for harmonizing current methodology for detecting BCR-ABL transcripts and kinase domain mutations and for expressing results. *Blood*, 108, 28-37.
- ICHIMURA, Y., KIRISAKO, T., TAKAO, T., SATOMI, Y., SHIMONISHI, Y., ISHIHARA, N., MIZUSHIMA, N., TANIDA, I., KOMINAMI, E., OHSUMI, M., NODA, T. & OHSUMI, Y. 2000. A ubiquitin-like system mediates protein lipidation. *Nature*, 408, 488-492.
- ISHIKAWA, F., YASUKAWA, M., LYONS, B., YOSHIDA, S., MIYAMOTO, T., YOSHIMOTO, G., WATANABE, T., AKASHI, K., SHULTZ, L. D. & HARADA, M. 2005. <div xmlns="http://www.w3.org/1999/xhtml">Development of functional human blood and immune systems in NOD/SCID/IL2 receptor γ chain^{null} mice</div>. *Blood*, 106, 1565-1573.
- ISHINO, Y., SHINAGAWA, H., MAKINO, K., AMEMURA, M. & NAKATA, A. 1987. Nucleotide sequence of the iap gene, responsible for alkaline phosphatase isozyme conversion in Escherichia coli, and identification of the gene product. *Journal of Bacteriology*, 169, 5429-5433.
- ITAKURA, E., KISHI, C., INOUE, K. & MIZUSHIMA, N. 2008. Beclin 1 Forms Two Distinct Phosphatidylinositol 3-Kinase Complexes with Mammalian Atg14 and UVRAG. *Molecular Biology of the Cell*, 19, 5360-5372.
- ITAKURA, E. & MIZUSHIMA, N. 2010. Characterization of autophagosome formation site by a hierarchical analysis of mammalian Atg proteins. *Autophagy*, 6, 764-776.
- IYER, S. P. & FOSS, F. F. 2015. Romidepsin for the Treatment of Peripheral T-Cell Lymphoma. *The Oncologist*, 20, 1084-1091.
- JABBOUR, E., CORTES, J. & KANTARJIAN, H. 2009a. Nilotinib for the treatment of chronic myeloid leukemia: An evidence-based review. *Core evidence*, 4, 207-213.
- JABBOUR, E., KANTARJIAN, H., JONES, D., TALPAZ, M., BEKELE, N., O'BRIEN, S., ZHOU, X., LUTHRA, R., GARCIA-MANERO, G., GILES, F., RIOS, M. B., VERSTOVSEK, S. & CORTES, J. 2006. Frequency and clinical significance of BCR-ABL mutations in patients with chronic myeloid leukemia treated with imatinib mesylate. *Leukemia*, 20, 1767-1773.
- JABBOUR, E., KANTARJIAN, H. M., JONES, D., SHAN, J., BRIEN, S., REDDY, N., WIERDA, W. G., FADERL, S., GARCIA-MANERO, G., VERSTOVSEK, S., RIOS, M. B. & CORTES, J. 2009b. Imatinib mesylate dose escalation is associated with durable responses in patients with chronic myeloid leukemia after cytogenetic failure on standard-dose imatinib therapy. *Blood*, 113, 2154.
- JACOB, B., OSATO, M., YAMASHITA, N., WANG, C. Q., TANIUCHI, I., LITTMAN, D. R., ASOU, N. & ITO, Y. 2010. Stem cell exhaustion due to Runx1 deficiency is prevented by Evi5 activation in leukemogenesis. *Blood*, 115, 1610-1620.
- JACOBSON, L. O., SPURR, C. L., BARRON, E., SMITH, T., LUSHBAUGH, C. & DICK, G. F. 1946. Nitrogen mustard therapy: Studies on the effect of methyl-bis (beta-chloroethyl) amine hydrochloride on neoplastic diseases and allied disorders of the hemopoietic system. *Journal of the American Medical Association*, 132, 263-271.
- JANSEN, R., EMBDEN, J. D. A. V., GAASTRA, W. & SCHOOLS, L. M. 2002. Identification of genes that are associated with DNA repeats in prokaryotes. *Molecular Microbiology*, 43, 1565-1575.
- JELINEK, J., GHARIBYAN, V., ESTECIO, M. R. H., KONDO, K., HE, R., CHUNG, W., LU, Y., ZHANG, N., LIANG, S., KANTARJIAN, H. M., CORTES, J. E. & ISSA, J.-P. J. 2011. Aberrant DNA Methylation Is Associated with Disease Progression, Resistance to Imatinib and Shortened Survival in Chronic Myelogenous Leukemia. *PLoS ONE*, 6, e22110.
- JENNINGS, B. A. & MILLS, K. I. 1998. c-myc locus amplification and the acquisition of trisomy 8 in the evolution of chronic myeloid leukaemia. *Leukemia Research*, 22, 899-903.
- JENUWEIN, T. & ALLIS, C. D. 2001. Translating the Histone Code. *Science*, 293, 1074-1080.

- JIANG, X., LOPEZ, A., HOLYOAKE, T., EAVES, A. & EAVES, C. 1999. Autocrine production and action of IL-3 and granulocyte colony-stimulating factor in chronic myeloid leukemia. *Proceedings of the National Academy of Sciences of the United States of America*, 96, 12804-12809.
- JIANG, X., SAW, K. M., EAVES, A. & EAVES, C. 2007. Instability of BCR-ABL Gene in Primary and Cultured Chronic Myeloid Leukemia Stem Cells. *Journal of the National Cancer Institute*, 99, 680-693.
- JIANG, Y., ZHAO, R. C. H. & VERFAILLIE, C. M. 2000. Abnormal integrin-mediated regulation of chronic myelogenous leukemia CD34(+) cell proliferation: BCR/ABL up-regulates the cyclin-dependent kinase inhibitor, p27(Kip), which is relocated to the cell cytoplasm and incapable of regulating cdk2 activity. *Proceedings of the National Academy of Sciences of the United States of America*, 97, 10538-10543.
- JINEK, M., CHYLINSKI, K., FONFARA, I., HAUER, M., DOUDNA, J. A. & CHARPENTIER, E. 2012. A Programmable Dual-RNA-Guided DNA Endonuclease in Adaptive Bacterial Immunity. *Science*, 337, 816-821.
- JINEK, M., EAST, A., CHENG, A., LIN, S., MA, E. & DOUDNA, J. 2013. RNA-programmed genome editing in human cells. *eLife*, 2, e00471.
- JOHANSSON, B., FIORETOS, T. & MITELMAN, F. 2002. Cytogenetic and Molecular Genetic Evolution of Chronic Myeloid Leukemia. *Acta Haematologica*, 107, 76-94.
- JONES, D., LUTHRA, R., CORTES, J., THOMAS, D., O'BRIEN, S., BUESO-RAMOS, C., HAI, S., RAVANDI, F., DE LIMA, M., KANTARJIAN, H. & JORGENSEN, J. L. 2008. BCR-ABL fusion transcript types and levels and their interaction with secondary genetic changes in determining the phenotype of Philadelphia chromosome-positive leukemias. *Blood*, 112, 5190-5192.
- JØRGENSEN, H. G., ALLAN, E. K., JORDANIDES, N. E., MOUNTFORD, J. C. & HOLYOAKE, T. L. 2007a. <http://www.w3.org/1999/xhtml> exerts equipotent antiproliferative effects to imatinib and does not induce apoptosis in CD34⁺ CML cells. *Blood*, 109, 4016.
- JØRGENSEN, H. G., ALLAN, E. K., JORDANIDES, N. E., MOUNTFORD, J. C. & HOLYOAKE, T. L. 2007b. Nilotinib exerts equipotent antiproliferative effects to imatinib and does not induce apoptosis in CD34⁺ CML cells. *Blood*, 109, 4016-4019.
- JUNG, C. H., JUN, C. B., RO, S.-H., KIM, Y.-M., OTTO, N. M., CAO, J., KUNDU, M. & KIM, D.-H. 2009. ULK-Atg13-FIP200 Complexes Mediate mTOR Signaling to the Autophagy Machinery. *Molecular Biology of the Cell*, 20, 1992-2003.
- KABAROWSKI, J. H., ALLEN, P. B. & WIEDEMANN, L. M. 1994. A temperature sensitive p210 BCR-ABL mutant defines the primary consequences of BCR-ABL tyrosine kinase expression in growth factor dependent cells. *The EMBO Journal*, 13, 5887-5895.
- KABEYA, Y., MIZUSHIMA, N., UENO, T., YAMAMOTO, A., KIRISAKO, T., NODA, T., KOMINAMI, E., OHSUMI, Y. & YOSHIMORI, T. 2000. LC3, a mammalian homologue of yeast Apg8p, is localized in autophagosome membranes after processing. *The EMBO Journal*, 19, 5720-5728.
- KAMITSUJI, Y., KURODA, J., KIMURA, S., TOYOKUNI, S., WATANABE, K., ASHIHARA, E., TANAKA, H., YUI, Y., WATANABE, M., MATSUBARA, H., MIZUSHIMA, Y., HIRAUMI, Y., KAWATA, E., YOSHIKAWA, T., MAEKAWA, T., NAKAHATA, T. & ADACHI, S. 2008. The Bcr-Abl kinase inhibitor INNO-406 induces autophagy and different modes of cell death execution in Bcr-Abl-positive leukemias. *Cell Death Differ*, 15, 1712-1722.
- KANG, M. R., KIM, M. S., OH, J. E., KIM, Y. R., SONG, S. Y., KIM, S. S., AHN, C. H., YOO, N. J. & LEE, S. H. 2009. Frameshift mutations of autophagy-related genes ATG2B, ATG5, ATG9B and ATG12 in gastric and colorectal cancers with microsatellite instability. *The Journal of Pathology*, 217, 702-706.
- KANTARJIAN, H., SAWYERS, C., HOCHHAUS, A., GUILHOT, F., SCHIFFER, C., GAMBACORTI-PASSERINI, C., NIEDERWIESER, D., RESTA, D., CAPDEVILLE, R., ZOELLNER, U., TALPAZ, M. & DRUKER, B. 2002. Hematologic and Cytogenetic Responses to Imatinib Mesylate in Chronic Myelogenous Leukemia. *New England Journal of Medicine*, 346, 645-652.
- KANTARJIAN, H., SHAH, N. P., HOCHHAUS, A., CORTES, J., SHAH, S., AYALA, M., MOIRAGHI, B., SHEN, Z., MAYER, J., PASQUINI, R., NAKAMAE, H., HUGUET, F., BOQUÉ, C., CHUAH, C., BLEICKARDT, E., BRADLEY-GARELIK, M. B., ZHU, C., SZATROWSKI, T., SHAPIRO, D. & BACCARANI, M. 2010. Dasatinib versus Imatinib in Newly Diagnosed Chronic-Phase Chronic Myeloid Leukemia. *New England Journal of Medicine*, 362, 2260-2270.
- KANTARJIAN, H. M., DEISSEROTH, A., KURZROCK, R., ESTROV, Z. & TALPAZ, M. 1993. Chronic myelogenous leukemia: a concise update. *Blood*, 82, 691-703.
- KANTARJIAN, H. M., HOCHHAUS, A., SAGLIO, G., DE SOUZA, C., FLINN, I. W., STENKE, L., GOH, Y.-T., ROSTI, G., NAKAMAE, H., GALLAGHER, N. J., HOENEKOPP, A., BLAKESLEY, R. E., LARSON, R. A. & HUGHES, T. P. 2011. Nilotinib versus imatinib for the treatment of patients with newly diagnosed chronic phase, Philadelphia chromosome-positive, chronic myeloid leukaemia: 24-month minimum follow-up of the phase 3 randomised ENESTnd trial. *The Lancet Oncology*, 12, 841-851.

- KANTARJIAN, H. M., KEATING, M. J., TALPAZ, M., WALTERS, R. S., SMITH, T. L., CORK, A., MCCREDIE, K. B. & FREIREICH, E. J. 1987. Chronic myelogenous leukemia in blast crisis. *The American Journal of Medicine*, 83, 445-454.
- KANTARJIAN, H. M., LARSON, R. A., GUILHOT, F., O'BRIEN, S. G., MONE, M., RUDOLTZ, M., KRAHNKE, T., CORTES, J., DRUKER, B. J., FOR THE INTERNATIONAL RANDOMIZED STUDY OF, I. & INVESTIGATORS, S. T. I. 2009. Efficacy of Imatinib Dose Escalation in Patients With Chronic Myeloid Leukemia in Chronic Phase. *Cancer*, 115, 551-560.
- KANTARJIAN, H. M., TALPAZ, M., O'BRIEN, S., GILES, F., GARCIA-MANERO, G., FADERL, S., THOMAS, D., SHAN, J., RIOS, M. B. & CORTES, J. 2003. Dose escalation of imatinib mesylate can overcome resistance to standard-dose therapy in patients with chronic myelogenous leukemia. *Blood*, 101, 473-475.
- KAPELLER, R. & CANTLEY, L. C. 1994. Phosphatidylinositol 3-kinase. *BioEssays*, 16, 565-576.
- KARVELA, M. 2013. *Investigation of autophagy as a survival factor for chronic myeloid leukaemia*. PhD, University of Glasgow.
- KARVELA, M., HELGASON, G. V. & HOLYOAKE, T. L. 2012. Mechanisms and novel approaches in overriding tyrosine kinase inhibitor resistance in chronic myeloid leukemia. *Expert Review of Anticancer Therapy*, 12, 381-392.
- KELLIHER, M. A., MCLAUGHLIN, J., WITTE, O. N. & ROSENBERG, N. 1990. Induction of a chronic myelogenous leukemia-like syndrome in mice with v-abl and BCR/ABL. *Proceedings of the National Academy of Sciences of the United States of America*, 87, 6649-6653.
- KELLY, P. A., GRUBER, S. A., BEHBOD, F. & KAHAN, B. D. 1997. Sirolimus, a New, Potent Immunosuppressive Agent. *Pharmacotherapy: The Journal of Human Pharmacology and Drug Therapy*, 17, 1148-1156.
- KHARAS, M. G. & FRUMAN, D. A. 2005. ABL Oncogenes and Phosphoinositide 3-Kinase: Mechanism of Activation and Downstream Effectors. *Cancer Research*, 65, 2047-2053.
- KIM, D.-H., SARBASSOV, D. D., ALI, S. M., KING, J. E., LATEK, R. R., ERDJUMENT-BROMAGE, H., TEMPST, P. & SABATINI, D. M. 2002. mTOR Interacts with Raptor to Form a Nutrient-Sensitive Complex that Signals to the Cell Growth Machinery. *Cell*, 110, 163-175.
- KIM, D.-H., SARBASSOV, D. D., ALI, S. M., LATEK, R. R., GUNTUR, K. V. P., ERDJUMENT-BROMAGE, H., TEMPST, P. & SABATINI, D. M. 2003. GβL, a Positive Regulator of the Rapamycin-Sensitive Pathway Required for the Nutrient-Sensitive Interaction between Raptor and mTOR. *Molecular Cell*, 11, 895-904.
- KIM, J., KUNDU, M., VIOLLET, B. & GUAN, K.-L. 2011. AMPK and mTOR regulate autophagy through direct phosphorylation of Ulk1. *Nature cell biology*, 13, 132-141.
- KIM, Y.-K., LEE, S.-S., JEONG, S.-H., AHN, J.-S., YANG, D.-H., LEE, J.-J., SHIN, M.-G. & KIM, H.-J. 2014. OCT-1, ABCB1, and ABCG2 Expression in Imatinib-Resistant Chronic Myeloid Leukemia Treated with Dasatinib or Nilotinib. *Chonnam Medical Journal*, 50, 102-111.
- KIRCHER, B., SCHUMACHER, P., PETZER, A., HOFLEHNER, E., HAUN, M., WOLF, A. M., NACHBAUR, D. & GASTL, G. 2009. Anti-leukemic activity of valproic acid and imatinib mesylate on human Ph+ ALL and CML cells in vitro. *European Journal of Haematology*, 83, 48-56.
- KIRISAKO, T., ICHIMURA, Y., OKADA, H., KABEYA, Y., MIZUSHIMA, N., YOSHIMORI, T., OHSUMI, M., TAKAO, T., NODA, T. & OHSUMI, Y. 2000. The Reversible Modification Regulates the Membrane-Binding State of Apg8/Aut7 Essential for Autophagy and the Cytoplasm to Vacuole Targeting Pathway. *The Journal of Cell Biology*, 151, 263-276.
- KLIONSKY, D. J., ABDELMOHSEN, K., ABE, A., ABEDIN, M. J., ABELIOVICH, H., ACEVEDO AROZENA, A., ADACHI, H., ADAMS, C. M., ADAMS, P. D., ADELI, K., ADHIHETTY, P. J., ADLER, S. G., AGAM, G., AGARWAL, R., AGHI, M. K., AGNELLO, M., AGOSTINIS, P., AGUILAR, P. V., AGUIRRE-GHISO, J., AIROLDI, E. M., AIT-SI-ALI, S., AKEMATSU, T., AKPORIAYE, E. T., AL-RUBEAI, M., ALBAICETA, G. M., ALBANESE, C., ALBANI, D., ALBERT, M. L., ALDUDO, J., ALGÜL, H., ALIREZAEI, M., ALLOZA, I., ALMASAN, A., ALMONTE-BECERIL, M., ALNEMRI, E. S., ALONSO, C., ALTAN-BONNET, N., ALTIERI, D. C., ALVAREZ, S., ALVAREZ-ERVITI, L., ALVES, S., AMADORO, G., AMANO, A., AMANTINI, C., AMBROSIO, S., AMELIO, I., AMER, A. O., AMESSOU, M., AMON, A., AN, Z., ANANIA, F. A., ANDERSEN, S. U., ANDLEY, U. P., ANDREADI, C. K., ANDRIEU-ABADIE, N., ANEL, A., ANN, D. K., ANOOPKUMAR-DUKIE, S., ANTONIOLI, M., AOKI, H., APOSTOLOVA, N., AQUILA, S., AQUILANO, K., ARAKI, K., ARAMA, E., ARANDA, A., ARAYA, J., ARCARO, A., ARIAS, E., ARIMOTO, H., ARIOSI, A. R., ARMSTRONG, J. L., ARNOULD, T., ARSOV, I., ASANUMA, K., ASKANAS, V., ASSELIN, E., ATARASHI, R., ATHERTON, S. S., ATKIN, J. D., ATTARDI, L. D., AUBERGER, P., AUBURGER, G., AURELIAN, L., AUTELLI, R., AVAGLIANO, L., AVANTAGGIATI, M. L., AVRAHAMI, L., AWALE, S., AZAD, N., BACHETTI, T., BACKER, J. M., BAE, D.-H., BAE, J.-S., BAE, O.-N., BAE, S. H., BAEHRECKE, E. H., BAEK, S.-H., BAGHDIGUIAN, S., BAGNIEWSKA-ZADWORNA, A., et al. 2016. Guidelines for the use and interpretation of assays for monitoring autophagy (3rd edition). *Autophagy*, 12, 1-222.

- KOMATSU, N., WATANABE, T., UCHIDA, M., MORI, M., KIRITO, K., KIKUCHI, S., LIU, Q., TAUCHI, T., MIYAZAWA, K., ENDO, H., NAGAI, T. & OZAWA, K. 2003. A Member of Forkhead Transcription Factor FKHRL1 Is a Downstream Effector of STI571-induced Cell Cycle Arrest in BCR-ABL-expressing Cells. *Journal of Biological Chemistry*, 278, 6411-6419.
- KONDO, M., WEISSMAN, I. L. & AKASHI, K. 1997. Identification of Clonogenic Common Lymphoid Progenitors in Mouse Bone Marrow. *Cell*, 91, 661-672.
- KONIG, H., HOLYOAKE, T. L. & BHATIA, R. 2008. Effective and selective inhibition of chronic myeloid leukemia primitive hematopoietic progenitors by the dual Src/Abl kinase inhibitor SKI-606. *Blood*, 111, 2329-2338.
- KONOPKA, J. B., WATANABE, S. M. & WITTE, O. N. 1984. An alteration of the human c-abl protein in K562 leukemia cells unmasks associated tyrosine kinase activity. *Cell*, 37, 1035-1042.
- KOO, E. H. & SQUAZZO, S. L. 1994. Evidence that production and release of amyloid beta-protein involves the endocytic pathway. *Journal of Biological Chemistry*, 269, 17386-17389.
- KOPTYRA, M., CRAMER, K., SLUPIANEK, A., RICHARDSON, C. & SKORSKI, T. 2008. BCR/ABL promotes accumulation of chromosomal aberrations induced by oxidative and genotoxic stress. *Leukemia*, 22, 10.1038/leu.2008.78.
- KURZROCK, R., GUTTERMAN, J. U. & TALPAZ, M. 1988. The Molecular Genetics of Philadelphia Chromosome-Positive Leukemias. *New England Journal of Medicine*, 319, 990-998.
- LAPLANTE, M. & SABATINI, D. M. 2013. Regulation of mTORC1 and its impact on gene expression at a glance. *Journal of Cell Science*, 126, 1713-1719.
- LARSON, R. A., DRUKER, B. J., GUILHOT, F., BRIEN, S. G., RIVIERE, G. J., KRAHNKE, T., GATHMANN, I. & WANG, Y. 2008. Imatinib pharmacokinetics and its correlation with response and safety in chronic-phase chronic myeloid leukemia: a subanalysis of the IRIS study. *Blood*, 111, 4022.
- LAURENTI, E., VARNUM-FINNEY, B., WILSON, A., FERRERO, I., BLANCO-BOSE, W. E., EHNINGER, A., KNOEPFLER, P. S., CHENG, P.-F., MACDONALD, H. R., EISENMAN, R. N., BERNSTEIN, I. D. & TRUMPP, A. 2008. Hematopoietic Stem Cell Function and Survival Depend on c-Myc and N-Myc Activity. *Cell Stem Cell*, 3, 611-624.
- LE COUTRE, P., MOLOGNI, L., CLERIS, L., MARCHESI, E., BUCHDUNGER, E., GIARDINI, R., FORMELLI, F. & GAMBACORTI-PASSERINI, C. 1999. In Vivo Eradication of Human BCR/ABL-Positive Leukemia Cells With an ABL Kinase Inhibitor. *Journal of the National Cancer Institute*, 91, 163-168.
- LE COUTRE, P., TASSI, E., VARELLA-GARCIA, M., BARNI, R., MOLOGNI, L., CABRITA, G., MARCHESI, E., SUPINO, R. & GAMBACORTI-PASSERINI, C. 2000. Induction of resistance to the Abelson inhibitor STI571 in human leukemic cells through gene amplification. *Blood*, 95, 1758-1766.
- LEE, S. M., BAE, J. H., KIM, M. J., LEE, H. S., LEE, M. K., CHUNG, B. S., KIM, D. W., KANG, C. D. & KIM, S. H. 2007. Bcr-Abl-Independent Imatinib-Resistant K562 Cells Show Aberrant Protein Acetylation and Increased Sensitivity to Histone Deacetylase Inhibitors. *Journal of Pharmacology and Experimental Therapeutics*, 322, 1084-1092.
- LEVINE, B., SINHA, S. & KROEMER, G. 2008. Bcl-2 family members: Dual regulators of apoptosis and autophagy. *Autophagy*, 4, 600-606.
- LEVY, G. D., MUNZ, S. J., PASCHAL, J., COHEN, H. B., PINCE, K. J. & PETERSON, T. 1997. Incidence of hydroxychloroquine retinopathy in 1,207 patients in a large multicenter outpatient practice. *Arthritis & Rheumatism*, 40, 1482-1486.
- LI, L., WANG, L., LI, L., WANG, Z., HO, Y., MCDONALD, T., HOLYOAKE, TESSA L., CHEN, W. & BHATIA, R. 2012. Activation of p53 by SIRT1 Inhibition Enhances Elimination of CML Leukemia Stem Cells in Combination with Imatinib. *Cancer Cell*, 21, 266-281.
- LI, S., ILARIA, R. L., MILLION, R. P., DALEY, G. Q. & VAN ETEN, R. A. 1999. The P190, P210, and P230 Forms of the BCR/ABL Oncogene Induce a Similar Chronic Myeloid Leukemia-like Syndrome in Mice but Have Different Lymphoid Leukemogenic Activity. *The Journal of Experimental Medicine*, 189, 1399-1412.
- LIANG, C., LEE, J.-S., INN, K.-S., GACK, M. U., LI, Q., ROBERTS, E. A., VERGNE, I., DERETIC, V., FENG, P., AKAZAWA, C. & JUNG, J. U. 2008. Beclin1-binding UVRAG targets the class C Vps complex to coordinate autophagosome maturation and endocytic trafficking. *Nature cell biology*, 10, 776-787.
- LIANG, X. H., JACKSON, S., SEAMAN, M., BROWN, K., KEMPKES, B., HIBSHOOSH, H. & LEVINE, B. 1999. Induction of autophagy and inhibition of tumorigenesis by beclin 1. *Nature*, 402, 672-676.
- LIN, S., STAAHL, B. T., ALLA, R. K. & DOUDNA, J. A. 2014. Enhanced homology-directed human genome engineering by controlled timing of CRISPR/Cas9 delivery. *eLife*, 3, e04766.
- LIPTON, J. H., CHUAH, C., GUERCI-BRESLER, A., ROSTI, G., SIMPSON, D., ASSOULINE, S., ETIENNE, G., NICOLINI, F. E., LE COUTRE, P., CLARK, R. E., STENKE, L., ANDORSKY, D., OEHLER, V., LUSTGARTEN, S., RIVERA, V. M., CLACKSON, T., HALUSKA, F. G., BACCARANI, M., CORTES, J. E., GUILHOT, F., HOCHHAUS, A., HUGHES, T.,

- KANTARJIAN, H. M., SHAH, N. P., TALPAZ, M. & DEININGER, M. W. 2016. Ponatinib versus imatinib for newly diagnosed chronic myeloid leukaemia: an international, randomised, open-label, phase 3 trial. *The Lancet Oncology*, 17, 612-621.
- LIU, F., LEE, J. Y., WEI, H., TANABE, O., ENGEL, J. D., MORRISON, S. J. & GUAN, J.-L. 2010. FIP200 is required for the cell-autonomous maintenance of fetal hematopoietic stem cells. *Blood*, 116, 4806-4814.
- LIU, Y., ELF, S. E., MIYATA, Y., SASHIDA, G., LIU, Y., HUANG, G., DI GIANDOMENICO, S., LEE, J. M., DEBLASIO, A., MENENDEZ, S., ANTIPIN, J., REVA, B., KOFF, A. & NIMER, S. D. 2009. p53 Regulates Hematopoietic Stem Cell Quiescence. *Cell Stem Cell*, 4, 37-48.
- LOMBARDO, L. J., LEE, F. Y., CHEN, P., NORRIS, D., BARRISH, J. C., BEHNIA, K., CASTANEDA, S., CORNELIUS, L. A. M., DAS, J., DOWEYKO, A. M., FAIRCHILD, C., HUNT, J. T., INIGO, I., JOHNSTON, K., KAMATH, A., KAN, D., KLEI, H., MARATHE, P., PANG, S., PETERSON, R., PITT, S., SCHIEVEN, G. L., SCHMIDT, R. J., TOKARSKI, J., WEN, M.-L., WITYAK, J. & BORZILLERI, R. M. 2004. Discovery of N-(2-Chloro-6-methyl-phenyl)-2-(6-(4-(2-hydroxyethyl)-piperazin-1-yl)-2-methylpyrimidin-4-ylamino)thiazole-5-carboxamide (BMS-354825), a Dual Src/Abl Kinase Inhibitor with Potent Antitumor Activity in Preclinical Assays. *Journal of Medicinal Chemistry*, 47, 6658-6661.
- LUGO, T. G., PENDERGAST, A. M., MULLER, A. J. & WITTE, O. N. 1990. Tyrosine kinase activity and transformation potency of bcr-abl oncogene products. *Science*, 247, 1079-1082.
- LUGO, T. G. & WITTE, O. N. 1989. The BCR-ABL oncogene transforms Rat-1 cells and cooperates with v-myc. *Molecular and Cellular Biology*, 9, 1263-1270.
- LUO, J., NIKOLAEV, A. Y., IMAI, S.-I., CHEN, D., SU, F., SHILOH, A., GUARENTE, L. & GU, W. 2001. Negative Control of p53 by Sir2 α Promotes Cell Survival under Stress. *Cell*, 107, 137-148.
- LY, C., ARECHIGA, A. F., MELO, J. V., WALSH, C. M. & ONG, S. T. 2003. Bcr-Abl Kinase Modulates the Translation Regulators Ribosomal Protein S6 and 4E-BP1 in Chronic Myelogenous Leukemia Cells via the Mammalian Target of Rapamycin. *Cancer Research*, 63, 5716.
- M ANDREEFF, S. J., X ZHANG, M KONOPLEVA, Z ESTROV, V E SNELL, Z XIE, M F OKCU, G SANCHEZ-WILLIAMS, J DONG, E H ESTEY, R C CHAMPLIN, S M KORNBLAU, J C REED, S ZHAO 1999. Expression of Bcl-2-related genes in normal and AML progenitors: changes induced by chemotherapy and retinoic acid. *Leukemia*, 13, 1881-1892.
- MA, L., SHAN, Y., BAI, R., XUE, L., EIDE, C. A., OU, J., ZHU, L. J., HUTCHINSON, L., CERNY, J., KHOURY, H. J., SHENG, Z., DRUKER, B. J., LI, S. & GREEN, M. R. 2014. A Therapeutically Targetable Mechanism of BCR-ABL-Independent Imatinib Resistance in Chronic Myeloid Leukemia. *Science translational medicine*, 6, 252ra121-252ra121.
- MACHOVA POLAKOVA, K., KOBLIHOVA, J. & STOPKA, T. 2013. Role of Epigenetics in Chronic Myeloid Leukemia. *Current Hematologic Malignancy Reports*, 8, 28-36.
- MAHON, F.-X., BELLOC, F., LAGARDE, V., CHOLLET, C., MOREAU-GAUDRY, F., REIFFERS, J., GOLDMAN, J. M. & MELO, J. V. 2003. <http://www.w3.org/1999/xhtml> MDR1 gene overexpression confers resistance to imatinib mesylate in leukemia cell line models. *Blood*, 101, 2368.
- MAHON, F.-X., HAYETTE, S., LAGARDE, V., BELLOC, F., TURCQ, B., NICOLINI, F., BELANGER, C., MANLEY, P. W., LEROY, C., ETIENNE, G., ROCHE, S. & PASQUET, J.-M. 2008. Evidence that Resistance to Nilotinib May Be Due to BCR-ABL, Pgp, or Src Kinase Overexpression. *Cancer Research*, 68, 9809.
- MAHON, F.-X., RÉA, D., GUILHOT, J., GUILHOT, F., HUGUET, F., NICOLINI, F., LEGROS, L., CHARBONNIER, A., GUERCI, A., VARET, B., ETIENNE, G., REIFFERS, J. & ROUSSELOT, P. 2010. Discontinuation of imatinib in patients with chronic myeloid leukaemia who have maintained complete molecular remission for at least 2 years: the prospective, multicentre Stop Imatinib (STIM) trial. *The Lancet Oncology*, 11, 1029-1035.
- MAHON, F. X., DEININGER, M. W. N., SCHULTHEIS, B., CHABROL, J., REIFFERS, J., GOLDMAN, J. M. & MELO, J. V. 2000a. <http://www.w3.org/1999/xhtml> Selection and characterization of BCR-ABL positive cell lines with differential sensitivity to the tyrosine kinase inhibitor STI571: diverse mechanisms of resistance. *Blood*, 96, 1070.
- MAHON, F. X., DEININGER, M. W. N., SCHULTHEIS, B., CHABROL, J., REIFFERS, J., GOLDMAN, J. M. & MELO, J. V. 2000b. Selection and characterization of BCR-ABL positive cell lines with differential sensitivity to the tyrosine kinase inhibitor STI571: diverse mechanisms of resistance. *Blood*, 96, 1070-1079.
- MAIRA, S.-M., STAUFFER, F., BRUEGGEN, J., FURET, P., SCHNELL, C., FRITSCH, C., BRACHMANN, S., CHÈNE, P., DE POVER, A., SCHOEMAKER, K., FABBRO, D., GABRIEL, D., SIMONEN, M., MURPHY, L., FINAN, P., SELLERS, W. & GARCÍA-ECHEVERRÍA, C. 2008. <http://www.w3.org/1999/xhtml> Identification and characterization of NVP-BEZ235, a new orally available dual phosphatidylinositol 3-

- kinase/mammalian target of rapamycin inhibitor with potent *in vivo* antitumor activity. *Molecular Cancer Therapeutics*, 7, 1851.
- MAIURI, M. C., LE TOUMELIN, G., CRIOLLO, A., RAIN, J.-C., GAUTIER, F., JUIN, P., TASDEMIR, E., PIERRON, G., TROULINAKI, K., TAVERNARAKIS, N., HICKMAN, J. A., GENESTE, O. & KROEMER, G. 2007. Functional and physical interaction between Bcl-X(L) and a BH3-like domain in Beclin-1. *The EMBO Journal*, 26, 2527-2539.
- MAJESKI, A. E. & FRED DICE, J. 2004. Mechanisms of chaperone-mediated autophagy. *The International Journal of Biochemistry & Cell Biology*, 36, 2435-2444.
- MAKAROVA, K. S., GRISHIN, N. V., SHABALINA, S. A., WOLF, Y. I. & KOONIN, E. V. 2006. A putative RNA-interference-based immune system in prokaryotes: computational analysis of the predicted enzymatic machinery, functional analogies with eukaryotic RNAi, and hypothetical mechanisms of action. *Biology Direct*, 1, 7-7.
- MALI, P., ESVELT, K. M. & CHURCH, G. M. 2013a. Cas9 as a versatile tool for engineering biology. *Nat Meth*, 10, 957-963.
- MALI, P., YANG, L., ESVELT, K. M., AACH, J., GUELL, M., DICARLO, J. E., NORVILLE, J. E. & CHURCH, G. M. 2013b. RNA-Guided Human Genome Engineering via Cas9. *Science*, 339, 823-826.
- MANLEY, P. W., BREITENSTEIN, W., BRÜGGEN, J., COWAN-JACOB, S. W., FURET, P., MESTAN, J. & MEYER, T. 2004. Urea derivatives of STI571 as inhibitors of Bcr-Abl and PDGFR kinases. *Bioorganic & Medicinal Chemistry Letters*, 14, 5793-5797.
- MANLEY, P. W., COWAN-JACOB, S. W., BUCHDUNGER, E., FABBRO, D., FENDRICH, G., FURET, P., MEYER, T. & ZIMMERMANN, J. 2002. Imatinib: a selective tyrosine kinase inhibitor. *European Journal of Cancer*, 38, S19-S27.
- MARIN, D., BAZEOS, A., MAHON, F.-X., ELIASSON, L., MILOJKOVIC, D., BUA, M., APPERLEY, J. F., SZYDLO, R., DESAI, R., KOZLOWSKI, K., PALIOMPEIS, C., LATHAM, V., FORONI, L., MOLIMARD, M., REID, A., REZVANI, K., DE LAVALLADE, H., GUALLAR, C., GOLDMAN, J. & KHORASHAD, J. S. 2010. Adherence Is the Critical Factor for Achieving Molecular Responses in Patients With Chronic Myeloid Leukemia Who Achieve Complete Cytogenetic Responses on Imatinib. *Journal of Clinical Oncology*, 28, 2381-2388.
- MARLEY, STEPHEN B. & GORDON, MYRTLE Y. 2005. Chronic myeloid leukaemia: stem cell derived but progenitor cell driven. *Clinical Science*, 109, 13-25.
- MARU, Y., KOBAYASHI, T., TANAKA, K. & SHIBUYA, M. 1999. BCR Binds to the Xeroderma Pigmentosum Group B Protein. *Biochemical and Biophysical Research Communications*, 260, 309-312.
- MATSUNAGA, K., MORITA, E., SAITOH, T., AKIRA, S., KTISTAKIS, N. T., IZUMI, T., NODA, T. & YOSHIMORI, T. 2010. Autophagy requires endoplasmic reticulum targeting of the PI3-kinase complex via Atg14L. *The Journal of Cell Biology*, 190, 511-521.
- MATSUSHITA, M., SUZUKI, N. N., OBARA, K., FUJIOKA, Y., OHSUMI, Y. & INAGAKI, F. 2007. Structure of Atg5·Atg16, a Complex Essential for Autophagy. *Journal of Biological Chemistry*, 282, 6763-6772.
- MATZKE, M., MATZKE, A. J. M. & KOOTER, J. M. 2001. RNA: Guiding Gene Silencing. *Science*, 293, 1080-1083.
- MAYCOTTE, P., ARYAL, S., CUMMINGS, C. T., THORBURN, J., MORGAN, M. J. & THORBURN, A. 2012. Chloroquine sensitizes breast cancer cells to chemotherapy independent of autophagy. *Autophagy*, 8, 200-212.
- MAYER, C. & GRUMMT, I. 2000. Ribosome biogenesis and cell growth: mTOR coordinates transcription by all three classes of nuclear RNA polymerases. *Oncogene*, 25, 6384-6391.
- MAYO, L. D. & DONNER, D. B. 2001. A phosphatidylinositol 3-kinase/Akt pathway promotes translocation of Mdm2 from the cytoplasm to the nucleus. *Proceedings of the National Academy of Sciences of the United States of America*, 98, 11598-11603.
- MCAFEE, Q., ZHANG, Z., SAMANTA, A., LEVI, S. M., MA, X.-H., PIAO, S., LYNCH, J. P., UEHARA, T., SEPULVEDA, A. R., DAVIS, L. E., WINKLER, J. D. & AMARAVADI, R. K. 2012. Autophagy inhibitor Lys05 has single-agent antitumor activity and reproduces the phenotype of a genetic autophagy deficiency. *Proceedings of the National Academy of Sciences of the United States of America*, 109, 8253-8258.
- MCGAHON, A., BISSONNETTE, R., SCHMITT, M., COTTER, K. M., GREEN, D. R. & COTTER, T. G. 1994. BCR-ABL maintains resistance of chronic myelogenous leukemia cells to apoptotic cell death [published erratum appears in *Blood* 1994 Jun 15;83(12):3835]. *Blood*, 83, 1179-1187.
- MCGLAVE, P., KIM, T., HURD, D., ARTHUR, D., RAMSAY, N. C. & KERSEY, J. 1982. Originally published as Volume 2, Issue 8299 SUCCESSFUL ALLOGENEIC BONE-MARROW TRANSPLANTATION FOR PATIENTS IN THE ACCELERATED PHASE OF CHRONIC GRANULOCYTIC LEUKAEMIA. *The Lancet*, 320, 625-627.

- MCGRATH, K. E., FRAME, J. M., FROMM, G. J., KONISKI, A. D., KINGSLEY, P. D., LITTLE, J., BULGER, M. & PALIS, J. 2011. A transient definitive erythroid lineage with unique regulation of the β -globin locus in the mammalian embryo. *Blood*, 117, 4600-4608.
- MCWEENEY, S. K., PEMBERTON, L. C., LORIAUX, M. M., VARTANIAN, K., WILLIS, S. G., YOCHUM, G., WILMOT, B., TURPAZ, Y., PILLAI, R., DRUKER, B. J., SNEAD, J. L., MACPARTLIN, M., O'BRIEN, S. G., MELO, J. V., LANGE, T., HARRINGTON, C. A. & DEININGER, M. W. N. 2010. A gene expression signature of CD34(+) cells to predict major cytogenetic response in chronic-phase chronic myeloid leukemia patients treated with imatinib. *Blood*, 115, 315-325.
- MCWHIRTER, J. R., GALASSO, D. L. & WANG, J. Y. 1993. A coiled-coil oligomerization domain of Bcr is essential for the transforming function of Bcr-Abl oncoproteins. *Molecular and Cellular Biology*, 13, 7587-7595.
- MEI HUANG, J. F. D., P K EPLING-BURNETTE, RAMADEVI NIMMANAPALLI, TERRY H LANDOWSKI, LINDA B MORA, GUILIAN NIU, DOMINIC SINIBALDI, FANQI BAI, ALAN KRAKER, HUA YU, LYNN MOSCINSKI, SHENG WEI, JULIE DJEU, WILLIAM S DALTON, KAPIL BHALLA, THOMAS P LOUGHRAN, JIE WU AND RICHARD JOVE 2002. Inhibition of Bcr-Abl kinase activity by PD180970 blocks constitutive activation of Stat5 and growth of CML cells. *Oncogene*, 21, 8804-8816.
- MEIR, W. & DAVID, S. 2011. Omacetaxine as an Anticancer Therapeutic: What is Old is New Again. *Current Pharmaceutical Design*, 17, 59-64.
- MELO, J. V. & BARNES, D. J. 2007. Chronic myeloid leukaemia as a model of disease evolution in human cancer. *Nat Rev Cancer*, 7, 441-453.
- MILLION, R. P. & VAN ETEN, R. A. 2000. The Grb2 binding site is required for the induction of chronic myeloid leukemia-like disease in mice by the Bcr/Abl tyrosine kinase. *Blood*, 96, 664-670.
- MINOT, G. R., BUCKMAN, T. E. & ISAACS, R. 1924. Chronic myelogenous leukemia: Age incidence, duration, and benefit derived from irradiation. *Journal of the American Medical Association*, 82, 1489-1494.
- MIOOTTO, E., SABBIONI, S., VERONESE, A., CALIN, G. A., GULLINI, S., LIBONI, A., GRAMANTIERI, L., BOLONDI, L., FERRAZZI, E., GAFÀ, R., LANZA, G. & NEGRINI, M. 2004. <http://www.w3.org/1999/xhtml> Aberrant Methylation of the $CDH4$ Gene Promoter in Human Colorectal and Gastric Cancer. *Cancer Research*, 64, 8156.
- MISHIMA, Y., TERUI, Y., MISHIMA, Y., TANIYAMA, A., KUNIYOSHI, R., TAKIZAWA, T., KIMURA, S., OZAWA, K. & HATAKE, K. 2008. Autophagy and autophagic cell death are next targets for elimination of the resistance to tyrosine kinase inhibitors. *Cancer Science*, 99, 2200-2208.
- MIYAMOTO, K., ARAKI, K. Y., NAKA, K., ARAI, F., TAKUBO, K., YAMAZAKI, S., MATSUOKA, S., MIYAMOTO, T., ITO, K., OHMURA, M., CHEN, C., HOSOKAWA, K., NAKAUCHI, H., NAKAYAMA, K., NAKAYAMA, K. I., HARADA, M., MOTOYAMA, N., SUDA, T. & HIRAO, A. 2007. Foxo3a Is Essential for Maintenance of the Hematopoietic Stem Cell Pool. *Cell Stem Cell*, 1, 101-112.
- MIZUSHIMA, N. 2007. Autophagy: process and function. *Genes & Development*, 21, 2861-2873.
- MIZUSHIMA, N., SUGITA, H., YOSHIMORI, T. & OHSUMI, Y. 1998. A New Protein Conjugation System in Human: THE COUNTERPART OF THE YEAST Apg12p CONJUGATION SYSTEM ESSENTIAL FOR AUTOPHAGY. *Journal of Biological Chemistry*, 273, 33889-33892.
- MOJICA, F. J. M., DÍEZ-VILLASEÑOR, C., SORIA, E. & JUEZ, G. 2000. Biological significance of a family of regularly spaced repeats in the genomes of Archaea, Bacteria and mitochondria. *Molecular Microbiology*, 36, 244-246.
- MOJICA, F. J. M., DÍEZ-VILLASEÑOR, C. S., GARCÍA-MARTÍNEZ, J. & SORIA, E. 2005. Intervening Sequences of Regularly Spaced Prokaryotic Repeats Derive from Foreign Genetic Elements. *Journal of Molecular Evolution*, 60, 174-182.
- MORI, S., NADA, S., KIMURA, H., TAJIMA, S., TAKAHASHI, Y., KITAMURA, A., ONEYAMA, C. & OKADA, M. 2014. The mTOR Pathway Controls Cell Proliferation by Regulating the FoxO3a Transcription Factor via SGK1 Kinase. *PLoS ONE*, 9, e88891.
- MORRISON, S. J., UCHIDA, N. & WEISSMAN, I. L. 1995. The Biology of Hematopoietic Stem Cells. *Annual Review of Cell and Developmental Biology*, 11, 35-71.
- MORRISON, S. J. & WEISSMAN, I. L. 1994. The long-term repopulating subset of hematopoietic stem cells is deterministic and isolatable by phenotype. *Immunity*, 1, 661-673.
- MORTENSEN, M., FERGUSON, D. J. P., EDELMANN, M., KESSLER, B., MORTEN, K. J., KOMATSU, M. & SIMON, A. K. 2010. Loss of autophagy in erythroid cells leads to defective removal of mitochondria and severe anemia in vivo. *Proceedings of the National Academy of Sciences of the United States of America*, 107, 832-837.
- MORTENSEN, M., SOILLEUX, E. J., DJORDJEVIC, G., TRIPP, R., LUTTEROPP, M., SADIGHI-AKHA, E., STRANKS, A. J., GLANVILLE, J., KNIGHT, S., W. JACOBSEN, S.-E., KRANC, K. R. &

- SIMON, A. K. 2011. The autophagy protein Atg7 is essential for hematopoietic stem cell maintenance. *The Journal of Experimental Medicine*, 208, 455-467.
- MUEHLECK, S. D., MCKENNA, R. W., ARTHUR, D. C., PARKIN, J. L. & BRUNNING, R. D. 1984. Transformation of Chronic Myelogenous Leukemia: Clinical, Morphologic, and Cytogenetic Features. *American Journal of Clinical Pathology*, 82, 1-14.
- MUKHERJEE, B., TOMIMATSU, N., AMANCHERLA, K., CAMACHO, C. V., PICHAMOORTHY, N. & BURMA, S. 2012. The Dual PI3K/mTOR Inhibitor NVP-BEZ235 Is a Potent Inhibitor of ATM- and DNA-PKCs-Mediated DNA Damage Responses. *Neoplasia (New York, N.Y.)*, 14, 34-43.
- NAGAR, B., BORNMANN, W. G., PELLICENA, P., SCHINDLER, T., VEACH, D. R., MILLER, W. T., CLARKSON, B. & KURIYAN, J. 2002. Crystal Structures of the Kinase Domain of c-Abl in Complex with the Small Molecule Inhibitors PD173955 and Imatinib (STI-571). *Cancer Research*, 62, 4236-4243.
- NAKATOGAWA, H., SUZUKI, K., KAMADA, Y. & OHSUMI, Y. 2009. Dynamics and diversity in autophagy mechanisms: lessons from yeast. *Nat Rev Mol Cell Biol*, 10, 458-467.
- NARALA, S. R., ALLSOPP, R. C., WELLS, T. B., ZHANG, G., PRASAD, P., COUSSENS, M. J., ROSSI, D. J., WEISSMAN, I. L. & VAZIRI, H. 2008. SIRT1 Acts as a Nutrient-sensitive Growth Suppressor and Its Loss Is Associated with Increased AMPK and Telomerase Activity. *Molecular Biology of the Cell*, 19, 1210-1219.
- NATIONAL INSTITUTE OF HEALTH, N. C. I. 2013. *FDA Approval for Ponatinib Hydrochloride* [Online]. <http://www.cancer.gov/about-cancer/treatment/drugs/fda-ponatinibhydrochloride> National Institute of Health, National Cancer Institute. [Accessed 08/08/2016 2016].
- NEUBAUER, H., CUMANO, A., MÜLLER, M., WU, H., HUFFSTADT, U. & PFEFFER, K. 1998. Jak2 Deficiency Defines an Essential Developmental Checkpoint in Definitive Hematopoiesis. *Cell*, 93, 397-409.
- NEVIANI, P., HARB, J. G., OAKS, J. J., SANTHANAM, R., WALKER, C. J., ELLIS, J. J., FERENCHAK, G., DORRANCE, A. M., PAISIE, C. A., EIRING, A. M., MA, Y., MAO, H. C., ZHANG, B., WUNDERLICH, M., MAY, P. C., SUN, C., SADDOUGH, S. A., BIELAWSKI, J., BLUM, W., KLISOVIC, R. B., SOLT, J. A., BYRD, J. C., VOLINIA, S., CORTES, J., HUETTNER, C. S., KOSCHMIEDER, S., HOLYOAKE, T. L., DEVINE, S., CALIGIURI, M. A., CROCE, C. M., GARZON, R., OGRETMEN, B., ARLINGHAUS, R. B., CHEN, C.-S., BITTMAN, R., HOKLAND, P., ROY, D.-C., MILOJKOVIC, D., APPERLEY, J., GOLDMAN, J. M., REID, A., MULLOY, J. C., BHATIA, R., MARCUCCI, G. & PERROTTI, D. 2013. PP2A-activating drugs selectively eradicate TKI-resistant chronic myeloid leukemic stem cells. *The Journal of Clinical Investigation*, 123, 4144-4157.
- NG, K. P., HILLMER, A. M., CHUAH, C. T. H., JUAN, W. C., KO, T. K., TEO, A. S. M., ARIYARATNE, P. N., TAKAHASHI, N., SAWADA, K., FEI, Y., SOH, S., LEE, W. H., HUANG, J. W. J., ALLEN, J. C., WOO, X. Y., NAGARAJAN, N., KUMAR, V., THALAMUTHU, A., POH, W. T., ANG, A. L., MYA, H. T., HOW, G. F., YANG, L. Y., KOH, L. P., CHOWBAY, B., CHANG, C.-T., NADARAJAN, V. S., CHNG, W. J., THAN, H., LIM, L. C., GOH, Y. T., ZHANG, S., POH, D., TAN, P., SEET, J.-E., ANG, M.-K., CHAU, N.-M., NG, Q.-S., TAN, D. S. W., SODA, M., ISOBE, K., NOTHEN, M. M., WONG, T. Y., SHAHAB, A., RUAN, X., CACHEUX-RATABOUL, V., SUNG, W.-K., TAN, E. H., YATABE, Y., MANO, H., SOO, R. A., CHIN, T. M., LIM, W.-T., RUAN, Y. & ONG, S. T. 2012. A common BIM deletion polymorphism mediates intrinsic resistance and inferior responses to tyrosine kinase inhibitors in cancer. *Nat Med*, 18, 521-528.
- NGUYEN, T., DAI, Y., ATTKISSON, E., KRAMER, L., JORDAN, N., NGUYEN, N., KOLLURI, N., MUSCHEN, M. & GRANT, S. 2011. HDAC INHIBITORS POTENTIATE THE ACTIVITY OF THE BCR/ABL KINASE INHIBITOR KW-2449 IN IMATINIB-SENSITIVE OR -RESISTANT BCR/ABL(+) LEUKEMIA CELLS IN VITRO AND IN VIVO. *Clinical cancer research : an official journal of the American Association for Cancer Research*, 17, 3219-3232.
- NGUYEN, T. T., MOHRBACHER, A. F., TSAI, Y. C., GROFFEN, J., HEISTERKAMP, N., NICHOLS, P. W., YU, M. C., LÜBBERT, M. & JONES, P. A. 2000. Quantitative measure of c-abl and p15 methylation in chronic myelogenous leukemia: biological implications. *Blood*, 95, 2990-2992.
- NICHOLS, G. L., RAINES, M. A., VERA, J. C., LACOMIS, L., TEMPST, P. & GOLDE, D. W. 1994. Identification of CRKL as the constitutively phosphorylated 39-kD tyrosine phosphoprotein in chronic myelogenous leukemia cells. *Blood*, 84, 2912-2918.
- NICOLINI, F. E., NOËL, M.-P., ESCOFFRE, M., CHARBONNIER, A., REA, D., DUBRUILLE, V., VARET, B. R., LEGROS, L., GUERCI, A., ETIENNE, G., GUILHOT, F., DULUCQ, S., ROUSSELOT, P. & GUILHOT, J. 2013. Preliminary Report Of The STIM2 Study: A Multicenter Stop Imatinib Trial For Chronic Phase Chronic Myeloid Leukemia De Novo Patients On Imatinib. *Blood*, 122, 654-654.
- NISHIMASU, H., RAN, F. A., HSU, PATRICK D., KONERMANN, S., SHEHATA, SORAYA I., DOHMAE, N., ISHITANI, R., ZHANG, F. & NUREKI, O. 2014. Crystal Structure of Cas9 in Complex with Guide RNA and Target DNA. *Cell*, 156, 935-949.

- NOENS, L., VAN LIERDE, M.-A., DE BOCK, R., VERHOEF, G., ZACHÉE, P., BERNEMAN, Z., MARTIAT, P., MINEUR, P., VAN EYGEN, K., MACDONALD, K., DE GEEST, S., ALBRECHT, T. & ABRAHAM, I. 2009. Prevalence, determinants, and outcomes of nonadherence to imatinib therapy in patients with chronic myeloid leukemia: the ADAGIO study. *Blood*, 113, 5401-5411.
- NOTTA, F., ZANDI, S., TAKAYAMA, N., DOBSON, S., GAN, O. I., WILSON, G., KAUFMANN, K. B., MCLEOD, J., LAURENTI, E., DUNANT, C. F., MCPHERSON, J. D., STEIN, L. D., DROR, Y. & DICK, J. E. 2016. Distinct routes of lineage development reshape the human blood hierarchy across ontogeny. *Science*, 351.
- NOVIKOFF, A. B. 1959. The Proximal Tubule Cell in Experimental Hydronephrosis. *The Journal of Biophysical and Biochemical Cytology*, 6, 136-138.
- NOWELL, P. C. & HUNGERFORD, D. A. 1960. Chromosome Studies on Normal and Leukemic Human Leukocytes. *Journal of the National Cancer Institute*, 25, 85-109.
- O'BRIEN, S. G. & DEININGER, M. W. N. 2003. Imatinib in patients with newly diagnosed chronic-phase chronic myeloid leukemia. *Seminars in Hematology*, 40, Supplement 2, 26-30.
- O'BRIEN, S. G., GUILHOT, F., LARSON, R. A., GATHMANN, I., BACCARANI, M., CERVANTES, F., CORNELISSEN, J. J., FISCHER, T., HOCHHAUS, A., HUGHES, T., LECHNER, K., NIELSEN, J. L., ROUSSELOT, P., REIFFERS, J., SAGLIO, G., SHEPHERD, J., SIMONSSON, B., GRATWOHL, A., GOLDMAN, J. M., KANTARJIAN, H., TAYLOR, K., VERHOEF, G., BOLTON, A. E., CAPDEVILLE, R. & DRUKER, B. J. 2003. Imatinib Compared with Interferon and Low-Dose Cytarabine for Newly Diagnosed Chronic-Phase Chronic Myeloid Leukemia. *New England Journal of Medicine*, 348, 994-1004.
- O'HARE, T., SHAKESPEARE, W. C., ZHU, X., EIDE, C. A., RIVERA, V. M., WANG, F., ADRIAN, L. T., ZHOU, T., HUANG, W.-S., XU, Q., METCALF III, C. A., TYNER, J. W., LORIAUX, M. M., CORBIN, A. S., WARDWELL, S., NING, Y., KEATS, J. A., WANG, Y., SUNDARAMOORTHY, R., THOMAS, M., ZHOU, D., SNODGRASS, J., COMMODORE, L., SAWYER, T. K., DALGARNO, D. C., DEININGER, M. W. N., DRUKER, B. J. & CLACKSON, T. 2009. AP24534, a Pan-BCR-ABL Inhibitor for Chronic Myeloid Leukemia, Potently Inhibits the T315I Mutant and Overcomes Mutation-Based Resistance. *Cancer Cell*, 16, 401-412.
- O'HARE, T., WALTERS, D. K., STOFFREGEN, E. P., JIA, T., MANLEY, P. W., MESTAN, J., COWAN-JACOB, S. W., LEE, F. Y., HEINRICH, M. C., DEININGER, M. W. N. & DRUKER, B. J. 2005. In vitro Activity of Bcr-Abl Inhibitors AMN107 and BMS-354825 against Clinically Relevant Imatinib-Resistant Abl Kinase Domain Mutants. *Cancer Research*, 65, 4500-4505.
- O'HARE, T., SHAKESPEARE, W. C., ZHU, X., EIDE, C. A., RIVERA, V. M., WANG, F., ADRIAN, L. T., ZHOU, T., HUANG, W.-S., XU, Q., METCALF, C. A., TYNER, J. W., LORIAUX, M. M., CORBIN, A. S., WARDWELL, S., NING, Y., KEATS, J. A., WANG, Y., SUNDARAMOORTHY, R., THOMAS, M., ZHOU, D., SNODGRASS, J., COMMODORE, L., SAWYER, T. K., DALGARNO, D. C., DEININGER, M. W. N., DRUKER, B. J. & CLACKSON, T. 2009. AP24534, a Pan-BCR-ABL Inhibitor for Chronic Myeloid Leukemia, Potently Inhibits the T315I Mutant and Overcomes Mutation-Based Resistance. *Cancer cell*, 16, 401-412.
- O'HARE, T., WALTERS, D. K., DEININGER, M. W. N. & DRUKER, B. J. 2005. AMN107: Tightening the grip of imatinib. *Cancer Cell*, 7, 117-119.
- O'REILLY, K. E., ROJO, F., SHE, Q.-B., SOLIT, D., MILLS, G. B., SMITH, D., LANE, H., HOFMANN, F., HICKLIN, D. J., LUDWIG, D. L., BASELGA, J. & ROSEN, N. 2006. mTOR Inhibition Induces Upstream Receptor Tyrosine Kinase Signaling and Activates Akt. *Cancer research*, 66, 1500-1508.
- ODA, T., HEANEY, C., HAGOPIAN, J. R., OKUDA, K., GRIFFIN, J. D. & DRUKER, B. J. 1994. Crkl is the major tyrosine-phosphorylated protein in neutrophils from patients with chronic myelogenous leukemia. *Journal of Biological Chemistry*, 269, 22925-22928.
- OKABE, S., TAUCHI, T., TANAKA, Y., KITAHARA, T., KIMURA, S., MAEKAWA, T. & OHYASHIKI, K. 2014. Efficacy of the dual PI3K and mTOR inhibitor NVP-BEZ235 in combination with nilotinib against BCR-ABL-positive leukemia cells involves the ABL kinase domain mutation. *Cancer Biology & Therapy*, 15, 207-215.
- OLIVER G. OTTMANN, G. A., DANIEL J. DEANGELO, YEOW-TEE GOH, MICHAEL C. HEINRICH, ANDREAS HOCHHAUS, TIMOTHY P. HUGHES, FRANCOIS-XAVIER MAHON, MICHAEL J. MAURO, HIRONOBU MINAMI, MARIE HUONG NGUYEN, DELPHINE REA, JUAN LUIS STEEGMANN, ARKENDU CHATTERJEE, VARSHA IYER, NOELIA MARTINEZ, GARY J. VANASSE, KIM DONG-WOOK. 2015. *ABL001, a Potent, Allosteric Inhibitor of BCR-ABL, Exhibits Safety and Promising Single-Agent Activity in a Phase I Study of Patients with CML with Failure of Prior TKI Therapy* [Online]. American Society of Hematology 57th Annual Meeting and Exposition. Available: <https://ash.confex.com/ash/2015/webprogram/Paper81180.html> [Accessed 08/08 2016].
- ORKIN, S. H. 2000. Diversification of haematopoietic stem cells to specific lineages. *Nat Rev Genet*, 1, 57-64.

- ORKIN, S. H. & ZON, L. I. 2008. Hematopoiesis: An Evolving Paradigm for Stem Cell Biology. *Cell*, 132, 631-644.
- OU, X., CHAE, H.-D., WANG, R.-H., SHELLEY, W. C., COOPER, S., TAYLOR, T., KIM, Y.-J., DENG, C.-X., YODER, M. C. & BROXMEYER, H. E. 2011. SIRT1 deficiency compromises mouse embryonic stem cell hematopoietic differentiation, and embryonic and adult hematopoiesis in the mouse. *Blood*, 117, 440-450.
- OYAMA, M., NAGASHIMA, T., SUZUKI, T., KOZUKA-HATA, H., YUMOTO, N., SHIRAIISHI, Y., IKEDA, K., KUROKI, Y., GOTOH, N., ISHIDA, T., INOUE, S., KITANO, H. & OKADA-HATAKEYAMA, M. 2011. Integrated Quantitative Analysis of the Phosphoproteome and Transcriptome in Tamoxifen-resistant Breast Cancer. *Journal of Biological Chemistry*, 286, 818-829.
- PACKER, L. M., RANA, S., HAYWARD, R., O'HARE, T., EIDE, C. A., REBOCHO, A., HEIDORN, S., ZABRISKIE, M. S., NICULESCU-DUVAZ, I., DRUKER, B. J., SPRINGER, C. & MARAIS, R. 2011. Nilotinib and MEK inhibitors induce synthetic lethality through paradoxical activation of RAF in drug-resistant chronic myeloid leukemia. *Cancer cell*, 20, 715-727.
- PANKIV, S., CLAUSEN, T. H., LAMARK, T., BRECH, A., BRUUN, J.-A., OUTZEN, H., ØVERVATN, A., BJØRKØY, G. & JOHANSEN, T. 2007. p62/SQSTM1 Binds Directly to Atg8/LC3 to Facilitate Degradation of Ubiquitinated Protein Aggregates by Autophagy. *Journal of Biological Chemistry*, 282, 24131-24145.
- PARK, I.-K., QIAN, D., KIEL, M., BECKER, M. W., PIHALJA, M., WEISSMAN, I. L., MORRISON, S. J. & CLARKE, M. F. 2003. Bmi-1 is required for maintenance of adult self-renewing haematopoietic stem cells. *Nature*, 423, 302-305.
- PARK, S. O., WAMSLEY, H. L., BAE, K., HU, Z., LI, X., CHOE, S.-W., SLAYTON, W. B., OH, S. P., WAGNER, K.-U. & SAYESKI, P. P. 2013. Conditional Deletion of Jak2 Reveals an Essential Role in Hematopoiesis throughout Mouse Ontogeny: Implications for Jak2 Inhibition in Humans. *PLoS ONE*, 8, e59675.
- PAUSE, A., BELSHAM, G. J., GINGRAS, A.-C., DONZE, O., LIN, T.-A., LAWRENCE, J. C. & SONENBERG, N. 1994. Insulin-dependent stimulation of protein synthesis by phosphorylation of a regulator of 5'-cap function. *Nature*, 371, 762-767.
- PAWSON, T. 1995. Protein modules and signalling networks. *Nature*, 373, 573-580.
- PELLICANO, F., SCOTT, M. T., HELGASON, G. V., HOPCROFT, L. E. M., ALLAN, E. K., ASPINALL-O'DEA, M., COPLAND, M., PIERCE, A., HUNTLY, B. J. P., WHETTON, A. D. & HOLYOAKE, T. L. 2014. The Antiproliferative Activity of Kinase Inhibitors in Chronic Myeloid Leukemia Cells Is Mediated by FOXO Transcription Factors. *STEM CELLS*, 32, 2324-2337.
- PENDERGAST, A. M., MULLER, A. J., HAVLIK, M. H., MARU, Y. & WITTE, O. N. 1991. BCR sequences essential for transformation by the BCR-ABL oncogene bind to the ABL SH2 regulatory domain in a non-phosphotyrosine-dependent manner. *Cell*, 66, 161-171.
- PENDERGAST, A. M., QUILLIAM, L. A., CRIPE, L. D., BASSING, C. H., DAI, Z., LI, N., BATZER, A., RABUN, K. M., DER, C. J., SCHLESSINGER, J. & GISHIZKY, M. L. BCR-ABL-induced oncogenesis is mediated by direct interaction with the SH2 domain of the GRB-2 adaptor protein. *Cell*, 75, 175-185.
- PENG, B., HAYES, M., RESTA, D., RACINE-POON, A., DRUKER, B. J., TALPAZ, M., SAWYERS, C. L., ROSAMILIA, M., FORD, J., LLOYD, P. & CAPDEVILLE, R. 2004. Pharmacokinetics and Pharmacodynamics of Imatinib in a Phase I Trial With Chronic Myeloid Leukemia Patients. *Journal of Clinical Oncology*, 22, 935-942.
- PERROTTI, D., JAMIESON, C., GOLDMAN, J. & SKORSKI, T. Chronic myeloid leukemia: mechanisms of blastic transformation. *The Journal of Clinical Investigation*, 120, 2254-2264.
- PETERSON, R. T. & SCHREIBER, S. L. 1998. Translation control: Connecting mitogens and the ribosome. *Current Biology*, 8, R248-R250.
- PICARD, S., TITIER, K., ETIENNE, G., TEILHET, E., DUCINT, D., BERNARD, M.-A., LASSALLE, R., MARIT, G., REIFFERS, J., BEGAUD, B., MOORE, N., MOLIMARD, M. & MAHON, F.-X. 2007. Trough imatinib plasma levels are associated with both cytogenetic and molecular responses to standard-dose imatinib in chronic myeloid leukemia. *Blood*, 109, 3496.
- PIETARINEN, P. O., PEMOVSKA, T., KONTRO, M., YADAV, B., MPINDI, J. P., ANDERSSON, E. I., MAJUMDER, M. M., KUUSANMAKI, H., KOSKENVESA, P., KALLIONIEMI, O., WENNERBERG, K., HECKMAN, C. A., MUSTJOKI, S. & PORKKA, K. 2015. Novel drug candidates for blast phase chronic myeloid leukemia from high-throughput drug sensitivity and resistance testing. *Blood Cancer Journal*, 5, e309.
- PIETRAS, E. M., WARR, M. R. & PASSEGUÉ, E. 2011. Cell cycle regulation in hematopoietic stem cells. *The Journal of Cell Biology*, 195, 709-720.
- PRINCE, H. M. & DICKINSON, M. 2012. Romidepsin for Cutaneous T-cell Lymphoma. *Clinical Cancer Research*, 18, 3509.

- PUIL, L., LIU, J., GISH, G., MBAMALU, G., BOWTELL, D., PELICCI, P. G., ARLINGHAUS, R. & PAWSON, T. 1994. Bcr-Abl oncoproteins bind directly to activators of the Ras signalling pathway. *The EMBO Journal*, 13, 764-773.
- PULLEN, N., DENNIS, P. B., ANDJELKOVIC, M., DUFNER, A., KOZMA, S. C., HEMMING, B. A. & THOMAS, G. 1998. Phosphorylation and Activation of p70s6k by PDK1. *Science*, 279, 707-710.
- PUTTINI, M., COLUCCIA, A. M. L., BOSCHELLI, F., CLERIS, L., MARCHESI, E., DONELLA-DEANA, A., AHMED, S., REDAELLI, S., PIAZZA, R., MAGISTRONI, V., ANDREONI, F., SCAPOZZA, L., FORMELLI, F. & GAMBACORTI-PASSERINI, C. 2006. In vitro and In vivo Activity of SKI-606, a Novel Src-Abl Inhibitor, against Imatinib-Resistant Bcr-Abl+ Neoplastic Cells. *Cancer Research*, 66, 11314-11322.
- QIAN, H., BUZA-VIDAS, N., HYLAND, C. D., JENSEN, C. T., ANTONCHUK, J., MÅNSSON, R., THOREN, L. A., EKBLUM, M., ALEXANDER, W. S. & JACOBSEN, S. E. W. 2007. Critical Role of Thrombopoietin in Maintaining Adult Quiescent Hematopoietic Stem Cells. *Cell Stem Cell*, 1, 671-684.
- QU, X., YU, J., BHAGAT, G., FURUYA, N., HIBSHOOSH, H., TROXEL, A., ROSEN, J., ESKELINEN, E.-L., MIZUSHIMA, N., OHSUMI, Y., CATTORETTI, G. & LEVINE, B. 2003. Promotion of tumorigenesis by heterozygous disruption of the beclin 1 autophagy gene. *Journal of Clinical Investigation*, 112, 1809-1820.
- QUENTMEIER, H., EBERTH, S., ROMANI, J., ZABORSKI, M. & DREXLER, H. G. 2011. BCR-ABL1-independent PI3Kinase activation causing imatinib-resistance. *Journal of Hematology & Oncology*, 4, 6-6.
- RAAIJMAKERS, M. H. G. P. 2007. ATP-binding-cassette transporters in hematopoietic stem cells and their utility as therapeutic targets in acute and chronic myeloid leukemia. *Leukemia*, 21, 2094-2102.
- RADICH, J. P., DAI, H., MAO, M., OEHLER, V., SCHELTER, J., DRUKER, B., SAWYERS, C., SHAH, N., STOCK, W., WILLMAN, C. L., FRIEND, S. & LINSLEY, P. S. 2006. Gene expression changes associated with progression and response in chronic myeloid leukemia. *Proceedings of the National Academy of Sciences of the United States of America*, 103, 2794-2799.
- RAITANO, A. B., HALPERN, J. R., HAMBUCH, T. M. & SAWYERS, C. L. 1995. The Bcr-Abl leukemia oncogene activates Jun kinase and requires Jun for transformation. *Proceedings of the National Academy of Sciences of the United States of America*, 92, 11746-11750.
- RAJALINGAM, K., SCHRECK, R., RAPP, U. R. & ALBERT, Š. 2007. Ras oncogenes and their downstream targets. *Biochimica et Biophysica Acta (BBA) - Molecular Cell Research*, 1773, 1177-1195.
- RAMALINGAM, S. S., KUMMAR, S., SARANTOPOULOS, J., SHIBATA, S., LORUSSO, P., YERK, M., HOLLERAN, J., LIN, Y., BEUMER, J. H., HARVEY, R. D., IVY, S. P., BELANI, C. P. & EGORIN, M. J. 2010. Phase I Study of Vorinostat in Patients With Advanced Solid Tumors and Hepatic Dysfunction: A National Cancer Institute Organ Dysfunction Working Group Study. *Journal of Clinical Oncology*, 28, 4507-4512.
- RAY, A., COWAN-JACOB, S. W., MANLEY, P. W., MESTAN, J. & GRIFFIN, J. D. 2007. Identification of BCR-ABL point mutations conferring resistance to the Abl kinase inhibitor AMN107 (nilotinib) by a random mutagenesis study. *Blood*, 109, 5011-5015.
- REGGIORI, F. & KLIONSKY, D. J. 2002. Autophagy in the Eukaryotic Cell. *Eukaryotic Cell*, 1, 11-21.
- REMSING RIX, L. L., RIX, U., COLINGE, J., HANTSCH, O., BENNETT, K. L., STRANZL, T., MULLER, A., BAUMGARTNER, C., VALENT, P., AUGUSTIN, M., TILL, J. H. & SUPERTI-FURGA, G. 2008. Global target profile of the kinase inhibitor bosutinib in primary chronic myeloid leukemia cells. *Leukemia*, 23, 477-485.
- REN, R. 2005. Mechanisms of BCR-ABL in the pathogenesis of chronic myelogenous leukaemia. *Nat Rev Cancer*, 5, 172-183.
- REUTHER, G. W., FU, H., CRIPE, L. D., COLLIER, R. J. & PENDERGAST, A. M. 1994. Association of the protein kinases c-Bcr and Bcr-Abl with proteins of the 14-3-3 family. *Science*, 266, 129-133.
- REXER, B. N., HAM, A. J. L., RINEHART, C., HILL, S., DE MATOS GRANJA-INGRAM, N., GONZALEZ-ANGULO, A. M., MILLS, G. B., DAVE, B., CHANG, J. C., LIEBLER, D. C. & ARTEAGA, C. L. 2011. Phosphoproteomic mass spectrometry profiling links Src family kinases to escape from HER2 tyrosine kinase inhibition. *Oncogene*, 30, 4163-4174.
- REYA, T., MORRISON, S. J., CLARKE, M. F. & WEISSMAN, I. L. 2001. Stem cells, cancer, and cancer stem cells. *Nature*, 414, 105-111.
- RINGSHAUSEN, I., SCHNELLER, F., BOGNER, C., HIPPEL, S., DUYSER, J., PESCHEL, C. & DECKER, T. 2002. Constitutively activated phosphatidylinositol-3 kinase (PI-3K) is involved in the defect of apoptosis in B-CLL: association with protein kinase C δ . *Blood*, 100, 3741-3748.
- ROMAN-GOMEZ, J., CASTILLEJO, J. A., JIMENEZ, A., CERVANTES, F., BOQUE, C., HERMOSIN, L., LEON, A., GRAÑENA, A., COLOMER, D., HEINIGER, A. & TORRES, A. 2003. Cadherin-13, a Mediator of Calcium-Dependent Cell-Cell Adhesion, Is Silenced by Methylation in Chronic Myeloid Leukemia and Correlates With Pretreatment Risk Profile and Cytogenetic Response to Interferon Alfa. *Journal of Clinical Oncology*, 21, 1472-1479.

- ROMAN-GOMEZ, J., JIMENEZ-VELASCO, A., AGIRRE, X., CASTILLEJO, J. A., NAVARRO, G., SAN JOSE-ENERIZ, E., GARATE, L., CORDEU, L., CERVANTES, F., PROSPER, F., HEINIGER, A. & TORRES, A. 2008. Repetitive DNA hypomethylation in the advanced phase of chronic myeloid leukemia. *Leukemia Research*, 32, 487-490.
- ROSENFELDT, M. T. & RYAN, K. M. 2009. The role of autophagy in tumour development and cancer therapy. *Expert Reviews in Molecular Medicine*, 11, e36.
- ROSS, D. M., BRANFORD, S., SEYMOUR, J. F., SCHWARER, A. P., ARTHUR, C., YEUNG, D. T., DANG, P., GOYNE, J. M., SLADER, C., FILSHIE, R. J., MILLS, A. K., MELO, J. V., WHITE, D. L., GRIGG, A. P. & HUGHES, T. P. 2013. Safety and efficacy of imatinib cessation for CML patients with stable undetectable minimal residual disease: results from the TWISTER study. *Blood*, 122, 515-522.
- ROWLEY, J. D. 1973. A New Consistent Chromosomal Abnormality in Chronic Myelogenous Leukaemia identified by Quinacrine Fluorescence and Giemsa Staining. *Nature*, 243, 290-293.
- ROWLEY, J. D. 1975. Nonrandom chromosomal abnormalities in hematologic disorders of man. *Proceedings of the National Academy of Sciences of the United States of America*, 72, 152-156.
- RUBIN, E. H., AGRAWAL, N. G. B., FRIEDMAN, E. J., SCOTT, P., MAZINA, K. E., SUN, L., DU, L., RICKER, J. L., FRANKEL, S. R., GOTTESDIENER, K. M., WAGNER, J. A. & IWAMOTO, M. 2006. A Study to Determine the Effects of Food and Multiple Dosing on the Pharmacokinetics of Vorinostat Given Orally to Patients with Advanced Cancer. *Clinical Cancer Research*, 12, 7039.
- SALESSE, S. & VERFAILLIE, C. M. 2002. BCR/ABL: from molecular mechanisms of leukemia induction to treatment of chronic myelogenous leukemia. *Oncogene*, 21, 8547-8559.
- SALGIA, R., LI, J. L., EWANIUK, D. S., PEAR, W., PISICK, E., BURKY, S. A., ERNST, T., SATTLER, M., CHEN, L. B. & GRIFFIN, J. D. 1997. BCR/ABL induces multiple abnormalities of cytoskeletal function. *Journal of Clinical Investigation*, 100, 46-57.
- SALGIA, R., UEMURA, N., OKUDA, K., LI, J.-L., PISICK, E., SATTLER, M., DE JONG, R., DRUKER, B., HEISTERKAMP, N., CHEN, L. B., GROFFEN, J. & GRIFFIN, J. D. 1995. CRKL Links p210BCR/ABL with Paxillin in Chronic Myelogenous Leukemia Cells. *Journal of Biological Chemistry*, 270, 29145-29150.
- SALOMONI, P. & CALABRETTA, B. 2009. Targeted therapies and autophagy: new insights from chronic myeloid leukemia. *Autophagy*, 5, 1050-1051.
- SANDRA, W. C.-J., VALERIE, G., GABRIELE, F., JAMES, D. G., DORIANO, F., PASCAL, F., JANIS, L., JURGEN, M. & PAUL, W. M. 2004. Imatinib (STI571) Resistance in Chronic Myelogenous Leukemia: Molecular Basis of the Underlying Mechanisms and Potential Strategies for Treatment. *Mini-Reviews in Medicinal Chemistry*, 4, 285-299.
- SANJANA, N. E., SHALEM, O. & ZHANG, F. 2014. Improved vectors and genome-wide libraries for CRISPR screening. *Nat Meth*, 11, 783-784.
- SARBASSOV, D. D., GUERTIN, D. A., ALI, S. M. & SABATINI, D. M. 2005. Phosphorylation and Regulation of Akt/PKB by the Rictor-mTOR Complex. *Science*, 307, 1098-1101.
- SATTLER, M., MOHI, M. G., PRIDE, Y. B., QUINNAN, L. R., MALOUF, N. A., PODAR, K., GESBERT, F., IWASAKI, H., LI, S., VAN ETEN, R. A., GU, H., GRIFFIN, J. D. & NEEL, B. G. 2002a. Critical role for Gab2 in transformation by BCR/ABL. *Cancer Cell*, 1, 479-492.
- SATTLER, M., PRIDE, Y. B., QUINNAN, L. R., VERMA, S., MALOUF, N. A., HUSSON, H., SALGIA, R., LIPKOWITZ, S. & GRIFFIN, J. D. 2002b. Differential expression and signaling of CBL and CBL-B in BCR/ABL transformed cells. *Oncogene*, 21, 1423-1433.
- SATTLER, M., SALGIA, R., SHRIKHANDE, G., VERMA, S., PISICK, E., PRASAD, K. V. S. & GRIFFIN, J. D. 1997. Steel Factor Induces Tyrosine Phosphorylation of CRKL and Binding of CRKL to a Complex Containing c-Kit, Phosphatidylinositol 3-Kinase, and p120CBL. *Journal of Biological Chemistry*, 272, 10248-10253.
- SATTLER, M., VERMA, S., SHRIKHANDE, G., BYRNE, C. H., PRIDE, Y. B., WINKLER, T., GREENFIELD, E. A., SALGIA, R. & GRIFFIN, J. D. 2000. The BCR/ABL Tyrosine Kinase Induces Production of Reactive Oxygen Species in Hematopoietic Cells. *Journal of Biological Chemistry*, 275, 24273-24278.
- SAWADA, M., SUN, W., HAYES, P., LESKOV, K., BOOTHMAN, D. A. & MATSUYAMA, S. 2003. Ku70 suppresses the apoptotic translocation of Bax to mitochondria. *Nat Cell Biol*, 5, 320-329.
- SAWYERS, C. L. 1993. Molecular Consequences of the BCR-ABL Translocation in Chronic Myelogenous Leukemia. *Leukemia & Lymphoma*, 11, 101-103.
- SAWYERS, C. L. 1999. Chronic Myeloid Leukemia. *New England Journal of Medicine*, 340, 1330-1340.
- SAWYERS, C. L., HOCHHAUS, A., FELDMAN, E., GOLDMAN, J. M., MILLER, C. B., OTTMANN, O. G., SCHIFFER, C. A., TALPAZ, M., GUILHOT, F., DEININGER, M. W. N., FISCHER, T., O'BRIEN, S. G., STONE, R. M., GAMBACORTI-PASSERINI, C. B., RUSSELL, N. H., REIFFERS, J. J., SHEA, T. C., CHAPUIS, B., COUTRE, S., TURA, S., MORRA, E., LARSON, R. A., SAVEN, A., PESCHEL, C., GRATWOHL, A., MANDELLI, F., BEN-AM, M., GATHMANN, I., CAPDEVILLE, R., PAQUETTE, R. L. & DRUKER, B. J. 2002. Imatinib induces hematologic

- and cytogenetic responses in patients with chronic myelogenous leukemia in myeloid blast crisis: results of a phase II study. *Blood*, 99, 3530-3539.
- SAWYERS, C. L., MCLAUGHLIN, J., GOGA, A., HAVLIK, M. & WITTE, O. 1994. The nuclear tyrosine kinase c-abl negatively regulates cell growth. *Cell*, 77, 121-131.
- SCHEMIONEK, M., HERRMANN, O., REHER, M. M., CHATAIN, N., SCHUBERT, C., COSTA, I. G., HANZELMANN, S., GUSMAO, E. G., KINTSLER, S., BRAUNSCHWEIG, T., HAMILTON, A., HELGASON, G. V., COPLAND, M., SCHWAB, A., MULLER-TIDOW, C., LI, S., HOLYOAKE, T. L., BRUMMENDORF, T. H. & KOSCHMIEDER, S. 2016. Mts1 is a critical epigenetically regulated tumor suppressor in CML. *Leukemia*, 30, 823-832.
- SCHEPERS, K., PIETRAS, E. M., REYNAUD, D., FLACH, J., BINNEWIES, M., GARG, T., WAGERS, A. J., HSIAO, E. C. & PASSEGUÉ, E. 2013. Myeloproliferative Neoplasia Remodels the Endosteal Bone Marrow Niche into a Self-Reinforcing Leukemic Niche. *Cell stem cell*, 13, 285-299.
- SCHINDLER, T., BORNMANN, W., PELLICENA, P., MILLER, W. T., CLARKSON, B. & KURIYAN, J. 2000. Structural Mechanism for STI-571 Inhibition of Abelson Tyrosine Kinase. *Science*, 289, 1938-1942.
- SCHOFIELD, R. 1978. The relationship between the spleen colony-forming cell and the haemopoietic stem cell. *Blood cells*, 4, 7-25.
- SCHULTHEIS, B., CARAPETI-MAROOTIAN, M., HOCHHAUS, A., WEIBER, A., GOLDMAN, J. M. & MELO, J. V. 2002. Overexpression of SOCS-2 in advanced stages of chronic myeloid leukemia: possible inadequacy of a negative feedback mechanism. *Blood*, 99, 1766-1775.
- SENN, N. 1903. Therapeutical value of Roentgen ray in treatment of pseudoleukaemia. *NY Med J*, 77, 665.
- SHAH, N. P., NICOLL, J. M., NAGAR, B., GORRE, M. E., PAQUETTE, R. L., KURIYAN, J. & SAWYERS, C. L. 2002. Multiple BCR-ABL kinase domain mutations confer polyclonal resistance to the tyrosine kinase inhibitor imatinib (STI571) in chronic phase and blast crisis chronic myeloid leukemia. *Cancer Cell*, 2, 117-125.
- SHAH, N. P., SKAGGS, B. J., BRANFORD, S., HUGHES, T. P., NICOLL, J. M., PAQUETTE, R. L. & SAWYERS, C. L. Sequential ABL kinase inhibitor therapy selects for compound drug-resistant BCR-ABL mutations with altered oncogenic potency. *The Journal of Clinical Investigation*, 117, 2562-2569.
- SHAH, N. P., TRAN, C., LEE, F. Y., CHEN, P., NORRIS, D. & SAWYERS, C. L. 2004. Overriding Imatinib Resistance with a Novel ABL Kinase Inhibitor. *Science*, 305, 399-401.
- SHALEM, O., SANJANA, N. E., HARTENIAN, E., SHI, X., SCOTT, D. A., MIKKELSEN, T. S., HECKL, D., EBERT, B. L., ROOT, D. E., DOENCH, J. G. & ZHANG, F. 2014. Genome-Scale CRISPR-Cas9 Knockout Screening in Human Cells. *Science*, 343, 84-87.
- SHANHAI XIE, H. L., TONG SUN AND RALPH B ARLINGHAUS 2002. Jak2 is involved in c-Myc induction by Bcr-Abl. *Oncogene*, 21, 7137-7146.
- SHANHAI XIE, Y. W., JIAXIN LIU, TONG SUN, MATTHEW B WILSON, THOMAS E SMITHGALL AND RALPH B ARLINGHAUS 2001. Involvement of Jak2 tyrosine phosphorylation in Bcr-Abl transformation. *Oncogene*, 20, 6188-6195.
- SHINGO DAN, M. N., TAKASHI TSURUO 1998. Selective induction of apoptosis in Philadelphia chromosome-positive chronic myelogenous leukemia cells by an inhibitor of BCR-ABL tyrosine kinase, CGP 57148. *Cell Death & Differentiation*, 5, 710-715.
- SHRIVASTAV, M., DE HARO, L. P. & NICKOLOFF, J. A. 2008. Regulation of DNA double-strand break repair pathway choice. *Cell Res*, 18, 134-147.
- SHUKLA, S., MACLENNAN, G. T., HARTMAN, D. J., FU, P., RESNICK, M. I. & GUPTA, S. 2007. Activation of PI3K-Akt signaling pathway promotes prostate cancer cell invasion. *International Journal of Cancer*, 121, 1424-1432.
- SHUNSUKE KIMURA, T. N., TAMOTSU YOSHIMORI 2007. Dissection of the Autophagosome Maturation Process by a Novel Reporter Protein, Tandem Fluorescent-Tagged LC3. *Autophagy*, 3, 452-460.
- SILLABER, C., MAYERHOFER, M., BÖHM, A., VALES, A., GRUZE, A., AICHBERGER, K. J., ESTERBAUER, H., PFEILSTÖCKER, M., SPERR, W. R., PICKL, W. F., HAAS, O. A. & VALENT, P. 2008. Evaluation of antileukaemic effects of rapamycin in patients with imatinib-resistant chronic myeloid leukaemia. *European Journal of Clinical Investigation*, 38, 43-52.
- SIMONSEN, A. & TOOZE, S. A. 2009. Coordination of membrane events during autophagy by multiple class III PI3-kinase complexes. *The Journal of Cell Biology*, 186, 773-782.
- SIMSEK, T., KOCABAS, F., ZHENG, J., DEBERARDINIS, R. J., MAHMOUD, A. I., OLSON, E. N., SCHNEIDER, J. W., ZHANG, C. C. & SADEK, H. A. 2010. The Distinct Metabolic Profile of Hematopoietic Stem Cells Reflects Their Location in a Hypoxic Niche. *Cell Stem Cell*, 7, 380-390.
- SKORSKI, T., BELLACOSA, A., NIEBOROWSKA-SKORSKA, M., MAJEWSKI, M., MARTINEZ, R., CHOI, J. K., TROTTA, R., WLODARSKI, P., PERROTTI, D., CHAN, T. O., WASIK, M. A., TSICHLIS, P. N. & CALABRETTA, B. 1997. Transformation of hematopoietic cells by BCR/ABL requires activation of a PI-3k/Akt-dependent pathway. *The EMBO Journal*, 16, 6151-6161.

- SKORSKI, T., KANAKARAJ, P., NIEBOROWSKA-SKORSKA, M., RATAJCZAK, M. Z., WEN, S. C., ZON, G., GEWIRTZ, A. M., PERUSSIA, B. & CALABRETTA, B. 1995a. Phosphatidylinositol-3 kinase activity is regulated by BCR/ABL and is required for the growth of Philadelphia chromosome-positive cells. *Blood*, 86, 726-736.
- SKORSKI, T., KANAKARAJ, P., NIEBOROWSKA-SKORSKA, M., RATAJCZAK, M. Z., WEN, S. C., ZON, G., GEWIRTZ, A. M., PERUSSIA, B. & CALABRETTA, B. 1995b. Phosphatidylinositol-3 kinase activity is regulated by BCR/ABL and is required for the growth of Philadelphia chromosome-positive cells. *Blood*, 86, 726.
- SMITH, A. G., PAINTER, D., HOWELL, D. A., EVANS, P., SMITH, G., PATMORE, R., JACK, A. & ROMAN, E. 2014. Determinants of survival in patients with chronic myeloid leukaemia treated in the new era of oral therapy: findings from a UK population-based patient cohort. *BMJ Open*, 4.
- SOLOMON, V. R. & LEE, H. 2009. Chloroquine and its analogs: A new promise of an old drug for effective and safe cancer therapies. *European Journal of Pharmacology*, 625, 220-233.
- SOVERINI, S., HOCHHAUS, A., NICOLINI, F. E., GRUBER, F., LANGE, T., SAGLIO, G., PANE, F., MÜLLER, M. C., ERNST, T., ROSTI, G., PORKKA, K., BACCARANI, M., CROSS, N. C. P. & MARTINELLI, G. 2011. BCR-ABL kinase domain mutation analysis in chronic myeloid leukemia patients treated with tyrosine kinase inhibitors: recommendations from an expert panel on behalf of European LeukemiaNet. *Blood*, 118, 1208-1215.
- SOVERINI, S., MARTINELLI, G., ROSTI, G., BASSI, S., AMABILE, M., POERIO, A., GIANNINI, B., TRABACCHI, E., CASTAGNETTI, F., TESTONI, N., LUATTI, S., DE VIVO, A., CILLONI, D., IZZO, B., FAVA, M., ABRUZZESE, E., ALBERTI, D., PANE, F., SAGLIO, G. & BACCARANI, M. 2005. ABL Mutations in Late Chronic Phase Chronic Myeloid Leukemia Patients With Up-Front Cytogenetic Resistance to Imatinib Are Associated With a Greater Likelihood of Progression to Blast Crisis and Shorter Survival: A Study by the GIMEMA Working Party on Chronic Myeloid Leukemia. *Journal of Clinical Oncology*, 23, 4100-4109.
- SPIERS, A. S. & BAIKIE, A. G. 1968. Cytogenetic evolution and clonal proliferation in acute transformation of chronic granulocytic leukaemia. *British Journal of Cancer*, 22, 192-204.
- SPIERS, A. S. D. 1979. METAMORPHOSIS OF CHRONIC GRANULOCYTIC LEUKAEMIA: DIAGNOSIS, CLASSIFICATION, AND MANAGEMENT. *British Journal of Haematology*, 41, 1-7.
- STAAL, S. P. 1987. Molecular cloning of the akt oncogene and its human homologues AKT1 and AKT2: amplification of AKT1 in a primary human gastric adenocarcinoma. *Proceedings of the National Academy of Sciences of the United States of America*, 84, 5034-5037.
- STABER, PHILIPP B., ZHANG, P., YE, M., WELNER, R. S., NOMBELA-ARRIETA, C., BACH, C., KERENYI, M., BARTHOLDY, BORIS A., ZHANG, H., ALBERICH-JORDÀ, M., LEE, S., YANG, H., NG, F., ZHANG, J., LEDDIN, M., SILBERSTEIN, LESLIE E., HOEFLER, G., ORKIN, STUART H., GÖTTGENS, B., ROSENBAUER, F., HUANG, G. & TENEN, DANIEL G. 2013. Sustained PU.1 Levels Balance Cell-Cycle Regulators to Prevent Exhaustion of Adult Hematopoietic Stem Cells. *Molecular Cell*, 49, 934-946.
- STERNBERG, S. H., REDDING, S., JINEK, M., GREENE, E. C. & DOUDNA, J. A. 2014. DNA interrogation by the CRISPR RNA-guided endonuclease Cas9. *Nature*, 507, 62-67.
- STOKLOSA, T., POPLAWSKI, T., KOPTYRA, M., NIEBOROWSKA-SKORSKA, M., BASAK, G., SŁUPIANEK, A., RAYEVSKAYA, M., SEFERYNSKA, I., HERRERA, L., BLASIAK, J. & SKORSKI, T. 2008. BCR/ABL Inhibits Mismatch Repair to Protect from Apoptosis and Induce Point Mutations. *Cancer Research*, 68, 2576-2580.
- STRATHDEE, G., HOLYOAKE, T. L., SIM, A., PARKER, A., OSCIER, D. G., MELO, J. V., MEYER, S., EDEN, T., DICKINSON, A. M., MOUNTFORD, J. C., JORGENSEN, H. G., SOUTAR, R. & BROWN, R. 2007. Inactivation of HOXA Genes by Hypermethylation in Myeloid and Lymphoid Malignancy is Frequent and Associated with Poor Prognosis. *American Association for Cancer Research*, 13, 5048-5055.
- SUDA, T., TAKUBO, K. & SEMENZA, GREGG L. 2011. Metabolic Regulation of Hematopoietic Stem Cells in the Hypoxic Niche. *Cell Stem Cell*, 9, 298-310.
- SUNAYAMA, J., MATSUDA, K.-I., SATO, A., TACHIBANA, K., SUZUKI, K., NARITA, Y., SHIBUI, S., SAKURADA, K., KAYAMA, T., TOMIYAMA, A. & KITANAKA, C. 2010. Crosstalk Between the PI3K/mTOR and MEK/ERK Pathways Involved in the Maintenance of Self-Renewal and Tumorigenicity of Glioblastoma Stem-Like Cells. *STEM CELLS*, 28, 1930-1939.
- SWARTS, D. C., MOSTERD, C., VAN PASSEL, M. W. J. & BROUNS, S. J. J. 2012. CRISPR Interference Directs Strand Specific Spacer Acquisition. *PLoS ONE*, 7, e35888.
- TAKAMURA, A., KOMATSU, M., HARA, T., SAKAMOTO, A., KISHI, C., WAGURI, S., EISHI, Y., HINO, O., TANAKA, K. & MIZUSHIMA, N. 2011. Autophagy-deficient mice develop multiple liver tumors. *Genes & Development*, 25, 795-800.
- TAKUBO, K., GODA, N., YAMADA, W., IRIUCHISHIMA, H., IKEDA, E., KUBOTA, Y., SHIMA, H., JOHNSON, R. S., HIRAO, A., SUEMATSU, M. & SUDA, T. 2010. Regulation of the HIF-1 α Level Is Essential for Hematopoietic Stem Cells. *Cell Stem Cell*, 7, 391-402.

- TALPAZ, M., MCCREDIE, K. B., MAVLIGIT, G. M. & GUTTERMAN, J. U. 1983. Leukocyte interferon-induced myeloid cytoreduction in chronic myelogenous leukemia. *Blood*, 62, 689-692.
- TALPAZ, M., SHAH, N. P., KANTARJIAN, H., DONATO, N., NICOLL, J., PAQUETTE, R., CORTES, J., O'BRIEN, S., NICAISE, C., BLEICKARDT, E., BLACKWOOD-CHIRCHIR, M. A., IYER, V., CHEN, T.-T., HUANG, F., DECILLIS, A. P. & SAWYERS, C. L. 2006. Dasatinib in Imatinib-Resistant Philadelphia Chromosome-Positive Leukemias. *New England Journal of Medicine*, 354, 2531-2541.
- TALPAZ, M., SILVER, R. T., DRUKER, B. J., GOLDMAN, J. M., GAMBACORTI-PASSERINI, C., GUILHOT, F., SCHIFFER, C. A., FISCHER, T., DEININGER, M. W. N., LENNARD, A. L., HOCHHAUS, A., OTTMANN, O. G., GRATWOHL, A., BACCARANI, M., STONE, R., TURA, S., MAHON, F.-X., FERNANDES-REESE, S., GATHMANN, I., CAPDEVILLE, R., KANTARJIAN, H. M. & SAWYERS, C. L. 2002. Imatinib induces durable hematologic and cytogenetic responses in patients with accelerated phase chronic myeloid leukemia: results of a phase 2 study. *Blood*, 99, 1928-1937.
- TANG, C., SCHAFRANEK, L., WATKINS, D. B., PARKER, W. T., MOORE, S., PRIME, J. A., WHITE, D. L. & HUGHES, T. P. 2011. Tyrosine kinase inhibitor resistance in chronic myeloid leukemia cell lines: investigating resistance pathways. *Leukemia & Lymphoma*, 52, 2139-2147.
- TANG, R., FAUSSAT, A.-M., MAJDAK, P., MARZAC, C., DUBRULLE, S., MARJANOVIC, Z., LEGRAND, O. & MARIE, J.-P. 2006. Semisynthetic homoharringtonine induces apoptosis via inhibition of protein synthesis and triggers rapid myeloid cell leukemia-1 down-regulation in myeloid leukemia cells. *American Association for Cancer Research*, 5, 723-731.
- TANIDA, I., MINEMATSU-IKEGUCHI, N., UENO, T. & KOMINAMI, E. 2005. Lysosomal Turnover, but Not a Cellular Level, of Endogenous LC3 is a Marker for Autophagy. *Autophagy*, 1, 84-91.
- TAVIAN, M., ROBIN, C., COULOMBEL, L. & PÉAULT, B. 2001. The Human Embryo, but Not Its Yolk Sac, Generates Lympho-Myeloid Stem Cells: Mapping Multipotent Hematopoietic Cell Fate in Intraembryonic Mesoderm. *Immunity*, 15, 487-495.
- TEACHEY, D. T., GRUPP, S. A. & BROWN, V. I. 2009. mTOR Inhibitors and Their Potential Role in Therapy in Leukemia and Other Haematologic Malignancies. *British journal of haematology*, 145, 569-580.
- TEN HOEVE, J., ARLINGHAUS, R. B., GUO, J. Q., HEISTERKAMP, N. & GROFFEN, J. 1994. Tyrosine phosphorylation of CRKL in Philadelphia+ leukemia. *Blood*, 84, 1731-1736.
- THOMAS, J., WANG, L., CLARK, R. E. & PIRMOHAMED, M. 2004. Active transport of imatinib into and out of cells: implications for drug resistance. *Blood*, 104, 3739.
- THOMAS, O., HARE, ZABRISKIE, M. S., EIDE, C. A., VELLORE, N. A., DRUKER, B. J. & DEININGER, M. W. 2015. Bull's-Eyes and Blind Spots: Pre-Clinical Studies with the Allosteric Inhibitor ABL001 in BCR-ABL1 Compound Mutation-Based Resistance. *Blood*, 126, 1565.
- TOKARSKI, J. S., NEWITT, J. A., CHANG, C. Y. J., CHENG, J. D., WITTEKIND, M., KIEFER, S. E., KISH, K., LEE, F. Y. F., BORZILLERRI, R., LOMBARDO, L. J., XIE, D., ZHANG, Y. & KLEI, H. E. 2006. The Structure of Dasatinib (BMS-354825) Bound to Activated ABL Kinase Domain Elucidates Its Inhibitory Activity against Imatinib-Resistant ABL Mutants. *Cancer Research*, 66, 5790-5797.
- TOOZE, S. A. & YOSHIMORI, T. 2010. The origin of the autophagosomal membrane. *Nat Cell Biol*, 12, 831-835.
- TROTTA, R., VIGNUDELLI, T., CANDINI, O., INTINE, R. V., PECORARI, L., GUERZONI, C., SANTILLI, G., BYROM, M. W., GOLDONI, S., FORD, L. P., CALIGIURI, M. A., MARAIA, R. J., PERROTTI, D. & CALABRETTA, B. 2003. BCR/ABL activates mdm2 mRNA translation via the La antigen. *Cancer Cell*, 3, 145-160.
- VAN ETTEN, R. A. 1999. Cycling, stressed-out and nervous: cellular functions of c-Abl. *Trends in Cell Biology*, 9, 179-186.
- VANHAESEBROECK, B., LEEVERS, S. J., AHMADI, K., TIMMS, J., KATSO, R., DRISCOLL, P. C., WOSCHOLSKI, R., PARKER, P. J. & WATERFIELD, M. D. 2001. Synthesis and Function of 3-Phosphorylated Inositol Lipids. *Annual Review of Biochemistry*, 70, 535-602.
- VARNUM-FINNEY, B., PURTON, L. E., YU, M., BRASHEM-STEIN, C., FLOWERS, D., STAATS, S., MOORE, K. A., LE ROUX, I., MANN, R., GRAY, G., ARTAVANIS-TSAKONAS, S. & BERNSTEIN, I. D. 1998. The Notch Ligand, Jagged-1, Influences the Development of Primitive Hematopoietic Precursor Cells. *Blood*, 91, 4084-4091.
- VASILIOU, V., VASILIOU, K. & NEBERT, D. W. 2009. Human ATP-binding cassette (ABC) transporter family. *Human Genomics*, 3, 281-290.
- VIATOUR, P., SOMERVILLE, T. C., VENKATASUBRAHMANYAM, S., KOGAN, S., MCLAUGHLIN, M. E., WEISSMAN, I. L., BUTTE, A. J., PASSEGUÉ, E. & SAGE, J. 2008. Hematopoietic Stem Cell Quiescence Is Maintained by Compound Contributions of the Retinoblastoma Gene Family. *Cell Stem Cell*, 3, 416-428.

- VON BUBNOFF, N., SCHNELLER, F., PESCHEL, C. & DUYSSTER, J. 2002. BCR-ABL gene mutations in relation to clinical resistance of Philadelphia-chromosome-positive leukaemia to STI571: a prospective study. *The Lancet*, 359, 487-491.
- WA, P. 1902. Report of cases treated with Roentgen rays. *JAMA*, 38, 911-919.
- WAGLE, M., EIRING, A. M., WONGCHENKO, M., LU, S., GUAN, Y., WANG, Y., LACKNER, M., AMLER, L., HAMPTON, G., DEININGER, M. W., O'HARE, T. & YAN, Y. 2016. A role for FOXO1 in BCR-ABL1-independent tyrosine kinase inhibitor resistance in chronic myeloid leukemia. *Leukemia*, 30, 1493-1501.
- WANDER, S. A., HENNESSY, B. T. & SLINGERLAND, J. M. 2011. Next-generation mTOR inhibitors in clinical oncology: how pathway complexity informs therapeutic strategy. *The Journal of Clinical Investigation*, 121, 1231-1241.
- WANG, C.-W. & KLIONSKY, D. J. 2003. The Molecular Mechanism of Autophagy. *Molecular Medicine*, 9, 65-76.
- WANG, L., GIANNOUDIS, A., LANE, S., WILLIAMSON, P., PIRMOHAMED, M. & CLARK, R. E. 2008. Expression of the Uptake Drug Transporter hOCT1 is an Important Clinical Determinant of the Response to Imatinib in Chronic Myeloid Leukemia. *Clinical Pharmacology & Therapeutics*, 83, 258-264.
- WANG, Y.-L., QIAN, J., LIN, J., YAO, D.-M., QIAN, Z., ZHU, Z.-H. & LI, J.-Y. 2010. Methylation status of DDIT3 gene in Chronic Myeloid Leukemia. *Journal of Experimental & Clinical Cancer Research : CR*, 29, 54-54.
- WARD, A. C., TOUW, I. & YOSHIMURA, A. 2000. The Jak-Stat pathway in normal and perturbed hematopoiesis. *Blood*, 95, 19-29.
- WARMUTH, M., DANHAUSER-RIEDL, S. & HALLEK, M. 1999. Molecular pathogenesis of chronic myeloid leukemia: implications for new therapeutic strategies. *Annals of Hematology*, 78, 49-64.
- WARR, M. R., BINNEWIES, M., FLACH, J., REYNAUD, D., GARG, T., MALHOTRA, R., DEBNATH, J. & PASSEGUE, E. 2013a. FOXO3A directs a protective autophagy program in haematopoietic stem cells. *Nature*, 494, 323-327.
- WARR, M. R., BINNEWIES, M., FLACH, J., REYNAUD, D., GARG, T., MALHOTRA, R., DEBNATH, J. & PASSEGUÉ, E. 2013b. FoxO3a Directs a Protective Autophagy Program in Hematopoietic Stem Cells. *Nature*, 494, 323-327.
- WEISBERG, E. & GRIFFIN, J. D. 2000. Mechanism of resistance to the ABL tyrosine kinase inhibitor STI571 in BCR/ABL-transformed hematopoietic cell lines. *Blood*, 95, 3498-3505.
- WEISBERG, E., MANLEY, P. W., BREITENSTEIN, W., BRÜGGEN, J., COWAN-JACOB, S. W., RAY, A., HUNTLY, B., FABBRO, D., FENDRICH, G., HALL-MEYERS, E., KUNG, A. L., MESTAN, J., DALEY, G. Q., CALLAHAN, L., CATLEY, L., CAVAZZA, C., MOHAMMED, A., NEUBERG, D., WRIGHT, R. D., GILLILAND, D. G. & GRIFFIN, J. D. 2005. Characterization of AMN107, a selective inhibitor of native and mutant Bcr-Abl. *Cancer Cell*, 7, 129-141.
- WELNER, R. S., AMABILE, G., BARARIA, D., CZIBERE, A., YANG, H., ZHANG, H., PONTES, L. L. D. F., YE, M., LEVANTINI, E., RUSCIO, A. D., MARTINELLI, G. & TENEN, D. G. 2015. Treatment of chronic myelogenous leukemia by blocking cytokine alterations found in normal stem and progenitor cells. *Cancer cell*, 27, 671-681.
- WENDEL, H.-G., DE STANCHINA, E., CEPERO, E., RAY, S., EMIG, M., FRIDMAN, J. S., VEACH, D. R., BORNMANN, W. G., CLARKSON, B., MCCOMBIE, W. R., KOGAN, S. C., HOCHHAUS, A. & LOWE, S. W. 2006. Loss of p53 impedes the antileukemic response to BCR-ABL inhibition. *Proceedings of the National Academy of Sciences of the United States of America*, 103, 7444-7449.
- WHITE, D. L., DANG, P., ENGLER, J., FREDE, A., ZRIM, S., OSBORN, M., SAUNDERS, V. A., MANLEY, P. W. & HUGHES, T. P. 2010. Functional Activity of the OCT-1 Protein Is Predictive of Long-Term Outcome in Patients With Chronic-Phase Chronic Myeloid Leukemia Treated With Imatinib. *Journal of Clinical Oncology*, 28, 2761-2767.
- WHITE, D. L., SAUNDERS, V. A., DANG, P., ENGLER, J., VENABLES, A., ZRIM, S., ZANNETTINO, A., LYNCH, K., MANLEY, P. W. & HUGHES, T. 2007. Most CML patients who have a suboptimal response to imatinib have low OCT-1 activity: higher doses of imatinib may overcome the negative impact of low OCT-1 activity. *Blood*, 110, 4064.
- WU, X., SENECHAL, K., NESHAT, M. S., WHANG, Y. E. & SAWYERS, C. L. 1998. The PTEN/MMAC1 tumor suppressor phosphatase functions as a negative regulator of the phosphoinositide 3-kinase/Akt pathway. *Proceedings of the National Academy of Sciences of the United States of America*, 95, 15587-15591.
- WULLSCHLEGER, S., LOEWITH, R. & HALL, M. N. 2006. TOR Signaling in Growth and Metabolism. *Cell*, 124, 471-484.
- WYLIE, A., SCHOEPFER, J., BERELLINI, G., CAI, H., CARAVATTI, G., COTESTA, S., DODD, S., DONOVAN, J., ERB, B., FURET, P., GANGAL, G., GROTZFELD, R., HASSAN, Q., HOOD, T., IYER, V., JACOB, S., JAHNKE, W., LOMBARDO, F., LOO, A., MANLEY, P. W., MARZINZIK, A., PALMER, M., PELLE, X., SALEM, B., SHARMA, S., THOHAN, S., ZHU, S., KEEN, N., PETRUZZELLI, L., VANASSE, K. G. & SELLERS, W. R. 2014. ABL001, a Potent Allosteric

- Inhibitor of BCR-ABL, Prevents Emergence of Resistant Disease When Administered in Combination with Nilotinib in an in Vivo Murine Model of Chronic Myeloid Leukemia. *Blood*, 124, 398-398.
- XIE, Z. & KLIONSKY, D. J. 2007. Autophagosome formation: core machinery and adaptations. *Nat Cell Biol*, 9, 1102-1109.
- YAMADA, Y., SUZUKI, N. N., HANADA, T., ICHIMURA, Y., KUMETA, H., FUJIOKA, Y., OHSUMI, Y. & INAGAKI, F. 2007. The Crystal Structure of Atg3, an Autophagy-related Ubiquitin Carrier Protein (E2) Enzyme that Mediates Atg8 Lipidation. *Journal of Biological Chemistry*, 282, 8036-8043.
- YAN, C.-H., LIANG, Z.-Q., GU, Z.-L., YANG, Y.-P., REID, P. & QIN, Z.-H. 2006. Contributions of autophagic and apoptotic mechanisms to CrTX-induced death of K562 cells. *Toxicol*, 47, 521-530.
- YANG, Z. & KLIONSKY, D. J. 2010. Mammalian autophagy: core molecular machinery and signaling regulation. *Current opinion in cell biology*, 22, 124-131.
- YE, M., ZHANG, H., AMABILE, G., YANG, H., STABER, P. B., ZHANG, P., LEVANTINI, E., ALBERICH-JORDÀ, M., ZHANG, J., KAWASAKI, A. & TENEN, D. G. 2013. C/EBP α controls acquisition and maintenance of adult haematopoietic stem cell quiescence. *Nat Cell Biol*, 15, 385-394.
- YECIES, J. L. & MANNING, B. D. 2011. Transcriptional Control of Cellular Metabolism by mTOR Signaling. *Cancer Research*, 71, 2815.
- YILMAZ, Ö. H., VALDEZ, R., THEISEN, B. K., GUO, W., FERGUSON, D. O., WU, H. & MORRISON, S. J. 2006. Pten dependence distinguishes haematopoietic stem cells from leukaemia-initiating cells. *Nature*, 441, 475-482.
- YOSHIHARA, H., ARAI, F., HOSOKAWA, K., HAGIWARA, T., TAKUBO, K., NAKAMURA, Y., GOMEI, Y., IWASAKI, H., MATSUOKA, S., MIYAMOTO, K., MIYAZAKI, H., TAKAHASHI, T. & SUDA, T. 2007. Thrombopoietin/MPL Signaling Regulates Hematopoietic Stem Cell Quiescence and Interaction with the Osteoblastic Niche. *Cell Stem Cell*, 1, 685-697.
- YUE, Z., JIN, S., YANG, C., LEVINE, A. J. & HEINTZ, N. 2003. Beclin 1, an autophagy gene essential for early embryonic development, is a haploinsufficient tumor suppressor. *Proceedings of the National Academy of Sciences of the United States of America*, 100, 15077-15082.
- ZHANG, B., LI, M., MCDONALD, T., HOLYOAKE, T. L., MOON, R. T., CAMPANA, D., SHULTZ, L. & BHATIA, R. 2013. Microenvironmental protection of CML stem and progenitor cells from tyrosine kinase inhibitors through N-cadherin and Wnt- β -catenin signaling. *Blood*, 121, 1824-1838.
- ZHANG, F., CONG, L., LODATO, S., KOSURI, S., CHURCH, G. M. & ARLOTTA, P. 2011. Efficient construction of sequence-specific TAL effectors for modulating mammalian transcription. *Nat Biotech*, 29, 149-153.
- ZHANG, X. & REN, R. 1998. Bcr-Abl Efficiently Induces a Myeloproliferative Disease and Production of Excess Interleukin-3 and Granulocyte-Macrophage Colony-Stimulating Factor in Mice: A Novel Model for Chronic Myelogenous Leukemia. *Blood*, 92, 3829-3840.
- ZHOU, T., COMMODORE, L., HUANG, W.-S., WANG, Y., THOMAS, M., KEATS, J., XU, Q., RIVERA, V. M., SHAKESPEARE, W. C., CLACKSON, T., DALGARNO, D. C. & ZHU, X. 2011. Structural Mechanism of the Pan-BCR-ABL Inhibitor Ponatinib (AP24534): Lessons for Overcoming Kinase Inhibitor Resistance. *Chemical Biology & Drug Design*, 77, 1-11.
- ZIMMERMANN, J., BUCHDUNGER, E., METT, H., MEYER, T. & LYDON, N. B. 1997. Potent and selective inhibitors of the Abl-kinase: phenylamino-pyrimidine (PAP) derivatives. *Bioorganic & Medicinal Chemistry Letters*, 7, 187-192.
- ZIMMERMANN, J., BUCHDUNGER, E., METT, H., MEYER, T., LYDON, N. B. & TRAXLER, P. 1996. Phenylamino-pyrimidine (PAP) — derivatives: a new class of potent and highly selective PDGF-receptor autophosphorylation inhibitors. *Bioorganic & Medicinal Chemistry Letters*, 6, 1221-1226.